Development of Monoaminergic Systems: Morphogenetic Roles and Early Specification

Tania Vitalis

Thesis submitted for the degree of Doctor of Philosophy in the Faculty of Medicine, University of Edinburgh

November 2000

PhD-The University of Edinburgh-November 2000

Disclaimer

All experiments presented in this thesis were performed by me unless clearly stated below.

1- In Chapter Two, measures with high-pressure liquid chromatography (HPLC) and fluorometric detection were performed by Drs. J. Callebert and J-M Launay.
2- In Chapter Three, K Gillies performed numerous genotyping required fore the study.
3- The study reported in Chapter Four was done in collaboration with Drs. P. Gaspar and O. Cases (INSERM U106, Paris, France) and with Dr. J. Shih (University of Southern California, California). These collaborators have cloned MAOA and MAOB and have performed additional in situ hybridization, some of which are shown in this report (Drs. P. Gaspar and O. Cases). They have also generated and characterised in vitro the specificity of the MAOB antibody (Dr. J. Shih) used in Chapter Four.
4- In Chapter Five, cryostat sectioning was mostly performed by G. Grant.

No part of this work has previously been or is being accepted for any other degree.

Tania Vitalis
November 2000

Acknowledgements

I would like to thank particularly Dr. David J. Price my PhD supervisor. David allowed me to build up my mind in complete freedom. Although sometimes I found it hard to be completely left to myself, I think that the experience was worthwhile. I feel that I have learned a lot about Science, people and myself, and that I am ready to pursue my scientific career knowing that this is what I really want to do. So thanks Dave and do not change.

I also would like to thank Dr. R. Ribchester my second supervisor and all the members of the "Price Lab" and "John Mason Lab" and the University of Edinburgh. Particularly my friends and those who have cheerfully helped me on a day to day basis and also in specific tasks. I would like to thank Katy Gillies for spending long hours at the bench genotyping a huge number of mice for me. I would like to thank Grace Grant for sectioning brains I gave her without measuring her time. I would like to thank Linda Sharp for her confocal assistance and Brendan McGrory for his enthusiasm during photographic assistance.

During my PhD, I have also received inestimable scientific and human help from Dr. Olivier Cases and Dr. Patricia Gaspar (INSERM U106, Paris, France). I met Patricia and Olivier in Paris, in 1995. Patricia supervised actively my "Veterinary Thesis" and was able to share and transmit her passion for Science, which will remain in my heart. Olivier, how should I thank Olivier? Olivier guided my path, encouraged me and explained to me so many things while preserving my freedom. We were and I hope we will continue to be "the dream team" in Science and life.

I would like to thank Catherine Verney (INSERM U106, Paris, France) and Luis Puelles (University of Murcia, Spain) who have been friendly and taken the time to introduce me to the world of dopaminergic neurons and to the "prosomeric model".

I would like to thank Dr. Linda Richards and Dr. Mickel Shipley who have invited me to spend working holidays in The University of Maryland (University of Maryland, Baltimore, USA). Linda taught me so much and so kindly, it was both a very nice scientific and human experience. I hope I will continue to collaborate with Linda, we have so many interesting questions to discuss...

I would like to thank the members of the "Pax6 meetings" in Edinburgh for their friendship and sharing freshly new data and ideas.

I would like to thank Marc Tessier-Lavigne and Andreas Puschel for their cheerful advice and encouragement.

I also would like to thank all the members of our BIOMED grant. I wish I could have met all of you more often to discuss even deeper on barrel field related topics. The few meetings we had brought me a lot of scientific information and updated data and ideas to carry on my research on barrel field and allow me to know your work and yourselves a bit more.

Finally, I would like to thank all my past, present and future collaborators for all their qualities and all the organisations that have sponsored my research and studies (The European Commission, The University of Edinburgh, The Physiological Society and The Brain Association).

Abstract

Development of Monoaminergic Systems:
Morphogenetic Roles and Early Specification

Although monoaminergic systems (serotonin, noradrenalin and dopamine) seem diffuse and unspecific, their actions on the refinement of the cerebral structure and wiring are crucial. Despite an abundant literature about monoamines actions on adult brain, little is known about monoaminergic development per se and its action on other developing structures. In my thesis, I wanted to investigate these different aspects by studying i) the influence of serotonin on the development of the murine somatosensory thalamocortical system, ii) the developmental expression pattern of monoamine oxidase A (MAOA) and B (MAOB): two major enzymes of degradation of monoamines and, iii) the influence of essential molecules such as the transcription factor Pax6 or the chemoattractive/chemorepellent molecule Netrin-1 on monoaminergic development.

Serotonin is often regarded as a powerful morphogen, however proofs of its action are often missing. In my thesis, I demonstrated that a transient excess of serotonin created pharmacologically by inhibition of MAOA enzyme altered the formation in barrels of both thalamocortical axons and granular neurons in the layer IV of the developing somatosensory cortex. Thalamocortical axon alterations are characterised by a state of exuberance. A small family of molecules, neurotrophins has been shown to control early events in the developing thalamus and cortex such as cell survival, neurite outgrowth, migration, or dendritic and axonal morphologies. I showed that trkB, an essential neurotrophin receptor was expressed in the cortex during the critical period of serotonin sensitivity. Analysis of mice lacking trkB showed subtle alterations in the thalamocortical projections, suggesting that trkB is not essential in the establishment of the barrel field. By obtaining mice lacking MAOA and trkB, I showed a synergistic altered phenotype in the thalamocortical projection, suggesting that in normal conditions serotonin and trkB signalling act synergistically in the refinement of the somatosensory thalamocortical map.

I also studied the spatio-temporal pattern of MAOA and MAOB and showed striking features during early development: MAOA is tightly linked to the serotoninergic and catecholaminergic phenotypes and MAOB is tightly linked to the glial cell lineage.

Analysis of mice lacking Pax6 showed that Pax6 was not essential to monoaminergic development but this study revealed that Netrin-1 was potentially important to the axonal pathfinding of dopaminergic neurons. Analysis of mice lacking Netrin-1 or its receptor *deleted in colorectal cancer* (DCC) confirmed that Netrin-1 is important but not essential for the axonal guidance of subsets of dopaminergic neurons. More interestingly, this study revealed that the interaction between Netrin-1 and DCC could be important for the cell survival of developing dopaminergic neurons.

Abbreviations

3-MT : 3-methoxytyramine
5, 7-DHT : 5, 7-dihydroxytryptamine
5-HIAA : acide-5-hydroxyindole acetic
5-HT : serotonin
5-HT1B/5-HT1b/5-HT_{1B} : serotonin receptor type 1b
5-MT : 5-methyl-N-tryptophane
6-OHDA : 6-hydroxydopamine
5n : trigeminal motor nucleus
7n : facial nucleus
10n : dorsal motor vagus nucleus
12n : hypoglossal nucleus
A1-A17 : catecholaminergic groups
A1 : primary auditory area
A6 : locus coeruleus
A6s : locus subcoeruleus
A8 : retrorubral field
A9 : substantia nigra
A10 : ventral tegmental area
A13 : zona incerta
A15d : bed nucleus
A15v : supraoptic nucleus
A : adrenaline/adrenalin
AA : anterior amygdala
AADC : aromatic L-amino acid decarboxylase
AB : anterobasal nuclei
ac : anterior commissure
ACB /Acb : accumbens nucleus
ACC : nucleus accumbens
ACh-E : acetylcholinesterase
ACX : archicortex
AEP : entopeduncular area
AH : anterior hypothalamus
Amb : ambiguus
AMPo : anterior medial preoptic nucleus
α-MPT : alpha-methylparatyrosine
AP : alar plate
AS : anterior snout
B1-B9 : serotoninergic groups
B1 : raphe pallidus
B2 : raphe obscurus
B 3 : raphe paragigantocellularis
B4 : raphe magnus
B5 : raphe pontis
B6-B7 : raphe dorsalis
B8 : raphe centralis superior
B9 : nucleus tegmenti reticularis ponti
BDNF : brain derived neurotrophic factor
BMP : bone morphogenetic protein
BP : basal plate
BrdU : bromodeoxyuridine
BST : bed nucleus of stria terminalis
C1-C3 : putative adrenergic neuronal groups
CA : catecholaminergic
CB : cerebellar primordium
cc : corpus callosum
Ce : central amygdaloid nucleus
CCK : cholecystokinin
CGEL : caudal ganglionic eminence, lateral part
CGEM : caudal ganglionic eminence, medial part
Ch(7) : cholinergic group (7)
Chp : choroid plexus
Cing : cingulate cortex
CL : central thalami nucleus
CM : central median thalamic nucleus
CNS : central nervous system
CO : cytochrome oxidase
Coll : collicullus
COMT : catecholamine-O-methyltransferase
cs : superior colliculus
CTX : cortex
D1-5 : dopamine receptors
DA : dopaminergic
DAB : diaminobenzidine
DBH : dopamine-b-hydroxylase
DCC : deleted in colorectal cancer
DMH : dorsal medial hypothalamic nucleus
DPMe : deep mesencephalic nucleus
dt /DT : dorsal thalamus
E15 : fifteenth day of postnatal life
EMT : thalamic eminence
ENK : enkephalin
ep/ET : epithalamus
FAD : flavine adenine dinucleotide
FGF : fibroblast growth factor
FP : floor plate
FP : fore paw
fr : fasciculus retroflexus
fx : fornix bundle
GABA : gamma aminobutiric acid
GDNF : glial derived neurotrophic factor
GNRH : growth hormone-realising hormone
Hb : habenula
HCC : hypothalamic cell cord
HDC : histidine decarboxylase
HP : hind paw
HPLC : high-pressure liquid chromatography
HVA : homovanylic acid:
ic : internal capsule
Ic : inferior colliculus
IMAO : monoamine oxidase inhibitor
IMD : intermediate thalamic nucleus
ION : infraorbital nerve lesion
ITA : intermediate telencephalic territory
Is : isthmus
LC/Lc : locus coeruleus
LD : lateral dorsal thalamic nucleus
L-DOPA : L-dihydroxyphenylalanine
LGE : lateral ganglionic eminence
LH : lateral hypothalamus
LH : luteinizing hormone
LL : lower lip
LL : lateral lemnisc
LTP : long term potentiation
M1 : primary motor area
M2 : secondary motor area
MA : mammillary region
MAO : monoamine oxidase
MAOA : monoamine oxidase type A
MAOB : monoamine oxidase type B

mb : mammillary body
mes : mesencephalon
mfb : medial forebrain bundle
MGE : medial ganglionic eminence
mGlur : metabotropic glutamate receptor
MHPG : 3-methoxy-4-hydroxyphenylglycol
mlf : medial longitudinal fasciculus
mm : mammillary body
MPTP : 1-methyl-4-phenyl-1,2,3,6-tetrahydropyridine
mtg : mammilotegmental tract
NA: noradrenaline
NGF : nerve growth factor
MHb : medial habenula
NMDA : N-methyl-D-aspartate
NMN : normetanephrin
MnPO : medial preoptic nucleus
MnR : raphe median nucleus
NPC : posterior commissure nucleus
NPY : neuropeptide Y
NT-(4) : neurotrphin (4)
OB : olfactory bulb
oe : olfactory epithelium
olf : olfactory nerve
OR : optic recess
OT : olfactory tubercle
OXT : oxytocin
p1-p6 : prosomeres; pc posterior commissure
PAVH : paraventricular hypothalamic nucleus
pc/ PC : posterior commissure
PC : paracentral thalamic nucleus
PCPA : parachlorophenylethylamine
PEP : posterior entopeduncular area
PF : prechordal floor plate
(S)PF : (sub)parafascicular thalamic nucleus
pir : piriform cortex
PLCβ1 : phospholipaseC-β1
PM : premotor area
PMBSF : posteromedial barrel subfield
PNMT : phenylethanolamine-N-methyltransferase
PNS : peripheral nervous system
POA : anterior preoptic area
POP : posterior preoptic area
PP : prechordal plate
PR : parietal rostral field
pt/PECT : pretectum
ptc : pretectal commissure
PV : paraventricular thalamic nucleus
PV : ventral sensory area
r1-r8 : rhombomeres
RCH : retrochiasmatic
Re : reuniens nucleus
REM : rapid eye movement sleep
RD : Raphe dorsal
Rh : rhomboid nucleus
RMg : Raphe magnus nucleus
Rsg : retrosplenial cortex
RP : roof plate
S1 : primary somatosensory cortex
S2 : secondary somatosensory cortex
sc : superior colliculus
SCH : suprachiasmatic
SDH : succinate dehydrogenase
SE : septum
SERT : serotonin transporter
Shh : sonic hedgehog
stm : stria medullaris
SN : substantia nigra
SNc : substantia nigra pars compacta
SNr : substantia nigra pars reticulata
SPV : supraoptico-paraventricular region
StHy : striato-hypothalamic nucleus
Str : striatum
sut/sth : subthalamic nucleus
tc/TC : thalamocortical axons
te : thalamic eminence
tect : midbrain tectum
TH : tyrosine-hydroxylase
TpOH : tryptophan hydroxylase
TrkB : tyrosine kinase receptor type B
Trp : tryptophan
TTX : tetrodotoxin
TU : tuberal hypothalamic region
V1 : primary visual area
V2 : secondary visual area
VB : ventrobosal thalamic nucleus (also VP)
VIP : vasopressin
VMAT : vesicular monoamine transporter
vt/VT : ventral thalamus
VTA : ventral tegmental area
Zi : zona incerta
Zli : zona limitans intrathalamica

CONTENTS

CHAPTER ONE: INTRODUCTION

CHAPTER TWO:
INFLUENCE OF SEROTONIN ON SPECIFIC DEVELOPING STRUCTURES: EFFECTS OF MONOAMINE OXIDASE A INHIBITION ON BARREL FORMATION IN THE MOUSE SOMATOSENSORY CORTEX: DETERMINATION OF A SENSITIVE DEVELOPMENTAL PERIOD

CHAPTER THREE:
IMPORTANCE OF TRKB SIGNALLING IN THE MURINE SOMATOSENSORY CORTEX

CHAPTER FOUR :
DEVELOPMENTAL EXPRESSION OF MONOAMINE OXIDASE A AND MONOAMINE OXIDASE B

CHAPTER FIVE:
SEARCH FOR MOLECULES THAT COULD INFLUENCE THE DEVELOPMENT OF MONOAMINERGIC SYSTEMS-I-: A ROLE FOR THE TRANCRIPTION FACTOR PAX6?

CHAPTER SIX:
SEARCH FOR MOLECULES THAT COULD INFLUENCE THE DEVELOPMENT OF MONOAMINERGIC SYSTEMS-II-: A ROLE FOR NETRIN-1?

CHAPTER SEVEN: CONCLUSION AND PERSPECTIVES

Chapter One:
Introduction

CHAPTER ONE:
INTRODUCTION

I Monoaminergic systems

1 The serotoninergic system

In the 1940s, scientists were aware of a substance present in the serum that induced powerful contractions of smooth muscles. In the 1970s, with the work of Page and his collaborators, a substance proposed to be a possible cause of high blood pressure (a serum tonic factor; Page, 1968, 1976) was isolated from platelets. At the same time, in Italy, a molecule present in high concentration in the intestinal mucosa and that caused contractions of gastrointestinal smooth muscle was characterised (Espaner, 1963). The molecule isolated from blood platelets was named "serotonin"; that from the intestinal tract was called "enteramine". Both molecules were purified, crystallised and shown to be the same indolamine, 5-hydroxytryptamine (5-HT). In the brain, 5-HT is a neurotransmitter implicated in various physiological and behavioural functions such as sleep, modification of circadian rhythms, nociception, eating, thermoregulation, arousal and sexual behaviour.

1.1 Localisation

The distribution of serotonin-containing cell bodies and their projections were originally described using fluorescent histochemical methods, first established by Falck and his collaborators (Swedish school) in the 1970s. In 1968, Falck and his collaborators first located the raphe nuclei and their projections (Dahlstrom and Fuxe, 1964; Fuxe et al, 1968). Later, the fluorescent method was supplanted by more sensitive immunohistochemical methods using antibodies generated against serotonin or tryptophan hydroxylase (TpOH). Using these techniques, Steinbusch and his collaborators provided a precise mapping of serotoninergic neurons and their projections (Steinbusch et al., 1978; Steinbusch, 1981).

Serotonin-containing cell bodies constitute the raphe nuclei and are classically distributed in nine groups (B1-B9), where B1 is the most posterior group and B9 the most anterior (Moore, 1981; Steinbusch and Nieuwhuys, 1983). Most of the

serotoninergic innervation arises from the most rostral components of the raphe: from the raphe dorsal (B6-B7) and from the raphe median (B5-B8) (Dahlstrom and Fuxe, 1964). The projections of these two raphe nuclei do not overlap completely and a relative specificity in the area of projection of each was reported. The innervation of the hippocampus arises mainly from B8 (fiber type M; Jacobs et al., 1974) whereas the innervation of the striatum arises principally from B7 (fiber type D). The serotoninergic innervation of the cortex arises from both nuclei but the projections of the neurons of these two groups are well separated (Tohyama et al., 1980). The posterior nuclei B1-B3 (overall B3 or nucleus of the raphe magnus) mainly project to the medulla. In addition, diffuse 5-HT containing terminals are found all over the central nervous system (cortex, hippocampus, striatum, accumbens, substantia nigra, hypothalamus) (Doucet et al., 1988). Figure I-1 provides a sagittal view of the different serotoninergic groups in adult rodent.

1.2 Metabolism

5-HT does not cross the blood brain barrier and the brain contains only 1-2% of the entire amount of 5-HT contained in the body (Bradley, 1989). In the central nervous system (CNS), 5-HT synthesis is located exclusively in serotoninergic neurons. In the peripheral nervous system (PNS), neurons of the gastro-intestinal plexus, the body of the pineal gland and enterochromaffin cells produce 5-HT whereas platelets only take up 5-HT.

The precursor of 5-HT is the essential amino acid tryptophan. In the blood, 90% of tryptophan is linked to serum-albumin and 10% of tryptophan is free to cross the brain blood barrier. Tryptophan is accumulated in serotoninergic neurons by a non-specific aminergic transporter (used by several uncharged amino acids). At this step, a competition between uncharged amino acids is possible.

In serotoninergic neurons, tryptophan is hydroxylated by tryptophan hydroxylase (TpOH) into 5-hydroxytryptophan that is then decarboxylated by the aromatic amino acid decarboxylase (AADC). AADC is not specifically located in serotoninergic neurons.

In serotoninergic cell bodies, 5-HT is stored into vesicles by a Ca^{2+}-dependent mechanism. Vesicles are then transported to dendritic and axonal terminals. Inside the vesicles, 5-HT is protected from the oxidative action of

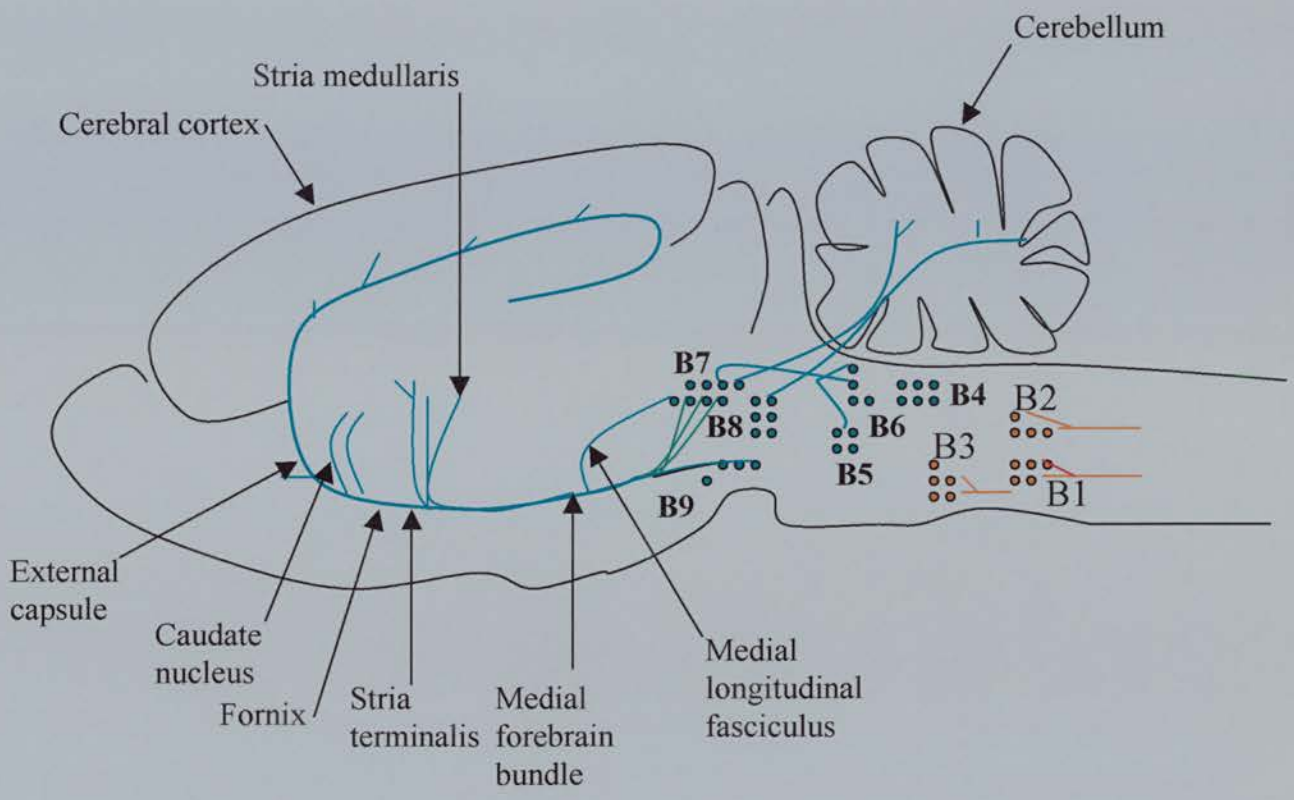

Figure I-1 Serotoninergic cell groups within the rodent brainstem. B1, nucleus raphe pallidus; B2, nucleus raphe obscurus; B3, nucleus paragigantocellularis; B4, nucleus raphe magnus; B5 nucleus raphe pontis; B6 and B7, nucleus raphe dorsallis; B8, nucleus centralis superior; B9, nucleus tegmenti reticularis pontis and adjacent tegmentum. Serotoninergic cell groups that belong to the caudal group appear in red whereas serotoninergic cell groups that belong to the rostral group appear in green. (From Kandel, Schwartz, and Jessel, (1991), third edition).

monoamine oxidase A (MAOA). Then, 5-HT is released into the synaptic cleft upon stimulation. 5-HT could be taken up into the terminals that released it by the serotonin transporter (SERT) located on the membrane. SERT is mainly located on serotoninergic neurons and platelets (Blakely et al., 1991; Hoffman et al., 1991; Lesch et al., 1993). However, during development SERT is also located on non-aminergic neurons (Hansson et al., 1998; Lebrand et al., 1998). This is consistent with the unexpected role of serotonin in the general development of the brain (i.e.: the thalamocortical system). Finally, 5-HT is either degraded enzymatically by MAOA to 5-hydroxyindole acetic acid (5-HIAA), or stored again in synaptic vesicles. 5-HIAA is the primary metabolite of serotonin and is excreted in urine. The brain accounts for only 5% of body production of 5-HIAA. Dosages of 5-HIAA concentration in urine offer a good evaluation of the metabolism of 5-HT when pathological alterations of the serotoninergic systems are suspected. Figure I-2 illustrates these metabolic steps.

Several mechanisms contribute to the regulation of serotonin synthesis. Serotoninergic neurons are sensitive to changes in plasma levels of tryptophan, and thus dietary changes can regulate serotonin levels in the brain. Increases in intracellular serotonin levels do not significantly alter serotonin synthesis in vivo. Short-term requirements for increases in serotonin synthesis appear to be accomplished by Ca^{2+}-dependent phosphorylation of TpOH. In contrast, situations which require a long-term increase in serotonin availability appear to induce TpOH synthesis.

1.3 Receptors and transduction pathway

Seven subtypes of serotonin receptors (5HT1-5HT7) have been identified, with further subdivision of the 5-HT1 subtype. With the exception of 5-HT3 receptor, which is ionotropic, all 5-HT receptors exhibit the typical seven transmembrane-spanning segments, and are all coupled to G proteins to exert their effects. They either modulate the activity of an enzyme linked to the membrane (adenylate cyclase, phospholipase C, phospholipase A2) or an ionic channel (Hoyer et al., 1994). For example, 5-HT1a, 5-HT1b, 5-HT1d and 5-HT4 either activate or inhibit adenylate cyclase and 5-HT1c and 5-HT2 receptors preferentially stimulate the activation of phospholipase C to produce increased levels of diacylglycerol and inositol 1,4,5-

Figure I-2 Metabolism of serotonin

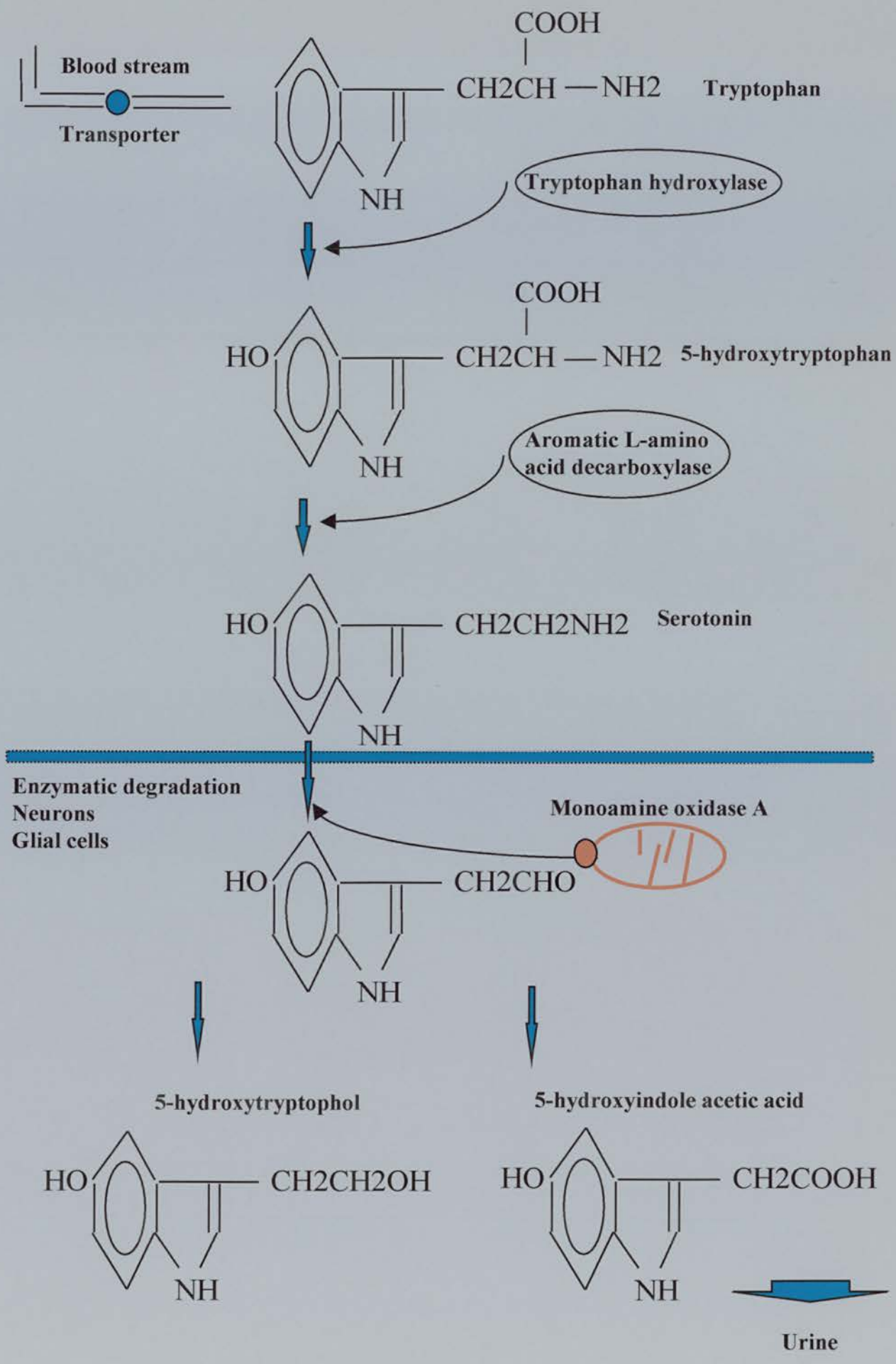

triphosphate. 5-HT1a, 5-HT1b, 5-HT1c, 5-HT1d have high affinity for 5-HT whereas 5-HT2 and 5-HT4 have 200-500% less affinity for 5-HT than the first group. Serotonin receptors can also be separated into two groups according to their gene structures. 5-HT1c and 5-HT2 are derived from genes that contain multiple introns. In contrast, 5-HT1 is encoded by a gene lacking introns. Interestingly, 5-HT1a is more closely related to the β-adrenergic receptor family than to the other members of the 5-HT receptor family. This helps to explain pharmacological results suggesting that 5-HT1a and 5-HT1b can bind certain adrenergic antagonists.

In the CNS, serotonin receptors are generally located post-synaptically. In addition, 5-HT1a, 5-HT1b and 5-HT1d are located on serotoninergic neurons themselves and the stimulation of these so-called "autoreceptors" inhibits the activity, the synthesis and the release of 5-HT (De Montigny et al., 1992).

1.4 Some biological effects of serotonin

Numerous pharmacological studies have elucidated the role of 5-HT in the modulation of a large number of stimulatory signals and in the coordination and the organisation of appropriate behaviours. Particularly, it was suggested that 5-HT plays a role in restraint of emotions such as fear, distress, depression and anguish (Vogt, 1982). Indeed, in several psychological disorders, sleep, circadian rhythms, mood, food intake, thermoregulation and sexual behaviour are altered (Meltzer and Lowy, 1987) and these functions are highly related to disorders of the serotoninergic system.

A role of 5-HT in the regulation of the mood was also strongly suggested. Studies of depressed (Shopsin et al., 1976; Delgado et al; 1990) or normal patients (Young et al., 1985; Smith et al., 1987) have shown that decreased levels of 5-HT in the brain are associated with mood disorders. Regimes low in tryptophan lead to slight depression in normal patients (Young et al., 1985; Smith et al., 1987) and lead to severe depression in patients already depressed before the regime (Smith et al., 1987)

Another characteristic feature of depression is the alteration of sleep. A latency in the state of sleep called rapid eye movement (REM) sleep is often observed in depressed patients and this was proposed to be due to a decrease of serotoninergic activity (Fornal and Radulavaki, 1983; Reyes et al., 1983). However, the cholinergic system may also be implicated in this symptom (Sitaram et al., 1982) and REM

alteration is observed in numerous psychiatric disorders not directly linked with alteration of 5-HT levels.

The alterations of circadian rhythms (Wehr and Goodwin, 1981) and of temperature regulation (Avery et al., 1982) observed in some depressed patients was suggested to be linked with perturbations of regulatory mechanisms in the suprachiasmatic nuclei. The suprachiasmatic nuclei have been shown to be strongly innervated by serotoninergic fibers (Moore et al., 1981). In addition, links were established between perturbation of serotoninergic systems and seasonal affective disorders, which are characterised by frequent periods of hypersomnia and boulimia in winter (Jacobson et al., 1987).

5-HT also plays an important role in motor function (Modigh et al., 1971), memory (Altman et al., 1984; Cross et al., 1988) and aggression (Valzelli et al., 1981; Cases et al., 1995). The existence of a transgenic mouse strain in which high levels of serotonin and aggression are associated provides further evidence for the role of 5-HT in the regulation of this behaviour (Cases et al., 1995).

2 The Dopaminergic system

For a long time, before the work of Carlson (Sweden, 1958), dopamine (DA) was only considered as an intermediate metabolite of the noradrenaline (NA) synthesis pathway. Because elevated DA levels were detected in the striatum even in the absence of NA, and because of its depletion due to reserpine (which antagonises the neuronal storage of amines into vesicles) DA was finally suggested to play a role as a neurotransmitter. Several studies have demonstrated its role as neurotransmitter, and today DA is considered as one of the most important and well-known neurotransmitters due to the diversity and importance of its functions and the number of pathologies in which it is implicated.

2.1 Localisation

In the CNS, dopaminergic neurons are classically organised in five systems: the tubero-infundibular and incerto-hypothalamic systems (A11-A14), the nigro-striatal system (A9), the meso-limbic (A10), the meso-striatal (A10) and the meso-

cortical (A10) systems (Bjorklund and Lindvall; 1984; 1986). The definition of these systems relies on the knowledge of their main area(s) of projection(s).

Nigro-striatal and meso-striatal systems include DA neurons of the substantia nigra (SN; A9) and of the ventral tegmental area (VTA; A10) which project to several striatal areas (the caudate, the globus pallidus, the accumbens, the olfactory tubercle and the stria terminalis). Meso-limbic and meso-cortical systems include neurons of the VTA which project to the limbic (i.e.: septum, locus coeruleus, habenula) and cortical areas. In addition, three discrete nuclei were described: A15 (dorsal and ventral preoptic areas), A16 (olfactory tubercle) and A17 (retina). Figure I-3 provides a sagittal view of the different dopaminergic groups in adult rodent.

2.2 Metabolism

Like other aminergic neurotransmitters, DA does not cross the brain-blood barrier. By contrast its precursor, tyrosine, crosses the brain blood barrier through an energy-dependent uptake process common to large neutral amino acids. The cytoplasmic enzyme, tyrosine hydroxylase (TH), catalyses the transformation of tyrosine to L-dihydroxyphenylalanine (L-DOPA). Under basal conditions, TH is the rate-limiting enzyme for DA synthesis and its physiological catalytic capacities are maximal. After TH, AADC decarboxylates L-DOPA and forms DA. AADC is not a rate limiting enzyme. After its synthesis, DA is actively concentrated by the vesicular monoamine transporter into vesicles. In the vesicles DA is protected from the oxidative activity of monoamine oxidases (MAOs) which could transform DA to DOPAC.

Several mechanisms are involved in the elimination of DA in the synaptic cleft: i) its uptake by DA terminals through specific DA transporters (Shimada et al., 1991; Kilty et al., 1991; Giros and Caron; 1993), ii) its capture by neighbouring glial cells, or iii) its inactivation by catecholamine-O-methyltransferase (COMT), into 3-MT (3-methoxytyramine). The combination of COMT and MAO leads to the formation of homovanylic acid (HVA). Figure I-4 sums up these steps.

2.3 Regulation of TH expression and activity

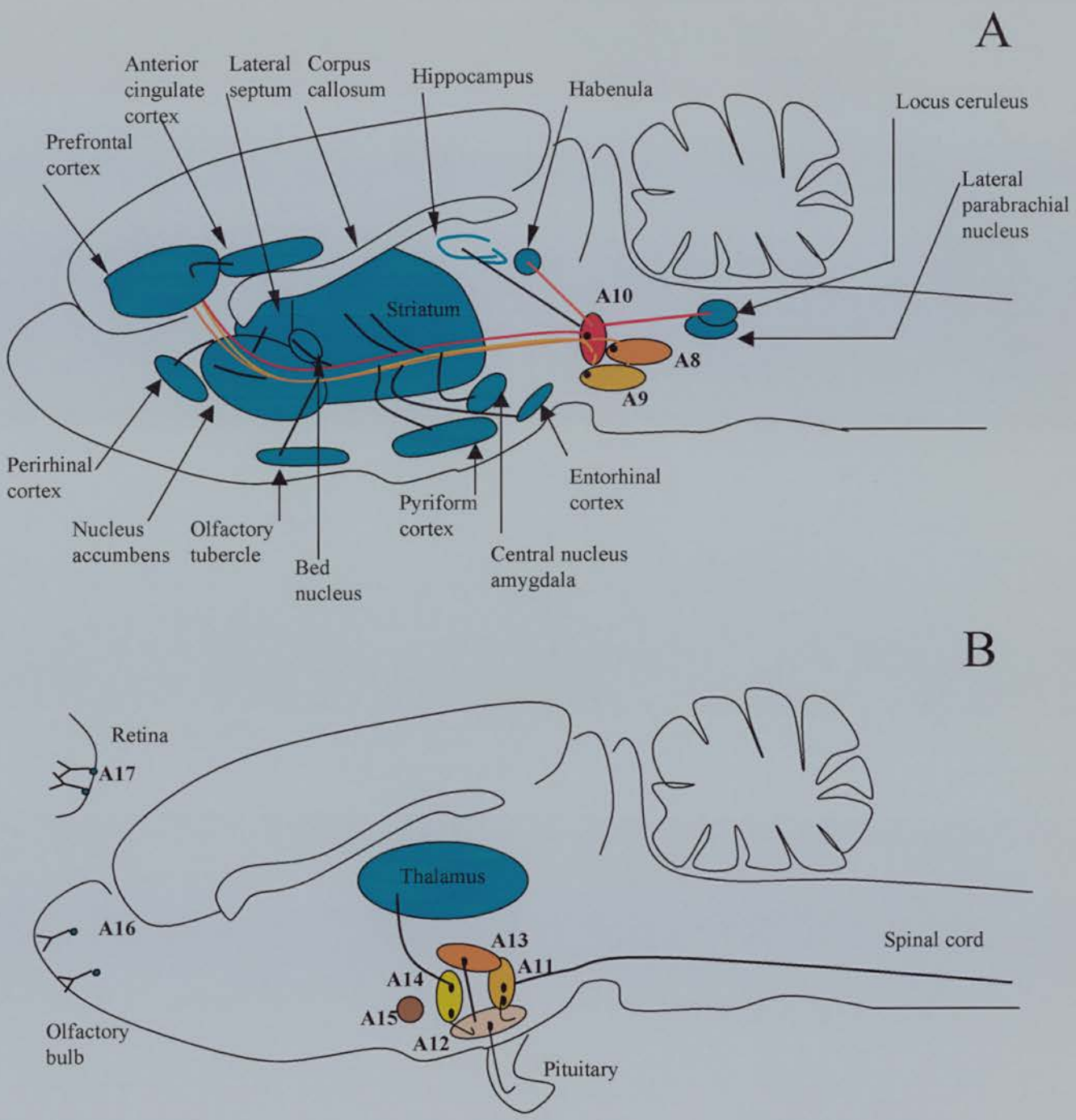

Figure I-3 Dopaminergic cell groups within the rat brainstem. A, The two major dopaminergic cell groups in the midbrain. The mesostriatal and mesolimbocortical systems are located in A8 (retrorubral nucleus), A9 (substantia nigra), and A10 (ventral tegmental area). **B,** Other dopaminergic cell groups of the central nervous system. Areas A11-A14 are the diencephalic dopaminergic cell groups, including the tuberohypophyseal incertohypothalamic and medullary periventricular neurons; area A15 includes cells in the dorsal and ventral preoptic areas and the hypothalamus; area A16 contains olfactory bulb and, area A17 the retinal dopaminergic neurons. (Adapted from Cooper, Bloom, and Roth, 1986)

Figure I-4 Metabolism of dopamine, noradrenaline and adrenaline

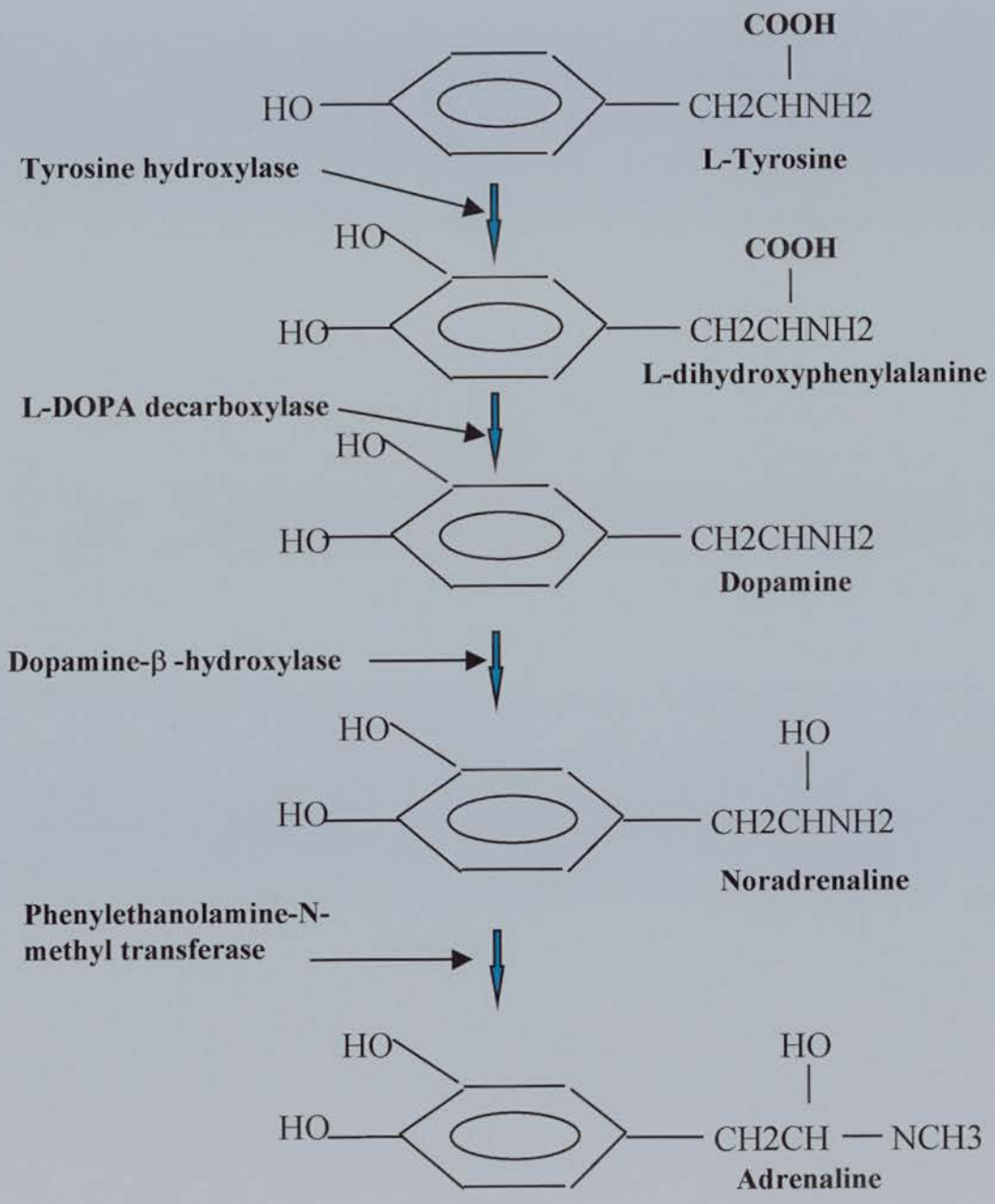

Regulation of TH expression is relatively complex and differs between species. In humans the TH gene gives rise to four TH mRNAs through alternative splicing, resulting in four TH isoforms (Nagatsu, 1995). By contrast, in monkey two TH isoforms are present, whereas in rat a single form of TH mRNA is detected. The different forms of TH in human may be associated with differences in activity of the enzyme, although this association remains unclear. TH function is determined by two factors: changes in enzymatic activity (the rate at which the enzyme converts the precursor into its product) and changes in the amount of the enzyme present. The regulation of the enzymatic activity is due in part to the phosphorylation of the enzyme which takes place at four different serine sites at the N-terminus of the protein. These residues are phosphorylated differently by different kinases. A second means of regulation of the enzymatic activity is through end-product inhibition: catecholamines can inhibit the activity of TH through competition for the required pterine cofactor of the enzyme.

An increased demand for catecholamine synthesis can be met by inducing TH protein or by activating (by phosphorylation) the enzyme. For instance, increase in NA synthesis in noradrenergic neurons of the locus coeruleus is accomplished primarily by increasing gene expression. In contrast, TH mRNA levels do not vary in dopaminergic neurons of the substantia nigra. In these neurons, TH synthesis is changed primarily by altering existing enzyme activity (post-translational events). (Glovinsky et al., 1976; Kumer and Vrana, 1996)

TH enzymatic activity requires the presence of a biopterin cofactor and Fe^{2+}. Because the levels of this cofactor are non-saturating under basal conditions, levels of cofactor are significant in regulating TH activity. Indeed, a genetic defect in the gene encoding GTP-cyclohydroxylase 1, the rate limiting enzyme in the synthesis of the biopterin cofactor, has been associated with a neurological disorder called dopa-responsive dystonia in which patients are impaired in specific movements (Ichinose et al., 1994).

Recently, the study of the TH promoter has shown the existence of distinct enhancer elements directing the region-specific expression of TH (Liu et al., 1997). For instance, a hypothalamus regulatory domain and a midbrain-specific element were located between -2.5 and -3.4kb and -0.8 and -5.5kb of the rat promoter respectively (Sakurada et al., 1999).

2.4 Receptors and transduction pathway

At least six types of DA receptors have been identified: D1, D2a, D2b, D3, D4, D5 and several isoforms exist for each receptor. All these receptors belong to a superfamily of seven helix transmembrane receptors coupled to a G protein. D1 and D5 are coupled with a Gs protein which increases cAMP by stimulating an adenylate cyclase. D1 receptors are located in neurons of the striatum and D5 receptors are located in cortical and hippocampal neurons. D2 and D4 receptors are located on neurons of the limbic system, in the accumbens, the hippocampus, the cortex, the caudate, the amygdala and the dopaminergic neurons of the substantia nigra. D2a receptors are coupled with a Gi protein, which inhibits adenylate cyclase and D2b receptors are coupled with a Gk protein, which stimulates the metabolism of phosphatidylinositol. D2a receptors are located on axonal terminals and on the cell bodies of dopaminergic neurons where they act as inhibitory autoreceptors. D3 and D4 receptors are mostly expressed in the limbic system and in the cortex.

2.5 Some biological effects of dopamine

Dopaminergic interneurons projecting over very short distances exert a neuromodulatory action on sensory input. This includes the interplexiform amacrine-like neurons, which link inner and outer plexiform layers of the retina and the periglomerular dopamine cells of the olfactory bulb which link mitral cell dendrites in separated adjacent glomeruli. For instance, it was shown that odor learning increases dopamine levels in the olfactory bulb, whereas odor deprivation increases D2 receptor density present on olfactory nerve terminals (Coopersmith et al., 1991).

In "intermediate length systems" (tuberohypophysal, tuberoinfundibular incertohypothalamic and periventricular systems) TH has been shown to be colocalised with several transmitters including growth hormone-realising hormone (GNRH), cholecystokinin (CCK), vasopressin (VIP), gamma aminobutiric acid (GABA/GAD), neuropeptide Y (NPY), enkephalin (ENK) and oxytocin (OXT) and, to play a role in the release of several transmitters (Tillet, 1991). The tubero-infundibular system participates in the regulation of the release of prolactin, luteinizing hormone (LH) and growth hormone. For instance, in this system, noradrenaline suppresses pulsatile release of LH in ovariectomized females rats, but stimulates the LH secretion in

oestrogen treated animals. During the preovulatory LH surge, noradrenaline and adrenaline (from A1/A2 group) stimulate the activity of LHRH neurons (Weiner et al., 1988). Dopamine (from A13/A14 groups) inhibits pulsatile release of LH with or without steroids (MacKenzie et al., 1988). In contrast to LH secretion prolactin is tonically inhibited by dopamine release from the tubero-infundibular system (Fuxe et al., 1969). In turn dopaminergic neuron activity is influence by prolactin. DA has also been directly implicated in promoting the release of vasopressin, oxytocin and corticotropin releasing factor from the supraoptic nucleus and the periventricular hypothalamic nucleus.

Systems formed by neurons projecting toward long distances, including the nigro-striatal, meso-limbic and meso-cortical systems have been extensively studied due to their implication in several diseases (see below). The nigro-striatal system is implicated in the coordination of voluntary movements. Meso-limbic and meso-striatal systems are implicated in the regulation of emotional behaviour, wakefulness and the initiation of voluntary movements. The meso-cortical system participates in cognition, attention, social behaviour and the organisation of memory

2.6 Dopamine and CNS pathologies

Parkinson's disease was the first illness associated with a lack of a specific neurotransmitter. In 1817, James Parkinson described motor disorders generated by an illness, which is nowadays associated with his name. Symptoms of Parkinson's disease are best characterised by: i) rhythmic trembling while at rest, ii) difficulties in the initiation of spontaneous movement (akinesia), iii) a very slow performance in voluntary movements and iv) muscle rigidity (bradykinesia). In the sixties, by studying the brains (post-mortem) of patients who died from Parkinson's disease, Oleh Hornykiewicz found decrease levels of 5-HT, NA and most importantly DA in those brains. Further, in 1966 Hornykiewicz demonstrated that brains of patients who died of Parkinson's disease displayed a 90% loss of dopaminergic neurons of the substantia nigra (Hornykiewicz, 1966). Extensive studies of human Parkinson's disease and of animals with dopaminergic-depleting brain lesions show that dopaminergic fibers of the nigro-striatal bundle are critical for initiation of voluntary movement. The fibers appear to mediate a non-specific component of arousal that is common to all motivated behaviours. The etiology of Parkinson's disease is

complex. Several genetic or epigenetic predispositions have been pointed out as key factors involved in the degeneration of mesencephalic dopaminergic neurons.

The fact that antipsychotic drugs block several dopaminergic receptors suggested that an excess of dopaminergic transmission could be associated with some schizophrenic symptoms. Indeed, indirect evidence strengthens this idea. First, the use of drugs increasing DA levels such as L-DOPA, cocaine or amphetamines could lead in some cases to psychotic states which resemble to some extent paranoic or schizophrenic states. Second, the post-mortem analysis of brains of patients suffering from schizophrenia displayed an increase in D2 receptors in the caudate and the accumbens (Kirch and Weinberger, 1986). This finding was corroborated by positron emission tomography in living patients (Wong et al., 1986). In fact, several models for schizophrenia in which DA plays a key role have been established. One of them implicates a defect of meso-cortical activity in the frontal lobe leading to the loss of the inhibitory feed-back of the frontal lobe on the meso-limbic system and limbic areas (Weinberger, 1987).

3 The Noradrenergic and Adrenergic systems

NA and adrenaline (A) are the oldest neurotransmitters known. NA acts as a neurotransmitter in the CNS and in the PNS and as an hormone in the adrenal. NA is implicated in various functions from the control of blood pressure to arousal and sleep.

3.1 Localisation

In the CNS, noradrenergic and adrenergic cell bodies are found in two main locations: i) in the region of the pons, at the level of the locus coeruleus (LC) and subcoeruleus (A5, A6, A7), ii) in the medulla at the level of the reticular nuclei (A1 and C1) and in the nuclei of the solitary tract (A2 and C2) (Moore and Bloom, 1979). LC projects widely to the cortex, the hippocampus, the amygdala, the septum, the thalamus, the hypothalamus and the medulla (Loughlin et al., 1986). Figure I-5 provides a general overview of the main noradrenergic projections arising from the LC. These neurons display an impressive number of collaterals. The noradrenergic groups A1 and A2 and their projections are partly mixed with the adrenergic groups

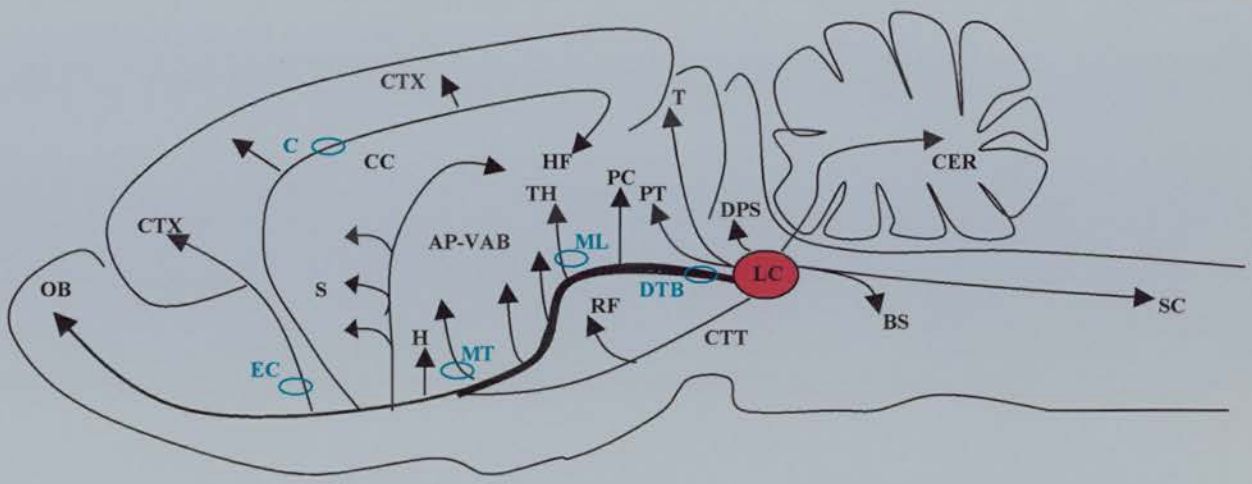

Figure I-5 Summary diagram of the projections of the locus coeruleus in the rat. AP-VAB, ansa penduncularis-ventral amygdaloid bundle system; BS, brain stem; C, cingulum; CC, corpus callosum; CER, cerebellum; CTT, central tegmental tract; CTX, cerebral cortex; DPS, dorsal periventricular system; DTB, dorsal tegmental bundle; EC, external capsule; F, fornix; H, hypothalamus; HF, hippocampal formation; LC, locus coeruleus; ML, medial lemniscus; MT, mammilothalamic tract; OB, olfactory bulb; PC, posterior commissure; PT, pretectal area; RF, reticular formation; S, septal area, SC, spinal cord; SM, stria terminalis; T, tectum; TH, thalamus. (From Kandel, Schwartz, and Jessel, 1991, third edition; adapted from Moore and Bloom, 1979).

(C1 and C2). A1 and C1 targets play an important role in the control of vegetative functions (regulation of the blood pressure, the heart rate and respiration frequency, of some neuro-hormonal secretions such as adrenocorticotrop hormones and growth hormone).

3.2 Metabolism

A and NA are synthesised from tyrosine, which is actively taken up by catecholaminergic neurons. Three enzymes: TH, AADC and dopamine-β-hydroxylase (DBH) are necessary for the synthesis of NA. Finally the conversion of NA to A is made by phenylethanolamine-N-methyltransferase (PNMT). The first two steps are done in the cytoplasm and lead to DA synthesis. The final step for NA or A synthesis takes place in the synaptic vesicles where DBH and PNMT are located. DA is actively taken-up and concentrated into vesicles by the vesicular monoamine transporter. Nerve terminals are depolarized by a calcium-dependent mechanism and vesicular contents are released into the synaptic cleft (NA) or into the blood (adrenal).

Several mechanisms are required for NA degradation. In the CNS, the most important event is the specific re-uptake of NA by terminals: this is an active step involving the specific NA transporter located on the membrane (Pacholczyk et al., 1991). In neurons (pre or post-synaptic) or glial cells, MAOA and COMT degrade NA to metabolites such as normetanephrin (NMN) and 3-methoxy-4-hydroxyphenylglycol (MHPG). Figure I-6 sums up the different steps involved in A and NA degradation.

The regulation of DBH, like that of AADC, is less understood than that of TH. However, it now appears that conditions that increase the activity of the locus coeruleus noradrenergic neurons increase TH activity, DBH (rather than TH) becomes saturated and is the rate limiting step in catecholamine synthesis (Scatton et al., 1984). This results in the accumulation of DA and acidic dopamine metabolites, which are then released from noradrenergic neurons.

3.3. Receptors and transduction pathway

Figure I-6 Degradation of noradrenaline

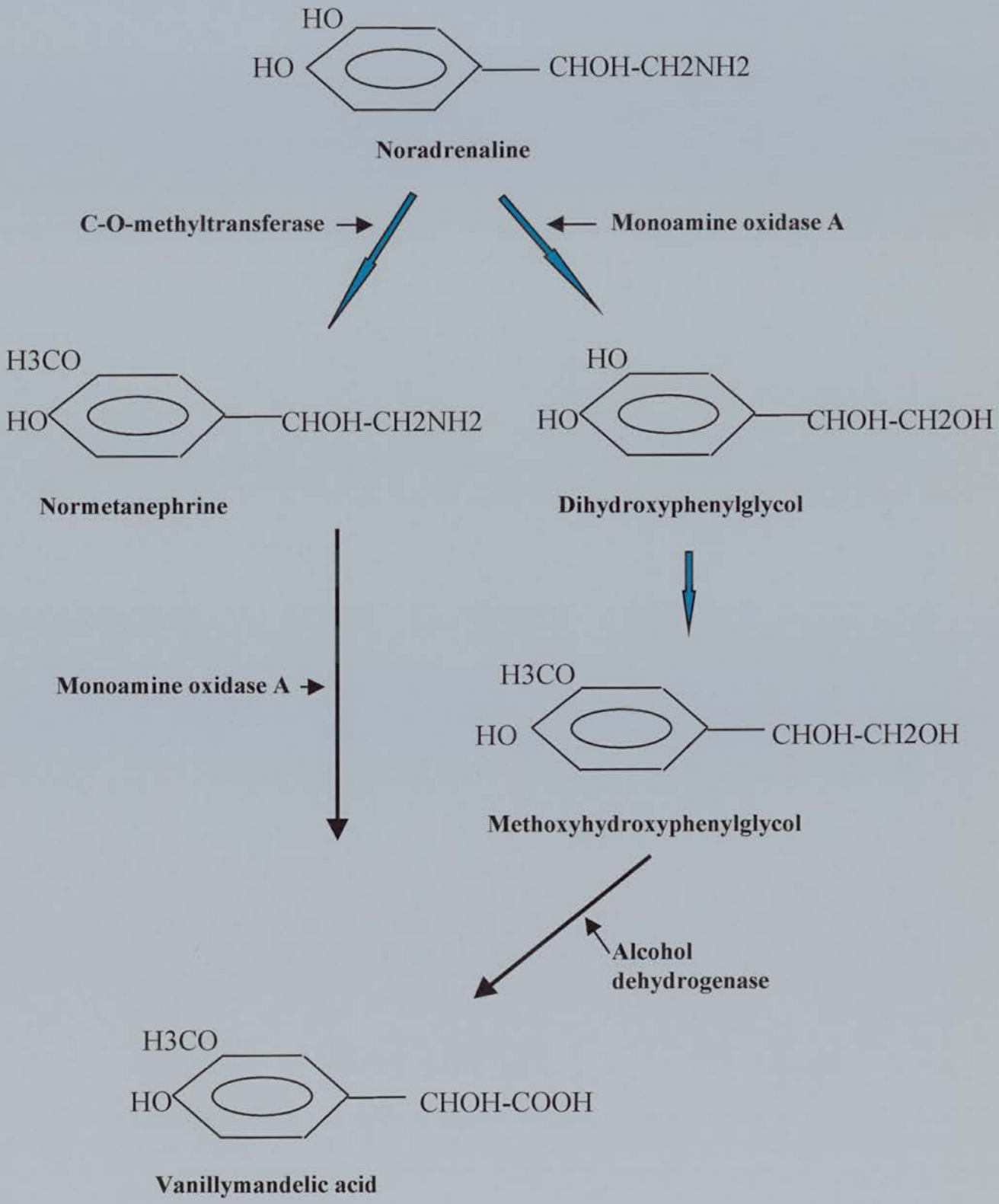

At least four types of receptors for NA have been identified: α1, α2, β1 and β2, with several isoforms for α1 (3), α2 (3), and β1 (2). These receptors belong to the superfamily of receptors coupled with a G protein (Jonowski and Sulser, 1987). β receptors are positively coupled with a Gs protein, which stimulates adenylate cyclase activity. They are expressed in the cortex and the cerebellum. β1 receptors are expressed in neurons whereas β2 receptors are expressed in glial cells. α1 receptors are coupled with a Gp protein, which increases phospholipase C activity. They are widely located in the brain (postsynaptically), in blood vessels (causing vasoconstriction) and in the spleen. α2 receptors are negatively coupled with a Gi protein, which inhibits adenylate cyclase activity. They are widely expressed in the brain and are mainly presynaptic.

3.4 Some biological effects of NA in the CNS

Biological effects of NA are mostly inhibitory: stimulation of the LC or iontophoretic injections of NA induce a decrease of the spontaneous activity of neurons. Conversely, NA potentiates the neuronal responses to auditory, visual and nociceptive stimulations. NA amplifies signals coming from the periphery over the background generated by the spontaneous activity of the neurons. This role is important in attention and arousal. Conversely, LC is in relative rest when only vegetative tasks or tasks related to species preservation are performed. During the state of REM sleep, LC neurons are actively suppressed, and with the end of REM sleep they show activation by novel sensory events. LC activation has been shown to be positively correlated with arousal.

3.5 Depression and noradrenergic and adrenergic systems

Evidence for the role of NA systems in depression are not direct. Most antidepressant drugs increase the half-life of monoamines, either by inhibiting their uptake (imipramines), or by decreasing the degradation of monoamines (monoamine oxidase inhibitors). Modifications in adrenergic receptors or in NA levels were observed in depressed patients, but results are often contradictory. Recently, the pharmacological administration of an antagonist of the α2 adrenoreceptor (raclopride) with or without a D2/3 dopamine receptor antagonist (idazoxan) has

shown the synergistic action of these two antagonists on cortical dopamine output and has suggested a role for α2 adrenoreceptor antagonists in the treatment of schizophrenia through its antipsychotic effects (Hertel et al., 1999).

4 Monoamine oxidases

4.1 Introduction

Monoamine oxidases (MAOs; monoamine: O2 oxydoreductase; EC 1.4.3.4) type A (MAOA) and type B (MAOB) are the major enzymes catalysing the oxidative degradation of biological amines such as catecholamines and 5-HT in the CNS and the PNS (liver, kidney, intestine). MAO also degrade xenobiotic amines such as tyramine found in the food and β-phenylethylamine. MAO are flavoproteins located in the external mitochondrial membrane (Weyler et al., 1990).

In vitro, MAOA degrades preferentially 5-HT and is irreversibly inactivated by clorgyline. In vitro, MAOB degrades preferentially β-phenylethylamine, telemethylhistamine and benzylamine. MAOB is irreversibly inactivated by L-deprenyl. In vitro, DA, NA, tyramine and tryptamine are common substrates for both enzymes. In vivo, MAOA preferentially degrades 5-HT, NA and A, whereas MAOB preferentially degrades DA, β-phenylethylamine, and telemethylhistamine in the brain. In addition, the xenobiotic 1-methyl-4-phenyl-1,2,3,6-tetrahydropyridine (MPTP) could be oxidised by MAOB into a neurotoxic product. In rat and monkey, MPTP injections cause permanently symptoms observed in Parkinson's disease (Strolin-Benedetti and Dostert; 1989; Srolin Benedetti et al., 1991) and are used as a model of this disease.

4.2 Localisation and organisation of genes coding for MAOA and MAOB

In human, mouse and probably most mammals, MAOs are located on the X chromosome. In the mouse, the MAOA and MAOB genes are located in a region of 240 Kb and are organised in a "tail-to-tail" configuration with their 3' ends separated by 50 Kb. The comparison of their genomic sequences showed that their exon-intron organisation is identical. The hypothesis is that the two genes were derived from the duplication of an initial ancestral gene (Grimsby et al., 1991). Nucleotidic sequences

show a very high homology between the two genes. In both genes, exon 12 encodes for the sequence allowing the fixation of the flavine adenine dinucleotide (FAD), the cofactor of MAO activity.

Although the promoters of MAOA and MAOB are highly homologous (Shih et al., 1993), the fixation sites for the transcription factors are not identical suggesting that the two promoters have functionally diverged during evolution. This would explain differences in their temporal expression and tissue distributions.

4.3 Tissue distribution of MAOA and MAOB

Numerous studies have been done to characterise the tissue distributions of MAO in several species including humans, primates, cats, sheeps, and rodents. However, only few developmental data are available.

In human, MAOA and MAOB are co-expressed in most tissues, with the exception of the placenta, which expresses only MAOA (Hsu et al., 1988; Grimsby et al., 1990) and of the platelets and lymphocytes which only express MAOB (Bond and Cundall, 1977). In the brain, MAOA is detected principally in noradrenergic neurons whereas MAOB is detected principally in serotoninergic neurons (Thorpe et al., 1987).

Luque et al. (1995) have recently shown that in the adult rat brain, the location and level of MAO mRNA expression is in tight correspondence with the quantity of MAO proteins. The highest level of MAOA expression is in noradrenergic neurons. Low levels of MAOA mRNA and protein are also reported in serotoninergic and dopaminergic neurons in several species including rat (Kitahama et al., 1994; Luque et al., 1995; Jahng et al., 1997). In addition, MAOA mRNA is also detected in non-aminergic neurons of the hippocampus and the cerebral cortex (Luque et al., 1995). MAOB mRNA and protein are principally located in serotoninergic and histaminergic neurons, ependymal cells and Bergmann's glial cells (Levitt et al., 1982; Kitahama et al., 1994; Luque et al., 1995; Jahng et al., 1997). In addition, MAOB mRNA is also observed in non-aminergic neurons of the hippocampus (CA1-2; Luque et al., 1995).

4.4 Temporal expression of MAO

The temporal expression of MAOA and MAOB are differently regulated during brain development. For instance, in human foetal brain MAOA activity precedes MAOB activity (Lewinsohn et al., 1980) whereas MAOB activity is higher than MAOA activity in adult brain (Garrick and Murphy, 1982).

In rodent brain, MAO activities first appear in the late stages of pregnancy (Liu et al., 1987). By using selective inhibitors of MAOA or MAOB activities and tyramine as the substrate, Mantel et al. (1976) were able to detected MAO activities in extracts of embryonic rat brain (E17). At this age, Mantel et al. (1976) have estimated the level of MAOB activity to be only 2.5-3% of the total activity of MAOA and MAOB. In mouse embryos, Melamed et al. (1990) have shown that MAOB activity is extremely low. Interestingly, these authors have linked these findings to developmental changes in MPTP sensitivity. MPTP damages dopaminergic neurons of the substantia nigra and MAOB is necessary for the activation of this toxin. When MPTP is injected to pregnant mice, a major decrease of dopaminergic neurons is observed in the mother but not in the embryos. This suggests that there is only a very low MAOB activity in the embryonic brain, which could explain the resistance of embryos to MPTP (Melamed et al., 1990).

Biochemical studies have shown that during the development of rodent brain, MAOA and MAOB activities follow different expression patterns. MAOA activity increases rapidly after birth and reaches a maximum by the fifteenth postnatal day (P15). At this age MAOB has only reached 30% of its maximal activity. In most regions of the brain, MAOB reaches its maximum by P45 (Jourdikian et al., 1975). The studies of Diez and Maderdrut (1977), Yu and Hertz (1982) and Cao Danh et al. (1984) have confirmed these results. In adult mice, in most brain regions, MAOA activity is stable from the second to the twenty-fourth month of age. MAOB activity increases during this period to reach a maximum at sixteen months of age (Strolin-Benedetti et al., 1991; Irwin et al., 1992)

In humans, MAOA activity is very high by birth, then decreases rapidly during the first two years of life, then remains stable during childhood and increases again with age. By contrast, MAOB activity is very low at birth, remains stable during childhood and increases progressively with age. The decrease of MAOA activity during development correlates with studies showing that the 5-HIAA and catecholamine metabolites are decreasing in the cerebrospinal fluid during the first two years of human life (Anderson et al., 1988). The rapid decrease of neuronal

density associated with the increase of synaptic density (Huttenlocher, 1979) during this period may account for this. The increase of MAOB activity during senescence has been well established (Fowler et al., 1980; Strolin-Benedetti and Dostert, 1989). Interestingly, it was suggested that this increase of MAOB could contribute to the neuronal degeneration observed in Parkinson's disease (Knoll et al., 1987). Indeed, MAOB antagonists are prescribed to Parkinson's patients (Suuronen et al., 2000). In addition, the recent generation of a transgenic mouse strain lacking MAOB (Shih et al., 1997) that is resistant to MPTP has clearly demonstrated the role of MAOB in the sensitivity to MPTP.

4.5 Monoamine oxidases and neurological and psychiatric disorders

The role of MAOB in psychiatric disorders has been studied extensively (Fowler et al., 1982; Giller et al., 1982; Sandler et al., 1981; Von Knorring et al., 1985; Zureick and Metzer, 1988). Most of these studies relied on measuring MAOB activity in platelets (Murphy and Donelly, 1974) or on the observation of drug side effects. Even though some results are contradictory, important studies have linked a deficiency in MAOB in the platelets with some neurological and psychiatric disorders. For instance, inherited alcoholism of type 2 is associated with a low MAOB activity in the platelets (Oreland; 1993; Devor et al., 1993, 1994).

The role of MAOA in neurobiologic disorders has been less extensively studied, for the reason that the diagnosis of MAOA deficiency requires a skin biopsy associated with fibroblast cultures (fibroblasts from normal patients possess a high level of MAOA activity). Nevertheless, MAOA deficiency was not found in patients suffering from delirium (Breakefield et al., 1980), schizophrenia (Giller et al., 1982), autism or Gilles de la Tourette syndromes (Giller et al., 1980).

The first evidence showing a link between neurological disorders and MAO deficiency were obtained by studying male patients carrying chromosomic deletions in the region of the MAO genes. These genes are located in the same region as the gene responsible for Norrie disease (Berger et al., 1992; Sims et al., 1992). The deletion of the Norrie gene causes a recessive illness characterised by blindness and progressive deafness sometimes associated with mild mental retardation (Warburg, 1966). Another form of this illness was characterised by severe mental retardation, growth delay, hypotonic crisis, mental seizures and biochemical alterations of

neurotransmitter metabolite levels in urine (Sims et al., 1989; Murphy et al., 1990; Collins et al., 1992). Genetic analysis of the patients revealed that they were carrying a deletion of the Norrie gene but also of MAOA and MAOB genes (De la Chapelle et al., 1985; Sims et al., 1989; Zhu et al., 1989).

Recently, the study of Brunner et al. (1993) has specifically associated MAOA deficiency with behavioural alterations (Brunner et al., 1993a,b) in a Dutch kindred. Indeed, four generations of males displayed the same behavioural alterations (mental retardation and impulsiveness including a verbal aggressive behaviour, aggressive attitudes and violence). In addition, these patients displayed biochemical alterations in the level of several neurotransmitter metabolites in the urine. For instance, they displayed a decrease of HVA, DOPAC, MHPG and 5-HIAA and an increase of 5-HT, NMN and 3-MT.

Recently, studies of mice lacking the gene encoding MAOA (Cases et al., 1995) allowed a deeper insight into the role of MAOA in development and behaviour. MAOA deficient males displayed an aggressive behaviour. Interestingly, preliminary results show that pharmacological treatments with parachlorophenylethylamine (PCPA), a serotonin synthesis inhibitor, are sufficient to reverse some aspects of the abnormal behaviour (I. Seif, unpublished results).

II Development of Monoaminergic systems

1 Genesis of monoaminergic neurons

The birth dates of discrete monoaminergic groups was investigated in several studies. In these studies, single or cumulative injections of ^{3}H-thymidine (Lauder and Bloom; 1974; Balan et al., 1996) or bromodeoxyuridine (BrdU) were used to label cells undergoing division. Heavily labelled cells were considered to be precursors that had not started to differentiate and that were undergoing S-phase at the time of injection. Double immunolabelling for BrdU and TH or 5-HT or detection of the radioactive ^{3}H-thymidine followed by TH or 5-HT immunolabelling revealed the monoaminergic phenotype of the labelled cells. It should be noted that most of these studies were done in rat (there is a two day delay between the development of rat embryos and mouse embryos; E12 rat in corresponds to E10 in mouse) and that these authors considered E1 as the plug date.

1.1Serotoninergic neurons

The development of the serotoninergic system was first described by Olsen and Seiger (1972; 1973) and later by Levitt and Moore (1978) in the rat embryo using fluorescence histochemistry (Olsen and Seiger, 1972; Seiger and Olson, 1973, Levitt and Moore, 1978). These studies provided topographic information concerning the appearance and the development of the different components of the raphe nuclei and their axonal projections. At the same time, the work of Lauder and her collaborators initiated studies to date the time of genesis of the raphe nuclei in rat embryos (Lauder and Bloom, 1974).

These studies have shown i) that raphe nuclei are generated between E11 and E15 with a peak of genesis at E13, the dorsal raphe being generated earlier than the median raphe (Lauder and Bloom, 1974), ii) that raphe nuclei are first detectable by fluorescence histochemistry or by immunocytochemistry between E12 or E14 with a precocity for the rostral group (B1-B7 complex), iii) that the onset of synaptogenesis in the raphe nuclei is E19 and iv) that dorsal and medial raphe neurons contain serotonin soon after they begin to differentiate and rapidly extend axons towards the forebrain (Olson and Seiger, 1972). Table I-1 sums up these findings.

1.2 Catecholaminergic neurons

Numerous studies have described the onset of TH expression in discrete catecholaminergic populations in different vertebrate species (i.e.: Medina et al., 1994 in sauropsides; Puelles and Medina, 1994, in chicks; Specht et al., 1977a,b in rats and Puelles and Verney, 1998 in humans). These studies have shown that catecholaminergic neurons start to express TH soon after they are generated. For instance, dopaminergic neurons of the SN-VTA complex start to express TH soon after they finish their last mitosis, while they are migrating to their final positions.

1.2.1.Dopaminergic neurons

TH-IR neurons of the substantia nigra are generated during a period extending from E12 to E16 in rats with a peak of genesis at E13 (Lauder and Bloom, 1974). TH-IR neurons of the retrorubral field and of the ventral tegmental area are

Table I-1 Development of serotoninergic neurons in the rat.

Serotonergic Groups		E11	E12	E13	E14	End of genesis	Time of midline fusion
CAUDAL	B1	*			o ◊		P6
	B2	*			o ◊		P6
	B3	*			o		none
ROSTRAL	B4		o				P3
	B5		o				P3
	B6		o				none
	B7	*	o ◊		**	E15	P1
	B8	*	o ◊	**	**	E15	P3
	B9		o ◊			E15	none

The terminology described in Wallace and Lauder (1983) is used in this table. The time of midline fusion was identified by Levitt and Moore (1978). Several features of the development of serotoninergic neurons are reported in this table: * the beginning of their mitosis, (Lauder and Bloom, 1974), ** their peak of mitosis (Lauder and Bloom, 1974), o the time of first observable fluorescence (Olson and Seiger, 1972) and, ◊ the time of first detection with 5-HT immunocytochemistry (Aitken and Tork, 1988; Konig et al., 1988).

generated simultaneously and a large majority of them (49% and 37% respectively) are born before E11 (Bayer et al., 1995). In rodents, a gradient in the genesis of TH-IR neurons of the SN-VTA was reported, such that the more anterior and dorsolateral neurons in the SN and the VTA are generated earlier than the posterior ventro-medial neurons (Bayer et al., 1995).

The birthdate of three CA groups, one located in the ventral thalamus (zona incerta; Zi-A13) and two in the hypothalamus (periventricular nucleus and arcuate nucleus) was studied by Balan et al. (1996). The authors showed that TH-IR neurons originate between E12 and E13 in Zi, between E12 and E14 in the periventricular nucleus and by E15 in the arcuate nucleus. In addition, they demonstrated a hormone-independent sexual dimorphism in the genesis of these groups, prior to the onset of a sex difference in androgen levels (E16).

In the telencephalon, TH-IR periglomerular interneurons of the main olfactory bulb are first generated by E18 and from this age they continue to be generated during the entire life of the animal by the subventricular zone of the lateral ventricles (Luskin and Boone, 1994; Betarbet et al., 1996). By contrast, TH-IR external tufted cells are generated locally in the ventricular zone of the olfactory bulb between E13 and E18.

1.2.2 Noradrenergic neurons

In rat, noradrenergic neurons of the locus coeruleus are generated from E11 to E13 with a sharp peak of genesis at E12 (Lauder and Bloom, 1974)

2 Specification and determination of monoaminergic neurons

The understanding of monoaminergic neuronal differentiation and specification rests on analysis of specific expression of transcription factors, or secreted proteins and use of chemicals that can directly interfere with these two steps. In the past few years, the mechanisms underlying the organisation of the mouse brain have been extensively studied and data are now available on the differentiation and specification of monoaminergic neurons of the PNS and CNS.

2.1 Patterning of the neural tube

In the CNS, grafting experiments have demonstrated that neural progenitors can acquire new identities if moved to ectopic locations (Alvarado-Mallart et al., 1990; Gardner and Barald, 1991; Simon, 1995; Grapin-Botton et al., 1997). In addition, transplantation and explant culture studies have confirmed the existence of signalling centres that can change the fate of juxtaposed neuronal progenitors. Signalling centres such as the dorsal ectodermal epidermis, roof plate, and notochord have been shown to instruct cells along the dorso-ventral axis (Tanabe and Jessel, 1996), whereas signalling centres located in the prechordal plate, paraxial mesoderm, midbrain-hindbrain boundary, and the anterior neural ridge can change cell fate along the antero-posterior axis of the neural tube (Lumsden and Krumlauf, 1996; Grapin-Botton et al., 1997; Muhr et al., 1997; Shimamura and Rubenstein, 1997, Houart et al., 1998). Finally, secreted proteins and chemicals were shown to modify cell fates in characteristic ways. For instance, Sonic hedgehog (Shh) and bone morphogenetic proteins (BMPs) were shown to modify cell fates along the dorso-ventral axis (Tanabe and Jessel, 1996) whereas the fibroblast growth factors, FGF2 and FGF8, retinoic acid, and wnt1 can change cell fate along the antero-posterior axis (Crossley et al., 1996; Lumsden and Krumlauf, 1996; Shimamura and Rubenstein, 1997).

In addition, gain-of-function experiments or conversely studies of transgenic deficient mice have provided insight in the role of transcription factors necessary for cell fate determination and specification.

2.2 Specification and determination of dopaminergic neurons

The nature of the signals that specify the fates and initial positions of dopaminergic and serotoninergic neurons was directly addressed in several studies. It was shown that the floor plate could induce the ectopic location of DA neurons when transplanted into both the midbrain and the rostral forebrain (Hynes et al., 1995a; Ye et al., 1998) and that transplantation of the isthmus induces DA neurons in ectopic ventrocaudal forebrain explants (Ye et al., 1998). Shh was shown to be in part responsible for these inductions (Hynes et al., 1995b; Ye et al., 1998) and to act in a dose and contact dependent fashion on the determination of cell fates. In addition, in vitro addition of Shh blocking antibody to the explants prevents the appearance of DA neurons in the forebrain (Ye et al., 1998). HNF3β, a Shh induced molecule, was

also reported to be able to induce DA neurons ectopically (Sasaki and Hogan, 1994; Hynes et al., 1995b). Finally, Ye et al. (1998) have shown that mesencephalic dopaminergic neurons develop at sites where Shh and FGF8 intersect and that these two molecules are necessary and sufficient for the expression of the DA phenotype in normal mice. However, the role of Shh in early and late stages of dopaminergic neuron differentiation may be different. Overexpression of Shh-N causes an increase in TH only if expressed in proliferating cells prior to differentiation (Sakurada et al., 1999). It is possible that the effect of Shh on dopaminergic neurons described by Ye et al. (1998) reflects the differential expansion of precursors via the mitogenic effects of Shh (Wechsler-Reya and Scott, 1999) or the effect of a ventral patterning influence of Shh that acts primarily in proliferative versus postmitotic precursors (Ye et al., 1998). Although Shh signalling is required beyond the final cell cycle in cholinergic differentiation (Ericson et al., 1996), results obtained by Sakurada et al. (1999) indicate that the later stages of dopaminergic neuronal differentiation may not depend on the protracted presence of Shh.

Few transcription factors have been clearly implicated in the determination of discrete dopaminergic populations. The specification of dopaminergic neurons of the SN-VTA complex have been shown to depend on the expression of Nurr1 and Ptx3. Nurr1 and Ptx3 are both specifically expressed in dopaminergic neurons of the SN-VTA complex and are thought to participate in the same regulatory cascade event (Zetterstom et al., 1997). Nurr1 is an orphan receptor belonging to the nuclear receptor superfamily (Law et al., 1992; Zetterstrom et al., 1996a) and Ptx3/Pitx3 is a bicoid-related homeobox factor (Semina et al., 1997, 1998; Smidt et al., 1997). In mice, Nurr1 is protractedly expressed in the midbrain from E10.5, just prior to the appearance of TH (Zetterstrom et al., 1996a,b). Nurr1 is not restricted to midbrain (A8, A9 and A10) dopaminergic neurons and it is also expressed in A11 and A2 catecholaminergic neurons (Baffi et al., 1999). Nurr1-null mice display a specific lack of midbrain dopaminergic neurons whereas A11 and A2 CA neurons are not affected (Zetterstrom et al., 1997; Saucedo-Cardenas et al, 1998, Castillo et al., 1998a) suggesting that Nurr1 plays different regulatory roles in the different catecholaminergic populations. In gain-of-function experiments, it was shown that Nurr1 is able to activate the transcription of the TH gene by binding a responsive element within a region of the TH promoter necessary for midbrain specific

expression. Interestingly, the action of Nurr1 upon dopaminergic neurons was shown to be independent of FGF8 and Shh signalling (Sakurada et al., 1999). TH and Nurr1 expressions potentiated by the accumulation of cAMP (Tinti et al.,1997; Castillo et al., 1997) and Shh inhibits adenylate cyclase suggesting that some of the TH-repressing activity of Shh-N are mediated by the inhibitory pathway of protein kinase A (Sakurada et al., 1999). In mouse, Ptx3 expression starts in the ventral midbrain by E11.5, just after Nurr1 expression and is exclusively and protractedly expressed in mesencephalic dopaminergic neurons in rodent and human (Smidt et al., 1997). In addition, Ptx3 expression is decreased in SN-VTA neurons of human Parkinson patients and in rat treated with 6-hydroxy-dopamine, an animal model for this disease (Smidt et al., 1997). Altogether, these results suggest that Ptx3 could play a specific role in the development of SN-VTA neurons down-stream to Nurr1 (Smidt et al., 1997).

The specification of discrete dopaminergic populations located in the paraventricular hypothalamus and the supraoptic nucleus have been shown to depend on the expression of Sim1.

In addition, in *Drosophila,* the transcription factor islet has been shown to be required for the expression of DA and 5-HT neurotransmitter phenotype (Thor and Thomas, 1997). In *islet* loss-of-function mutants, TH expression is lost and a great reduction in the number of 5-HT-IR neurons is observed. Interestingly, ectopic expression of *islet* induces ectopic TH-IR cells but not ectopic 5-HT-IR cells.

2.3 Specification of serotoninergic neurons in the CNS

Both the specification of serotoninergic and dopaminergic neurons depends on FGF8 and Shh (see above). However, the specification of serotoninergic requires the additional presence of FGF4. Low levels (5ng/ml) of FGF4 and FGF2 can induce ectopically 5-HT neurons in areas of the brain containing endogenous sources of Shh and FGF8 (Ye et al., 1998). Interestingly, the ectopic genesis of 5-HT neurons was observed to the detriment of DA neurons suggesting that FGF4 can change the fate of early neural progenitors (Ye et al., 1998).

Several mediators for Shh's effects have been identified in vertebrates, such as the members of the Gli and Nkx families, and studies in *Drosophila* have pointed out the necessity of several additional transcription factors.

A member of the Gli family (zinc finger family), Gli1, which is expressed in the midline neural plate from the stage of gastrulation, has been shown to act as a target and mediator of Shh signalling in floor plate and ventral neuronal differentiation (Lee et al., 1997). Misexpression of Gli1 protein (but not of Gli2 and Gli3 proteins) in frog and mouse embryos leads to ectopic transcription of Shh and to the ectopic differentiation of serotoninergic neurons (Hynes et al., 1997; Lee et al., 1997). Interestingly, Gli2 and Gli3 have been shown to participate in Gli1 regulation (Ding et al., 1998). Mainly, Gli3 and Shh repress each other whereas Gli2 and Gli1 are targets for Shh signalling (Sasaki et al., 1997; Ding et al., 1998; Ruiz i Aetaba, 1998). It is possible that in the absence of Gli3, Shh territory would expand and generate ectopic serotoninergic neurons, showing the requirement for Gli3 in the mediation of Shh signalling. I have tested this hypothesis in Gli3 knockout mice but found no ectopic serotoninergic neurons at any stage studied. Interestingly, it was recently shown that shh expression is not ectopically activated in the brain of mice lacking Gli3 suggesting that Gli3 fulfils a Shh-independent pathway (Theil et al., 1999). This may explain my result.

Recently, the role of another transcription factor, Nkx2.2, in the genesis of a subpopulation of serotoninergic neurons was also pointed out. Briscoe et al. (1999) have shown that mice lacking Nkx2.2 display a specific loss of serotoninergic neurons located adjacent to the floor plate but not of serotoninergic neurons of the dorsal raphe. They showed that these serotoninergic neurons arise from Nkx2.2-positive progenitors.

Studies on *Drosophila* have pointed to the requirement for four genes encoding for transcription factors essential for the development of serotoninergic neurons: the homeobox genes *engrailed (en)* and *islet*, the zinc-finger-protein-encoding gene *huckenbein (hkb)*, and *eagle (eg,* a member of the steroid receptor gene superfamily*)* (for review see Goridis and Brunet, 1999).

Lundell and Hirsh (1998) have shown that loss-of-function of *eagle* in *Drosophila* leads to a dramatic reduction in the number of serotonin-producing neurons (Lundell and Hirsh; 1998). The authors have demonstrated that *eagle* is necessary for the maintenance of engrailed and Zinc-finger-2 expression in serotoninergic neurons.

The *en* gene probably acts early in the lineage, as it is required for the proper formation and development of the neuroblast from which 5-HT neurons are derived in *Drosophila*. However, *en* is dispensable for 5-HT expression in neurons expressing both *eg* and *hkb*. In fact the combined action of *en* and *hkb* is responsible for the specification of the serotoninergic phenotype (Dittrich et al., 1997). Ectopic expression of *eg* throughout the embryonic nervous system drives ectopic expression of 5-HT in one or two cells in each segment of the *Drosophila*. In a *hkb* mutant background, the number of these ectopic 5-HT neurons decreases dramatically suggesting a co-operative effect of *eg* and *hkb* in the specification of serotoninergic neurons (Dittrich et al., 1997).

2.4 Specification of Noradrenergic neurons in the CNS and the PNS

Several groups of researchers have contributed very important insights into the specification of noradrenergic neurons of the sympathetic ganglia in several species. In chick, the work of Groves et al. (1995) has examined the expression of transcription factors and their implication in the noradrenergic phenotype. They have shown that sympathetic progenitor cells sequentially express the bHLH transcriptional regulator Cash-1, Phox2, a paired homeodomain protein, GATA-2, a zinc finger protein, and finally SCG10, a panneuronal membrane protein before tyrosine hydroxylase. In addition, depletion experiments have shown that GATA-2, Phox2 and TH, but not Cash1 and SCG10, expressions depend on the presence of the notochord. Together, these results suggest that the development of sympathetic neurons involves multiple transcriptional regulatory cascades: one depending on notochord or floor plate derived signals, involving Phox2 (renamed Phox2a) and GATA2 which is assigned to the expression of the neurotransmitter phenotype; the other independent of the notochord, involving CASh-1 which is assigned to the expression of pan-neuronal properties (Groves al., 1995). The generation of mice lacking Phox2a demonstrated the role of Phox2a in the differentiation of the noradrenergic phenotype in the locus coeruleus, a subset of sympathetic and parasympathetic ganglia and the VIIth, IXth, and Xth cranial sensory ganglia (Valarche et al., 1993; Tiveron et al., 1996; Morin et al., 1997). In mice lacking Phox2a, the transient expression of DBH in neuroblasts is abolished and the expression of the GDNF receptor subunit c-ret is greatly reduced. Consequently,

there is a massive increase of GDNF-dependent apoptosis in ganglion cells (Oppenheim et al., 1995; Trupp et al., 1996; Morin et al., 1997). The overexpression of Phox2 in chick neural crest culture leads *in vitro* to an apparent increase in number of sympathoadrenergic cells and *in vivo* to the generation of additional neurons expressing the noradrenergic markers, TH and DBH, and the cholinergic markers ChAT and VAChT. New insight into the cascade of Phox2a expression was brought by the work of Lo et al. (1998) showing that BMP2 and then MASH1 expression were upstream of Phox2. Culture of neural crest stem cells in the presence of the bone morphogenetic protein BMP2 leads to the induction of MASH1 expression which in turn leads to Phox2a expression. Targeted mutation of Mash1 showed that Mash1 is necessary for the development of all (except cranial sensory ganglia) central and peripheral neurons that express permanently or transiently noradrenergic traits (Hirsh et al., 1998). In mice lacking Mash1, Phox2a is abolished. In mice lacking Phox2a, the expression of DBH is not abolished in all NA neurons and NA neurons expressing Phox2b continue to express DBH. The regulation of DBH through the Phox2 genes is thought to be direct since Phox2a and Phox2b bind to regulatory elements of the DBH promoter and stimulate DBH promoter activity in cultured cells. Interestingly, the overexpression of Phox2a in chick embryos has been shown to result in ectopic TH expression (Goridis and Brunet; 1999).

3 Development and guidance of monoaminergic projections

The molecular signals that guide and confer target specificity on different monoaminergic neurons are poorly understood. So far, only a few molecules have been shown to play a direct role in dopaminergic axon guidance. Recently, the receptor EphB1 and its ligand ephrin-B2 have been shown to play a role in the guidance of discrete dopaminergic projections of the SN and the VTA (Yue et al., 1999). EphB1 and ephrin-B2 are expressed in a complementary pattern in the midbrain dopaminergic neurons and their targets (Yue et al., 1999) during the early postnatal period, when dopaminergic innervation primarily occurs (Loizou, 1969; 1972; Coyle and Axelrod, 1972a,b; Olson and Seiger, 1972; Seiger and Olson, 1973). EphB1 is detected at high levels in the SN and not in the VTA and, complementarily, its ligand is highly expressed in the developing striatum, the nucleus accumbens and the olfactory tubercle and only weakly in the caudate putamen (Yue et al., 1999). In addition, ephrin-B2 specifically inhibits the neuritic outgrowth and induces cell loss

of SN but not VTA neurons (Yue et al., 1999). Together, these results suggest that the interaction between EphB1 and ephrin-B2 may result in an inhibitory signal that restricts SN axons from innervating the ventromedial striatum and promotes cell death in mistargeted neurons, thus contributing to the establishment of the mesostriatal and mesolimbic pathways (Yue et al., 1999). In addition, in mice, ephrin-B2 is upregulated after cocaine treatments (Yue et al., 1999) suggesting that it could play a role in plasticity of the dopaminergic brain reward circuit and consequently be involved in drug addiction mechanisms (Nestler et al., 1993; Hyman and Nestler, 1996).

Interestingly, it was suggested that the development of a transient catecholaminergic phenotype could play a role in the maturation of brain circuitry. Several neuronal populations have been described to transiently express tyrosine hydroxylase. These neurons are mainly located in the telencephalon (piriform cortex, neocortex, amygdala, bed nucleus of the stria terminalis, anterior olfactory nucleus, and the inferior colliculus). Most of these neurons are only observed with TH but not with AADC, DBH or PNMT immunocytochemistry and it is therefore possible that these neurons use L-DOPA as a neurotransmitter. No signs of morphological degeneration were reported in these neurons or in the surrounding tissues. In addition the association of TH with somatostatin or substance P in these neurons suggests that these neurons could progressively loose TH expression and remain somatostatin- and substance P-immunoreactive. It is strongly suggested that the transient TH immunoreactivity observed in those neurons could be associated with the maturation of early limbic circuits (Jaeger and Joh; 1983; Verney et al., 1988).

4 Maturation and survival of monoaminergic neurons

Neurodegeneration of dopaminergic neurons in the ventral mesencephalon projecting to the dorsal striatum (meso-striatal system) plays a major role in Parkinson's disease. Thus the finding of candidate molecules able to promote the survival capacities of dopaminergic neurons is a major area of investigation and hope in the therapy of Parkinson's disease. Several factors have been implicated in enhancing the late development of DA neurons. They could play a role in the maturation, the late specification and the survival of DA neurons.

Cultured DA neurons are responsive to the serine protease thrombin, which changes the length, the number of branches, and the pattern of neurites (Debeir et al., 1998). Similarly, morphological changes could be induced in DA neurons by members of the nerve growth factor protein family, by brain-derived neurotrophic factor (BDNF), neurotrophin-3, neurotrophin-4/5, and by the members of the FGF, TGF and GDNF families (Horger et al., 1998). Studies of mice deficient for the TGFα gene revealed that these mice have a 50% reduction in the number of DA neurons in the SN, but a normal complement of other midbrain DA neurons. This indicates that TGFα may participate in the expansion or differentiation of this particular subtype of DA neurons (Blum; 1998).

Two members of the neurotrophic factor family, neurturin (NTN) and BDNF have been shown to play important roles in the survival of mesencephalic dopaminergic neurons. *In vivo*, neurturin, a glial cell-line derived neurotrophic factor, protects dopaminergic neurons from lesion-induced degeneration and increases the survival of embryonic DA neurons transplanted into postnatal rats (Eggert et al., 1999; Rosenblad et al., 1999). *In vitro*, BDNF has been implicated in the survival and differentiation of dopaminergic neurons. *In vivo*, mice overexpressing BDNF in DBH positive neurons display a 52% increase of tyrosine-hydroxylase positive neurons in the substantia nigra pars compacta (Alonso-Vanegas et al., 1999). The authors suggest that an increased anterograde transport of BDNF via the coerulo-nigral projection could rescue dopaminergic neurons from the perinatal period of developmental cell death (Alonso-Vanegas et al., 1999).

In addition, several factors have been shown to influence the development, survival and maturational state of DA neurons in vitro, such as the pituitary adenylate cyclase-activating polypeptide (PACAP; Webber et al., 1998), neurotensin (Sotty et al., 1998), oestrogen and progesterone (Kritzer and Kohama; 1998), substance P (Futami et al., 1998), retinoic acid (Samad et al., 1997), and opioid peptides (Tsao et al., 1998). However, little is known about the function of these factors. They could participate in the late specification or serve as mitogenic or survival factors for discrete DA progenitors.

III Development and organisation of the cerebral cortex

1 Development of the cerebral cortex and cortical lamination

In mammals, the cerebral cortex is organised into six cortical layers. This histological laminar appearance of the cerebral cortex is due to variations of cell densities and of cell types throughout the thickness of the cortex. For instance, i) afferents from the sensory thalamus stop in layer IV; ii) pyramidal neurons located in the supragranular region of the cortex project to other cortical regions, including the contra-lateral cortex; iii) layers V and VI project outside of the cortex, sending their axons toward the thalamus, the striatum, the claustrum and the brainstem. In addition to this laminar organisation, the cortex is divided into discrete areas more or less well-defined (Figure I-7). After the discredited works of the phrenologists of the XVIII century, who tried to associate patriotic thoughts to discrete regions on the cortical surface, numerous works followed. The works of de Broca and Wernicke on language, studies of alterations due to genetic disorders (Clarke and O'Malley, 1969; Blakemore, 1977) and more recently electrophysiological stimulations of specific cortical regions have progressively confirmed the existence of cortical topographical maps.

The main difference between the different cortical regions and that determines their functional specificity is the origins of their afferents. The thalamus is, by far, the major origin of cortical afferents. Both sensory organs (with the exception of the olfactory system) and subcortical motor areas send their information to one or several specific thalamic nuclei, which possess well-defined reciprocal interconnections with specific cortical areas. For instance, the entirety of the rodent's neocortex receives thalamic afferents (Caviness and Frost, 1980), and there is a precise isomorphic correspondence between the topographical organisation of thalamic nuclei and the organisation of cortical areas (Caviness et al., 1988).

In all mammals, the mechanisms of cortical neurogenesis appear to be the same (Uylings et al., 1990). Neurons and glial cells originate in the telencephalic neuroepithelium. As rapid cell division thickens the proliferative zone, the emerging cortical structure progresses from a simple neuroepithelial sheet into a complex laminar structure. The first step in this process involves the creation of a marginal zone, a cell-sparse zone from which nuclei are excluded during interkinetic movements in the epithelium (Marin-Padilla, 1978). Shortly thereafter, by the thirteenth day of embryonic life (E13) in the rat, the first neurons to be generated exit the ventricular zone and form a single layer called the preplate. Together with the

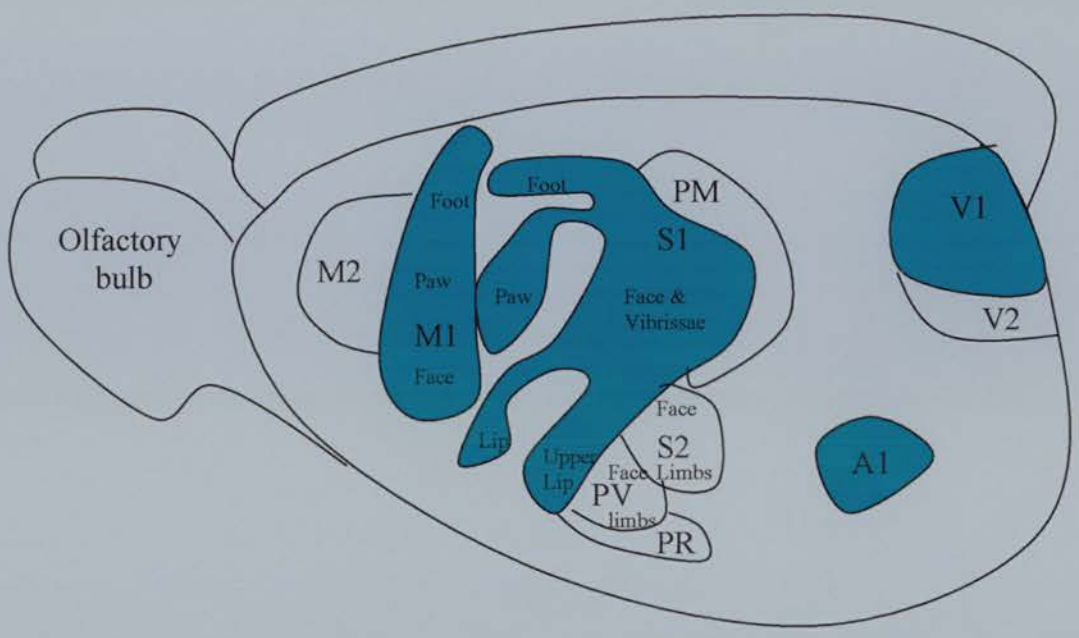

Figure I-7 Cortical areas in rats. Rodent's isocortex is constituted by discrete functional areas. These include the first (S1) and second (S2) somatosensory areas, the more ventrally located ventral sensory area (PV), the primary motor area (M1), the primary auditory area (A1), the primary (V1) and secondary (V2) visual areas, the supplementary motor areas (M2) and the premotor area (PM). The parietal rostral field (PR) is included for orientation. Primary sensory areas appear in green in this schematic representation (adapted from Northcutt and Kaas, 1995).

axons growing into the cortex, the axons of preplate neurons form the intermediate zone, which separates the ventricular zone from the preplate. Collectively, these axons pioneer the connections in both directions between the cortex and the thalamus. The progressive thickening of the developing cortex continues in an inside-out fashion (Lund and Mustari, 1977; Rakic, 1981) and a three-layered cortex appears by E16. It is constituted by a ventricular zone containing proliferative cells, the intermediate zone containing axons and migrating neurons, and the preplate containing postmitotic neuronal precursors that will be subdivided later into the subplate and the marginal zone (Marin-Padilla, 1978; Boulder Committee, 1970). Then, the ventricular zone begins to produce neurons destined for different layers of the cortex. These cells migrate through the intermediate zone and form the cortical plate, a structure that splits the embryonic preplate into two domains: the marginal zone (future layer I); and the subplate, a transient population of neurons that largely disappears by programmed cell death in early postnatal life (Shatz et al., 1988). Finally during the middle and the latter stages of neurogenesis (E21 in rat), a subventricular zone containing mitotically active cells forms between the ventricular zone and the intermediate zone. Figure I-8 sums up these developmental steps.

Preplate neurons seem to play an important role during corticogenesis. They are the first to express a large variety of receptors for several neurotransmitters (Shatz et al., 1988), and to send axons outside of the cortex. In addition, the earliest thalamic axons to penetrate the cortex accumulate under the subplate, over several days in the rodent brain to a few weeks in primates (Rakic, 1977; Lund and Mustari, 1977; Shatz and Luskin, 1986). However in the somatosensory system of the rodent, thalamic axons penetrate the deeper cortical areas without a waiting period (Catalano et al., 1991).

An important issue in cortical development is the understanding of the mechanisms leading to the specification of the cortical areas. According to the work of Rakic (1988) and Reznikov et al. (1984), the cytoarchitectonic characteristics of specific cortical areas are predetermined in the ventricular zone (Smart and McSherry, 1982; Rakic, 1988). Others, like O'Leary (1989), have proposed that the cortical plate is not predetermined and that the determination of specific cortical areas is due to external signals. For instance, the arrival of topographically organised thalamocortical axons in the sensory cortices would determine the characteristics of the different cortical areas (O'Leary et al., 1988). In favour of the hypothesis

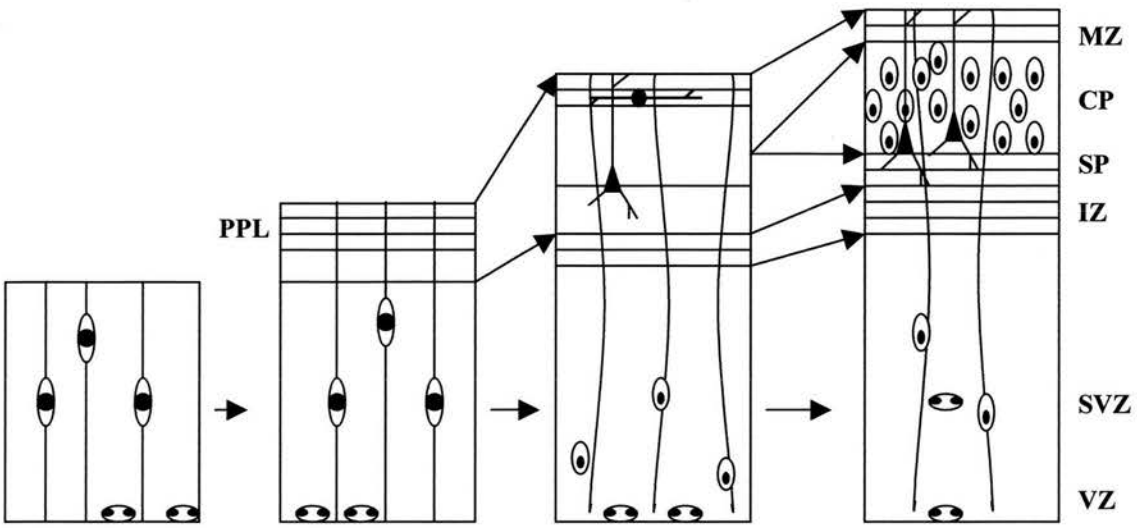

Figure I-8 Stratification of the cerebral wall. Neurogenesis in the mouse neocortex occurs from embryonic day E12 (left) to E17 (right). Cortical development begins with the appearance of a population of cells along the lateral ventricle, known as the ventricular zone (VZ; E12 mice mice). This population of cells gives rise to most of the neurons and glial cells of the cerebral cortex. Once generated, neurons migrate towards the pial surface and complete their differentiation in the cortical plate. Neurons for the deeper layers of the cortex are generated and then migrate away form the VZ earlier than the neurons destined for progressively more superficial layers. On E13-E14, the cerebral wall is bilaminar consisting of the VZ and overlying primitive plexiform layer. CP, cortical plate; IZ, intermediate zone; MZ, marginal zone; PPL, primordial plexiform layer; SP, subplate; SVZ, subventricular zone (From Uylings et al., 1990).

described by O'Leary is the observation that the organisation of some sensory cortical areas is tightly linked to the distribution of thalamocortical axons. This is particularly well illustrated by the organisation of the primary visual cortex into ocular dominance columns in the monkey (Hubel and Wisel, 1977) and by the organisation of the primary somatosensory cortex into the barrel field in rodents (Van der Loos and Woolsey, 1973). In addition, these cytoarchitectonic characteristics only appear after the arrival of thalamocortical axons in the cortical plate (Rakic, 1976; Jhaveri et al., 1991). The most convincing experiment in favour of this hypothesis is that in which one cortical region was grafted into another cortical area (Schlaggar and O'Leary, 1991). Presumptive embryonic rat visual cortex grafted into the presumptive somatosensory cortex develops cytoarchitectonic characteristics of the somatosensory cortex. In the same way, if this region is grafted into a rostral cortical region not belonging to the somatosensory cortex, it will adopt cytoarchitectonic characteristics of the host region (O'Leary and Stanfield, 1989). Recently, the generation of mice lacking *Gbx-2* whose thalamic differentiation is disrupted and lack thalamocortical axons was used to provide a definitive answer on the requirement for thalamocortical axons on neocortical regionalisation (Miyashita-Lin et al., 1999). This study shows that despite the lack of thalamocortical innervation, neocortical lamination and neocortical region-specific gene-expressions (i.e.: *cadherin-6, EphA-7, Id-2 and RZR-beta*) developed normally. This study provides the first evidence that cortical lamination is largely independent of thalamic influence. However, it is likely that thalamic inputs regulates later steps in neocortical development such as neuronal maturation, formation of neocortical modules (such as barrels) and association cortices. Unfortunately *Gbx-2* mutants died at birth making it impossible to investigate the role of thalamic afferents on postnatal neocortical development (Miyashita-Lin et al., 1999).

Studies on cortical development have shown that each developmental step in its construction is plastic and consequently could be influenced by external signals coming from the periphery. The nature of the signals is not known. One hypothesis, that will be developed in Chapter II, is that cortical development could be controlled or at least influenced by aminergic and thalamic afferents via the release of neurotransmitters such as serotonin, dopamine, noradrenaline, glutamate and acetylcholine.

2 The somatosensory system

The following paragraph briefly summarises the numerous studies that have elucidated the organisation of the rodent primary somatosensory cortex, a very attractive system in which to study the formation and plasticity of the somatosensory map.

2.1 Organisation of the somatosensory system

In rodents, the tactile hairs located on the snout, the lower lip, the paws and the trunk are isomorphically represented in the primary somatosensory cortex in a topographic map "the barrel field" (Van Der Loos and Welker, 1985; Van Der Loos et al., 1991) where the size of the representation depends on the functional importance of the receptor field (Figure I-9). For instance, the main whiskers located on the posterior snout are precisely organised into five parallel rows and each row is constituted by four to height large whiskers. The most caudal whiskers are the largest and the more thick; the caudal most are the smallest (Figure I-10). Each whisker receives a strong sensory innervation from the infra-orbital nerve.

Sensory information from the whiskers is conducted through a series of relays to the somatosensory cortex. The successive relays are located in: i) the trigeminal ganglion, ii) the trigeminal nuclei (the principalis, interpolaris and caudalis nuclei, Erzurumulu and Jhaveri, 1992) and ii) the ventrobasal thalamic nucleus. Each relay, with the exception of the trigeminal ganglion, maintains the precise topographical organisation observed on the snout (Figure I-11). In these nuclei, neurons are organised in discrete structural units called barrelettes in the trigeminal nuclei (Ma, 1993) and barreloids in the ventrobasal (or ventro posterior) thalamic nucleus. Barreloids project to the primary somatosensory cortex via thalamocortical axons. This isomorphic representation is first established in the trigeminal nuclei.

2.2 The barrel field

De Vries first observed the barrel field, in 1912. After toluidine blue coloration of preparations fixed in alcohol, De Vries reported the presence of "square

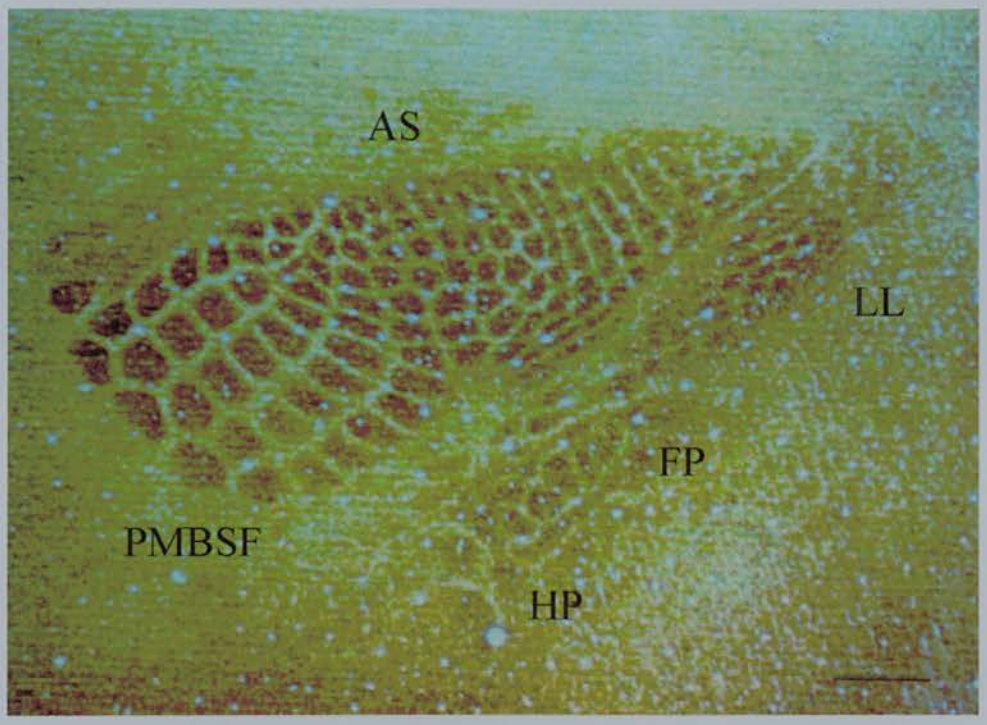

Figure I-9 Isomorphic organisation of the barrel field. On flattened preparations stained for cytochrome oxidase each whisker located on the snout of the mice has a unique and isomorphic representation in the somatosensory cortex of the animal. The size of the representation depends on the functional importance of the barrel field. The posteromedial barrel subfield (PMBSF) corresponds to the main whiskers located on the snout. Whiskers located in the anterior snout (AS), lower lip (LL), hind paw (HP) and forepaw (FP) are also represented in the barrel field. Note that the representation of the main whiskers (PMBSF) which are the most important for the behaviour of the animal proportionally occupy a larger brain area than the representation of the other tactile hairs. Scale bar = 400 μm.

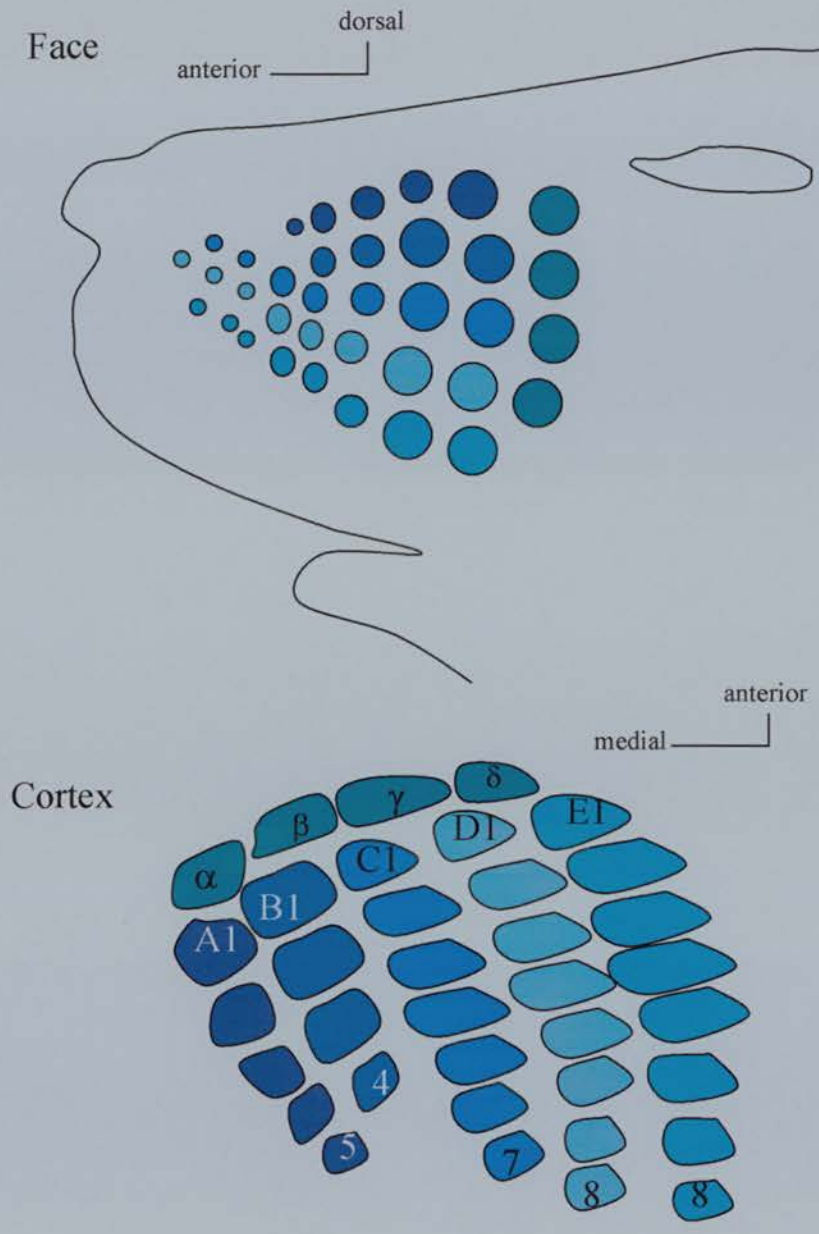

Figure I-10 Organisation of the whiskers on the face of the mice and of the barrels in the cortex of the mice. Schematic representation of the organisation of the mystacial vibrissae on the face and the barrel field in the first somatosensory cortex (S1). On the face (top), the whiskers are arranged in the five principal rows labeled A-E from dorsal to ventral, and numbered 1-4+ from caudal to rostral within the rows, with four straddler whiskers located caudally between the principal rows and labeled α–δ. This arrangement is seen in the cortex (bottom), where each barrel is a cytoarchitectonically distinct area that is one-to-one correspondence with a whisker on the animal's contralateral face. In the barrel cortex, barrels for row E whiskers are anterior to those for row D whiskers, and lower-numbered and straddler barrels are medial to higher-numbered barrels within a row.

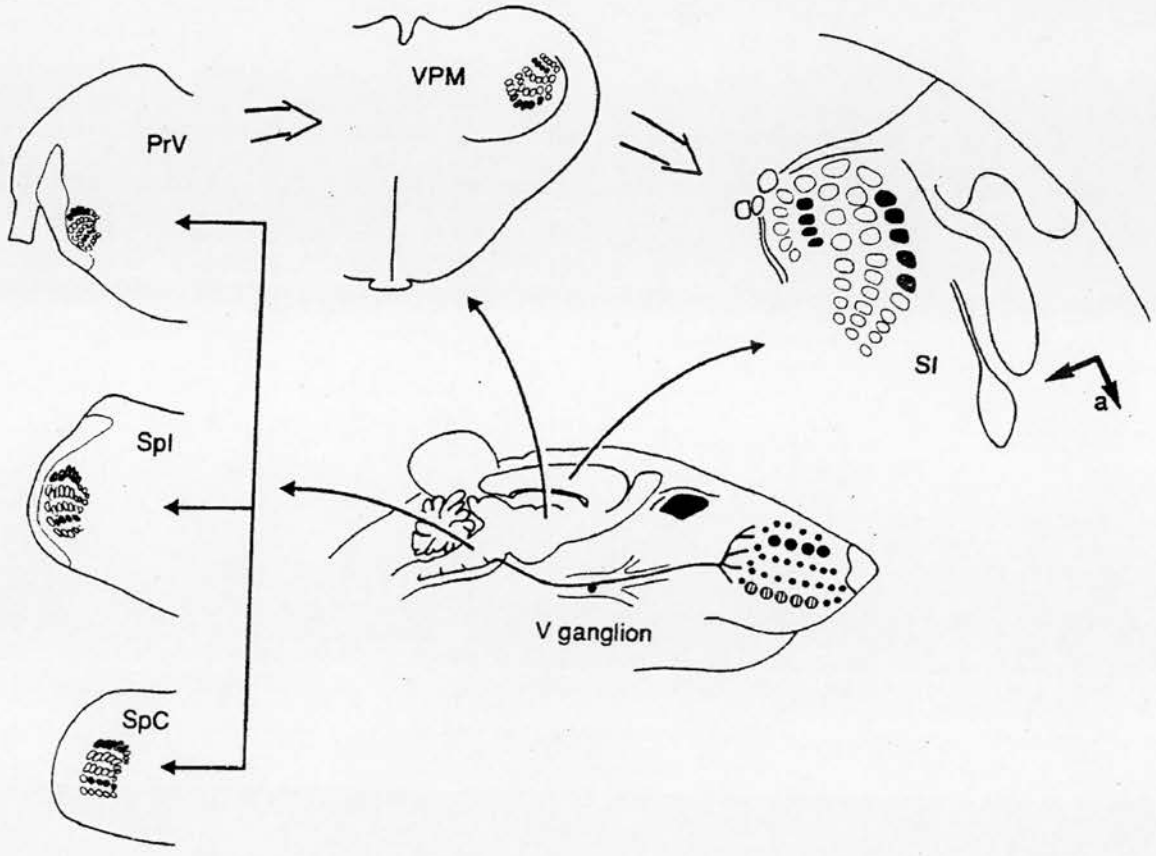

Figure I-11 The five vibrissae-related maps of the trigeminal portion of the somatosensory system of the rat. Three anatomically demonstrable maps are found in the trigeminal complex of the brainstem of the rat which receives input from the trigeminal ganglion (V ganglion). These are found the principal trigeminal nucleus (PrV), the subnucleus interpolaris (SpI) and subnucleus caudalis (Spc) of the spinal trigeminal nucleus. These brainstem nuclei in turn project into the contralateral thalamus where they terminate in the medial portion of the ventral posterior nucleus (VPM), which contains the fourth vibrissae-related map. During development, formation of the map in the ventral posterior is dependent on an intact principal sensory nucleus, and not on other parts of the trigeminal complex of the brainstem. The ventral posterior nucleus in turn projects into the primary somatosensory cortex (S1). (From Killackey et al., 1995).

spaces" and "small islands" in layer IV of the cortical area that he described as "H^2" (De Vries, 1912). Then, rapidly the extensive studies of Droogleever Fortuny, Lorente de No', Rose, Van Erp Taalman Kip and more recently Woolsey and Van Der Loos, contributed to the precise description of the barrel field and to its scientific popularity (Droogleever Fortuny, 1914; Lorente de No', 1922; Rose, 1929; Van Erp Taalman Kip, 1938; Woolsey and Van Der Loos, 1970).

According to the work of Woolsey and Van Der Loos, which serves as a reference today, the cytoarchitectonic organisation of layer IV of the primary somatosensory cortex is called the "barrel field". On tangential sections stained for Nissl, a barrel appears to comprise a ring of granular neurons (the wall) around a sparse cell space (the hollow). Two neighbouring barrels are separated by a septum (Figure I-12).

In the barrel field, thalamocortical axons occupy the cell sparse hollows of the barrels. They have been identified by the activity of several mitochondrial enzymes. In 1968, Ladesky and Lierse first analysed the cortex of the mouse using the activity of succinate dehydrogenase (SDH) and first described layer IV of the somatosensory cortex as having blobs of high SDH activity and suggested that they corresponded to the barrels. Today the activity of cytochrome oxidase and acetylcholinesterase (O'Leary et al., 1994; Broide et al., 1996) is also extensively used to visualise the peripheral related afferents.

In the barrel field, the "posteromedial barrel subfield" or PMBSF is the cortical correspondence of the main whiskers on the snout. The barrels of the PMBSF are organised in same five rows than the whiskers. The correspondence between the PMBSF and the whiskers has been established by electrophysiology and was extended to the entirety of the barrel field.

3 Influence of the thalamocortical and serotoninergic afferents on barrel field formation.

The formation of the barrel field requires both thalamocortical afferents coming from the ventrobasal thalamus and serotoninergic afferents coming from the raphe nuclei. Thalamocortical axons are the first topographically organised structures. Their organisation is determined during embryonic life (Erzurumlu and Jhaveri, 1990; Schlaggar and O'Leary, 1994). The arrival of thalamocortical axons in

the layer IV of the cortex is followed, one day later, by the arrival of serotoninergic axons (Rhoades et al., 1990; Blue et al., 1991). Glial barriers form two to three days after the arrival of thalamocortical axons (Jhaveri et al., 1991; Rice and Van Der Loos; 1977).

3.1 Influence of thalamocortical axons on the formation of the barrel field

Using acetylcholinesterase (ACh-E) activity, Schlaggar and O'Leary (1994) and Broide et al. (1996) have examined the emergence of the somatosensory map in the rat cortex. They described the existence of a dense region of ACh-E activity in layer VI of the developing somatosensory cortex by E20 rapidly followed at E21 by the separation of the main domains of the representation (the snout, the paws and the trunk). At the end of P0, the rows are distinguished in the cortical plate. Then, thalamocortical axons project from the deep cortical plate into layer IV of the somatosensory cortex following a radial trajectory developing rapidly a barrel-like organisation (Agmon et al., 1993; 1995). By P1, thalamocortical axons reach their neuronal targets in presumptive layer IV.

The use of lipophilic dyes has defined the timing of thalamocortical development and shown that thalamocortical axons develop without a waiting period in the rodent cortex (Senft and Woolsey, 1991a; Agmon et al., 1993). The precise morphology of individual thalamocortical axons has shown their precise degree of addressage since E16 (Catalano et al., 1991; Agmon et al., 1993). Thus, there is a strong correlation between the arrival of thalamocortical axons and the emergence of the blobs of ACh-E enzymatic activities.

The study of the topographical organisation of the thalamocortical axons in the adult rat brain was first performed by Lorente de No' His work has defined the existence of two types of thalamocortical axons i) the "non-specific thalamocortical axons" sending collaterals in the white matter ii) the specific thalamocortical axons characterised by a dense plexus of collaterals restricted to a small area of layer IV (Lorente de No', 1949). Recently, Jensen and Killackey (1987a) have described the morphological organisation of thalamocortical axons of the somatosensory cortex (Figure I-13). They have shown that i) their plexus extends into layer III and, rarely, into layer II, ii) the size of their arborisations depends on the region of the somatosensory cortex and on the whisker-barrel relation, iii) thalamocortical axons

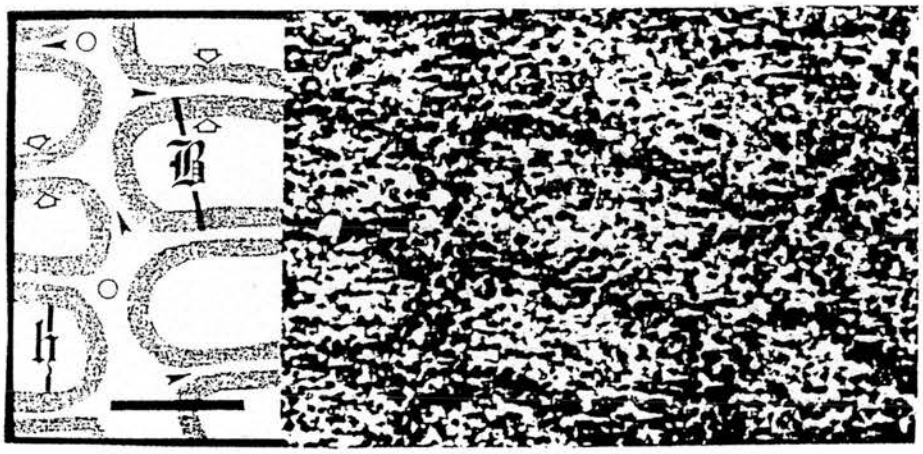

Figure I-12 Organisation of granular neurons in the barrel field. In the layer IV of the somatosensory cortex granular neurons form cylindrical aggregates called "barrels". On flattened preparation stained for Nissl, barrels (*B*) appear as ring of granular neurons "the wall" (*white arrows*) separated by cell spare regions "the septae*"(thin black arrows*). Inside the barrel is the "hollow" (*h*). Scale bar is 100 μm. (From Woolsey and Van der Loos, 1970).

which have a large area of projection in the tangential plane belong to the PMBSF. Previous studies have also shown that the number of neurons in a barrel depends on the number of myelinated axons innervating the corresponding barrel (Killackey, 1973; Killackey and Leshin, 1975; Lee and Woolsey, 1975, Welker and Van Der Loos, 1986).

3.2 Influence of serotonin on the formation of the barrel field

Several studies have shown that cholinergic and aminergic projections are necessary for normal cortical development. Cholinergic alterations lead to alterations of the cytoarchitectonic organisation of the cortex (Hohmann et al., 1988a) and pre- or postnatal lesions in dopaminergic and noradrenergic afferents lead to alterations in the cortical dendritic trees or in the kinetics of cortical synaptogenesis (Ebersole et al., 1981; Loeb et al., 1987; Parnavelas and Blue, 1982).

The role of serotonin on cortical development has been addressed in several studies. These studies were motivated in part by the description of a "transient serotoninergic hyperinnervation" observed in rodent sensory cortices (Fujimiya et al., 1986; Rhodes et al., 1990; Bennett-Clarke et al., 1991; Blue et al., 1991). Indeed, Fujimiya et al. (1986) reported the presence of strong immunolabelling for serotonin in the murine somatosensory cortex during the first ten days of postnatal life (P1 to P10; with a maximum around P5). They proposed that the diffuse serotoninergic innervation observed at birth becomes progressively organised into barrels and disappears after P10. At the same time, D'Amato et al. (1987) observed the same transient hyperinnervation in the rat and showed the presence of sites of uptake of serotonin in the somatosensory cortex. Recent studies have shown that this hyperinnervation is due to the uptake and the storage of serotonin by thalamocortical axons (Lebrand et al., 1996) and that this phenomenon could be generalised to all sensory cortices (Cases et al., 1998). Figure I-14 illustrates these observations.

These observations suggest a role for serotonin in the formation of the somatosensory cortex. In addition, during the transient serotoninergic hyperinnervation period, 5-HT1b receptors (Leslie et al., 1992; Bennett-Clarke et al., 1993), the serotonin transporter and the vesicular monoamine transporters are expressed (Lebrand et al., 1996; Hansson et al., 1996) by thalamic neurons.

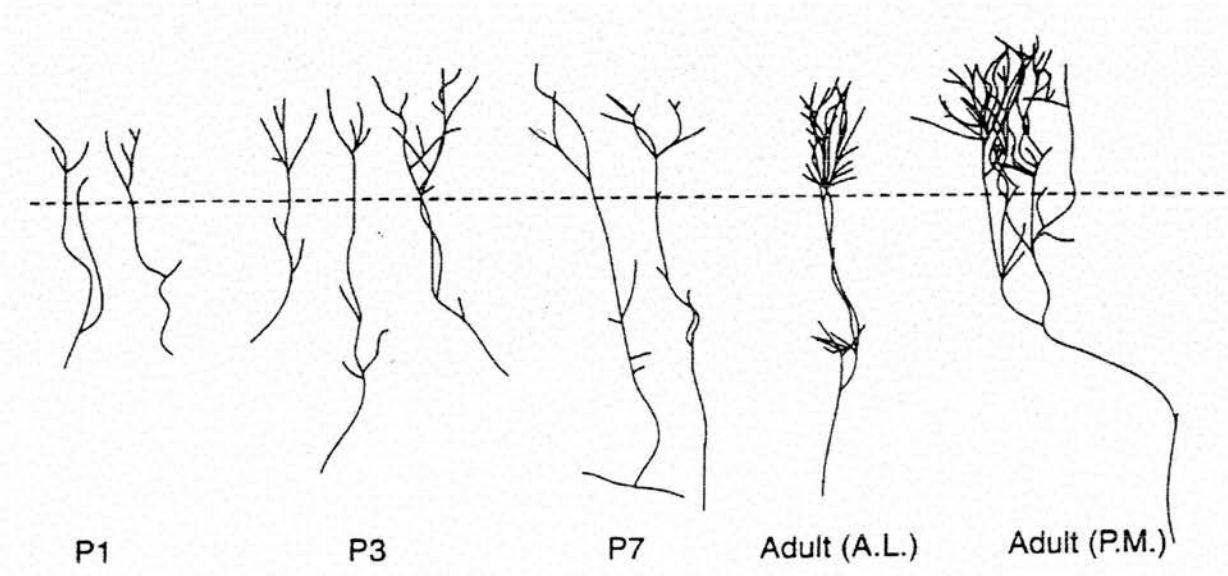

Figure I-13 Individual reconstructed terminals of thalamocortical afferents. Normal terminal arbors of animals of various ages from P1 (first day after birth) to adulthoood are illustrated. In addition, terminal arbors of normal adults found in the anterolateral (A.L.) portion of the surface map of the body, where small rostral vibrissae are represented, and from the posteromedial (P.M.) portion of the map, were the large caudal mystacial vibrissae are represented, are illustrated (From Killackey et al., 1994).

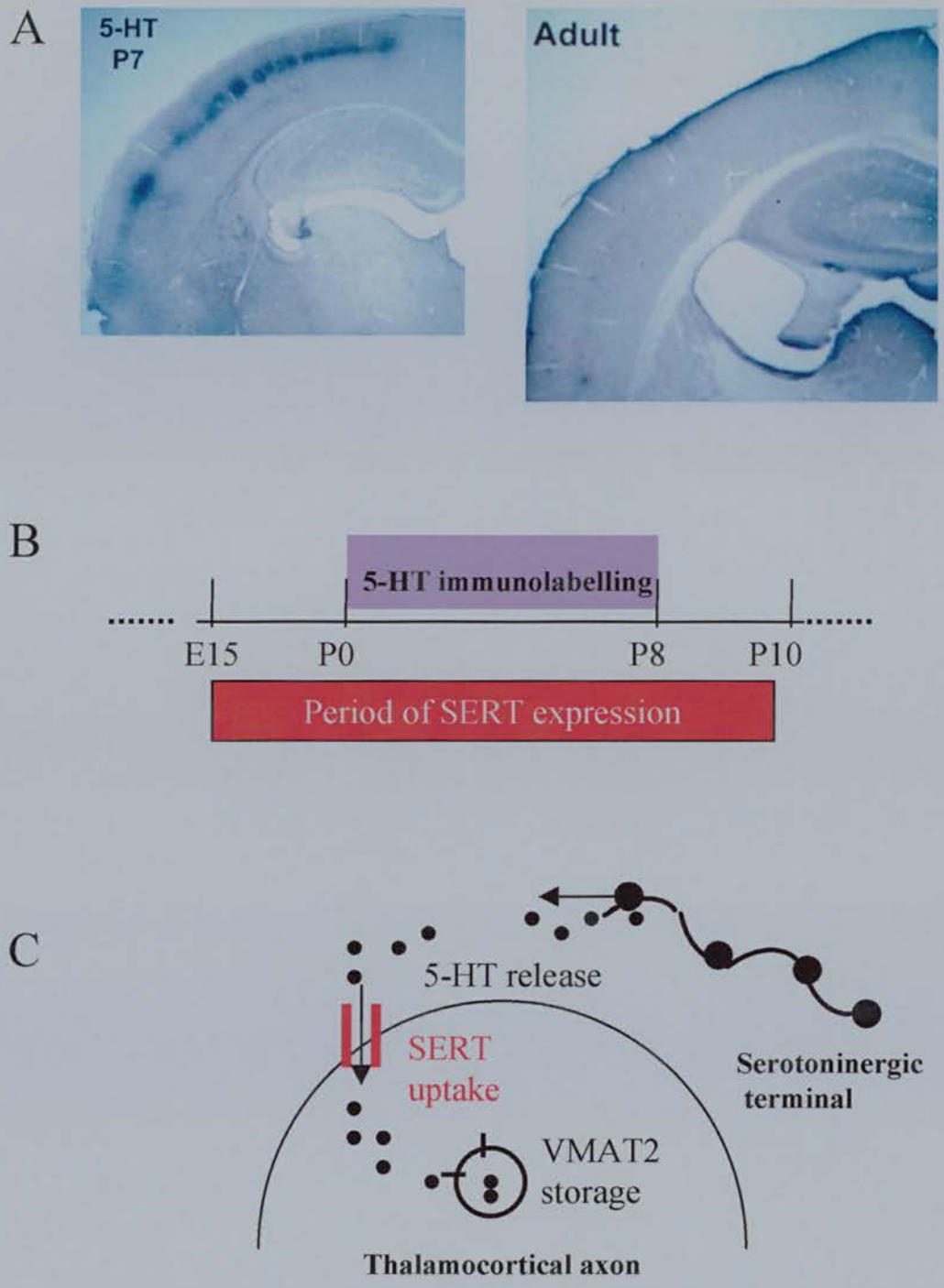

Figure I-14 Serotoninergic hyperinnervation of the barrel field: observation and interpretation. A, During a transient period (P0-P8), barrels display a strong and transient 5-HT-immunolabelling. 5-HT-immunolabelling is strongest by P5-P7 and rapidly decrease to completely disappear by P10. Adult mice show no remaining 5-HT-immunolabelling in the somatosensory cortex. **B,** SERT is expressed from E15 to P10 in the somatosensory cortex. **C,** SERT is able to uptake 5-HT released by serotoninergic terminals and also by thalamocortical axons (to a lower extent). 5-HT is then transported into vesicles by the vesicular monoamine transporter type 2 (VMAT2). The model proposed to explain the so-called "transient serotoninergic hyperinnervation of the somatosensory cortex" is now based on this recent finding rather then on a progressive degeneration of the serotoninergic terminals.

Surprisingly, lesions of the serotoninergic systems had only few effects on barrel field formation and organisation. Permanent lesions of the serotoninergic system by pharmacological injection of 5,7-DHT at birth induced only a delay in the apparition of the barrel field (Blue et al., 1991; Osterheld-Haas et al., 1994) and a 20% reduction in the size of the barrels (Bennett-Clarke et al., 1994). These results suggest that serotonin does not play an instructive role but rather a modulatory or trophic role in barrel field formation.

Is an excess of serotonin during the period of formation of sensory cortices playing an instructive role in the barrel field formation? Recently, a transgenic mouse line deficient for the gene encoding MAOA was generated (Cases et al., 1995; Cases et al., 1996) and shown to display increased levels of serotonin during a period covering the critical period of barrel field formation and alterations of the organisation of the somatosensory cortex (Figure I-15). Studies on dissociated thalamic neurons have recently shown that serotonin can increase the growth of thalamic neurites (Lotto et al., 1999). It is possible that 5-HT could act by enhancing the production of neurotrophic factors (Whitaker-Azmitia and Azmitia, 1989; Whitaker-Azmitia et al., 1990) or by reducing the production of factors that inhibit growth. But it is also possible that serotonin is related to the modulation of neuronal activity in the developing cortex. In this case, its action upon 5-HT1b receptors, that are expressed on glutamatergic thalamic axons (Bennett-Clark et al., 1993), could mediate strong presynaptic inhibitory effects upon thalamocortical transmission (Rhoades et al., 1994). In MAOA-knockout mice it is possible that excessive amounts of serotonin could result in a functional silencing of thalamic neurons, which would be reversed when 5-HT levels are normalised. This possible role of an excess of 5-HT on barrel field formation is still speculative since a clear effect of neuronal activity on the formation of the barrel field has not been clearly demonstrated (review in O'Leary et al., 1994).

It is interesting to note that a similar transient hyperinnervation was described from the noradrenergic neurons of the locus coeruleus in the mouse parietal cortex (Lidov et al., 1978; Lidov and Molliver, 1982a,b; Levin et al., 1988) suggesting that NA stimulation could also play a modulatory role in the formation of cortical organisation. In addition, lesion of the catecholaminergic system by pharmacological injection of 6, OHDA induced a delay in the appearance of the barrel field similar to

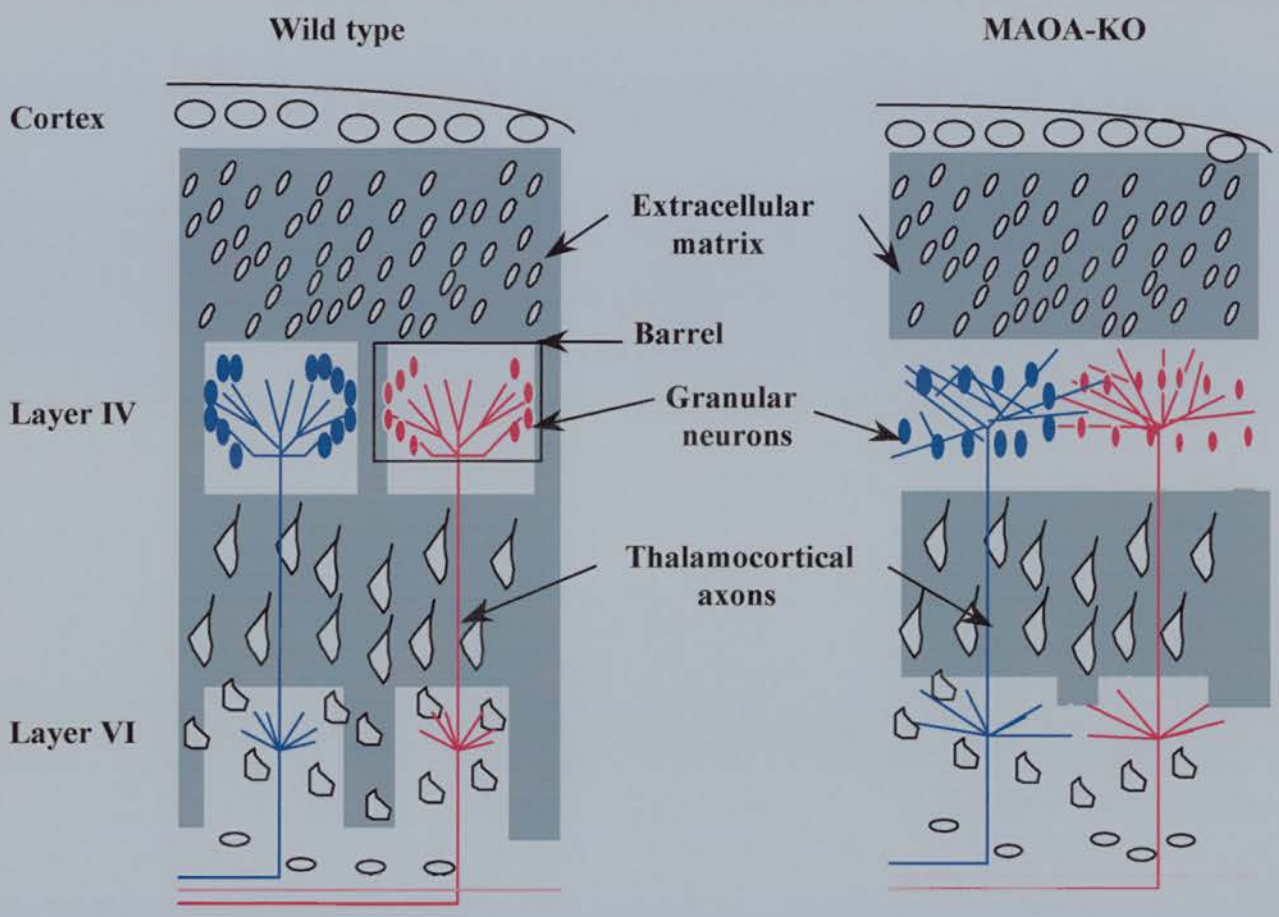

Figure I-15 Schematic representation of the barrel field in wild type and MAOA-knockout mice. In wild types, thalamocortical axons arborize in layers VI and IV and granular neurons are clustered into barrels in the layer IV of the somatosensory cortex. Barrels are separated by septa containing the extracellular matrix protein, tenascin. In MAOA-knockout mice, thalamocortical axons and granular neurons are not clustered into barrels and boundaries of tenascin are lacking.

that observed after 5,7-DHT lesion. This strongly suggests a role for catecholamine in the development of the barrel field. MAOA-knockout mice display also an excess of NA during the period of barrel field formation which was shown not to be responsible for the altered formation of the barrel field (Cases et al., 1996). Catecholaminergic innervation may participate in the formation of other cortical regions.

4 The somatosensory system and plasticity

4.1Plasticity of the somatosensory system

The organisation of the somatosensory system is dependent on the integrity of the peripheral system during development (Van Der Loos and Woolsey, 1973; Woolsey, 1990). Each synaptic level from the periphery to the cortex can be altered in neonates (Killackey et al., 1976; Belford and Killackey, 1979a,b, 1980; bates et al., 1982). Early thalamic lesions (Wise and Jones, 1978), or lesions of peripheral receptors by section of the infraorbital nerve or by cauterisation of the whiskers from P0 to P5 (Belford and Killackey, 1980; Jeanmonod et al., 1981; Jensen and Killackey, 1987b), lead to permanent alteration of the barrel field. Thalamic lesions and lesions of the infraorbital nerve reduce the thickness of the layer IV and induce fusion in the row of the PMBSF (Wise and Jones, 1978, Jensen and Killackey, 1987b, Rhoades et al., 1990).

4.2 Plasticity of the somatosensory system versus that of the visual system: a role for activity?

Classically, the cat visual system and the rodent somatosensory system have been confronted in considering the process involved in their plasticity. The plasticity of the visual system is dependent on activity whereas for the somatosensory system there is no direct evidence to show the same dependence. Contrary to what is observed in the visual system, blockade of afferents (Henderson et al., 1992) or of cortical activity in the somatosensory system (Chiaia et al., 1992; 1994a,b) by tetrodotoxin (TTX), or with D-2-amino-5-phosphovalerate (APV; an N-methyl-D-aspartate (NMDA) antagonist; Schlaggar et al., 1993), do not lead to

cytoarchitectonic alterations of the somatosensory cortex. However, Fox et al. (1996) have recently shown that electrophysiological properties of the barrel field were modified after APV treatment, the receptor field of each whisker was enlarged tangentially both in layers IV and II/III (Fox et al., 1996).

The difference between these two systems could be explained on the basis of the results of several experiments. First, spontaneous and evoked activities are stronger in the cat visual system than in the rodent somatosensory system (Armstrong-James, 1975; Chiaia et al., 1994a). It is possible that the blockage or decrease of activity in a system where the spontaneous activity is low is less important than in a system where activity is more intense. Secondly, ocular dominance columns in cats form over a longer period (ten postnatal weeks) than the barrel field (3 postnatal days). Therefore, in rodent the postnatal blockade of activity can have only a short period of action upon barrel field formation. However, several studies have explored this idea and the blockade of activity (with TTX or NMDA antagonist) in hamster, in which the period of barrel field formation is longer (2 weeks), has no effect on barrel field representation (Chiaia et al., 1994a). Interestingly, mice lacking the NMDA-R1 receptor lack the characteristic topographical organisation of the first sensory relay in the trigeminal ganglion (Li et al., 1994). Unfortunately, these mice die at birth and they provide no real information on the formation of the somatosensory system.

CHAPTER TWO:
INFLUENCE OF SEROTONIN ON SPECIFIC DEVELOPING STRUCTURES: EFFECTS OF MONOAMINE OXIDASE A INHIBITION ON BARREL FORMATION IN THE MOUSE SOMATOSENSORY CORTEX: DETERMINATION OF A SENSITIVE DEVELOPMENTAL PERIOD

CHAPTER TWO:
INFLUENCE OF SEROTONIN
ON SPECIFIC DEVELOPING STRUCTURES

EFFECTS OF MONOAMINE OXIDASE A INHIBITION
ON BARREL FORMATION IN THE MOUSE SOMATOSENSORY CORTEX:
DETERMINATION OF A SENSITIVE DEVELOPMENTAL PERIOD

I Abstract

Genetic inactivation of monoamine oxidase A (MAOA) in mice with a C3H/HeJ genetic background causes a complete absence of barrels in the somatosensory cortex. Likewise, in normal C3H/HeJ mice, pharmacological inhibition of MAOA during the first postnatal week causes permanent alterations of the barrel field. To further determine the sensitive period during which developmental alterations of the barrel field can be produced in normal mice, I administered the MAOA inhibitor clorgyline to mice of the outbred strain OF1 for various time periods between embryonic day 15 (E15) and postnatal day 7 (P7). The optimal dose and schedule for clorgyline administration (10mg/kg/8h) was selected after testing different protocols of drug administration. High-pressure liquid chromatography measures of brain serotonin (5-HT) showed three to eight-fold increases during the periods of clorgyline administration. Perinatal mortality was increased and weight gain was slowed between P3 and P6. Cytochrome oxidase and Nissl stains showed a disorganised barrel field in P10 or adult mice treated with clorgyline during the periods E15-P7 or P0-P7: barrels did not form in the anterior snout representation, and the posteromedial barrel subfield (PMBSF) displayed various fusions of barrels, both along and across barrel rows. Administration of clorgyline from P0 to P4 caused similar though less severe barrel field alterations, indicating that MAOA inhibition continues to be effective on barrel development after P4. However, when started on P4, administration of clorgyline caused no detectable abnormalities. Similarly, treatment from E15 to P0 caused no observable changes. In the cases with barrel field alterations, a rostral to caudal gradient of changes was noted: rostral barrels of the PMBSF were most frequently fused and

displayed an increased size tangentially (P0-P4 treated pups). Within S1, the area of the trigeminal representation was increased (10-20%) in the most affected cases (E15-P7 and P0-P7 treated pups), while the thickness of layer IV was reduced by 10-20%.

Altogether, these results indicate that MAOA inhibition, resulting in increased brain levels of brain 5-HT, affects barrel development during the entire first postnatal week but that there is a sensitive period for this effect between P0 and P4. The rostral to caudal gradient of changes in the barrel field parallels known developmental gradients in the sensory periphery and in the maturation pattern of thalamocortical afferents. The observed barrel fusions reflect a reduced clustering of thalamic afferents, that could correspond to a default in the initial segregation of these fibers at the time when they contact their cortical targets and/or to a continued exuberant growth, after they have reached these targets, which overrides the tangential domain that is normally devoted to individual whiskers.

II Introduction

1 Trophic role of monoamines

5-HT, DA and acetylcholine influence, in vitro, the growth of their targets (Haydon et al., 1984; McCobb et al., 1988; Lipton and Kater, 1989). This is either an inhibitory or a stimulatory regulation depending on the developmental stage, of the secondary messengers implicated, the presence of glial cells and of the method of administration.

In *Heliosoma*, 5-HT and NA directly applied to their targets inhibit neurite outgrowth and increase the intracellular concentration of Ca^{2+} (Lipton and Kater, 1989). In larvae of *Heliosoma,* 5-HT depletion by 5,7-DHT causes an increase of dendritic outgrowth among the cellular targets of 5-HT, suggesting that serotoninergic afferents inhibit the growth. However, 5-HT can initiate neurite outgrowth from a sub-population of neurons (Goldberg and Kater, 1989). It was suggested that the nature (inhibitory or stimulatory) of 5-HT's effect was directly dependent on the developmental stage of the target cells and on their intracellular concentration of Ca^{2+}. Acetylcholine also inhibits neurite outgrowth when it is directly applied to appropriate neurons, but could also inhibit the inhibitory effects of

5-HT on target cells by acting on the intracellular concentration of Ca^{2+} and the resting membrane potential (Lipton and Kater; 1989).

Glial cells can influence the effect of neurotransmitters on other neurons. Neurite outgrowth is inhibited by micromolar concentrations of 5-HT applied to dissociated cultures of cortical (Sikich et al., 1990) and raphe neurons. Like 5-HT, DA inhibits cortical and retinal neurite outgrowth (McCobb et al., 1998). These inhibitory effects of 5-HT and DA have been associated with the activation of 5-HT1a and D1 receptors respectively (Lankford et al., 1988; Santos Rodrigues and Dowling, 1990; Todd, 1992). However, in cortical or hippocampal organotypic cultures, neural differentiation and synaptogenesis are stimulated by the same concentration of 5-HT and a proliferation of glial cells is also observed (Lauder, 1990). The presence of glial cells in organotypic cultures versus dissociated cultures can account for the opposite effect of 5-HT. Glial cells can release neurotrophic factors in response to monoamines. Astrocytes bear a large variety of monoaminergic receptors (Lauder and McCarthy, 1986) and send neurotrophic signals for afferent neurons (Qian et al., 1992: Liu and Lauder, 1992a). Neuronal activity and monoamines could regulate the synthesis and the release of growth signals. Indeed, interactions between glial cells and neurons transmit some neurotrophic functions during development.

The trophic interactions between neurons and glial cells are best exemplified by the regulation of the protein S100β. This protein captures the calcium and functions like a growth factor for serotoninergic neurons (Whitaker-Azmitia, 1992). During the development of the serotoninergic system, interactions between the neurons of the raphe and glial cells bearing the 5-HT1a receptors induce the release of S100β. S100β is released by glial cells on serotoninergic neurons of the raphe and along the serotoninergic pathways (Van Hartesfeldt et al., 1986; Bledsoe and Zhou, 1992). 5-HT1a agonists induce the release of S100β by astrocytes and serotoninergic outgrowth (Liu and Lauder, 1992b). After 5-HT1a stimulation, APMc is activated and the transcription of S100β is initiated. This is due to the presence of a CRE responsive element on the promoter of the gene coding for S100β. In addition, AMPc is increased in glial cells treated with 8-OH-DPAT (Liu and Lauder, 1982b). It is possible that the release of monoamines from developing axons stimulates, in vivo, the release of neurotrophic factors from glial cells. Then, the expression of specific receptors for monoamines on glial cells could add a degree of specificity to neuronal connections.

2 Serotonin

2.1 Role of serotonin on development of serotoninergic neurons

Several in vitro and in vivo experiments have demonstrated that alteration of 5-HT levels are critical for the development of serotoninergic neurons. In vitro, 5-HT regulates the growth of serotoninergic neurons of the raphe in a dose-dependant fashion (Lauder et al., 1990; Whitaker-Azmitia et al., 1990). 5-HT is also able to initiate and to auto-amplify its own synthesis. This was shown in hypothalamic cultures (De Vitry et al., 1986). In vivo evidence of the role of 5-HT in its own development was given by the characterisation of *Drosophila* mutants unable to synthesise serotonin (Budnik et al., 1989). These mutants display an aberrant growth of their serotoninergic projections (Budnik et al., 1989). In addition, rats treated with 5-MT, a 5-HT agonist, displayed abnormal growth of their serotoninergic axons (Whitaker-Azmitia, 1992).

2.2 On the development of other structures

2.2.1 Lack of serotonin

The alteration of the serotoninergic system is also deleterious to the development of its targets systems. PCPA injections into pregnant rats or mice induce 5-HT depletion in the embryonic neurons of the raphe. This depletion is followed by a delay in the neurogenesis of areas normally receiving precociously serotoninergic afferents (Lauder et al., 1990). This effect is transmitted by a variety of serotoninergic receptors (Hellendahl et al., 1992) and their number seems to be modulated by 5-HT. Indeed, PCPA or 5-MT treatment during pregnancy alters the level of 5-HT receptors expressed postnatally.

2.2.2 Excess of serotonin

The effect of an excess of 5-HT on barrel field formation was clearly established in MAOA-knockout mice (Cases et al., 1996). During the sensitive period of barrel field formation, MAOA-knockout mice display an increase in 700-

900% of serotonin levels whereas NA levels, which are also affected in this mouse strain, display only a 35-70% increase. In addition, pharmacological treatment with α-MPT, an inhibitor of catecholamine synthesis, during the first postnatal week caused no cortical alterations, whereas reduction of 5-HT synthesis by administration of PCPA restored the normal development of the barrel field. The phenotype of MAOA knockout mice is best characterised by a fusion of the barrels in each main domain of the barrel field representation and an alteration of the organisation of the periphery related afferents. Granular neurons of layer IV are not organised into barrels but in a continuous and homogeneous band. Thalamocortical axons are not segregated in layers VI and IV of the barrel field. In the somatosensory area, layer IV displayed a 20% decrease of its thickness whereas the total cortical thickness is unchanged and the total size of the barrel field is increased by 20%. In layer IV, tenascin immunoreactivity is decreased. Interestingly, trigeminal and thalamic relays display no obvious alteration in their organisation and thalamocortical axons bear 5-HT1b receptors as normal. These alterations are summarised in figure I-15.

3 Effects of monoamine oxidase A inhibition on barrel formation in the mouse somatosensory cortex: Determination of a sensitive developmental period

A number of mechanisms underlying the formation and plasticity of cortical sensory maps have been uncovered by studying the barrel field in the rodent somatosensory cortex. The appeal of this system for developmental analyses lies in the fact that its precise topographical organization can be readily visualised: the peripheral tactile receptors associated with the whiskers are isomorphically represented as discrete elements called barrelettes in the sensory relays of the brainstem, barreloids in the thalamic relay, and barrels in the primary somatosensory cortex (S1). In S1, barrels form clear units in layer IV, consisting of a ring of granular cells that surrounds a cell-sparse hollow containing the clustered terminal arbors of thalamic neurons (Woolsey and Van der Loos, 1970; Jensen and Killackey, 1987a). The crucial role of the sensory periphery in the formation of barrels was demonstrated early on. Lesioning a row of whiskers early in postnatal development causes defective formation of barrels in the corresponding cortical representation (Van der Loos and Woolsey 1973; Woolsey and Wann, 1976; Belford and Killackey, 1980; Jeanmonod et al., 1981). Conversely, the presence of additional whiskers on the snout induces additional barrels to form in the cortex (Welker and Van der Loos,

1986). However, the nature of the signal conveyed by the periphery is still unclear since blockade of neural activity with tetrodotoxin or bupivacaine does not alter barrel formation (Chiaia et al., 1992; Henderson et al., 1992; Chiaia et al., 1994). Nevertheless, normal glutamatergic neurotransmission appears to be necessary for the refinement of topographic order in the thalamocortical projection, since whisker-related patterns fail to develop in the brainstem, thalamus, and cortex of mice genetically deficient for the key subunit of the N-methyl-D-aspartate (NMDA) receptors (Li et al., 1994; Iwasato et al., 1996), and since pharmacological blockade of NMDA receptors in normal S1 disrupts the topographic refinement of the thalamocortical projection and the functional columnar organization of barrels (Fox et al., 1996).

Recently, defective formation of barrels has been shown to occur, despite the presence of normal peripheral receptors, in two other strains of mice. One strain is characterized by a spontaneous mutation, named "barrelless", located on the proximal segment of chromosome 11 (Welker et al., 1996). The other strain has a serendipitous knockout for the gene encoding monoamine oxidase A (MAOA) located on the X chromosome (Cases et al., 1995). In these two strains of mice, the tangential clustering of thalamocortical afferents is lacking and granular neurons in layer IV do not form the characteristic rings. An excess of brain serotonin (5-HT) amounts during early postnatal development appears to be responsible for the abnormalities in the MAOA knockout mice, since lowering 5-HT amounts in the brain of developing pups allows normal barrels to form in S1 (Cases et al., 1996). Excess of 5-HT could alter two components of the normal developmental processes that underlie cortical barrel formation: the ingrowth of thalamocortical fibers and the differentiation of cortical neurons in layer IV. In mice, thalamocortical fibers reach the cortical anlage as early as embryonic day 15 (E15), invade the deep cortical layers (V-VI) in late embryonic life (Catalano et al., 1996), and the cortical plate around birth (postnatal day 0, P0) (Senft and Woolsey, 1991 a,b; Agmon et al., 1993), reaching the nascent layer IV in the lower cortical plate by P2. Barrel-like periodicities of the thalamocortical afferents become detectable on P3 (Senft and Woolsey, 1991 a,b; Agmon et al., 1993) and are soon accompanied by changes in the distribution of the layer IV neurons: in Nissl-stained tangential sections, barrels first appear by P3.5 as oval-shaped patches of decreased packing density of perikarya.

Clear ring-like arrangements of granular neurons are observed by P5 (Rice and Van der Loos, 1977).

Although the exact targets of 5-HT in this intricate developmental process remain to be determined, there are strong arguments for a direct effect of 5-HT on the thalamocortical neurons originating from the ventrobasal (VB) thalamic nuclei. Serotonin receptors of the 5-HT_{1B} subtype are transiently located on VB terminals in the somatosensory cortex (Bennett-Clarke et al., 1993) and pre-synaptically inhibit the excitatory thalamocortical transmission, at least *in vitro* in brain slices (Rhoades et al., 1994). Furthermore, developing VB neurons transiently express the genes encoding the serotonin transporter (SERT) and the vesicular monoamine transporter (VMAT2). As a result, 5-HT is taken up and stored in thalamocortical axons innervating S1 (Lebrand et al., 1996), giving the picture of a dense 5-HT-positive innervation of the barrel field during the first postnatal week (Fujimiya et al., 1986; D'Amato et al., 1987; Rhoades et al., 1990; Blue et al., 1991; Lebrand et al., 1996).

In the present study, I sought to obtain more precise information on the sensitive period during which increased levels of brain 5-HT are affecting barrel development. In previous work, focusing on the absence of barrels in MAOA knockouts, I had shown that in wild-type C3H/HeJ mice, transient pharmacological inactivation of MAOA with clorgyline from P0 to P6 caused important and permanent barrel field abnormalities (Cases et al., 1996). The purpose of the present study, performed on another strain of mice, the outbred OF1 strain, was to compare the extent of changes following a variety of clorgyline dosages and schedules in prenatal and early postnatal life and to provide a more detailed analysis of the pattern of barrel field abnormalities. I also analyzed the general physiological effects of the pharmacological treatments, to determine whether any observed alterations of the barrel field could be related to effects of MAOA inhibition on overall growth and development of the mice.

III Material and methods

1 Animals

Experiments were carried out on mice of the outbred strain OF1. All animal procedures were conducted in strict compliance with approved institutional

protocols, and in accordance with the provisions for animal care and use described in the "Scientific procedures on living animals ACT 1986". The day of birth was counted as postnatal day 0 (P0).

2 Pharmacological treatments

Clorgyline (5, 10, or 30 mg/kg; Sigma-Aldrich, M-3778, France) or physiological saline were administered intraperitoneally to pregnant dams and subcutaneously to mouse pups using a 30-gauge needle. Injections were given either daily or every 8 hours over the following developmental periods: E15-P0, E15-P7, P0-P4, P4-P7, and P0-P7 (Fig. II-1). The first injection at P0 was made 4 to 8 hours after delivery. Each day, surviving pups were numbered and weighed. The total number of OF1 mice that were treated with the different dosages and schedules is indicated in Table II-1.

3 Biochemical analysis

Embryos (E19) and P7 pups treated for various times with clorgyline (10 mg/kg/8h) or saline were decapitated after cold-anesthesia, three hours after the dams or the pups received their last injection. P0 pups born form treated mothers were killed in the same way but in this case the delay with the last clorgyline injection to the mother was uncertain (between 3 and 10 hours). In addition, P3 pups were killed 3.5, 8, and 24 hours after a single clorgyline injection (10 mg/kg). The brains were rapidly frozen in liquid nitrogen, and kept at -80°C. After homogenization of the whole brains, 5-HT, 5-hydroxyindoleacetic acid (5-HIAA), and tryptophan (Trp) amounts were measured with high-pressure liquid chromatography (HPLC) and fluorometric detection (Kema et al., 1993).

4 Histology

For Nissl and cytochrome oxidase (CO) stains, most animals were killed at P8 and P10 (Table II-1). Some treated mice were killed as adults (2 months). Mice were deeply anesthetized with ether at P8 and P10, and with chloral hydrate (0.5 g/kg) as adults, and perfused transcardially with 4% paraformaldehyde in 0.1M

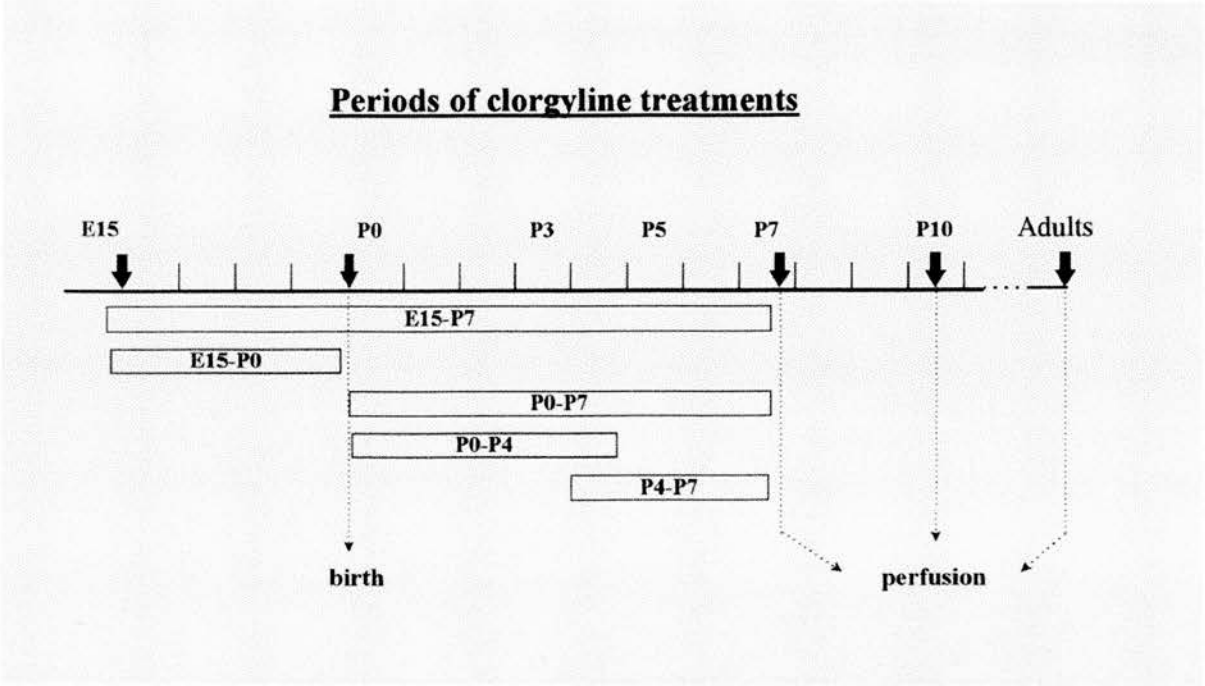

Figure II-1 Schedules of clorgyline treatment. The different schedules of clorgyline treatment used in the present study are indicated with bars along a time-scale that marks the days of pre- and postnatal development.

Table II-1. Clorgyline and saline treated pups and dams used in the different experiments in this report.

Treatment	Dose (mg/kg)	Interval between injections	Period of the treatment	Dams *n*	P0 pups *n*	Animals Analysed *n*	Ages
Experiment 1: Optimization of clorgyline dosage							
saline			E15⟶P7	4	51	10	P8, P10, P15
clorgyline	5	24h	E15⟶P7	3	37	14	P8, P15
clorgyline	30	24h	E15⟶P7	2	24	7	P8, P15
clorgyline	5	8h	E15⟶P7	2	16	5	P8, P15
clorgyline	10	8h	E15⟶P7	7	60	9	P8, P10
[1]**Experiment 2: Varying the period of clorgyline administration**							
clorgyline	10	8h	P0⟶P7	6	50	17	P0, P10, Adults
clorgyline	10	8h	P0→P4	3	16	9	P10
clorgyline	10	8h	E15⟶P0	3	15	11	P10
clorgyline		8h	P4→P7	2	24	5	P10

Animals that have been used for biochemical analyses are not counted in this Table. [1] For all these periods saline-treated controls (n = 6) were analyzed in parallel with the clorgyline-treated mice.

phosphate buffer (pH 7.4). After perfusion, brains were removed from the skull and weighed. One hemisphere was separated from the rest of the brain by a section through the internal capsule and flattened between two glass slides separated by spacers. The rest of the brain was kept as one block. Blocks were postfixed overnight in the same buffered paraformaldehyde and cryoprotected in 30% sucrose phosphate buffer. Serial, 40 micron-thick, frozen sections were obtained in the coronal or tangential planes. Alternate series of sections were used for CO, as described by Wong-Riley and Welt (1980), and Nissl (0.025% thionine in acetate buffer pH 5.5).

5-HT immunocytochemistry (rat monoclonal antibody from Harlan-Sera-lab, clone YC5/45, 1:50; Consolazione et al., 1981) was performed on frozen sections from animals killed at P0 and P7, as previously described in Lebrand et al. (1996).

5 Histological analysis

Barrels were examined in Nissl- or CO-stained coronal sections, and the entire barrel field was reconstructed from serial CO-stained tangential sections. The outlines of the CO-dense clusters (barrels, abnormally shaped barrels, or fused barrels) were drawn using a camera lucida and the drawings from consecutive sections were aligned using blood vessels. Reconstructions from four to six animals were made for each administration schedule at 10 mg/kg/8h clorgyline.

From the reconstructions made with the x6.3 objective, I determined the total number of CO-dense clusters (barrels, abnormally shaped barrels, and fused barrels) in the posteromedial barrel subfield (PMBSF). To evaluate the topographical distribution of changes, the number of normal barrels were counted: a) along the 5 longitudinal rows (A to E) of the PMBSF; b) along the eight transversal arcs (1-8) of the PMBSF (see Rice and Van der Loos, 1977 for the nomenclature). The most caudal barrels α, β, γ, δ, that straddle barrel rows, were not counted in this scheme.

The surface area covered by the PMBSF and the anterior snout (AS) was outlined on reconstructions made with the x2.5 objective and measured using a morphometric software (Image Tool, The University of Texas Health Science Center in San Antonio). The surface area of individual barrels was measured from reconstructions made with the x10 objective. Only unfused barrels in B1-B4, C1-C5, and D1-D5 in P0-P4 saline- or clorgyline-treated mice could be evaluated.

The thickness of cortical layers II-IV and layers II-VI were measured in Nissl-stained coronal sections, using an eyepiece graticule (x10 objective). The thickness of layer IV was measured in CO-stained coronal sections (x16 objective). Measurements were taken along a line perpendicular to the pial surface, at two different levels: one in the PMBSF, (level -1 posterior and -3.1 lateral to the Bregma), and the other in AS, (level +0.7 anterior and -3 lateral to the Bregma).

IV Results

1 Optimization of clorgyline dosage regime

I determined the minimal dose and frequency of administration of clorgyline capable of producing major alterations in the formation of the barrel field. After each of the various protocols listed in Table II-1 (Experiment 1), the barrel field was examined with Nissl and CO stains at P8. I started with a 5 mg/kg daily injection of clorgyline, a dose known to acutely inhibit MAOA activity by nearly 100% in adult rats and which does not produce obvious behavioral alterations (Green and Youdim, 1975; Sleight et al., 1988). After daily administrations from E15 to P7, a few abnormally shaped barrels were observed in CO-stained coronal sections (4 out of 14 pups). Increasing the daily dose to 30 mg/kg did not produce more substantial modifications of the barrel field. Taking into account the higher rate of MAOA synthesis in pups (Nelson et al., 1979; Samsa et al., 1979), I then increased the frequency of clorgyline administration. Treating animals from E15 to P7 with 5 mg/kg/8h of clorgyline produced alterations in rostral barrels but had little effect on the posteromedial barrel subfield (PMBSF). The 10 mg/kg/8h regime led to constant and severe abnormalities throughout the barrel field. The following report will therefore mainly deal with the latter dosage regime.

2 General developmental and behavioral effects of clorgyline administration

In mothers treated from E15 to P0 (5 mg/kg/24h or 10 mg/kg/8h), I observed no effects of the clorgyline treatment on the duration of pregnancy, nor on the survival and weight increase during pregnancy (Fig. II-2A). However, the size of the litters, evaluated 4 to 8 hours after delivery, was reduced by 30% (Fig. II-2B)

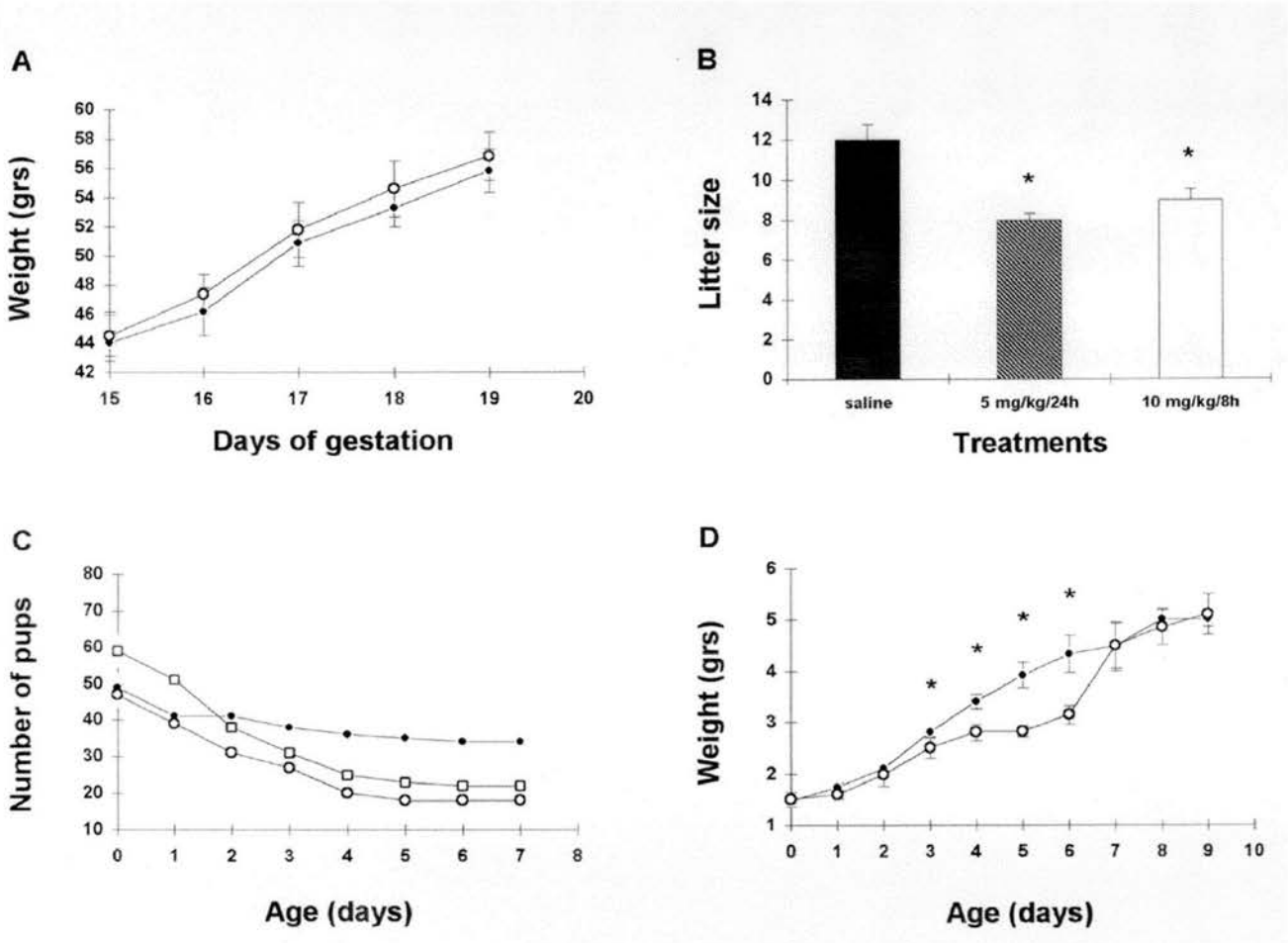

Figure II-2 General developmental effects of clorgyline administrations. A, Weight increase in gram units (gr.) during pregnancy in dams injected with saline (filled circles, n = 5) and 10 mg/kg/8h clorgyline (open circles, n = 7). Mean ± SEM. **B**, Litter size at birth in mice treated with saline (n = 7), 5 mg/kg/24h clorgyline (n = 3), or 10 mg/kg/8h clorgyline (n = 7) from E15 to P0. Mean ± SEM. **C**, Survival of pups receiving injections of saline (filled circles) or 10 mg/kg/8h clorgyline from E15 to P7 (open squares) or from P0 to P7 (open circles). **D**, Weight increase in gr. of 10 mg/kg/8h clorgyline-treated pups from 6 litters (open circles) versus saline-treated pups from 5 litters (filled circles). Injections were administered during the P0-P7 period. Mean ± SEM. Significant differences between groups ($p < 0.05$; Student's *t* test) are indicated with an asterisk* in (**B**) and (**D**).

reflecting an increased perinatal mortality. Mortality of clorgyline-treated pups was considerably increased during the subsequent 4 days of postnatal life (Fig. II-2C) with a survival rate at P7 of 30% and 36% in the E15-P7 and P0-P7 administration schedules, respectively. Surviving clorgyline-treated pups aged P3-P6 displayed a slight, temporary retardation of their growth curve relative to controls, but their growth returned to normal at P7 (Fig. II-2D). Clorgyline-treated pups displayed some of the behavioral abnormalities described in the MAOA knockout pups (Cases et al., 1995) such as agitation, trembling, hunched posture, increased righting time (15-20 seconds, instead of 1 second in controls), and abnormal rooting reflex. However, these behavioral alterations were less intense and were no longer observable 24 hours after the last injection. By contrast, saline-treated pups showed no changes in survival, weight gain, and behavior compared to non-injected animals.

Clorgyline-treated dams, contrary to saline-treated dams, showed almost constantly increased locomotor activity and excitability, even after the end of the treatment, which were probably due to the long-lasting effects of clorgyline in adults (Maitre et al., 1976). This could explain in part the high mortality rate of the pups observed in the E15-P7 group. Nursing and nurturing defects have also been noted previously when rat pups were treated with inhibitors of MAOs (IMAOs) (Whitaker-Azmitia et al., 1994).

3 Biochemical abnormalities

To evaluate the duration of MAOA inhibition provoked by the administration of clorgyline, I measured the amounts of 5-HT and its metabolite, 5-HIAA, 3.5, 8, and 24 hours after a single subcutaneous injection at P3 (10 mg/kg) (Fig. II-3A). As judged by the reduction in the amounts of 5-HIAA, MAOA inhibition was maximal 3.5 hours after the injection (55% reduction from controls) and a partial recovery was observed by 8 hours (20-25% reduction from controls). 5-HT amounts were increased by three-fold 3.5 and 8 hours after the injection.

Repeated injections of clorgyline (10 mg/kg/8h) over the P0-P7 period led to a more complete inhibition of MAOA. There was a larger increase in 5-HT (eight-fold; Fig. II-3B), a larger decrease in 5-HIAA (80% reduction; Fig. II-3C), and a 6% increase in tryptophan levels (not shown). Pharmacological inhibition with clorgyline was also effective in embryos. In E19 embryos taken from treated pregnant dams, or

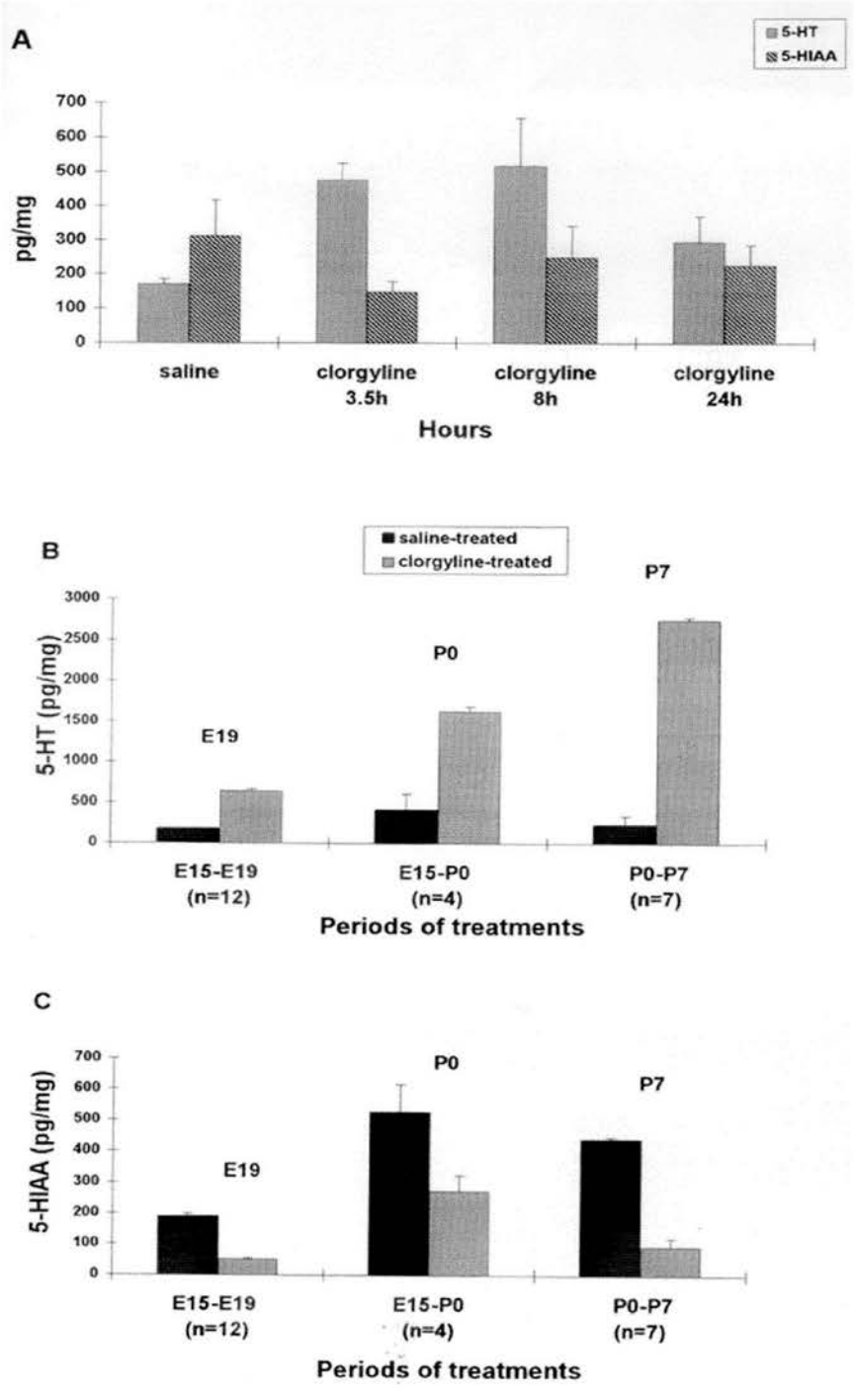

Figure II-3. Serotonin levels in the brains of clorgyline-treated pups compare to wild types. **A**, Whole brain amounts of serotonin (5-HT; shaded bars) and 5-hydroxyindolacetic acid (5-HIAA; cross-hatched bars) in P3 pups after a single 10 mg/kg clorgyline injection. Pups were killed 3.5, 8, or 24 hours later (n = 5 for each point). Saline-treated controls were killed at the beginning, t = 0 (n = 3), and at the end of the experiment, t = + 24 hours (n = 3), and no difference was observed between these two control groups, which are pooled in the first histogram. Values are expressed in picograms per milligram of wet brain and represent the mean ± SEM. Asterisk indicates that the results are statistically significant ($p < 0.005$; Student's *t* test). **B**, 5-HT and **C**, 5-HIAA amounts in whole brains of mice receiving repeated injections of saline (filled bars) or 10 mg/kg/8h clorgyline (shaded bars) following the E15-P7 schedule. Measures were performed at E19 (n = 12), P0 (n = 4), and P7 (n = 7). In graphs A and B, all values of the clorgyline-treated group were statistically different from controls ($p < 0.005$; Student's *t* test).

in P0 pups born from treated mothers the amounts of brain 5-HT were four-fold higher than in controls, while 5-HIAA was reduced by 70%, or 50% of the controls (Fig. II-3C).

4 5-HT immunostaining

5-HT immunostaining at P7 was increased in the brainstem, diencephalon, and cerebral cortex of P0-P7 clorgyline-treated pups. This increase was also visible in P0 pups born from clorgyline-treated mothers. In tangential sections of the cerebral cortex of P7 clorgyline-treated pups, 5-HT immunolabeling was markedly increased in S1, as well as in the primary auditory and primary visual cortices. In S1, the frontiers between cortical barrels were blurred (Fig. II-4B).

5 Effects on the barrel field

The patterning of the barrels was diversely affected by the different schedules of clorgyline administration. In animals that had received clorgyline treatments only during the embryonic period E15-P0, cortical barrels had a normal appearance on CO- and Nissl-stained coronal sections. On reconstructions from CO-stained tangential sections, the organization of S1 was similar to that of controls (Figs. II-5A and II-5B). Barrels and other characteristic CO-dense elements were distinguished in the four main domains of S1: the PMBSF, AS, the lower lip (LL), and the forepaw (FP). They normally have different aspects and sizes in these different parts: they are largest and quadrangular in the PMBSF, smaller and roughly circular in the caudal part of AS, have a stripe-like organization in the rostral part of AS, and are the least sharply defined in LL and FP, where ovoid blobs are visible.

Severe alterations of the barrel field were observed in all pups that received clorgyline from E15 to P7 or from P0 to P7. On CO-stained coronal sections, barrels were distinguished only in a few cases: large patches with blurred outlines were observed in the most caudal part of the PMBSF (Fig. II-6E). Tangential reconstructions of S1 were made in 12 cases. In AS, barrels or stripes were completely absent in 11 cases, and in one case showed a few disorganized clusters. In LL, CO-positive clusters or blobs were completely lacking in 8 cases (Figs. II-5C and II-5D). In the PMBSF, some barrels were visible in all the cases but there were

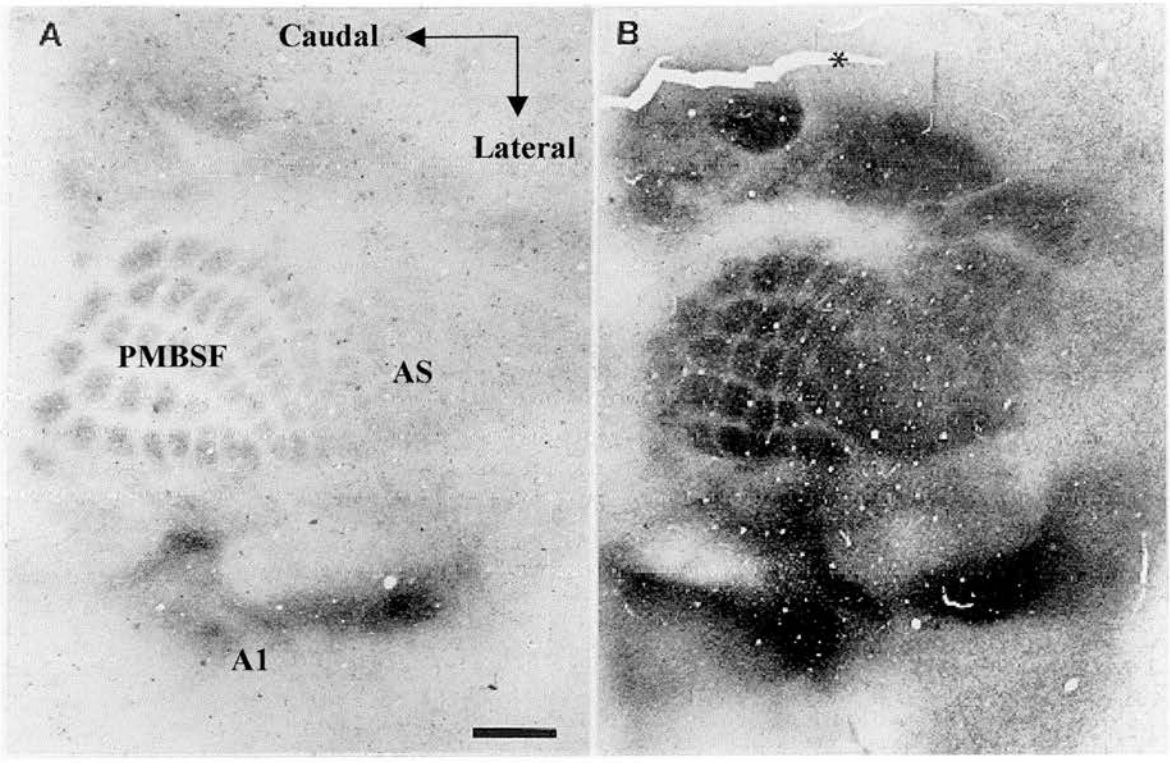

Figure II-4 5-HT immunostaining in tangential sections of the flattened cortex at P7. **A**, In saline-treated pup, moderate 5-HT immunostaining delineates S1 with a barrel pattern visible in the PMBSF and AS; the auditory cortex (A1) is also visible. **B**, In P0-P7 clorgyline-treated pup, 5-HT immunostaining is more intense, obliterating the normal pattern of some barrels in S1. An artefactual crack on this section is indicated with an asterisk (*) Scale bar = 330 μm.

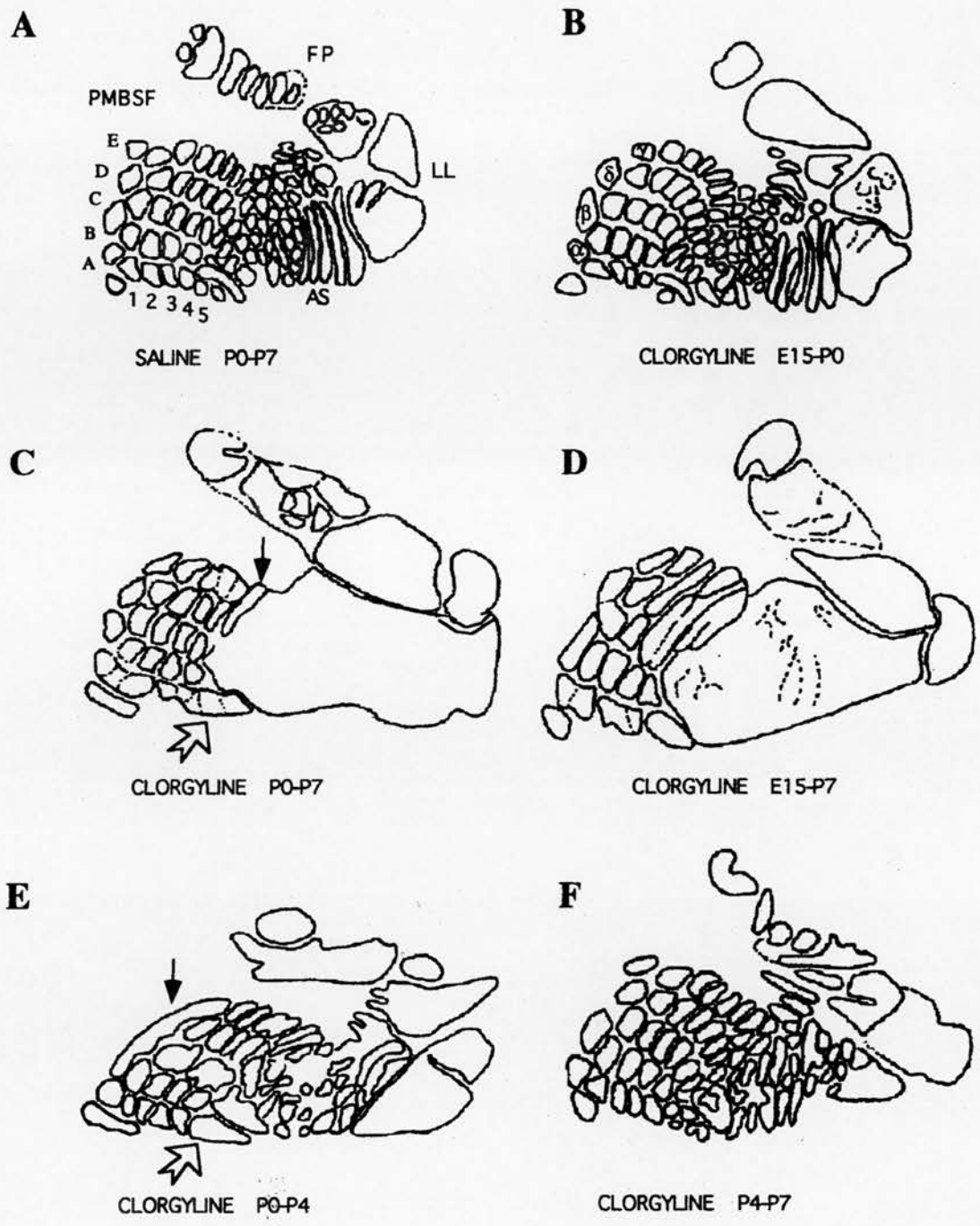

Figure II-5 Representative reconstructions of S1 were made from complete series of cytochrome oxidase (CO)-stained tangential sections of flattened cortex. A, In a saline-treated pup, the different regions of the somatosensory representation are indicated: the large mystachial vibrissae (PMBSF), the anterior snout (AS), the lower lip (LL), and the forepaw (FP); these regions are separated by large septa. Each division is subdivided into barrels and stripes. **B**, Embryonic clorgyline injections (E15-P0) have no effects. **C** and **D**, Severe alterations are seen in protracted postnatal clorgyline treatments. A complete barrel fusion is seen in the AS and partial row-fusions (open arrow) or arc-fusions (closed arrow) are visible in the PMBSF. **E**, Early postnatal clorgyline administration (P0-P4) causes barrel disorganization and fusions in the LL, AS, and to a lesser extent in the PMBSF. **F**, P4-P7 clorgyline injections have no visible effects on formation of barrels in the different subfields.

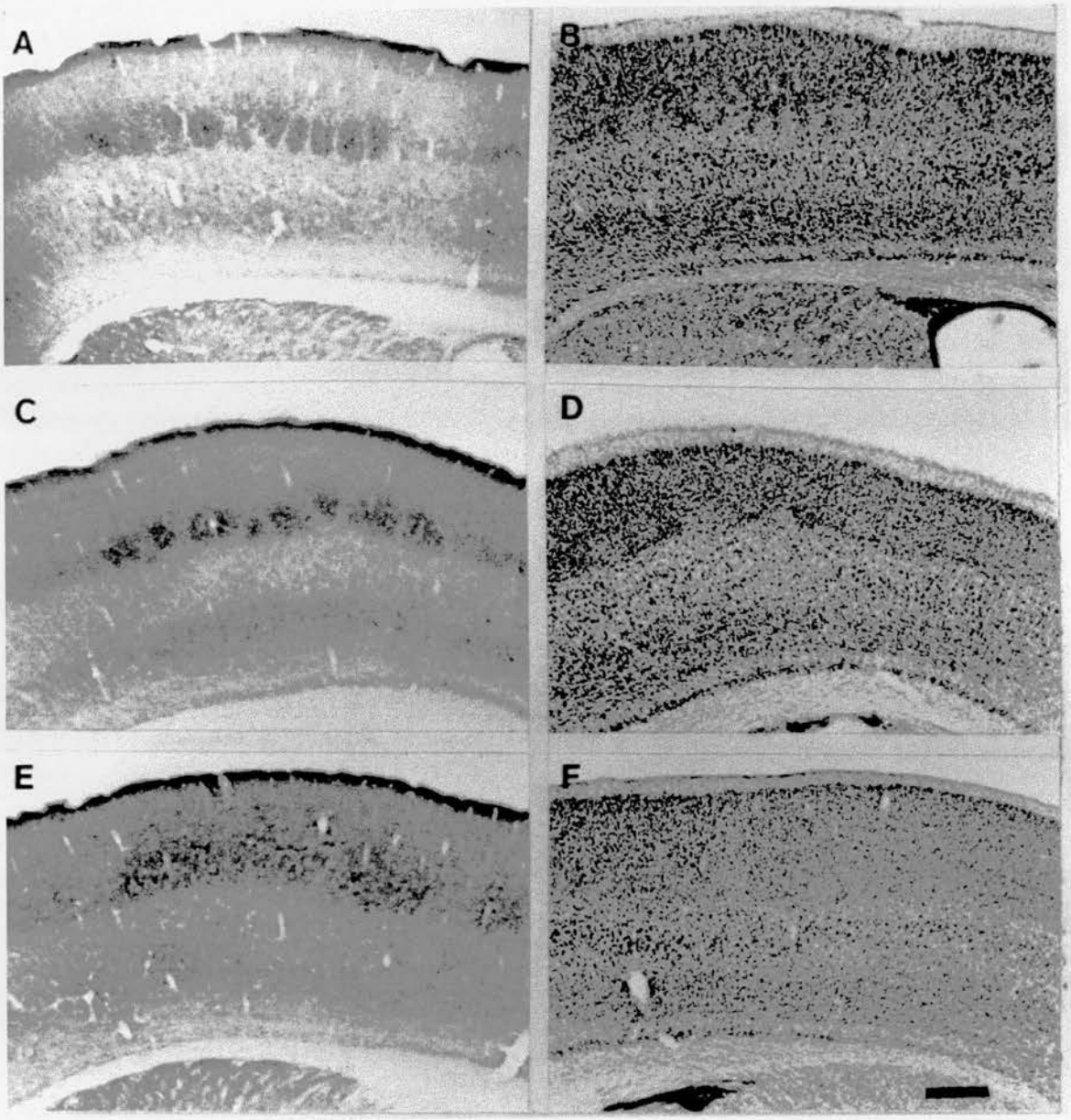

Figure II-6 Gradual alterations of the cortical barrels according to the period and the duration of the clorgyline treatment. **A**, Normal barrels are visible as blobs of increased CO activity or **B**, as clustered granular cells in layer IV, surrounding a cell sparse hollow, with Nissl staining. **C**, In P0-P4 clorgyline-treated pups, barrels appear larger than in controls on CO stains and **D**, are less clearly defined cytoarchitecturally on Nissl stains. **E**, In P0-P7 clorgyline-treated pups, increased CO activity and **F**, granular neurons form a continuous band in layer IV. Scale bar = 320 μm.

fusions of barrels within a given row, mainly in row A, or along the barrel arcs, mainly between the rostral barrels of rows C, D, and E (Fig. II-7). Nissl-stained coronal sections did not show the characteristic clusters in layer IV of S1 (Fig. II-6B); instead, granular neurons formed a uniform band with a moderate packing density (Fig. II-6F). These cortical alterations were not accompanied by any obvious abnormalities in the barrelette or barreloid patterns of the lower sensory stations (Fig. II-8). Furthermore, cortical changes were permanent, as no barrels were distinguished on CO- and Nissl-stained coronal sections from four adult mice that had been treated with 10 mg/kg/8h of clorgyline from P0 to P7 (Figs. II-9A and II-9B).

Less severe alterations of the barrel field were visible in P0-P4 clorgyline-treated pups. In coronal sections, clustered CO-stained blobs were observed in the caudal PMBSF (Fig. II-6C) and also occasionally in coronal sections, though the anterior part of the barrel field. These CO-clusters had irregular shapes and blurred contours. Tangential reconstructions of S1 were done in 6 cases. In AS, barrels were completely lacking in only one case, the other 5 cases displaying barrel-like CO-positive clusters, albeit with a disorganized appearance compared to controls (Fig. II-5E). In LL, segregation as blobs was absent in 4 cases. In the PMBSF, barrels were always distinguishable, but with some barrel fusions similar to those previously described, along arcs or rows (Fig. II-5E, and Fig. II-7). Nissl-stained coronal sections through S1 revealed a disorganized distribution of granular cells in layer IV; with periodic differences in cellular density (Fig. II-6D), suggesting that some architectonic differentiation had occurred.

In P4-P7 treated pups, barrels appeared to be normal on coronal sections, and in all the 5 reconstructed cases, all PMBSF barrels could be identified, and barrels were found in AS (Fig. II-5E). In the case illustrated, the patterning of AS differs slightly from controls, but this is difficult to interpret because there are some variations in the patterning of this subfield in normal animals.

To provide a quantitative comparison of the effect of these different treatments, I counted the total number of CO-positive clusters as well as the number of clearly formed barrels in the PMBSF (see Materials and Methods). These counts confirmed that clorgyline had more potent effects when administered during the E15-P7 and P0-P7 periods, rather than just during the P0-P4 period, while a prenatal treatment did not significantly augment clorgyline's deleterious developmental effect

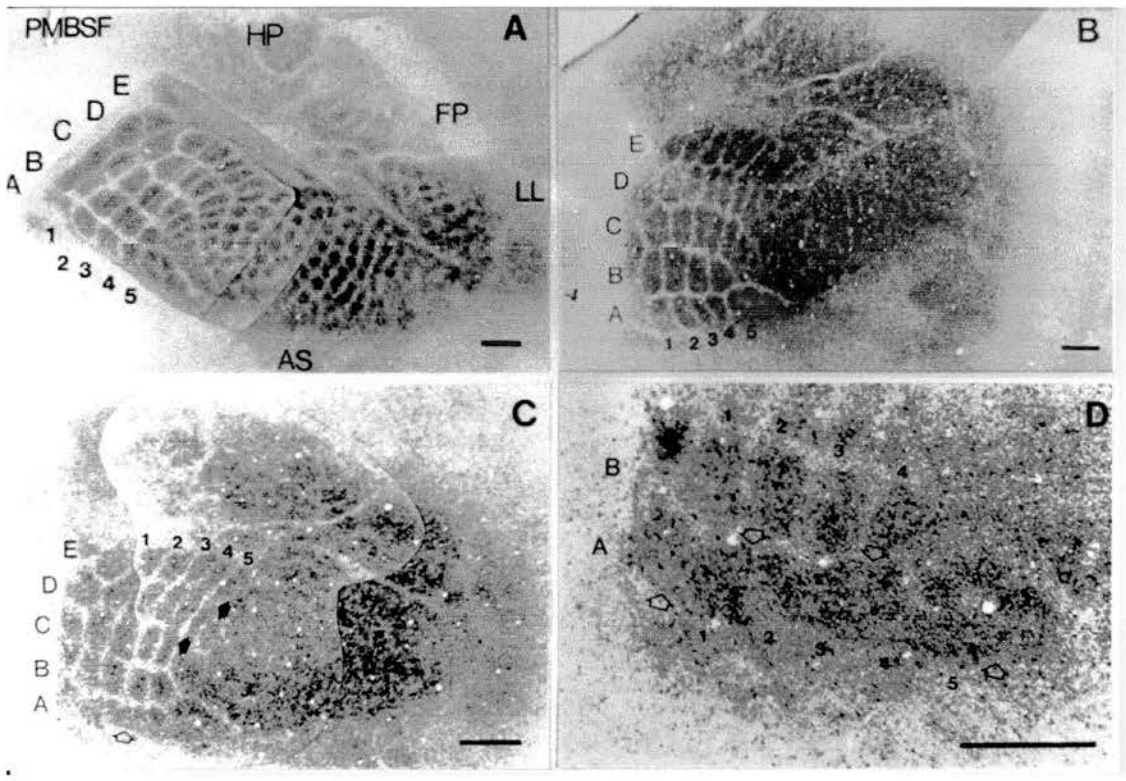

Figure II-7 Pattern of barrel field alterations caused by MAOA inhibition viewed on CO-stained tangential sections. A, Reconstruction of S1 in a control case killed at P10, showing the different trigeminal subfields, PMBSF, AS, and LL as well as the hindpaw (HP) and forepaw (FP) representations. The 5 rows in the PMBSF are indicated with letters from A to E, and the first five barrel arcs are indicated with numbers. **B**, E15-P7 clorgyline-treated mouse killed at P8: note the lack of barrels or CO-positive clusters in AS, LL, and FP. In the PMBSF, the most rostral barrels are lacking with arc-like fusions of barrels along arc 4 (C4, D4, and E4) and 5 (arrow). A row-like fusion is also visible along row A (open arrow). **C**, A similar pattern of barrel field alterations is visible in another case that received a clorgyline treatment from P0 to P7 and was killed at P8. **D**, higher magnification of C. Scale bar = 320 μm.

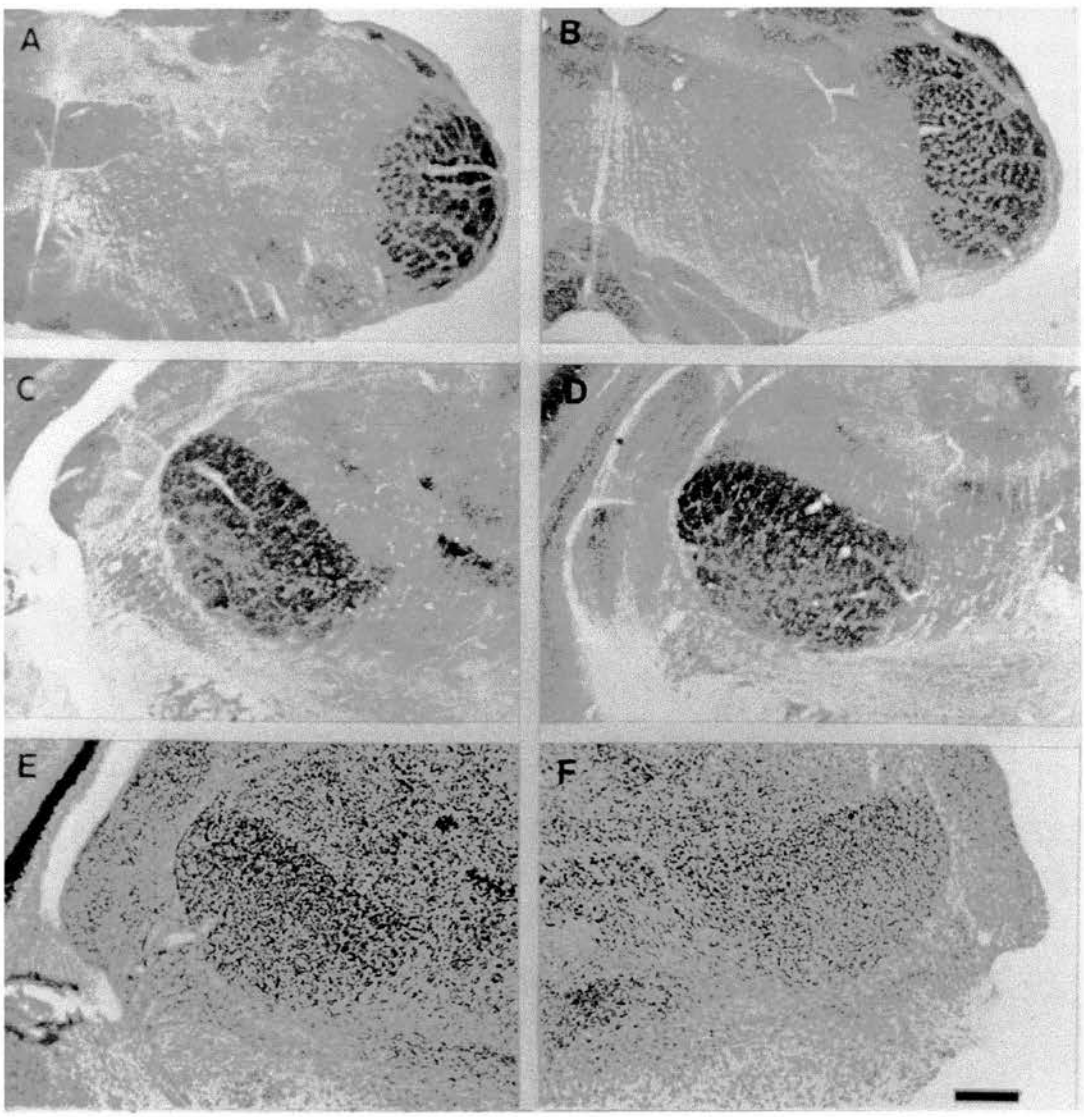

Figure II-8 Normal patterning in the lower stations of the somatosensory pathway, in P10 pups. Different relays of the somatosensory pathway are shown with CO activity (**A-D**) and Nissl (**E**, **F**). Barrelettes have similar staining and distribution patterns in the trigeminal nucleus principalis of (**A**) controls, and (**B**) P0-P7 clorgyline-treated-pups. Barreloids have similar staining and distribution in the ventrobasal thalamic nucleus of (**C**, **E**) controls and (**D**, **F**) P0-P7 clorgyline-treated pups. Scale bar = 320 μm.

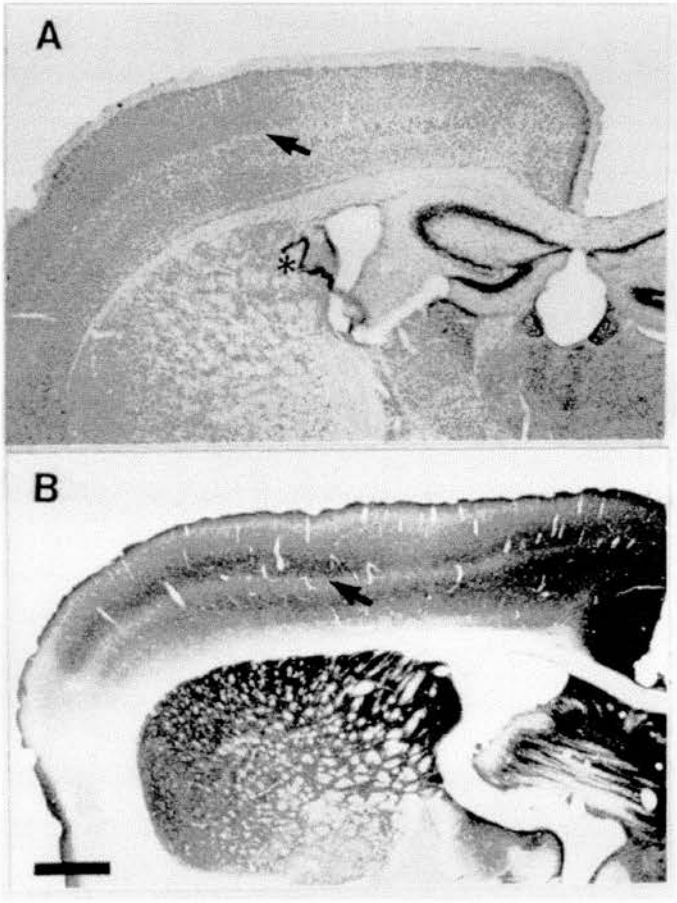

Figure II-9 Permanent alterations of layer IV in a two-month-old mouse treated with 10 mg/kg/8h clorgyline from P0 to P7: granular neurons observed with Nissl staining (the asterisk indicates a displaced fragment of the choroid plexus) (**A**) and CO activity (**B**) form a continuous band in layer IV instead of clustered granular cells (Fig. 7A) or blobs of increased CO activity (Fig. 7B). Scale bar = 640 µm.

(Table II-2). Furthermore, counts of the number of the normally formed barrels along the rows and arcs confirmed the impression of a topographical distribution of the barrel alterations: the reduction in the number of barrels was most severe in row A. Row B, which is formed of four caudal barrels in the normal PMBSF, appeared to be relatively spared by clorgyline treatments. Normal barrels were also less frequent within rostral barrel arcs, comprizing arcs 3 to 8, in the E15-P7 and P0-P7 clorgyline-treated pups, and arcs 5 to 8 in the P0-P4 clorgyline-treated pups (Table II-3). Barrel straddlers (α,β,γ, δ), not included in the counts appeared to be fused in about half the clorgyline-treated cases (E15-07, P0-P7, and P0-P4).

6 Morphometry

Brain weights were similar in P0-P7 clorgyline-treated (308 ± 30 mg) and controls (310 ± 7 mg) P10 mice. On Nissl-stained coronal sections, neither the thickness of cortical layers II-VI, nor the thickness of the layers (II-IV) were significantly changed by any of the treatments (Table II-4). By contrast, the thickness of layer IV, measured as the reactive CO-dense zone, was reduced by 10-20% (Table II-5).

The surface area comprising the PMBSF and AS in the tangential sections, showed a significant 10-20% increase in the P0-P7 and E15-P7 clorgyline-treated pups, but appeared unchanged with the E15-P0, P0-P4, and P4-P7 treatments (Fig. II-10A). Measurements of the individual barrel areas were done in the P0-P4 clorgyline-treated pups, considering only the unfused barrels that could be identified in rows B, C, and D. Significant increases in size were noted for barrels C3 to C5 and D3 to D5, whereas changes were non-significant for the more caudal barrels C1, C2, D1, and D2 and for barrels B1 to B4 (Fig. II-10B). Measurements of individual barrel areas in the P4-P7 treated mice showed no significant difference with controls. Such measures were not feasible in the other treated groups because of the frequency of fusioned barrels.

V Discussion

The present study shows that pharmacological inhibition of MAOA activity during development irreversibly alters the formation of barrels in the mouse

Table II-2 Number of CO positive clusters (normal barrels, abnormal shaped barrels, and fused barrels) and number of clearly defined barrels that can be identified in the PMBSF of P10 pups treated with saline or clorgyline (10 mg/kg/8h) during different periods. These counts were obtained from flattened reconstructions. Mean ± SEM. Asterisk indicates a statistical difference with the control group (* $p < 0.05$; Student's *t* test). Circles indicates a statistical difference between the different clorgyline schedules and the P0-P7 treated group (° $p < 0.05$; Student's *t* test).

	saline			**clorgyline**		
	P0-P7 (n = 5)	E15-P0 (n = 5)	E15-P7 (n = 4)	P0-P7 (n = 5)	P0-P4 (n = 6)	P4-P7 (n = 4)
CO-clusters in the PMBSF	30	29.5 ± 0.7 °	17 ± 1.3 *	19.4 ± 1.5 *	23.8 ± 2.3 * °	29.7 ± 0.6 °
Clearly defined barrels in the PMBSF	30	29.5 ± 0.7 °	12.3 ± 1.8 *	14 ± 0.4 *	19 ± 1.8 * °	29.7 ± 0.6 °

Table II-3 Topographical distribution of barrel alterations. Number of clearly defined barrels along rows and arcs of the PMBSF as identified on complete S1 reconstructions. Analysis was done in P10 pups treated with saline or clorgyline (10 mg/kg/8h). Values represent the mean ± SEM of n cases. Asterisk indicates a statistical difference with the saline group (** $p < 0.01$, * $p < 0.05$; Student's *t* test).

	saline	**clorgyline**				
Rows	P0-P7 (n = 5)	E15-P0 (n = 6)	E15-P7 (n = 4)	P0-P7 (n = 5)	P0-P4 (n = 6)	P4-P7 (n = 4)
A	5	5	1 ± 0.7 **	1.6+0.9 **	3± 1.3 *	4.7 ± 0.5
B	4	4	4	4	4	4
C	6	6	2 **	3.2 ± 0.6 **	4.2 ± 0.6 *	6
D	7	7.5 ± 0.7	2.7 ± 0.9 **	2.2 ± 0.3 **	3.3 ± 1 **	7
E	8	8	3 ± 0.7 **	2.8 ± 0.6 **	4.3 ± 0.7 **	8
Arcs						
1	5	5	4.3 ± 0.9	4.4 ± 0.5	4.5 ± 0.6	5
2	5	5	4	4.4 ± 0.5	4 ± 0.7	5
3	5	5	2.3 ± 0.4 **	2.8 ± 0.6 **	4 ± 0.3 *	5
4	5	5	1.7 ± 0.9 **	2 ± 0.4 **	4.3 ± 0.7	5
5	4	4	0	2 ± 0.4 **	1.3 ± 1.0 **	3.7 ± 0.4
6	3	2.7 ± 0.4	0	0.2 ± 0.3 **	0.5 ± 0.5 **	3
7	2	2	0	0	0.5 ± 0.7 *	2
8	1	1	0	0	0.2 ± 0.3 *	1

Table II-4 Cortical thickness in P10 pups treated with saline or clorgyline (10 mg/kg/8h) during different periods. Measures were obtained from Nissl-stained coronal sections at the level -1 mm posterior, -3.1 mm lateral to the Bregma. Mean ± SEM.

Treatment (number of pups)	Period of treatment	Thickness of layers (μm)	
		II-IV	**II-VI**
saline (n=3)	P0-P7	467 ± 20	1195 ± 34
clorgyline (n=6)	E15-P0	413 ± 32	1023 ± 22
clorgyline (n=6)	P0-P4	410 ± 39	1088 ± 90
clorgyline (n=6)	P0-P7	462 ± 24	1169 ± 64

Table II-5 Thickness of cortical layer IV in P10 pups treated with saline or clorgyline (10 mg/kg/8h) during different periods. Measures were obtained from CO-stained coronal sections at two different stereotaxic levels: -1 mm posterior and -3.1 mm lateral, and + 0.7 mm anterior and -3 mm lateral, to the Bregma. Mean ± SEM.

Treatment (number of pups)	**Period of treatment**	**Thickness of layer IV (μm) at level to the Bregma**	
		-1 ; -3.1 mm	**+0.7; -3 mm**
saline (n=2)	P0-P7	203 ± 17	201 ± 2
clorgyline (n=6)	E15-P0	189 ± 20	207 ± 12
clorgyline (n=6)	P0-P4	169 ± 16	209 ± 14
clorgyline (n=6)	P0-P7	168 ± 8	177 ± 7

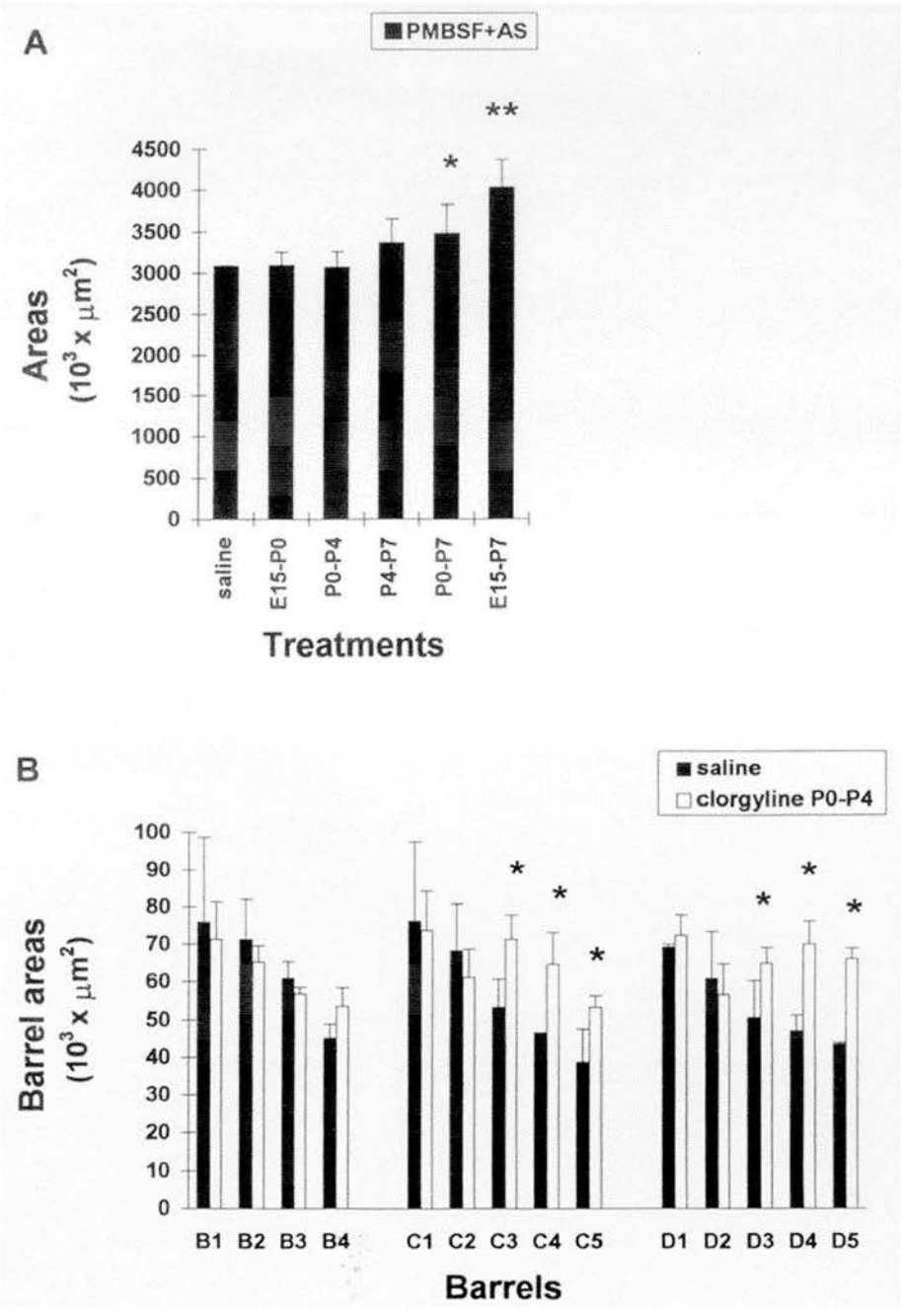

Figure II-10. Morphometric analysis of the barrel field of clorgyline-treated pups. **A**, Area of the PMBSF plus the AS measured on CO stains from pups treated with saline (n = 4) or 10 mg/kg/8h clorgyline during different periods: E15-P0 (n = 6), P0-P4 (n = 6), P4-P7 (n = 5), P0-P7 (n = 6), and E15-P7 (n = 4). ** = $p < 0.005$, *= $p < 0.025$ (Student's *t* test). **B**, Histograms representing the area of individual CO-stained barrels after saline (n = 4) and P0-P4 clorgyline treatment (n = 6). * indicates significant differences ($p < 0.05$; Student's *t* test) between saline- and clorgyline-treated pups.

somatosensory cortex. The degree of cortical abnormality is strongly related to the time period during which MAOA activity is inhibited, with a sensitive period during the first 4 days of postnatal life, but with more pronounced effects when MAOA inhibition is maintained throughout the first postnatal week.

1 Pharmacological blockade of MAOA activity: evaluation of the present model and comparison with MAOA knockout mice

Monoamine oxidases (MAOs) are key enzymes in the degradation pathway of monoamines. Two MAOs exist in the brain, MAOA and MAOB (review in Weyler et al., 1990). Although closely related in their gene structure (Shih, 1991), MAOA and MAOB differ in several characteristics: MAOA is abundant in noradrenergic neurons (Luque et al., 1995; Jahng et al., 1997), has a preferential affinity for 5-HT, and is selectively inhibited by clorgyline, whereas MAOB is abundant in serotoninergic neurons and glial cells, has a lower affinity for 5-HT, and is selectively inhibited by deprenyl. Compounds that inhibit MAOA exhibit antidepressant activity (review in Tipton, 1989). In rodents, developmental studies have shown that MAO activity in the brain appears early in ontogeny, by E15 (Bourgoin et al., 1977), with MAOA activity initially predominating over MAOB (Mantle et al., 1976). By P15, MAOA is maximal, whereas MAOB activity reaches 50% of adult values (Jourdikian et al., 1975).

In a transgenic mouse line characterized by the deletion of exons 2 and 3 of the gene encoding MAOA, and resulting in the absence of measurable MAOA activity, I observed a peculiar developmental abnormality in the primary somatosensory cortex, where layer IV cortical neurons and afferent thalamic fibers failed to organize in barrels (Cases et al., 1995; 1996). Similar though less extensive alterations were produced when the corresponding wild-type mice (inbred strain C3H/HeJ) were treated with the MAOA inhibitor clorgyline (Cases et al., 1996). In order to generalize these findings, an important first step was to show that similar effects could be obtained in other mouse strains. In the present study, abnormalities in barrel formation were observed after MAOA inhibition in the OF1 mouse strain. I found that these alterations were similar to those observed in the C3H/HeJ mice. However, in parallel unpublished studies, I observed variations of the effects of MAOA inhibition among different mouse strains. In F1 hybrids between the

C57BL/6 and C3H/HeJ strains, clorgyline treatments from P0 to P7 induced only minor changes in the AS field, while treatment from P0 to P4 produced no visible cortical alterations (T. Vitalis and O. Cases, unpublished observations). Correspondingly, MAOA knockouts with a C57BL/6 genetic background, obtained by repeated backcrossing, have some, ill-defined barrels in the caudal PMBSF (I. Seif and P. Gaspar, unpublished observations). This suggests that according to the mouse strain, factors that modulate the levels or effects of 5-HT are differently regulated. Indeed, amounts of MAOs (Voitenko, 1992), tryptophan hydroxylase (Knapp et al., 1981; Daszuta et al., 1984; Kulikov et al., 1995), 5-HT receptors, 5-HT transporter, as well as the number of serotonergic raphe neurons (Daszuta and Portalier, 1985) appear to differ among inbred mouse strains.

The milder severity of alterations in clorgyline-treated mice as compared with MAOA knockouts with identical genetic background could be due to incomplete inhibition of MAOA. Incomplete inhibition of MAOA might be particularly critical during specific periods such as the perinatal period. Clorgyline is an irreversible inhibitor of MAOA and the duration of its effects is linked to its elimination and the rate of synthesis of MAOA, with a replacement rate in MAO activity varying from 24 hours in rat or mouse pups (Nelson et al., 1979; Samsa et al., 1979), to 10-12 days in adult rats (Maitre et al., 1976). Present observations indicate that a partial recovery of MAOA activity occurs as soon as 8 hours after a single clorgyline administration at P3. Thus, although chronic administration of clorgyline every 8 hours resulted in a near-complete inhibition of MAOA at P7, as reflected by the increased levels of brain 5-HT that mirrored those observed in the MAOA knockouts, there could be fluctuations in these levels. For instance, at P0, brain levels of 5-HT increased four-fold in pharmacologically treated versus nine-fold in MAOA knockouts, probably reflecting the difficulty of drug administrations during the perinatal period. A continuous mode of administration of clorgyline, such as afforded by minipumps, would be needed to evaluate the importance of these fluctuations. A critical threshold of brain 5-HT may exist, above which cortical abnormalities occur. Below such a level, compensatory mechanisms might be active: for instance other neurotransmitters could antagonize the effects of 5-HT, or changes in number or affinity of 5-HT receptors and monoaminergic transporters could dampen the effects of 5-HT increase. Such compensations would become ineffective when the brain is overwhelmed with large amounts of 5-HT.

The present protocol is potentially flexible and could be applied to other useful experimental species, such as rats or felines, to determine whether similar effects of MAOA inhibition on the formation of cortical maps can be observed. The variability of effects observed between different mouse strains is however an indication that interspecies differences are to be expected.

2 Period sensitive to MAOA inhibition: relationship to stages in barrel field development

The present pharmacological study, together with previous observations in the MAOA knockout mice, allows me to narrow down the sensitive period during which MAOA inhibition can alter the development of barrels.

In the rodent trigeminal system, the formation of the cortical map and its differentiation into barrels results from a precisely timed sequence of events, which can be separated into three main epochs. The first period corresponds to the formation of a topographic map of the VB in the cortex. During fiber outgrowth, VB axons maintain a strictly ordered topography (Molnar and Blakemore, 1995; Catalano et al., 1996) that is in register with the peripheral topography initiated in the trigeminal nerve and transmitted to the trigeminal nerve nuclei and to the VB (Erzurumlu and Killackey, 1983). All these processes which occur during embryonic life are not affected by MAOA inhibition. Indeed, clorgyline treatments during embryonic life caused no visible effects and did not increase significantly the postnatal effects of MAOA inhibition (comparison of E15-P7 with P0-P7 clorgyline treatments). Accordingly, in MAOA knockouts, inhibition of 5-HT synthesis during postnatal life (P0-P6) suffices to reverse the barrel field abnormalities (Cases et al.,1996). Furthermore, the topographic organization of the thalamocortical projection, revealed with anterograde tracers in adult MAOA knockouts, appeared to be normal (Cases et al.,1996).

The second major step is the formation of periphery-related clusters in S1. This process seems to be dictated by a tendency of thalamic terminal axons carrying information from a functional group of peripheral receptors (large vibrissa, sinus hair, or digits) to cluster together, first in layer VI, then in layer IV, where they induce the characteristic cellular ring-like cytoarchitectonic differentiation (Rice and Van der Loos, 1977; Senft and Woolsey, 1991 a,b; Agmon et al., 1993). These

processes which occur essentially during the first 4-5 days of postnatal life appear to be most affected by the clorgyline treatments. Indeed, clorgyline treatments during the first five days of life sufficed to cause alterations in the barrel field while clorgyline treatments after P4 caused no visible changes of the barrels. This time limit coincides with that disclosed for the effects of lesions of peripheral receptors (Woolsey and Wann, 1976; Belford and Killackey, 1980; Jeanmonod et al., 1981) indicating that the cytoarchitectonic differentiation of granular neurons in layer IV is an irreversible process once it has been initiated. The exact step that is disrupted by excess 5-HT during this 4-day period remains to be determined.

The third and last phase of barrel development extends until probably P21 and is characterized by the functional maturation of the barrels, coinciding with an extensive collateral arborization of the thalamic axonal arbors within the confines of a given barrel (Agmon et al., 1993). A corresponding maturation of the cortical targets occurs with extensive dendritic remodeling, formation of dendritic spines and synapses (White et al., 1997). The general resultant of these cellular events is a growth in the size of individual barrels and in the total area of S1 (Rice and Van der Loos, 1977; Riddle et al., 1992). I could not detect a clear effect of clorgyline treatments between P4 to P7. However, the histological methods used in the present study do not allow me to monitor more subtle developmental events that could be affected by the excess of brain 5-HT, such as the fine topographic arrangement of thalamocortical afferents. For instance, early sensory deprivation, or application of an NMDA-receptor antagonist, to the cortex, caused no cytoarchitectonic changes of the barrel field although electrophysiological studies demonstrated the presence of topographically inappropriate thalamic projections (Fox, 1992; Fox et al., 1996).

An observation for which I have as yet no clear interpretation is that barrel field changes were more important when MAOA inhibition was maintained until the end of the first postnatal week rather than just during the first five postnatal days. This difference could be interpreted as resulting from a delay in the cellular processes of barrel formation, that could still be re-initiated when MAOA inhibition ceases at P4, but not when it ceases at P7. However, in other experimental situations where a delay in barrel formation was observed, such as caused by 5-HT neurotoxins (Blue et al., 1991; Osterheld-Haas et al., 1994; Osterheld-Haas and Hornung, 1996), or protein malnutrition (Vongdokmai et al., 1980) a normal barrel field eventually formed, whereas the patterning of the barrel field remained abnormal after P0-P4

clorgyline treatments. The synergism of P4-P7 clorgyline treatments with the P0-P4 treatment could indicate that there are some later effects of 5-HT on barrel development, but that these become apparent only when primed by an early effect during the initial stages of barrel development.

3 Gradients of changes in the barrelfield

Barrel alterations in the representation of the whisker pad were not uniformly distributed, effects were more marked in the rostral fields where the small vibrissae are represented than in the posterior field where the large caudal vibrissae are represented. Indeed, barrel fusions were more frequent in the AS representation and in the rostral part of the PMBSF, where significant enlargments of « intact » individual barrels was also seen. Exceptions to this general trend were the largest and caudal-most barrels (α, β, γ, and δ), which were frequently fused.

Several hypotheses can be proposed to explain this phenomenon. The sequence of development of the face vibrissae proceeds from ocular to nasal and this temporal sequence is replicated at least at the level of the trigeminal nerve and the brainstem (Erzurumlu and Killackey, 1983). A caudal to rostral sequence of emergence of periphery-related patterns has also been described in the somatosensory cortex. This can be seen in the ACh-E preparations of Schlaggar and O'Leary (1994), where barrel-like patterning is visible in the PMBSF before it emerges in AS. Using 5-HT immunostaining, that also reveals the thalamocortical afferents, Rhoades et al. (1990), described a clear caudal to rostral sequence of fiber clustering in S1. Later in development, boundary patterns of cortical glia (McCandlish et al., 1989) and markers of synaptogenesis (Stettler et al., 1996), were described as following a similar gradient of maturation. In this view, excess 5-HT would have more pronounced effects on the rostral, relatively immature thalamic fibers compared with the more mature caudal ones, and the fact that I were not able to disrupt the caudalmost barrels even when administering clorgyline before birth, could be due to an unsufficient MAOA inhibition during late embryonic and early postnatal life.

These gradients should also be considered in the context of a difference in the geometry and function of the peripheral receptors that are mapped in the caudal versus the rostral parts of S1: the large vibrissae mapped in the PMBSF are more

widely separate on the snout than the anterior sinus hair of the AS. Large PMBSF vibrissae could thus be expected to be functionally autonomous and to have asynchronous activity compared to their neighbours. This would provide a larger drive for segregation of afferents than in the case of the small AS vibrissae. If excess 5-HT, antagonizes this process, one could therefore have more visible effects in the AS than in the PMBSF. This hypothesis derives from the general hypothesis that activity-dependent mechanisms are regulating the segregation of sensory afferents following the principle that "cells that fire together wire together" (review in Shatz, 1990).

4 Mechanisms of MAOA inhibition

It is important to consider whether the effects of clorgyline on barrel field development are due to a general effect on growth, since clorgyline administration caused a deficit in weight gain between P3 and P6. This is an unlikely explanation however, because protein malnutrition in mice causes only a two-day delay in the development of the barrels and in the sensitive period to neonatal vibrissal damage (Vongdokmai et al., 1980), and not a persistent absence of barrels as observed in this study.

Despite the ignorance about the precise mechanism of 5-HT action in the developing somatosensory thalamocortical system, the developmental pattern of expression of 5-HT receptors in this system should be a good indication of the potential cellular targets of 5-HT.

In the cortex, pyramidal cells in layers II-III express functional 5-HT2 receptors during development and their activation reduces gap junction coupling (Rörig and Sutor, 1996). Scattered cortical neurons have been shown to express 5-HT3 receptor gene (Tecott et al. 1995). However, these neurons would constitute unlikely targets in the process of barrel formation within layer IV, and it has not yet been determined whether layer IV neurons or glia express any 5-HT receptors, during the sensitive period of barrel development.

On the other hand, developing VB thalamic fibers express both SERT (Lebrand et al., 1996) and 5-HT_{1B} receptor subtype between E15 and P10 (Lebrand et al., in preparation). SERT causes 5-HT to accumulate in large excess in VB neurons when MAOA is inhibited (Cases et al.,1998) and thereby, could cause an

abnormal development. Indeed, an abnormal tangential distribution of the thalamocortical fibers in the clorgyline-treated mice was presently visualized with 5-HT immunocytochemistry. Excessive stimulation of the presynaptic 5-HT_{1B} receptor subtype might cause a complete inhibition of the excitatory neurotransmission in the thalamocortical circuit, interrupting any activity-dependent mechanism that could be responsible for the segregation of the thalamocortical axons. Alternatively, activation of the 5-HT_{1B} receptor subtype or internalization of 5-HT might also have a direct trophic action on axonal growth, that would mask the underlying segregation processes.

Indirect clues on the mechanisms underlying 5-HT's effects may be drawn from comparing the effects of MAOA inhibition with that of different types of lesions. The fact that 5-HT has no instructive effects *per se* on barrel formation is demonstrated by the early lesions of the 5-HT system that cause no disruption in the general patterning of the barrel field (Blue et al., 1991; Bennett-Clarke et al., 1994, Osterheld-Haas et al., 1994). On the other hand, these studies suggest that 5-HT may have a trophic effect on thalamocortical and barrel development. In neonatal rat pups, 5,7-dihydroxytryptamine (5,7-DHT) or fenfluramine administration caused a decrease in the tangential area covered by individual barrels in the PMBSF (Bennett-Clarke et al., 1994; 1995) and a delay in the laminar differentitation of layer IV was noted in 5,7-DHT treated mice (Osterheld-Haas and Hornung, 1996). These findings are however hampered by the possibility that 5-7 DHT could have a direct toxic effect on the developing thalamic neurons, because it may be taken up in these neurons by SERT.

5-HT could be acting as a modulator of peripheral influences derived from the periphery. Lesions of the infraorbital nerve (ION), the trigeminal branch that supplies the whisker pad, produce effects similar to that of MAOA inhibition in that there is loss of the characteristic thalamocortical clustering and a lack of cytoarchitectonic differentiation in layer IV. However, the pattern of PMBSF alterations resulting from such lesions differed: the deprived territory appeared atrophic and disorganized with a main outline of the 5 barrel rows (Jensen and Killackey, 1987b; Killackey et al., 1994) (Figure II-11). By contrast, clorgyline treatment during the sensitive period results in barrel fusions, both within and across rows with a general trend for hypertrophy as there was an increase in the size of the trigeminal representation, or of individual barrels. Furthermore, MAOA inhibition

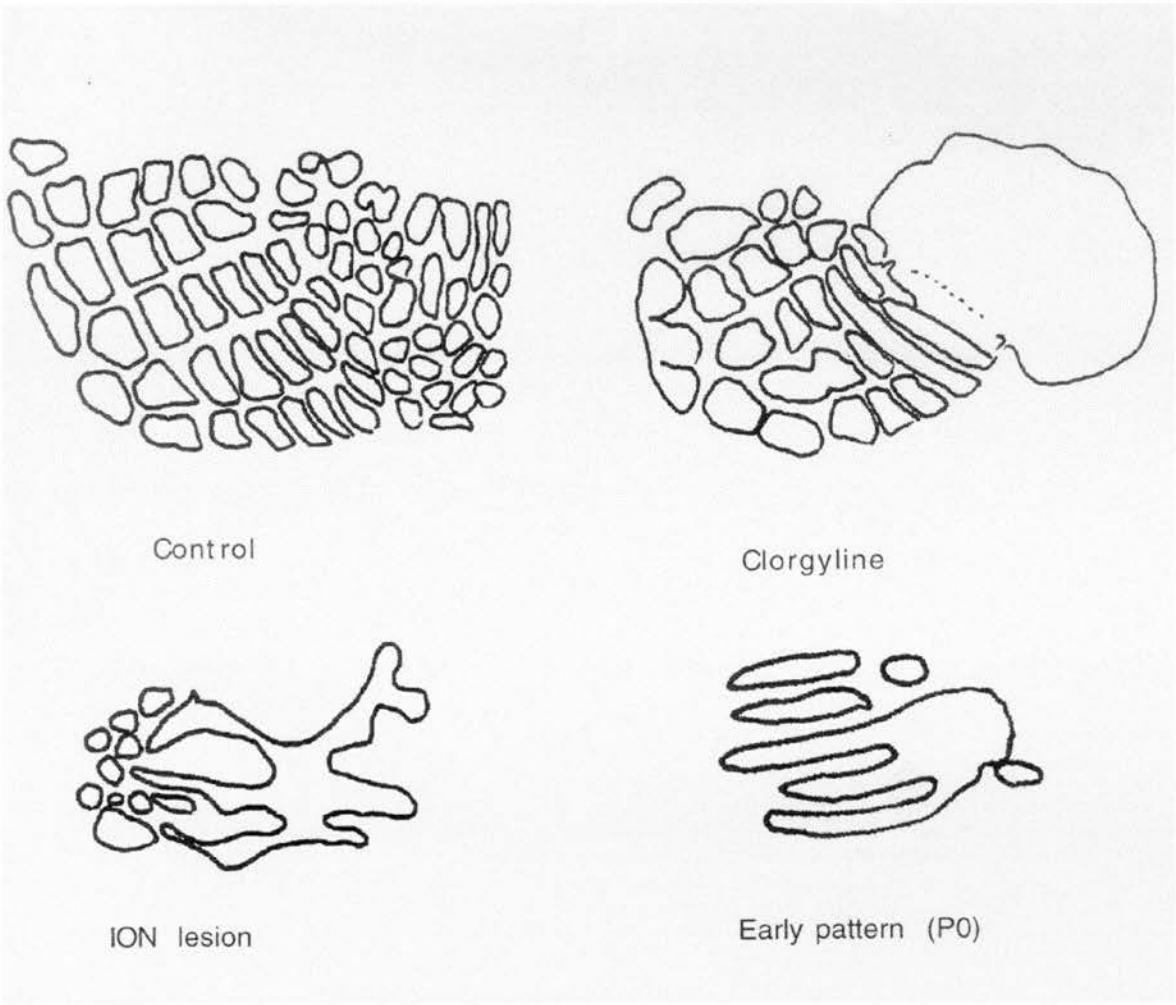

Figure II-11 Schematic representation of the barrel field (PMBSF and AS) pattern after MAOA inhibition, in comparison with reported changes after infraorbital nerve transection (Killackey et al., 1994), and with described patterns of thalamocortical afferents in P0 rat pups (redrawn from Schlaggar and O'Leary, 1994).

caused no visible alterations in the trigeminal nerve nucleus and VB, contrary to the effects of lesions (Killackey et al.,1994; Durham and Woolsey, 1984). These different patterns of alterations could indicate that peripheral lesions interrupt a trophic influence originating from the peripheral receptors whereas excess 5-HT does not. Anterograde transport of neurotrophic molecules from the periphery has been recently demonstrated in the chick developing visual system (Von Bartheld et al., 1997) and could well exist in the rodent somatosensory system, as suggested by recent observations (Wilkinson et al., 1996; Chiaia et al., 1996). In this respect, the effects of 5-HT may be viewed as being limited to the distalmost component of this ascending sensory pathway, which is the synaptic interaction of ingrowing terminals with their maturing cortical targets. Direct evidence derived from electrophysiological studies, pharmacology, single axonal reconstructions, and electron microscopy will be necessary to comprehend what these effects precisely are.

CHAPTER THREE:
IMPORTANCE OF TRKB SIGNALLING IN THE MURINE SOMATOSENSORY CORTEX

CHAPTER THREE:
IMPORTANCE OF TRKB SIGNALLING IN THE MURINE SOMATOSENSORY CORTEX.

I Abstract

In this chapter, I show that the catalytic trkB tyrosine kinase receptor is strongly expressed in layer IV of the somatosensory cortex from P0 to P10. This period corresponds to the sensitive period of establishment of both granular neurons and thalamocortical axons in barrels. To elucidate if trkB has a role in these processes, I have analysed the somatosensory thalamocortical system in mice lacking trkB. I show that trkB is not essential in the clustering of granular neurons in barrels, although thalamocortical axons display subtle morphological alterations, expanding abnormally in layer II-III but not tangentially. This suggests that cortical trkB signalling participates in the fine clustering of thalamocortical axons.

I also wanted to evaluate the effects of trkB signalling in MAOA knockout mice. MAOA knockout mice display both an abnormal exuberant tangential thalamocortical projection and an abnormal clustering of granular neurons in layer IV. I showed that trkB mRNA levels are normal in MAOA knockout mice, suggesting that abnormal expression of trkB is not essential in the phenotype displayed by MAOA knockout mice. Interestingly, the lack of trkB in MAOA knockout mice induced a much more expanded tangential thalamocortical projection as revealed by 5-HT, SERT and VMAT2 immunolabelling. In addition, MAOA-trkB double knockout mice displayed also an abnormal vertical expansion of SERT immunolabelling in layers II-III, similar to those observed in trkB knockout mice. These results suggest that the mechanisms inducing the abnormal phenotypes in MAOA knockout mice are independent of trkB, although knock out of both genes can act synergistically.

Interestingly, MAOA-trkB double knockout mice displayed a much better survival rate than trkB knockout mice. However, similar reductions in body and brain weights and cortical thickness between both strains were observed by P8.5. I have also compared the cell death in the CNS of MAOA-trkB double and trkB knockout mice. I showed decreased numbers of pyknotic profiles in specific brain regions of MAOA-trkB knockout mice compared to trkB knockout mice. This

suggests that increasing monoamines (5-HT and NA) levels in the brain of trkB knockout mice prevents or delays the cell death of discrete neuronal populations such as the accumbens and cingulate cortex.

II Introduction

Excess of 5-HT affects late events in the development of the somatosensory thalamocortical system, such as the morphology of axonal terminals and dendritic processes or migration of cortical neurons. Candidate molecules that may be affected are unknown. In this chapter, I have explored the hypothesis that 5-HT could directly or indirectly modulate the actions of trophic factors, such as neurotrophins, in the somatosensory thalamocortical system. Second, I have tested whether the signalling through one of the neurotrophin receptor, TrkB, is requiered for the effects of excess 5-HT. Neurotrophins are trophic factors expressed in the CNS and have a wide spectrum of effects, such as neuronal survival, axonal guidance or neurite outgrowth. A hypothesis tested in this chapter is that an excess of 5-HT could induce an excess of "neurotrophic effects" that lead to an abnormal exuberant growth of thalamic fibers in the somatosensory cortex.

1 Neurotrophins and their receptors

Several neurotrophins have been identified, all of which are able to promote the survival of a large range of neuronal populations: nerve growth factor (NGF; Levi-Montacini, 1987), brain-derived neurotrophic factor (BDNF; Barde et al., 1982), and neurotrophins 3 (NT-3; Ernfors et al., 1990) and 4/5 (NT-4/5; Berkemeier et al., 1991; Hallbook et al., 1991). Neurotrophins act through membrane receptors whose activation leads to a cascade of intracellular phosphorylations. Three high affinity receptors have been identified, and belong to a family of tyrosine kinase proteins. TrkA binds preferentially NGF, TrkB binds both BDNF and NT-4/5 with the same affinity and TrkC binds preferentially NT-3 (Barbacid, 1994). In addition, a low affinity receptor, p75, which binds all the neurotrophins with the same affinity has been identified (Chao, 1994).

2 Neurotrophins and critical periods during sensory development

Several observations suggest that neurotrophins play important roles in the control of developmental plasticity; for instance, exogenous supply of neurotrophins counteracts the effects of monocular deprivation and dark rearing, and blocking their activity prevents the formation of ocular dominance columns. They can modulate synaptic transmission and, like NMDA receptors, their expression is developmentally regulated and dependent on electrical activity (Caleo et al., 1999; Berardi and Maffei, 1999). This reciprocal regulation between neurotrophins and neural activity may provide means by which active neuronal connections are selectively strengthened. Indeed, neurotrophins seem to require the presence of electrical activity in order to exert their effects (McAllister et al., 1999). Particularly compelling evidence for this comes from Caleo et al. (1999), who have shown that NGF signalling via trkA receptor must be coupled with afferent electrical activity to prevent the effects of molecular deprivation. In addition, there is clear evidence that neurotrophins control the duration of the critical period; in fact, they are the first molecules for which a causal relation has been established between their action and the duration of critical periods in mammals. The first evidence came from the finding that blockade of endogenous NGF through the use of antibodies prolongs the duration of the critical period, an effect similar to that of dark-rearing (Domenici et al., 1994). Very recently, in an elegant study using transgenic mice that overexpress BDNF in the forebrain, Huang et al. (1999) have found accelerated visual development and early cessation of synaptic plasticity that is enabled by LTP in the visual cortex. These findings suggest that BDNF controls the time course of the critical period by accelerating the maturation of GABAergic inhibition.

To summarise, BDNF regulates GABAergic inhibitory interneurons (Carnahan and Nawa, 1995), potentiates GABA release (Sala et al., 1995), and mediates the activity-dependent regulation of synaptic inhibition (Rutherford et al., 1998). In addition to these actions, BDNF has been repeatedly found to affect excitatory transmission; also, modulation of NMDA responses by BDNF has been recently suggested (Carmignoto et al., 1997; Levine et al., 1998).

3 Neurotrophins and the somatosensory system

In the somatosensory cortex, several studies have shown that neurotrophins can rapidly modulate activity-dependant stimulation; for instance in adult rats, levels of BDNF mRNA in non-GABAergic neurons are increased after sensory stimulation of the whiskers (Rocamora et al., 1996). In addition, exogenous supply of BDNF to the surface of the somatosensory cortex leads to a decrease in the size of the receptive field of a whisker and to a decrease in the amplitude of cortical activity-dependent signals (Prakash et al., 1996). It is important to note that mice deficient for trkA, trkB, trkC, p75, BDNF or NT4/5 display no obvious alteration of the barrel field (Henderson et al., 1995).

4. TrkB signalling in the neocortex

The effects of trkB signalling on the development of neocortical neurons has been of particular interest due to the correlation between the spatial and temporal patterns of expression of the trkB receptor and its ligands during corticogenesis, and the known effects of trkB activation on neuronal survival and function in vitro. Immunocytochemical and in situ hybridisation analyses have shown that expression of trkB receptors and/or ligands are increased during corticogenesis. TrkB activation has been shown to influence the survival (Nawa et al., 1994), differentiation (McAllister et al., 1995, 1997; Horch et al., 1999), connectivity (Katz and Shatz, 1996) and neurotransmitter release (Wang and Poo, 1997) of neocortical neurons both in vivo and in vitro. Finally, one well known action of trkB in developing neocortical neurons is the regulation of dendritic growth (Yacoubian and Lo, 2000). Together, these findings led to the hypothesis that trkB signalling may be critical for neocortical neuronal development.

Determining the effects of the deletion of trkB on neocortical neuronal survival, differentiation, and function has been difficult with mutant mice alone due to the neonatal lethality caused by the trkB gene deletion. While gross anatomical analysis of trkB knockout mice suggests normal neocortical cytoarchitecture within neonatal mice (Silos-Santiago et al., 1997), other studies point to a significant increase in apoptotic cell death and reduced cell numbers in layer II/III, V, and VI of the developing mutant cortex (Alcantara et al., 1997). Recently, subtle anatomical abnormalities have been observed in mutant cortex such as reduced survival and neurite outgrowth in vitro, and delayed neuronal migration and differentiation in vivo

(Gates et al., 2000). Limitations on the importance of trkB in neocortical development are potentially confounded by unrelated cranofacial sensory and suckling defects that greatly reduce the health and postnatal lifespan of mutant mice. This early death occurs before the more superficial neocortical layers II/III and IV fully develop, and before the processes of axon pathfinding, fiber pruning and synaptogenesis in the neocortex are complete. Recently, this problem has been circumvented obtaining viable conditional trkB knockout mice. In these mutant mice, only layer V neurons display a lack of trkB. Following trkB deletion in layer V pyramidal cells, their dendritic arbors are altered, and cortical layers II/III and V are compressed, after which there is an apparent loss of mutant neurons expressing the transcription factor SCIP but not of those expressing Otx1 (Xu et al., 2000). Taken together, this shows that trkB is required for the differentiation and maintenance of specific populations of cells in the developing and adult neocortex.

5 Aim of the work

In this chapter, I wanted to show if trkB signalling has a role in the critical period of the somatosensory thalamocortical system. In the first place, I studied the spatio-temporal pattern of catalytic trkB during the critical period of the somatosensory thalamocortical system. Then, I characterised subtle alterations in the somatosensory cortex of trkB knockout mice. Moreover, I wanted to know if there was a link between 5-HT and trkB signalling in the alterations displayed by MAOA knockout mice. The basic hypothesis would be that 5-HT could regulate a trkB-promoted outgrowth of thalamic fibers in the somatosensory cortex. First, I obtained the pattern of expression of trkB in MAOA knockout mice to evaluate if 5-HT could act on the transcription of this molecule. Then, I obtained MAOA-trkB double knockout mice to see if the alterations observed in MAOA knockout mice were unchanged.

II Material and methods

1 Mice

trkB knockout mice were generated with a targeted mutation in the tyrosine kinase domain (Klein et al., 1993). trkB knockout mice were maintained on a mixed C57/Bl6-Sv129 genetic background. MAOA knockout mice displayed a deletion of exon 2 and 3 in the gene encoding MAOA (Cases et al., 1995). MAOA knockout mice were originally obtained and maintained on a C3H/He genetic background. Mice double knockout for trkB and MAOA were obtained in the F2 progeny from crosses between females heterozygous for MAOA and trkB and males hemizygous for MAOA and heterozygous for trkB. trkB knockout, MAOA knockout and wild type mice were obtained from the same crosses. Genitors and pups were genotyped for trkB and MAOA mutations. For trkB genotyping, the same primers as previously described by Klein et al. (1993) were used. For MAOA genotyping, two couples of primers were used. The first couple was used to detect the presence of the transgene (5': CTCAGAAGTCGGATCTGAT in the H2-Kb and 3': CAGTAGATTCACTACCAGTC in the interferon-β gene). The other couple of primers corresponded to a sequence that is only present in the normal allele (5': GATTCTCTCCTATTGTCTCTG and 3': AAAGACAGTTGTGAAGCCTCA).

2 Immunocytochemistry and histochemistry

Postnatal mice were analysed at postnatal day 0 (P0) and P8.5 (the day of birth was counted as P0). Pups were anaesthetised and fixed in 4% paraformaldehyde in 0.12M phosphate buffer, pH 7.4. All mice were perfused transcardially and postfixed in fresh fixative overnight. After perfusion, brains were removed from the skull and weighed. One hemisphere was separated from the rest of the brain by a section through the internal capsule and flattened between two glass slides separated by spacers. The rest of the brain was kept as one block. Blocks were postfixed overnight in the same buffered paraformaldehyde and cryoprotected in 30% sucrose phosphate buffer. Serial, 40 μm-thick, frozen sections were obtained in the coronal or tangential planes. Alternate series of sections were used for CO, as described by Wong-Riley and Welt (1980), and Nissl (0.05% thionine in acetate buffer pH 5.5).
5-HT immunocytochemistry (rat monoclonal antibody from Harlan-Seralab, clone YC5/45, 1:20 to 1:50; Consolazione et al., 1981) was performed on frozen sections as previously described in Lebrand et al. (1996). VMAT2 (1:4000, Phoenix

Immunochemicals) and SERT (1:2000, Calbiochem) immunocytochemistries were also performed on sections from P8.5 animals.

3 In situ hybridisation for trkB

trkB cRNA probes, corresponding to the tyrosine kinase domain of the protein were used (Klein et al., 1993). The plasmid was linearised with BamH1 for antisense RNA synthesis by T7 polymerase and with EcoRI for sense RNA synthesis by T3 polymerase. The in vitro transcription was carried out using the Promega kit and probes were labelled with ^{35}S-UTP (>1000 Ci/mmol; Amersham). In situ hybridisation for cRNA probes was performed on fresh frozen brain sections (15 µm thick). Tissue sections were postfixed for 15 mn in 4% paraformaldehyde, washed in PBS, acetylated, washed in PBS, dehydrated, and air-dried. Sections were covered with hybridisation buffer containing $5x10^4$ cpm μl^{-1} of the ^{35}S-trkB probes (12.5 µl/section), and then incubated overnight in a humid chamber at 48°C. Washes were then performed as previously described in Fontaine and Changeux, 1989. Autoradiograms were obtained by apposing the sections to hyperfilms (β-max, Amersham) for several days. Autoradiographic films were developed in D19 (Kodak) for 3 min at 20°C, and fixed in A14 (Ilford) for 5 min. For histological analyses, the slides were dipped in photographic emulsion (NTB2, Kodak) and exposed for about 10 days. After development of the emulsion, the sections were counterstained with cresyl violet.

4 Morphometric analysis

Counts. Coronal sections stained for Nissl (one section out of three) were analysed using a 20x objective and a millimetric eyepiece. The number of pyknotic nuclei was counted in the cingulate cortex (Cing), restrosplenial cortex (Rsg), striatum (Str), Accumbens (Acb), ventrobasal thalamic nucleus (VB), somatosensory cortex (S1) and superior colliculus (Coll). Counts were performed in 5 to 7 sections per animal (100,000 μm^2 fields per section for each region). Values derived from trkB and MAOA-trkB double knockout mice were compared with those of the various controls using an unpaired Student's *t* test.

Neuronal size. For determination of neuronal cross-sectional areas, profile of neurons in layer V (somatosensory cortex) of trkB, MAOA-trkB double knockout and wild type mice (P8.5, 4 animals each, 30 neurons per animal) were drawn using camera lucida tracing. Areas were quantified with Image Tool software (The University of Texas Health Science Centre in San Antonio).

Areas. Trigeminal ganglion and facial nuclei of wild type, trkB knockout and MAOA-trkB double knockout mice were outlined using a camera lucida. Areas of the trigeminal ganglion and facial nucleus were estimated using the Image tool software (The University of Texas Health Science Centre in San Antonio). One section out of three was analysed from two pups of each genetic background (analysis of additional animals would be necessary for statistical analyses).

5 Cortical analysis

The barrel field was analysed from sections obtained from tangentially sectioned hemispheres. Reconstruction of the PMBSF was obtained either from CO-reacted sections or from 5-HT- reacted sections (Vitalis et al., 1998-Chapter II). The thickness of cortical layers II-IV and layers II-VI were measured in Nissl-stained coronal sections, using an eyepiece graticule (x10 objective). The thickness of layer IV was measured in CO-reacted coronal sections (x16 objective). Measurements were taken along a line perpendicular to the pial surface, at two different levels: one in the PMBSF, (level –1.94 posterior and -3.1 lateral to the Bregma), and the other in AS, (level –0.82 anterior and –3.1 lateral to the Bregma).

III Results

1 TrkB expression in MAOA knockout mice during the critical period of barrel field formation

In order to test whether high levels of 5-HT were playing a role in modulating the expression of trkB in the cortex and the thalamus, I first analysed trkB mRNA expression in wild type and MAOA knockout mice. This study was mainly conducted during the period of barrel field formation at P0, P4, P6 and P15. In situ

hybridisations with riboprobes corresponding to the tyrosine kinase domain of trkB in wild type and MAOA knockout pups showed that MAOA knockout mice displayed a normal pattern of trkB expression in the ventrobasal thalamic nucleus and somatosensory cortex. In the isocortex and allocortex, most neurons were strongly labelled at birth. This expression progressively decreased during development. Interestingly, trkB expression was high in layer IV of sensory cortices from P0 to P10. In S1, trkB was expressed in a barrel-like pattern from P4 to P7 (Fig. III-1). Then, the distribution of trkB was diffuse all cortical layers, except layer I. In the thalamus, the ventrobasal thalamic nucleus displayed low to moderate levels of expression at P0, P4 and P7. From P15, levels of trkB expression were low. These results are in agreement with previous studies done in rat (Masana et al., 1993). At the level of the cortex and the thalamus, similar patterns and levels of trkB expression were observed in MAOA knockout mice (data not shown).

These results failed to reveal any striking differences in trkB levels between controls and MAOA knockout mice during postnatal development (P0-P15). I decided to test the hypothesis that trkB is requiered for MAOA phenotype by generating mice double knockout for trkB and MAOA.

2 General development of MAOA-trkB double knockout mice

MAOA-trkB double knockout and trkB knockout mice and their various controls were obtained in the F2 progeny from crosses between females heterozygous for both MAOA and trkB and males hemizygous for MAOA and heterozygous for trkB. The size of the litter and the weight of pups of the different genotypes were evaluated prior to perfusion, at P0 and P8.5. At P0, the size of the litter was similar to controls (10 ± 1.3 pups; values are mean ± SEM) with a normal sex ratio. MAOA-trkB double knockout and trkB knockout mice were obtained with an expected frequency and there was no statistical difference in pup's weights (MAOA-trkB, 1.2 g ± 0.2, n=6; trkB, 1.1 g ± 0.1, n=5; MAOA, 1.2 g ± 0.1, n=5; wild type, 1.3 g ± 0.2, n=5). By P3, a reduction of 20% in weight was observed for both MAOA-trkB double knockout and trkB knockout pups. Few pups died around this age. By P8.5, most trkB knockout mice had died whereas MAOA-trkB double knockout mice survived (n=13 litters analysed). Surviving trkB and MAOA-trkB double knockout pups displayed both a reduction in body weight (MAOA-trkB, 2.3 ±

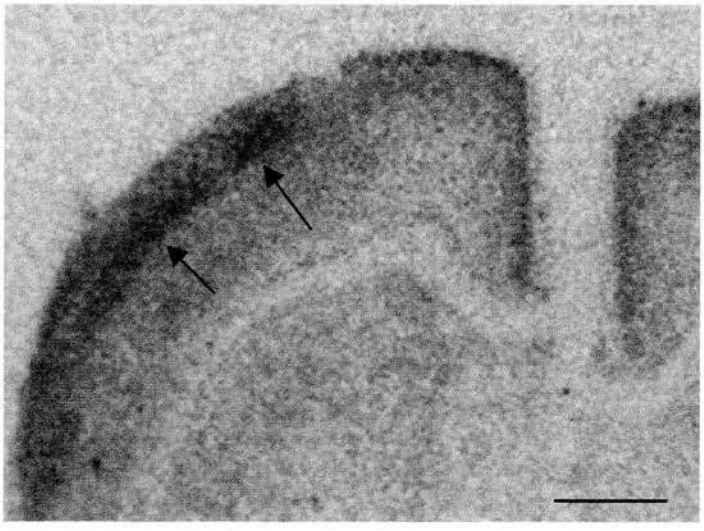

Figure III-1 Coronal section of a P7 pup showing trkB expression at the level of the somatosensory cortex. *White arrow* point to lower layer IV. Scale bar = 600 μm.

0.3 g, n=14; trkB, 2.5 ± 0.2 g, n=4; MAOA; 5.2 ± 0.4 g, n=10; wild type, 5.5 ± 0.6 g, n=10) and in brain weight (trkB-MAOA, 0.26 ± 0.03 g, n=14; trkB, 0.22 ± 0.02 g, n=4; MAOA; 0.31 ± 0.02 g, n=10; wild type, 0.32 ± 0.03 g, n=10).

trkB knockout mice died as a result of feeding problems due probably to the increased cell death observed in the central (facial motor nucleus) and peripheral (trigeminal) nervous system (Klein et al., 1993). Since 5-HT has been shown to have a survival- and growth-promoting role for some neuronal populations, it is conceivable that subsets of cells, which die in trkB knockout mice, are at least temporally rescued by elevated levels of serotonin in the brain. I have investigated this possibility. Evidence for this role will be presented later.

3 Deficiency of trkB in MAOA knockout mice does not rescue the alterations of the barrel field observed in MAOA knockout mice

3.1 Abnormal organisation of granular neurons

In wild type mice, the structural differentiation of layer IV neurons into barrels is visible with Nissl staining as cylindrical shaped aggregates (Fig. III-2*A*). Barrels consist of a dense ring of granular neurons surrounding a hollow (area of less cell density) and are separated by septae. This cytoarchitectonic differentiation occurs normally in trkB knockout mice (Fig. III-2*B*). In contrast, MAOA-trkB double knockout mice display the same cortical alterations as those previously described in MAOA knockout mice (Fig. III-2*C,D*). The granular cells in layer IV do not cluster into barrels but instead form a continuous band with homogeneous density (Cases et al., 1996 and present study).

3.2 Cortical thickness

As measured on coronal sections of P8.5 mice at the level of the posteromedial barrel subfield (PMBSF) and the anterior snout (AS), the thickness of layers II-IV and layers II-VI displayed a significant reduction in trkB and MAOA-trkB double knockout mice (Table III-1). Layers II-IV were the most affected layers and the reduction was more severe in the anterior region of the brain. At this level,

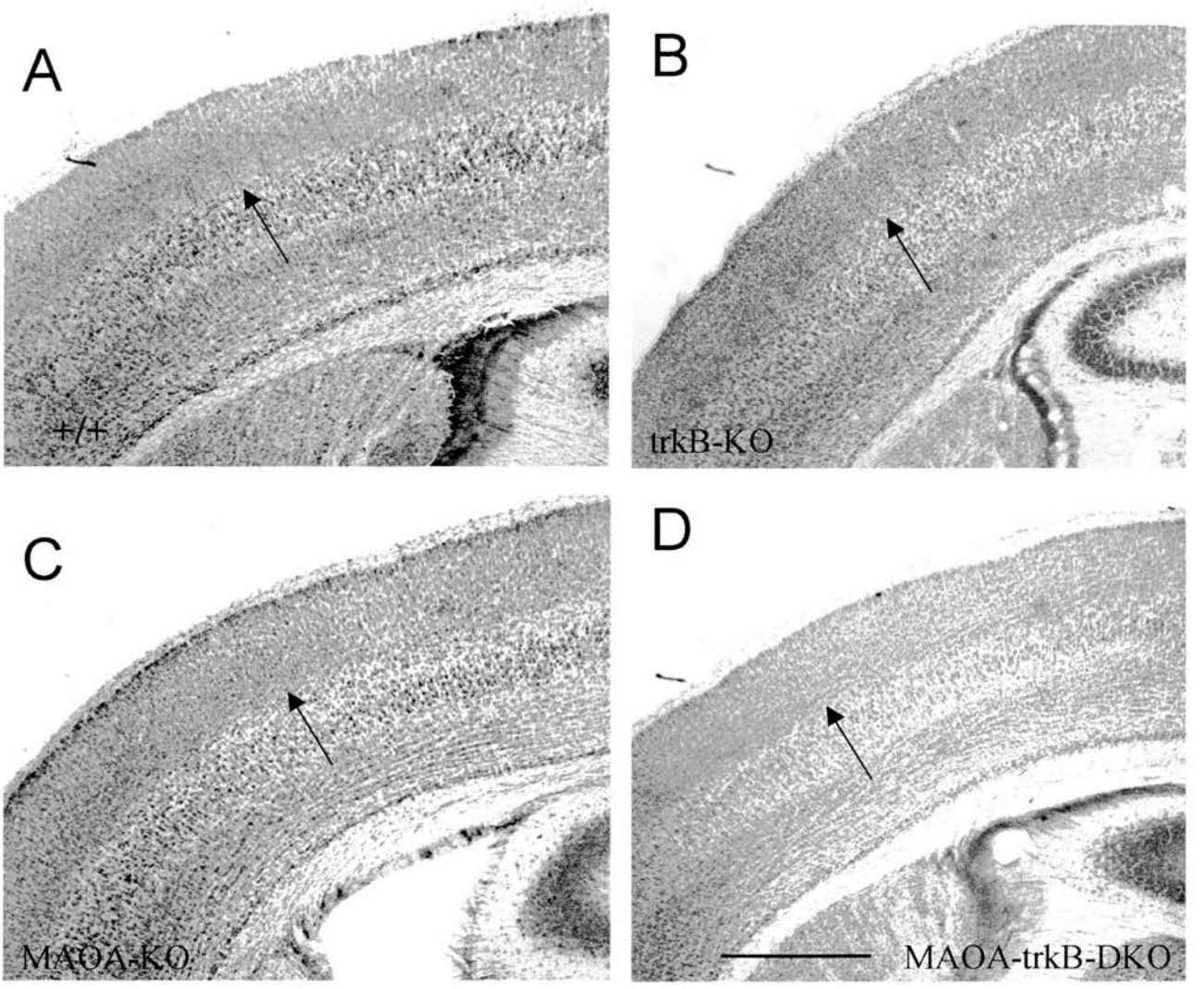

Figure III-2 ***A-D,*** Organisation of granular neurons in layer IV of the somatosensory cortex in P8.5 (A) wild type, (B) trkB knockout, (C) MAOA knockout and (D) MAOA-trkB double knockout mice. ***A-D,*** *Black arrow* points to lower layer IV. Note that both (A) wild type and (B) trkB knockout mice show a discrete clustering of granular neurons in the layer IV of the somatosensory cortex whereas (C) MAOA knockout and (D) MAOA-trkB double knockout mice do not. Note also the slight decrease in the cortical thickness of (B) trkB and (D) MAOA-trkB double knockout mice. Scale bar = 640 μm.

the thickness of Layers II-IV displayed a 25% reduction in trkB knockout mice and a 18% reduction in MAOA-trkB double knockout mice compared to wild types.

3.3 Cytochrome oxidase histochemistry

Cytochrome oxidase (CO) histochemistry allows the visualisation of neurons with heightened metabolic activity in the centre of the cortical barrels. At this level, CO is localised mainly in dendrites of cortical neurons, but also in axon terminals (Wong-Riley et al., 1980). In trkB knockout mice, the intensity of CO activity was similar than that of wild types (Fig. III-3*A,B*). Barrels were observed in the entirety of the barrel field, in the representations corresponding to the main whiskers (PMBSF), tactile hairs located on AS, the lower lip, the hind paw and the fore paw. However, there was a 26%-29% reduction in the area of the barrel field representation. This decreased area was proportional to the reduction of the size of the flattened hemisphere, suggesting that the reduction of the barrel field area was due to hypotrophism. Individual barrels displayed similar shrinkage in proportion to the entire barrel field representation (wild type: B2 length, 280 μm ± 2.3, n=5; B2 width, 190 μm ± 1.8, n=5; B1-B4 length, 840 μm ± 4.6, n=5; A1-A4 width, 730 μm ± 5.0, n=5; trkB knockout: B2 length, 200 μm ± 2.3, n=4; B2 width, 150 μm ± 2, n=4; B1-B4 length, 650 μm ± 4.5, n=4; A1-A4 width, 550 μm ± 5.0, n=4). In MAOA knockout mice, the somatosensory map was profoundly modified as previously reported (Cases et al., 1996 and Fig. III-3*C*). Most of the PMBSF and AS representations were fused, with only separations maintained between the AS, the lower lip and the fore paw, the trunk and the hind paw. In the mixed genetic background used in this study, there was a variation in the intensity of the phenotype. In most cases, some barrels located in the PMBSF and blobs of CO activity corresponding to the fusion of several barrels in PMBSF and in AS were identified. Differences in phenotype displayed by MAOA knockout mice were previously reported depending on the genetic background (Vitalis et al., 1998). In double knockout mice, the intensity of CO activity was greatly reduced in the cortex compared to wild type, trkB or MAOA knockout mice (Fig. III-3). On coronal sections, the lower part of layer IV displayed a stronger CO activity that progressively faded in the upper part of layer IV. No barrels could be identified on these sections (data not shown). On flattened sections, the edges of the barrel field

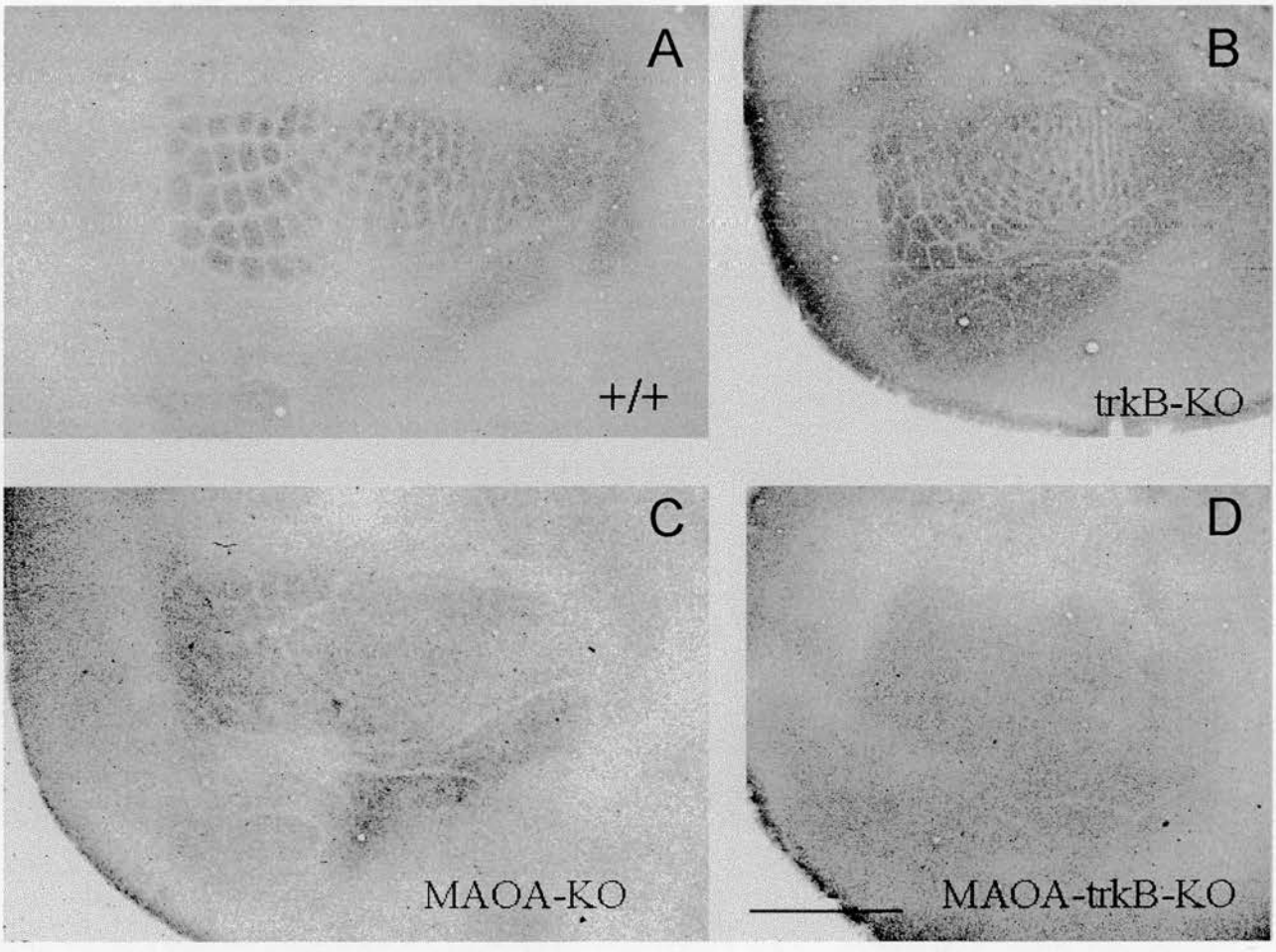

Figure III-3 ***A-D,*** Flattened sections of P8.5 (A) wild type, (B) trkB knockout, (C) MAOA knockout, and (D) MAOA-trkB double knockout mice stained for cytochrome oxidase (CO). ***A, B,*** Note blobs of cytochrome (CO) oxidase activity in the posteromedial barrel subfiled (PMBSF) and the anterior snout representation (AS) in (A) wild type and (B) trkB knockout mice. ***C,*** Section showing a complete blurring of the AS representation and a remainder of barrel-like organisation in the PMBSF of a MAOA knockout pup. ***D,*** Section showing a complete lack of barrel and barrel-like CO blobs in the PMBSF and AS representations of a MAOA-trkB double knockout pup. Note also the decrease in CO activity. Scale bar = 960 μm.

Table III-1 Cortical thickness in wild type, MAOA knockout, trkB knockout and MAOA-trkB double knockout pups aged P8.5. Measures were obtained from Nissl-stained coronal sections at two different stereotaxic levels: –1.94 mm posterior and -3.1 mm lateral, and –0.82 mm anterior and -3.1 mm lateral, to the Bregma. Mean ± SEM.

Genotype	Thickness of cortical layers (μm)			
	II-IV		II-VI	
	-0.82	-1.94	-0.82	-1.94
Wild type (n = 4)	403 ± 16	386 ± 17	1122 ± 30	1071 ± 50
MAOA-KO (n = 4)	395± 20	360 ± 25	1100 ± 40	1091 ± 30
trkB-KO (n = 4)	305 ± 7	305 ± 21	937 ± 15	935 ± 50
MAOA-trkB-DKO (n = 8)	328 ± 15	303 ± 20	1024 ± 27	943 ± 36

representation were difficult to identify precisely in most cases (Fig. III-3*D*). However, separations between the anterior snout, the lower lip and the fore paw, the trunk and the hind paw were visible in the cases presenting a sufficient CO activity. These alterations appeared similar, although more severe than those observed in MAOA knockout mice of the same genetic background.

3.4 Abnormality of 5-HT immunolabelling

Thalamic neurons do not synthesise 5-HT but accumulate exogenous 5-HT through 5-HT high affinity uptake sites located on thalamocortical axons and terminals from E15 to P10 (Lebrand et al., 1996). I have taken advantage of this transient mechanism to specifically visualise and compare thalamocortical axons in trkB knockout and MAOA-trkB double knockout mice. On flattened 5-HT immunolabeled sections, trkB knockout mice have normally individualised barrels in the PMBSF (Fig. III-4*A*,*B*) and AS representations. In MAOA knockout mice, strong 5-HT immunolabeling delineates the three sensory cortices. In the somatosensory cortex, the barrel field representation is blurred although in several cases few barrels and blobs of immunolabeling remained (Fig. III-4*C*), similarly to what was observed with CO activity (see above). In MAOA-trkB double knockout mice, the barrel field representation was altered more than in MAOA knockout mice (Fig. III-4*D*). Interestingly, the 5-HT immunostaining of the presumptive auditory and somatosensory cortices were fused whereas limits between the primary visual cortex and the sensory or the auditory cortices were defined in most cases (Fig. III-4*D*). Moreover, on coronal sections, 5-HT immunolabeling extended abnormally in layers II-III, (Fig. III-5) below the region of CO activity. This suggested that either thalamocortical axons extended abnormally far radially in proportion to the thickness of the cortex in layers II-III and tangentially in layer IV or that 5-HT was abnormally released from thalamocortical axons or serotoninergic varicosities in layers II-III and IV.

3.5 Abnormality of SERT immunolabeling

The serotonin transporter is specifically expressed on thalamocortical arbors from E15 to P10 (Lebrand et al., 1998). At P8.5, in the wild type cortex, a dense

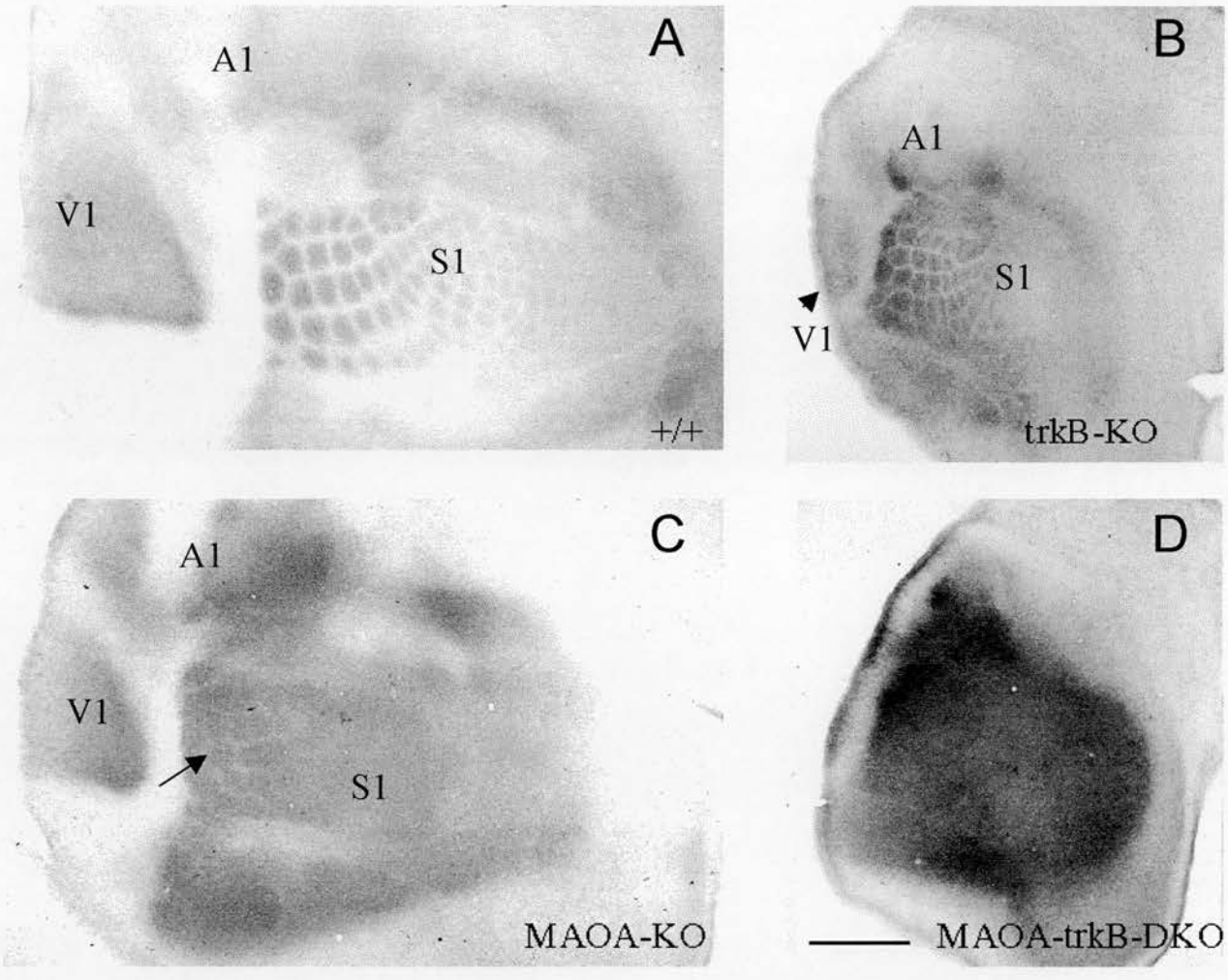

Figure III-4 ***A-D,*** Flattened sections of P8.5 (A) wild type, (B) trkB knockout, (C) MAOA knockout and (D) MAOA-trkB double knockout mice stained for 5-HT. ***A,*** The primary sensory cortices (visual, V1; auditory, A1; somatosensory, S1) are delineated and in S1, barrels are individualised. ***B,*** Sections of trkB knockout mice showing V1 and normally segregated barrels in the PMBSF. AS do not appear on this plane of section. ***C,*** Section of MAOA knockout mouse showing V1, A1, S1. Note the presence of clusters corresponding to fused barrels in PMBSF (*black arrow*). ***D,*** Section of MAOA-trkB double knockout mouse showing a complete fusion of 5-HT immunolabelled regions. ***A-D,*** Note the similar reduction in the size of the flattened cotex in both (B) trkB knockout and (D) MAOA-trkB knockout mice compared to (A) wild type or (C) MAOA knockout mice. Scale bar = 700 μm.

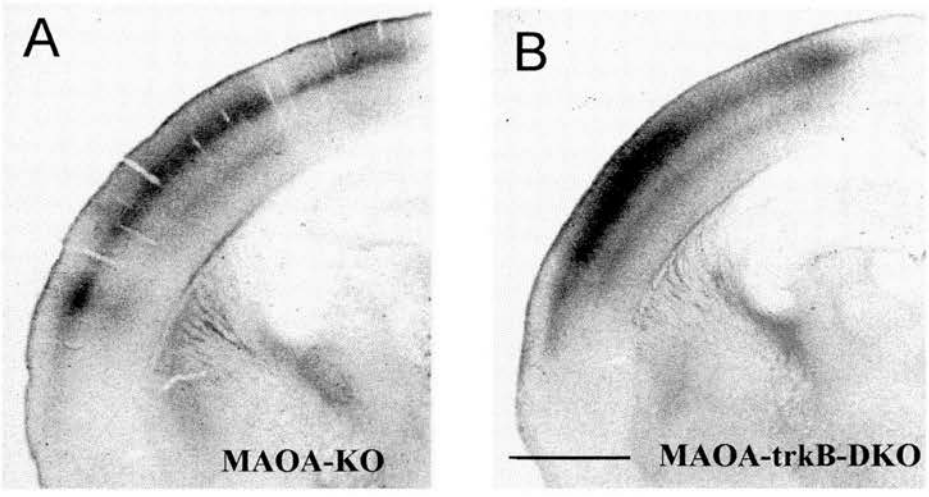

Figure III-5 ***A, B,*** Coronal section of P8.5 (A) MAOA knockout and MAOA-trkB double knockout mice immunolabeled for 5-HT. ***A,*** Coronal section of a MAOA knockout pup showing three distinct areas displaying strong 5-HT-immunolabeling in layer IV: in the premotor cortex (dorsal), the primary somatosensory cortex (medial) and, the primary auditory cortex (ventral). Note that 5-HT-immunolabeling is strongest in layer IV. Note also 5-HT immunolabeling in layer VI which mirrors the 5-HT-immunolabeling in layer IV. ***B,*** Coronal section of a MAOA-trkB double knockout pup showing an homogeneous band of 5-HT immunolabeling in layer IV and an extension of the staining in upper layers II-III. Note also 5-HT immunolabeling in layer VI which appears as a single band of staining. Scale bar = 640 μm.

network of SERT-immunolabeled terminals was visible in the primary somatosensory cortex (S1), the secondary somatosensory areas (S2, PV and PR), the auditory (A1) and the primary visual (V1) areas. In S1, barrels were clearly delineated in PMBSF, AS, FP, HP and LL. In trkB knockout mice, tangential sections of flattened cortex showed that sensory cortices were normally immunolabeled and barrels were clearly defined in S1 similarly to what was observed with 5-HT immunolabeling (see above). Interestingly, on coronal sections SERT-immunolabeled thalamocortical axons showed abnormal extensions in layers II-III (Fig. III-6). In MAOA knockout mice, SERT and 5-HT immunolabeling showed similar alterations (see below): a blurring of the barrel field representation on flattened sections and a decrease in the thickness of SERT immunolabeling on coronal sections (Fig. III-6*C*). In MAOA-trkB double knockout mice, SERT immunolabeling partially mirrored 5-HT immunolabeling (Fig. III-6*D*). On flattened sections, the auditory and somatosensory cortices were fused as observed with 5-HT-immunolabeling showing that thalamocortical axons extended abnormally in the tangential plane. On coronal sections, there was also a relative increase in the thickness of SERT immunolabeling, expanding radially in layers II-III. Together, these results show that trkB knockout mice have subtle alterations of thalamocortical projections. Moreover, thalamocortical alterations are increased in MAOA-trkB double knockout mice compared to MAOA or trkB knockout mice both in the radial and tangential plane indicating that the lack of trkB signalling and excess of 5-HT act synergistically on thalamocortical axonal morphology.

3.6 Organisation of the sensory relays

Previous studies have shown that the lower stations of the somatosensory system, the barrelettes, in the brainstem and the barrelloids, in the ventrobasal thalamic nuclei were normally organised in MAOA knockout mice (Cases et al., 1996). No alterations in their organisation were observed in trkB knockout and MAOA-trkB double knockout mice (Fig. III-7).

4 Do 5-HT excess prevents cell death induced by a lack of trkB ?

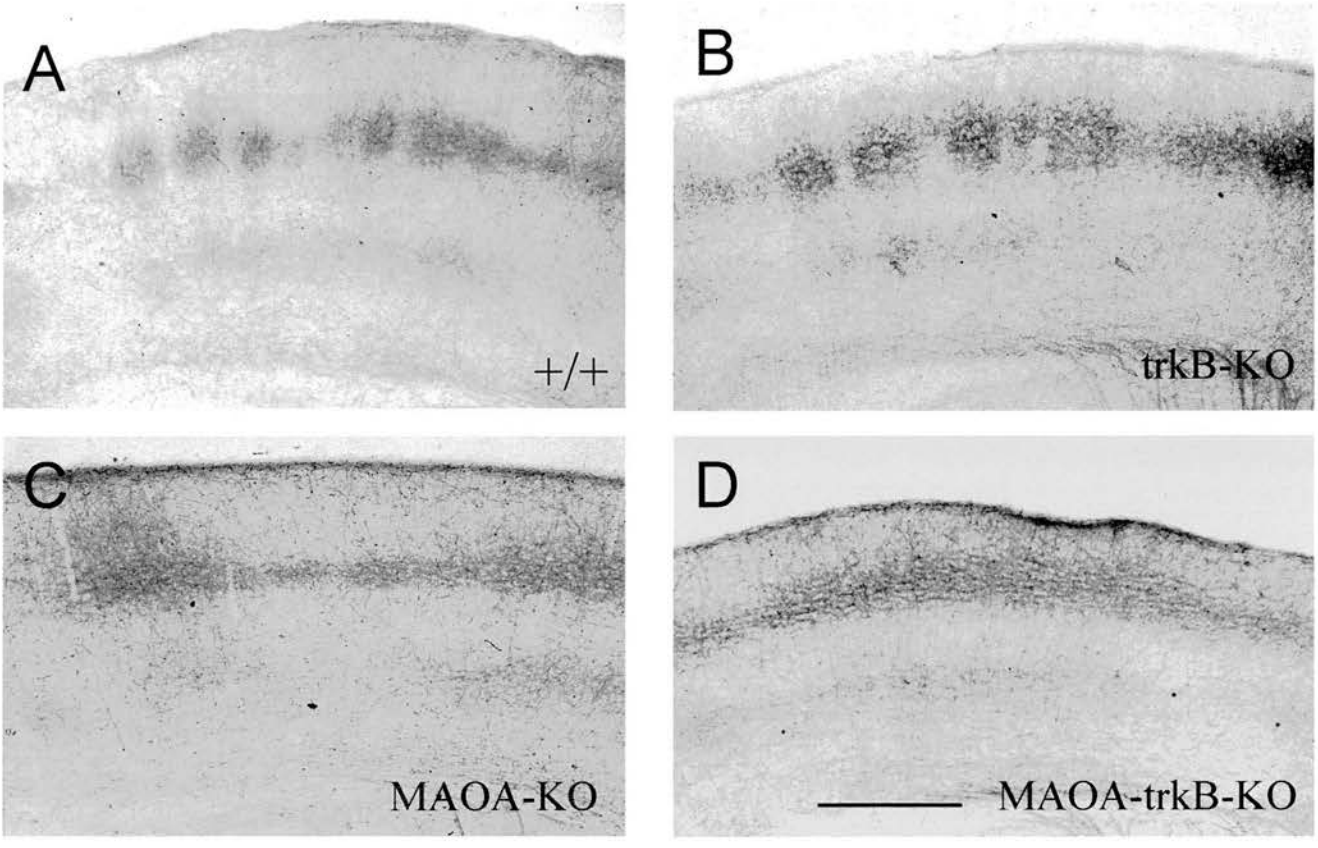

Figure III-6 ***A-C,*** Coronal sections of P8.5 (A) wild type, (B) trkB knockout, (C) MAOA knockout and, (D) MAOA-trkB double knockout pups immunolabeled for SERT. ***A,*** Section of wild type pup showing SERT immunolabeled barrels. ***B,*** SERT immunolabeled barrels appear larger and slightly extended radially in trkB knockout pup. ***C,*** In MAOA knockout mouse, SERT immunolabeling appears as a band of staining which is restricted to layer IV. ***D,*** In MAOA-trkB double knockout pup, SERT immunolabeling defines a homogeneous band that extends radially in layers II-III. Scale bar = 600 μm.

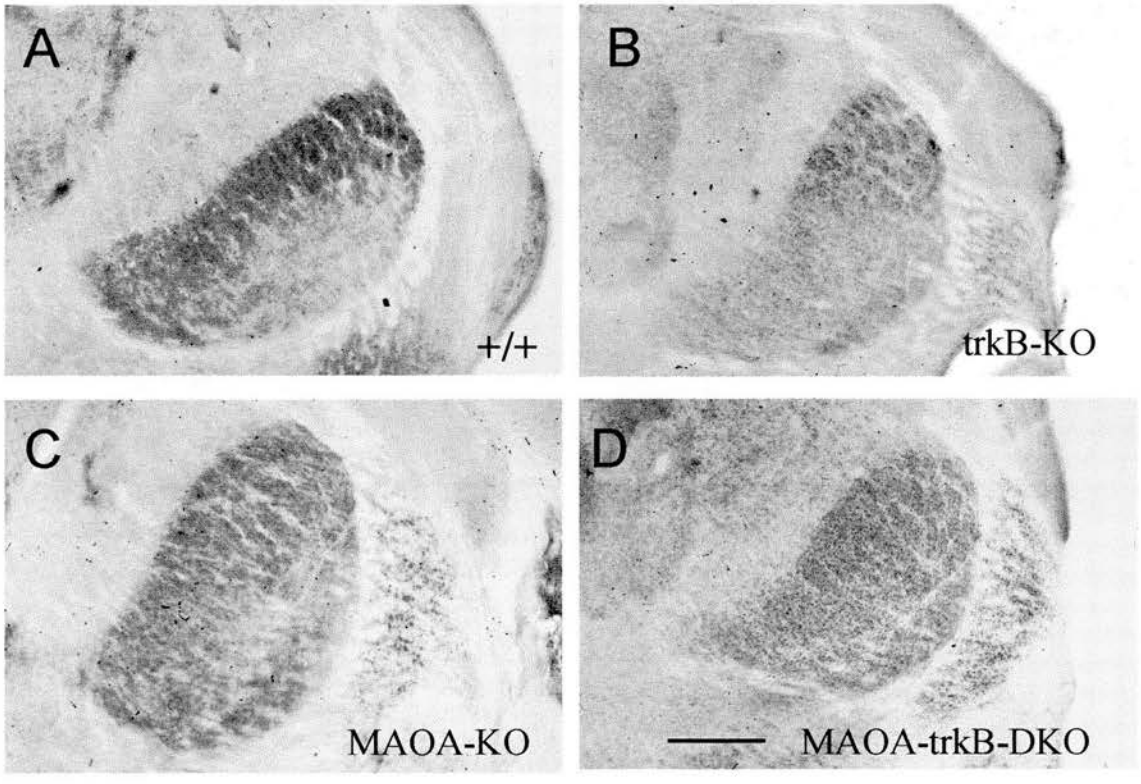

Figure III-7 ***A-C,*** Normal organisation in barreloids in the thalamus, of (A) wild type, (B) trkB knockout, (C) MAOA knockout and, (D) MAOA-trkB double knockout P8.5 pups. Barreloids are shown with cytochrome oxidase activity. Barreloids have similar distribution in the ventrobasal thalamic nucleus of (A) wild type, (B) trkB knockout, (C) MAOA knockout and (D) MAOA-trkB double knockout pups. Scale bar = 320 μm.

trkB knockout mice display severe neuronal deficits in the peripheral nervous system (Klein et al., 1993) and an increased apoptosis in the central nervous system of several brain regions (Alcantara et al., 1997). Serotonin is regarded as a strong candidate molecule having a role in the maturation and survival of several neuronal populations (Lauder, 1993). Since MAOA-trkB double knockout mice displayed an increased survival, I have tested whether the increase in 5-HT levels could prevent or delay the cell death of specific populations affected in trkB knockout mice (Klein et al., 1993; Alcantara et al., 1997).

I have analysed Nissl-stained sections of P8.5 animals and counted the number of pyknotic nuclei in several brain regions (accumbens, caudate putamen, cingulate cortex, somatosensory cortex, retrosplenial cortex, ventrobasal thalamic nucleus, ventral lateral geniculate thalamic nucleus and superior colliculus). Pyknotic nuclei were extremely shrunken, dark, and surrounded by an almost absent cytoplasm, suggesting that they corresponded to apoptotic cells. I found that wild type and MAOA knockout mice displayed a similar number of pyknotic nuclei in most of these brain areas. A significant increase in cell death of both trkB knockout and MAOA-trkB double knockout mice was observed in these areas (Fig III-8). However, a significantly lower number of pyknotic nuclei was counted in the accumbens and the cingulate cortex of MAOA-trkB double knockout mice compared to trkB knockout mice (Fig III-8). The location of pyknotic profiles was similar in trkB knockout and MAOA-trkB double knockout mice. They were randomly distributed in the accumbens, striatum and ventrobasal thalamic nucleus. However, in the superior colliculus they were mainly located in the stratum zonale and superficial grey layer. In the somatosensory cortex, pyknotic profiles were mainly located in layers II-III and layer V. In the cingulate and retrosplenial cortex, they were mainly located in upper layer II and lower layer VI.

Preliminary data obtained from newborn pups show a similar reduction in the size of the facial nucleus and trigeminal ganglion in trkB knockout and MAOA-trkB double knockout mice (20% estimated).

IV Discussion

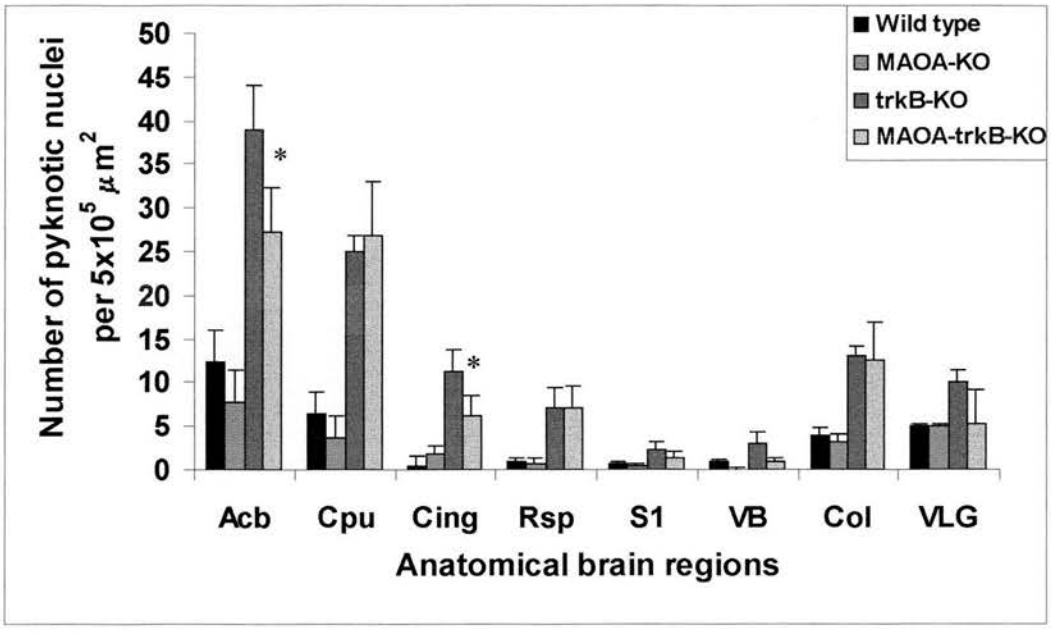

Figure III-8 Number of pyknoctic nuclei in different brain regions of wild type, MAOA knockout, trkB knockout and MAOA-trkB double knockout P8.5 pups. No significant differences were obtained between wild type and MAOA knockout mice. A significant increase in cell death in both trkB knockout and MAOA-trkB double knockout mice was observed in the different regions analysed (except for the VLG) compare to wild type mice ($p< 0.05$, Student's *t* test). A significant lower number of pyknotic nuclei was observed in the accumbens and the cingulate cortex in MAOA-trkB double knockout mice compare to trkB knockout mice (* $p< 0.05$, Student's *t* test).

Acb: accumbens; Cing: cingulate cortex; Cpu: caudate putamen; Col: superior colliculus; Rsp: retrosplenial cortex; S1: primary somatosensory area; VB: ventrobasal thalamic nuleus; VLG: ventral lateral geniculate thalamic nucleus.

1 Analysis of trkB deficiency on somatosensory thalamocortical development

This study reports that trkB is strongly expressed by layer IV neurons from P0 to P7, suggesting a potential role of trkB in the establishment of the somatosensory cortex. The period of the strongest trkB expression corresponds to the critical period of differentiation of immature neurons arranged homogeneously in the cortical plate (prospective layer IV) into mature neurons arranged in barrels. The known effects of trkB in the developing cortex are numerous, including neuronal survival (Alcantara et al., 1997; Xu et al., 2000), dendritic growth (Yacoubian and Lo, 2000) and the control of the expression of LTP (Sermasi et al., 2000). It has been already reported that the deficiency in trkB does not increase cell death (Alcantara et al., 1997) and does not alter the development of granular neurons in barrels (Henderson et al., 1995). This study confirms that the development of the topographic arrangement of granular neurons into barrels is not affected in trkB deficient mice. Indeed, despite an increased expression of trkB during the first postnatal week, no significant increase in cell death is observed in the somatosensory cortex of trkB knockout mice. In a preliminary study, I looked at the dendritic morphology of granular neurons using mGluRV immunoreactivity. mGluRV is transiently located on dendrites of granular neurons, forming clear barrels from P4 to P9 (Munoz et al., 1999). Data indicate that dendritic organisation is grossly altered in trkB knockout mice. To have further details of the dendritic morphology adopted by granular neurons in trkB knockout mice, I would like to use fluorescent marker/gene-transfer method. This method allows the labelling of individual neurons in slices of the cortex in vitro (Lo et al., 1994). Then using a Neurolucida system, the dendritic morphology can be reconstructed and compared to normal or mutant cases.

Moreover, as judged by SERT- and 5-HT-IR, thalamocortical axons are subtly altered in trkB mutant mice. Indeed, somatosensory thalamocortical axons are arranged in barrels but display a surprisingly vertical expansion in the superficial layer II/III rather than a tangential expansion in layer IV. Since trkB is only very slightly expressed in somatosensory thalamic neurons, this suggests that the alteration of thalamocortical axons is induced by the lack of trkB in cortical cells.

2 Role of an excess 5-HT and trkB signalling deficiency

MAOA knockout mice display increased 5-HT levels during the early postnatal period (Cases et al., 1995) and this excess alters permanently the clustering in barrels of both granular neurons and thalamocortical axons (Cases et al., 1996; Vitalis et al., 1998). I have tested the hypothesis that these alterations could be related to an alteration in trkB signalling. In first place, I have determined the levels of trkB mRNAs in the somatosensory thalamocortical system. No changes of mRNA expression was observed in the cortex or the thalamus of MAOA knockout mice. Second, since it has been reported that BDNF and trkB signalling play crucial roles in the regulation of the serotoninergic phenotype both in vitro (Galter and Unsicker, 2000a,b) and in vivo (Lyons et al., 1999; Mamounas et al., 2000), I have verified that trkB deficiency did not induce low number of serotoninergic neurons or low 5-HT levels in trkB knockout mice. Interestingly, the lack of trkB does not induce dramatic changes in the number of serotoninergic neurons or 5-HT levels, suggesting that in vivo trkB signalling is not crucial at least for the early development and differentiation of serotoninergic neurons. The number of serotoninergic neurons in MAOA-trkB double knockout mice is normal but 5-HT levels are similar to those displayed by MAOA knockout mice (complete study in progress). Surprisingly, the consequences of excess 5-HT in the somatosensory thalamocortical system of MAOA-trkB double knockout mice are not similar to those displayed by MAOA knockout or trkB knockout mice alone. Whereas the abnormal homogenous band of granular neurons in layer IV is present in MAOA-trkB double knockout, as in MAOA knockout mice, thalamocortical axons display a much more widely tangential and vertical expansion. Indeed, sensory thalamocortical axons of auditory and somatosensory cortices overlap and have abnormally invaded tangentially the premotor and limbic areas. Radially, sensory thalamocortical axons have invaded the superficial layers II/III. Thus, the lack of trkB signalling worsens the MAOA phenotype at least at the level of thalamocortical projections in the cortex. The mechanisms underlying this increased alteration are unknown and may be related to a lack of cortical neurons to release a trkB-induced factor facilitating the clustering of thalamocortical axons. This trkB-induced factor could be also per se insensitive to 5-HT levels. Then, deficiency in trkB signalling alone induces subtle changes in thalamocortical projections and excess of 5-HT alone induces only a limited tangential expansion. However, when these two alterations are together, they can act synergistically to produce a totally aberrant pattern, as observed in MAOA-trkB

double knockout mice. I would like also to look at the dendritic morphology adopted by granular neurons in trkB knockout, MAOA knockout, MAOA-trkB double knockout and wild type mice. To do that, I will use the same methods described above (mGluRV immunoreactivity and fluorescent marker/gene-transfer).

3 Excess 5-HT has potential recovery effects in cell death of specific populations

The analysis of mice lacking TrkB has illustrated the critical role of TrkB signalling in the generation and/or survival of a variety of sensory neurons in the peripheral nervous system (Klein et al., 1993; Minichiello et al., 1995; Schimmang et al., 1995, Pinon et al., 1996). More recently, Alcantara et al. (1997) have demonstrated that TrkB signalling plays a similar role in the central nervous system. Their study showed that trkB knockout mice undergo a period of increased cell death during early postnatal life in various cell populations. Interestingly, the authors correlated the onset of cell death with the peak of expression of the catalytic trkB tyrosine kinase receptor observed during the second postnatal week (Dugich-Djordjevic et al., 1993; Knusel et al., 1994). My study confirmed this finding and extended the analysis to other brain regions such as the accumbens, the cortex or the collicullus. Interestingly, MAOA-trkB double knockout mice display a substantial recovery from cell death in specific brain regions such as the accumbens or the cingulate cortex. This suggests that increased levels of 5-HT can prevent the increased cell death observed in specific brain regions of mice lacking TrkB. Indeed, serotonin is regarded as a strong candidate for a molecule having a role in the maturation and survival of several neuronal populations (Lauder, 1993). For instance, serotonin promotes the differentiation and the survival of glutamatergic neurons in organotypic slice cultures of the developing cerebral cortex (Dooley et al., 1997; Lavdas et al., 1997). 5-HT acts upon specific high affinity receptors and it has been shown that some of them can support cell survival (Dooley et al., 1997; Galter and Unsicker, 2000). Then, one can think that in some cases 5-HT could act in synergy with trkB signalling to ensure a correct development of specific structures.

CHAPTER FOUR :
DEVELOPMENTAL EXPRESSION OF MONOAMINE OXIDASE A AND MONOAMINE OXIDASE B

CHAPTER FOUR:
DEVELOPMENTAL EXPRESSION OF MONOAMINE OXIDASE A AND MONOAMINE OXIDASE B

This study was performed in collaboration with Drs. P. Gaspar and O. Cases (INSERM U106, Paris, France) and with Dr. J. Shih (University of Southern California, California). These collaborators have cloned the MAOA and MAOB probes and have performed additional in situ hybridizations, some of which are shown in this report (Drs. P. Gaspar and O. Cases). They have also generated and characterised in vitro the specificity of the MAOB antibody (Dr. J. Shih) used in this study.

I Abstract

Monoamine oxidase A (MAOA) and B (MAOB) are key players in the inactivation pathway of monoaminergic transmitters and of xenobiotic amines. Although there is a wide literature about MAOA and MAOB location in adults, nothing is known concerning the localisation of both enzymes during development. This present study combines in situ hybridization, histochemistry and immunocytochemistry to locate precisely MAOA and MAOB in the developing nervous system.

I found that MAOA expression is tightly linked to the noradrenergic phenotype. MAOA is expressed early (from embryonic day 12) in all noradrenergic and adrenergic neurons in the hindbrain and peripheral nervous system, as well as in neurons that transiently express the noradrenaline synthesising enzyme, dopamine-β-hydroxylase: the autonomic motor nuclei of the hindbrain, and the sensory ganglia of cranial nerves. By E12, MAOA is also expressed in the serotoninergic neurons of the raphe, soon after they start producing 5-HT. Then, during early postnatal life, serotoninergic neurons shift progressively from MAOA to MAOB expression. I also found that most dopaminergic groups, as well as neurons that display a transient tyrosine hydroxylase phenotype, express MAOA. Besides its link with histaminergic neurons, this study points out that MAOB is expressed in most forebrain cholinergic neurons, in the septum, the striatum, the ventral pallidum, and the tegmental nuclei.

MAOB-expressing neurons were also detected in structures that did not contain monoaminergic or cholinergic neurons such the accumbens or the thalamus. MAOB expression was also associated with non-neuronal cells such as the ventricular ependymal cells and astrocytes. In addition, I found two novel localizations of MAOB: i) in the olfactory placode and olfactory epithelium where MAOB is expressed from E10 to adulthood, and ii) in astrocytes at the spinal and cranial nerve interface between the CNS and PNS, where the period of MAOB expression coincides with the period of crossing and arborization of nerves into the CNS.

II Introduction

Monoamine oxidase A (MAOA) and B (MAOB) are membrane-bound mitochondrial flavoproteins that oxidatively deaminate a broad range of biogenic amines, including monoaminergic neurotransmitters in neurons, glial cells, and other cell types (Weyler et al., 1990; Shih, 1997). In CNS, MAOs are thought to be involved in maintaining low cytosolic and extracellular levels of monoamines, and in preventing various natural substrates from accumulating in monoaminergic neurons to act as false neurotransmitters. In rodent brain, MAOA mainly metabolises monoaminergic neurotransmitters such as serotonin (5-HT), dopamine (DA), noradrenaline (NA) or adrenaline (A) whereas MAOB mainly metabolises trace amines such as tyramine or β-phenylethylamine (Strolin-Benedetti and Dostert, 1992). These functions could be particularly important during development since the lack of MAOA causes enhanced levels of 5-HT and NA during embryonic and early postnatal life (Cases et al., 1995; Lajard et al., 1998) and an abnormal development of the somatosensory (Cases et al., 1996; Vitalis et al., 1998) and visual systems (Upton et al., 1999).

MAOA and MAOB have been localised in rodent, cat, primate, and human adult brain by a variety of techniques, including immunohistochemistry (Levitt et al., 1982; Westlund et al., 1985; 1988), histochemistry (Kitahama et al., 1994), enzyme autoradiography (Saura et al., 1992; 1996), and in situ hybridisation (Luque et al., 1995; Jahng et al., 1997). Generally, MAOA is most abundant in (nor)adrenergic neurons, moderate in serotoninergic neurons and very low in histaminergic neurons (Luque et al., 1995; Jahng et al., 1997) whereas MAOB is most abundant in histaminergic and serotoninergic neurons (Levitt et al., 1982; Saura et al., 1992;

Luque et al., 1995; Jahng et al., 1997). Surprisingly, MAOs are also present in non-aminergic cell populations. Indeed, MAOA is abundant in neurons of the cerebral cortices, the hippocampal formation and the cerebellar granule cell layer whereas MAOB is abundant in non-neuronal cells such as astrocytes, Bergmann glial cells or circumventricular organs (Luque et al., 1995). So far no developmental studies have been done and indirect evidence derived from studies in MAOA knockout mice suggests that MAOA could be expressed in other locations during development. Indeed, during embryonic and early postnatal life, 5-HT immunolabeling is considerably increased in MAOA knockout mice, compared to wild type mice, not only in monoaminergic neurons, but also in a number of structures that transiently express the serotonin transporter (SERT) (Cases et al., 1998, Lebrand et al., 1998). This indicates that, in normal conditions, 5-HT is internalized in non-aminergic neurons where it could be rapidly degraded.

In this study, in situ hydridization, histochemistry and immunocytochemistry were combined to study the developmental distribution of MAOA and MAOB in CNS. MAOA expression started by E12 and increased dramatically in embryonic life. By birth, MAOA expression decreased sharply and the adult pattern of expression was reached by P10. MAOB expression appeared later, by E14 and increased progressively to reach the adult pattern of expression by P15. I found two striking characteristics of MAOA distribution in embryonic and early postnatal life. The first is its association with a (nor)adrenergic phenotype: MAOA is expressed in all neurons that permanently or transiently express dopamine-β-hydroxylase, the biosynthetic enzyme of NA and A. The second is its association with a serotoninergic phenotype: MAOA is strongly expressed in all serotoninergic neurons. From birth, MAOA expression progressively decreased to reach a minimum by P10. In the meantime, MAOB expression increased progressively in serotoninergic neurons to reach a maximum by P10. This study corroborates mostly the documented locations of MAOA and MAOB in adults, i.e.: in dopaminergic neurons and in the hippocampus for MAOA and in histaminergic neurons and in astrocytes for MAOB. In addition, I have shown new and interesting locations of MAOA and MAOB, such as astrocytes at the interface between the CNS and the PNS from E12 to P4, during the entire period when peripheral nerves enter into the CNS, or in the olfactory epithelium thoughout life.

III Material and methods

1 Animals

Experiments were carried out on E11, E12, E14, E15, E16, E17, and E18 embryos and P0, P4, P7, P10, P13, P21 and 5-months-old C3H/He and MAOA knockouts (Cases et al., 1995). The day of the vaginal plug was counted as E1, and the day of birth as P0.

2 In situ hybridization

Partial murine cDNAs encoding from exon 1 to exon 8 of MAOA and MAOB were amplified by RT-PCR, cloned into the pCRII-TOPO vector (Invitrogen, Carlsbad, USA) and verified by sequencing. The plasmid containing MAOA was linearised with HindIII (Amersham, IL) for antisense RNA synthesis by T7 RNA polymerase (Boehringer-Mannheim) and the plasmid containing MAOB was linearised with EcoRV (Amersham) for antisense RNA synthesis by SP6 RNA polymerase (Boehringer-Mannheim). For whole mount in situ hybridization (ISH), antisense digoxigenin (DIG)-labelled riboprobes for MAOA and MAOB were produced using a DIG-RNA labelling kit (Boehringer-Mannheim), following the manufacturer's instructions. For radioactive ISH, antisense riboprobes were labelled with ^{35}S-UTP (Amersham). Mice were sacrified by deep anesthesia and brains were immediately removed and frozen in isopentane. Coronal and sagittal sections (20 µm) were cut on a cryostat, collected onto SuperFrost slides and stored at -80°C until ISH. Tissue sections were post-fixed for 15 minutes in 4% paraformaldehyde, washed in PBS, acetylated, washed, dehydrated in ascending alcohols and air-dried. Sections were covered with hybridation buffer (50% formamide, 10% dextran sulfate, 4 X SSC, 1 X Denhardt's solution, 10 mM dithiotreitol, 0.5 mg/ml sonicated denatured herring sperm DNA and 1.5 ng/ml RNA total) containing riboprobes (500,000 cpm/slide) and then incubated overnight in a humid chamber at 48°C. Washes were then performed as previously described (Fontaine and Changeux, 1989). Sections were dehydrated, air-dried and exposed onto Kodak-MR films (Eastman-Kodak, Rochester, NY) at room temperature for 1-4 days. For histological analyses, slides were dipped in NTB-2 radioautographic emulsion (Eastman-Kodak)

and exposed at 4°C for up to 1 week. Emulsion-dipped slides were counterstained with Nissl.

Levels of MAOA mRNA expression were estimated on emulsion-dipped slides. High, moderate and weak levels of expression were distinguished as exemplified: i) the locus coeruleus displayed strong level of MAOA mRNA expression (Fig. IV-1), ii) the substantia nigra displayed moderate level of MAOA mRNA expression at P10 (Fig. IV-4*C*) and iii) the facial and trigeminal nuclei displayed low level of MAOA mRNA expression at P0 (Fig. IV-6*C*).

3 Immunocytochemistry

To identify monoaminergic neurons, I used antibodies to 5-HT (1:50; rat monoclonal; Harlan), tyrosine hydroxylase (1:5000; rabbit polyclonal; gift from A. Vigny), aromatic amino-acid decarboxylase (1:1000; rabbit polyclonal; Protos Biotech, New-York, NJ), and dopamine-β-hydroxylase (1:1000; rabbit polyclonal; Protos Biotech, New-York, NJ). Anaesthetised animals were transcardially perfused with saline followed by 4% paraformaldehyde in PB. Whole embryos or brains were post-fixed 2-5 days in the same fixative and cryoprotected in 30% sucrose in PB. Serial coronal sections (50 μm) were cut on a freezing microtome and immediately processed for immunocytochemistry as previously described (Cases et al., 1996). In brief, sections were washed in PB, incubated 1 hr in PBS+ (0.1M PBS with 0.2% gelatine and 0.25% Triton X-100). Sections were incubated sequentially with the primary antibodies (24 hrs at 4°C), PBS+ (30 min), secondary antibodies (biotinylated goat anti-rat; biotinylated swine anti-rabbit; 1:200; DAKO, Denmark) (2 hrs at room temperature), PBS+, streptavidin-biotin-peroxidase complex (1:200; Amersham) (2 hrs at room temperature) and finally reacted with a solution containing 0.02% diaminobenzidine, 0.6% nickel ammonium sulfate (Carlo Erba), and 0.003% H_2O_2 in 0.05M Tris buffer, pH 7.6. All sections were mounted on TESPA-coated slides, air-dried overnight, dehydrated, and coverslipped in DePeX.

4 Histochemistry of MAOA and MAOB activities

E12 and E13 embryos were fixed for 2 hours by immersion in an ice-cold mixture of 1.5% paraformaldehyde and 1.5% glutaraldehyde in PB. Older embryos

were perfused transcardially with 0.9% saline followed by the same ice-cold fixative and 1h post-fixation. Pups and adults were perfused with a mixture of 1% paraformaldehyde and 1% glutaraldehyde. Brains were removed and cryoprotected overnight in 30% sucrose in PB at 4°C. Serial sections were cut (50-60 μm) on a freezing microtome, collected in cold PB, and processed immediately. MAO activities were revealed according to Dunning et al. (1997). Briefly, sections were rinsed three times for 1 min each in PB, preincubated for 15 min in 50 mM Tris buffer pH 7.6, incubated for 4 hr to 24 hr at 22-25°C in a solution containing 0.07% tyramine-HCl (Sigma), 0.005% diaminobenzidine-HCl, 0.05% horseradish peroxidase Type II (Sigma), 0.065% sodium azide and 0.6% nickel sulfamate (Aldrich, Germany) in 50 mM Tris buffer, pH 7.6. During the entire procedure, sections were kept in the dark and gently agitated. Since the specific inhibitor of MAOB, L-deprenyl (Research Biochemicals, Natick, MA), can partially inhibit MAOA activity, I used MAOA knock-outs to determine the minimal concentration of L-deprenyl necessary to inhibit completely the remaining MAOB activity.

5 Characterisation of a novel polyclonal MAOB antibody and immunocytochemistry for MAOB

To determine the location of MAOB in several populations, I used a specific polyclonal antibody raised against the full length of the mouse MAOB protein (clone 110-1). This antibody was obtained in collaboration with Dr. J. Shih (University of Southern California, California) and Drs. P. Gaspar and O. Cases (INSERM U106, Paris). The specificity of the antibody was confirmed on western blot by Dr. J. Shih and collaborators. In addition the staining obtained on sections from wild type mice and MAOA knockout mice was compared. I found no difference in the location of the protein in wild type and MAOA knockout mice showing that in vivo the antibody was likely to recognise only type B monoamine oxidase. However, MAOA knockout mice may not be perfect controls since a truncated protein corresponding to exon 1 of the MAOA gene could still be generated in these mice (Cases et al., 1995; I. Seif, personal communication). The rabbit polyclonal MAOB antibody (1:2000) was used as described in "3 Immunocytochemistry". Double labeling for MAOB and 5HT (rat monoclonal anti-5HT, 1:30, Harlan-Sera-Lab) or MAOB and GFAP (mouse monoclonal anti-GFAP, 1:200, Sigma) were performed on free floating sections.

Sections were incubated overnight at room temperature with two primary antibodies diluted in PBS+. Then, sections were washed in PB and incubated for 1 hr with two secondary antibodies (TRITC anti-mouse antibody, 1:200, molecular probe or Cy3 anti-rat antibody, 1:200, Sigma and FITC anti-rabbit antibody, 1:200; Molecular Probe).

IV Results

The location of MAOA and MAOB mRNA expressions was determined during embryonic and postnatal development. The nomenclature is taken from Paxinos et al. (1994) for embryonic stages and from Franklin and Paxinos (1994) for postnatal ages.

1 MAOA and MAOB mRNA expressions in classical monoaminergic neurons

The neuronal populations described in the following paragraph were reported to express permanently the monoamine synthesizing enzymes, tyrosine hydroxylase (TH), dopamine-β-hydroxylase (DBH), tryptophan hydroxylase (TpOH), or histidine decarboxylase (HDC).

1.1 Noradrenergic and Adrenergic cell groups

By E12 a strong MAOA mRNA expression was already detected in most of the noradrenergic and adrenergic cell groups: A4, A5, the locus coeruleus (A6), the locus subcoeruleus (A6s), C3 and A1/C1 and A2/C2 complexes (A1 and C1, and A2 and C2 are located in similar anatomical regions; this does not allow there complete distinction; Jacobowitz and Abbott, 1998) (Table IV-1, Fig. IV-1). Then, MAOA mRNA expression remained very high during all embryonic and postnatal life (Fig. IV-1). In the PNS, by E12, all noradrenergic neurons of the sympathetic ganglia already displayed a strong MAOA mRNA expression. By far, MAOA mRNA expression was the highest in noradrenergic neurons of the CNS and PNS.

MAOB mRNA was not detected in noradrenergic and adrenergic neurons in normal mice at any age studied.

Table IV-1 Locations of MAOA mRNA expression in monoaminergic neurons during development

Location	Labeling intensity of neurons at pre- and postnatal ages								
	E12 (n = 3)	E14 (n = 3)	E16 (n = 3)	E18 (n = 3)	P0 (n = 3)	P4 (n = 3)	P7 (n = 4)	P10 (n = 4)	Adults (n = 2)
Serotoninergic groups									
Raphe pallidus, obscurus, magnus (B1-B3)	+++	+++	+++	+++	++	++	+	-	-
Raphe dorsal, median, pontis (B4-B9)	+++	+++	+++	+++	++	++	+	+	+
Noradrenergic groups									
CNS									
A6 Locus Coeruleus, A6s Subcoeruleus	+++	+++	+++	+++	+++	+++	+++	+++	+++
A1, A2, A4, A5	+++	+++	+++	+++	+++	+++	+++	+++	+++
PNS									
Sympathetic ganglia	+++	+++	+++	+++	+++	+++	+++	+++	+++
Adrenergic groups									
C1, C2, C3	++	+++	+++	+++	+++	+++	+++	+++	+++
Dopaminergic groups									
A16 Olfactory bulb	-	+	+++	+++	+++	+++	+++	+++	+++
A15v Supraoptic n.	-	-	-	-	-	-	**nd**	+	+
A14 Dorsomedial hyp. n.	-	-	-	+	+	**nd**	**nd**	-	-
A14 Paraventricular n.	-	-	+	+	+	+	**nd**	-	-
A13 Zona incerta	-	-	+	+	++	++	++	++	++
A10 Ventral tegmental area	-	-	-	-	+	++	++	++	++
A9 Substantia nigra	-	-	-	-	+	++	++	++	++
Histaminergic group	-	-	-	-	-	+	+	+	+

Intensity of the labeling at prenatal and postnatal ages according to locations in the brain: - none; + weak; ++ moderate ; +++ high; nd not defined.

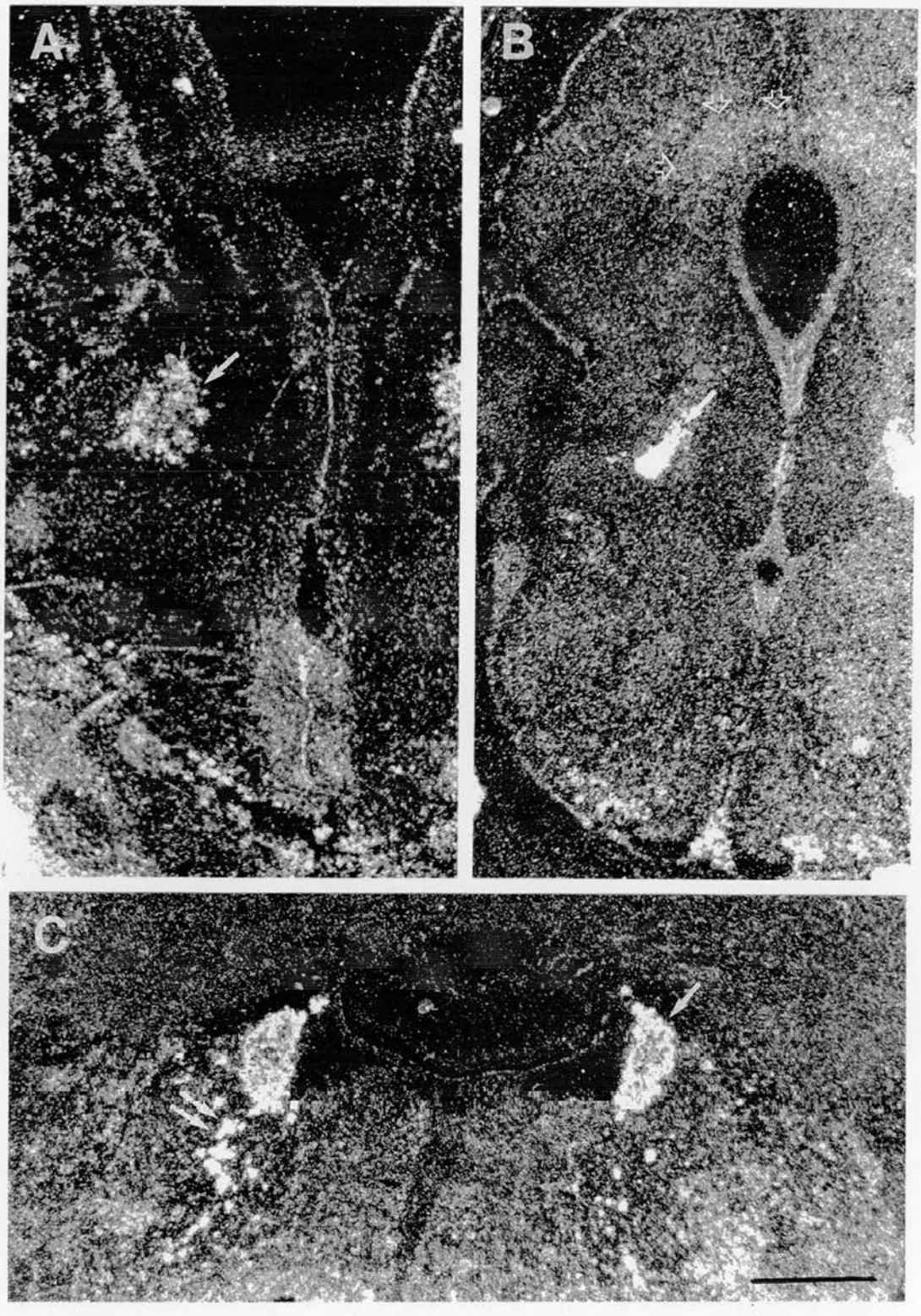

Figure IV-1 Coronal sections of (A) E12 embryo and (B) P0 and (C) P15 postnatal pups showing MAOA expression in noradrenergic neurons of the locus coeruleus. ***A-C,*** The *white arrow* points to the locus coeruleus. ***A,*** Note the strong intensity of the signal as early as E12. ***B,*** *Open arrows* point to the periaqueductal gray that display a low level of MAOA expression. ***C,*** *Double white arrows* point to the locus subcoeruleus. Scale bar: A, 2mm; B,C, 1mm.

1.2 Serotoninergic cell groups

Strong MAOA mRNA expression was first detected by E12 near the midline where serotoninergic neurons are normally located (Fig. IV-2 and Table IV-1). By E14, all serotoninergic neurons displayed strong MAOA mRNA expression (Fig. IV-2, Fig. IV-5*B* and Table IV-1). This expression remained high until P0-P4, when MAOA mRNA expression decreased to reach a minimum from P15 (Fig. IV-2 and Table IV-1). The decrease of MAOA mRNA expression was heterogenous in 5-HT neurons since some neurons in the dorsal raphe retained MAOA mRNA expression whereas 5-HT neurons in caudal raphe nuclei (B1-B3) stopped expressing MAOA (Table IV-1).

Low MAOB mRNA expression was first detected in caudal and rostral serotoninergic neurons by E12 (Fig. IV-10*A* and Table IV-2). Then MAOB mRNA expression increased progressively to reach a maximum by P10. MAOB mRNA expression remained strong during the entire postnatal period (Fig. IV-3*A,C* and Table IV-2).

1.3 Dopaminergic cell groups

The isthmic neuroepithelium, a region where midbrain dopaminergic neurons of the substantia nigra-ventral tegmental (SN-VTA) complex are generated, displayed moderate MAOA mRNA expression from E12 (data not shown). By P0, low levels of MAOA mRNA expression were seen at the level of the SN(A9)-VTA(A10) complex (Fig IV-3A,B and Table IV-1). Then, MAOA mRNA expression increased progressively to reach a maximum by P4 (Table IV-1). This expression remained stable during all postnatal life in SN-VTA neurons (Fig. IV-4C and Table IV-1). Low to moderate MAOA mRNA expression was also detected in several other dopaminergic cell groups: in the ventral thalamus at the level of the zona incerta (A13) from E16, in the hypothalamus at the level of the paraventricular nucleus from E16 and the dorsal medial hypothalamic nuclei (A14) from E18, and in the telencephalon at the level of the supraoptic nucleus (A15v) from P10 (Table IV-1). In the olfactory bulb, A16 dopaminergic external tufted cells displayed a strong MAOA mRNA expression from E16 (Fig. IV-4D,E) and A16 dopaminergic periglomerular interneurons from P0 (Table IV-1).

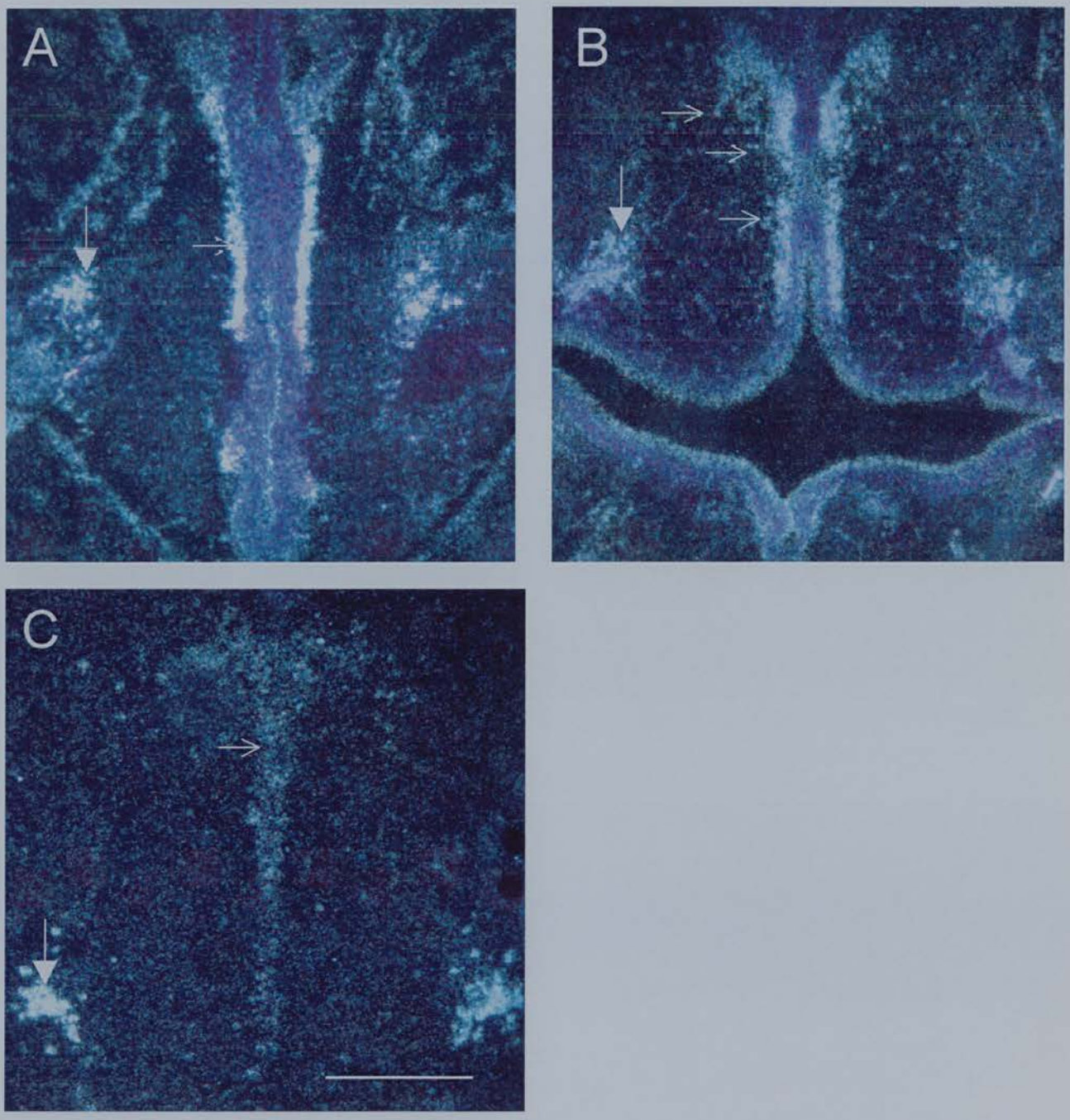

Figure IV-2 Coronal sections of (A) E12 and (B) E14 embryos and of (C) P0 pups showing MAOA expression in serotoninergic neurons of the B4-B9 complex. ***A-C,*** *Open arrows* point to serotoninergic neurons and *filled arrows* point to noradrenergic neurons of the locus coeruleus. ***A,*** Note that MAOA expression is already intense and mainly located in postmitotic neurons, in close proximity with the proliferating region of the B4-B9 complex (*white open arrow*). ***B,*** *White open arrows* point to serotoninergic neurons, that have migrated away from their region of genesis. ***C,*** Note the general decrease in MAOA expression in serotoninergic neurons in comparison to (A) and (B). Note also the relative decrease of MAOA expression in serotoninergic neurons versus noradrenergic neurons. Scale bar = 2mm.

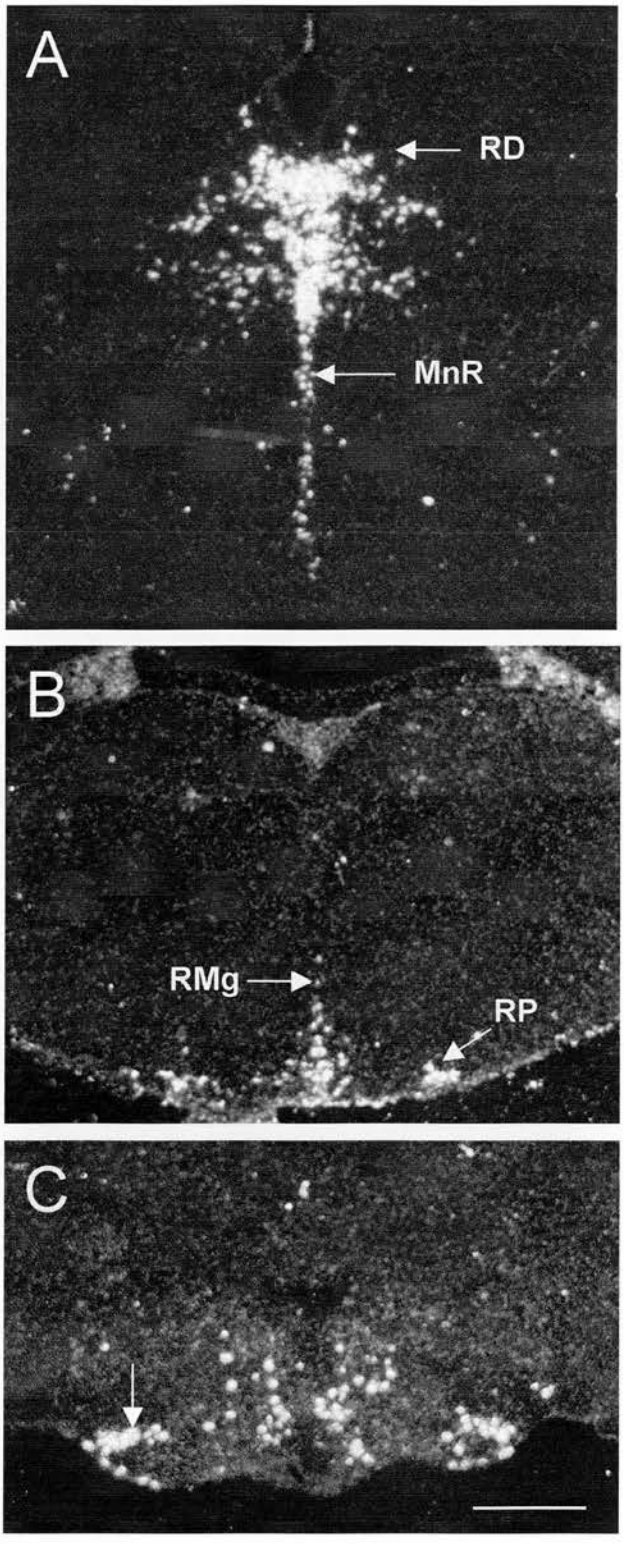

Figure IV-3 ***A-C,*** Coronal sections of P21 pups showing MAOB mRNA expression (A,B) in serotoninergic neurons of (A) the dorsal (RD) and median (MnR) raphe nuclei and (B) the magnus (RMg) and pallidus (RP) raphe nuclei and (C) in histaminergic neurons (*white arrow*) in the tubero-mammilar region. Scale bar: A,B, 2mm; C, 1mm.

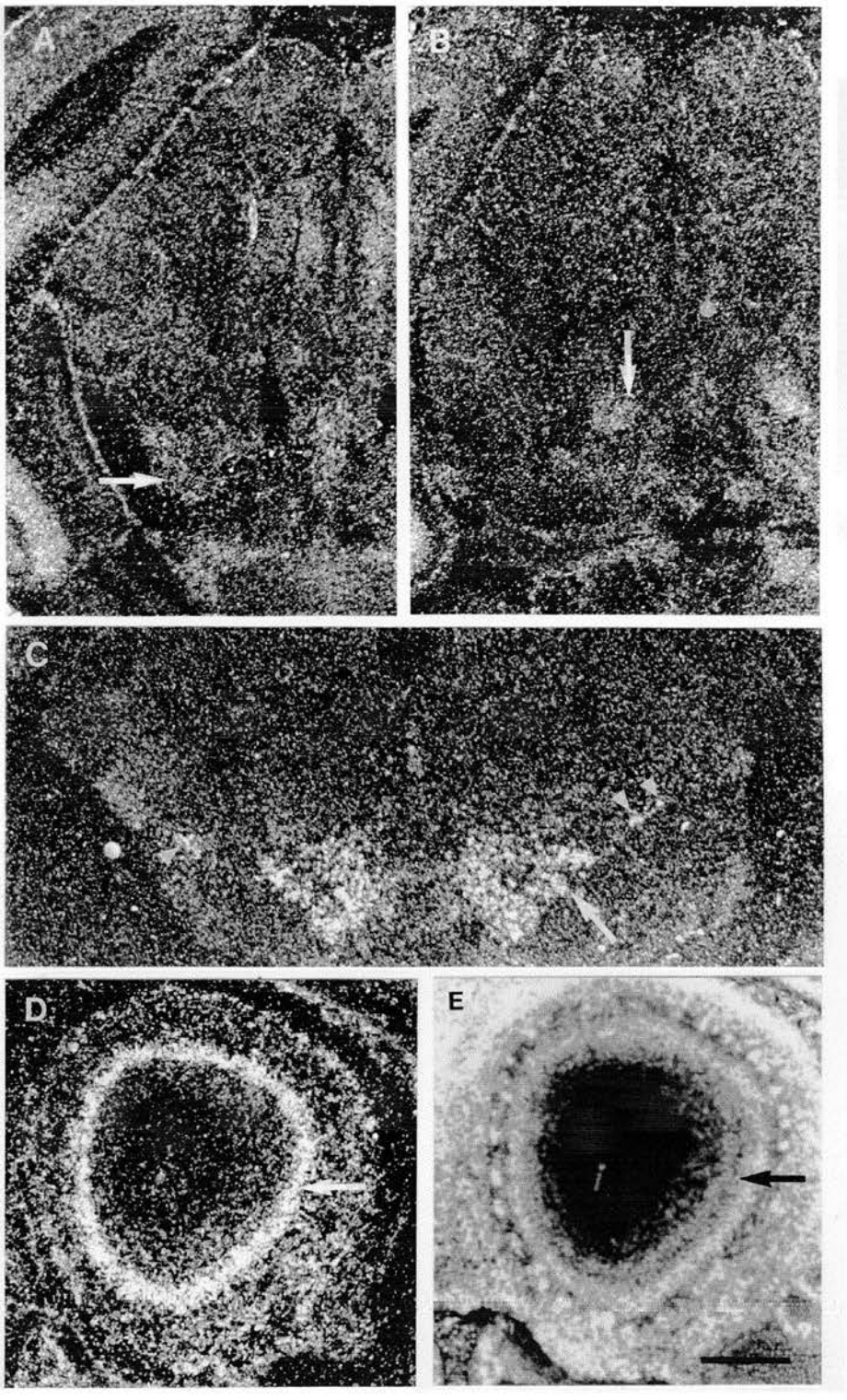

Figure IV-4 Coronal sections of (A,B) P0, (C) P10 and (D) E16 animals showing MAOA expression in dopaminergic cell groups of the (A-C) substantia nigra (SN)-ventral tegmental area (VTA) complex and (D) in the olfactory bulb. ***A,*** *White arrow* points to the SN-VTA where a low level of MAOA expression is seen. ***B,*** More caudal section than shown in (A). *White arrow* points to the dorsal part of the VTA which displays a higher level of MAOA expression. ***C,*** *White arrow* points to the VTA that expresses moderate level of MAOA expression. *Arrowheads* point to dopaminergic neurons of the SN. ***D,*** *White arrow* points to the mitral cell layer where dopaminergic external tufted cells are located. ***E,*** Bright field photomicrograph of the section shown in (D) pointing to the mitral cell layer (*black arrow*). Scale bar: A-C, 1mm; D,E, 0.5mm.

Table IV-2 Location of MAOB mRNA expression in monoaminergic and cholinergic neurons during development

Location	Labeling intensity of neurons at pre- and postnatal ages								
	E12 (n = 3)	E14 (n = 3)	E16 (n = 3)	E18 (n = 3)	P0 (n = 3)	P4 (n = 3)	P7 (n = 4)	P10 (n = 4)	Adults (n = 2)
Serotoninergic groups									
(B1-B3) Raphe pallidus, obscurus, magnus	-	++	++	++	++	++	++	+++	+++
(B4-B9) Raphe dorsal, median, pontis	-	++	++	++	++	++	++	+++	+++
Histaminergic cells	-	-	-	-	+	++	+++	+++	+++
Melatoninergic cells	-	-	++	++	+++	+++	+++	+++	+++
Dopaminergic group									
A15v Supraoptic n.	-	-	-	-	-	-	-	++	++
Preoptic area	-	-	-	-	-	-	-	++	++
Cholinergic groups									
Ch1-Ch3,	-	-	-	-	-	++	++	++	++
Ch5-Ch6	-	-	-	-	-	+	+	++	++
Ch7	-	++	++	++	++	++	++	++	++
Striatum, Ventral pallidum	-	-	-	-	++	++	++	++	++

Intensity of the labeling at prenatal and postnatal ages according to locations in the brain: - none; + weak; ++ moderate ; +++ high.

From P10, moderate MAOB mRNA expression was only detected in dopaminergic neurons located in the supraoptic (A15v) and preoptic areas (Table IV-2).

1.4 Histaminergic cell group

Scattered neurons displaying a low MAOB mRNA expression were first detected by P0 in the caudal hypothalamus (Table IV-2). By P4, these neurons displayed moderate MAOB mRNA expression and were clearly distributed at the level of the tubero-mammillary nucleus, they corresponded to histaminergic neurons (Table IV-2). Then MAOB mRNA expression remained very high in histaminergic neurons (Fig. IV-3*C*). Interestingly, a weak MAOA mRNA expression was detected in few histaminergic neurons from P4 (Table IV-1).

1.4 Melatoninergic cell group

From E16, melatoninergic cells of the pineal gland displayed already moderate MAOB mRNA expression (Table IV-2) in parallel with a strong tryptophan hydroxylase expression (data not shown). Then MAOB mRNA expression increased to reach a maximum by P0 and remain high throughout life (Table IV-2).

2 MAOA mRNA expression in neurons displaying a transient monoaminergic phenotype

The neuronal populations described in this following section are not classified as classical monoaminergic cell groups but have been shown to express transiently at least one particular monoamine synthesizing enzyme.

2.1 Transient TH-expressing neurons

I and others have reported that during development discrete neuronal populations express transiently the catecholamine synthetisizing enzyme, tyrosine hydroxylase (TH). Indeed, transient TH-expressing neurons have been located in the cortex (Berger et al.,1985), piriform cortex (Vitalis et al., 2000), amygdala (Verney et al., 1988 ; Vitalis et al., 2000), or inferior colliculus (Jaeger and Joh, 1983; Vitalis

et al., 2000). I showed that some of these transient TH-expressing neurons display a parallel transient MAOA mRNA expression. In the developing amygdala, neurons of the central, medial and cortical amygdaloid nuclei display both a moderate TH immunoreactivity and a weak to moderate MAOA mRNA expression from E16-E18 to P0-P4 (Fig. IV-5*D-F* and Table IV-3). In the developing mesencephalon, neurons in the inferior colliculus displayed a weak TH immunoreactivity and a moderate MAOA mRNA expression from E14 to E16 (Fig. IV-5*A-C* and Table IV-3).

2.2 Transient DBH-expressing neurons

It has been reported that motor neurons of the hindbrain express transiently DBH (Tiveron et al., 1996) but not TH (unpublished results) from E12 to birth. From E12-16 to P0-P4, a weak to moderate MAOA mRNA expression was detected in motor neurons of the oculomotor, trochlear, trigeminal motor, abducens, facial, ambiguus, dorsal motor vagus, and hypoglossal nuclei (Fig. IV-6 and Table IV-3). In facial and ambiguus motor nuclei low levels of MAOA mRNA expression were observed protractedly (Fig. IV-6*F* and Table IV-3).

2.3 Transient DBH and TH-expressing neurons

Cranial sensory ganglia serving the trigeminal (Vth), facial (VIIth), glossopharyngeal (IXth), and vagus (Xth) have been reported to express transiently during embryonic development selected catecholaminergic traits, such as TH or DBH expression or NA uptake (Son et al., 1996). Interestingly, cranial sensory neurons expressed also moderate to strong levels of MAOA mRNA from E12 to at least birth (Table IV-3). Low to moderate MAOA mRNA expression was also found from E12 to at least P0 in sensory neurons of the dorsal root ganglia (Table IV-3).

3 MAOB mRNA expression in discrete cholinergic populations

Cholinergic neurons are found in seven major projections systems (Ch), and at least three major areas containing intrinsic neurons, contained wholly within the CNS. Earlier reports have shown that cholinergic neurons of the pedunculopontine tegmental (Ch5) and laterodorsal tegmental (Ch6) (Ikemoto et al., 1999), and small cholinergic interneurons intrinsic to the caudate-putamen (Nakamura et al., 1993)

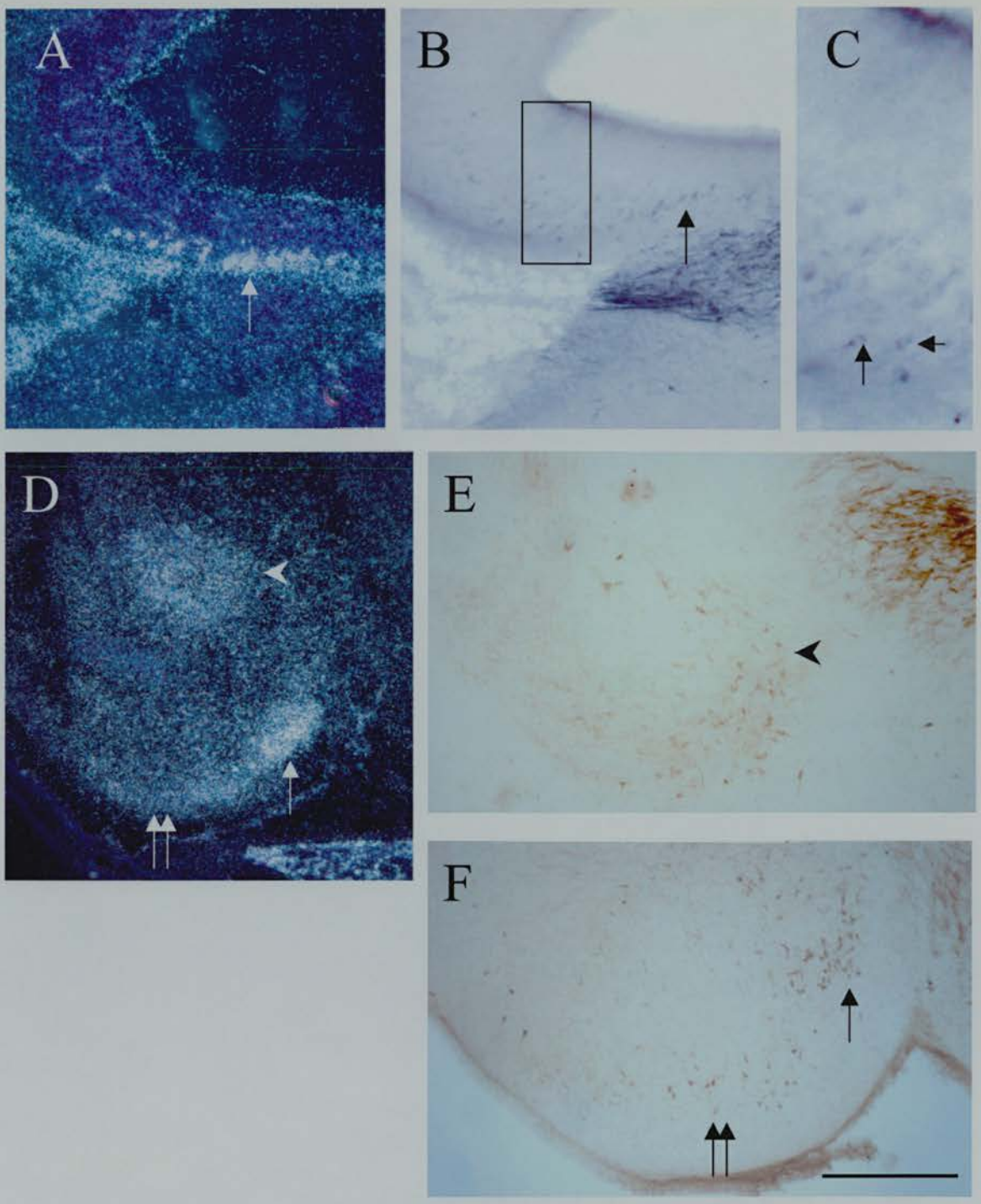

Figure IV-5 MAOA expression in neurons displaying a transient tyrosine hydroxylase (TH) immunoreactivity in the (A-C) inferior colliculus and the (D-F) amygdala. ***A,*** MAOA expression and ***B,*** TH immunoreactivity at the level of the caudal inferior colliculus at E14. ***A,B,*** *arrows* point to individual neurons at the same level. ***C,*** Higher magnification in box inset in (B), *arrows* show small and lightly stained TH-immunoreactive neurons. ***D,*** MAOA expression and ***E-F***, TH immunoreactivity in the developing amygdala at P0. ***D,*** MAOA expression is located at the level of the medial cortical amygdaloid nucleus (*arrow*), the central nucleus (*arrowhead*) and the basal cortical amygdaloid nucleus (*double arrow*). ***E,*** Numerous TH-immunoreactive neurons are located in the central nucleus (*arrowhead*), ***F,*** the medial cortical amygdaloid nucleus (*arrow*), and the cortical amygdaloid nucleus (*double arrow*). Scale bar: A,B,E,F, 2mm; C, 0.5mm; D, 3mm.

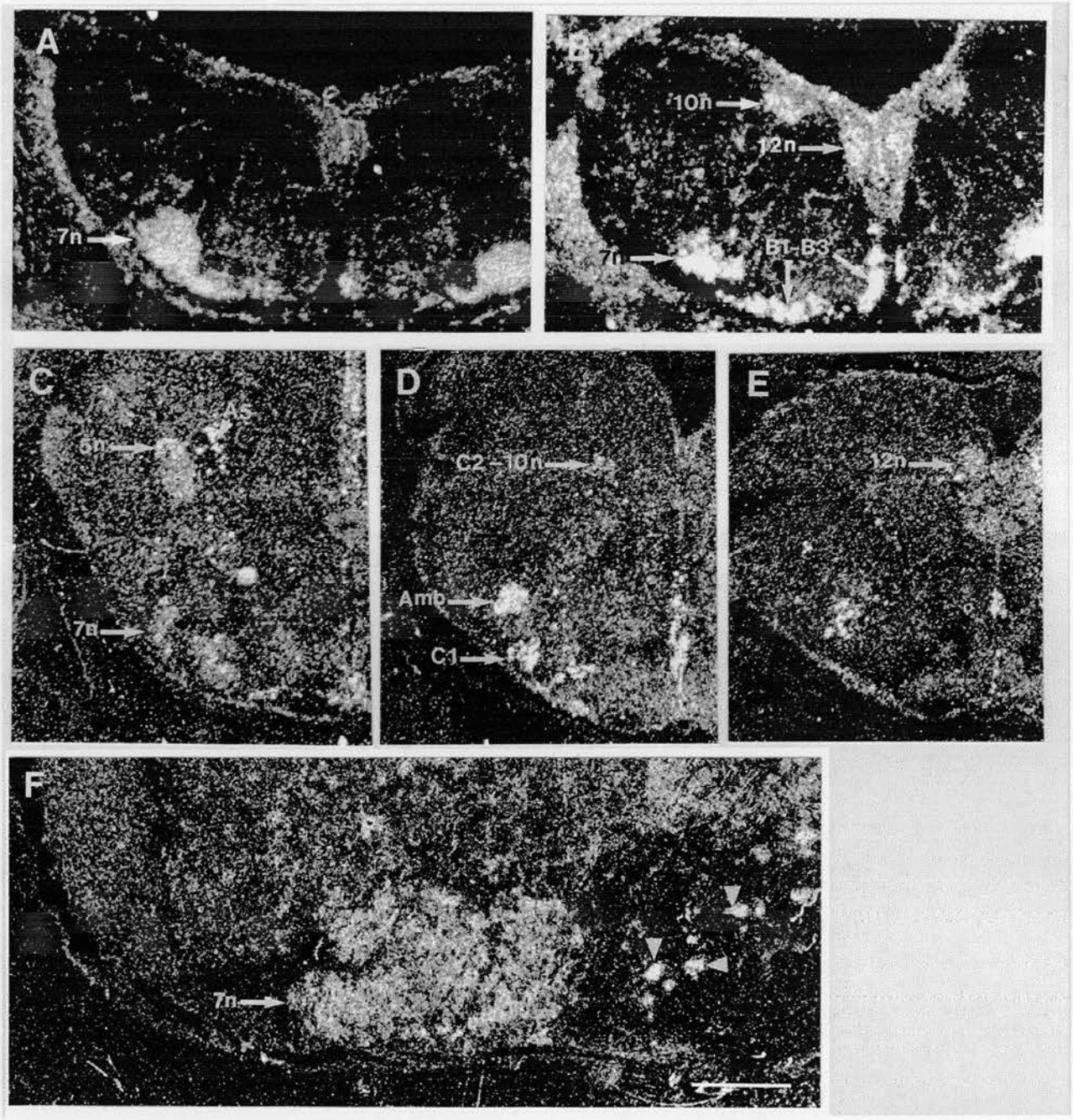

Figure IV-6 MAOA expression in motor neurons of the hindbrain. ***A, B*** Sections of E14 embryos showing strong MAOA expression in (A,B) the facial nucleus (7n) and (B) the dorsal motor vagus (10n) and the hypoglossal nucleus (12n). ***B,*** Note also MAOA expression in serotoninergic neurons of the B1-B3 complex (B1-B3). ***C-E***, MAOA expression in sections from new born pups, note the decrease of MAOA expression in motor neurons in comparison to (A-B). ***C,*** MAOA expression at the level of the trigeminal motor nucleus (5n) and the facial nucleus (7n). Note also MAOA expression in adrenergic neurons of the A5 group (A5). ***D,*** MAOA expression at the level of the dorsal motor vagus and the neighbouring adrenergic group C2 (C2), the ambiguus (Amb) and the adrenergic group C1 (C1). ***E,*** moderate MAOA expression in the hypoglossal nucleus (12n). ***F,*** Section of P15 pups showing protracted MAOA expression in the facial nucleus. *Arrowheads* point to serotoninergic neurons of the B1-B3 complex. Scale bar: A,B, 2mm; C-E, 1mm; F, 0.5mm.

Table IV-3 Location of MAOA mRNA expression in neurons expressing transiently a catecholaminergic phenotype

Location	Labeling intensity of neurons at pre- and postnatal ages								
	E12 (n = 3)	E14 (n = 3)	E16 (n = 3)	E18 (n = 3)	P0 (n = 3)	P4 (n = 3)	P7 (n = 4)	P10 (n = 4)	Adults (n = 2)
TH-positive									
Central n. of amygdala	-	-	+	+	+	+	-	-	-
Medial amygdaloid n.	-	-	-	++	++	-	-	-	-
Cortical amygdaloid n.	-	-	-	+	+	-	-	-	-
Inferior colliculus	-	++	++	-	-	-	-	-	-
DBH-positive									
Oculomotor n.	-	-	+	+	+	-	-	-	-
Trochlear n.	-	-	+	+	+	-	-	-	-
Trigeminal motor n.	-	+	++	++	+	-	-	-	-
Abducens n.	+	++	++	++	++	+	-	-	-
Hypoglossal n.	+	++	++	++	+	+	-	-	-
Dorsal motor vagus n.	+	++	++	++	+	+	-	-	-
Facial n.	+	++	++	++	++	+	+	+	+
Ambiguus n.	-	+	+	++	++	+	+	+	+
TH-positive and DBH-positive									
Cranial sensory ganglia									
V, VII, IX, X	++	+++	+++	+++	+++	++	**nd**	**nd**	**nd**
Dorsal root ganglia	+	++	++	++	++	++	**nd**	**nd**	**nd**

Intensity of the labeling at prenatal and postnatal ages according to locations in the brain: - none; + weak; ++ moderate ; +++ high; nd not defined.

display MAOB activity. I confirmed these findings by in situ hybridization and extended the notion of MAOB location in cholinergic neurons by showing MAOB mRNA expression in additional cholinergic groups (Table IV-2).

From P4, weak MAOB mRNA expression was found in cholinergic neurons of Ch5 and Ch6 (Table IV-2). In the basal telencephalon, large cholinergic neurons in the medial septal nucleus (Ch1), vertical limb of the diagonal band of Broca (Ch2) and horizontal limb of the diagonal band of Broca (Ch3) displayed moderate MAOB mRNA expression from P4 (Table IV-2). In the epithalamus, the medial habenular nucleus (Ch7) displayed strong MAOB mRNA expression from E14 (Table IV-2). Moderate MAOB mRNA expression was also detected in small cholinergic interneurons of the striatum and ventral pallidum by P0 (Table IV-2).

4 MAOA and MAOB mRNA expression in non-aminergic neuronal populations

The neuronal populations described below never express transiently the monoamine synthesizing enzymes, TH, TpOH, DBH, HDC or L-amino acid decarboxylase.

4.1 Telencephalon

From E12 to E16, low MAOA mRNA expression was found throughout the ventricular and subventricular zone of the neocortical, striatal, amygdal and pallidal anlages (Table IV-4). Then MAOA mRNA expression became restricted to discrete neuronal populations. Low MAOA mRNA expression was detected from E16 in the cortical plate and the hippocampal formation (Table IV-4). In the cortex, MAOA mRNA expression was stronger in layer VIb and V (Fig IV-6 and Table IV-4). In the hippocampal formation MAOA mRNA expression was located at the level of the CA1-CA3 fields, the strongest expression being in CA3 (Fig. IV-8 and Table IV-4). From E16, the ventral part of the basal amygdaloid nucleus displayed low levels of MAOA mRNA expression (Table IV-4).

Low MAOB mRNA expression was detected by P0 in the basal telencephalon, particularly at the level of the medial and lateral nucleus accumbens shell. In these structures MAOB mRNA expression progressively increased to reach maximal levels in adults.

Table IV-4 Location of MAOA and MAOB expressions in non-monoaminergic neurons and glial cells during development

Location	Labeling intensity at pre- and postnatal ages								
	E12 (n = 2)	E14 (n = 2)	E16 (n = 3)	E18 (n = 3)	P0 (n = 3)	P4 (n = 3)	P7 (n = 4)	P10 P15 (n = 4)	Adult (n = 6)
MAOA									
Telecephalon									
Neocortex									
SVZ-VZ	+	+	+	-					
Cortical plate	-	-	+	+	+				
Layer VI b				+	+	+	+	+	+
Layer V				+	+	+	+	+	+
Piriform Cortex		-	-	-	+	++	++	++	++
Anterior olfactory n.		-	-	+	+	+	+	+	+
LGE-MGE									
SVZ-VZ	+	+	+	-					
Hippocampus									
SVZ-VZ	-	+	+	+					
CA1			+	+	+	-	-	-	-
CA3			++	++	++	++	++	++	++
Amygdala									
Basal amygdaloid nucleus		-	+	+	+	+	+	+	+
Diencephalon									
Zona incerta, caudal part			-	+	+	+	+	+	-
Habenula	-	+	++	++	++	++	++	++	++
Paraventricular th. n.	-	-	-	+	+	+	+	+	+
Lateral dorsal th. n.	-	-	-	-	**nd**	**nd**	**nd**	+	+
(sub)Parafascicular th. n.	-	-	-	+	+	+	+	+	+
Central th. system	-	-	-	+	+	+	+	+	+
Rhomboid n., Reuniens n.	-	-	-	+	+	+	+	+	+
Ventromedial hyp. n.	-	-	-	+	+	+	+	-	-
Brainstem									
Ventral Cochlear n.	-	-	-	-	+	**nd**	**nd**	**nd**	**nd**
Lateral Vestibular n.	-	-	-	-	+	**nd**	**nd**	**nd**	**nd**
Solitary tract n.	-	++	++	++	++	++	++	++	++
MAOB									
Neuronal cells									
Accumbens	-	-	-	-	+	+	++	++	+++
Lateral habenula	-	-	-	-	+	+	++	++	+++
Paraventricular th. n.	-	-	-	-	+	+	++	++	+++
Central th. system	-	-	-	-	-	+	++	++	++
Rhomboid n., Reuniens n.	-	-	-	-	-	+	+	+	+
Ventral th. system	-	-	-	-	-	+	+	+	+
Non-neuronal cells									
Nerve entry zone	++	+++	+++	+++	++	+	-	-	-
Astrocytes	-	-	-	-	-	+	++	+++	+++
Circumventricular organs	-	-	-	-	+	++	+++	+++	+++

Intensity of the labeling at prenatal and postnatal ages according to locations in the brain: - none; + weak; ++ moderate ; +++ high.; nd not defined.

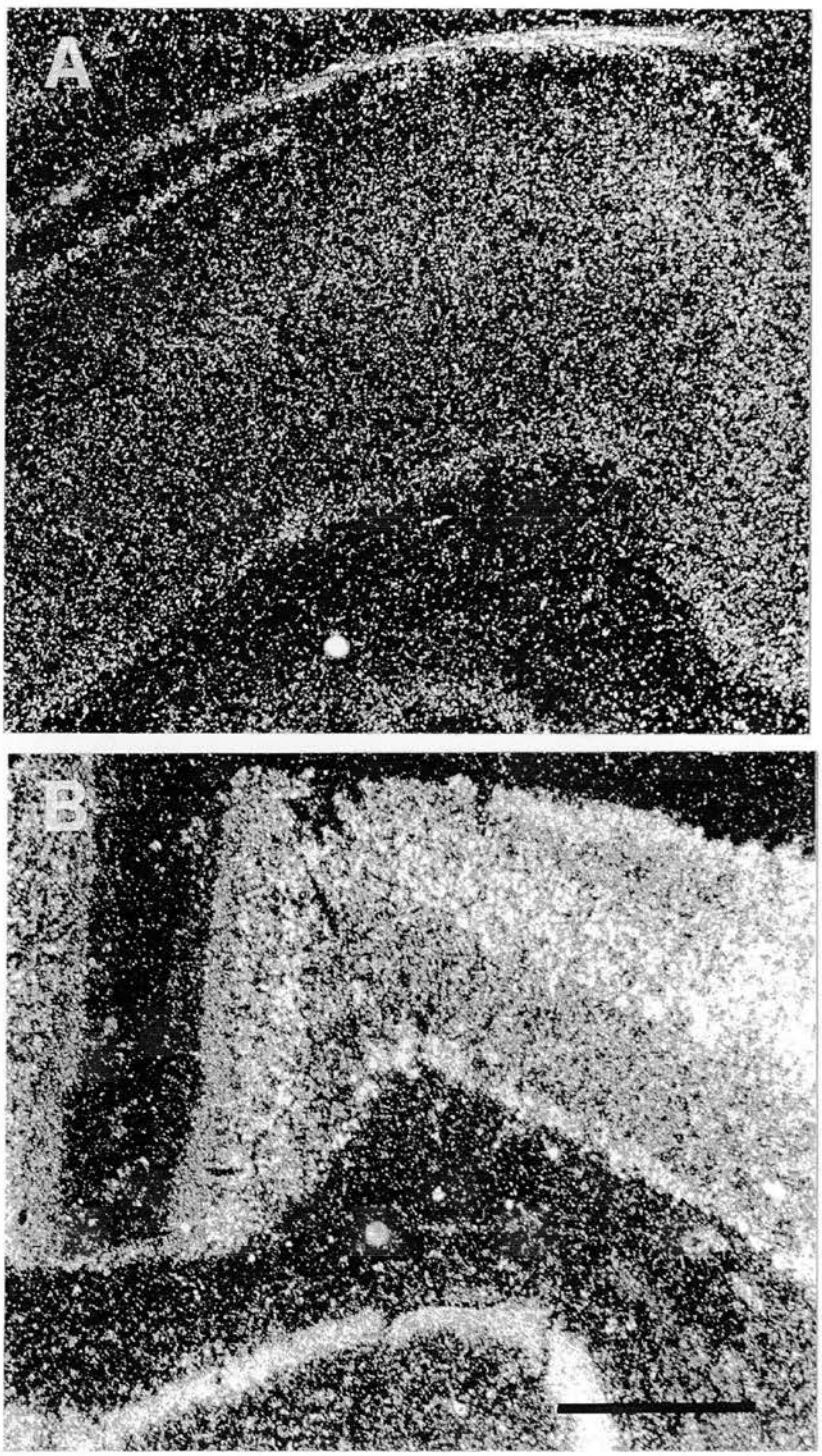

Figure IV-7 MAOA expression in the developing cerebral cortex. ***A,*** MAOA expression in a E18 embryo showing a moderate expression in lower layer IV, upper layer V and in the pia. ***B,*** MAOA expression in a P15 pup. Note the strongest MAOA expression in lower layer VI and layer V. Scale bar: A, 0.25mm; B, 0.5mm.

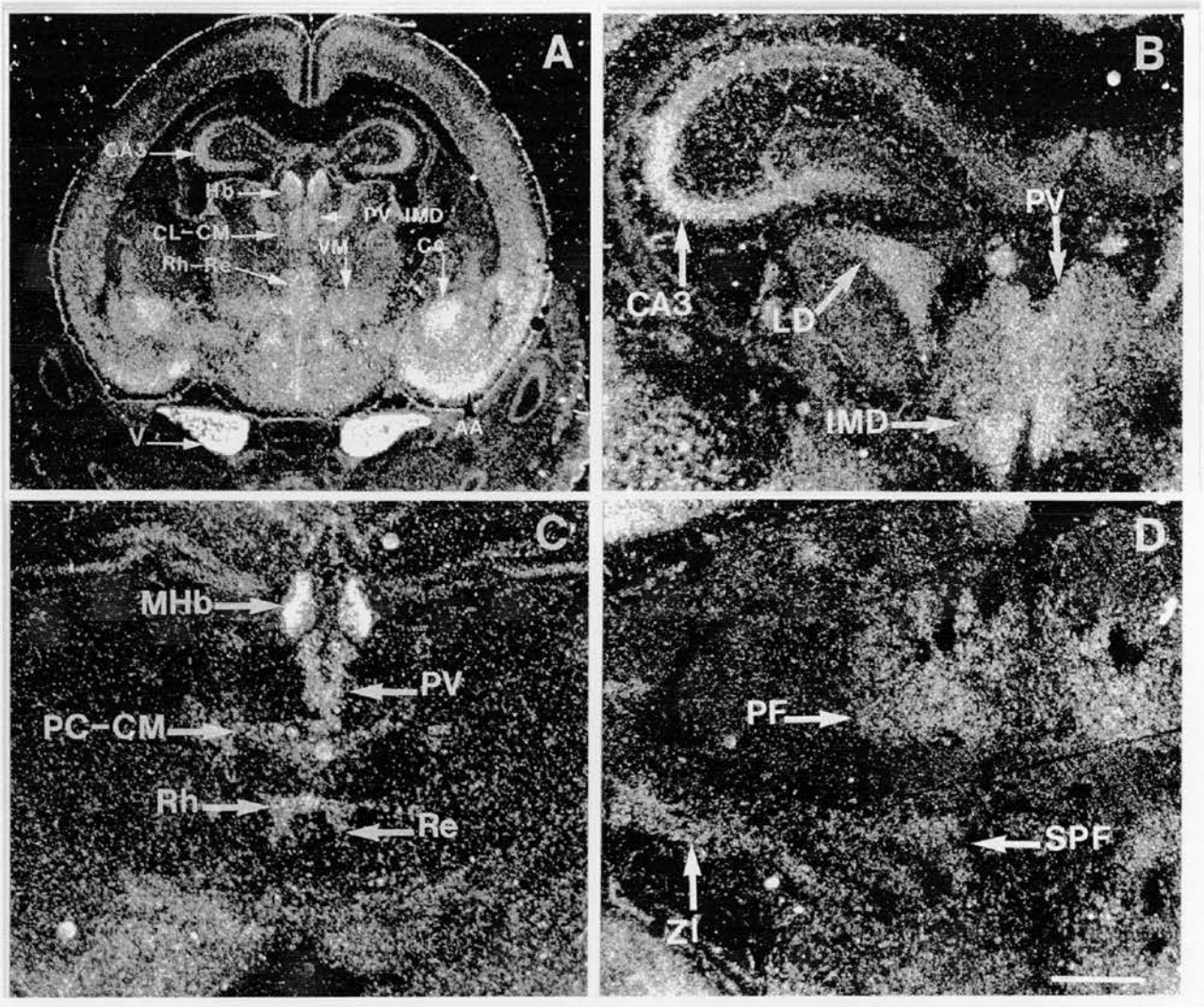

Figure IV-8 MAOA mRNA expression in thalamic nuclei. ***A,*** Coronal section of E18 embryo showing MAOA expression in the thalamus: in intralaminar thalamic nuclei (central (CL), central median (CM), paraventricular (PV) and intermediate dorsal thalamic nuclei (IMD) thalamic nuclei), the rhomboid (Rh), the reuniens (Re), and the ventral medial (VM) thalamic nuclei. Note also MAOA expression in the hippocampus with higher levels of expression in CA3, the habenula (Hb), the amygdala with higher level of expression in the central (Ce) and the anterior amygdala (AA) and in the trigeminal ganglion (V). ***B-D,*** Coronal sections of P15 pups showing protracted MAOA expression in thalamic nuclei. ***B,*** Rostral section showing MAOA expression in the lateral dorsal (LD), paraventricular (PV) and intermediate thalamic nuclei (IMD). Note also the strong and protracted MAOA expression in CA3. ***C,*** more caudal section showing MAOA expression in intralaminar thalamic nuclei (paracentral (PC), CM and PV), Rh and Re and the medial habenula (MHb). ***D,*** Caudal section showing MAOA expression in the parafascicular (PF) and subparafascicular (SPF) thalamic nuclei and in the zona incerta (ZI). Scale bar: 2 mm.

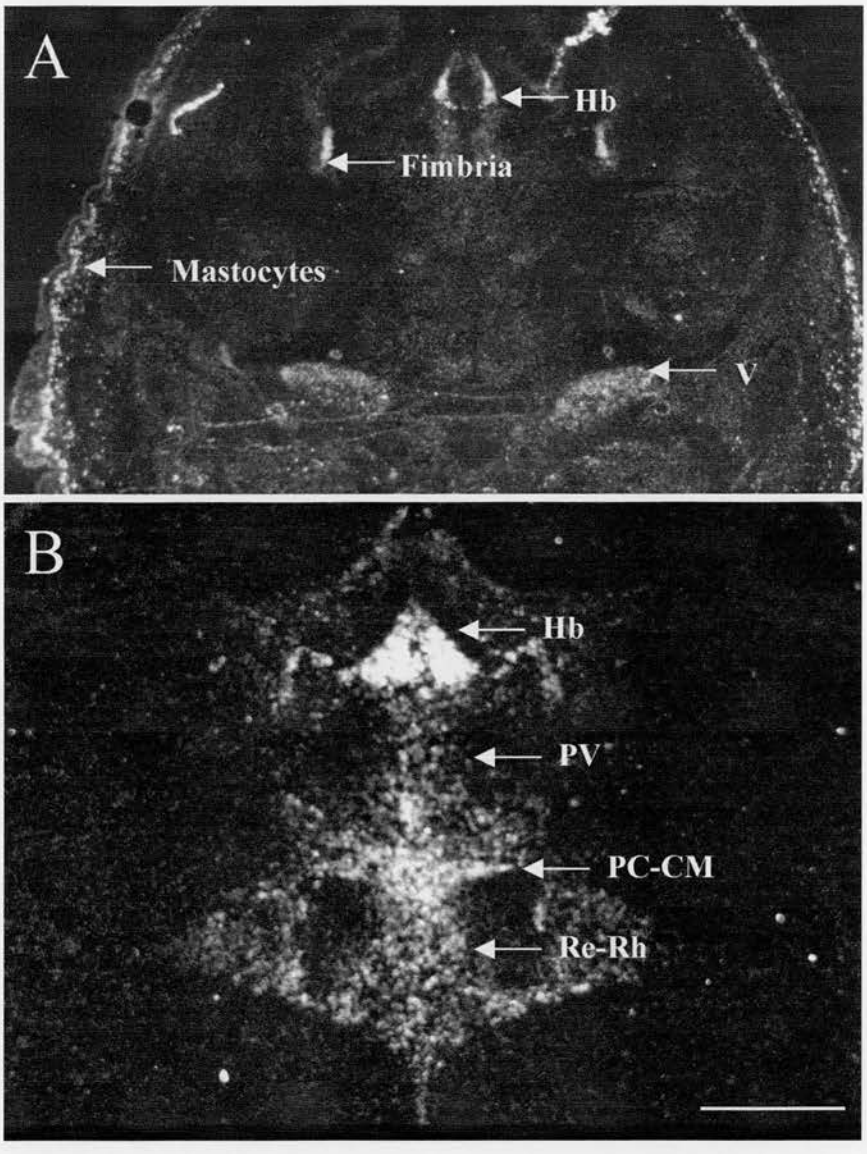

Figure IV-9 MAOB mRNA expression at the level of the thalamus and habenula. ***A,*** Coronal section of a E18 embryo showing MAOB mRNA expression in the fimbria and the mastocytes. Note also MAOB mRNA expression in the habenula (Hb) and the trigeminal ganglion (V). ***B,*** Coronal scetion of a P21 pup showing MAOB mRNA expression in the habenula and thalamic nuclei: in the paraventricular (PV), the paracentral (PC) and central median (CM) and, in the rhomboid (Rh) and reuniens (Re) thalamic nuclei. Scale bar = 2mm.

4.2 Diencephalon

In the epithalamus, the habenula displayed low MAOA mRNA expression by E14. From E16, the entire medial habenula displayed moderate MAOA mRNA expression (Fig. IV-8 and Table IV-4). From E18, low MAOA mRNA expression was detected in the paraventricular thalamic, the lateral dorsal, the (sub)parafascicular, the rhomboid and reuniens nuclei and in discrete nuclei of the central system (central, central median and paracentral) (Fig. IV-8 and Table IV-4).

From E18-P0, strong MAOB mRNA expression was detected in the lateral habenula (E18; Fig. IV-9*A*) and paraventricular thalamic nucleus (P0). From P4, the rhomboid and reuniens nuclei and all dorsal thalamic nuclei of the central and ventral systems (ventroanterior, ventromedian, ventrolateral, and ventroposterior) displayed low to moderate MAOB mRNA expression (Fig. IV-9*B* and Table IV-4).

From E18 to P7, the ventromedial hypothalamic nucleus displayed low MAOA mRNA expression (Table IV-4). From E18 to P10, low MAOA mRNA expression was also detected in the caudal zona incerta (Fig. IV-8 and Table IV-4).

4.3 Brainstem

From E18, MAOA mRNA was detected in the periaqueductal central grey (Fig. IV-1*B*) and the nucleus of the solitary tract (Table IV-4). In the superior colliculus, the stratum zonale contained low levels of MAOA mRNA from P0 (Table IV-4). Low levels of MAOA mRNA expression were also detected by P0 in the ventral cochlear and the lateral vestibular nuclei (Table IV-4).

5 Non-neuronal cells

5.1Glial cells

From E12 to P4, cells at the interface between the CNS and the PNS displayed strong MAOB mRNA expression (Fig. IV-10*A* and Table IV-4). The nature of the cells is not clear but might correspond to astrocytes. From E14, glial cells of the tectal glia limitans displayed strong levels of MAOB mRNA. From E12, there was a strong MAOB mRNA expression in the olfactory epithelium (Fig. IV-10*B)*. From E14, ensheating astrocytes of the olfactory nerve and olfactory bulb

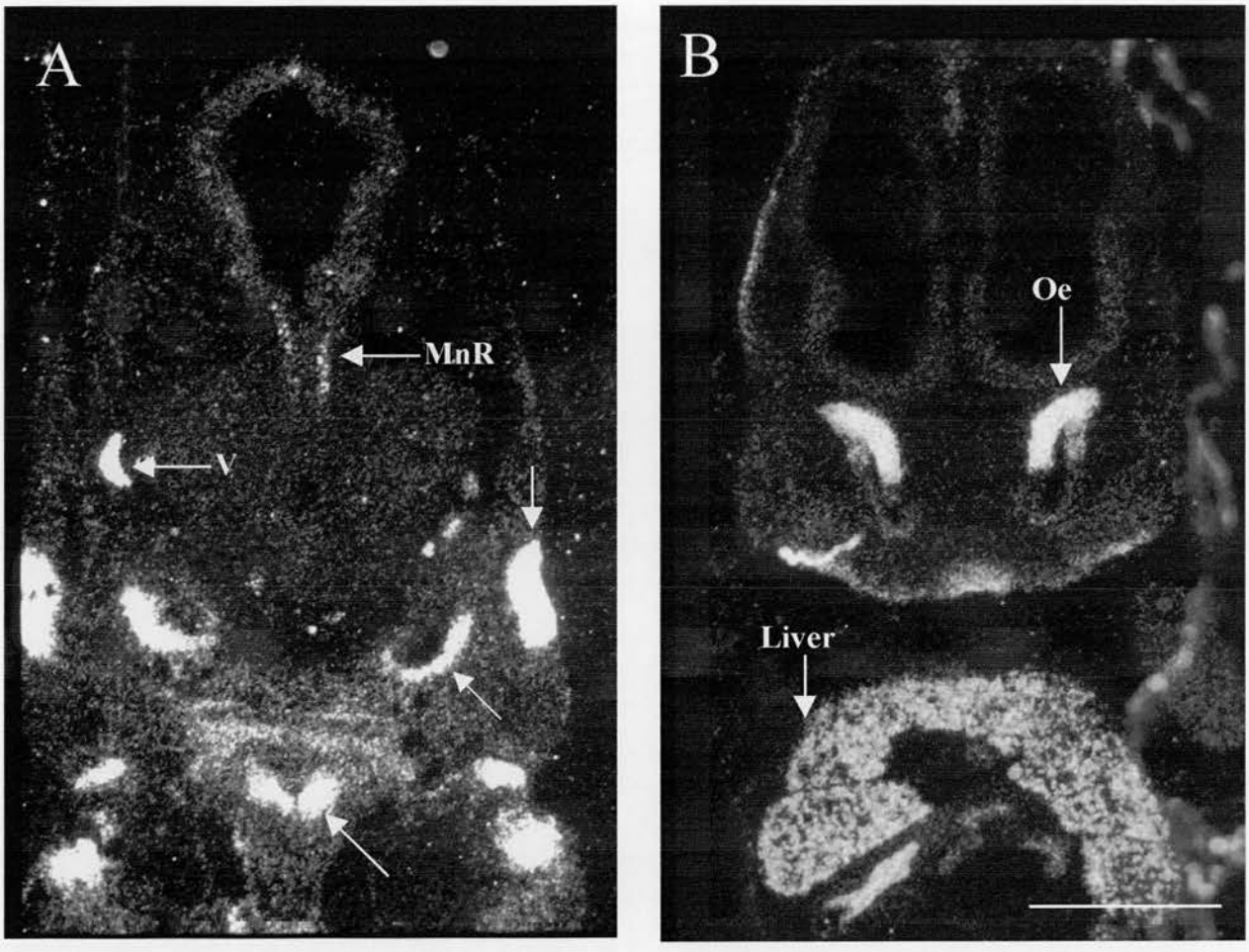

Figure IV-10 MAOB mRNA expression in glial cells. ***A,*** MAOB mRNA expression at the interface between the CNS and the PNS at the level of nerve V (V). Note also MAOB mRNA expression in serotoninergic neurons of the raphe median (MnR). *Arrows* point to MAOB mRNA expression in several cartilages. ***B,*** Coronal section showing MAOB mRNA expression in the olfactory epithelium (Oe). Note also MAOB mRNA expression in the liver. Scale bar = 4mm.

nerve layer expressed high levels of MAOB. From E17 the fimbria display high level of MAOB (Fig. IV-9*A*). Finally, astrocytes displayed moderate MAOB mRNA expression in all brain regions from P0-P4.

5.2 Ependymocytes and circumventricular organs

A moderate level of MAOB mRNA expression was detected from E17 in all circumventricular organs: the subfornical and subcommissural organs, the area postrema and the choroid plexus. Then MAOB mRNA expression increased to reach a maximum by P7. A high level of MAOB mRNA expression was also detected from P4 throughout all ventricular ependyma (Table IV-4).

5-3 Blood vessels

From E15, blood vessels displayed low levels of MAOA mRNA expression in all brain regions. MAOB mRNA was never detected in blood vessels. This is in contrast to what was reported in rat in which MAOB but not MAOA is expressed in blood vessels (Kitahama et al., 1994).

6 MAO activity

I used clorgyline, a selective inhibitor of MAOA, and deprenyl, a selective inhibitor of MAOB, to determine the specific pattern of MAOA and MAOB activity during development. I used MAOA knockouts to determine the minimal concentration of deprenyl necessary to inhibit completely the remaining MAOB activity. I found that 10^{-7} M deprenyl was sufficient to inhibit MAOB activity. I found also that 10^{-7} M clorgyline was sufficient to block MAOA activity. On the whole, I found a good spatio-temporal correlation between MAO activity and MAO mRNA expression, especially with noradrenergic, serotoninergic, histaminergic, melatoninergic, and some dopaminergic neurons where MAO proteins are largely concentrated into cell bodies and dendrites and allow a clear visualisation (Arai et al., 1986 and Figure IV-11). However, exceptions were found such as SN-VTA neurons that never displayed MAO activity. Cholinergic neurons also displayed a good spatio-temporal correlation between MAOB mRNA and MAOB activity. I found also a rather good spatio-temporal correlation between MAO activity and MAO

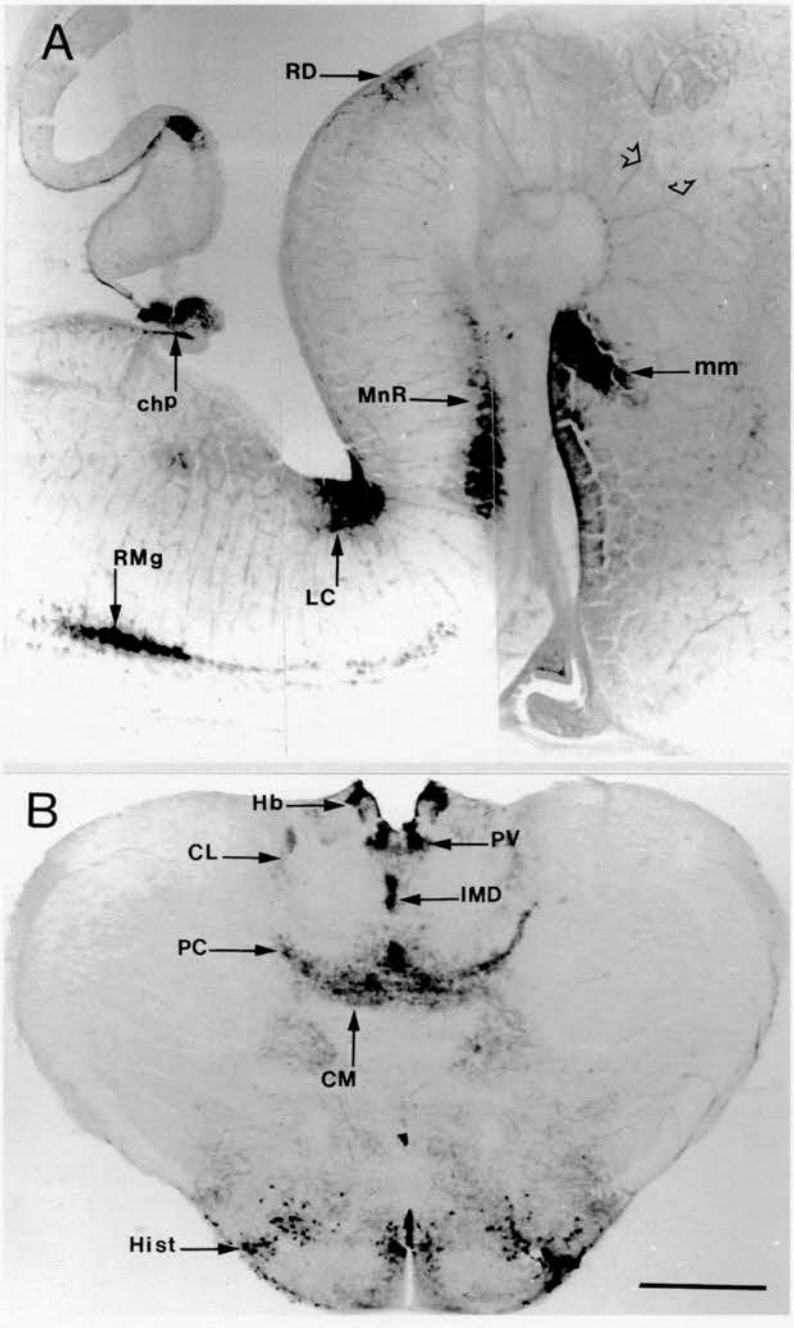

Figure IV-11 MAO activity in aminergic, histaminergic and thalamic neurons. ***A,*** Sagittal section of a E14 embryo showing strong MAO activity in serotoninergic neurons (RD, MnR, RMg), in noradrenergic neurons of the locus coeruleus (LC), in the mammilary body (mm) and the choroid plexus (chp). *Open arrows* point to individual blood vessels. Note that numerous blood vessels display MAO activity. ***B,*** Coronal section of a P4 pup showing MAO activity in histaminergic neurons in the tubero-mammilar region (hist), in the habenula (Hb) and in several intralaminar thalamic nuclei (PV, CL, IMD, PC, CM). CL, central lateral; CM, central median, MnR, raphe median nucleus; PC, paracentral; RD, Raphe dorsal; RMg, Raphe magnus nucleus. Scale bar: A, 3mm; B, 4mm.

mRNA in non-monoaminergic neurons and neurons displaying a transient monoaminergic phenotype. For instance, TH-IR neurons of the inferior colliculus displayed MAOA activity until E14 and neurons of the thalamic intralaminar system by P4 (Fig. IV-11). However, I failed to detect any MAO activity in the hippocampus or cortex. Finally, an excellent spatio-temporal correlation was found between MAOB activity and MAOB mRNA in non-neuronal cells (Fig. IV-12).

7 MAOB immunocytochemistry

I have used MAOB immunocytochemistry to determine the cell types containing MAOB. The complete analysis of the cellular and subcellular locations of the MAOB protein is not completed. Some preliminary results are presented below.

So far I was able to show that most serotoninergic neurons express MAOB as early as E14. At this age MAOB immunolabeling was more intense in neurons that had migrated away from their area of genesis (Fig. IV-13). The difference of intensity in MAOB labelling was maintained throughout development. The high intensity of the signal obtained could be attributed to the long life of the protein and to its accumulation. In other neuronal populations there was a good correlation with in situ hybridization and activity.

MAOB labelled numerous astroglial and glial cells that were scattered all over the brain. Double labelling for GFAP and MAOB revealed that MAOB was an earlier and more general marker for astrocytes than GFAP. MAOB was observed in numerous astrocytes as early as E17 and was also observed in astrocytes that were not GFAP-positive (i.e.: at the level of the fimbria) (Fig. IV-14).

V Discussion

I provide here the first description of the developmental localisation of MAOA and MAOB. Unexpectedly, in serotoninergic neurons I found that MAOA is the principal enzyme of degradation of serotonin in embryonic ages whereas MAOB is the principal enzyme of degradation in postnatal ages. In addition, I report that there is a transient expression of MAOA in proliferating neuroepithelia and in several non-monoaminergic structures, a notion that is of importance to comprehend the actions of monoamines and related psychoactive drugs during development.

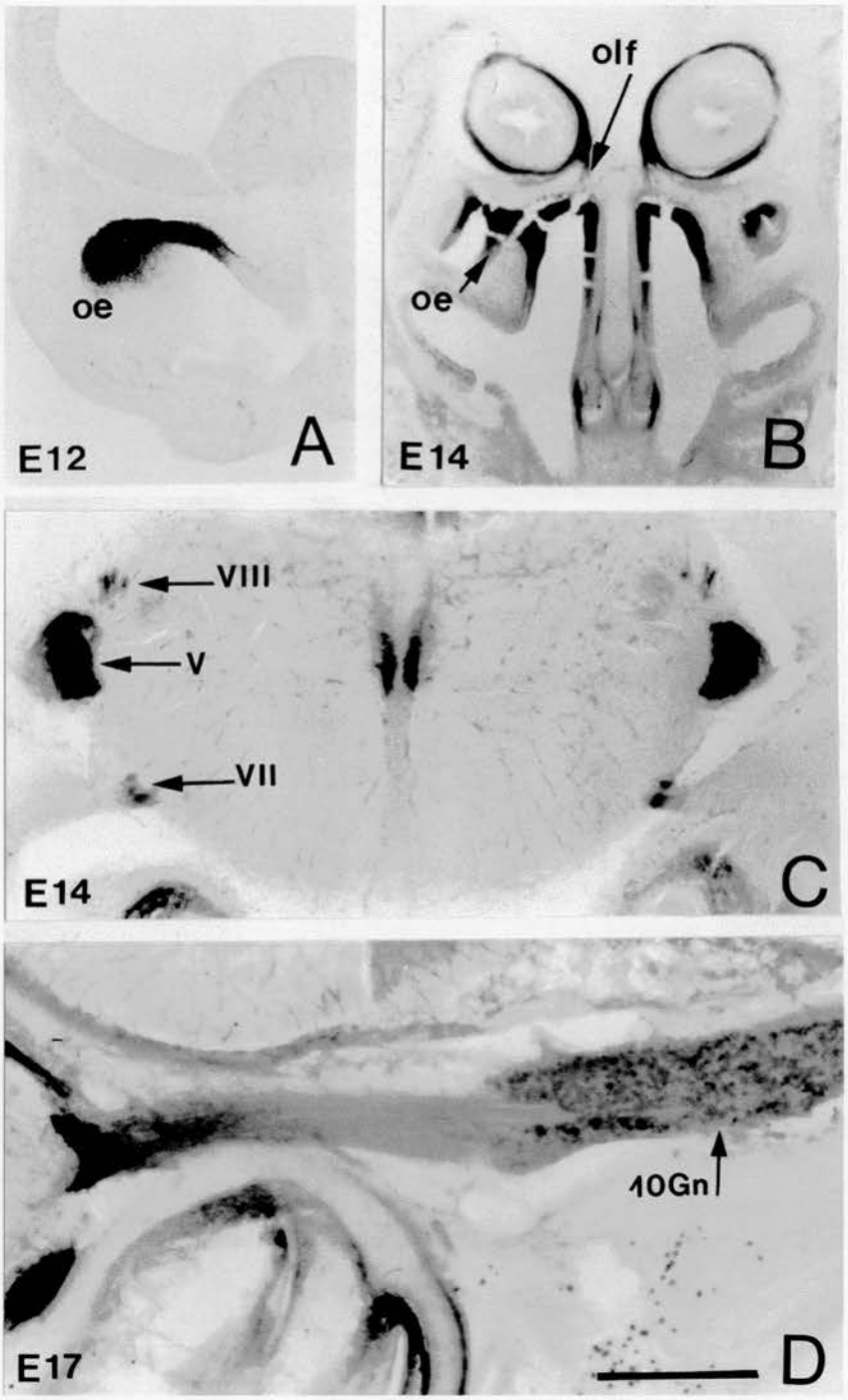

Figure IV-12 ***A,*** Sagittal section of E12 embryo showing a strong MAO activity at the level of the olfactory epithelium (oe). ***B,*** Coronal section of E14 embryo showing MAO activity in the olfactory epithelium and the olfactory nerve (olf). ***C,*** Coronal section of E14 embryo showing strong MAOA activity at the interface between the CNS and the PNS at the levels of nerves VIII, V and VII. ***D,*** Sagittal section of E17 embryo showing MAO activity in individual cells in the ganglion of the nerve X (10Gn). Scale bar: A, 1mm; B, 4mm; C, 2mm; D, 0.5mm.

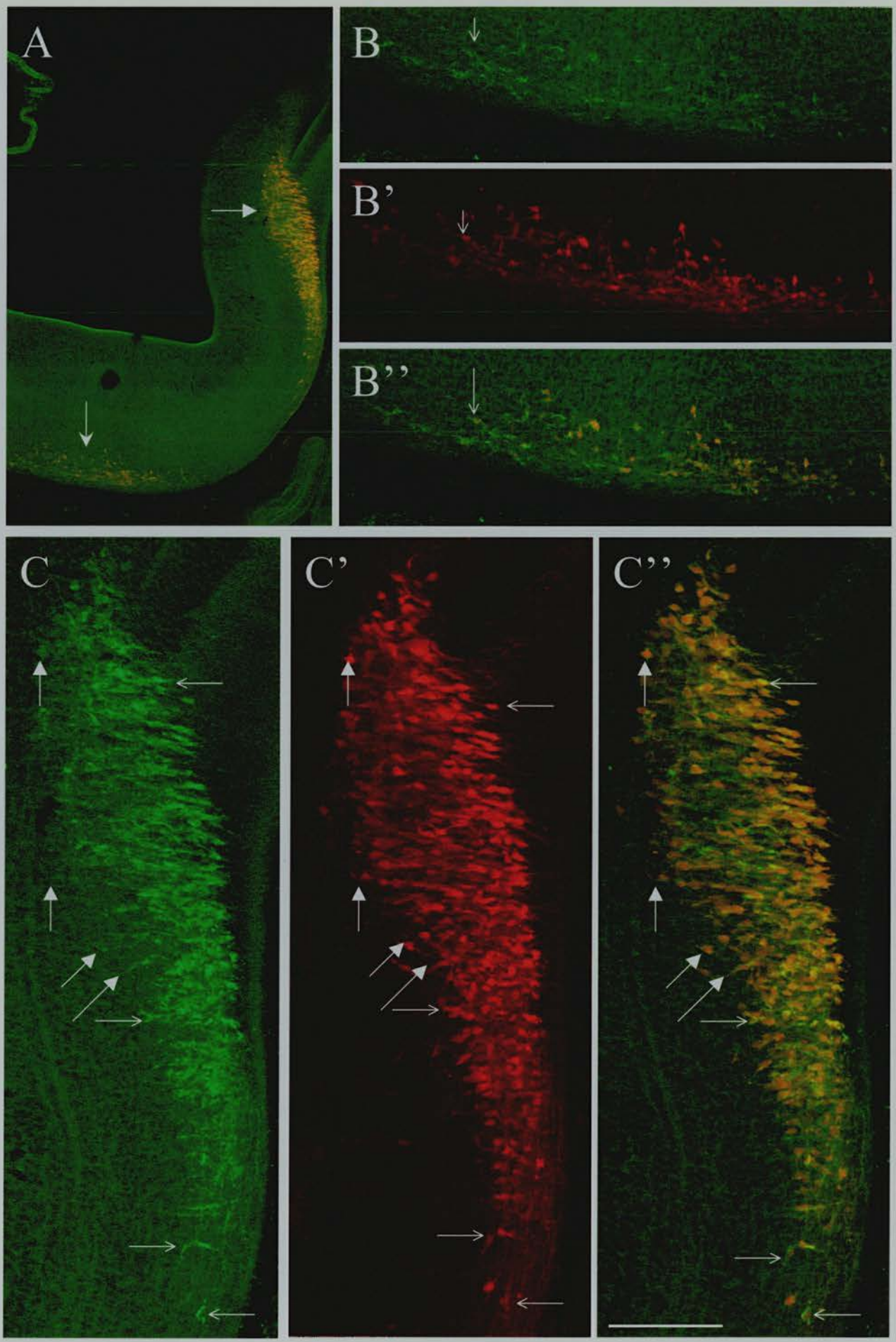

Figure IV-13, Please see following page for figure legend

Figure IV-13 Colocalisation of MAOB and 5-HT in sagittal section of E14 embryo. ***A,*** 5-HT and MAOB are colocalised in both B1-B3 (ventral) and B4-B9 (medial) serotoninergic complexes. ***B-C''***, Higher magnification of areas pointed out in (A) showing (B,C) MAOB-immunolabeled serotoninergic neurons, (B',C') 5-HT immunolabeled neurons, (B'',C'') the overlay of (B and B') and (C and C') respectively. ***B-C''***, *Arrows* and *filled arrows* point to single neurons. Note that most serotoninergic neurons contain MAOB. Note also that in both serotoninergic groups (B1-B3) and (B4-B9) some serotoninergic neurons contain lower levels of MAOB than others. ***B-C''***, *Arrows* point to serotoninergic neurons displaying a strong MAOB immunolabeling. ***C-C',*** *Filled arrows* point to serotoninergic neurons displaying a less strong MAOB immunolabelling. Note that these neurons are closer to their area of genesis than those displaying higher level of MAOB immunolabeling. Scale bar: A, 1mm; B-B'', 0.4mm; C-C'', 0.3mm.

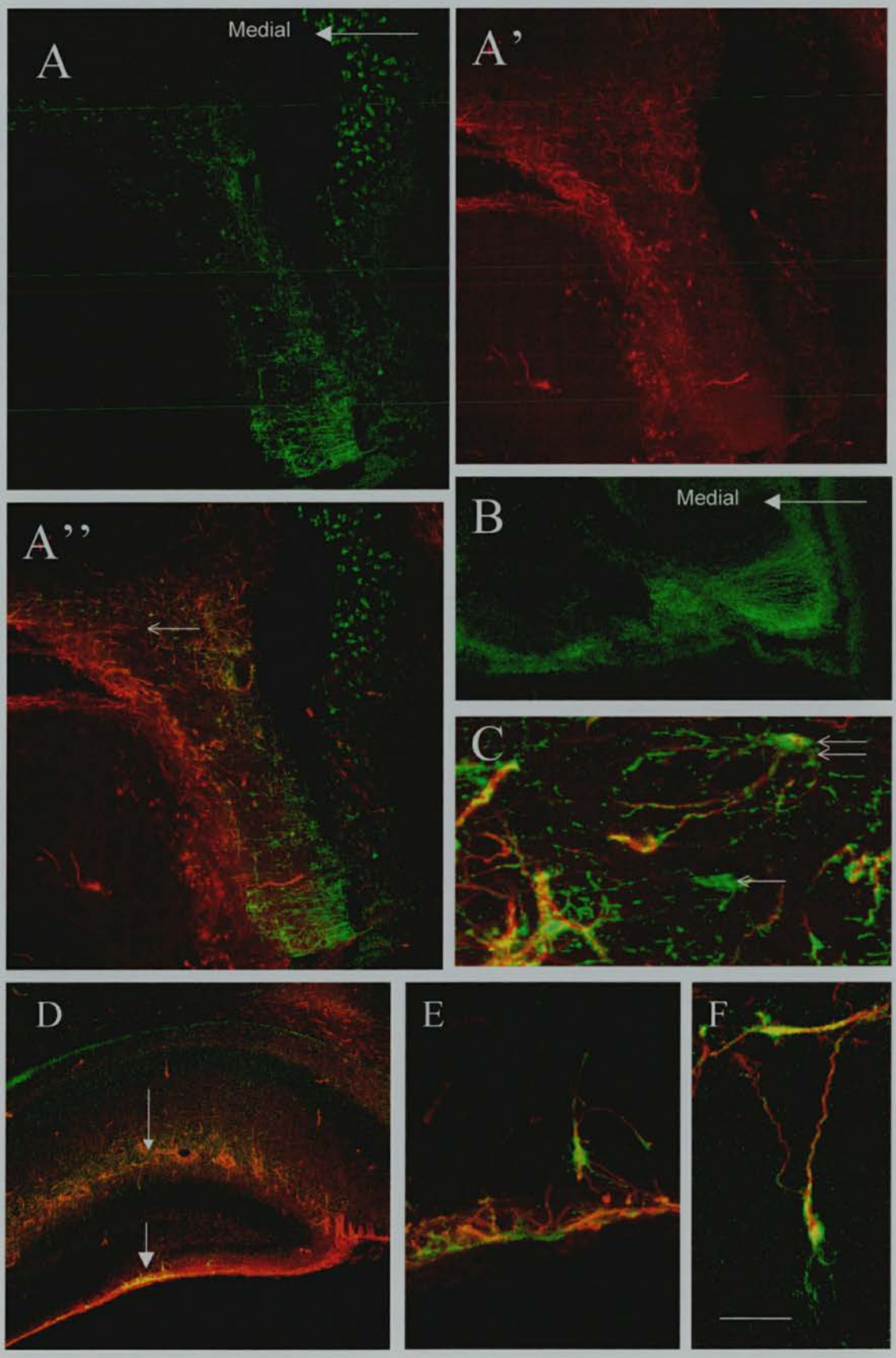

Figure IV-14 Please, see figure legend on the following page

Figure IV-14 Colocalisation of MAOB and GFAP at the level of (A-C) the fimbria and (D-F) the hippocampus. ***A-A''***, Coronal section of a P15 pup showing immunolabeling for (A) MAOB, (A') GFAP and (A'') the overlay. Note that the ventral part of the fimbria is immunolabeled for MAOB but not for GFAP. ***B,*** Coronal section of E17 embryo showing a strong MAOB immunolabeling but no GFAP immunolabeling. Please, see FigIV-9A for the location of the fimbria on coronal section. ***C,*** Higher power of the region pointed in (A'') showing an astrocyte double labelled for MAOB and GFAP (*double arrow*) and another astrocyte displaying a single label for MAOB (*arrow*). ***D,*** Coronal section of a P15 pup double labelled for MAOB and GFAP. ***E,F,*** Higher power of the areas pointed by the (E) *large arrow* and (F) *thin arrow* in (D) respectively, showing astrocytes immunolabeled for MAOB and GFAP. Scale bar: A-B, 0.5mm; C, 0.2mm; D, 1mm; E,F, 0.3mm.

Finally, beside its important role in scavenging monoamines by non-neuronal cells, this study shows a surprising coexistence of MAOB in cholinergic neurons.

1 MAOA expression is linked to the noradrenergic phenotype

Previous localization studies in the adult have shown that in all species studied, humans (Westlund et al., 1985), cats (Kitahama et al., 1994) and rats (Luque et al., 1995), MAOA is most abundantly expressed in noradrenergic neurons of the central and peripheral nervous system. In this study, I show that typical noradrenergic neurons express MAOA soon after they differentiate by embryonic day 12. Interestingly, MAOA is also transiently expressed in neurons that display a transient noradrenergic phenotype such as motor nuclei of the brainstem and Vth, VIIth, IXth and Xth cranial sensory ganglia. All these nuclei express the biosynthetic enzyme of NA, DBH (Tiveron et al., 1996) during the same developmental period as MAOA, suggesting that both genes could be co-regulated. Interestingly, recent studies have implicated two transcription factors, MASH1 and Phox2a, in the control of (nor)adrenergic differentiation (Morin et al., 1997; Hirsch et al., 1998). In particular, Phox2a has been shown to be a positive regulator of the DBH gene (Zellmer et al., 1995) and inactivation of Phox2a leads to a complete agenesis of neurons that display either a permanent or a transient noradrenergic phenotype: the LC and parasympathetic ganglia are absent, while the cranial sensory ganglia and the superior cervical ganglion are atrophic or altered (Morin et al., 1997). It is tempting to speculate that, in addition to its control of the DBH gene, Phox2a could be a positive regulator of the MAOA gene in (nor)adrenergic cell groups. Surprisingly, the other biosynthetic enzymes of NA, tyrosine hydroxylase and L-DOPA decarboxylase, are not expressed in motor nuclei suggesting that either NA could be produced from DA by specific uptake of DA or DBH could have another substrate.

2 MAOA is the principal degradative enzyme of serotonin in serotoninergic neurons during early development

Previous descriptions done in rat adult brain have already shown a moderate MAOA mRNA expression in some serotoninergic neurons (Luque et al., 1995). This study confirms this observation in mice. Interestingly, MAOA is also strongly

expressed in all serotoninergic neurons during early development. MAOA is expressed and active in all serotoninergic neurons soon after they differentiate and start producing 5-HT. Serotoninergic neurons start producing 5-HT when neurons are still in the process of migrating to their final destination (E10-E12 in mice, present study; E12 to E14 in rats, Lauder and Bloom, 1974, Lidov and Molliver, 1982a). Concomitantly, serotoninergic neurons express SERT (Schroeter and Blakely, 1996), and VMAT2 (Hansson et al., 1998, Lebrand et al. 1998). Thus, soon after they are generated, developing serotoninergic neurons are already able to produce, store, release, uptake and degrade 5-HT. Unexpectedly, with respect to previous observations in adults (Levitt et al., 1982), serotoninergic neurons express strongly MAOA during embryogenesis and early postnatal life. The shift toward the adult pattern begins by P0, when serotoninergic neurons start to co-express MAOA and MAOB. MAOB gene expression then increases progressively, while MAOA gene expression decreases to reach low levels in adult serotoninergic neurons. Since MAOA degrades more efficiently 5-HT than MAOB, the predominant presence of MAOA in serotoninergic neurons during embryonic life could be important for regulating the levels of this amine. Indirect evidences for this are the high levels of 5-HT during embryonic development and the progressive decrease of these high levels during early postnatal development in mice lacking MAOA (Cases et al., 1995 ; Lajard et al., 1999) and the fact that 5-HT levels are unchanged in mice lacking MAOB (Grimsby et al., 1997). It will be important to know whether similar mechanisms occur in humans. MAOA deficiency has been associated with mild mental retardation and behavioural abnormalities (Brunner et al., 1993a,b) whereas MAOB deficiency has not been associated with behavioural alterations. This suggests that the same mechanisms could be conserved in humans.

3 MAOB in cholinergic neurons

Earlier reports have already shown the existence of MAOB in subsets of cholinergic neurons (Nakamura et al., 1993; Ikemoto et al., 1999) and identified MAOB-expressing cells in regions containing cholinergic neurons (Ikemoto et al., 1997). This study shows the striking expression of MAOB in most of forebrain cholinergic neurons. Only cholinergic neurons of the basalis nucleus of Meynert (Ch4) do not display MAOB expression. Despite no biochemical data upon the specificity of MAOB to acetylcholine, it appears very unlikely that acetylcholine

represents a substrate for MAOB. The more likely explanation would be the elimination of trace amines that interfere with acetylcholine synthesis or storage in vesicles, although the nature of these trace amines remains unknown. Alternatively, MAOB could degrade monoamines such histamine or serotonin internalised with their own receptors. In the cytoplasm, monoamines could interfere with acetylcholine storage by acting upon the vesicular acetylcholine transporter that display a substantial resemblance with vesicular monoamine transporters (Roghani et al., 1994). However, in vitro studies have shown that monoamines are not transported by the vesicular acetylcholine transporter (Clarkson et al., 1993). Although the role of MAOB in cholinergic neurons remains speculative, its inhibition could be of importance in neurodegenerative conditions involving cholinergic neurons such as Alzheimer's disease or even aging. In Alzheimer's disease, several trials have shown the benefit of the MAOB inhibitor, deprenyl used in a low dosage; in particular it improves cognition (Birks and Flicker, 2000). Interestingly, there is a 40% decrease in MAOB activity in the brains of smokers and smoking has been shown to protect to some extent against Alzheimer's disease (Fowler et al., 1996). The mechanisms inducing neuroprotection by MAOB inhibition are not known but could include a delay in cell death (Magyar et al., 1998; Paterson and Tatton, 1998).

4 MAOB as a multipurpose scavenger

In the adult brain MAOB has been shown to be located to all ependymal and astroglial cell populations and this pattern is already present during development. I found that MAOB mRNA expression in the ventricular ependymal system, and the circumventricular organs (plexus choroid, subcommissural organs, area postrema, and pineal gland), appeared on the day of birth and increased progressively until adulthood. The known physiological role of MAOB in these structures is to protect the CNS from trace amines present in the cerebrospinal fluid (Levitt et al., 1982; Willoughby et al., 1988; Saura et al., 1992). Astrocytic expression of MAOB had the same temporal pattern of expression, starting after birth. In astrocytes the role of MAOB might be dual: i) in the vicinity of monoaminergic nerve terminals, it could degrade transmitters taken up, by the glial cells and ii) throughout the brain, it could inactivate trace amines in the extracellular space. Recent reports have shown that astrocytes are capable of high-affinity 5-HT uptake (Bel et al., 1997) and possess a

facilitated diffusion system for dopamine (Hosli and Hosli, 1997). In addition to these known locations, I found two novel and interesting locations of MAOB during development. MAOB was intensely expressed in the developing cranial and spinal nerve entry zones, in a very particular population of cells, that are most likely astrocytes (Golding et al., 1997; Golding and Cohen, 1997). It is tempting to speculate that, at this transitional zone between the CNS and the penetrating nerves these cells produce MAOB to prevent amines of the cerebrospinal fluid from penetrating into the CNS. MAOB expression in this area is transient, from E10 to P4, a period when cranial and spinal nerves cross the nerve entry zones to arborize into the CNS (Golding et al., 1997; Golding and Cohen, 1997). It has been shown that regenerating axons are able to cross the dorsal root entry zone when a dorsal root is crushed neonatally whereas they fail to re-enter the spinal cord when the crush is effected one week postnatally (Carlstedt, 1985; Carlstedt et al., 1987). This temporal coincidence suggests that MAOB could be used as a marker of astrocytic permissivity at nerve entry zones. The other new localization of MAOB uncovered by the present analysis is the expression in the olfactory epithelium. The olfactory epithelium is exposed to a variety of xenobiotic chemicals, including odorants, pheromones and airborne toxic compounds. Recently, several novel, highly abundant, olfactory-specific biotransformation enzymes have been identified: the cytochrome P-450olf (Nef et al., 1990), the olfactory UDP-glucoronosyl transferase (Lazard et al., 1990) and glutathion-S-transferase (Rama-Krishna et al., 1992). These enzymes are particularly important in the rapid termination of odorant signals and detoxification (Thornton-Manning et al., 1997). It is tempting to speculate that the physiological role of MAOB in the olfactory epithelium might also be the termination of aminergic odorant signals and the detoxification of a broad range of airborne amines. Interestingly, all these enzymes have an exceptionally high activity in the olfactory system, comparable or even higher to that measured in the liver. The increasing popularity of the nose as a route of drug administration and the increased incidences of nasal tumour associated occupations makes the study of MAOB as a xenobiotic-metabolising enzyme of the nasal cavity an important are of health-related research. Interestingly in humans DA is metabolised by MAOB whereas in rodents it is oxidised by MAOA (Neff and Yang, 1974). As a consequence, increased oxidation of dopamine (DA) by MAOB may be associated with the loss of dopaminergic neurons in the substantia nigra, which underlies Parkinson's disease.

Indeed, patients with Parkinson's disease have elevated MAOB activity in striatal astroglial cells, and the MAOB inhibitor, deprenyl, delays the progression of symptoms (Knoll et al., 1989). However, it has been suggested that deprenyl may have neuroprotective effects independent of MAOB inhibition (Tatton and Chalmers-Redman, 1996).

CHAPTER FIVE:
SEARCH FOR MOLECULES THAT COULD INFLUENCE THE DEVELOPMENT OF MONOAMINERGIC SYSTEMS-I-: A ROLE FOR THE TRANCRIPTION FACTOR PAX6?

CHAPTER FIVE :
SEARCH FOR MOLECULES THAT COULD INFLUENCE THE DEVELOPMENT OF MONOAMINERGIC SYSTEMS: A ROLE FOR THE TRANSCRIPTION FACTOR PAX6?

Note that in this study the word specification should be read TH-specification

I Abstract

In the central nervous system, the lack of the transcription factor Pax6 has been associated with early defects in cell proliferation, cell specification and axonal pathfinding of discrete neuronal populations. In this study, I show that Pax6 is expressed in discrete catecholaminergic neuronal populations of the developing ventral thalamus, hypothalamus and telencephalon. In mice lacking Pax6, these catecholaminergic populations develop abnormally: those in the telencephalon are reduced in cell number or absent whereas those in the ventral thalamus and hypothalamus are greatly displaced and densely packed. Catecholaminergic neurons of the substantia nigra (SN) and the ventral tegmental area (VTA) do not express Pax6 protein. Nevertheless, mice lacking Pax6 display an altered pathfinding of SN-VTA projections: instead of following the route of the medial forebrain bundle ventrally, most of the SN-VTA projections are deflected dorso-rostrally at the pretectal-dorsal thalamic transition zone and in the dorsal thalamic alar plate. Moreover, some catecholaminergic neurons are displaced dorsally to an ectopic location at the pretectal-dorsal thalamic transition zone. Interestingly, from the pretectal-dorsal thalamic to the dorsal thalamic-ventral thalamic transition zones, mice lacking Pax6 display an ectopic ventral to dorsal expansion of the chemorepellant/chemoattractive molecule, Netrin-1. This may be responsible for both the altered pathway of catecholaminergic fibers and the ectopic location of catecholaminergic neurons in this region.

II Introduction

1 The transcription factor Pax6

Pax6 is a member of the Pax gene family, which has nine members (Dressler et al., 1988; Walter and Gruss, 1991). All share a conserved paired box-sequence which encodes a protein that binds the DNA and influences its transcription (Kessel and Gruss, 1990). These transcription factors are highly conserved during evolution. The same DNA-binding motif has been identified in a variety of organisms such as zebrafish (Krauss et al., 1991a,b; Puschel et al., 1992), chicken (Goulding et al., 1992), nematodes, frog, turtle, mouse and human (Dressler et al., 1988; Burri et al., 1989). The paired sequence of the mouse and the human Pax6 genes share 90% homology. In addition, the sites of splicing in both the paired domain and the homeodomain are conserved in different species of vertebrates suggesting that vertebrate Pax6 genes are homologues.

Interestingly, in vitro studies have shown that Pax6 can bind and transactivate its own promoter (Plaza et al., 1993). Pax6 is able to stimulate Pax6-responsive reporter constructs in transient transfection assays and this response is critically dependent on Pax6 concentration (Czerny and Busslinger, 1995). Few genes have been identified as candidate targets for Pax6. Chalepakis et al. (1994) have identified three in vitro binding sites of Pax6 in the promoter region of the neural cell adhesion molecule L1 suggesting that Pax6 could play a direct role in regulating L1. In vitro, the gene coding for the neural cell adhesion molecule NCAM, several Pax genes and crystallin genes (Witsow and Piatigorsky, 1988) have also been shown to be direct targets of Pax6.

Mutations of the Pax genes have been associated with three congenital disorders in humans: mutations in PAX2 with autosomal dominant renal abnormalities, and optic colobomas (Sanyanusin et al., 1995); mutations in PAX3 with Wardenburg's syndrome type 1 and Klein-Wardenburgh syndrome (Baldwin et al., 1992, Hoth et al., 1993; Morell et al., 1992); and mutations in PAX6 with aniridia (Ton et al., 1991).

The role of Pax6 in the developing nervous system is far from completely understood. However, several studies have shown its direct role on eye induction, on nose and craniofacial development, in the dorso-ventral organisation of the spinal chord (Ericson et al., 1997) in the specification of neuromeric boundaries (Stoykova et al., 1996) and in thalamic development (Stoykova et al., 1996; Warren and Price, 1997). All these events (which represent a non-exhaustive list) are altered in the

several strains of mice and rat lacking Pax6. Unfortunately, the lack of Pax6 is lethal and mice lacking Pax6 die at birth limiting the possible analysis of the role of Pax6.

In the mouse, Pax6 is expressed from E8.5 (Walther and Gruss, 1991; Grindley et al., 1995) and its expression is protracted in several region of the developing brain. Interestingly, Pax6 is protractedly expressed in regions known to contain a high concentration of dopaminergic neurons such as: the olfactory bulb, the amygdala, the zona incerta and the paraventricular hypothalamic region (Stoykova and Gruss, 1994). In addition, Pax6 expression was reported in the isthmus, the presumptive region of mesencephalic dopaminergic neuron genesis and decribed in P45 mouse brain in the region of the substantia nigra (pars reticulata and pars lateral) (Stoykova and Gruss, 1994).

The pattern of Pax6 expression led me to further analyse the possible co-localisation of Pax6 and tyrosine hydroxylase, the rate-limiting enzyme for cathecholamine synthesis. I also wanted to assess the possible deleterious effect of the lack of Pax6 on catecholaminergic neurons by studying the genesis and development of catecholaminergic neurons in mice lacking Pax6.

2 Defects of tyrosine hydroxylase-immunoreactive neurons in the brains of mice lacking the transcription factor Pax6

Catecholaminergic neurons (dopaminergic, noradrenergic and adrenergic) express the rate-limiting biosynthesis enzyme, tyrosine-hydroxylase (TH), as soon as they are generated, allowing a relatively easy study of their development. Recently, a neuromeric model for catecholaminergic (CA) neuronal development has been proposed in several species, including lizard (Medina et al., 1994), chick (Puelles and Medina, 1994) and human (Puelles and Verney, 1998). In this model, it is proposed that permanent or transient CA neurons are generated in or near the region that they occupy in the adult, rather than being generated at a few localized sources and distributed through migration (Olson and Seiger; 1972). As a consequence, complex CA entities such as the substantia nigra (SN), the ventral tegmental area (VTA) or the incerto-hypothalamic axis (Hokfelt et al., 1984) are generated along several neuromeric components. Despite the apparent anatomical diversity of noradrenergic (NA) and dopaminergic (DA) neurons, it appears that their early specification relies on a small number of molecules. For instance, essential

transcription factors such as Mash1, Phox2a and Phox2b have been implicated in controlling the specification of all noradrenergic neurons (Pattyn et al., 1997; Hirsh et al., 1998). It appears that the two secreted molecules sonic hedgehog (SHH) and fibroblast growth factor 8 (FGF8) are critical for the specification of DA neurons, and the stereotypic location of most DA neurons along the antero-posterior and dorso-ventral axes is defined by the integration of these two signals (Ye et al., 1998; Hynes et al., 2000).

Gene expression studies have shown that the transcription factor Pax6 is transiently expressed in areas containing discrete CA neurons in the mesencephalon, the ventral thalamus, the hypothalamus (Stoykova and Gruss, 1994), and the olfactory bulb (Dellovade et al., 1998). *Pax6* is a member of a highly conserved gene class and encodes a transcription factor containing a paired domain and an homeodomain (Callaerts et al., 1997). The spatiotemporal expression of *Pax6*, from E8.5 to adulthood, suggested that Pax6 plays key roles in central nervous system development (Walther and Gruss, 1991; Stoykova and Gruss, 1994). Indeed, mice lacking Pax6 display early defects in axonal pathfinding (Mastick et al., 1997), in the specification of several prosomeric transition zones (Grindley et al., 1995, 1997; Stoykova et al., 1996), in cell proliferation (Warren and Price, 1997), in the specification of motor (Ericson et al., 1997) and diencephalic (Stoykova et al., 1996) cell subtypes and in cell migration (Caric et al., 1997; Brunjes et al., 1998; Engelkamp et al., 1999).

In the present study, I first defined the localisation of the Pax6 protein in TH-immunoreactive (TH-IR) populations during development. I then investigated the role of Pax6 in these populations by looking at their development in mice lacking Pax6. I found that developing TH-IR neurons of the ventral thalamus (zona incerta), hypothalamus (paraventricular nucleus), olfactory bulb and basal telencephalon (anterior olfactory nucleus, piriform cortex, anterior amygdala and olfactory tubercle) display high levels of Pax6 protein during a critical period of their development. Despite severe positional alterations, diencephalic and hypothalamic TH-IR neurons were identified in mice lacking Pax6, showing that Pax6 is not necessary for their specification. In contrast, TH-IR neurons were greatly reduced in number in the basal telencephalon and the remaining olfactory bulb. In addition, I found ectopic TH-IR neurons distributed ventro-dorsally along the pretectal-dorsal thalamic transition zone, and that TH-IR fibers and fibers immunoreactive for the

cell adhesion molecules NCAM (neural cell adhesion molecule) and L1 were misguided in this zone and in the dorsal thalamic alar plate. Interestingly, this region displayed an increased and ectopic expression of the SHH induced chemorepellant/chemoattractive molecule Netrin-1 (Leonardo et al., 1997a; Lauderdale et al., 1998) which might contribute to its having altered cues for cell migration and axonal navigation.

III Material and methods

1 Animals

The original small-eye ($Pax6^{sey}$) mutation arose spontaneously in a stock called "CSR" and was subsequently out-crossed. The genetic background of the small-eye strain used in this study was derived from the outbred Swiss background. The mating of $Pax6^{sey}/+$ (small-eye heterozygotes) was confirmed by the presence of a vaginal plug the following morning. This was designated embryonic day 0.5 (E0.5). Experiments were carried out on E11.5, E12.5, E13.5, E14.5, E16.5, E17.5 and E18.5 embryos. Embryos were dissected from deeply anaesthetised mothers into cold phosphate buffered saline (PBS) on ice and examined under a dissecting microscope. Homozygous $Pax6^{sey}/Pax6^{sey}$ embryos were easily distinguished by their absence of eyes and characteristic craniofacial phenotype of foreshortened upper jaw (Hogan et al., 1986). From E12.5, heterozygotes ($Pax6^{sey}/+$) were distinguished by the characteristic appearance of their iris lacking its inferior margin (Kaufman et al., 1995). In each experiment, wild type and $Pax6^{sey}/Pax6^{sey}$ embryos were obtained from the same litter. Some additional experiments were also carried out on embryos, postnatal and adult mice of the Swiss genetic background. Animal procedures were conducted in strict compliance with approved institutional protocols and in accordance with the provisions for animal care and use described in the "Scientific procedures on living animals ACT 1986". In all the experiments, adult mice were anaesthetised with 0.3 ml 25% urethane injected intraperitoneally.

2 Immunocytochemistry

E11.5, E12.5 and E13.5 embryos were fixed by immersion in 4% paraformaldehyde in 0.1M phosphate buffer pH 7.6 (PB). Embryos from E14.5 to

E19.5 and postnatal mice were perfused transcardially with saline followed by 4% paraformaldehyde in PB. Whole embryos or brains were post-fixed for 2-5 days in the same fixative and cryoprotected in 30% sucrose in PB. Serial coronal or sagittal sections (40 μm) were cut on a freezing microtome and immediately processed for immunocytochemistry as previously described (Cases et al., 1996). In brief, sections were incubated with the primary antibodies diluted in PBS+ (0.1M PBS with 0.2% gelatine and 0.25% Triton X-100) overnight at 4°C. Rabbit polyclonal anti-TH antibodies (1:8000; a kind gift of A.Vigny or 1:800; Protos Biotech, New-York), rabbit polyclonal anti-calretinin antibody (1:10000: Swant, Switzerland), rabbit polyclonal anti-calbindin antibody (1:20000; Swant), rat monoclonal anti-L1 antibody (1:50; Roche-Diagnostics, USA) and rat monoclonal anti-NCAM antibody (1:50; Roche-Diagnostics) were used. Biotinylated goat anti-rabbit and biotinylated goat anti-rat (1:200; DAKO, Denmark) were used as secondary antibodies and were revealed with a streptavidin-biotin-peroxidase complex (1:200; Amersham, UK). Sections were then reacted with a solution containing 0.02% diaminobenzidine, 0.6% nickel ammonium sulfate, and 0.003% H_2O_2 in 0.05M Tris buffer, pH 7.6 (DAB-Ni). From these sections, the total number of TH-IR neurons in A14PAVH and the diameters of randomly selected TH-IR neurons (n = 20) were measured in A14PAVH from E17.5 wild type (n = 4) and $Pax6^{sey}/Pax6^{sey}$ (n = 4) embryos.

3 Double Pax6 and TH immunocytochemistry

Whole embryos (E11.5, E12.5, E14.5, E16.5, E17.5 and E18.5) and dissected postnatal (P0, P2, P4 and P9) and adult brains (5 week- and 16 week-old) were immediately frozen in isopentane (-40°C) and stored at -80°C until sectioning. Coronal and sagittal sections (10 to 14 μm) were cut on a cryostat and processed the same day. Sections were dried at room temperature, fixed 10 min in methanol-acetone (1/1; -20°C), dried 15 min at room temperature, hydrated 5 min in PBS, and blocked 15 min in a solution containing 2% bovine serum albumin, 2% sheep serum, 7% glycerol and, 0.2% Tween-20 (BS). Sections were then incubated overnight at room temperature with three different antibodies: a rabbit polyclonal anti-TH antibody (1:5000; a kind gift of A. Vigny) and two mouse monoclonal anti-PAX6 antibodies (AD1.5.6 and AD2.35; 1:50 in embryos and 1:30 in adults; Engelkamp et al., 1999) diluted in BS. Sections were washed in PBS 0.2% Tween-20 (PBST) and

incubated 1 hr with secondary antibodies (TRITC anti-mouse antibody, 1:200; Vector Labs, and FITC anti-rabbit antibody, 1:200; Sigma) diluted in PB. Sections were washed in PBST and analyzed with a Leica confocal microscope (Leica TCNS, Germany). In addition, alternate sections immunostained with anti-TH antibody or anti-PAX6 antibody or Nissl-stained were analyzed in parallel.

4 Morphometric analysis

Free floating sections (45 μm) were processed for TH immunocytochemistry as described above, except that immunolabeling was revealed using a FITC anti-rabbit antibody (1:200; DAKO). Propidium iodide, a nuclear dye (1:10000; Molecular Probes, USA), was added during the last 10 minutes of incubation with the secondary antibody. This analysis was carried out on sections obtained from four wild type and four $Pax6^{sey}/Pax6^{sey}$ embryos. In each case, 7 sections from wild type embryos and 5 sections from $Pax6^{sey}/Pax6^{sey}$ embryos taken through the zona incerta (Zi) and the dorsomedial hypothalamic (DMH) nucleus were selected. By confocal microscopy (Leica TCNS, Germany), each section was re-sectioned into serial 7 μm-thick sections. To estimate the volume of A13 and A14DMH in wild type and $Pax6^{sey}/Pax6^{sey}$ embryos, the surface area of these nuclei in each section was measured using LEICA TCNS software. For each brain, volumes were obtained by multiplying each area by the thickness of tissue between sections and summing the values. To estimate cell densities in A13 and A14DMH, the same sections were analysed. In the areas defined by TH-immunoreactivity, all propidium-labelled nuclei and all cells with a visible TH-immunostaining were counted and the averages of total cell density and of TH-IR neuronal density (per mm^3) were calculated for each nucleus. From these sections, the diameters of randomly selected TH-IR neurons (n = 30) were measured in A13 and A14DMH in wild type and $Pax6^{sey}/Pax6^{sey}$ embryos using the same software.

5 Proliferation of tyrosine hydroxylase neurons

Pregnant mice were injected with a single dose of bromodeoxyuridine (BrdU; 25mg/kg in sterile saline i.p.) on E9.75, E10.5, E11.5 and E12.5 and were killed when embryos reach E17.5. Embryos were perfused transcardially with saline

followed by 4% paraformaldehyde in PB, brains were dissected, post-fixed overnight in the same fixative and cryoprotected in 10% sucrose in PB. Brains were embedded in a solution containing 7% gelatine and 10% sucrose and frozen in isopentane. Alternate coronal sections (20 μm) were cut on a cryostat and processed for sequential immunolabeling. Half of the alternate sections were reacted for both TH and BrdU. Sections were first processed for TH immunocytochemistry as described above except that only DAB was used (0.03% DAB, 0.01% hydrogen peroxide in 0.1M PBS). Then, sections were washed in TBS (0.09% NaCl, 50mM Tris, pH 7,6), incubated 8 min in 1M HCl at 60°C, washed 4 min with tap water, rinsed in TBS, incubated 10 min in 20% rabbit serum in TBS and finally incubated overnight with a solution containing mouse anti-BrdU (1:200; Becton-Dickinson, Maryland) in 20% rabbit serum-TBS. Sections were washed in TBS, incubated for 2hr with a biotinylated rabbit anti-mouse (1:200; DAKO) in 20% rabbit serum-TBS, washed in TBS, incubated with a streptavidin-biotin-peroxidase complex (1:200; Amersham) for 2 hr at room temperature and revealed with the DAB-Ni protocol (see above). The other half was Nissl-stained. To estimate the number of BrdU-labelled cells, a minimum of 6 sections taken through Zi and DMH were selected. On each section, A13 and A14DMH were identified and the number of TH-IR neurons heavily labelled (HL; defined as having more than 50 % of the nucleus immunolabeled) for BrdU was estimated using 40x and 100x objectives. Only heavily labelled cells were counted since they would have been generated at the time of BrdU administration, whereas many lightly labelled cells would have been the products of further progenitor cell divisions (Gillies and Price, 1993). For each age of BrdU injection, wild type (n = 4) and $Pax6^{sey}/Pax6^{sey}$ (n = 4) embryos were obtained from at least 2 independent litters. In addition, the total number of TH-IR neurons in A13 and A14DMH was estimated from these sections in wild type (n = 6) and $Pax6^{sey}/Pax6^{sey}$ (n = 6) embryos.

6 Nissl staining and counterstaining

Complete series of parasagittal and coronal paraffin sections (10 μm) obtained from E11.5, E12.5, E14.5, E16.5 and E18.5 wild type and $Pax6^{sey}/Pax6^{sey}$ embryos were Nissl-stained in a solution containing 0.05% thionin in acetic acid (pH 5.5).

7 In situ hybridization

E11.5, E12.5, E13.5, E14.5, E16.5 and E19.5 wild type and $Pax6^{sey}/Pax6^{sey}$ embryos were dissected in PBS, fixed and cryoprotected overnight in 4% paraformaldehyde-30% sucrose. 80-100 μm thick-sections were obtained on a freezing microtome, washed in PBS 0.1% Tween-20 (PTW), dehydrated 20 min in methanol and rehydrated in PTW before hybridization. Hybridization was performed as described in Henrique et al. (1995). Briefly, sections were treated with proteinase K (10 mg/ml) for 10 min, rinsed in PTW, fixed for 20 min in 4% paraformaldehyde-0.2% glutaraldehyde, rinsed in PTW, rinsed in the hybridization medium (50% formamide, 1.3XSSC, 50 mM EDTA, 0.2% Tween-20, 10% CHAPS, 100 mg/ml heparin) at room temperature until the sections settled and rinsed in the hybridization medium (HM) at 65°C before hybridization. Sections were then hybridized overnight at 65°C with digoxigenin-labeled (Roche Diagnostics) riboprobes for Netrin-1 (a kind gift of M. Tessier-Lavigne; EcoRI, T3: antisense; SacI, T7: sense) or Pax6 (a kind gift of S. Saule; PstI, T3: antisense; HindIII, T7: sense). The following day, sections were rinsed in HM (2 X 30 min, 65°C), washed in a 1:1 mixture of HM and MABT (100 mM maleic acid, 150 mM NaCl, pH 7.5, 0.1% Tween-20) for 10 min at 65°C and 15 min at room temperature, incubated for 1 hr in MABT with 2% blocking reagent (Roche Diagnostics) and incubated 4 hr in MABT with 2% blocking reagent and 20% of heat-treated sheep serum (MABT+) and finally incubated overnight with anti-digoxigenin antibody conjugated with alkaline-phosphatase (1:2000; Roche Diagnostics) in MABT+. Sections were washed in MABT for 4 hr and in NTMT (100 mM NaCl, 100 mM Tris-HCl pH 9.5, 50 mM $MgCl_2$, 0.1% Tween-20) for 20 min before the enzymatic color detection with the NBT/BCIP substrate (Roche Diagnostics).

8 Nomenclature

On the basis of gene expression domains and anatomical features (constrictions in the neural wall and regions of low cell density), the brain has been subdivided into neuromeres. The rhombomeric and mesencephalic organisation have been described by Lumsden (1990), Krumlauf (1994) and Guthrie (1996) and the

prosomeric organisation has been described in Rubenstein et al. (1994) and Puelles (1995). Eight consecutive rhombomeres (r1-r8), the isthmus (Is) and the mesencephalon (mes) are identified in the rhombencephalon and midbrain. Note that rhombomere 1 and isthmus are represented as a single entity (r1-Is) in this scheme. According to the prosomeric model, the forebrain is subdivided into six transverse domains called prosomeres (p1-p6). The diencephalon develops in prosomeres 1-3 (p1-p3) and the secondary prosencephalon (hypothalamus, preoptic areas and its hyper-alar extension, the telencephalon) develops in p4-p6. In addition, these transverse domains are subdivided dorso-ventrally into roof plate, alar plate, basal plate and floor plate or prechordal plate (from p4; Shimamura at al., 1995). Telencephalic organisation refers also to the work of Fernandez et al. (1998). The anatomical description refers to the atlas of the developing rat brain (Paxinos; 1991), the atlas of the mouse brain (Franklin and Paxinos, 1995) and the chemoarchitectonic atlas of the developing mouse brain (Jacobowitz and Abbott, 1998). To describe the permanent TH-IR cell groups (A1 to A17), I have mainly used the nomenclature of Hokfelt et al. (1984) and Jacobowitz and Abbott (1998). The description of the distribution of TH-IR neurons in the hypothalamus and preoptic regions also refers to the work of Ruggiero et al. (1984) and Foster (1994). A14 complex was subdivided into subgroups relative to their main anatomical locations. In addition, some transient TH-IR neuronal populations have already been described in the developing central nervous system (Jaeger and Joh, 1983; Verney et al., 1988; Nagatsu et al., 1990).

IV Results

1 Neuromeric location of TH immunoreactive groups in E14.5 wild type embryos

So far, no description of the neuromeric location of permanent and transient TH-IR groups is available in developing mice despite the increasing references to the neuromeric organisation of the brain (Bulfone et al., 1993; Rubenstein et al., 1994; Puelles, 1995; Shimamura et al., 1995; 1997). In this study I first provide a comprehensive neuromeric location of the different TH-IR groups in E14.5 wild type mice. At this age, most of the permanent TH-IR groups (A1 to A17; Hokfelt et al., 1984) occupy their definitive position, some transient TH-IR groups are detected and

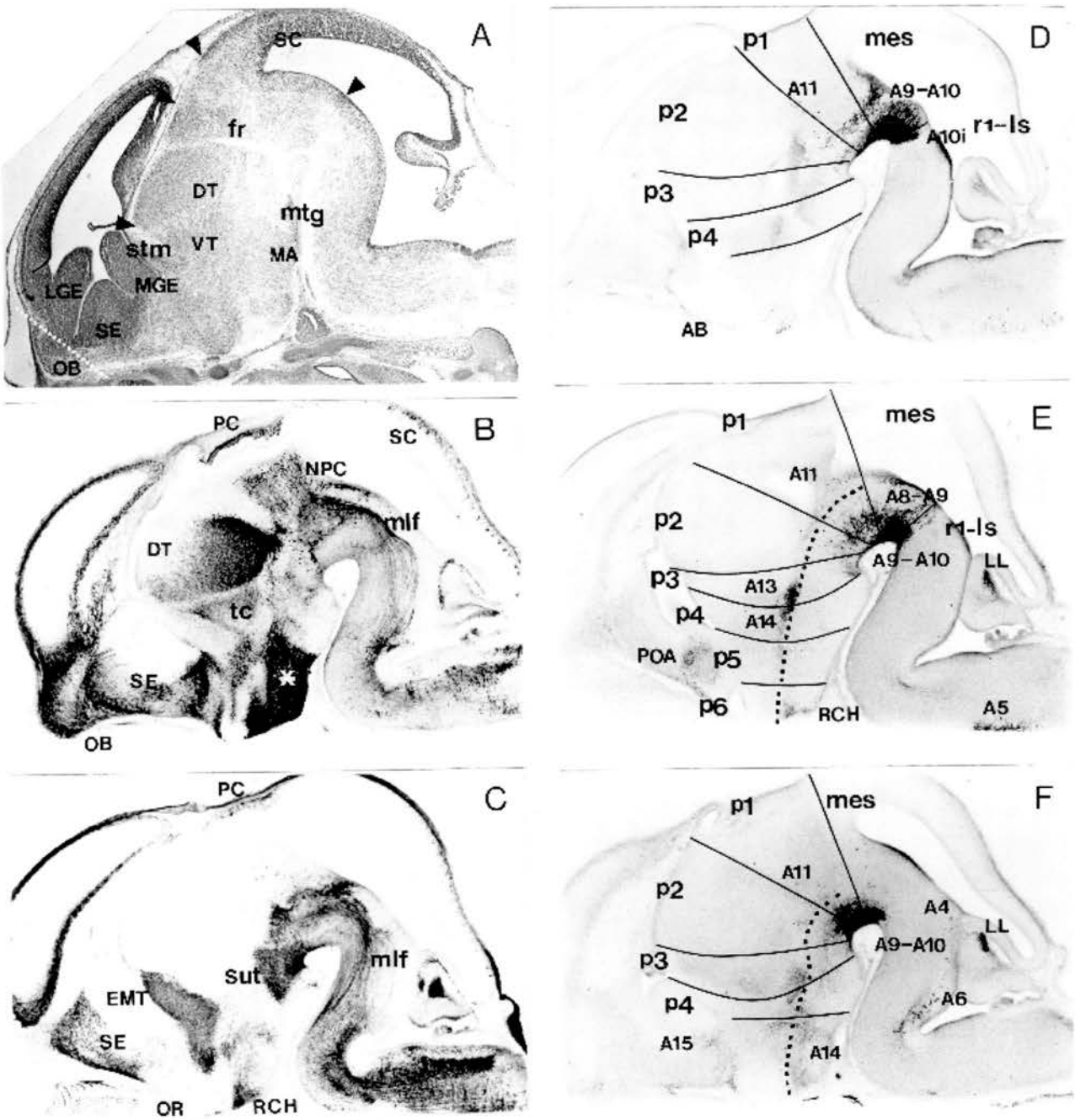

Figure V-1 Please, see figure legend on the following page.

Figure V-1 Determination of the neuromeric organisation of TH-IR neurons in E14.5 wild type embryos. Sagittal sections stained for Nissl (*A*) or immunoreacted for calbindin (*B*) or calretinin (*C*) have provided the prosomeric landmarks used for the determination of the segmental organisation of TH-IR groups as shown in (*D-F*). ***A***, The section shows constrictions in the neural wall and regions of low cell densities associated with prosomeric boundaries. *Arrowheads* indicate, from caudal to rostral, the isthmic constriction, the caudal limit of the posterior commissure (PC) at the mesencephalic (mes)-p1 boundary, the fasciculus retroflexus (fr) at the p1-p2 boundary (in p2), and the stria medullaris (stm) at the p3-p4 boundary. The *dotted line* represents the angle used for coronal sectioning. ***B***, Calbindin immunoreactivity shows the posterior commissure in the roof of p1, the nucleus of the posterior commissure (NPC) in p1, the dorsal thalamus (DT) in p2 alar plate, and thalamocortical axons (tc) running through p3 alar plate. The *asterisk* marks a strong immunoreactive hypothalamic region in p5 and p6 basal plate. The septum (SE) and olfactory bulb (OB) are also strongly immunoreactive. ***C***, Calretinin immunoreactivity shows the posterior commissure, the subthalamic nucleus (Sut) in p4 basal plate, the thalamic eminence (EMT) in p4 alar plate and the retrochiasmatic area (RCH) in p6 basal plate. The septum (SE) is also strongly immunolabelled. ***D-F***, The prosomeric boundaries (*continuous black lines*) and basal-alar limit (*dotted lines*) are deduced from the adjacent sections stained for calretinin or calbindin. Note that *B, C, E* are alternate sections. ***D***, Medial section showing a subgroup of A11 organised along the fasciculus retroflexus and the A9-A10 complex. Note that A9 is located in the basal plate and extends from mes to p2 whereas A10 is located in the floor plate and extends from the isthmic (A10i) region to p3. ***E***, A more lateral section than shown in (*D*) showing A11 extending from mes to p2 and the diencephalic and hypothalamic groups: A13 in p3, A14 in p4 and RCH and anterior preoptic (POA) areas in p6. ***F***, A lateral section shows additional groups in the hypothalamus (A14 subgroups in p5 basal and alar plates) and in the telencephalon (A15).
AB: anterobasal nucleus; Is: isthmus; LGE: ganglionic eminence, lateral part; LL: lateral lemniscal area; MA: mammillary region; mes: mesencephalon; MGE ganglionic eminence, medial part; mlf: medial longitudinal fasciculus; mtg: mammillotegmental tract; OR: optic recess; p1-p3: prosomeres; r1: rhombomere 1; SC: superior colliculus. Scale bar: *A-F*, 4 mm.

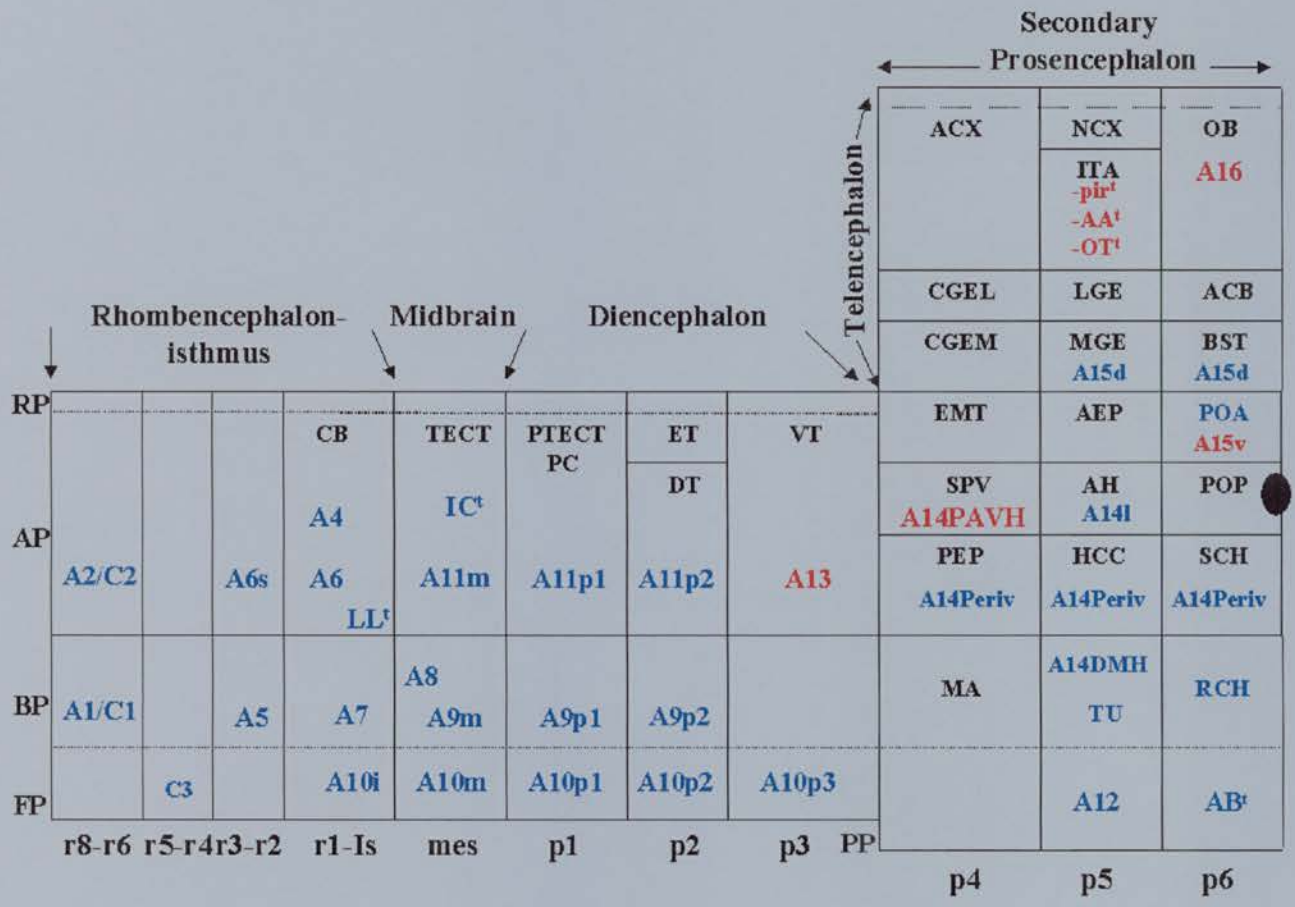

Table V-1 Please, see figure legend on the following page.

Table V-1 Mapping of the main TH-IR groups in E14.5 mouse brain. The same neuromeric criteria as those applied to describe the early neuromeric TH-IR neurons in human embryos (Puelles and Verney, 1998) were used here. According to the models described in Lumsden (1990), Krumlauf (1994), Rubenstein et al. (1994), Puelles (1995), Guthrie (1996), see also "Material and Methods: Nomenclature", the different neuromeres are individualised by longitudinal and transverse *black bars* and the different histogenetic fields are labelled in *black capitals*. The optic recess is marked with a *black circle*. In this scheme, the different TH-IR groups are mapped and appear in blue or red. Groups displaying a transient tyrosine-hydroxylase immunoreactivity are labelled with a superscript "t". Each subgroup was labelled according to its location; for instance, the isthmic component of A10 is labelled A10i where "i" stands for the isthmus, except for the transient TH-IR groups located in the piriform cortex (pir), the anterior amygdala (AA) and the olfactory tubercle (OT) which appear in the intermediate telencephalic territory (ITA), the region from which they are supposed to be derived (Fernandez et al., 1998). TH-IR groups displaying Pax6 immunoreactivity appear in red. TH-IR groups not displaying Pax6 immunoreactivity appear in blue.

A1-A17: catecholaminergic groups; AB: anterobasal nuclei; ACB: nucleus accumbens; ACX: archicortex; AEP: entopeduncular area; AH: anterior hypothalamus; AP: alar plate; BP: basal plate; BST: bed nucleus of stria terminalis; C1-C3: putative adrenergic groups; CB: cerebellar primordium; CGEL: caudal ganglionic eminence, lateral part; CGEM: caudal ganglionic eminence, medial part; DMH: dorsal medial hypothalamic nucleus; DT: dorsal thalamus; ET: epithalamus; FP: floor plate; HCC: hypothalamic cell cord; IC: inferior colliculus; Is: isthmus; LGE: lateral ganglionic eminence; LL: lateral lemniscus; MA: mammillary region; mes: mesencephalon; MGE: medial ganglionic eminence; OB: olfactory bulb; p1-p6: prosomeres; PC: posterior commissure; PAVH: paraventricular hypothalamic nucleus; PEP: posterior entopeduncular area; PF: prechordal floor plate; POA: anterior preoptic area; POP: posterior preoptic area; PP: prechordal plate; PTECT: pretectum; r1-r8: rhombomeres; RCH: retrochiasmatic nucleus; RP: roof plate; SCH: suprachiasmatic nucleus; SPV: supraoptic/paraventricular region; EMT: thalamic eminence; TECT: midbrain tectum; TU: tuberal hypothalamic region; VT: ventral thalamus.

the neuromeric limits are still visible. The topological landmarks necessary for the description of the neuromeric organisation were obtained by studying alternate sections stained for Nissl (Fig. V-1*A*) or for several differentiation markers, principally, the two calcium-binding proteins calbindin (Fig. V-1*B*) and calretinin (Fig. V-1*C*) which display complementary immunoreactive patterns (Jacobowitz and Abbott, 1998, and Figure V-1). The neuromeric location of the main discrete TH-IR groups is shown in Figure V-1*D-F* and detailed in Table V-1. The description of TH-IR groups that did or did not display Pax6 immunoreactivity in wild type mice is presented within this framework (see below and Table V-1).

2 Colocalisation of Pax6 and TH immunoreactivities

2.1 TH immunoreactive neurons displaying Pax6 immunoreactivity (Table V-1)

Pax6 immunoreactivity was detected in three dopaminergic groups of the forebrain. In the alar plate of the ventral thalamus, a subpopulation (around 40%) of TH-IR neurons of the zona incerta (A13) displayed a strong and transient Pax6 immunoreactivity from E12.5 to P9 (Fig. V-2*D,E*). This subpopulation corresponds to the body of A13. In the hypothalamus, TH-IR neurons of the magnocellular part of the hypothalamic paraventricular nucleus displayed transient Pax6 immunoreactivity from E14.5 to P2 (A14PAVH in Table V-1; data not shown). TH-IR neurons of the supraoptic nucleus (A15v) display also a transient Pax6 immunoreactivity from P0 to P9 (Table V-1; data not shown). In the telencephalon, transient TH-IR neurons located in the anterior olfactory nucleus (A16AON) displayed Pax6 immunoreactivity from E14.5 to E18.5 (Table V-1; data not shown). Transient TH-IR neurons of the piriform cortex, the olfactory tubercle and the anterior amygdala display Pax6 immunoreactivity from E14.5 to E18.5 (Fig. V-2 *G-I*). In the olfactory bulb (A16OB), TH-IR external tufted cells displayed Pax6 immunoreactivity from E14.5 and TH-IR periglomerular interneurons from E18.5 (Fig. V-2*J,K* and Table1).

2.2 TH immunoreactive neurons not displaying Pax6 immunoreactivity (Fig. V-2 and Table V-1)

Noradrenergic (A1-A7) and adrenergic (C1-C3) neurons of the brainstem never displayed Pax6 immunoreactivity (Table1). Dopaminergic neurons of the

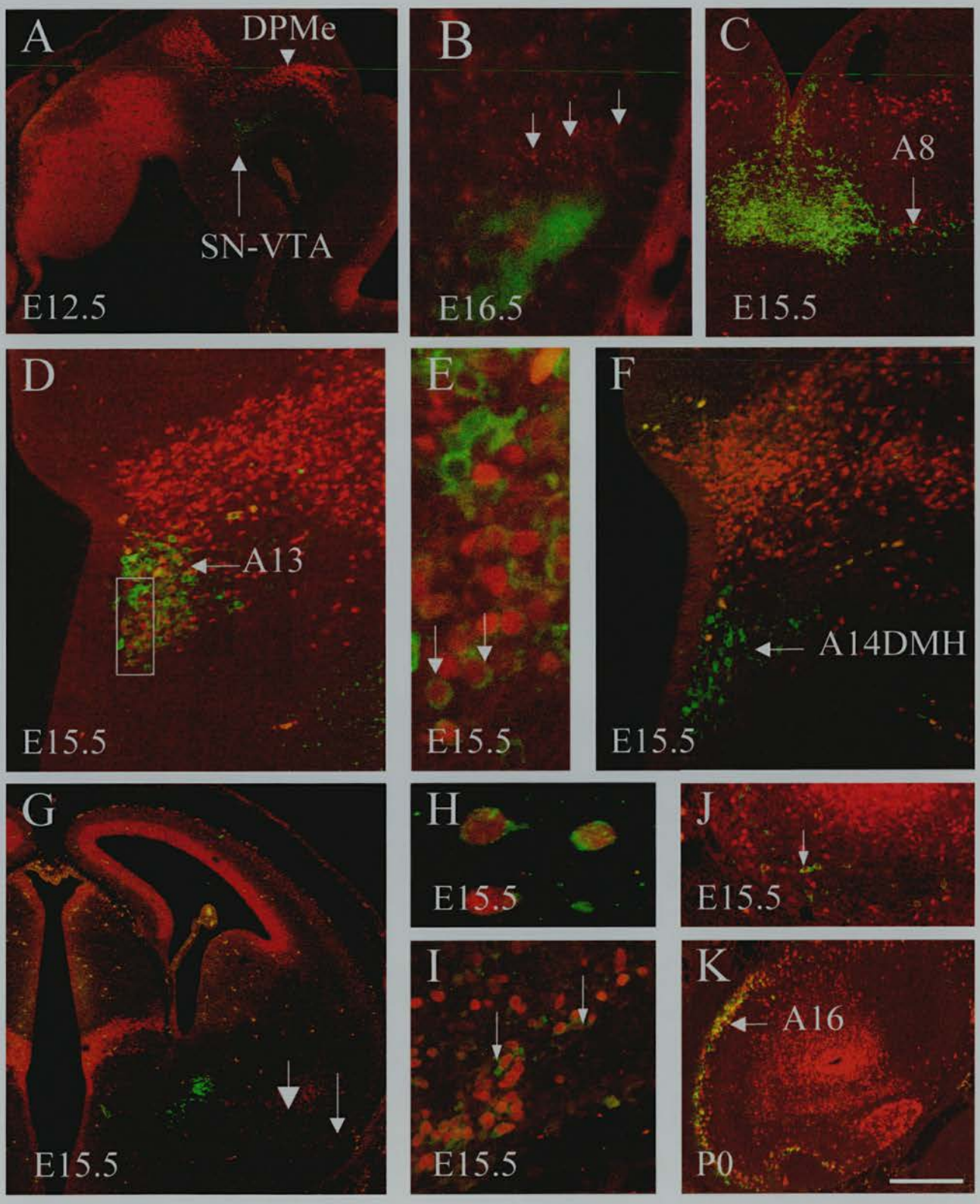

Figure V-2 Please, see figure legend on the following page.

Figure V-2 Pax6 protein expression in discrete developing TH-IR groups. Sections through the A8-A10 complex (*A-C*), the diencephalon and the hypothalamus (*D-F*), and the telencephalon (*G-K*) were double immunostained with antibodies to TH (green; cytoplasmic staining) and Pax6 (red; nuclear staining). ***A-C,*** Absence of Pax6 and TH colocalization in SN-VTA (A9-A10) complex and the retrorubral field (A8). ***A,*** The sagittal section shows a lack of Pax6 immunoreactivity in the developing SN-VTA of E12.5 embryo. Note the strong Pax6 immunolabeling of the deep mesencephalic nucleus (DPMe). ***B,*** The coronal section shows Pax6 immunoreactive cells (*short arrows*) in close proximity with TH-IR neurons of the dorsal part of the SN in E16.5 embryo. ***C,*** The coronal section shows Pax6 immunoreactive cells in the retrorubral field close to A8 neurons. ***D,*** The coronal section shows the colocalisation of TH and Pax6 in A13 neurons of the zona incerta in the ventral thalamus. ***E,*** Higher magnification of the box shown in (*D*) showing individual double immunolabeled cells *(white arrows)*. Note the presence of TH-IR neurons (A13d) that do not express Pax6 (*white arrowhead*). ***F,*** The coronal section shows the lack of Pax6 immunoreactivity in A14DMH neurons of the hypothalamus. **G,** Coronal section showing Pax6 immunoreactive cells in the basal telencephalon, Pax6 immunoreactive cells are located in the anterior amygdala (*large arrowhead*) and the region of the piriform cortex (*small arrowhead*). Note Pax6 immunoreactive cells also in the cerebral cortex, hypothalamus and ventral thalamus. ***H,*** Higher magnification of (*G)* showing individual double labelled neurons at the level of the anterior amygdala. *I,* Higher magnification of (*G*) showing individual double labelled neurons at the level of the piriform cortex (*arrows*). ***J, K,*** Coronal sections of the olfactory bulb. ***J,*** TH-IR external tufted cells display a strong Pax6 immunostaining in E15.5 embryo (*small arrow*). ***K,*** Both TH-IR periglomerular neurons and TH-IR external tufted cells in A16 display Pax6 immunoreactivity at P0. Scale bar: *A, G,* 6 mm; *B, C,* 4 mm; *D, F, J,* 1 mm; *E,* 0.25 mm; *H,* 0.12 mm; *I,* 0.5 mm, *K,* 5mm.

ventral tegmental area (A10i, A10m, A10p1, A10p2 and, A10p3) in the floor plate, of the substantia nigra (A9m, A9p1 and, A9p2) and of the retrorubral field (A8) in the basal plate, and of A11 complex (A11m, A11p1, A11p2) in the alar plate did not display Pax6 immunoreactivity throughout development (Fig. V-2*A-C*). In the hypothalamus, the TH-IR groups listed below did not display Pax6 immunolabeling at any stage of development: the lateral hypothalamic nucleus (A14l), the medial preoptic area (POA and A14d), the arcuate nucleus (A12). In the telencephalon, TH-IR neurons of the bed nucleus of the stria terminalis (A15d) did not display Pax6 immunoreactivity. Although no colocalization of TH and Pax6 was observed in TH-IR neurons of the dorsal medial hypothalamic nucleus (A14DMH, Fig. V-2*F*), Pax6 was expressed in the neuroepithelium of A14DMH during its period of genesis (from E9.75 to E12.5; see below).

3 An overview of defects in $Pax6^{sey}/Pax6^{sey}$ embryos

From E10.5 to E14.5, $Pax6^{sey}/Pax6^{sey}$ embryos displayed a delay in their growth. A marked difference in their crown-rump length was observed at E11.5 (wild type: 4.8 ± 0.3 mm, n = 15; $Pax6^{sey}/Pax6^{sey}$: 3.8 ± 0.33 mm, n = 15). By E14.5 wild type and $Pax6^{sey}/Pax6^{sey}$ embryos displayed no significant difference in their crown-rump length (wild type: 11.7 ± 0.07 mm, n = 30; $Pax6^{sey}/Pax6^{sey}$: 11.1 ± 0.1 mm, n = 30). By E17.5 brain weights were similar in wild type and $Pax6^{sey}/Pax6^{sey}$ embryos (wild type: 0.76 ± 0.07 g, n = 30; $Pax6^{sey}/Pax6^{sey}$: 0.74 ± 0.06 g, n = 25).

TH-IR groups that did or did not display Pax6 immunoreactivity were described in $Pax6^{sey}/Pax6^{sey}$ embryos within the same framework used above (see Figure V-3 for a general overview at E14.5). I observed several alterations in both Pax6-expressing TH-IR populations and TH-IR neurons that did not express Pax6, such as SN and VTA neurons. Noradrenergic (A1-A7) and adrenergic (C1-C3) neurons, and mesencephalic dopaminergic neurons of A8, which did not express Pax6 (Table V-1), displayed no delay and appeared normally organised in $Pax6^{sey}/Pax6^{sey}$ embryos. The following description will focus on TH-IR groups displaying alterations.

4 Defects in Pax6 immunoreactive components of the incerto-hypothalamic axis

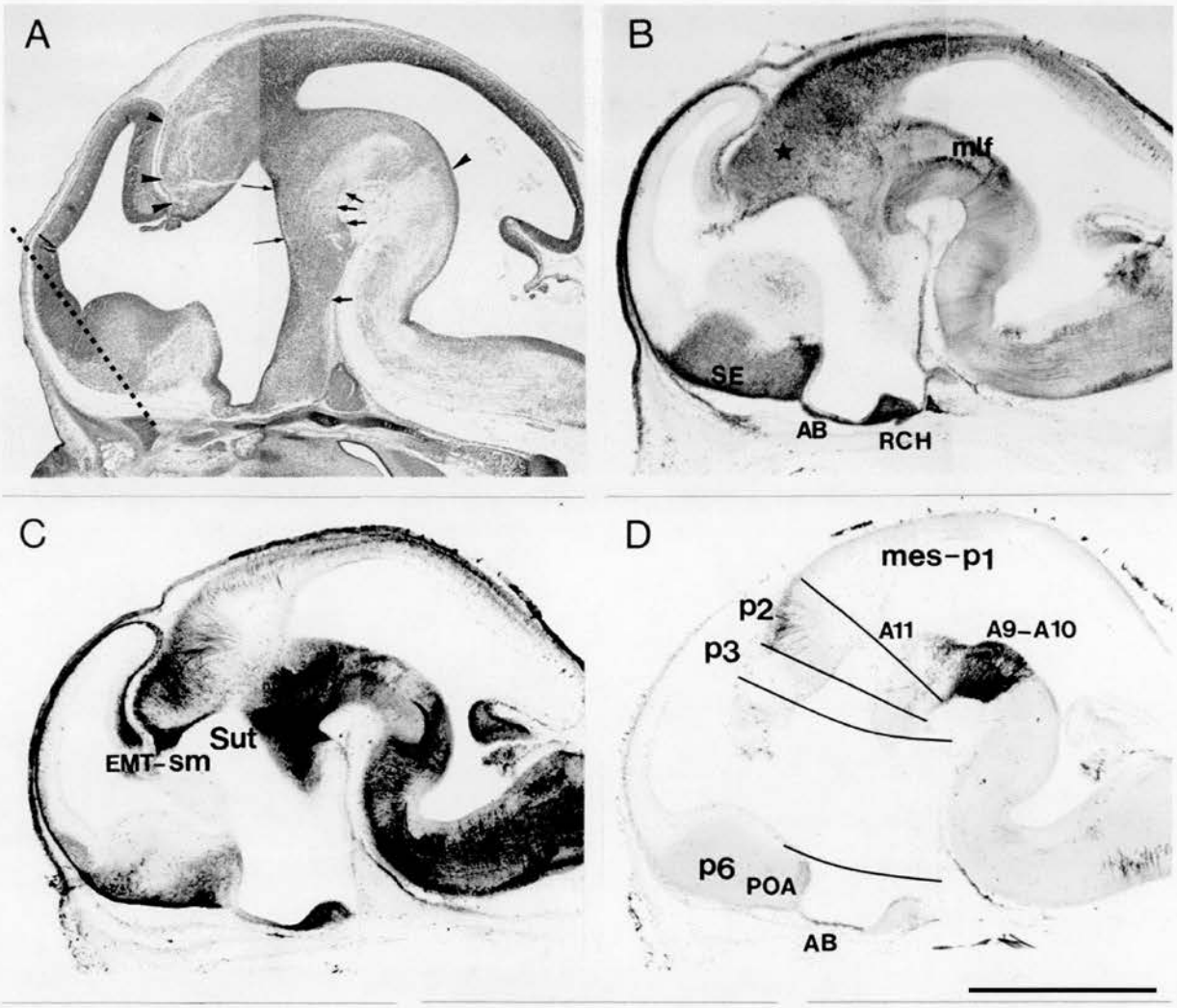

Figure V-3 Determination of the presumptive neuromeric organisation of TH-IR groups in E14.5 Pax6^{sey}/Pax6^{sey} embryos. Nissl-staining (*A*) and immunolabelling for calbindin (*B*) or, calretinin (*C*) have provided prosomeric landmarks used for the determination of the segmental organisation of TH-IR groups (*D*). ***A***, The sagittal section shows constrictions in the neural wall and regions of low cell densities associated with neuromeric boundaries. From caudal to rostral, *arrowheads* point to the isthmic constriction and the presumptive, p1-p2, p2-p3 and p3-p4 boundaries. *Thin arrows* point to the presumptive p2-p3 and p3-p4 boundaries. Arrows point to the presumptive p1-p2, p2-p3, p3-p4 and p4-p5 boundaries. The *dotted line* represents the angle used for coronal sectioning. ***B***, The sagittal section immunoreacted for calbindin shows a normal medial longitudinal fasciculus (mlf), retrochiasmatic (RCH) and anterobasal (AB) areas, and septum (SE). The *black star* indicates the lack of clustering of the presumptive dorsal thalamus and the lack of thalamocortical axons. ***C***, Sagittal section immunoreacted for calretinin shows normal immunoreactivity in the thalamic eminence (EMT), the stria medullaris (sm) and the subthalamic nucleus (Sut) in p4. ***D***, The sagittal section immunoreacted for TH shows numerous groups and complexes: A11, A9-A10 and in anterobasal and preoptic (POA) areas. The limit between mes and p1 is not indicated since this neuromeric limit is altered in the mutant (Mastick et al., 1997). Scale bar: *A-D*, 4 mm.

The incerto-hypothalamic axis (Bjorklund et al., 1975) includes TH-IR neurons of A11-A14. In this structure in normal animals, TH-IR neurons appear fused together along an axis extending from the mesencephalon to the anterior hypothalamus. In this structure, TH-IR neurons are arranged either in discrete nuclei (A12, A13, A14PAVH and A14DMH) or in a periventricular position (A11, A14Periv). A13 and A14PAVH express Pax6 transiently during development whereas A11, A12, A14DMH, A14Periv and A14l do not express Pax6.

4.1 Cell generation

In E11.5 wild type embryos, it was possible to identify scattered TH-IR neurons in the ventral thalamus at the level of the primordium of A13 and a few medium-sized TH-IR neurons of the A14 complex in p4 and p5. These cells were more numerous by E12.5 (Fig. V-4*A*). In $Pax6^{sey}/Pax6^{sey}$ embryos, the A13 and A14 primordia appeared with a two-days delay (Fig. V-4*A,B*) and, when they did first appear, they contained fewer TH-IR neurons than in wild type embryos (50% reduction estimated). This delay did not persist: by E17.5 the total numbers of TH-IR profile counts in mutants and wild types were similar in A13 (n = 600 ± 65, from 6 wild types; n = 524 ± 60, from 6 mutants; values are means ± SEM), in A14DMH (n = 510 ± 40, from 6 wild types; n = 486 ± 60, from 6 mutants) and in A14PAVH (n = 40 ± 4, from 4 wild types; n = 38 ± 3, from 4 mutants). Since the mean diameters of TH-IR neuronal cell bodies were similar in wild type (A13, n = 10 μm ± 0.7; A14DMH, n = 11 μm ± 0.7; A14PAVH, n = 12 μm ± 0.9; values are means ± SEM from 30 TH-IR neurons from 4 wild types) and $Pax6^{sey}/Pax6^{sey}$ embryos (A13, n = 11 μm ± 0.6; A14DMH, n = 10.5 μm ± 1.0; A14PAVH, n = 11.5 μm ± 0.4, values are means ± SEM from 30 TH-IR neurons from 4 mutants), this indicates that there is no difference in TH-IR cell number in these structures.

Although Pax6 is expressed in differentiated TH-IR neurons of A13 and A14PAVH but not A14DMH, Pax6 is expressed during the time of genesis of all these TH-IR populations. I have investigated a possible delay in cell generation of the cells destined for these groups in $Pax6^{sey}/Pax6^{sey}$ embryos. Cell proliferation was studied by analyzing BrdU incorporation into S-phase cells and visualizing them at E17.5 using anti-BrdU and anti-TH antibodies (Fig. V-4*C-F*). To identify the embryonic stages at which the neurons of these nuclei are generated, a single

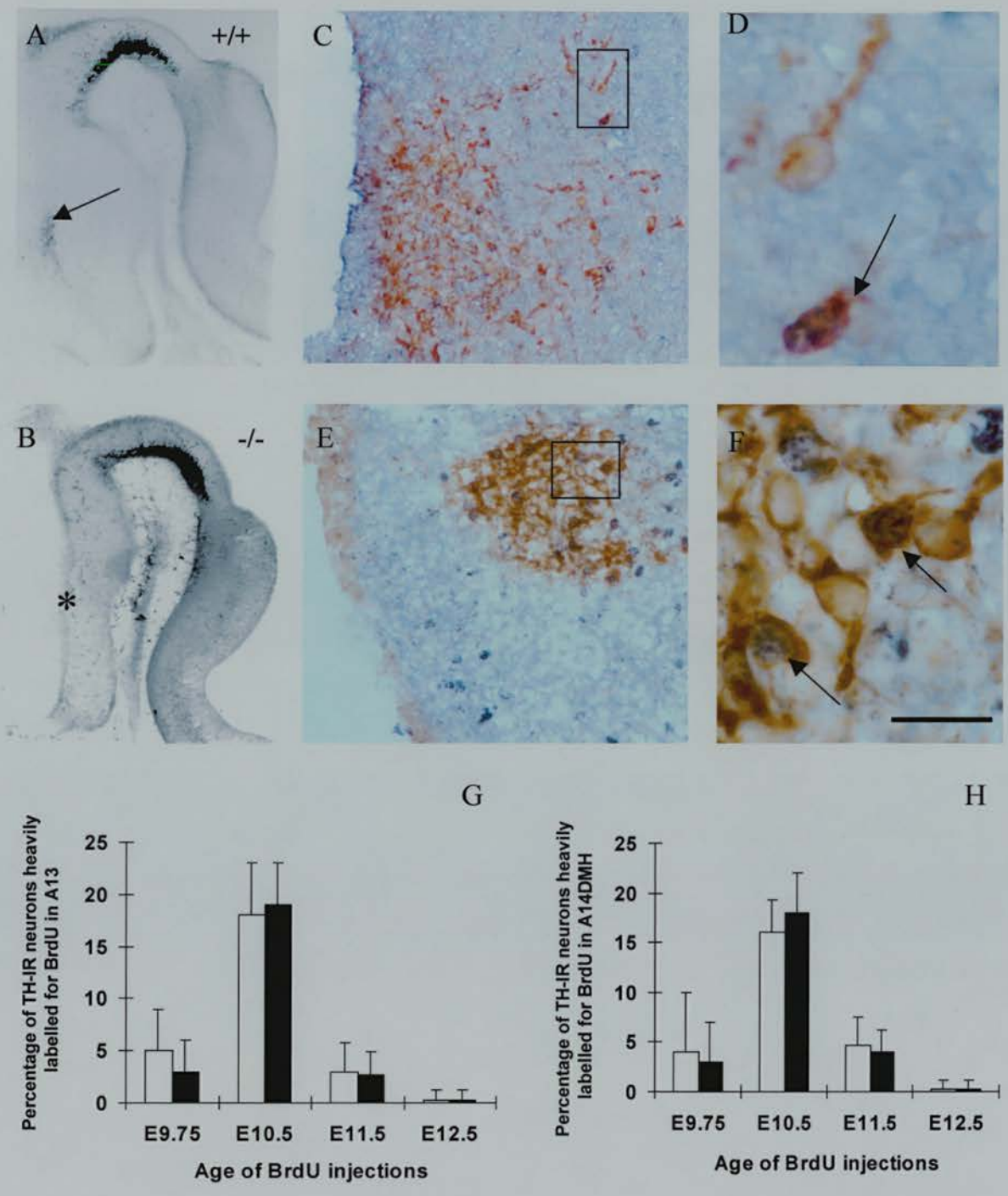

Figure V-4 Please, see figure legend on the following page.

Figure V-4 Delay in the appearance of a TH phenotype in A13 and A14DMH is not due to a cell proliferation defect. ***A, B,*** Sagittal sections of E12.5 wild type (*A*) and $Pax6^{sey}/Pax6^{sey}$ (*B*) embryos immunolabelled for TH. *A*, *arrow* points to the A13 and A14 primordia. ***B,*** The *black asterisk* indicates the presumptive location of the A13 and A14 primordia in the mutant; note the lack of TH-IR neurons in these regions. ***C-F,*** Double immunolabeling for TH and BrdU of E17.5 wild type (*C,D*) and $Pax6^{sey}/Pax6^{sey}$ embryos (*E,F*) at the level of A13. BrdU was injected on E10.5. ***D, F,*** *Arrows* point to TH-BrdU double labelled neurons. ***G, H*** Histograms showing similar mean percentages (± SEM) of TH-IR neurons darkly labelled for BrdU in A13 (*G*) and A14DMH (*H*) in wild type (*white bars*) and $Pax6^{sey}/Pax6^{sey}$ (*black bars*) E17.5 embryos following injections of BrdU on E9.75-E12.5. Scale bar: *A, B*, 2 mm; *C, E*, 0.5 mm; *D, F*, 0.1 mm.

injection was applied at four different developmental stages: E9.75, E10.5, E11.5 and, E12.5. The number of BrdU-TH-positive cells and TH-positive cells was determined on coronal sections at E17.5. The labelling index was calculated as the percentage of the total number of TH-positive cells that were BrdU-TH-positive. In wild type embryos, A13 and A14DMH are generated from E9.75 to E11.5 with a peak at E10.5 (*White bars*, Fig. V-4*G,H*). In $Pax6^{sey}/Pax6^{sey}$ embryos, the labelling index following each injection was unchanged and no delay was observed (*Black bars*, Fig. V-4*G,H*) suggesting that cell generation is unaffected in A13 and A14DMH.

4.2 Positional alterations

In wild type embryos, A13, A14DMH and A14PAVH were populated by large TH-IR neurons and appeared fused with each other from E14.5 (Fig. V-1*F*, Fig. V-5*A,C*). In $Pax6^{sey}/Pax6^{sey}$ embryos, A13, A14DMH and A14PAVH appeared greatly disjoined and abnormally shaped (Fig. V-5*E-G*). In wild type embryos, three distinct A13 subgroups were observed from E16.5 (Hokfelt et al, 1984): a dorsal group (A13d), a lateral group (Fig. V-5*B*; A13L) and a medial group (A13) (Fig. V-5*B*). In $Pax6^{sey}/Pax6^{sey}$ embryos, only two subgroups were identified in A13; they were displaced laterally from the third ventricle and appeared as a ventral round shaped group (Fig. V-5*E,F*) and as a dorsal group (Fig. V-5*F*). The presumptive A14PAVH was observed more rostrally, as a small nucleus densely packed with few TH-IR neurons (Fig. V-5*G*). The presumptive A14DMH group was laterally displaced and organised as an ovoid shaped nucleus (Fig. V-5*E,F*).

4.3 Cellular segregation

In wild type embryos, the structures of the incerto-hypothalamic axis, Zi, DMH and PAVH are each composed of several neuronal groups with different phenotypes, such as TH, neurotensin, or vasopressin neurons. In these structures, TH-IR neurons are mixed with other cell types that do not express TH (Fig. V-6*A*). In $Pax6^{sey}/Pax6^{sey}$ embryos, TH-IR neurons constituting A13, A14DMH and A14PAVH appeared more highly clustered (Fig. V-6*B*). As described above, the total number of TH-IR neurons in A13, A14DMH and A14PAVH are the same in the wild type and $Pax6^{sey}/Pax6^{sey}$ embryos (Fig. V-6*C-F*). However, the volume

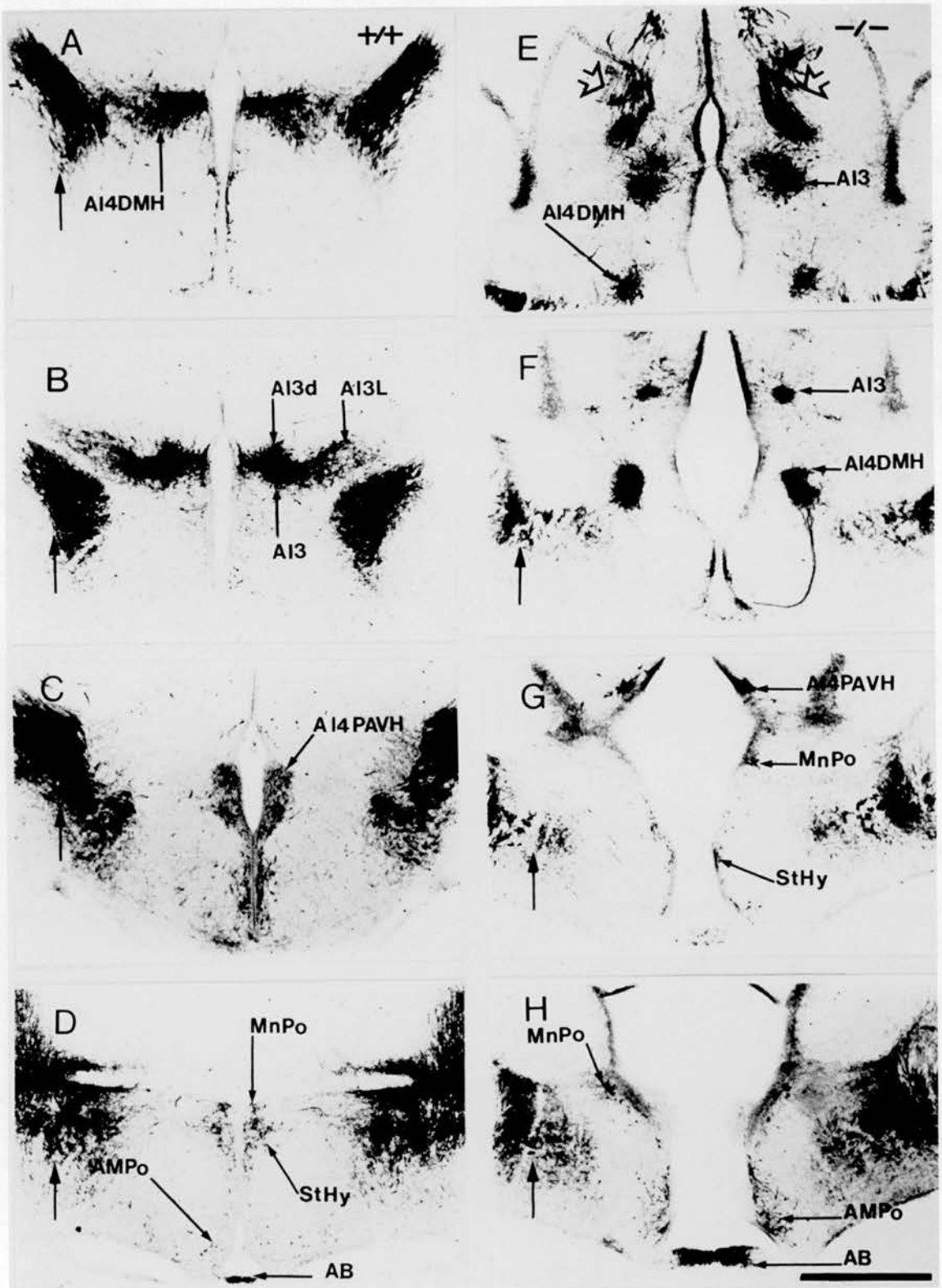

Figure V-5 Please, see figure legend on the following page.

Figure V-5 Alterations of the incerto-hypothalamic axis in E18.5 Pax6^{sey}/Pax6^{sey} embryos. Coronal sections are shown for wild type (*A-D*) and Pax6^{sey}/Pax6^{sey} (*E-H*) embryos and are organized from caudal (top) to rostral (bottom). ***A-C,*** The components of the incerto-hypothalamic axis, A13, A14PAVH and A14DMH appear fused together in wild type embryos. The medial forebrain bundle is also indicated in *A-D* and *F-H* (*large unlabelled arrows*). ***A,*** *Arrow* indicates TH-IR neurons of the A14DMH complex. *B,* TH-IR neurons of A13 are divided in three distinct groups: a dorsal group (A13d), a lateral group (A13L) and a medial group A13 (A13). **C,** *Arrow* indicates TH-IR neurons of the paraventricular hypothalamic nucleus (A14PAVH). ***D,*** Rostral section at the level of the anterior commissure showing TH-IR neurons located in the medial preoptic nucleus (MnPo), the striato-hypothalamic nucleus (StHy) and the anterobasal region (AB). ***E-G***, In Pax6^{sey}/Pax6^{sey} embryos, the components of the incerto-hypothalamic axis are completely disjoined and display abnormally high packing of the neurons. ***E,*** *Arrows* indicate A13 and A14DMH. *Open arrows* indicate abnormally located TH-IR fibers originating from the SN-VTA. ***F,*** *Arrows* indicate A13 and A14DMH. Projections from A14DMH to the area of the arcuate nucleus-median eminence are abnormally highly fasciculated. ***G, H,*** *Arrows* indicate the location of A14PAVH, StHy, the anterior medial preoptic nucleus (AMPo), MnPo and AB. Scale bar: *A-H*, 2 mm.

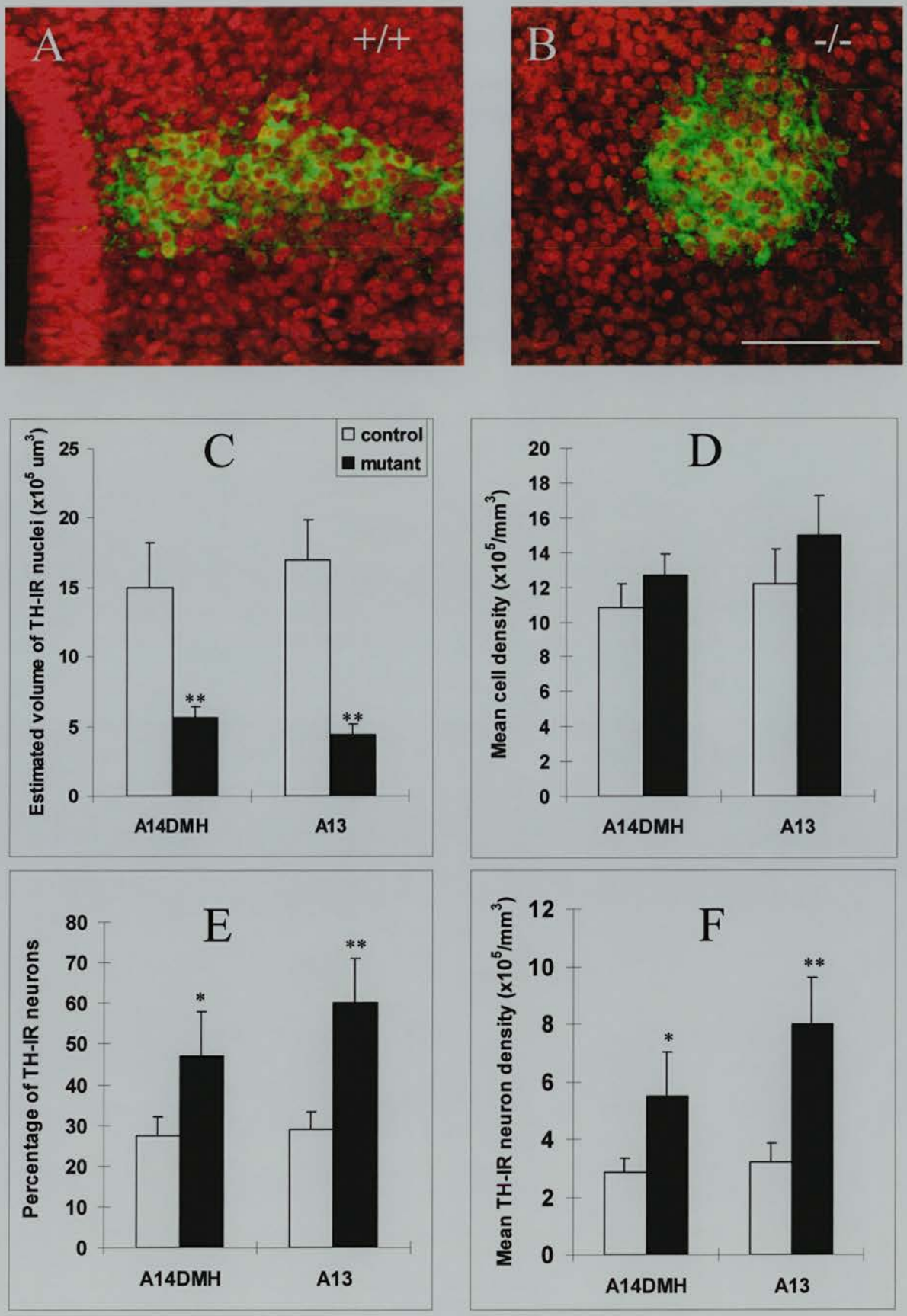

Figure V-6 Please, see figure legend on the following page.

Figure V-6 Increased cellular segregation of TH-IR neurons in A13 and A14DMH of mice lacking Pax6. TH was revealed with fluorescein-coupled antibodies (green in *A* and *B*) and nuclei were revealed on the same sections with propidium iodide (red in *A* and *B*). Pictures show the addition of two confocal images acquired simultaneously with a two-channel excitation beam. ***A***, In A13 in the wild-type embryo, TH-IR neurons were mixed with non TH-IR neurons. ***B***, In $Pax6^{sey}/Pax6^{sey}$ embryo, TH-IR neurons of A13 appeared more densely clustered and more segregated from the non TH-IR neurons. ***C***, Histogram shows the estimated volume occupied by TH-IR neurons in A14DMH and A13 in wild type (*white bars*) and $Pax6^{sey}/Pax6^{sey}$ (*black bars*) embryos. ***D***, Histogram shows that the mean cell density of propidium-positive nuclei in A14DMH and A13 was similar in wild type (*white bars*) and $Pax6^{sey}/Pax6^{sey}$ (*black bars*) embryos. ***E***, Histogram shows a significant increase of the percentage of TH-IR neurons compared to the total number of propidium-positive nuclei in A14DMH and A13 of $Pax6^{sey}/Pax6^{sey}$ embryos. ***F***, Histogram shows a significant increase in the density of TH-IR neurons in A14DMH and A13 in $Pax6^{sey}/Pax6^{sey}$ embryos. ***C-F***, Significant differences with Student's t-test between groups are indicated: $*P < 0.05$; $**P < 0.01$. Scale bar: *A, B,* 0.75 mm.

occupied by A13 and A14DMH was smaller in Pax6^{sey}/Pax6^{sey} embryos (Fig. V-6*C*). Interestingly, whereas the mean cellular density was similar between wild type and Pax6^{sey}/Pax6^{sey} embryos (Fig. V-6*D*), the cellular density of TH-IR neurons in these structures was higher in Pax6^{sey}/Pax6^{sey} embryos (Fig. V-6*F*), indicating a higher segregation of TH-IR neurons in these structures as estimated by the increased percentage of TH-IR neurons within them (Fig. V-6*E*). TH-IR neurons were more clustered or less mixed with cell types that did not express TH. This suggests altered adhesive properties of cells composing the Zi and DMH in Pax6^{sey}/Pax6^{sey} embryos.

5 Defects of TH immunoreactive neurons in the telencephalon of Pax6^{sey}/Pax6^{sey} embryos

In wild type embryos, from E14.5, TH-IR neurons were observed at the level of the bed nucleus (A15d; Fig. V-7*A*) and the anterior olfactory nucleus (A16AON; Nagatsu et al., 1990; Fig. V-8*C*). In Pax6^{sey}/Pax6^{sey} embryos, A15d was greatly reduced in cell number (Fig. V-7*C*), whereas A16AON was absent by E14.5 (Fig. V-8*G*). In wild type embryos, TH-IR neurons were also observed in the olfactory bulb as soon as E16.5 (Fig. V-8*D*). Based on their age, large soma size and the location in the developing glomerular layer, these neurons probably correspond to external tufted cells. By E18.5, a large number of TH-IR neurons were observed in the glomerular layer of the olfactory bulb, corresponding to both external tufted cells and the earliest population of periglomerular interneurons. In Pax6^{sey}/Pax6^{sey} embryos, from E16.5, only a few lightly labelled TH-IR neurons were observed at the level of the residual olfactory bulb (Fig. V-8*G*). Evidence for the development of a residual olfactory structure is provided by calretinin and calbindin immunoreactivities (Fig. V-8*E,F*). In this structure, TH-IR neurons were scattered but differentiated: they were large with angular shapes and short processes probably corresponding to the external tufted cells (Fig. V-8*H*). The reduction in the mutant of TH-IR neurons in A15d (Fig. V-7*C*) and A16 (Data not shown) persisted in older Pax6^{sey}/Pax6^{sey} embryos. No small TH-IR neurons corresponding to the periglomerular interneurons were observed in older Pax6^{sey}/Pax6^{sey} embryos.

In wild type embryos, from E16.5, TH-IR neurons were observed at the level of the strio-hypothalamic nuclei (Fig. V-5*D*). In Pax6^{sey}/Pax6^{sey} embryos, despite the

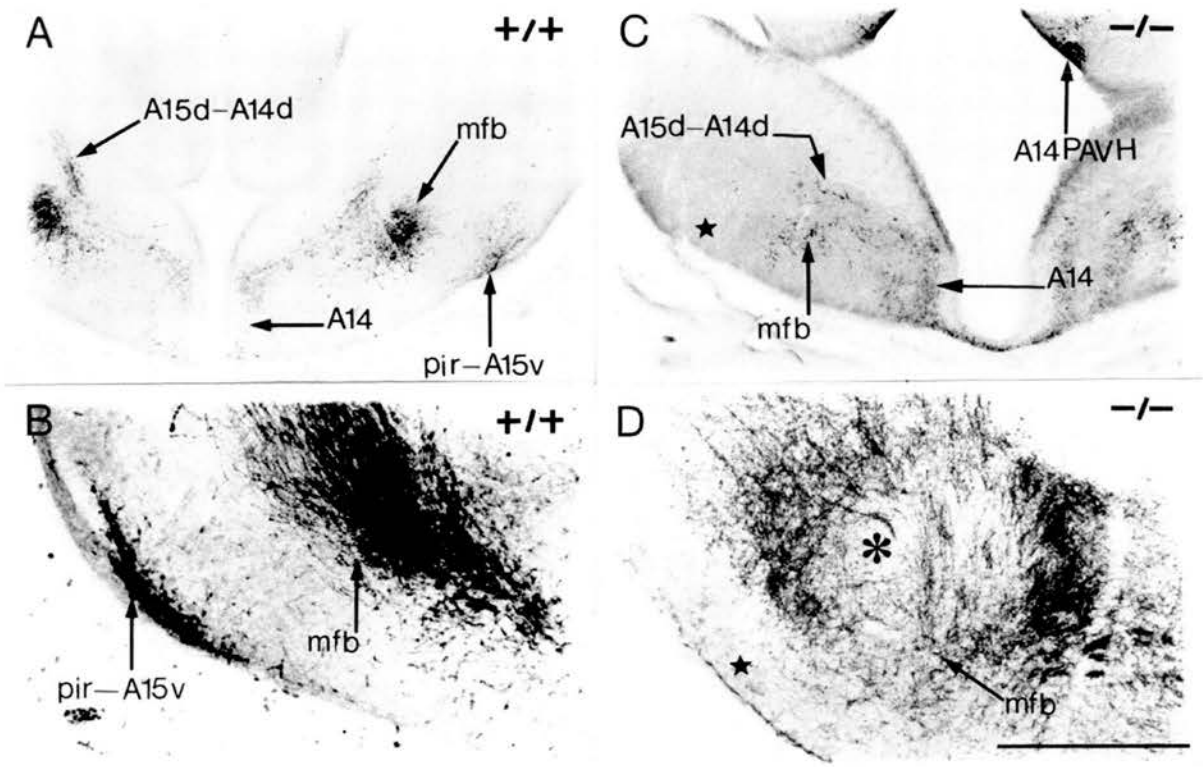

Figure V-7 Defects of the telencephalic TH-IR neurons in Pax6^{sey}/Pax6^{sey} embryos. Coronal sections through the basal telencephalon and hypothalamus of E14.5 (*A, C*) and E18.5 (*B, D*) wild type (*A, B*) and Pax6^{sey}/Pax6^{sey} (*C, D*) embryos. ***A***, The section shows both the transient TH-IR neurons of the piriform cortex (pir) and the permanent TH-IR groups of A15v and A15d in continuation with A14d. Note the location of the medial forebrain bundle (mfb). ***B***, High magnification of the pir-A15v area. ***C***, The section shows a reduced A15d still in continuation with A14d. The *black star* indicates the lack of pir-A15v at the presumptive level of the rhinal fissure. ***D***, The lack of pir-A15v persists in older age embryos (*black star*). The *large asterisk* indicates the abnormal swirl of TH-IR fibers at the medial forebrain bundle (mfb). Scale bar: *A-E*, 2 mm.

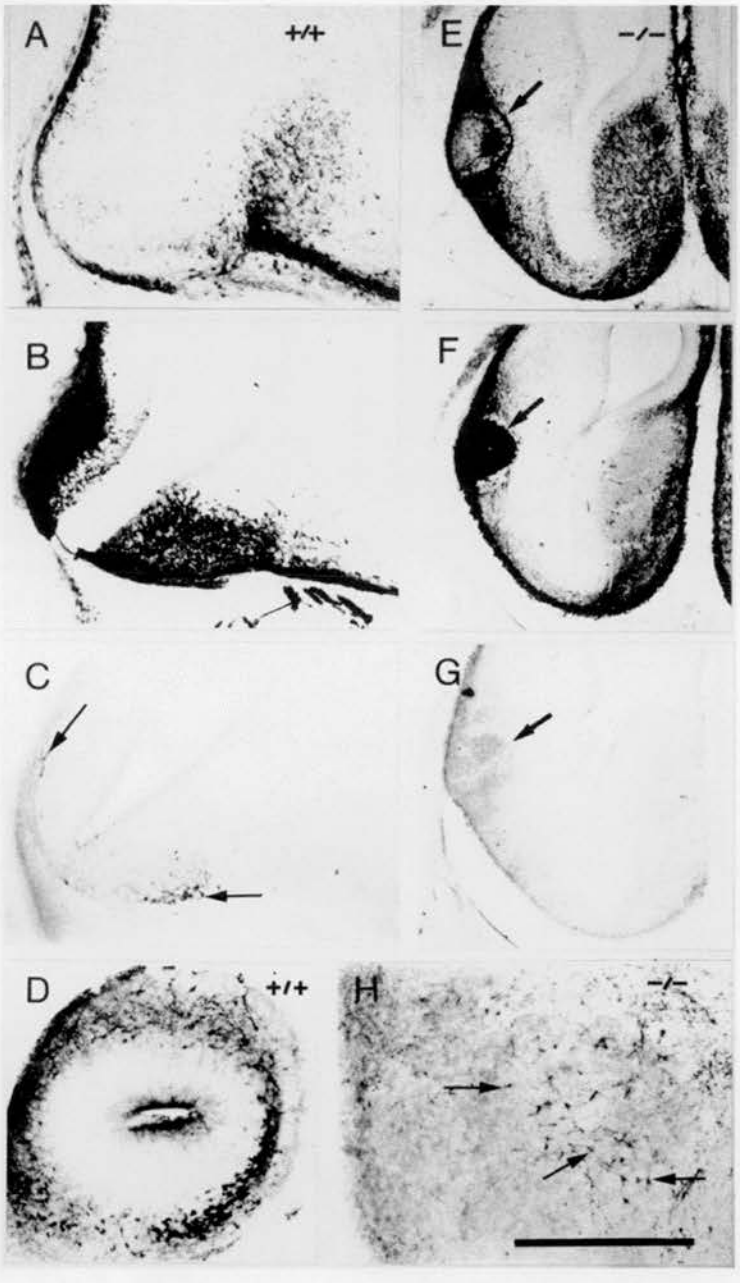

Figure V-8 Delay and diminution in the number of A16 neurons in the anterior olfactory nucleus and the residual olfactory structure of Pax6^{sey}/Pax6^{sey} embryos. Sagittal (*A-C*) and coronal (*D-H*) sections are shown for E14.5 (*A-C, E-G*) and E16.5 (*D, H*) wild type (*A-D*) and Pax6^{sey}/Pax6^{sey} (*E-H*) embryos. Alternate sections are immunostained for calbindin (*A, E*), calretinin (*B, F*) or TH (*C, F*). ***A***, Calbindin immunoreactivity labels short axon cells of the olfactory bulb. ***B***, Calretinin immunoreactivity labels mitral and tufted cells of the olfactory bulb. ***C***, *Arrows* indicate neurons of A16 in the anterior olfactory bulb in A16AON. ***D***, Section showing TH-IR external tufted cells in the olfactory bulb of E16.5 wild type embryo. ***E***, Calbindin immunoreactivity strongly labels cells that may correspond to short axon cells. ***F***, Calretinin immunoreactivity strongly labels cells that may correspond to the mitral and tufted cells of the remaining olfactory bulb. ***G***, TH-IR neurons are absent in the remaining olfactory structure of E14.5 Pax6^{sey}/Pax6^{sey} embryo. *E-G Arrow* points to the residual olfactory structure. ***H***, High magnification shows scattered TH-IR neurons with short processes (*arrows*) in the residual olfactory bulb of E16.5 Pax6^{sey}/Pax6^{sey} embryo. Scale bar: *A-C, E-G,* 2 mm; *D, H*, 1 mm.

lack of the anterior commissure, TH-IR neurons were observed at the presumptive level of the strio-hypothalamic nucleus (Fig. V-5*H*).

In addition, transient TH-IR neurons were observed in the piriform cortex (nearby to A15v, Fig. V-7*A,B*) from E14.5 to E18.5 and in the anterior amygdala (data not shown) and olfactory tubercle (data not shown) from E16.5 to E18.5 in wild type embryos. In $Pax6^{sey}/Pax6^{sey}$ embryos, TH-IR neurons were rare round and pale (n = 15 ± 4, values are mean ± SEM from 4 mutants; n = 90 ± 10, values are mean ± SEM from 4 wild types) at the presumptive level of the anterior amygdala. By E18.5, TH-IR neurons were not detected and no pyknotic profiles were observed in this region. This suggests that these neurons were generated and had progressively lost their ability to maintain TH expression. TH-IR neurons were never observed in the presumptive olfactory tubercle, the piriform cortex (Fig. V-7*C,D*) and the neighbouring hypothalamic A15v (Fig. V-7*C*) and at any age studied in $Pax6^{sey}/Pax6^{sey}$ embryos.

6 Defects in TH immunoreactive groups not expressing Pax6

6.1 Defects in the SN-VTA (A9-A10) and A11 complex

In wild type embryos, from E11.5 to E13.5, TH-IR neurons of the primordium of the ventral tegmental area (A10i, A10m, A10p1, A10p2 and, A10p3) and of the substantia nigra (A9m, A9p1, and A9p2) migrate radially from their proliferative zones to more superficial positions (Kawano et al., 1995). These cells are shown in Figure V-9*A*. In $Pax6^{sey}/Pax6^{sey}$ embryos, by E11.5, TH-IR neurons of A9m and A9p1 and of A10m and A10p1 were normally radially organised suggesting that they were normally migrating to their ventral positions (data not shown). At this age, TH-IR neurons of A10p2 and A10p3, in the p2-p3 floor plate of the mutants, were less numerous than in wild type (75% reduction estimated). By E12.5, whereas sagittal medio-lateral sections of wild type embryos showed that the oldest TH-IR neurons of A9p1 and A9p2 were oriented caudo-rostrally in p1 and p2, in $Pax6^{sey}/Pax6^{sey}$ embryos, very few radially oriented TH-IR neurons were observed on medial-most sections in mes, p1, p2 and p3. Strikingly, in medio-lateral and lateral sections TH-IR neurons of A9 were abnormally positioned along the presumptive p1-p2 transition zone (Fig. V-9*E* compare with Fig. V-9*A*).

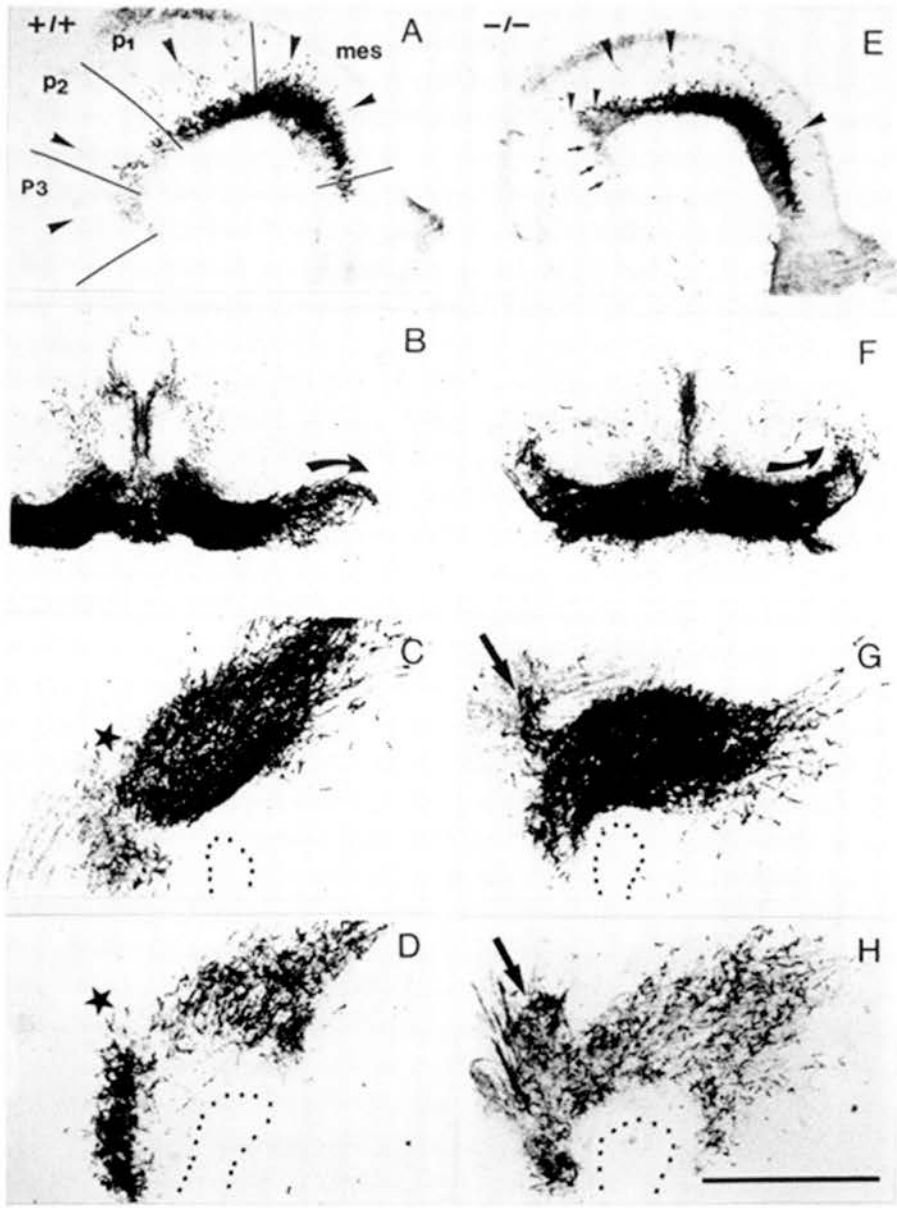

Figure V-9. Developmental defects of the SN-VTA complex in Pax6^{sey}/Pax6^{sey} embryos. ***A***, Sagittal section showing the developing SN-VTA complex of E12.5 wild type embryo. *Arrowheads* indicate the radially oriented TH-IR neurons from mes to p3. Note that TH-IR neurons of A10 in p3 (A10p3) display a less intense immunoreactivity. ***B***, Coronal section of E18.5 wild type embryo showing the characteristic topographical "inverted fountain-like" organisation of the SN-VTA complex. ***C, D,*** Medial (*C*) and lateral (*D*) sagittal sections of E18.5 wild type embryo showing the organisation of the SN-VTA complex. ***E***, Sagittal section of the developing SN-VTA complex in E12.5 Pax6^{sey}/Pax6^{sey} embryo showing the abnormal topographical organisation of TH-IR neurons in p1 and p2 (*small arrowheads*). *Small arrows* point to A10p3. *Large arrowheads* point to radially migrating TH-IR neurons. ***F***, The coronal section shows the abnormal topographical organisation of the SN-VTA complex in an E18.5 Pax6^{sey}/Pax6^{sey} embryo. *B, F*, *Curved arrows* emphasise the topographical organisation of dopaminergic neurons of the SN and the main direction of their neuropils. *G, H*, Medial (G) and lateral (H) sagittal sections of E18.5 Pax6^{sey}/Pax6^{sey} embryo. The *arrows* point to TH-IR neurons abnormally located along the p1-p2 border and in p2. *C, D,* The *black star* indicates the lack of TH-IR neurons in wild type embryo at the corresponding location where ectopic TH-IR neurons are seen in the mutant. Scale bar: *A, E,* 2 mm; *B, F,* 1 mm; *C, D, G, H,* 0.5 mm.

In wild type embryos, the number of radially oriented TH-IR neurons detected in the vicinity of the ventricular surface gradually decreased by E13.5. By E14.5, most A9 and A10 neurons had reached their final locations in more superficial positions of the ventral floor plate and basal plate, respectively, and were oriented parallel to the ventral pial surface. From E16.5, TH-IR neurons of the A9 complex displayed their characteristic "inverted fountain" pattern (Hanaway et al., 1971; Kawano et al., 1995). This arrangement was even more striking in embryos of older stages (Fig. V-9B). Strikingly, in $Pax6^{sey}/Pax6^{sey}$ embryos, from E16.5, defects in the topography of A9 neurons were accentuated at the p1-p2 border and, in p2, A9 did not show its characteristic "inverted fountain" organisation (compare Fig. V-9*F* and Fig. V-9*B*). On sagittal sections TH-IR neurons accumulated abnormally at the p1-p2 border in $Pax6^{sey}/Pax6^{sey}$ embryos (Compare Fig. V-9*C* with Fig. V-9*G* and, Fig. V-9*D* with Fig. V-9*H*). Taken together, these results suggest defects in the migration of TH-IR A9 and A10 neurons in the mutant.

6.2 TH-IR fiber pathway alterations in $Pax6^{sey}/Pax6^{sey}$ embryos

In wild type embryos, by E11.5, nigrostriatal and mesocortical fibers originating from A9 and A10 followed the pathway of the medial forebrain bundle (mfb) in mes, p1, p2, p3, and p4 basal plate. By E14.5, nigrostriatal fibers terminated in the lateral portion of the caudate-putamen (Fig. V-10*A*) whereas mesocortical fibers continued rostrally to reach the prefrontal cortex and the striatum by E15.5. In addition, a few TH-IR fibers originating from A10 were observed running along the fasciculus retroflexus toward the epithalamus (Skagerberg et al., 1984). By E18.5, the caudate-putamen and the globus pallidus were homogeneously labelled and a denser band of terminals was visible under the external capsule (Fig. V-10*K*). Mesocortical fibers emerged from mfb entered the olfactory tubercle or ramified into the ventral lateral part of the nucleus accumbens (Fig. V-10*K*). The remaining mesocortical TH-IR fibers turned dorsally to enter the medial, prefrontal, and anterior cingulate cortices (Schlumpf et al., 1980; Verney et al.,1982; Voorn et al., 1988, and present study).

In $Pax6^{sey}/Pax6^{sey}$ embryos, by E11.5, most TH-IR fibers did not follow the pathway of mfb. Fibers were misguided along the presumptive p1-p2 transition zone where they followed a straight ventro-dorsal course (Fig. V-10*B,C*). A few fibers

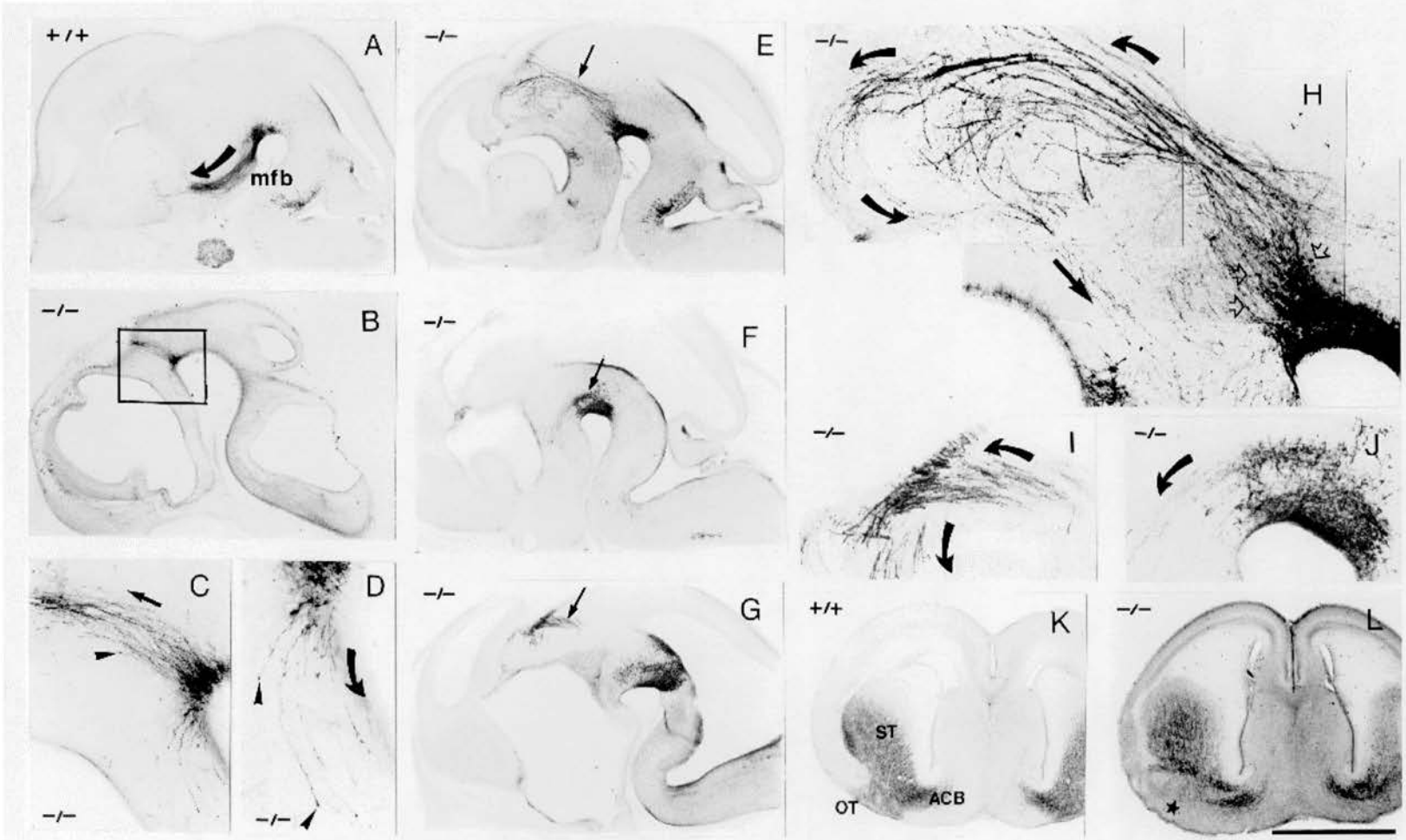

Figure V-10 Please, see figure legend on the following page.

Figure V-10 Alterations of TH-IR fibers pathway in Pax6^{sey}/Pax6^{sey} embryos. Sagittal (*A-J*) and coronal (*K-L*) sections are shown for wild type (*A, K*) and Pax6^{sey}/Pax6^{sey} (*B-J; L*) embryos. Embryos were sectioned at E11.5 (*B-D*), E14.5 (*A, E-J*) and E18.5 (*K, L*). *Large arrows* indicate the direction of the fibers. ***A***, *Large arrow* indicates the direction of the medial forebrain bundle (mfb), the major fiber pathway originating from TH-IR neurons of the SN-VTA complex. ***B***, The sagittal section shows early alterations of TH-IR fiber pathway. ***C, D*** *Small arrowheads* point to growth cones. ***C***, Higher magnification of area outlined in (*B*), showing that most of the TH-IR fibers are abnormally deflected dorsally following the presumptive pretectal-dorsal thalamic boundary. ***D***, Higher magnification of area outlined in (B) shows that some TH-IR fibers are not deflected dorsally. ***E***, A lateral section shows a high number of fibers from the SN-VTA complex misguided in the diencephalic alar plate (*arrow*). *F*, A medio-lateral section of Pax6^{sey}/Pax6^{sey} embryos indicating neurons of the SN and their projections. *Arrow* indicates some TH-IR neurons of the SN that are not misguided. ***G***, A medial section shows TH-IR fibers looping in the roof of the diencephalon (*arrow*). ***H, I, J,*** are higher magnifications of (*E, G, F*) respectively. *H*, Reconstruction of TH-IR fiber pathway. ***K***, The coronal section shows the main projecting areas of TH-IR fibers, the striatum (ST), the nucleus accumbens (ACB) and the olfactory tubercle (OT). ***L***, TH-IR fibers terminated normally in the striatum and the nucleus accumbens of Pax6^{sey}/Pax6^{sey}embryo. The *black star* indicates a lack of terminals in the olfactory tubercle. Scale bar: *A, E*-G, *K, J,* 4 mm; *B*, 2 mm; *C, H-J,* 1 mm; *D*, 0.5 mm.

originating from the more rostral and ventro-medial neurons of the A9-A10 complex followed the pathway of the presumptive mfb (Fig. V-10*D*), although they only reached p4 by E12.5. By E14.5, misguided TH-IR fibers looped in the roof of p2, plunged medio-laterally following the presumptive p2-p3 border and turned rostro-ventrally in p3 basal plate to reach and follow the pathway of the presumptive mfb in p4 and p5 (Fig. V-10*E-J*). In addition, few TH-IR fibers looped rostrally in presumptive p2 alar plate (Fig. V-10*E,G*). In their ascending and descending courses, TH-IR fibers appeared abnormally highly fasciculated (Fig. V-10*H*). At the presumptive level of the internal capsule and the optic tract, TH-IR fibers swirled just before they entered the caudate putamen (Fig. V-7*D*). From E18.5, at least some TH-IR fibers reached the same rostral levels as observed in wild type embryos, although the number of terminals was greatly reduced, particularly in the olfactory tubercle (Fig. V-10*L*).

7 General fiber pathway alterations in Pax6^{sey}/Pax6^{sey} embryos

Using the neuronal cell adhesion molecules NCAM and L1 as general markers of most axonal pathways, I analyzed whether alterations of TH-IR axons in the presumptive diencephalon were a selective defect of catecholaminergic fibers or a general defect of all ascending and descending fibers.

NCAM (from E11.5 to E13.5) and L1 (from E14.5) immunoreactivities revealed most of the fiber pathways travelling in the diencephalon. In wild type embryos, the posterior, pretectal and tectal commissures, the fasciculus retroflexus and the stria medullaris were labelled with NCAM (Fig. V-11*B*) or L1 (Fig. V-11*E*). In addition, the zona limitans intrathalamica (Zli) at the p2-p3 boundary displayed NCAM immunoreactivity from E11.5 to E13.5 (Fig. V-11*B*).

In Pax6^{sey}/Pax6^{sey}embryos, fibers travelling medially followed a normal trajectory in the basal plate of the rhombencephalon, mes, p1, p2 and p3 whereas fibers located laterally in basal plate and alar plate were misguided at the presumptive p1-p2 transition zone and in p2 alar plate (Fig. V-11*D,F*). In p2, most of the L1 immunoreactive fibers were highly fasciculated into several straight and parallel bundles (Fig. V-11*F*). In the roof of p2, most fibers looped and descended at the presumptive p2-p3 limit.

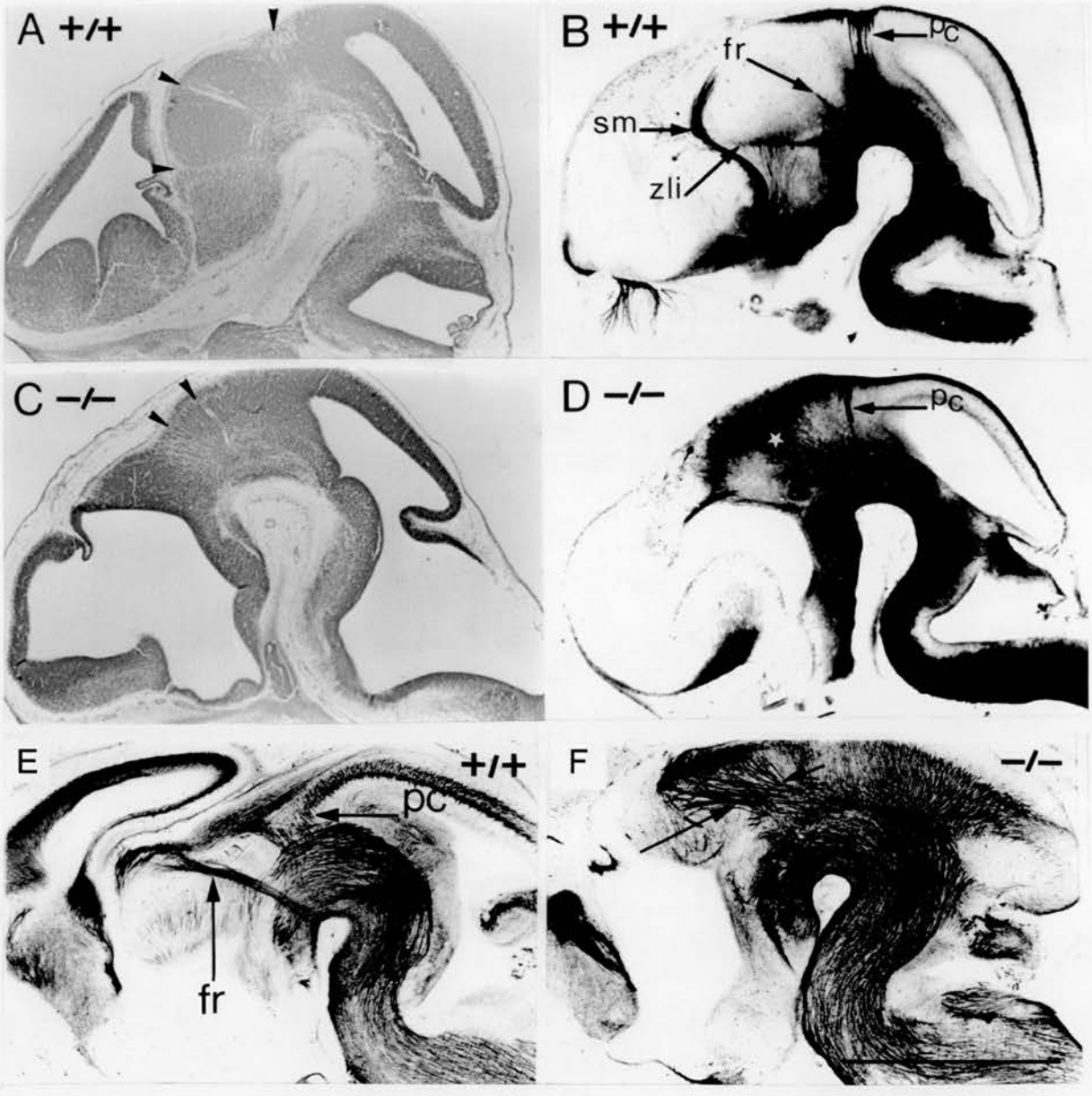

Figure V-11 Alterations of specific fiber pathways in Pax6^{sey}/Pax6^{sey}embryos. Sagittal sections are shown for E12.5 wild type (*A, B*) and Pax6^{sey}/Pax6^{sey} (*C, D*) embryos. Nissl-stained sections (*A, C*) are shown in parallel with sections immunoreacted for NCAM (*B, D*). ***A, C,*** The sagittal section shows constrictions and regions of low cell densities associated with prosomeric boundaries. ***A, C,*** *Arrows* indicate, from caudal to rostral, the mes-p1 boundary and the p1-p2 boundary. ***B,*** NCAM immunoreactivity reveals ascending and descending fibers of the posterior commissure (pc), the fasciculus retroflexus (fr), the stria medullaris (sm) and thalamic axons. A cellular labelling also reveals the zona limitans intrathalamica (Zli). ***D,*** A remaining pc is distinguishable in p1 but most of the fiber tracts are misguided in the diencephalon (*white arrowhead*). ***E, F*** Sagittal sections immunoreacted for L1 are shown for E18.5 (E) wild type and (F) Pax6^{sey}/Pax6^{sey} embryos. ***E,*** The sagittal section shows the posterior commissure (pc) in the caudal part of the pretectum and the fasciculus retroflexus (fr) at the pretectal-dorsal thalamic transition zone. ***F,*** The sagittal section shows aberrant fiber pathways in the pretectal and dorsal thalamic alar plate (*between the arrows*). Note that fibers travelling in the lower part of the basal plate and in the floor plate maintain a normal trajectory. Scale bar: *A-D,* 4 mm; *E, F,* 8 mm.

8 Altered expression of the chemorepellent/chemoattractive molecule Netrin-1 in Pax6^{sey}/Pax6^{sey} embryos

In Pax6^{sey}/Pax6^{sey} embryos, from E11.5, the developmental expression of Netrin-1 was roughly normal in the rhombencephalic and mesencephalic floor plate, along the floor of the fourth ventricle and along the wall of the lateral ventricle (Fig. V-12). From E13.5, Netrin-1 was normally expressed in the striatum and from E14.5 in the vicinity of the SN-VTA complex (Livesey and Hunt, 1997; Fig. V-12*A,C*). However, an abnormally high and expanded expression of Netrin-1 was observed from the presumptive p1-p2 transition zone to the p2-p3 transition zone. Instead of being expressed in the ventral part of the diencephalic basal plate and in the zona limitans intrathalamica (Fig. V-12*C*), Netrin-1 expression was expanded in all the basal plate and the most ventral part of the presumptive alar plate (Fig. V-12*D*). This altered Netrin-1 expression persisted and was correlated with increased and expanded expression of SHH previously reported (Grindley et al., 1997; and data not shown). The comparison of the pattern of Netrin-1 expression with TH-IR immunoreactivity (compare Fig. V-12*D* and Fig. V-10*E,H*) showed that TH-IR fibers and neurons seemed orientated abnormally toward the increased and ectopic Netrin-1 expression located at the pretectal-dorsal thalamic transition zone.

V Discussion

The results obtained in normal mice are in good agreement with previous comparative analyses on catecholaminergic systems in sauropsides (Medina et al, 1994) and humans (Puelles and Verney, 1998). The main TH-IR neurons clearly arise independently along the whole brain axis. Table V-1 shows the resulting topological map of these groups. This mosaic pattern strongly suggests that this phenotype is generated by the combinatorial effects of regionally expressed transcription factors, such as Pax6, and diffusable morphogens such as SHH or FGF8. Differences between groups of TH-IR neurons may be caused by differences in the factors they express and the signals they receive.

It has been suggested that the transcription factor Pax6 could be a good candidate for controlling the proliferation, specification, or the maintenance of discrete catecholaminergic populations (Stoykova and Gruss, 1994; Dellovade et al.,

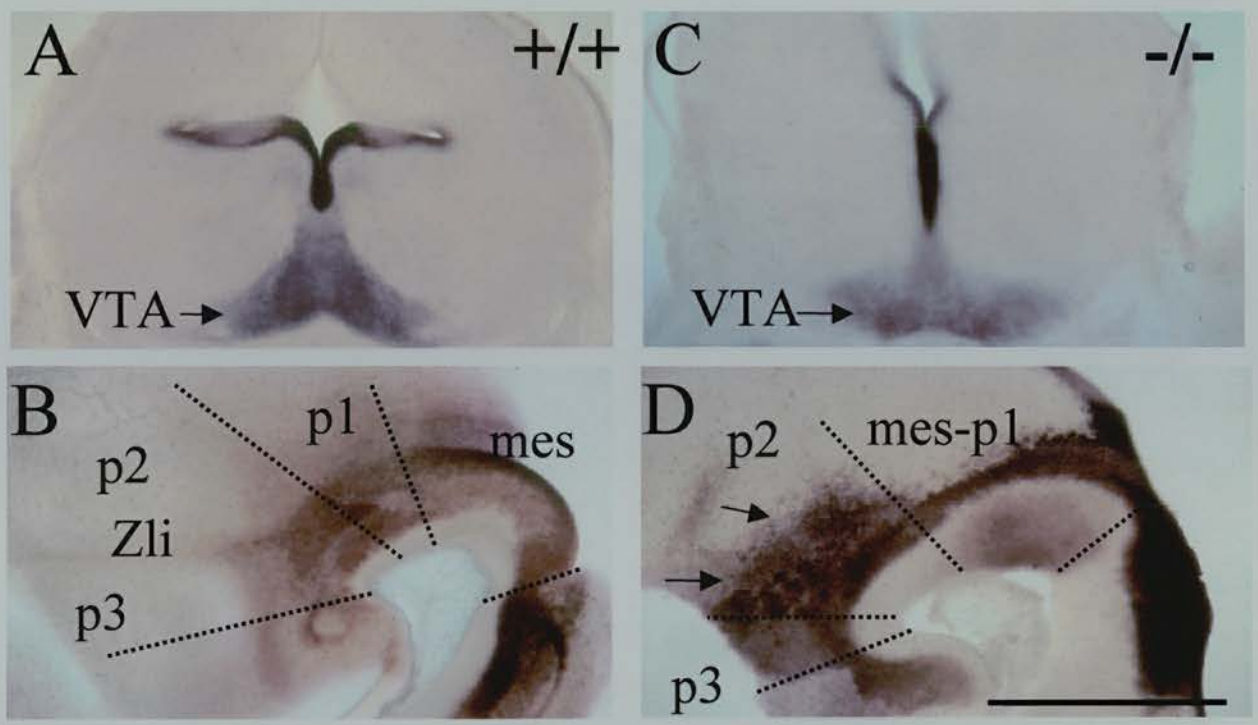

Figure V-12 Alteration of Netrin-1 expression in the diencephalon of Pax6^{sey}/Pax6^{sey} embryos. Coronal (*A, C*) and sagittal (*B, D*) sections of E14.5 (*B, D)* and E16.5 (*A, C*) wild type (*A, B*) and Pax6^{sey}/Pax6^{sey} (*C, D*) embryos. ***A*,** In the mesencephalon, Netrin-1 is expressed at the level of the SN-VTA complex. ***B*,** The sagittal section shows Netrin-1 expression in the floor of the fourth ventricle and in the basal plate of p1, p2 and p3. Note also a weak expression along the zona limitans intrathalamica (Zli). ***C*,** The coronal section shows a normal Netrin-1 expression at the level of the SN-VTA complex. ***D*,** In the diencephalon, Netrin-1 expression is increased and expanded dorsally. *Arrows* indicate the dorsal expansion in the ventral and dorsal thalamic alar plates. mes: mesencephalon. Scale bar: *A, C*, 4 mm; *B, D,* 2 mm

1998). This study indicates that discrete catecholaminergic populations in the diencephalon, the hypothalamus and the basal telencephalon express Pax6, either permanently or transiently. By analysing mice lacking Pax6, I show that Pax6 is not necessary for the specification and time of generation of diencephalic and hypothalamic dopaminergic neurons but is needed for the normal packing and segregation of these cells. The lack of Pax6 leads also to a virtual absence of TH-IR neurons in the basal telencephalon. I also describe non-cell autonomous defects among dopaminergic neurons of the SN-VTA complex: some are abnormally located and the medial forebrain bundle, the major ascending pathway of dopaminergic neurons, is misrouted.

1 Dopaminergic populations expressing Pax6

1.1 Diencephalic and hypothalamic TH-IR neurons : cell adhesion defect

The neuroepithelium of prosomeres 3, 4 and 5 expresses Pax6 during the time of genesis of diencephalic and hypothalamic TH-IR neurons. This study indicates that differentiated TH-IR neurons of A13 and A14PAVH continue to express Pax6 until the first postnatal days whereas A14DMH does not. In mice lacking Pax6, these populations differentiate but display a one to two days delay in their appearance. Since previous studies have shown abnormally low proliferative rates in the entire diencephalic alar plate of mice lacking Pax6 (Warren and Price, 1997), I looked for a delay in the genesis of two of these TH-IR groups (A13 and A14DMH). My results indicate no significant delay in genesis in A13 and A14DMH and no reduction in cell number of TH-IR neurons in A13, A14PAVH and A14DMH. It is unlikely that Pax6 is required for the specification and the regulation of proliferation of TH-IR neurons in these groups.

In mice lacking Pax6, A13, A14PAVH and A14DMH TH-IR neurons display an increase in cell density, suggesting altered adhesive properties. Previous studies have suggested that Pax6 regulates the expression of adhesion molecules such as R-cadherin (Matsunami and Takeichi, 1995; Stoykova et al., 1997). In mice lacking Pax6, there is a loss of R-cadherin expression in areas in which this gene is normally co-expressed with Pax6 (Stoykova et al., 1997). Moreover, it has been shown that the segregation normally observed in aggregates of cortical and striatal cells in an *in vitro* assay is lost in mice lacking Pax6 (Stoykova et al., 1997). This could be

explained by a model in which loss of Pax6 disrupts the Ca^{2+}-dependent adhesive mechanisms involving R-cadherin, thereby increasing cell mixing and leading to some of the morphological disruptions observed in the mutant. Interestingly, TH-IR neurons in A13, A14PAVH and A14DMH do not display a particular scattering or increased cell mixing, as might be expected, but paradoxically they are more densely packed in roundish cell clusters. I suggest that the selective loss of some adhesion molecules (such as R-cadherins) may alter the balance between heterophilic and homophilic interactions in such a way that some cells may have reduced ability to adhere to other types of cells and may have a tendency to adhere more strongly to cells of their own type.

1.2 Telencephalic populations: cell migration/ maintenance defect

In the olfactory bulb, Pax6 is expressed from E15.5 in TH-IR external tufted cells and from E18.5 in TH-IR periglomerular interneurons. In mice, external tufted cells are born between E13 and E18 (Hinds; 1968a,b) and proliferate in the ventricular zone of the olfactory bulb. In mice lacking Pax6, I observe rare TH-IR neurons in the region of the olfactory structure whose onset of TH expression and morphology correspond to those expected for external tufted cells. This suggests that Pax6 is important for the specification of external tufted cells in the olfactory bulb. Proliferation defects may account for the low number of external tufted cells. Alternatively, since mice lacking Pax6 fail to develop a nasal olfactory epithelium, this dramatic reduction could be due to the lack of induction by primary olfactory afferents. Indeed, it has been shown that activity-dependent processes from primary olfactory nerves are necessary for the initiation and maintenance of TH expression (McLean and Shipley, 1988; Baker and Farbman, 1993; Cigola et al., 1998).

In contrast to external tufted cells, periglomerular cells are born from E18 and arise along the anterior subventricular zone (Hinds, 1968a,b; Betarbet et al., 1996) from which they migrate in a large subventricular stream to the main olfactory bulb (Alvarez-Buylla, 1997). In mice lacking Pax6, no TH-IR periglomerular interneurons are observed in late embryos or neonatal pups. Interestingly $Pax6^{sey}/+$ heterozygote mice display a dramatic and specific decrease of TH-IR periglomerular interneurons whereas external tufted cells are preserved (Dellovade et al., 1998). This reduction

has been correlated to a progressive diminution in primary afferents (Dellovade et al., 1998).

Pax6 is strongly and transiently expressed in all TH-IR neurons of the piriform cortex, olfactory tubercle and anterior amygdala. Recently, it has been suggested that cells populating these structures may be derived in part from a transient structure, the intermediate telencephalic territory (ITA), located at the transition zone between the neocortex and the lateral ganglionic eminence. Pax6 is expressed (from E12.5 to E14.5) in both proliferating cells and cells located near or in migrating neurons of the lateral cortical migratory stream derived from ITA (Fernandez et al., 1998; unpublished results). When cells reach their targets, most of them express Pax6 during the formation of the different structures of the basal telencephalon. In mice lacking Pax6, ITA is dramatically altered: radial glial fascicles do not form at the cortical-ganglionic eminence transition zone, the normal expression of R-cadherin and the extracellular matrix molecule tenascin-C is lost and an ectopic expression of Dlx1 is found (Stoykova et al., 1997; Gotz et al., 1998). Interestingly, cellular migration in the lateral cortical migratory stream occurs in $Pax6^{sey}/Pax6^{sey}$ embryos, although cells fail to stop in their final locations in the basal telencephalon and continue to migrate to the pial surface of the brain (Brunjes et al., 1998). I observe that the transient TH-IR neurons of the piriform cortex, the anterior amygdala and the olfactory tubercle are decreased in number and fail to maintain TH expression in $Pax6^{sey}/Pax6^{sey}$ embryos. I suggest that the absence of TH immunoreactivity in these cells may be due to the failure of TH induction or maintenance of TH expression in these migrating neurons that do not recognize a "stop signal " in the basal telencephalon. Whereas proliferative defects may account for the absence of TH-IR neurons, BrdU studies suggest a normal proliferation from the lateral ventricles (data not shown; Brunjes et al., 1998).

2 Defects in catecholaminergic populations not expressing Pax6

Although TH-IR neurons of the SN-VTA complex, from the isthmus to p3, never display Pax6 immunoreactivity, I show in mice lacking Pax6 an abnormal location of TH-IR neurons and an altered pathway of catecholaminergic fibers along the pretectal-dorsal thalamic transition zone and in the alar plate of the dorsal thalamus. The abnormal location of TH-IR neurons might be due to either an ectopic

genesis induced by altered expression of morphogenetic molecules or to an altered migratory behavior induced by changes in the navigational environment.

2.1 Ectopic genesis of TH-IR neurons

$Pax6^{sey}/Pax6^{sey}$ mice display an early abnormal ventral to dorsal expansion of expression of the signaling secreted morphogen SHH and the SHH-induced gene, the winged helix transcription factor hepatocyte nuclear factor 3β (HNF-3β) at the level of the pretectal-dorsal thalamic transition zone and in the alar plate of the dorsal thalamus (Grindley et al., 1997; unpublished observation). There is evidence that HNF-3β, SHH and FGF8 create induction sites for TH-IR neurons along the dorso-ventral axis (Hynes et al., 1995b; Wang et al., 1995; Ye et al., 1998; Sasaki and Hogan, 1994; Hynes et al., 1995a). It is possible that the early ectopic SHH and HNF-3β expression domains in $Pax6^{sey}/Pax6^{sey}$ mice induce ectopic catecholaminergic neurons. Additional experiments will be required to answer this question.

2.2 Changes in navigational environment

Clearly a complex set of attractive and repulsive guidance molecules are provided in the environment. Ectopic expression of SHH or FGF8 could induce an ectopic expression of guidance cues such as netrin, ephrin, semaphorin, or slit proteins, leading to the misrouting of growth cones or defects in cellular migration. For instance, it has been shown recently that ectopic expression of Hedgehog molecules induces ectopic Netrin-1 expression in the CNS of zebrafish embryos (Lauderdale et al., 1998). In mice lacking Pax6, the early ventral to dorsal expansion of SHH (Grindley et al., 1997) coincides with the ventral to dorsal expansion of Netrin-1 along the pretectal-dorsal thalamic transition zone and in the dorsal thalamus. Netrin-1 is a laminin-related secreted protein with critical roles in axon guidance (Leonardo et al., 1997a) and cell migration (Przyborski et al., 1998; Bloch-Gallego et al., 1999) which induces either attractive or repulsive responses, depending on the netrin receptor expressed. Activation of DCC family receptors (DCC and neogenin in vertebrates) produces attraction (Fazeli et al., 1997; Ming et al., 1999) whereas activation of UNC5 family receptors (UNC5H1, UNC5H2, and

UNC5H3) produces repulsion (Ackerman et al., 1997; Leonardo et al., 1997b). Normally, TH-IR neurons of the SN-VTA complex migrate in two phases, first radially along tenascin-bearing glial processes and, secondly, tangentially giving the SN its characteristic "inverted fountain" shape (Hanaway et al., 1971; Kawano et al., 1995). In $Pax6^{sey}/Pax6^{sey}$ embryos, the radial migration of SN-VTA neurons occurs normally along tenascin-bearing glial processes (unpublished results). Later, the rostral pretectal SN-VTA neurons are disorientated at the pretectal-dorsal thalamic transition zone near the expansion of Netrin-1 expression and ectopic TH-IR neurons in the dorsal thalamus are disorientated and appear to be migrating away from the expanded Netrin-1 expression. The SN-VTA neurons in the mesencephalon and the caudal pretectum display a normal orientation, suggesting a normal tangential migration.

Nearly all SN-VTA projections are also misrouted at the pretectal-dorsal thalamic transition zone. Instead of following the medial forebrain bundle ventrally, SN-VTA projections are deflected rostro-dorsally away from the expanded Netrin-1 expansion. Taken together, this suggests that Netrin-1 has a chemorepulsive activity on both the tangential migration and the pathfinding of SN-VTA neurons.

In conclusion, this study indicates that Pax6 is directly or indirectly involved in the adhesion and migration of discrete catecholaminergic populations and the maintenance of their phenotype. Second, Pax6 has a primordial role in determining the correct navigational environment for early diencephalic axonal pathfinding.

CHAPTER SIX:
SEARCH FOR MOLECULES THAT COULD INFLUENCE THE DEVELOPMENT OF MONOAMINERGIC SYSTEMS-II-: A ROLE FOR NETRIN-1?

CHAPTER SIX:
SEARCHING FOR MOLECULES THAT COULD INFLUENCE THE DEVELOPMENT OF MONOAMONERGIC SYSTEMS-II: A ROLE FOR NETRIN-1?

I Abstract

First, this study confirmed that Netrin-1 is expressed in the floor plate of mes-p3 where mesencephalic dopaminergic neurons are generated and later on in the vicinity of dopaminergic neurons of the substantia nigra (SN) and ventral tegmental area (VTA). Furthermore, I showed for the first time that numerous SN-VTA dopaminergic neurons coexpress protractedly tyrosine hydroxylase (TH), the rate limiting enzyme for DA synthesis, and Netrin-1.

Then, I investigated whether Netrin-1 plays a role in the axon guidance and/or neuronal migration of discrete dopaminergic populations of the SN and VTA. VTA explants obtained from E14 embryos co-cultured in the presence of a gradient of Netrin-1 showed a slight but significant increase in neurite outgrowth toward the source of Netrin-1 whereas explants from E14 SN, E17 SN or E17 VTA did not. In parallel, the analysis of E15 Netrin-1 knockout mice showed a reduction in the density of TH-IR fibers at the level of the olfactory tubercule, a major target that expresses high levels of Netrin-1. Together this suggests that, in vivo, Netrin-1 could play a role in promoting outgrowth of VTA projections. In vitro, SN and VTA explants showed no neuronal migration toward a source of Netrin-1. However, Netrin-1 knockout embryos and pups (E15-P0) displayed ectopic TH-IR neurons in mes-p3. At the moment, it is difficult to attribute to Netrin-1 a role in the migratory behavior of SN-VTA neurons. Netrin-1 could act early by guiding specific subpopulations of dopaminergic neurons and/or later in the maintenance of dopaminergic neurons. Interestingly, mice lacking the Netrin-1 receptor, *deleted in colorectal cancer* (DCC) displayed larger numbers of SN and VTA TH-IR neurons indicating a potential role for DCC and Netrin-1 in the survival of SN-VTA neurons.

Additional experiments such as BrdU injections in mice lacking DCC or Netrin-1 would be required to support those findings.

II Introduction

1 Role of Netrin-1 in axonal guidance

Netrins are secreted molecules closely related in structure to the non-diffusible molecule laminin-1. Netrins mediate long-range attraction and repulsion of axons. They were identified as proteins that can mimic the diffusible outgrowth-promoting activity of floor plate cells on commissural axons (Kennedy et al., 1994). Netrin-1 is produced by floor plate cells, and is believed to be present in the spinal cord in a decreasing ventral-to-dorsal gradient that attracts commissural axons to the ventral midline of the spinal cord (Kennedy et al., 1994; Serafini et al., 1996). Interestingly, Netrin-1 also appears to function as a long range repellent (Colamario et al., 1995; Tucker et al., 1996). Thus, netrins appear to guide axons in both dorsal and ventral directions in the neural tube. Netrins are the vertebrate homologs of the UNC-6 protein of the nematode *Caenorhabditis elegans*, which plays similar roles in the nematode (Hedgecock et al., 1990; Wadsworth et al., 1996).

Interestingly, Netrin-1 is expressed in the region of the ventral tegmental area and substantia nigra (Livesey and Hunt, 1997), suggesting that dopaminergic neurons located in these areas could be influenced in their migration or in their axonal projections.

The action of Netrin-1 is mediated by cell membrane receptors. So far, five Netrin-1 receptors have been identified, neogenin and DCC (*deleted in colorectal cancer*), and three members of the UNC-5 family (Unc5H1, Unc5H2 and, Unc5H3). Neogenin and DCC are expressed in the region where mesencephalic dopaminergic neurons are differentiating from E12 to adults (Livesey and Hunt; 1997), whereas only Unc5H2 is transiently expressed in the basal mesencephalon (Leonardo et al., 1997). So far, no colocalisations of TH and Netrin-1 or any of these receptors have been reported.

Thus, it is highly possible that DCC, neogenin and/or Unc5H2 mediate several actions of Netrin-1 on mesencephalic dopaminergic neurons but what are these effects?

2 Role of Netrin-1 in neuronal migration

Recently, Netrin-1 has been implicated in neuronal migration. Bloch-Gallego et al. (1999) have shown that the expression of Netrin-1 and several Netrin-1 receptors, DCC, neogenin and a member of the Unc5 family, was consistent with a possible role of netrins in directing the migration of precerebellar neurons from the rhombic lip. Their analysis of mice deficient in Netrin-1 revealed a decrease in the number of inferior olivary neurons (Bloch-Gallego et al., 1999). In addition, they showed that ablations of the midline lead to a fusion of two olivary masses suggesting that the floor plate may function as a specific stop signal for inferior olivary neurons. Together, these studies demonstrate a requirement for Netrin-1 in the migration of inferior olivary neurons. Interestingly, the authors also support the idea that Netrin-1 plays a direct or indirect role in the survival of inferior olivary neurons.

In addition, the study of a natural mutant deficient for Unc5H3 (*rcm* mutant) has shown a direct role of Unc5H3 in the neuronal migration occuring in cerebellar development. Rcm mutants display, from E13.5, an ectopic location and accumulation of granule cells and Purkinje cell precursors (Przyborski et al., 1998). This suggests that the establishment of the rostral cerebellar boundary may rely on chemorepulsive signalling events requiring UNC5H3 and Netrin-1. In mice lacking Pax6, Unc5H3 is absent in the cerebellar granule cells and these mice display similar cerebellar alterations to those described in rcm mutants (ectopic granule cells in the inferior colliculus).

To conclude, Netrin-1 is involved in other mechanisms than axonal guidance such as neuronal migration or survival.

3 A role for Netrin-1 in the migration and axonal guidance of dopaminergic SN-VTA neurons?

Because i) Netrin-1 is expressed in the ventral tegmental area and the substantia nigra (Livesey and Hunt, 1997) and because ii) I reported that altered Netrin-1 expression was associated with abnormal topographical organisation of SN-VTA neurons and their projections in mice lacking Pax6, I wanted to investigate the role of Netrin-1 in the development of mesencephalic dopaminergic neurons.

The role of netrin-1 has been assessed *in vivo* by studying the phenotype of mice lacking Netrin-1. I have also developed in the laboratory of Dr. Linda Richards (The University of Maryland, Baltimore) an *in vitro* approach by co-culturing SN-

VTA explants with EBNA-293 cells expressing Netrin-1 (Keino-Mazu et al., 1996). I have also tried to find the receptor mediating the effects of Netrin-1. DCC appeared to be a good candidate since it has been shown that DCC is expressed in the SN-VTA complex (Shu et al., 2000). The time-course of expression of DCC and the phenotype of mice lacking DCC were studied for these reasons.

III Material and methods

1 Animals

Netrin-1 knockout mice and their control littermates were analysed at embryonic day (E) E14, E15, E16, and E17 and postnatal day 0 (P0). DCC knockout pups were also analysed at P0. Both strains were maintained on a C57/Bl6 genetic background.

2 Immunocytochemistry

Embryos were perfused transcardially with saline followed by 4% paraformaldehyde in PB. Brains were postfixed for 2-5 days in the same fixative and cryoprotected in 30% sucrose in PB. Serial coronal or sagittal sections (40 μm) were cut on a freezing microtome and immediately processed for immunocytochemistry as previously described (Chapter II). Some brains were also embedded in a solution containing 3% agarose and cut in the coronal plane (40 μm) using a Leica vibratome. In brief, sections were incubated with the primary antibodies diluted in PBS+ (0.1M PBS with 0.2% gelatin and 0.25% Triton X-100) overnight at 4°C. Rabbit polyclonal anti-TH antibodies (1:200, Pel-Freez; 1:800, Protos Biotech, New-York), rabbit polyclonal anti-calretinin antibody (1:10000: Swant, Switzerland), rabbit polyclonal anti-calbindin antibody (1:20000; Swant), rabbit anti-neurofilament (1:50000, DAKO, Denmark), rabbit polyclonal anti-βgalactosidase (1:50000, DAKO), rat monoclonal anti-tenascin (1:20000, Sigma, USA) and rat monoclonal anti-L1 antibody (1:50, Roche-Diagnostics, USA) were used. Biotinylated goat anti-rabbit and biotinylated goat anti-rat (1:200; DAKO) were used as secondary antibodies and were revealed with a streptavidin-biotin-peroxidase complex (1:200, Amersham, UK). Sections were then reacted with a solution containing 0.02% diaminobenzidine, 0.6% nickel ammonium sulfate, and 0.003% H_2O_2 in 0.05M Tris buffer, pH 7.6

(DAB-Ni) or with a solution containing 0.04% diaminobenzidine, and 0.003% H_2O_2 in PBS (DAB).

3 In situ hybridization

In situ hybridization for Netrin-1 was either performed on 80-100 μm thick sections that were obtained on a freezing microtome or on 10 μm thick-paraffin sections. Sections were processed for in situ hybridization as described in Chapter V.

4 Sequential in situ hybridization for Netrin-1 and immunolabelling for TH

In situ hybridization for Netrin-1 was performed on 10 μm thick-paraffin sections as described in Chapter V. Sections were then rinsed in PBS and directly processed for TH immunolabelling as described above. TH immunolabelling was revealed with DAB.

5 Collagen gel assays and quantification

5.1 Explant cultures:

Experiments were carried out on E14 and E17 mouse embryos of the C57/Bl6 background. Brains were removed from the skull, embedded in 3% low melt agarose diluted into Leibovitz's L-15 medium (GIBCO, USA) supplemented with 10% glucose (Sigma) (L15+) and sectioned into 300 μm thick coronal sections. The substantia nigra and ventral tegmental area were dissected out from these sections and collected in L15+. The delineation of regional boundaries of the SN, VTA and striatum was performed according to Jacobowitz and Abbott (1998). A cut was made in the lateral top region of the explants as an indication of the topographic orientation of the explant (Fig. VI-1). Explants were co-cultured at a distance of 200 to 600 μm with aggregates of EBNA-293 cells stably transfected with a construct encoding netrin-1-c-myc, or with a construct encoding c-myc alone (Keino-Masu et al., 1996). Explants were embedded into a solution containing 40% dialysed rat-tail collagen (Collaborative Biomedical Products, USA), 50% matrigel (Collaborative Biomedical Products), 5% 10x MEM (GIBCO), 7.5% Na2CO3, and cultured in DMEM/F-12 (ICN/Flow) supplemented with 4% glucose, for 36 h in a 5% CO2, 95% humidity

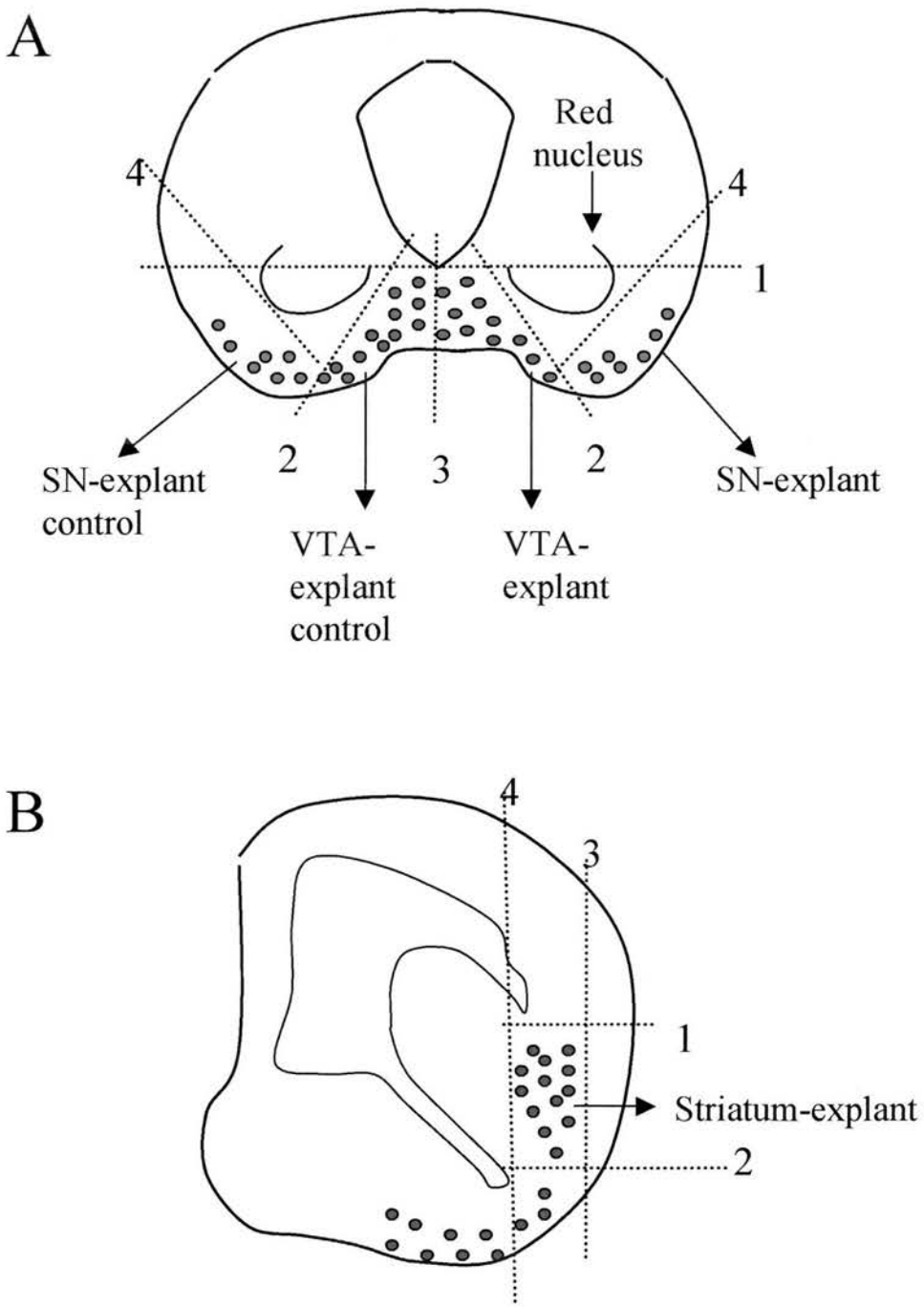

Figure VI-1 Schematic drawing illustrating the origin and dissection of the explants chosen in the co-culture experiments. ***A, B,*** The *dotted lines* indicate the sections made to isolate the explants and the numbers indicate the order of sectioning. ***A,*** Schematic representation of a section from which explant containing dopaminergic neurons of the substantia nigra (SN, *red)* or the ventral tegmental area (VTA, *green*) were obtained. Note that the shape of the section and the location of the red nucleus were useful indicators of the SN and VTA areas. ***B,*** Schematic representation of a section from which striatal explant were obtained. The blue dots represent the area of Netrin-1 expression.

incubator at 37°C. Netrin-1 expression was previously reported to be obtained in a gradient over a distance of about 300-400 μm away from the EBNA-293 aggregates after 2 days in similar conditions (Alcantara et al., 2000).

5.2 Analysis and quantification

Explants were photographed and fixed at 4°C in 4% paraformaldehyde diluted in PBS. Some explants were micro-injected with 1 μl of a solution containing 10% of DiI (DiI was diluted in N-N-dimethyl formamide, Sigma) using a picospritzer apparatus. DiI was allowed to diffuse until entire explants were labelled. For quantification, explants were scanned using a Leica confocal microscope and the halo of outgrowth was divided into four quadrants as illustrated in figure VI-2. To determine the preferential direction of the outgrowth, the longest axons (to a maximum of 10) were measured in each quadrant and for each explant.

IV Results

1 Netrin-1 expression in the region of the developing SN-VTA complex

Netrin-1 expression is detected in the area of differentiation of SN-VTA dopaminergic neurons as soon as E12.5 (Livesey and Hunt; 1997). At this age few dopaminergic neurons co-expressed TH and Netrin-1 (data not shown). By E14, the ventral tegmental area displayed a strong Netrin-1 expression. Co-expression of Netrin-1 and TH was observed in numerous TH-IR neurons in the VTA (Fig. VI-3). By E17, Netrin-1 expression increased in SN. At this age, at the level of the SN-VTA complex, Netrin-1 expression was observed in subsets of dopaminergic neurons located close to the midline and the basalmost region of mes. By P4, most dopaminergic neurons in SN-VTA complex (estimated 75%) co-expressed TH and Netrin-1. Netrin-1 was also expressed by non-TH-IR cells in the vicinity of SN-VTA dopaminergic neurons at all ages studied (Fig. VI-3). This pattern of expression was protracted in adults (data not shown). This suggests that Netrin-1 could play several roles during the development of SN-VTA TH-IR neurons: in their proliferation, migration and axonal pathfinding. Interestingly, Netrin-1 has a protracted expression

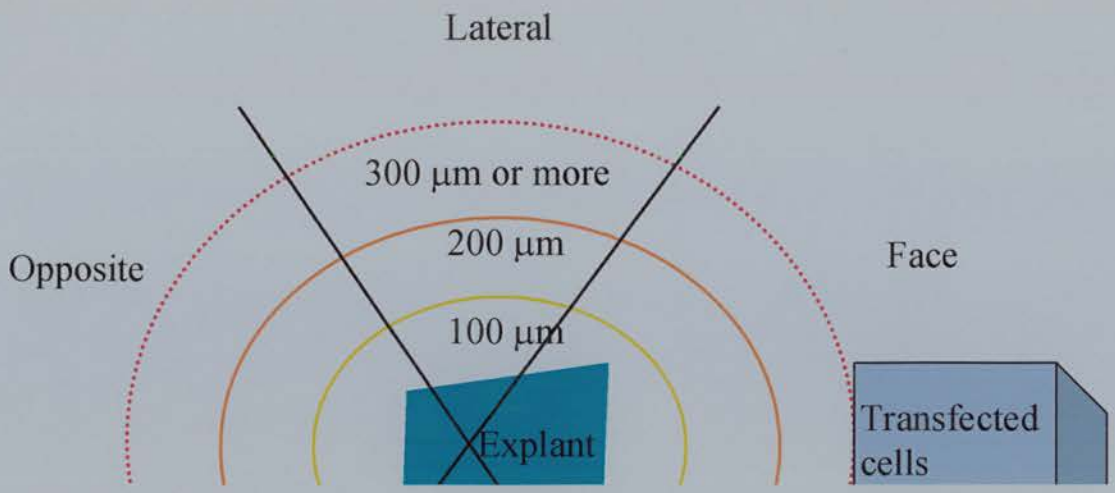

Figure VI-2 Schematic representation of a co-culture explaining how the explants were analysed. The explant is divided into four quadrants and the halo of outgrowth was analysed in three of them: one facing the transfected cells (face), one opposite to the transfected cells (opposite) and an intermediate one (lateral). Concentric circles symbolize the distances from the edges of the explant (100 µm, 200 µm and 300 µm and more).

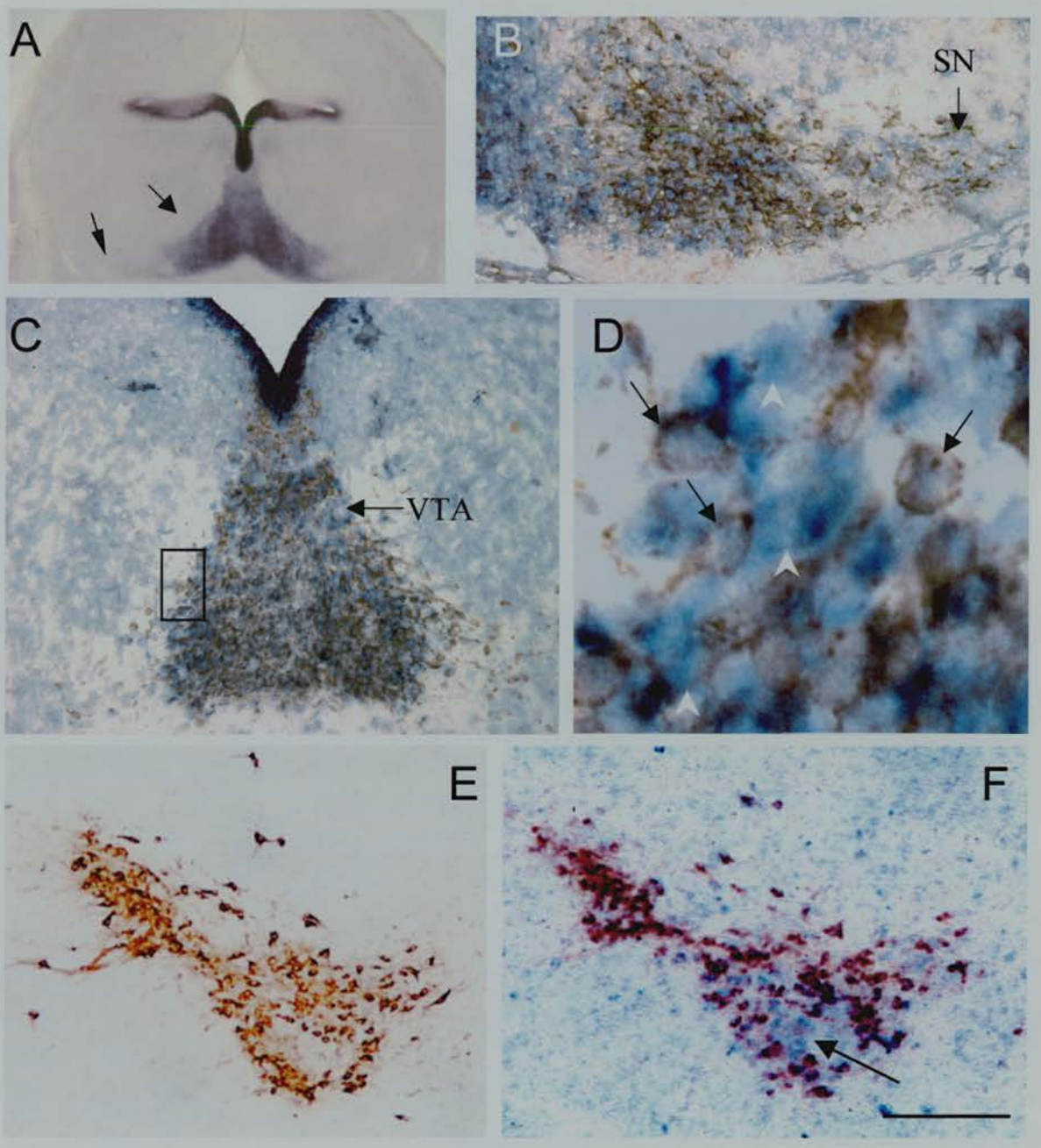

Figure VI-3 Netrin-1 expression at the level of the SN-VTA: in dopaminergic neurons and in the vicinity of dopaminergic neurons. ***A,*** Strong expression of Netrin-1 in the VTA (*large arrow*) and low expression of Netrin-1 in the SN *(thin arrow*) of E14 embryo. ***B-D,*** Colocalization of Netrin-1 expression (*blue*) and tyrosine hydroxylase immunoreactivity (TH-IR, *brown*) in E14 embryo. ***B,*** *Arrow* points to low level of Netrin-1 expression in SN. ***C,*** Colocalisation of Netrin-1 and TH-IR in dopaminergic neurons of the VTA. ***D,*** Higher magnification of the *box* shown in (C). *Black arrows* point to dopaminergic neurons coexpressing Netrin-1 and TH and *white arrows* point to cells expressing only Netrin-1. ***E-F***, Alternate coronal sections of the substantia nigra of a P4 pup stained for (E) TH (*brown-red*) and (F) TH and Netrin-1 (*blue*). ***F,*** *Black arrow* points to Netrin-1 expression located in the vicinity of dopaminergic neurons of the substantia nigra. Scale bar: *A*, 3.5 mm; *B, C,* 1.2 mm; *D*, 0.1 mm; *E, F*, 0.5 mm.

in adults (Livesey and Hunt; 1997 and data not shown) indicating a potential role in survival and plasticity of dopaminergic neurons.

Target neurons in the basal telencephalon (caudate-putamen, accumbens, and olfactory tubercle) also expressed high levels of Netrin-1 during their period of innervation by SN-VTA neurons, suggesting that Netrin-1 produced by striatal neurons could be used as a chemo-attractant for SN-VTA TH-IR neurons. Conversely, it is also possible that Netrin-1 produced by dopaminergic neurons could be used to guide striato-nigral projections toward the mesencephalon.

2 Co-culture experiments

In vitro experiments with E17 striatal explants cultured alone or co-cultured with E17 SN or E17 VTA or Netrin-1 secreting cells showed no neurite outgrowth. However, numerous cells were seen migrating radially out of the striatal explants in all the conditions tested. A similar result was obtained with E14 striatal explants facing E14 SN, E14VTA or Netrin-1 secreting cells. It is difficult to conclude from these experiments whether I failed to optimise the culture conditions necessary to obtain striatal outgrowth or whether striatal projections are not attracted by a gradient of Netrin-1. However, this suggests that Netrin-1 is not playing a crucial role in the initial establishment of striato-nigral projections.

I have also tested whether the neurite outgrowth of SN or VTA neurons from E14 or E17 embryos was affected by a maintained gradient of Netrin-1. I found that E17 SN and VTA explants displayed little neurite outgrowth (a few short processes) and that they showed no selective outgrowth toward Netrin-1 secreting cells. I considered that the failure to observe significant neurite outgrowth was due to the old stage of the explants. Indeed, dopaminergic neurons of the SN-VTA complex have already established a mature pattern of innervation in their targets (striatum and olfactory tubercle) by E17. I have therefore repeated my experiments using younger tissues obtained from E14 embryos, ages at which SN-VTA projections start to reach their telencephalic targets. At E14, VTA explants displayed a significant increase of neurite outgrowth directed towards Netrin-1 secreting cells compared to control cells (Fig VI-4) whereas SN explants did not. The neurites were thin and straight. This suggests that developing projections of VTA neurons could be directed or attracted, in vivo, by local sources of Netrin-1.

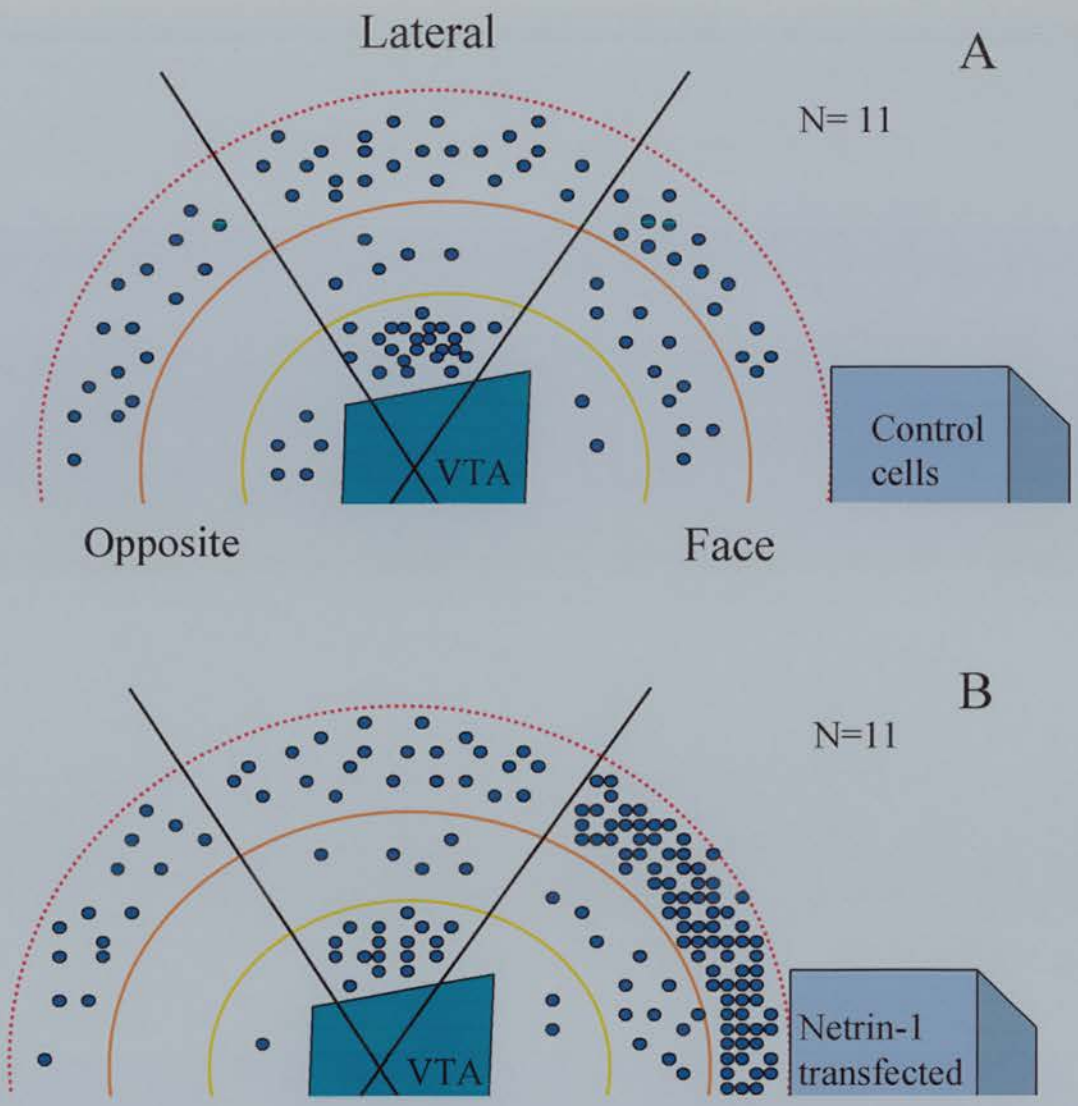

Figure VI-4 Schematic representation showing the outgrowth observed in VTA explants cultured with (A) control cells or with (B) cells secreting Netrin-1. Data of all explants (Controls, N=11; Netrin-1, N=11) are added together to give the diagram above. *Blue dots* show the distribution of the growth cones of the longest axons (with a maximum of 10 axons counted per quandrant and per explant). ***A,*** Note that there is no selectivity in the direction of growth from VTA explants cultured with control cells. ***B***, Note that there is a significant (χ^2, $P< 0.01$) increase in the number of axons and their length from VTA explants co-cultured with Netrin-1 secreting cells.

Using the same experimental paradigm, I tested the migratory behaviour of SN or VTA neurons toward Netrin-1 secreting cells. I found no migration of dopaminergic neurons toward Netrin-1 secreting cells in these experimental conditions. It is therefore unlikely that SN-VTA neurons require Netrin-1 for their migratory behaviour. However, it is possible that the conditions required to observe SN-VTA neuronal migration was not reached in my experiments. For instance, it is possible that endogenous secretion of Netrin-1 in the explants would prevent the establishment of a gradient of Netrin-1 in these co-cultures.

3 Analysis of dopaminergic neurons and fiber pathways in Netrin-1 knockout mice

I used Netrin-1 knockout mice to test whether, in vivo, Netrin-1 could play a role in the guidance of dopaminergic neuronal projections arising from the SN and the VTA and in the migration of these neuronal populations.

3.1 Altered topographic organisation of mesencephalic and diencephalic dopaminergic neurons in Netrin-1 knockout mice

In wild type embryos, by E15, TH-IR neurons of the SN-VTA complex have reached their final superficial position. SN neurons are located in the basal plate of mes-p2 and VTA neurons are located in the floor plate of mes-p3 (Vitalis et al., 2000). By E15, SN neurons are migrating tangentially and start to display their characteristic "inverted fountain" pattern (Hanaway et al., 1971; Kawano et al., 1995). In mes, p1 and p2, TH-IR neurons are also located along the third ventricle (A11), the floor of the aqueduct (A10dc) and in the retrorubral field (A8).

From E15, the earliest age analysed, Netrin-1 knockout mice displayed an ectopic location of several TH-IR neurons (Fig. VI-5). Coronal sections of Netrin-1 knockout newborns showed the existence of ectopic TH-IR neurons (n=1115 and 1145 neurons estimated from 2 pups) in mes, p1, p2 and p3. Ectopic TH-IR neurons were located dorsally to A8, A9 and A10 and laterally to A11 and A10dc (Fig. VI-6). In some sections, ectopic neurons were abnormally located around the red nucleus (Fig. VI-6). Their morphology resembled those adopted by the most differentiated A8, A9 or A11 neurons: they were large with long bipolar or multipolar processes

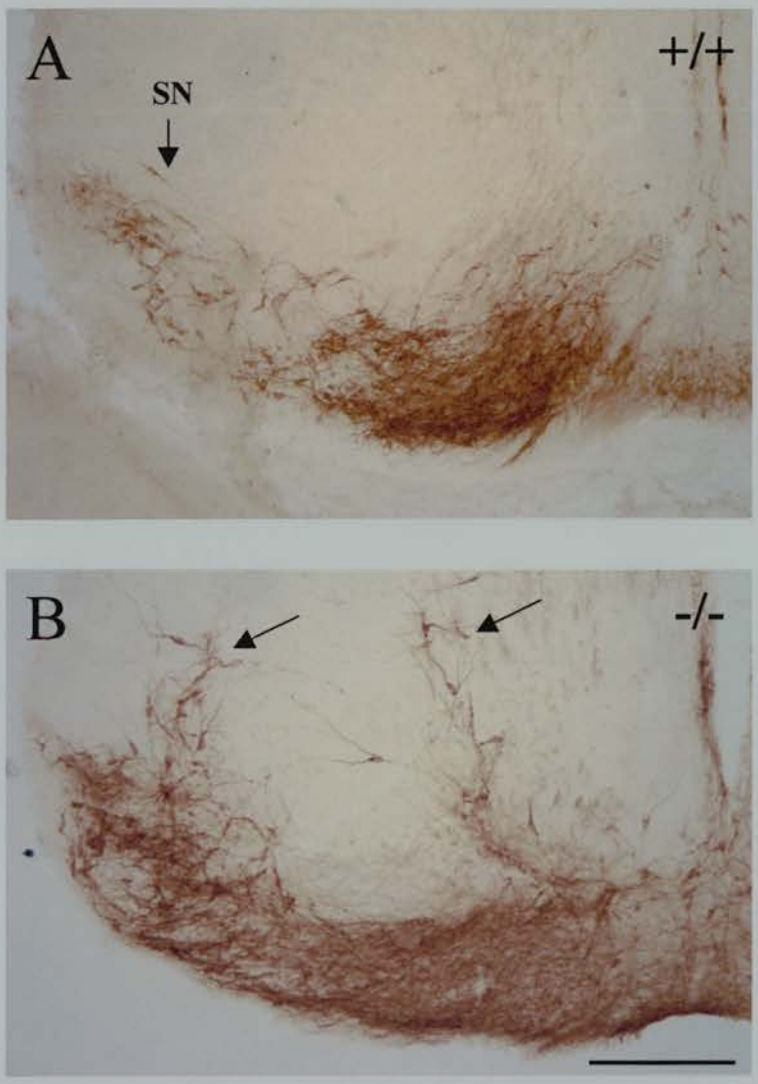

Figure VI-5 Topographical alterations of tyrosine-hydroxylase neurons in E15 Netrin-1 knockout embryo. ***A,*** Coronal section of a E15 wild type embryo at the level of the SN-VTA complex. *Arrow* points to dopaminergic neurons of the substantia nigra (SN). ***B,*** Coronal section of a E15 Netrin-1 knockout embryo at a similar level than shown in (A). *Arrows* point to ectopically located TH-IR neurons. Scale bar = 0.5 mm.

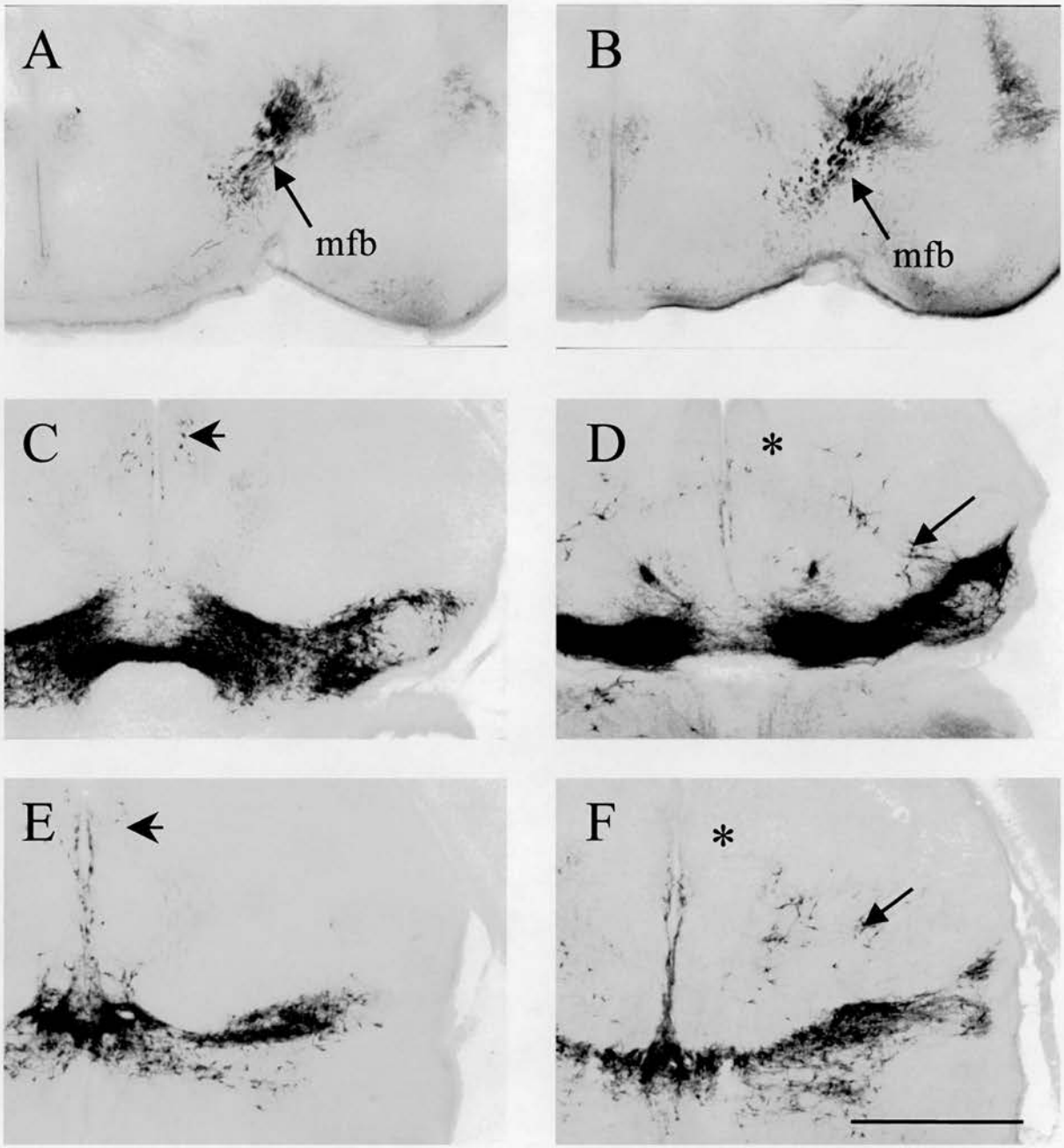

Figure VI-6 Normal pathfinding of the medial forebrain bundle and ectopic location of tyrosine-hydroxylase neurons in the pretectum and the mesencephalon of Netrin-1 knockout mice. ***A, B,*** Coronal sections showing the pathfinding of the medial forebrain bundle (mfb) in wild type (A) and Netrin-1 knockout mice (B). Note that there is no obvious alteration in the organisation of the mfb. ***C-F,*** Coronal sections of the (C, D) substantia nigra and the ventral tegmental area or (E, F) the retrorubral field in (C, E) wild type mice and (D, F) Netrin-1 knockout mice. ***C, E*** *Short arrows* point to A11 neurons. ***D, F,*** *Stars* point out the region were A11 neurons are normally located in wild type mice. Note the reduction of A11 neurons in Netrin-1 knockout mice. *Long arrows* point to ectopic tyrosine-hydroxylase neurons in Netrin-1 knockout mice. ***D,*** Note that ectopic tyrosine-hydroxylase neurons are in close contact with the substantia nigra. Scale bar = 2 mm.

(Fig. VI-6). These ectopic neurons never displayed the morphology adopted by A10 neurons at the age studied (small and roundish appearance). Their long processes were mostly oriented laterally toward the dorsal part of the SN and sometimes medially toward A11 neurons. Fewer A11 TH-IR neurons were observed in Netrin-1 knockout mice compare to wild type mice (wild type, n=1026 and n=1050; Netrin-1 knockout, n=357 and n= 390 values were obtained from 2 wild type and 2 Netrin-1 knockout mice). At this stage of the analysis, I can not be sure of the identity of these TH-IR neurons but from their location, morphology and number it is highly possible that they could belong to A8, A9 or/and A11 groups.

It has been reported that tenascin-bearing glial processes may guide SN-VTA neurons while they migrate radially and that L1- and neurofilament-bearing neuronal processes could support the tangential migration of SN-VTA neurons (Kawano et al., 1995; Ohyama et al., 1998). I have analysed the pattern of expression of these molecules in Netrin-1 knockout mice. I found no gross alteration in tenascin-, L1- or neurofilament immunoreactivity in the mesencephalon of Netrin-1-knockout mice (data not shown).

Interestingly, the analysis of the location of cells that would normally express Netrin-1 in Netrin-1 knockout mice (using immunolabeling for β-Gal) revealed a dorsal expansion of the β-Gal/Netrin-1-positive region, the region where SN-VTA neurons are generated (Fig. VI-7). It is therefore conceivable that, in Netrin-1 knockout mice, some TH-IR positive neurons are generated too far from cues that would normally guide them (i.e.: tenascin-bearing processes, see also figure VII-3) and therefore appear ectopically located later on. Additional analysis of their genesis and cell lineage would be required.

3. 2 Analysis of SN-VTA fibers pathway in Netrin-1 knockout mice

In wild type mice, mesocortical fibers reached the prefrontal cortex and the striatum by E15. In addition, a few TH-IR fibers originating from A10 were observed running along the fasciculus retroflexus toward the epithalamus (Skagerberg et al., 1984). By E18.5, the caudate-putamen and the globus pallidus were homogeneously labelled and a denser band of terminals was visible under the external capsule. Mesocortical fibers emerged from mfb, entered the olfactory tubercle or ramified into the ventral lateral part of the nucleus accumbens. The remaining mesocortical

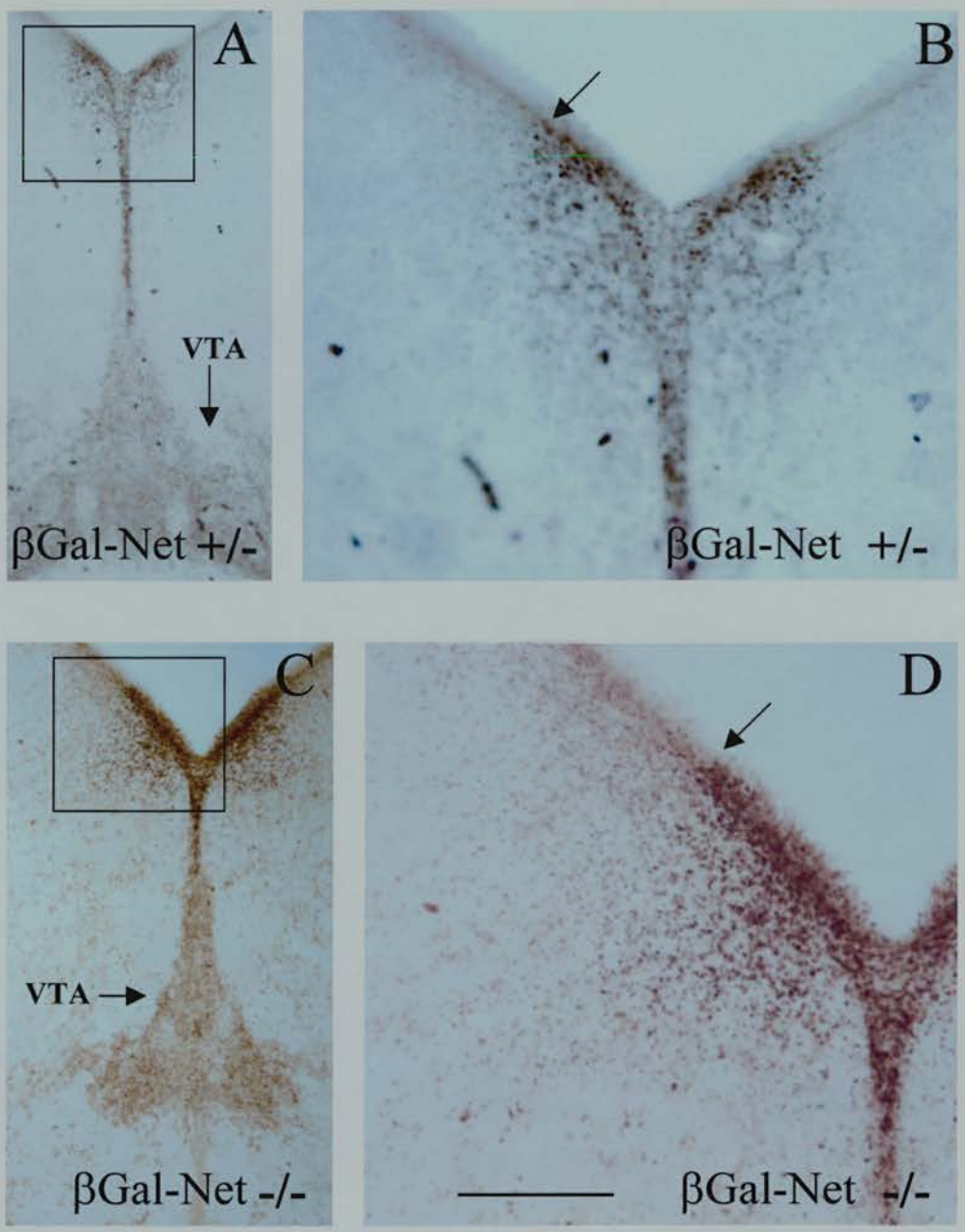

Figure VI-7 ***A-D,*** Coronal sections of (A,B) E15 embryo heterozygote for Netrin-1 mutation and (C, D) E15 Netrin-1 knockout embryo at the level of the floor of the aqueduct and the ventral tegmental area (VTA). Sections are immunostained for βGal which reveals the location of Netrin-1 expressing cells. ***B, D*** Higher magnification of boxes shown in (A) and (C) respectively. *Arrows* point to the dorsal limit of strong βGal immunolabeling. Note that βGal immunolabeling extends more dorsally in (D) than in (B). Scale bar: *A,C,* 1 mm; *B,D,* 0.25 mm.

TH-IR fibers turned dorsally to enter the medial, prefrontal, and anterior cingulate cortices (Schlumpf et al., 1980; Verney et al.,1982; Voorn et al., 1988, and present study). By P0, cortical and septal regions started to display a more refined innervation. In the septum, TH-IR innervation was mostly refined to the lateral and lateral-dorsal regions. The innervation of the cingulate cortex was denser in regions lateral to the indusium griseum, above the corpus callosum (data not shown).

In Netrin-1 knockout mice, TH-IR fibers originating from the SN and the VTA display minor alterations in the telencephalon whereas they appeared normal in other brain regions. By E15, Netrin-1 knockout mice displayed a decrease in TH-IR fiber density in the ventral pallidum, mainly at the level of the olfactory tubercle (Fig. VI-8). By E17, Netrin-1 knockout mice showed a 34% reduction in the thickness of olfactory tubercle (OT) as revealed by TH immunoreactivity (TH-IR-OT) and βGal immunoreactivity (βGal-IR-OT) (wild type: TH-IR-OT, 280 μm +/- 8 μm; βGal-OT, 210 μm +/- 16 μm; Netrin-1 knockouts: TH-IR-OT, 180 μm +/- 8 μm, βGal-OT, 160 μm +/- 20 μm, values are mean +/- SEM of four wild type and four Netrin-1 knockout mice- TH-IR-OT is a measure of the thickness of the TH-IR fibers at the level of the olfactory tubercle and βGal-OT is a measure of the thickness of the βGal-immunopositive region of the olfactory tubercle). This difference was no longer observed at P0, suggesting that Netrin-1 may have an early outgrowth promoting effect on VTA projections toward the olfactory tubercle in vivo. However, it is also possible that this defect is secondary to an hypomorphism of the region and to the lack of anterior commissure. By P0, TH-IR fiber alterations were observed in the innervation of the septum and cingulate cortex where fibers appeared tangled instead of being organised in parallels (data not shown). This alteration is probably secondary and due to the lack of the corpus callosum and the abnormal formation of Probst's bundles in the septum. Taken together, this suggests that Netrin-1 is not essential to the axonal guidance of SN-VTA TH-IR neurons. However, Netrin-1 may have an outgrowth promoting effect on VTA projections innervating the olfactory tubercle.

3 Analysis of mice lacking DCC

DCC is protractedly expressed at the level of the SN-VTA (Gad et al., 1997), and pharmacological alterations of dopaminergic neurons induce the down-

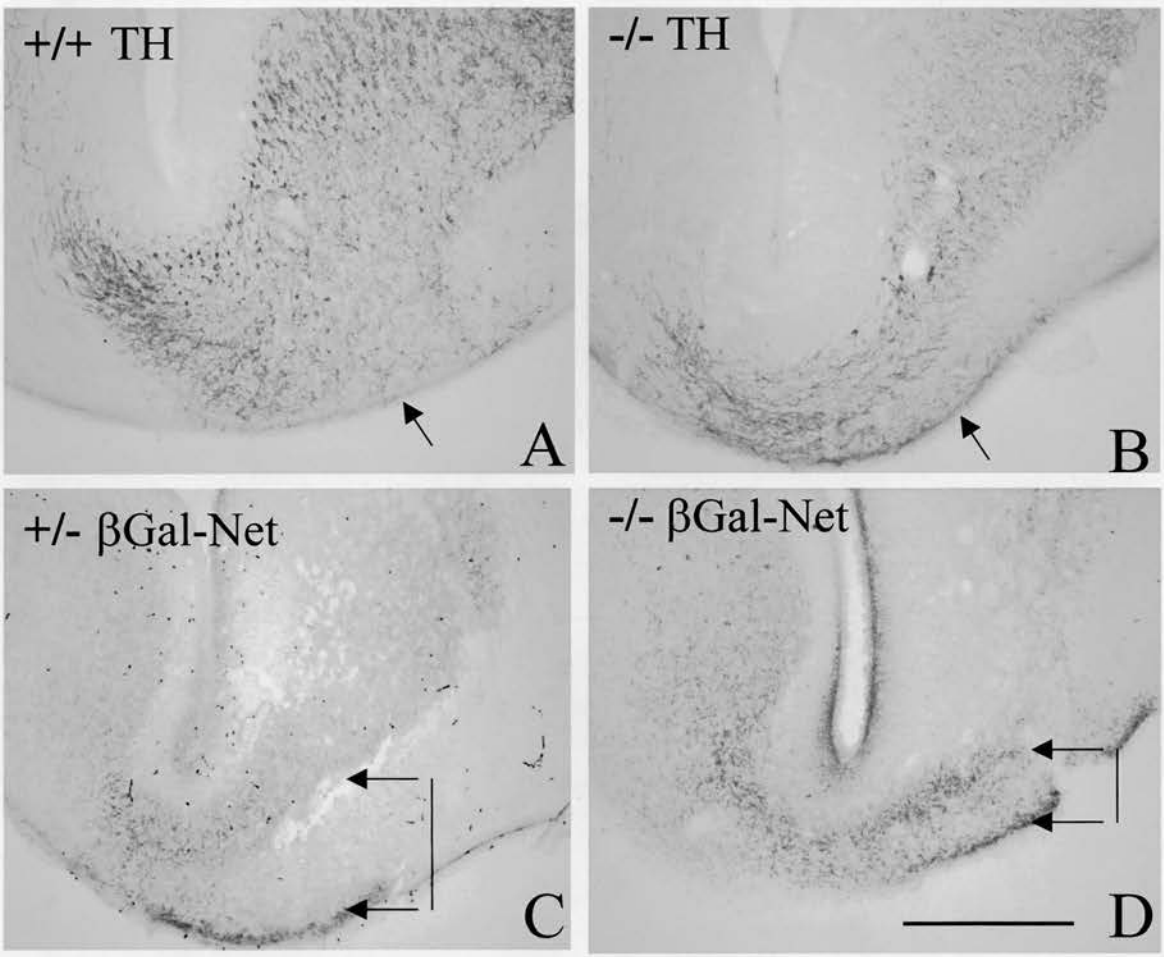

Figure VI-8 ***A, D,*** Coronal sections at the level of the olfactory tubercle of E17 (A) wild type (C) Netrin-1 heterozygote and (B,D) Netrin-1 knockout embryos. Sections were immunostained for (A,B) tyrosine hydroxylase or for (C,D) βGal which reveals the location of Netrin-1 expressing cells. ***A, B,*** Coronal sections showing the decrease in the density of tyrosine hydroxylase immunoreactive fibers in the olfactory tubercle of (B) Netrin-1 knockout embryo in comparison to (A) wild type embryo. *Arrow* points to the olfactory tubercle. ***C, D,*** Arrows define the thickness of the olfactory tubercle. Note the reduction in the thickness of the olfactory tubercle in (E) Netrin-1 knockout embryo in comparison to (D) Netrin-1 heterozygote embryo. Scale bar = 1 mm.

regulation of DCC expression (Volenec et al., 1998), suggesting that DCC is expressed by dopaminergic neurons. In addition, it has been recently reported that DCC is transiently expressed from E15 to E17 in the nigrostriatal bundle (Shu et al., 2000) and mesocortical fibers (data not shown). This suggests that DCC could be a good candidate in mediating the role of Netrin-1 in dopaminergic neurons.

I have tested whether DCC- and Netrin-1-knockout mice displayed similar alterations. Like Netrin-1 knockout mice, mice lacking DCC displayed no gross alterations in SN-VTA projections and I have observed similar alterations to those displayed by Netrin-1 knockout mice. By contrast, DCC-knockout mice displayed only few ectopic TH-IR neurons in mes-p2 which were located dorsally to A10. Interestingly, we found that DCC knockout mice displayed an increased number of SN and VTA TH-IR neurons as judged by the higher density and higher surface occupied by the SN-VTA complex (Figure VI-9). However, additional experiments such BrdU injections would be necessary to provide a quantitative analysis of this phenotype.

V Discussion

1 Expression of Netrin-1 in dopaminergic neurons of the A9-A10 complex

The roles of the morphogen sonic hedgehog (Shh) in the spinal cord have been well described: SHH protein is first produced by the notochord and induces the formation of the floor plate in the ventral midline of the neural tube, which then goes on to express Netrin-1 (Ingh, 1995; Placzek, 1995). At the level of the midbrain, Shh has been implicated in the differentiation of dopaminergic neurons (Hynes et al., 1995; Wang et al., 1995; Wu et al., 1999). It is conceivable that the expression of Netrin-1 by nigral and ventral tegmental dopaminergic neurons reflects the role of Shh in their development. In this view, Netrin-1 expression could be regarded as an early marker of differentiation of SN-VTA dopaminergic neurons. In this study, I pointed out that a subset of A9-A10 dopaminergic neurons, mostly located in VTA, express Netrin-1. This suggests that dopaminergic neurons of the A9-A10 complex are not equally influenced by Shh while they are generated, and that Netrin-1 expression in specific dopaminergic neurons may provide additional qualities to these neurons, such as those involved in migration, axonal outgrowth or survival.

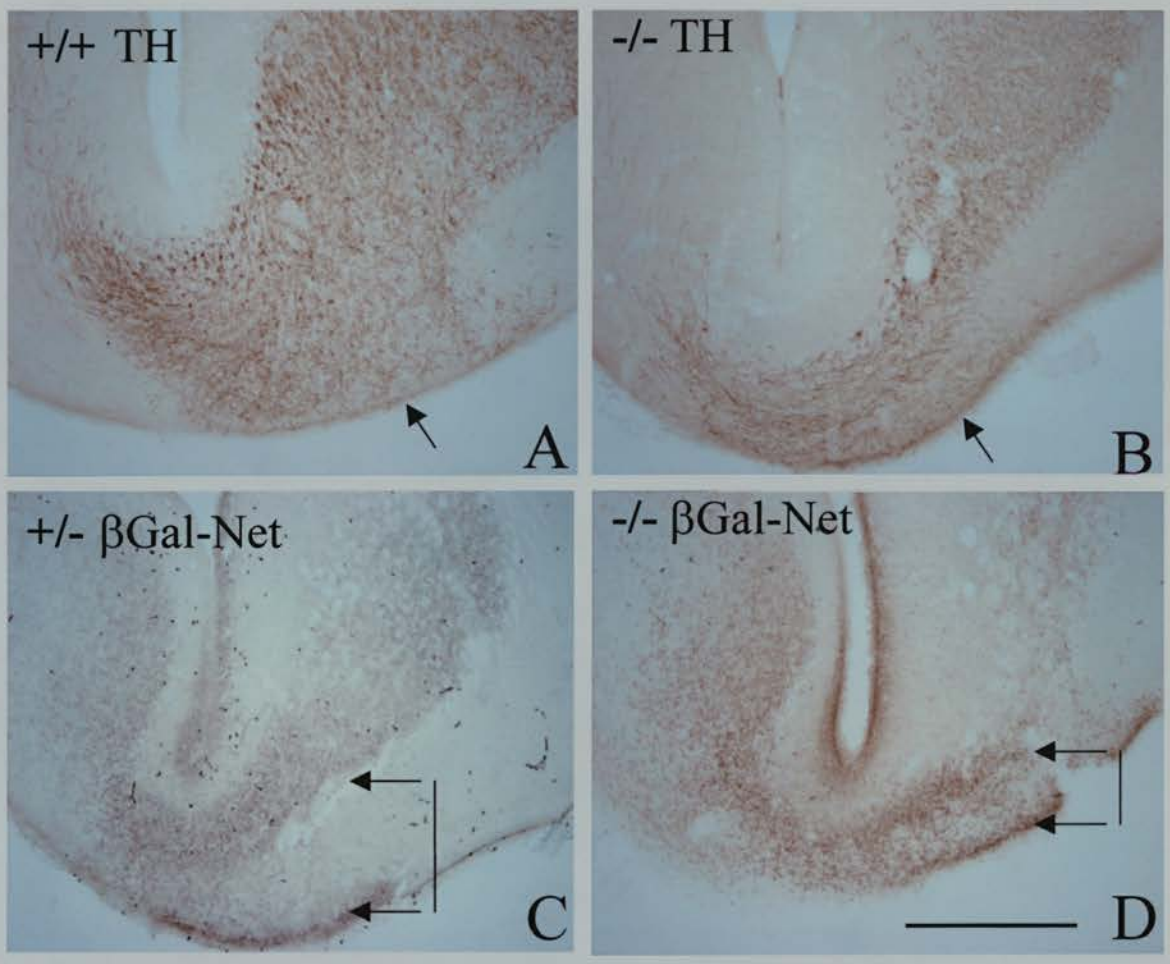

Figure VI-8 ***A, D,*** Coronal sections at the level of the olfactory tubercle of E17 (A) wild type (C) Netrin-1 heterozygote and (B,D) Netrin-1 knockout embryos. Sections were immunostained for (A,B) tyrosine hydroxylase or for (C,D) βGal which reveals the location of Netrin-1 expressing cells. ***A, B,*** Coronal sections showing the decrease in the density of tyrosine hydroxylase immunoreactive fibers in the olfactory tubercle of (B) Netrin-1 knockout embryo in comparison to (A) wild type embryo. *Arrow* points to the olfactory tubercle. ***C, D,*** Arrows define the thickness of the olfactory tubercle. Note the reduction in the thickness of the olfactory tubercle in (E) Netrin-1 knockout embryo in comparison to (D) Netrin-1 heterozygote embryo. Scale bar = 1 mm.

2 Role of Netrin-1 in neuronal migration

Several studies have pointed out the role of Netrin-1 in the migration of different neuronal populations in non-vertebrates (Chan et al., 1996) and vertebrates (Block-Gallego et al., 1999; Alcantara et al., 2000). Dopaminergic neurons have a biphasic migratory behavior, first they migrate radially from the proliferative (ventricular) zone to the superficial zone of the midbrain and then they migrate tangentially from caudal to rostral. The radial migration starts from E10.5 to finish roughly by E13.5 whereas the tangential migration starts from E14 to finish by E17. In early developmental stages from E12 to E14, I found a strong expression of Netrin-1 both in the proliferative zone where SN-VTA neurons are generated and in the marginal zone where postmitotic SN-VTA neurons are migrating radially from the ventricular zone to the superficial zone. From E15, Netrin-1 expression decreased strongly in the proliferative and radial migration zone whereas Netrin-1 expression increased in the regions of tangential migration. It is conceivable that Netrin-1 controls both the radial and tangential migration of newly generated postmitotic neurons away from the germinal zones. My in vitro experiments with E14 and E17 explants failed to support a role for Netrin-1 in the migratory behavior of SN-VTA neurons. Additional co-culture experiments performed with younger explants including germinal zones would be required to fully answer this question. In addition, it is possible that the endogenous expression of Netrin-1 in the explants has prevented the gradient of Netrin-1 established from the EBNA-Netrin-1 aggregates in co-cultures, leading to the failure of SN-VTA neurons to migrate toward Netrin-1 secreting cells. The use of explants obtained from Netrin-1 knockout mice would prevent such artefacts from happening. Interestingly, in mice lacking Netrin-1, I found ectopic TH-IR neurons in the midbrain. The existence of these ectopic TH-IR neurons could originate from either an abnormal migratory behavior of some dopaminergic neurons or an abnormal increase of the proliferative zone that could induce supernumerary TH-IR neurons. Interestingly, Netrin-1 knockout mice displayed a normal expression of Shh and HNF3-β, two molecules able to induce the generation of dopaminergic neurons. Taken together, my results suggest that Netrin-1 could be a factor important for the migratory behavior of some dopaminergic neurons.

3 Axonal outgrowth

The data obtained from my in vitro assay show that E14 VTA explants display an increase and preferential axonal outgrowth towards Netrin-1 secreting cells. This suggests that Netrin-1 could play a role as a guidance molecule for TH-IR fibers from the VTA to their target tissues or alternatively that Netrin-1 could play an outgrowth-promoting role on dopaminergic neurons of the VTA. It is believed that in vivo, Netrin-1 mediates its effects locally rather than over long distances. Since Netrin-1 is expressed in the target tissues but also all along the pathway of the medial forebrain bundle where most dopaminergic projections are travelling it is conceivable that Netrin-1 could guide VTA fibers which express DCC. My data support also the possibility of an outgrowth promoting effect of Netrin-1. Indeed, the number of growth cones facing the transfected cells is increased if the cells were transfected with Netrin-1 rather than c-myc alone. However, the nature of the VTA projections affected by Netrin-1 has not been identified in these experiments and it would be crucial to do it.

Netrin-1 and DCC knockout mice display an overall normal organisation of TH-IR fibers travelling along the medial forebrain bundle and the fasciculus retroflexus. Alterations in the organisation of TH-IR terminals are only seen in the ventral pallidum, septum and cingulate cortex and they are most likely secondary to the lack of the anterior commissure and corpus callosum and the abnormal presence of Probst's bundles in the septum. This suggests that Netrin-1 and DCC are not likely to play a major role in the initial guidance of TH-IR fibers in the brain. However, this study does not present the quantitative data necessary to provide a definite answer and it is possible that terminals reaching the specific targets of the SN or VTA (i.e.: the olfactory tubercle) are reduced in number. Finally, this study shows that other molecules than Netrin-1 are playing roles in the guidance of TH-IR fibers.

Since Netrin-1 is protractedly expressed in adults, it is also possible that Netrin-1 could be important in the plasticity of the dopaminergic system (i.e.: in the plasticity of the dopaminergic brain reward circuit).

4 Neuronal survival and DCC

In the midbrain, DCC is expressed from E13.5 in postmitotic dopaminergic neurons (Gad et al., 1997; Volonec et al., 1998). Interestingly, this period corresponds to the tangential migration, axonal guidance and survival of dopaminergic neurons. Interestingly, DCC knockout mice displayed no gross alterations in TH-IR fiber pathway or migratory behavior. However, DCC knockout showed an obvious increase in the number of SN-VTA dopaminergic neurons at P0 suggesting a role for DCC either in the cell proliferation or the cell survival of these dopaminergic populations. DCC is a candidate tumour-suppressor gene (Fearon and Pierceall, 1995). Indeed, loss of DCC expression has been associated with tumorigenicity of several tissue types (i.e.: colon, uterus; Schmitt et al., 1998) including brain (Ekstrand et al., 1995). Furthermore, reestablishment of DCC expression in tumours cells has been shown to suppress tumorigenicity (Kato et al., 2000). One mechanism by which DCC could have its tumor suppressor activity would be that DCC induces apoptosis when engaged by Netrin-1. DCC is a caspase substrate and mutation of the site at which caspase-3 cleaves DCC suppresses the pro-apoptotic effect of DCC completely (Mehlen et al., 1998). Apoptosis in SN-VTA dopaminergic neurons has only been reported to occur postnatally, from P2 (Jackson-Lewis et al., 2000) and so far there is no evidence for embryonic cell death in SN-VTA dopaminergic neurons. Interestingly, the caspase-3 pathway has been shown to be implicated in early cell death of SN dopaminergic neurons (Jackson-Lewis et al., 2000). Altogether, this suggests that DCC could participate in the regulation of SN-VTA dopaminergic neuron cell number throught the caspase-3 pathway. Further experiments such caspase-3 localisation or BrdU injections in DCC knockout mice are required to answer that question.

CHAPTER SEVEN:
CONCLUSION AND PERSPECTIVES

CHAPTER SEVEN:
DISCUSSION AND PERSPECTIVES

I Chapter II and Chapter III

In Chapter Two, I showed that an excess of serotonin during the critical period P0-P4 was sufficient to produce permanent thalamocortical and cortical alterations of the barrel field. This demonstrates that a transient rather than a permanent excess of serotonin (as observed in MAOA-knockout mice) produces these permanent alterations. Moreover, soon after this study had started, colleagues showed that sensory thalamic neurons were able to take up and store 5-HT, reinforcing the idea of a primordial role of serotonin during the development of the thalamocortical system.

The targets that mediate the effects of serotonin in the thalamocortical somatosensory system are still not clearly defined and much work has to be done to elucidate the molecular and cellular mechanisms through which serotonin acts. So far, several targets have been identified and a few mechanisms could be proposed.

1 5-HT action mediated through 5-HT receptors and 5-HT transporter

1.1 Presynaptic action

5-HT could act presynaptically on two main targets: the 5-HT1B receptor subtype and the plasma membrane serotonin transporter (SERT). Both are expressed by thalamic neurons and are located at the level of the axonal arbors during the critical period of barrel field formation.

5-HT1B is a member of the seven transmembrane domains family and is coupled to a Gi protein. Its activation by 5-HT inhibits the adenylate cyclase activity leading to a decrease in cAMP levels. Physiologically, 5-HT1B activation leads to a decrease of neurotransmitter release (i.e. 5-HT or acetylcholine). In the thalamocortical system, 5-HT1B activation could lead to a decrease in glutamate release. Indeed, electrophysiological studies have shown that glutamate release was decreased by applying 5-HT or 5-HT1B antagonists in the bath of a thalamocortical preparation in vitro (Rhoades et al., 1994). In vivo, 5-HT1B knockout mice display a

normal barrel field and recently, mice double knockout for MAOA and 5-HT1B have been generated. MAOA-5HT1B double knockout mice display both a normal barrel field and an excess of 5-HT (as observed in MAOA knockout mice), indicating a direct role of 5-HT1B in mediating the effects of 5-HT excess (Salichon et al., submitted). Moreover, it has been shown that adenylate cyclase 1 knockout mice display a barrelless phenotype. Taken together, this indicates that 5-HT acting on 5-HT1B modulates in vivo the release of glutamate by inhibiting the cAMP transduction pathway (Fig. VII-1). It is not known presently what targets are involved in this transduction pathway.

SERT and VMAT2 are also transiently expressed by thalamocortical axons. SERT takes up 5-HT from extracellular space to intracellular cytosol. Then, 5-HT is stored into vesicles through VMAT2. It is possible that 5-HT could be released by thalamocortical axons after budding of the vesicles. 5-HT could act locally on presynaptic (5-HT1B) and postsynaptic targets. The role of SERT in the formation of the barrel field is important since SERT knockout mice display a barrelless phenotype. This could be explained by the fact that 5-HT is not cleared from the synaptic cleft and could act in a long lasting time on 5-HT1B receptors. Moreover, it is unlikely that VMAT2 plays an important role in S1 formation since VMAT2 knockout mice did not display alteration in the barrel field organisation (O. Cases, unpublished observations).

1.2 Postsynaptic action

So far, no 5-HT receptors have been identified in S1 layer IV cells. At least 5-HT1A, 1B, 1D, 2A and 2C are not expressed in S1 layer IV cells during the critical period (O. Cases, unpublished observation). In addition, mice knockout for 5-HT2A, 1B, 1A, 5A, and 5B have a normal barrel field organisation (J.P. Hornung, unpublished observations). However, other 5-HT receptor subtypes are still to be studied such as the 5-HT3 or 5-HT2B.

Moreover, it has been described that cortical astrocytes display a low affinity uptake for serotonin. This study was done in vitro and there is no evidence for such a mechanism in vivo.

2 5-HT action mediated through activity-dependent mechanisms

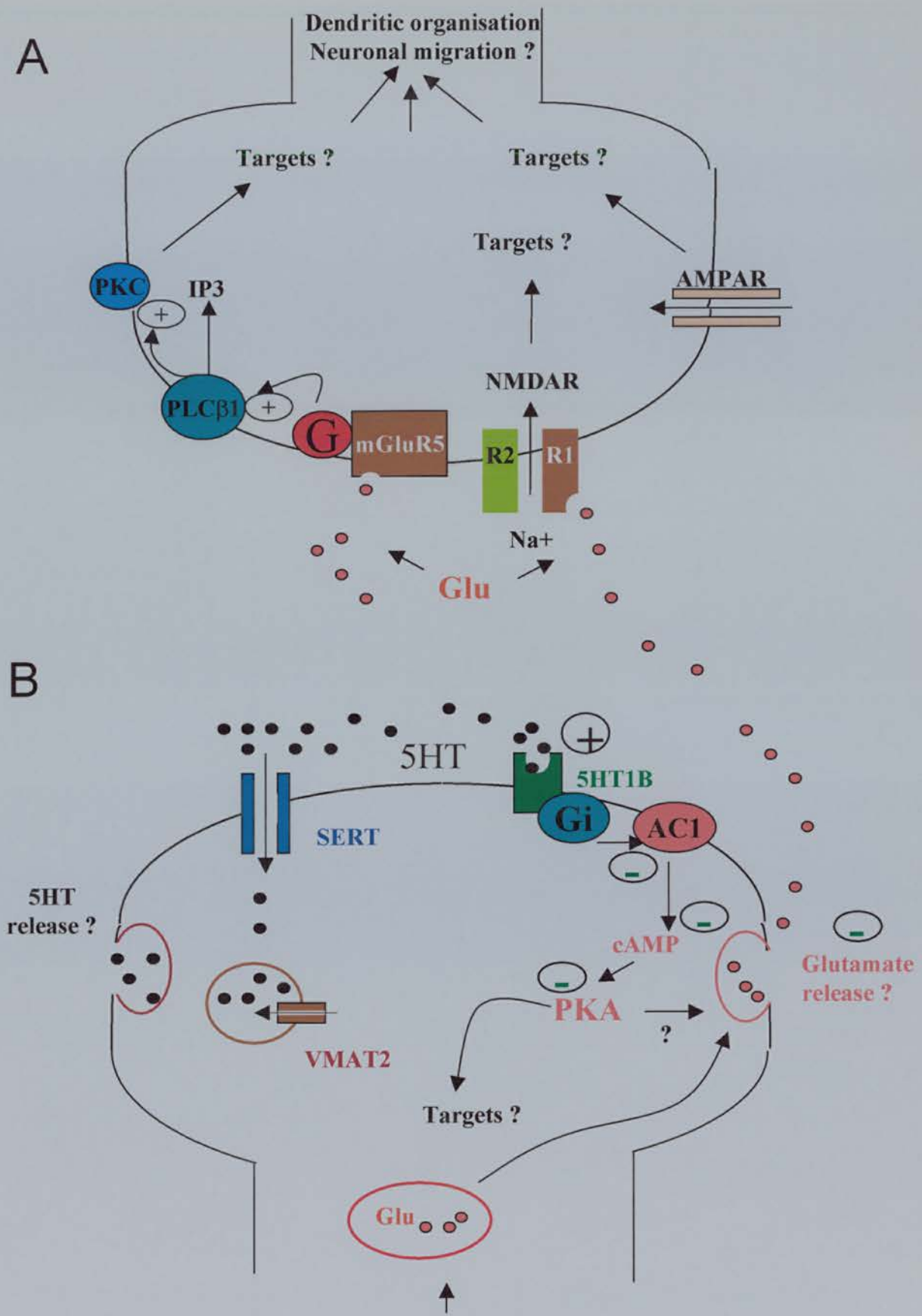

Figure VII-1: Please, see figure legend on the following page

Figure VII-1: A, Action of glutamate on granular neurons. Glutamate (Glu) can act via the metabotropic glutamate receptor type V (mGluR5), the NMDA receptor and AMPA receptor that are expressed by granular neurons during the critical period. **B, Presynaptic action of 5HT on thalamocortical axons**. 5HT1B receptors are transiently expressed on thalamocortical axons, 5HT action is to inhibit adenylate cyclase 1 (AC1). Inhibition of AC1 leads possibly to the inhibition of glutamate (Glu) release through the cAMP transduction pathway. 5HT uptake through the serotonine transporter (SERT) and storage through the vesicular monoamine transposter type 2 (VMAT2) leads to the accumulation of 5HT that could be released.

Table VII-1 Barrel-like expression of several markers-non exhaustive list.

Components and Markers	Species	Age of first detection	Pattern	Period of expression	References
Thalamocortical afferents					
Acetylcholinesterase	Rat	E21 0 hr 11 hr P3	Nascent Row Barrels Barrels	Permanent	Schlaggar and O'Leary (1991) Kristt (1979)
DiI (anterograde)	Rat	25 hr 49hr	Row Barrel	Permanent	Jhaveri et al., 1991 Erzurumlu and Jhaveri (1990)
anti-GAP-43	Rat	P3	Barrel	Transient until P7	Erzurumlu et al., 1990
Cytochrome oxidase	Rat	P3	Barrel	Permanent	Erzurumlu et al., 1990
anti-5HT	Rat	25 hr 60 hr 73 hr	Nascent Row Barrels	Transient until P10	Rhoades et al., 1990
anti-SERT	Mouse Rat		Barrels	Transient until P10 Transient until P15	Lebrand et al., 1998 Hanson et al., 1998
anti-VMAT2	Mouse		Barrels	Transient until P12	Lebrand et al., 1998
5HT1B	Mouse	P3	Barrels	Transient until P10	Boschert et al., 1994

	Rectificator of inward currents anti-GIRK-1 KV3	Rat	-	Barrels	-	Ponce et al., 1996 Weiser et al., 1994
Cortical glycogonjugates						
	Peanut agglutinin (Lectin)	Rat	P3	Barrels Septae		McCandish et al., 1989
	Cytotactin or Tenascin		P3	Barrels Septae		Crossin et al., 1989
	Neurocan		P2 P4	Nascent Barrels Septae	Permanent	Watanabe et al., 1995
Cortical cells						
	Nissl	Mice	P3	Barrels Walls	Permanent	Wise and Jones, (1978) Rice et al., 1985
	anti-mGluR1	Mice	P2	Barrel Hollow	(P7-P9 max)	Munoz et al., 1999
	anti-mGluR2,3	Mice			Transient P4-P9 max	Munoz et al., 1999
	anti-mGluR5	Rat Mice	P5 P4	Barrels Hollow	(P5-P14 max) (P7-P9 max)	Blue et al., 1997 Munoz et al., 1999
	anti-AMPAR GluR1 GluR2,3	Rat	P10	Barrels Septae high	(P14 max)	Blue et al., 1997

	anti-KainateR GluR5,6	Mice		Barrel center high	(P14-P21 max)	Brennan et al., 1997
	NADPH diaphorase	Mice	P0	Barrels Septae	Transient (P0-P15)	Mitrovic and Schachner (1996)
	Synaptic Vesicle Protein	Rat		Barrels	during synaptogenesis	Stettler et al., 1996
	SV2		P3			
	Synaptophysin I		P4			
	Synapsin		P4			
	Rab3a		P7			
	anti-GIRK-1	Rat	-	Barrels	-	Ponce et al., 1996

Table VII-2: Some knockout mice displaying alteration(s) of the somatosensory system

Molecule	Abnormality	Clustering of granular neurons	Clustering of thalamocortical axons	Lower stations	Other informations and References
Presynaptic					
MAOA	Degradation of 5HT and NA	Absent	absent (after P3)	Normal	rescue by crossing with 5HT1B-KO (1)
SERT	Uptake of 5-HT	Absent	Partially altered	Normal	(2)
VMAT2	Storage of monoamines	Partially altered	Partially altered	Normal	(3)
Adenylate cyclase 1	AMPc	Absent	Absent (before P4)	Normal	enlargment of the receptive field of a whisker (4)
GAP-43	Cytoskeletal organisation in nerve ending presynaptic substrate for PKC	Absent	Absent	Normal	(5)
Postsynaptic					
NMDAR1-conditional KO (cortical)		Absent	Mostly preserved	Normal	(6)
PLC-β1	IP3	Altered	Mostly preserved	no data	(7)
mGluR5		Altered	Partially preserved	no data	(7)

(1) N. Salichon, I Seif et al., personal communication; (2 and 3) P. Gaspar, O. Cases et al., personal communication; (4) Welker et al., 1996; (5) Maier et al., 1999; (6) Iwasato et al., 2000; (7) Hannan et al., submitted.

The hypothesis is that 5-HT inhibits presynaptically the release of glutamate (Figure VII-1). Glutamate acts on three families of receptors: the AMPA, the NMDA and the metabotropic glutamate receptors. The AMPA and NMDA receptors are ionotropic types. Metabotropic glutamate receptors (mGluRs) are coupled to G proteins and mediate slow action of glutamate through modulation of second messenger pathways. It has been shown that granular neurons express during the critical period the AMPAR, the NMDAR1 and R2 subunits and mGluR1and R5 subtypes. Both mGluR1 and mGluR5 stimulate phosphatidyl inositol hydrolysis and mobilisation of Ca2+ from intracellular stores. Group I-mediated PI hydrolysis is enhanced in early development (Casabona et al., 1997) and mGlur1α and mGluR5 expression is differentially regulated during the same time period (Romano et al., 1996). In the kitten primary visual cortex, peaks in mGluR1 and mGluR5 expression and in mGluR-mediated PI turnover overlap the critical period of development (Reid et al., 1997). Hence, mGluRs may make a substantial contribution to the activity-dependent establishment of somatopic patterns of representation in the developing central nervous system. Mice lacking mGluR5 have recently been shown to lack granular neuronal clustering (J.P. Hornung, unpublished observation and Hannan, submitted). In addition, it has been shown that mGluR5 mediates the activation of phospholipaseC-β1 (PLCβ1) and that mice lacking PLCβ1 display similar alterations than those observed by mGluR5 knockout mice (P. Kind, personal communication and Hannan et al., submitted).

Intense NMDAR1 immunoreactivity is also present in layer IV during the critical period and recent data show that conditional knockout mice for NMDAR1 in the cortex display altered granular neurons clustering (Iwasato et al., 2000).

In conclusion, glutamate is necessary to the clustering in barrels of granular neurons. Cytoplasmic or membrane targets of mGluR5 or NMDA activation have not been identified so far.

3 5-HT action mediated through other mechanism

In addition, several expression studies have also pointed out that several molecules are expressed in a barrel-like pattern either transiently or permanently (Table VII-1). Several knockout mice have been done to explore the involvement of these molecules in barrel field formation (Table VII-2). None of these molecules shows a direct relationship with the serotoninergic phenotype. A way to explore their

role would be to create in vitro assays in which slices containing normal thalamus and cortex would be cultured in presence of diffusible molecules and the clustering of granular neurons and the segregation of thalamic axons would be assessed.

II Chapter IV

To understand how monoamines could act on the developing brain, it is crucial to have a clear picture of the location of molecules that could participate in the regulation of monoamines levels such as the 5-HT transporter, the vesicular monoamine transporter types I and II, and monoamine oxidases types A and B. Recently, the developmental studies of the monoamine transporters have been completed, suggesting an unexpected role of monoamine during development (Hansson et al., 1997; Lebrand et al., 1998). Since I have started my "scientific career" by studying some of the phenotypes caused by altered MAOA activity (Cases et al., 1996; Vitalis et al., 1998), I have decided to provide deeper insights into the developmental course of the monoamine oxidases in the murine central (Chapter IV) and peripheral nervous system (Chapter IV and data not reported).

In Chapter IV, I have combined in situ hybridization, histochemistry and immunocytochemistry to locate precisely MAOA and MAOB in the developing nervous system. Several important points emerged from this study which have been extensively discussed in Chapter IV. Briefly, I showed that MAOA mRNA expression was tightly linked to the catecholaminergic (transient or permanent) and serotoninergic phenotypes. This showed that the regulation of embryonic serotonin levels is, at least in part, performed by the embryo itself soon after the genesis of its own serotoninergic neurons. Interestingly, whereas MAOA expression decreased dramatically in serotoninergic neurons during early postnatal development, MAOB expression increased strongly during the same period and reached its maximum expression by P21. This differential pattern of expression of MAOA and MAOB in serotoninergic neurons could explain the normalisation of 5-HT levels in MAOA knockout mice. I also showed that MAOB mRNA expression was located in most forebrain cholinergic neurons and all non-neuronal cells, such as the ventricular ependymal cells or astrocytes. In addition, I found two novel localizations of MAOB: i) in the olfactory placode and olfactory epithelium where MAOB is expressed from

E10, and ii) in astrocytes at the spinal and cranial nerve interface between the CNS and PNS.

To my point of view, one of the most interesting perspective of research would be to elucidate the role of MAOB activity in these two novel locations that I have described. For instance, it would be exciting to find out whether MAOB activity is playing a physiological role during the period of crossing and arborization of the nerves in the CNS and whether a re-expression of MAOB could help the re-growth of peripheral nerves after lesions into the CNS. The other interesting perspective would be to investigate the physiological role of MAOB activity in the olfactory epithelium using MAOB knockout mice.

III Chapter V and Chapter VI

The studies reported in Chapters V and VI aimed initially to give deeper insights into the development of dopaminergic populations notably those progressively lost in Parkinson's disease (i.e.: the substantia nigra). This would have both satisfied my scientific curiosity and interest and provided, I hoped, the seeds for future therapeutic researches. More precisely, I wanted to elucidate what were the "factors" necessary for a normal proliferation, specification and migration of dopaminergic neurons of the substantia nigra.

Pax6 was previously suggested to be a strong candidate in regulating the proliferation of isthmic progenitors (the isthmus is the proliferative region where dopaminergic neurons of the substantia nigra and ventral tegmental area originate) and the maintenance of dopaminergic neurons where its expression was protracted (Stoykova and Gruss, 1995). I was therefore strongly attracted to study the location of Pax6 in dopaminergic neurons and the phenotype displayed by mice lacking Pax6. This study is described in Chapter V and leads me to conclusions and hypothesis that I started to explore and are reported in Chapter VI.

Briefly, in Chapter V, I showed that Pax6 is expressed in discrete catecholaminergic neuronal populations of the developing ventral thalamus, hypothalamus and telencephalon and that in mice lacking Pax6, these catecholaminergic populations develop abnormally: those in the telencephalon are reduced in cell number or absent whereas those in the ventral thalamus and hypothalamus are greatly displaced and densely packed. My study suggested that Pax6 may be involved directly or indirectly in regulating adhesive properties, cell

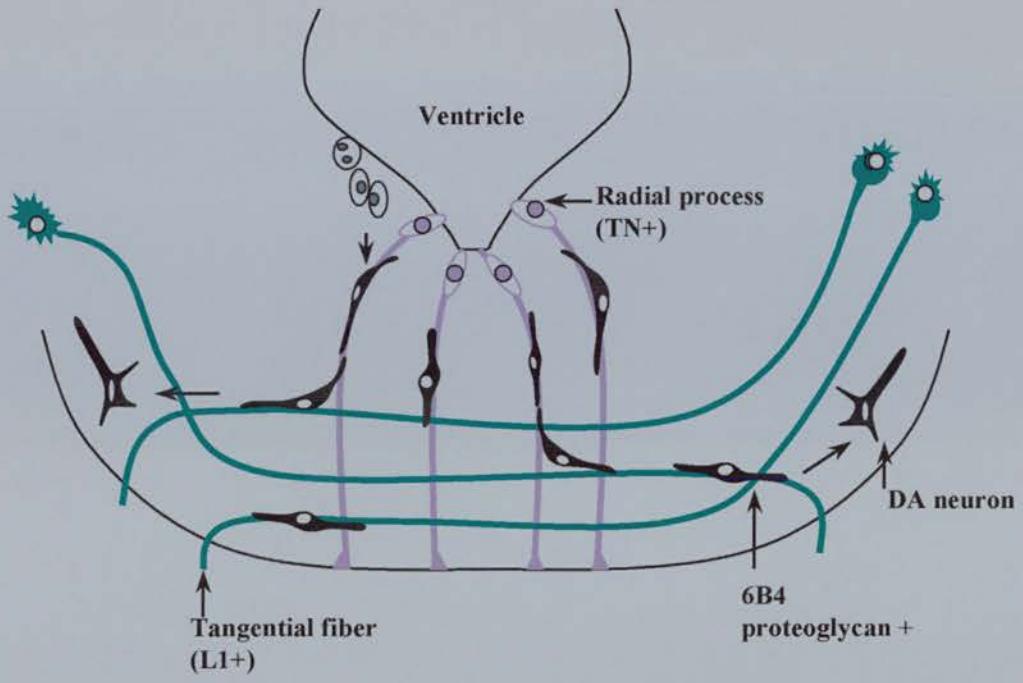

Figure VII-2 A schematic drawing of the migratory process of mesencephalic dopaminergic (DA) neurons in mice. DA neurons are generated at the ventricular surface of the ventral mesencephalon. The neurons migrate in two phases: first they migrate toward the ventromedial part of the mesencephalon along tenascin (TN)-immunoreactive processes of the neuroepithelial cells (Kawano et al., 1995); second they migrate laterally in the basal part of the mesencephalon along L1-positive tangentially arranged nerve fibers. The migratory DA neurons are immunoreactive for 6B4 proteoglycan, which bind L1 (From Ohyama et al., 1998).

migration but not cell proliferation of discrete catecholaminergic populations expressing Pax6. In addition, I found that catecholaminergic neurons of the substantia nigra (SN) and the ventral tegmental area (VTA) do not express Pax6 protein. Nevertheless, mice lacking Pax6 display an altered pathfinding of SN-VTA projections: instead of following the route of the medial forebrain bundle ventrally, most of the SN-VTA projections are deflected dorso-rostrally at the pretectal-dorsal thalamic transition zone and in the dorsal thalamic alar plate. Moreover, some catecholaminergic neurons are displaced dorsally to an ectopic location at the pretectal-dorsal thalamic transition zone. Interestingly, from the pretectal-dorsal thalamic to the dorsal thalamic-ventral thalamic transition zones, mice lacking Pax6 display a ventral to dorsal expansion of the chemorepellant/chemoattractive molecule, Netrin-1.

This study opened new perspectives regarding the development of SN-VTA dopaminergic neurons and I was interested to test whether Netrin-1 was playing a role in guiding the pathway and the migration of catecholaminergic populations. I have therefore started to analyse the phenotype displayed by Netrin-1 and DCC knockout mice and established an in vitro essay to directly test whether Netrin-1 gradients could guide/attract SN-VTA projections or SN-VTA migrating neurons. Preliminary results presented in Chapter VI showed that VTA but not SN projections display an increase growth toward Netrin-1 secreting cells. In addition, the analysis of Netrin-1 knockout mice show that dopaminergic neurons, most likely corresponding to A9-A11 groups are ectopically located in the mutant brain suggesting a direct or indirect role for Netrin-1 in the migration and/or survival of these dopaminergic populations. Preliminary analysis of DCC knockout mice suggests that DCC may play a role in early apoptosis of dopaminergic neurons.

Additional experiments would be required to fully analyse the phenotype displayed by Netrin-1 and DCC knockout mice and to explore more widely, in vitro, the role of Netrin-1 on dopaminergic neurons. It would be important to precisely determine the emergence of the phenotypes displayed by both Netrin-1 and DCC mutants. This would allow to relate the alterations to the different phases of development that SN-VTA dopaminergic neurons undergo: genesis (E10-E15), migration (radial: E10-E14, tangential: from E14) and cell death (believed to start in neonates; Jackson-Lewis et al., 2000). The analysis of the repartition of BrdU labelled progenitors may also help to give a clear picture of the mutants phenotype. It

would also be necessary to repeat in vitro experiments with younger tissues to test whether newly postmitotic dopaminergic neurons migrate toward Netrin-1 secreting cells. Finally, it is likely that DCC participates in the regulation of apoptosis in dopaminergic neurons of the SN-VTA complex. The generation of mice over-expressing DCC in SN-VTA neurons or alternately the use of in vitro assays in which SN-VTA explant would be transfected with DCC under the control of a specific promoter (using the gene-gun technique) may answer this important question.

During my PhD, I was surprised by the lack of data available on migration and cell death of dopaminergic neurons. So far, only descriptive and coincidental evidences are available to support the molecular basis of the migratory behavior of dopaminergic neurons of the SN-VTA complex (Fig. VII-2). Recent and preliminary analysis of L1 knockout mice which display ectopic dopaminergic neurons appear to confirm these observations (Demyanenko et al., 2000). Interestingly, Pax6 mutant mice display abnormal organisation of L1-positive fibers associated with an abnormal topographical organization of DA neurons and one of my hypothesis was that dopaminergic neurons had abnormally migrated along abnormally guided L1-fibers. These two independent observations seems to reinforce the idea that L1 is playing a direct role in the tangential migration of SN-VTA dopaminergic neurons. However, only a small proportion of the dopaminergic population seems to be affected by L1 alterations suggesting that other molecules are likely to be involved in tangential migration of DA neurons. Regarding cell death of dopaminergic neurons of the SN-VTA complex, few and controversial data are available but recent findings support the idea that SN-VTA neurons are subject to a regressive event that begins before birth (Jackson-Lewis et al., 2000). The regulation of the number of SN dopaminergic neurons seems therefore to be influence by several events: i) one which takes place during late embryonic development and which is not described, ii) one which takes place between P7 and P21 and which tend to match the number of dopaminergic neurons and target cells and iii) a later one which may be involved in Parkinson's disease. Indeed, it has been proposed that in Parkinson's disease neuronal cell death may result from the inappropriate re-activation of the developmental cell death process (Burke and Kholodilov, 1998).

General Point

Science offers an incredible number of fields in which one can dig and find one's own satisfaction in discovering new elements that could help to cure disease or simply contribute to the general knowledge.

REFERENCES

REFERENCES

• Ackerman SL, Kozak LP, Przyborski SA, Rund LA, Boyer BB, Knowles BB (1997) The mouse rostral cerebellar malformation gene encodes an UNC-5-like protein. Nature 386: 838-842.

• Aitken AR, Tork I (1988) Early development of serotonin-containing neurons and pathways as seen in wholemount preparations of the fetal rat brain. J Comp Neurol 274: 32-47.

• Alcantara S, Frisen J, del Rio JA, Soriano E, Barbacid M, Silos-Santiago I (1997) TrkB signaling is requiered for postnatal survival of CNS neurons and protects hippocampal and motor neurons from axotomy-induced cell death. J Neurosci 17: 3623-3633.

• Alcantara S, Ruiz M, De Castro F, Soriano E, Sotelo C (2000) Netrin 1 acts as an attractive or as a repulsive cue for distinct migrating neurons during the development of the cerebellar system. Development 127:1359-1372

• Agmon A, Yang LT, O'Dowd DK, Jones EG (1993) Organized growth of thalamocortical axons from the deep tier of terminations into layer IV of developing mouse barrel cortex. J Neurosci 13: 5365-5382.

• Agmon A, Yang LT, Jones EG, O'Dowd DK (1995) Topographical precision in the thalamic projection to neonatal mouse barrel cortex. J Neurosci 15: 549-561.

• Altman HJ, Nordy DA, Ogren SO (1984) Role of serotonin in memory: facilitation by aloproclate and zimelidine. Psychopharmacology 84: 496-502

• Alonso-Vanegas MA, Fawcett JP, Causing CG, Miller FD, Sadikot AF (1999) Characterization of dopaminergic midbrain neurons in a DBH:BDNF transgenic mouse. J Comp Neurol 413: 449-462.

• Alvarado-Mallart RM, Martinez S, Lance-Jones CC (1990) Pluripotentiality of the 2-day-old avian germinative neuroepithelium. Dev Biol 131:75-88

• Anderson GM, Riddle MA, Hoder EL, Feibel FC, Shaywitz BA, Cohen DJ (1988) The ontogeny of 3,4-dihydroxyphenylacetic acid in human cerebrospinal fluid. J Neurol Neurosurg Psychiatry 51: 1100-1102.

• Arai R, Kimura H, Maeda T (1986) Topographic atlas of monoamine oxidase-containing neurons in the rat brain studied by an improved histochemical method. Neuroscience 19: 905-925.

• Arai R, Karasawa N, Nagatsu T, Nagatsu I (1995) Exogenous L-hydroxytryptophan is decarboxylated in neurons of the substantia nigra pars compacta and locus coeruleus of the rat. Brain Res 669: 145-149.

• Armstrong-James M (1975) The functional status and columnar organization of single cells responding to cutaneous stimulation in neonatal rat somatosensory cortex S1. J Physiol 246: 501-538.

• Avery DH, Wildschiodtz G, Rafaelsen OJ (1982) Nocturnal temperature in affective disorder. J Affective Disord 4: 61-71.

• Baffi JS, Palkovits M, Castillo SO, Mezey E, Nikodem VM (1999) Differential expression of tyrosine hydroxylase in catecholaminergic neurons of neonatal wild-type and Nurr1-deficient mice. Neuroscience 93: 631-642.

• Baker H, Farbman AI (1993) Olfactory afferent regulation of the dopamine phenotype in the fetal rat olfactory system. Neuroscience 51: 115-134.

• Balan IS, Ugrumov MV, Borisova NA, Calas A, Pilgrim C, Reisert I, Thibault J (1996) Birthdates of the tyrosine hydroxylase immunoreactive neurons in the hypothalamus of male and female rats. Neuroendocrinology 64: 405-411.

• Baldwin CT, Hoth CF, Amos JA, da-Silva EO, Milunsky A (1992) An exonic mutation in the HuP2 paired domain gene causes Waardenburg's syndrome. Nature 355: 637-638.

• Barbacid M (1994) The trk family of neurotrophin receptors. J Neurobiol 25: 1386-1403.

• Barde YA, Edgar D, Thoenen H (1982) Purification of a new neurotrophic factor from the mammalian brain. EMBO J 1: 549-553.

• Bates CA, Erzurumlu RS, Killackey HP (1982) Central correlates of peripheral pattern alterations in the trigeminal system of the rat. Dev Brain Res 5: 108-113.

• Bates CA, Killackey HP (1985) The organisation of the neonatal rat's brainstem trigeminal complex and its role in the formation of central trigeminal pattern. J Comp Neurol 240: 265-287.

• Bayer SA, Wills KV, Triarhou LC, Ghetti B (1995) Time of neuron origin and gradients of neurogenesis in midbrain dopaminergic neurons in the mouse. Exp Brain Res 105:191-199.

• Bel N, Figueras G, Vilaro MT, Sunol C, Artigas F (1997) Antidepressant drugs inhibit a glial 5-hydroxytryptamine transporter in rat brain. Eur J Neurosci 9: 1728-1738.

• Belford GR, Killackey HP (1979a) Vibrissae representation in subcortical trigeminal centres of the neonatal rat. J Comp Neurol 183: 305-322.

• Belford GR, Killackey HP (1979b) The development of vibrissae representation in subcortical trigenimal centres of the neonatal rat. J Comp Neurol 188: 63-74.

• Belford GR, Killackey HP (1980) The sensitive period in the development of the trigeminal systems of the neonatal rat. J Comp Neurol 193: 335-350.

• Bennett-Clarke CA, Chiaia NL, Crissman RS, Rhoades RW (1991) The source of the transient serotoninergic input to the developing visual and somatosensory cortices in rat. Neuroscience 43: 163-183.

• Bennett-Clarke CA, Leslie MJ, Chiaia NL, Rhoades RW (1993) Serotonin 1B receptors in the developing somatosensory and visual cortices are located on thalamocortical axons. Proc Natl Acad Sci USA 90: 153-157.

• Bennett-Clarke CA, Leslie MJ, Lane RD, Rhoades RW (1994) Effect of serotonin depletion on vibrissa-related patterns of thalamic afferents in the rat's somatosensory system. J Neurosci 14: 7594-7607.

• Bennett-Clarke CA, Lane RD, Rhoades RW (1995) Fenfluramine depletes serotonin from the developing cortex and alters thalamocortical organization. Brain Res 702: 255-260.

• Berardi N, Maffei L (1999) From visual experience to visual function: roles of neurotrophins. J Neurobiol 41: 119-126.

• Berger B, Verney C, Gaspar P, Febvret A (1985) Transient expression of tyrosine hydroxylase immunoreactivity in some neurons of the rat neocortex during postnatal development. Brain Res 355: 141-144

• Berger W, Meindl A, Van de Pol TRJ (1992) Isolation of a candidate gene for Norrie disease by positional cloning. Nature Genet 1: 199-203.

• Berkemeier LR, Winslow JW, Kaplan DR, Nikolics K, Goeddel DV, Rosenthal A (1991) Neurotrophin-5: a novel neurotrophic factor that activates trk and trkB. Neuron 7: 857-866.

• Betarbet R, Zigova T, Bakay RA, Luskin MB (1996) Dopaminergic and GABAergic interneurons of the olfactory bulb are derived from the neonatal subventricular zone. Int J Dev Neurosci 14: 921-930.

• Birks J, Flicker L (2000) Selegiline for Alzheimer's disease. Cochrane database Syst Rev 2: CD000442.

• Bjorklund A, Lindvall O, Nobin A (1975) Evidence of an incerto-hypothalamic dopamine neurone system in the rat. Brain Res 89: 29-42.

• Bjorklund A, Lindvall O (1984) Dopamine-containing systems in the CNS. In "Handbook of chemical anatomy, Vol2: Classical transmitters in the CNS, Part1". Bjorklund A, Hokfelt T (Eds) Amsterdam, Elsevier, pp 55-122.

• Bjorklund A, Lindvall O (1986) Catecholamine brain stem regulatory systems. In "Handbook of physiology, Section1: The nervous system, Vol IV". Bloom FE (Ed). Bethesda, American physiological society, pp 155-235.

• Blakely RD, Berson HE, Fremau RT, Caron MG, Peek MM, Prince HK, Bradley CC (1991) Cloning and expression of a functional serotonin transporter from rat brain. Nature 354: 66-70.

• Blakemore C (1977) Mechanisms of the mind. Cambridge University Press, Cambridge.

• Bledsoe S, Zhou FC (1992) S100 and ontogenesis of radial glia-like cells and astrocytes during development of the rat. Soc Neurosci Abstr 18, 1117.

• Bloch-Gallego E, Ezan F, Tessier-Lavigne M, Sotelo C (1999) Floor plate and netrin-1 are involved in the migration and survival of inferior olivary neurons. J Neurosci 19: 4407-4420.

• Blue ME, Parnavelas JG (1982) The effect of neonatal 6-hydroxydopamine treatment on synaptogenesis in the visual cortex. J Comp Neurol 205: 199-205.

• Blue ME, Erzurumlu RS, Jhaveri S (1991) A comparison of pattern formation by thalamocortical and serotonergic afferents in the rat barrel field cortex. Cereb Cortex 1: 380-389.

• Blue ME, Martin LJ, Brennan EM, Johnston MV (1997) Ontogeny of non-NMDA glutamate receptors in rat barrel field cortex : I. Metabotropic receptors. J Comp Neurol 386: 16-28.

• Blum M (1998) A null mutation in TGF-alpha leads to a reduction in midbrain dopaminergic neurons in the substantia nigra. Nat Neurosci 1: 374-377.

• Bond PA, Cundall RL (1977) Properties of monoamine oxidase (MAO) in human blood platelets, plasma lymphocytes, and granulocytes. Clin Chim Acta 80: 317-326.

• Boulder Committee (1975) Embryonic vertebrate nervous system: revised terminology. Anat Rec 166: 257-262.

• Bradley PB (1989) Introduction to neuropharmacology. Butterworth and Co.

• Breakefield XO, Giller ELJ, Nurnberger JI, Castiglione CM, Buchsbaum MS, Gershon ES (1980) Monoamine oxidase type A in fibroblasts from patients with bipolar depressive illness. Psychiatr Res 2: 307-314.

• Brennan EM, Martin LJ, Johnston MV, Blue ME (1997) Ontogeny of non-NMDA glutamate receptors in rat barrel field cortex: II. α-AMPA and kainate receptors. J Comp Neurol 386: 29-45

• Briscoe J, Sussel L, Serup P, Hartigan-O'Connor D, Jessell TM, Rubenstein JL, Ericson J (1999) Homeobox gene Nkx2.2 and specification of neuronal identity by graded Sonic hedgehog signalling. Nature 398: 622-627.

• Broide RS, Robertson RT, Leslie FM (1996) Regulation of α-7 nicotinic acetylcholine receptors in the developing rat somatosensory cortex by thalamic afferents. J Neurosci 16: 2956-2971.

• Brunjes PC, Fisher M, Grainger R (1998) The small-eye mutation results in abnormalities in the lateral cortical migratory stream. Dev Brain Res 110:121-125.

• Brunner HG, Nelen MR, van Zandvoort P, Abeling NGGM, van Gennip AH, Wolters EC, Kuiper MA, Ropers HH, van Oost BA (1993a) X-linked borderline mental retardation with prominent behavioral disturbance: phenotype, genetic localization, and evidence for disturbed monoamine metabolism. Am J Hum Genet 52: 1035-1039.

• Brunner HG, Nelen M, Breakefield XO, Ropers HH, van Oost BA (1993b) Abnormal behavior associated with a point mutation in the structural gene for monoamine oxidase A. Science 262: 578-580.

• Budnik V, Wu CF, White K (1989) Altered branching of serotonin-containing neurons in drosophila mutants unable to synthesize serotonin and dopamine. J Neurosci 9: 2866-2877.

• Bulfone A, Puelles L, Porteus MH, Frohman MA, Rubenstein JLR (1993) Spatially restricted expression of Dlx-1, Dlx2 (Tes-1), Gbx-2 and Wnt-3 in the embryonic day 12.5 mouse forebrain defines potential transverse and longitudinal segmental boundaries. J Neurosci 13: 3155-3172.

• Burri M, Tromvoukis Y, Bopp D, Frigerio G, Noll M (1989) Conservation of the paired domain in metazoans and its structure in three isolated human genes. EMBO J 8: 1183-1190.

• Burke and Kholodilov (1998) Programmed cell death: does it play a role in Parkinson's disease? Ann Neurol 44: S126-S133.

• Buznikov GA (1991) The biogenic monoamines as regulator of early (pre-nervous) embryogenesis: new data. Adv Exp Med Biol 296: 33-48.

• Caleo M, lodovichi C, Maffei L (1999) Effects of nerve growth factor on visual cortical plastivity require afferent electrical activity. Eur J Neurosci 11: 2979-2984.

• Callaerts P, Halder G, Gehring WJ (1997) PAX-6 in development and evolution. Annu Rev Neurosci 20: 483-532.

• Cao Danh H, Strolin-Benedetti M, Dostert P (1984) Differential changes in monoamine oxidase A and B activity in aging rat tissues. In "Monoamine oxidase and disease. Prospects for therapy with reversible inhibitors". Tipton KF, Dostert P, Strolin-Benedetti M (Eds). London, Academic Press, pp 301-317.

• Caric D, Gooday D, Hill RE, McConnell SK, Price DJ (1997) Determination of the migratory capacity of embryonic cortical cells lacking the transcription factor Pax-6. Development 124: 5087-5096.

• Carlstedt T (1985) Regenerating axons from nerve terminals at astrocytes. Brain Res 347: 188-191.

• Carlstedt T, Dalsgaard CJ, Molander C (1987) Regrowth of lesioned dorsal root nerve fibers into the spinal cord of neonatal rats. Neurosci Lett 74: 14-18.

• Carmignoto G, Pizzorusso T, Tia S, Vicini S (1997) Brain-derived neurotrophic factor and nerve growth factor potentiate excitatory synaptic trnasmission in the rat visual cortex. J Physiol 418: 153-164.

• Casabona G, Knopfelt T, Kuhn R, Gasparini F, Baumann P, Sortino MA, Copani A, Nicoletti F (1997) Expression and coupling to polyphosphoinositide hydrolysis of group I metabotropic glutamate receptors in early postnatal and adult rat brain. Eur J Neurosci 9: 12-17.

• Cases O, Seif I, Grimsby J, Gaspar P, Chen K, Pournin S, Muller U, Aguet M, Babinet C, Shih JC, De Maeyer E (1995) Aggressive behavior and altered amounts of brain serotonin and norepinephrine in mice lacking MAOA. Science 268: 1763-1766.

• Cases O, Vitalis T, Seif I, De Maeyer E, Sotelo C, Gaspar P (1996) Lack of barrels in the somatosensory cortex of monoamine oxidase A-deficient mice: role of a serotonin excess during the critical period. Neuron 16: 297-307.

• Cases O, Lebrand C, Giros B, Vitalis T, De Maeyer E, Caron MG, Price DJ, Gaspar P, Seif I (1998) Plasma membrane transporters of serotonin, dopamine, and norepinephrine mediate serotonin accumulation in atypical locations in the developing brain of monoamine oxidase A knock-outs. J Neurosci 18: 6914-6927.

• Castillo SO, Xiao Q, Lyu MS, Kozak CA, Nikodem VM (1997) Organization, sequence, chromosomal localization, and promoter identification of the mouse orphan nuclear receptor Nurr1 gene. Genomics 41: 250-257.

• Castillo SO, Baffi JS, Palkovits M, Goldstein DS, Kopin IJ, Witta J, Magnuson MA, Nikodem VM (1998a) Dopamine biosynthesis is selectively abolished in substantia nigra/ventral tegmental area but not in hypothalamic neurons in mice with targeted disruption of the Nurr1 Gene. Mol Cell Neurosci 11: 36-46.

• Catalano SM, Robertson RT, Killackey HP (1991) Early ingrowth of thalamocortical afferents to the noecortex of the prenatal rat Proc Natl Acad Sci USA 88: 2999-3003.

• Catalano SM, Robertson RT, Killackey HP (1995) Rapid alteration of thalamocortical axons morphology follows peripheral dammage in the neonatal rat. Proc Natl Acad Sci USA 92: 2549-2552.

• Catalano SM, Robertson RT, Killackey HP (1996) Individual axon morphology and thalamocortical topography in developing rat somatosensory cortex. J Comp Neurol 367: 36-53.

• Carnahan J, Nawa H (1995) Regulation of neuropeptide expression in the brain by neurotrophins. Potential role in vivo. Mol Neurobiol 10: 135-149.

• Caviness VS, Frost DO (1980) Tangential organization of thalamic projections to the neocortex of the mouse. J Comp Neurol 194: 335-367.

• Caviness VS (1988) Architecture and development of the thalamocortical projection in the mouse. In "Cellular thalamic mechanisms" Bentivoglio M, Spreafico R (Eds). Elsevier, Amsterdam, pp 489-499.

• Cellerino A, Maffei L, Domenici L (1996) The distribution of brain-derived neurotrophic factor and its receptor trkB in parvalbumin-containing neurons of the rat visual cortex. Eur J Neurosci 8: 1190-1197.

• Chalepakis G, Wijnholds J, Giese P, Schachner M, Gruss P (1994) Characterization of Pax-6 and Hoxa-1 binding to the promoter region of the neural cell adhesion molecule L1. DNA Cell Biol 13: 891-900.

• Chao MV (1994) The p75 neurotrophin receptor. J Neurobiol 25: 1380-1385.

• Chiaia NL, Fish SE, Bauer WR, Bennett-Clarke CA, Rhoades RW (1992) Postnatal blockade of cortical activity by tetrodotoxin does not disrupt the formation of vibrissae-related patterns in the rat's somatosensory cortex. Dev Brain Res 66: 244-250.

• Chiaia NL, Fish SE, Bauer WR, Figley BA, Eck M, Bennett-Clarke CA, Rhoades RW (1994a) Effects of postnatal blockade of cortical activity with tetrodotoxin upon the development and plasticity of vibrissae-related patterns in the somatosensory cortex of hamster. Somatosens Mot Res 11: 219-228.

• Chiaia NL, Fish SE, Bauer WR, Figley BA, Eck M, Bennett-Clarke CA, Rhoades RW (1994b) Effects of postnatal blockade of cortical activity with tetrodotoxin upon lesion-induced reorganization of vibrissae-related patterns in the somatosensory cortex of the rat. Dev Brain Res 79: 301-306.

• Chiaia NL, Bennett-Clarke CA, Rhoades RW (1994c) Transection of, and axoplasmic transport blockade in the infraorbital nerve in newborn rats reduce expression of acetylcholinesterase by somatosensory axons. Soc Neurosci Abstr 20: 1699.

• Chiaia NL, Bennett-Clarke CA, Crissman RS, Zheng L, Chen M, Rhoades RW (1996) Effect of neonatal axoplasmic transport attenuation in the infraorbital nerve on vibrissae-related patterns in the rat's brainstem, thalamus and cortex. Eur J Neurosci 8: 1601-1612.

• Chubakov AR, Gromova EA, Konovalov GV, Sarkisova EF, Chubakov EI (1986) The effects of serotonin on the morpho-functional development of rat cerebral neocortex in tissue culture. Brain Res 369: 285-297.

• Cigola E, Volpe BT, Lee JW, Franzen L, Baker H (1998) Tyrosine hydroxylase expression in primary cultures of olfactory bulb: role of L-type calcium channels. J Neurosci 19: 7638-7649.

• Clarke E, O'Malley CD (1969) The human brain and spinal cord: a historical study illustrated by writings from antiquity to the twentieth century. University of California Press, Berkeley.

• Clarkson ED, Bahr BA, Parsons SM. (1993) Classical noncholinergic neurotransmitters and the vesicular transport system for acetylcholine. J Neurochem 61: 22-28.

• Colamarino SA, Tessier-Lavigne M (1995) The axonal chemoattractant netrin-1 is also a chemorepellent for trochlear motor axons. Cell 84: 621-629.

• Collins FA, Murphy DL, Reiss AL, Sims KB, Lewis JG, Freund L, Karoum F, Zhu D, Maumenee IH, Antonarakis SE (1992) Clinical, biochemical, and neuropsychatric evaluation of a patient with a contiguous gene syndrome due to a microdeletion Xp11.3 including the Norrie disease locus and monoamine oxidase (MAOA and MAOB) genes. Am J Med Genet 42: 127-134.

• Cooper RJ, Bloom FE, Roth RH (1991) The biochemical basis of neuropharmacology. 6th ed, New York, Oxford University Press.

• Coopersmith R, Weihmuller FB, Kristein CL, Marshall JF, Leon M (1991) Extracellular dopamine increases in the neonatal olfactory bulb during odor preference training. Brain Res 564: 149-153.

• Coppen A, Swade C (1988) 5-HT and depression: the present position. In "New concepts in depression" Briley M, Fillion G (Eds) London, Macmillan Press. 120-136

• Consolazione A., Milstein C, Wright B, Cuello AC (1981) Immunocytochemical detection of serotonin with monoclonal antibodies. J Histochem Cytochem 29: 1425-1430.

• Coyle JT, Axelrod J (1972a) Dopamine-hydroxylase in the rat brain: developmental characteristics. J Neurochem 1972 19: 449-459.

• Coyle JT, Axelrod J (1972b) Tyrosine hydroxylase in rat brain: developmental characteristics. J Neurochem 19:1117-1123.

• Croll SD, Wiegand SJ, Anderson KD, Lindsay RM, Nawa H (1994) Regulation of neuropeptides in adult rat forebrain by neurotrophins BDNF and NGF. Eur J Neurosci 6: 1343-1353.

• Cross AJ (1988) Serotonin in neurodegenerative disorders. In "Neuronal serotonin". Osborn NN, Hamon M (Eds) Chichester, John Wiley and Sons, pp 231-253.

• Crossin K, Hoffman S, Tan SS, Edelman GM (1989) Cytotactin and its proteoglycan ligand mark structural and functional boundaries in somatosensory cortex of the early postnatal mouse. Dev Biol 136: 381-392.

• Crossley PH, Martinez S, Martin GR (1996) Midbrain development induced by FGF8 in chick embryo. Nature 380: 66-68.

• Czerny T, Busslinger M (1995) DNA-binding and transactivation properties of Pax-6:three amino acids in the paired domain are responsible for the different sequence recognition of Pax-6 and BSAP (Pax-5). Mol Cell Biol 15: 2858-2871.

• D'Amato R, Blue ME, Largent BL, Lynch DR, Ledbetter DJ, Molliver ME, Snyder SH (1987) Ontogeny of the serotonergic projection to rat neocortex: transient expression of a dense innervation to primary sensory areas. Proc Natl Acad Sci USA 84: 4322-4326.

• Dahlstrom A, Fuxe K (1964) Evidence for the existence of monoamine-containing neurons in the central nervous system. I. Demonstration of monoamines in cell bodies of brain neurons. Acta Physiol Scand 62 (Suppl 232): 1-55.

• Daszuta A, Hery F, Faudon M (1984) In vitro 3H-serotonin (5-HT) synthesis and release in BALBc and C57BL mice. I. Terminal areas. Brain Res Bull 12: 559-563.

• Daszuta A, Portalier P (1985) Distribution and quantification of 5-HT nerve cell bodies in the nucleus raphe dorsalis area of C57BL and BALBc mice. Relationship between anatomy and biochemistry. Brain Res 360: 58-64.

• Dawson DR, Killackey HP (1985) Distinghuishing topography and somatotopy in the thalamocortical projections of the developing rat. Dev Brain Res 17: 309-313.

• Debeir T, Benavides J, Vige X (1998) Involvement of protease-activated receptor-1 in the in vivo development of mesencephalic dopaminergic neurons. Neuroscience 82: 739-752.

• De la Chapelle A, Sankila E-M, Lindlof M, Aula O, Norio R (1985). Norrie disease caused by a gene deletion allowing carrier detection and prenatal diagnosis. Clin Genet 28: 317-320.

• Delgado PL, Charney PS, Price LH, Aghajanian GK, Andes HL, Heninger GR (1990) Serotonin function and the mechanism of antidepressant action. Reversal of antidepressant induced remission by rapid depletion of plasma tryptophan. Arch Gen Psychiatry 47: 411-418.

• Dellovade TL, Pfaff DW, Schwanzel-Fukuda M (1998) Olfactory bulb development is altered in small-eye (Sey) mice. J Comp Neurol 402:402-418.

• De montigny C, Blier P (1992) Potentiation of 5-HT neurotransmission by short-term lithium: in vivo electrophysiological studies. Neuropharmacology 15 (suppl 1): 610-611.

• Demyanenko GP, Shibata Y, Maness PF (2000) Altered migration and cell loss of dopaminergic neurons in the L1 knockout mice. American Neuroscience Abstract.

• De Vitry F, Hamon M, Catelon J, Dubois M, Thibault J (1986) Serotonin initiates and autoamplifies its own synthesis during mouse central nervous system development. Proc Natl Acad Sci USA 83: 8629-8633.

• Devor EJ, Cloninger R, Hoffman PL, Tabakoff B (1993) Association of monoamine oxidase (MAO) activity with alcoholism and alcoholic subtypes. Am J Med Genet 48: 209-213.

• Devor EJ, Abell CW, Hoffman PL, Tabakoff B, Cloninger R (1993) Platelet MAO activity in type I and type II alcoholism. Ann NY Acad Sci 708: 119-128.

• De Vries I (1912) Uber die zytoarchitektonik der grosshirnrinde der maus und uber die beziehungen der einzelnen zellschishten zum corpus callosum auf grund von experimentellen lasionen. Folia neuro-biol (Lpz) 6: 288-322.

• Diez JA, Maderdrut JL (1977) Development of multiple forms of mouse brain monoamine oxidase *in vivo* and *in vitro*. Brain Res 128: 187-192.

• Ding J, Yang L, Yan Y-T, Chen A, Desai N, Wynshaw-Boris A, Shen MM (1998) *Cripto* is required for correct orientation of the anterior-posterior axis in the mouse embryo. Nature 395: 702-707.

• Dittrich R, Bossing T, Gould AP, Technau GM, Urban J (1997) The differentiation of the serotonergic neurons in the Drosophila ventral nerve cord depends on the combined function of the zinc finger proteins Eagle and Huckebein. Development 124: 2515-2525.

• Domenici L, Cellerino A, Berardi N, Cattaeno A, Maffei L (1994) Monoclonal antibodies to NGF prolong the sensitive period for monocular deprivation in the rat. Neuroreport 5: 2041-2044.

• Dooley AE, Pappas IS, Parnavelas JG (1997) Serotonin promotes the survival of cortical glutamatergic neurons in vitro. Exp Neurol 148: 205-214.

• Doucet G, Descarries L, Audet MA, Garcia S, Berger B (1988) Radioautographic method for quantifying regional monoamine innervation in the rat brain. Application to the cerebral cortex. Brain Res 441: 223-259.

• Dourish CTM, Clark ML, Iversen SD (1988) 8-OH-DPAT elicits feeding and not chewing: evidence from liquid diet study and diet choice test. Psychopharmacology 95: 185-188.

• Dressler GR, Deutsch U, Balling R, Simon D, Guenet J-L, Gruss PD (1988) Murine genes with homology to *Drosophila* segmentation genes. Development 104: 181-186 (Suppl.) .

• Droogleever Fortuyn AB (1914) Cortical cell-lamination of the hemispheres of some rodents. Arch Neurol Psychiat (Mott's) 6: 221-354.

• Dugich-Djordjevic MM, Ohsawa F, Hefti F (1993) Transient elevation in catalytic trkB mRNA during postnatal development of the rat brain. Neuroreport 4: 1091-1094.

• Dunning DD, McHaffie JG, Stein BE (1997) A simple enzyme histochemical method for the simultaneous demonstration of acetylcholinesterase and monoamine oxidase in fixed-frozen sections. J Histochem Cytochem 45: 895-902.

• Durham D, Woolsey TA (1984) Effects of neonatal lesions on mouse central trigeminal pathways. J Comp Neurol 223: 424-447.

• Ebersole P, Parnavelas JG, Blue ME (1981) Development of visual cortex of rats treated with 6-hydroxydopamine in early life. Anat Embryol 162: 489-492.

• Eggert K, Schlegel J, Oertel W, Wurz C, Krieg JC, Vedder H (1999) Glial cell line-derived neurotrophic factor protects dopaminergic neurons from 6-hydroxydopamine toxicity in vitro. Neurosci Lett 269: 178-182.

• Eichenbaum H, Shedlack KJ, Eckmann KW (1980) Thalamocortical mechanisms in odor-guided behavior. I. Effects of lesions of the mediodorsal thalamic nucleus and frontal cortex and olfactory discrimination in the rat. Brain Behav Evol 17: 255-275.

• Engelkamp D, Rashbass P, Seawright A, van Heyningen V (1999) Role of *Pax6* in development of the cerebellar system. Development 126: 3583-3596.

• Ericson J, Morton S, Kawakami A, Roelink H, Jessell TM (1996) Two critical periods of Sonic Hedgehog signalling required for the specification of motor neuron identity. Cell 87: 661-673.

• Ericson J, Rashbass P, Schedl A, Brenner-Morton S, Kawakami A, Van Heyningen V, Jessel TM, Briscoe J (1997) Pax6 controls progenitor cell identity and neuronal fate in response to graded Shh signalling. Cell 90:169-180.

• Ernfors P, Ibanez CF, Ebendal T, Olson L, Persson H (1990) Molecular cloning and neurotrophic activities of a protein with structural similarities to nerve growth factor: developmental and topographical expression in the brain. Proc Natl Acad Sci USA 87: 5454-5458.

• Espaner V (1963) 5-hydroxytryptamine. In "Comparative endocrinology". Von Euler US, Heller H (Eds), pp 159-181.

• Erzurumlu RS, Killackey HP (1983) Development of order in the rat trigeminal system. J Comp Neurol 213: 365-380.

• Erzurumlu RS, Jhaveri S (1990) Thalamic axons confer a blueprint of sensory periphery onto the developing rat somatosensory cortex. Dev Brain Res 56: 229-234.

• Erzurumlu RS, Jhaveri S (1992) Trigeminal ganglion cell processes are spatially ordered prior to the differentiation of the vibrissa pad. J Neurosci 12: 3946-3955.

• Falck B, Hillarp NA, Thieme G, Torp A (1962) Fluorescence of catecholamines and related compounds condensed with formaldehyde. J Histochem Cytochem 10: 348-354.

• Fawcett JW, O'Leary DD, Cowan WM (1984) Activity and the control of ganglion cell death in the rat retina.

• Fazeli A, Dickinson SL, Herminston ML, Tighe RV, Steen RG, Small CG, Stoeckli ET, Keino-Masu K, Masu M, Rayburn H, Simons J, Bronson RT, Gordon JI, Tessier-Lavigne M, Weinberg RA. (1997) Phenotype of mice lacking functional Deleted in colorectal cancer (Dcc) gene. Nature 386: 796-804.

• Fernandez AS, Pieau C, Reperant J, Boncinelli E, Wassef M (1998) Expression of the Emx-1 and Dlx-1 homeobox genes define three molecularly distinct domains in the telencephalon of mouse, chick, turtle and frog embryos: implications for the evolution of telencephalic subdivisions in amniotes. Development 125: 2099-2111.

• Fontaine P, Changeux JP (1989) Localization of nicotinic acetylcholine receptor alpha-subunit transcripts during myogenesis and motor endplate development in the chick. J Cell Biol 103: 1025-1037.

• Fornal C, Radulavaki M (1983) Sleep suppressant action of fenfluramine in rats. I. relation to postsynaptic serotoninergic stimulation. J Pharmacol Exp Ther 225: 667-674.

• Foster GA (1994) Ontogeny of catecholaminergic neurons in the central nervous system of mammalian species: general aspects. In: Phylogeny and development of catecholamine systems in the CNS of vertebrates. Smeeths WJAJ, Reiners A (Eds), Cambridge, Cambridge University Press, pp 405-434.

• Fowler CJ, Wiber A, Oreland L, Marcusson J, Winblad B (1980) The effects of age on the activity and molecular properties of human brain monoamine oxidase. J Neural Transm 49: 1-20.

• Fowler CJ, Tipton KF (1982) Deamination of 5-hydroxytryptamine by both forms of monoamine oxidase in the rat brain. J Neurochem 38: 733-736.

• Fowler CJ, Mc Gregor, Wolf AP, Arnett CD, Dewey SL, Schlyer D, Christman D, Logan J, Smith M, Sachs H, Aquilonius SM, Bjurling P, Halldin C, Hartig P, Leeders KL, Lundqvist H, Oreland L, Stalnacke CG, Langstrom B (1987). Mapping human brain monoamine oxidase A and B with 11C-labeled suicide inactivators and PET. Science 235: 481-485.

• Fowler JS, Fazzini E, Volkow ND (1996) Deprenyl and levodopa and Parkinson's disease progression. Ann Neurol 40: 267-268.

• Fox K (1992) A critical period for experience-dependent synaptic plasticity in rat barrel cortex. J Neurosci 12: 1826-1838.

• Fox K, Schlaggar BL, Glazewski S, O'Leary DDM (1996) Glutamate receptor blockade at cortical synapses disrupts development of thalamocortical and columnar organization in somatosensory cortex. Proc Natl Acad Sci USA 93: 5584-5589.

• Franklin KBJ, Paxinos G (1995) The atlas of the mouse brain. San Diego, CA: Academic Press.

• Franquinet R, Martelly I (1981) Effects of serotonin and catecholamines on RNA synthesis in planarians: in vitro and in vivo studies. Cell Diff 10: 201-209.

• Fujimiya M, Kimura H, Maeda T (1986) Postnatal development of serotonin nerve fibers in the somatosensory cortex of mice studied by immunohistochemistry. J Comp Neurol 246: 191-201.

• Futami T, Hatanaka Y, Matsushita K, Furuka S (1998) Expression of substance P receptor in the substantia nigra. Mol Brain Res 54: 183-198.

• Fuxe K, Hokfelt T, Ungerstedt U (1968) Localization of indolealkylamine in the CNS. Adv Pharmacol 6: 235-251.

• Fuxe K, Hokfelt T, Nilsson O (1969) actors involved in the control of the activity of the tubero-infundibular dopamine neurons during pregnancy and lactation. Neuroendocrynology 5: 257-270.

• Gad JM, Keeling SL, Wilks AF, Tan SS, Cooper HM (1997) The expression patterns of guidance receptors, DCC and neogenin are spatially and temporally distinct throughout mouse embryogenesis. Dev Biol 192: 258-273.

• Galter D, Unsicker K (2000a) Brain-derived neurotrophic factor and trkB are essential for cAMP-mediated induction of the serotoninergic neuronal phenotype. J Neurosci Res 61: 295-301.

• Galter D, Unsicker K (2000b) Sequential activation of the 5-HT1(A) serotonin receptor and TrkB induces the serotonergic neuronal phenotype. Moll Cell Neurosci 15: 446-455.

• Gardner CA, Barald KF (1991) The cellular environment controls the expression of engrailed-like protein in the cranial neuroepithelium of quail-chick chimeric embryos. Development 113: 1037-1048.

• Garrick NA, Murphy DL (1982) Monoamine oxidase type A: Differences in selectivity toward norepinephrin compare to serotonin. Biochem Pharmacol 31: 4061-4066.

• Gates MA, Tai CC, Macklis JD (2000) Neocortical neurons lacking the protein-tyrosine kinase B receptor display abnormal differentiation and process elongation in vitro and in vivo. Neuroscience 98: 437-447.

• Giller ELJ, Young JG, Breakfield XO, Carbonari C, Braverman M, Cohen DJ (1980) Monoamine oxidase and catecholamine-O-methyltransferase activities in cultured fibroblasts and blood cells from children with autism and Gilles de la Tourette syndrome. Psychiat Res 2: 307-314.

• Giller ELJ, Castiglione CM, Wojciechowski J, Breakefeiled XO (1982) Molecular properties of platelet MAO in psychiatric patients and controls. In "Biological markers in psychiatry and neurology". Pergamon press, New York.

• Gillies K, Price DJ (1993) The fates of cells in the developing cerebral cortex of normal and methylazoxymethanol acetate-lesioned mice Eur J Neurosci 5: 73-83.

• Giros B, Caron MG (1993) Molecular characterization of the dopamine transporter. Trends Pharmacol Sci 14: 43-49.

• Glowinski J (1976) Regulation of synthesis and release processes in central catecholaminergic neurons. Monograph p, 187-203.

• Goldberg JI, Kater SB (1989) Expression and function of the neurotransmitter serotonin during development of the *Heliosoma* nervous system. Dev Biol 131: 483-495.

• Goldberg JI, Mills LR, Kater SB (1991) Novel effects of serotonin on neurite outgrowth in neurons cultured from embryos of Helisoma trivolvis. J Neurobiol 22: 182-194.

• Golding JP, Shewan D, Cohen J (1997) Maturation of the mammalian dorsal root entry-zone - from entry to no entry. Trends Neurosci 20: 303-308.

• Golding JP, Cohen J (1997) Border controls at the mammalian spinal cord: Late-surviving neural crest boundary cap cells at dorsal root entry sites may regulate sensory afferent ingrowth and entry zone morphogenesis. Mol Cell Neurosci 9: 381-396.

• Goridis C, Brunet JF (1999) Transcriptional control of neurotransmitter phenotype. Curr Opin Neurobiol 9: 47-53.

• Gotz M, Stoykova A, Gruss P (1998) Pax6 controls radial glia differentiation in the cerebral cortex. Neuron 21: 1031-1044.

• Grapin-Botton A, Bonnin MA, Le Douarin NM (1997) Hox gene induction in the neural tube depends on three parameters: competence, signal supply and paralogue group. Development 124: 849-859.

• Green AR, Youdim MBH (1975) Effects of monoamine oxidase inhibition by clorgyline, deprenyl or tranylcypromine on 5-hydroxytryptamine concentrations in rat brain and hyperactivity following subsequent tryptophan administration. Br J Pharmacol 55: 415-422.

• Grimsby J, Lan NS, Neve R, Chen K Shih JC (1990) Tissue distribution of human monoamine oxidase A and B mRNA. J Neurochem 55: 1166-1169.

• Grimsby J, Chen K, Wang LJ, Lan NC, Shih JC (1991) Human monoamine oxidase A and B genes exhibit identical exon-intron organisation. Proc Natl Acad Sci USA 88: 3637-3641.

• Grimsby J, Toth M, Chen K, Kumazawa T, Klaidman L, Adams JD, Karoum F, Gal J, Shih JC (1997) Increased stress-response and beta-phenylethylamine in MAOB-deficient mice. Nat Genet 17: 206-210.

• Grindley JC, Davidson DR, Hill RE (1995) The role of Pax-6 in eye and nasal development. Development 121: 1433-1442.

• Grindley JC, Hargett LK, Hill RE, Ross A, Hogan BLM (1997) Disruption of Pax6 function in mice homozygous for the Pax6Sey-1Neu mutation produces

abnormalities in the early development and regionalization of the diencephalon. Mechs Dev 64: 111-126.

• Groves AK, George KM, Tissier-Seta JP, Engel JD, Brunet JF, Anderson DJ (1995) Differential regulation of transcription factor gene expression and phenotypic markers in developing sympathetic neurons. Development 121: 887-901.

• Guthrie S (1996) Patterning the hindbrain. Curr Opin Neurobiol 6: 41-48.

• Hallbook F, Ibanez CF, Persson H (1991) Evolutionary studies on the nerve growth factor family reveal a novel member abundantly expressed in *Xenopus* ovary. Neuron 6: 845-858.

• Hanaway J, McConnell JA, Netsky MG (1971) Histogenesis of the substantia nigra, ventral tegmental area of Tsai and interpeduncular nucleus: an autoradiographic study of the mesencephalon in the rat. J Comp Neurol 142: 59-74.

• Haydon PG, McCobb DP, Kater SB (1984) Serotonin selectivity inhibits growth cone mobility and the connection of identified neurons. Science 226: 561-564.

• Hedgecock EM, Culotti JG, Hall DH (1990) The *unc-5, unc-6,* and *unc-40* genes guide circumferential migrations of pioneers axons and mesothelial cells on epidermis in *C. elegans.* Neuron 2: 61-85.

• Hellendahl RP, Schambra U, Liu J. Breese GR, Millhorn DE, Lauder JM (1992) Detection of serotonin receptor transcripts in the developing nervous system. J Chem Neuro Anat 5: 299-310.

• Henderson TA, Woolsey TA, Jacquin MF (1992) Infraorbital nerve blockade from birth does not disrupt central trigeminal pattern formation in the rat. Dev Brain Res 66: 146-152.

• Henderson TA, Rhoades RW, Bennett-Clarke CA, Johnson EM, Jacquin MF (1993) NGF augmentation rescues trigeminal ganglion and principalis neurons, but not brainstem or cortical whisker patterns after infraorbital nerve injury at birth. J Comp Neurol 336: 243-260.

• Henderson TA, Mosconi TM, Foschini DR, Silos-Santiago I, Barbacid M, Jacquin MF (1995) Whisker-related patterning in the cerebral cortex of trkA, trkB, or trkC knockout mice. Soc Neurosci Abstr 119-8, 279.

• Henrique D, Adam J, Myat A, Chitnis A, Lewis J, Ish-Horowicz D (1995) Expression of a Delta homologue in prospective neurons in the chick. Nature 375: 787-790.

• Hensson SR, Mezey E, Hoffman BJ (1998) Serotonin transporter messenger RNA in the developing brain: early expression in serotonergic neurons and transient expression in non-serotonergic neurons. Neuroscience 83: 1185-1201.

• Hertel P, Fagerquist MV, Svensson TH (1999) Enhanced cortical dopamine output and antipsychotic-like effects of raclopride by alpha2 adrenoreceptor blokade. Science 286: 105-107.

• Hirsch M-R, Tiveron M-C, Guillemot F, Brunet JF, Goridis C (1998) Control of noradrenergic differentiation and Phox2a expression by MASH1 in the central and peripheral nervous system. Development 125: 599-608.

• Hoffman BJ, Mezey MJ, Brownstein MJ (1991) Cloning of serotonin transporter affected antidepressant. Science 254: 579-580.

• Hogan BL, Horsburgh G, Cohen J, Hetherington CM, Fisher G, Lyon MF (1986) Small eye (Sey): a homozygous lethal mutation on chromosome 2 which affects the differentiation of both lens and nasal placodes in the mouse. J Embryol Exp Morph 97:95-110.

• Hohmann CF, Brooks AR, Coyle JT (1988a) Neonatal lesions of the basal cholinergic neurons result in abnormal cortical development. Dev Brain Res 42: 253-264.

• Hohmann CF, Hamon R, Batshaw ML, Coyle JT (1988b) Transient postnatal elevation of serotonin levels in mouse neocortex. Dev Brain Res 43: 163-166.

• Hokfelt T, Matensson A, Bjorklund S, Kleinau S, Goldstein M (1984) Distributional maps of tyrosine hydroxylase-immunoreactive neurons in the rat brain. In: Handbook of chemical neuroanatomy. Classical transmitters in the CNS. Vol 2. Bjorklund A, Hokfelt T (Eds), Amsterdam, Elsevier, pp 227-379.

• Horch HW, Kruttgen A, Portbury SD, Katz LC (1999) Destabilization of cortical dendrites and spines by BDNF. Neuron 23: 353-364.

• Horger BA, Nishimura MC, Armanini MP, Wang LC, Poulsen KT, Rosendlad C, Kirik D, Moffat B, Simmons L, Jhonson E et al. (1998) Neurturin exerts potent actions on survival and function of midbrain dopaminergic neurons. J Neurosci 18: 4929-4937.

• Hornykiewicz O (1966) Metabolism of brain dopamine in human parkinsonism: neurochemical and clonical aspects. In "Biochemistry and pharmacology of the basal ganglia". Costa E, Cote LJ, Yarh MD (Eds). New York, Raven Press, pp 171-185.

• Houart C, Westerfield M, Wilson SW (1998) A small population of anterior cells patterns the forebrain during zebrafish gastrulation. Nature 391: 788-792.

• Hosli E, Hosli L (1997) Autoradiographic studies on the uptake of ^{3}H-dopamine by neurons and astrocytes in explant and primary cultures of rat CNS: effects of uptake inhibitors. Int J Dev Neurosci 15: 45-53.

• Hoth C, Milunskyn A, Lipsky N, Sheffer R, Claren SK, Baldwin CT (1993) Mutations in the paired domain of the human PAX3 gene cause Klein-Waardenburg Syndrome (WS-III) as well as Waardenburg Syndrome Type I (WS-I). Am J Genet 52: 455-462.

• Hoyer D, Clarke DE, Fozard JR, Martin GR, Mylecharane EJ, Saxena PR, Humphrey PPA (1994) VII. International pharmacology of receptors for 5-hydroxytryptamine (serotonin). Pharmacological Reviews 46: 157-203.

• Hsu YP, Weyler W, Chen S, Sims KB, Rinehart WB, Utterback M, Powell JF, Breakefield XO (1988) Structural features of human monoamine oxidase A elucidated from cDNA and peptide sequences. J Neurochem 51: 1321-1324.

• Huang ZJ, Kikwood A, Pizzorusso T, Porciatti V, Morales B, Bear MF, Maffei L, Tonegawa S (1999) BDNF regulates the maturation of inhibition and the critical period of plasticity in mouse visual cortex. Cell 98: 739-735.

• Hubel DH, Wiesel TN (1977) Functional architecture of macaque monkey visual cortex. Proc R Lond B Biol Sci 198: 1-59.

• Huttenlocher PR (1979) Synaptic density in human frontal cortex-Developmental changes and effects of ageing. Brain Res 163: 195-205.

• Hyman C, Juhasz M, Jackson C, Wright P, Ip NY, Lindsay RM (1994) Overlapping and distinct actions of the neurotrophins BDNF, NT-3, and NT-4/5 on cultured dopaminergic and GABAergic neurons of the ventral mesencephalon. J Neurosci 14: 335-347.

• Hyman SE, Nestler EJ (1996) Initiation and adaptation: a paradigm for understanding psychotropic drug actio. Am J Psychiatry 153: 151-162.

• Hynes M, Poulsen K, Tessier-Lavigne M, Rosenthal A (1995a) Control of neuronal diversity by the floor plate: Contact-mediated induction of midbrain dopaminergic neurons. Cell 80: 95-101.

• Hynes M, Porter JA, Chiang C, Chang D, Tessier-Lavigne M, Beachy PA (1995b) Induction of midbrain dopaminergic neurons by sonic hedgehog. Neuron 15: 35-44.

• Hynes M, Stone DM, Dowd M, Pitts-Meek S, Goddard A, Gurney A, Rosenthal A (1997) Control of cell pattern in the neural tube by the zinc finger transcription factor and oncogene Gli-1. Neuron 19: 15-26.

• Hynes M, Ye W, Wang K, Stone D, Murone M, Sauvage FD, Rosenthal A (2000) The seven-transmembrane receptor smoothened cell-autonomously induces multiple ventral cell types. Nat Neurosci 31: 41-46.

• Ichinose H, Ohye T, Takahashi E, Seki N, Hori T, Segawa M, Nomura Y, Endo K, Tanaka H, Tsuji S et al., (1994) Hereditary progressive dystonia with marked diurnal fluctuation caused by mutations in the GTP cyclohydrolase I gene. Nat Genet 8: 236-242.

• Innocenti GM, Kaas JH (1995) The cortex. Trends in Neurosci 9: 371-373.

• Ikemoto K, Kitahama K, Seif I, Maeda T, De Maeyer E, Valatz JL (1997) Monoamine oxidase B (MAOB)-containing structures in MAOA-deficient transgenic mice. Brain Res 771: 121-132.

• Ikemoto K, Kitahama K, Maeda T, Jouvet M, Nagatsu I (1999) Cholinergic neurons with monoamine oxidase type B (MAOB)-activity in the laterodorsal tegmental nucleus of the mouse. Neurosci Lett 271: 53-56.

• Irwin I, Finnegan KT, Delanney LE, Di Monte D, Langston JW (1992) The relationship between aging, monoamine oxidase, striatal dopamine and the effects of MPTP in C57BL/6 mice: A critical reassessment. Brain Res 572: 224-231.

• Iwasato T, Datwani A, Wolf AM, Nishiyama H, Taguchi Y, Tonegawa S, Hnopfel T, Erzurumlu RS, Itohara S (2000) Cortex-restricted disruption of NMDAR1 impairs neuronal patterns in the barrel cortex. Nature 406: 726-731.

• Jackson-Lewis V, Vila M, Djaldetti R, Guenan C, Liberatore G, Liu J, O'Malley K, Burke K, Przedbobrski S (2000) Developmental cell death in dopaminergic neurons of the substantia nigra in mice. J Comp Neurol 424: 476-488.

• Jacobs BL, Wise WD, Taylor KM (1974) Differential behavioural and neurochemical effects following lesions of the dorsal and median raphe nuclei in rats. Brain Res 79: 353-361.

• Jacobson FM, Sack DA, Wehr TA, Rogers S, Rosenthal NA (1987) Neuroendocrine response to 5-hydroxytryptophan in seasonal affective disorder. Arch Gen Psychiatry 44: 1086-1091.

• Jacobson CD, Adam DE, Fields J, Sladek JR (1989) Simultaneous catecholaminergic histofluorescence and thymidine autoradiography of sexually dimorphic nucleus of the preoptic area in the rat. Exp Neurol 104: 257-263.

• Jacobowitz DM, Abbott LC (1998) Chemoarchitectonic atlas of the developing mouse brain. CRC press.

• Jaeger CB, Joh TH (1983) Transient expression of tyrosine hydroxylase in some neurons of the developing inferior colliculus of the rat. Dev Brain Res 11: 128-132.

• Jaeger CB, Ruggiero DA, Albert VR, Joh TH, Reis DJ (1984) Immunocytochemical localization of aromatic-L-aminoacid decarboxylase. In: Handbook of chemical neuroanatomy. Vol.2: Classical transmitters in the CNS, Part I. A. Bjorklund, T. Hokfelt, (Eds), Amsterdam, Elsevier, pp 387-408.

• Jahng JW, Houpt TA, Wessel TC, Chen K, Shih JC, Tong JH (1997) Localization of monoamine oxidase A and B mRNA in the rat brain by in situ hybridization. Synapse 25: 30-36.

• Jeanmonod D, Rice FL, Van der Loos H (1981) Mouse somatosensory cortex: alterations in the barrelfield following receptor injury at different early postnatal ages. Neuroscience 6: 1503-1535.

• Jensen KF, Killackey HP (1987a) Terminal arbors of axons projecting to the somatosensory cortex of the adult rat. I. The normal morphology of specific thalamocortical afferents. J Neurosci 7: 3529-3543.

• Jensen KF, Killackey HP (1987b) Terminal arbors of axons projecting to the somatosensory cortex of the adult rat. II. The altered morphology of thalamocortical afferents following neonatal infraorbital nerve cut. J Neurosci 7: 3544-3553.

• Jhaveri S, Erzurumlu RS, Crossin K (1991) Barrel construction in the rodent neocortex: role of thalamic afferences versus extracellular matrix molecules. Proc Natl Acad Sci USA 88: 4489-4493.

• Jonakait GM, Markey KA, Goldstein M, Black IB (1984) Transient expression of selected catecholaminergic traits in cranial sensory and dorsal root ganglia of the embryonic rat. Dev Biol 101: 51-60.

• Jones KR, Farinas I, Backus C, Reichardt LF (1994) Targeted disruption of the BDNF gene perturbs brain and sensory neuron development but not motor neuron development. Cell 76: 989-999.

• Jonowsky A, Sulser A (1987) Alpha and beta adrenergic receptors in brain. In "Psychopharmacology, the third generation of progress". Melzer HT (Ed), New York, Raven-Press, pp 249-256.

• Jourdikian F, Tabakoff B, Alivisatos SGA (1975) Ontogeny of multiple forms of monoamine oxidase in mouse brain. Brain Res 93: 301-308.

• Kandel ER, Schwartz JH, Jessel TM (1991) Principles of neural science. Third edition. Kandel ER, Schwartz JH, Jessel TM (Eds), Prentice-Hall Int Inc.

• Kaplan GP, Hartman BK, Creveling CR (1981) Localization of catechol-O-methyltransferease in the leptomeningies, choroid plexus, and cilliary epithelium: implications for the separation of central and peripheral catechols. Brain Res. 204: 353-360.

• Kaufman MH, Chang HH, Shaw JP (1995) Craniofacial abnormalities in homozygous Small eye (Sey/Sey) embryos and newborn mice. J Anat 186: 607-617.

• Kasamatsu T, Pettigrew JD (1976) Depletion of brain catecholamines: failures of ocular dominance shift after monocular occlusion in kittens. Science 194: 206-209.

• Kasamatsu T, Pettigrew JD, Avry M (1979) Restoration of visual cortical plasticity by local microperfusion of norepinephrine. J Comp Neurol 28: 189-201.

• Kato H, Zhou Y, Asanoma K, Kondo H, Yoshikawa Y, Watanabe K, Matsuda T, Wake N, Barett JC (2000) Suppressed tumorigenicity of human endometrial cancer cells by the restored expression of the DCC gene. Br J Cancer 82: 459-466.

• Katz LC, Shatz CJ (1996) Synaptic activity and the construction of cortical circuits. Science 274: 1133-1138.

• Kawano H, Ohyama K, Kawamura K, Nagatsu I (1995) Migration of dopaminergic neurons in the embryonic mesencephalon of mice. Dev Brain Res 86: 101-113.

• Kema IP, Schellings AM, Hoppenbrouwers CJ, Rutgers HM, de Vries EGE, Muskiet FAJ (1993) High performance liquid chromatographic profiling of tryptophan and related indoles in body fluids and tissues of carcinoid patients. Clin Chim Acta 221: 143-158.

• Kennedy TE, Serafini T, de la Torre JR, Tessier-Lavigne M (1994) Netrins are diffusible chemotropic factors for commissural axons in the embryonic spinal cord. Cell 78: 425-35

• Kessel M, Gruss P (1990) Murine developmental control genes. Science 249: 374-379.

• Killackey HP (1973) Anatomical evidence for subdivisions based on vertically thalamic projections from the ventroposterior nucleus to the cortical barrel in the rat. Brain Res 51: 326-331.

• Killackey HP, Leshin S (1975) The organisation of specific thalamocortical projections to the posteromedial barrel subfield of the rat somatic sensory cortex. Brain Res 86: 469-472.

• Killackey HP, Belford G, Ruygo R, Ruygo DK (1976) Anomalous organization of thalamocortical projections consequent to vibrissae removal in the newborn rat or mouse. Brain Res 104: 309-315.

• Killackey HP, Chiaia NL, Bennett-Clarke CA, Eck M, Rhoades RW (1994) Peripheral influences on the size and organization of somatotopic representations in the fetal rat cortex. J Neurosci 14: 1496-1506.

• Killackey HP, Rhoades RW, Bennett-Clarke CA (1995) The formation of a cortical somatotopic map. Trends in Neurosci 9: 402-408.

• Kilty J, Lorang D, Amara SG (1991) Cloning and expression of cocaine sensitive rat dopamine transporter. Science 254: 578-579.

• Kirch DG, Weinberger DR (1986) Anatomical neuropathology in schizophrenia: post-mortem findings. In "The neurology of schizophrenia" Nasrallah HA, Weinberger DR (Eds), Amsterdam, Elsevier, pp 325-348.

• Kitahama K, Maeda T, Denney RM, Jouvet M (1994) Monoamine oxidase: distribution in the cat brain studied by enzyme- and immunohistochemistry: recent progress. Prog Neurobiol 42: 53-78.

• Klein R, Smeyne RJ, Wurst W, Long LK, Auerbach BA, Joyner AL, Barbacid M (1993) Targeted disruption of the trkB neurotrophin receptor gene results in nervous system lesions and neonatal death. Cell 75: 113-122.

• Knapp S, Mandell AJ, Russo PV, Vitto A, Stewart KD (1981). Strain differences in kinetic and thermal stability of two mouse brain tryptophan hydroxylase activities. Brain Res 230: 317-336.

• Knoll J (1987) Critical role of MAO inhibition in Parkinson's disease. Advances in Neurology 45: 107-110.

• Knoll J (1989) The pharmacology of selegiline ((-)deprenyl). New aspects. Acta Neurol Scand Suppl 126: 83-91.

• Knusel B, Rabin SJ, Hefti F, Kaplan DR (1994) Regulated neurotrophin receptor responsiveness during neuronal migration and early differentiation. J Neurosci 14: 1542-1554.

• Konig N, Wilkie MB, Lauder JM (1988) Tyrosine hydroxylase and serotonin containing cells in embryonic rat rhombencephalon: a whole-mount immunocytochemical study. J Neurosci Res 20: 202-223.

• Kritzer MF, Kohama SG (1998) Ovarian hormones influence the morphology, distribution, and density of tyrosine hydroxylase immunoreactive axons in the dorsolateral prefrontal cortex of adult rhesus monkeys. J Comp Neurol 395: 1-17.

• Kruesi MJP, Rappaport JL, Hamburger S, Hibbs E, Potter WZ, Lenane M, Brown GL (1990) Cerebrospinal fluid monoamine metabolites, aggression, and impulsivity in disruptive behaviour disorders of children and adolescents. Arch Gen Psychiatry 47: 419-426.

• Kulikov AV, Kozlachkova EY, Kudryavstseva NN, Popova NK (1995) Correlation between tryptophan hydroxylase activity in the brain and predisposition to pinch-induced catalepsy in mice. Pharmacol Biochem Behav 50: 431-435.

• Kumer SC, Vrana KE (1996) Intricate regulation of tyrosine hydroxylase activity and gene expression. J Neurochem 67: 443-62.

• Krauss S, Johansen T, Korzh V, Fjose A (1991a) Expression pattern of zebrafish pax genes suggests a role in early brain regionalisation. Nature 353: 267-270.

• Krauss S, Johansen T, Korzt V, Moens U, Ericson JU, Fjose A (1991b) Zebrafish pax (zf-a) : a paired box containing gene expressed in the neural tube. EM BO J 10: 3609-3619.

• Kristt DA (1979) Somatosensory cortex: acetylcholinesterase staining of barrel neuropil in the rat. Neurosci Lett 12: 177-182.

• Krumlauf R (1994) Hox genes in vertebrate development. Cell 78:191-201.

• Lajard AM, Christolomme A, Bou C, Monteau R, Seif I, Lanoir J, Hilaire G (1998) Serotonin levels and 5-HT1A receptor expression in the central nervous system of monoamine oxidase-A deficient Tg8 mice. Eur J Neurosci 10 (S10).

• Lajard AM, Bou C, Monteau R, Hilaire G (1999) Serotonin levels are abnormally elevated in the fetus of the monoamine oxidase-A-deficient transgenic mouse. Neurosci Lett 261: 41-44.

• Lankford KL, DeMello FG, Klei WL (1988) D1-type monoamine receptors inhibit growth cone motility in cultured retina neurons: evidence that neurotransmitters act as morphogenic growth regulators in the developing central nervous system. Proc Natl Acad Sci USA 85: 2839-2843.

• Lauder JM, Bloom FE (1974) Ontogeny of monoamine neurons in the locus coeruleus, raphe nuclei and substantia nigra of the rat. I. Cell differentiation. J Comp Neurol 155: 469-481.

• Lauder JM (1983) Hormonal and humoral influences on brain development. Psychoneuroendocrinology 8: 121-155.

• Lauder JM, McCarthy KD (1986) In "Astrocytes". Federoff S and Vernadakis A. (Eds), Academic press, Oxford, pp 295-314

• Lauder JM (1988) Neurotransmitters as morphogens. Prog Brain Res 73: 365-387.

• Lauder JM (1990) Ontogeny of the serotoninergic system in the rat: serotonin as a developmental signal. Ann NY Acad Sci. 600: 297-314

• Lauder JM (1993) Neurotransmitters as growth regulatory signals: role of receptors and second messengers Trends in Neurosci 16: 233-239.

• Lauderdale JD, Pasquali SK, Fazel R, van Eeden FJ, Schauerte HE, Haffter P, Kuwada JY (1998) Regulation of netrin-1a expression by hedgehog proteins. Mol Cell Neurosci 11: 194-205.

• Lavdas AA, Blue ME, Lincoln J, Parnavelas JG (1997) Serotonin promotes the differentiation of glutamate neurons in organotypic slice cultures of the developing cerebral cortex. J Neurosci 17: 7872-7880.

• Law SW, Conneely OM, DeMayo FJ, O'Malley BW (1992) Identification of a new brain-specific transcription factor NURR1. Mol Endocrinol 6: 2129-2135.

• Lazard D, Tal N, Rubenstein M, Khen M, Lancet D, Zupko K (1990) Identification and biochemical analysis of novel olfactory-specific cytochrome P-450IIA and UDP-glucoronosyl transferase. Biochemistry 29: 7433-7440.

• Lebrand C, Cases O, Aldebrecht A, Doye A, Alvarez C, El Mestikawy S, Seif I, Gaspar P (1996) Transient uptake and storage of serotonin in developing thalamic neurons. Neuron 17: 823-835.

• Lebrand C, Cases O, Werhle R, Blakely R, Edwards J, Gaspar P (1998) Transient developmental expression of monoamine transporters in the rodent brain. J Comp Neurol: 506-524.

• Lee KL, Woolsey TA (1975) A proportional relationship between peripheral innervation density and cortical neuron number in the somatosensory system of the mouse. Brain Res 99: 349-353.

• Lee SM, Danielan PS, Fritzsch B, McMahon AP (1997) Evidence that FGF8 signalling from the midbrain-hindbrain junction regulates growth and polarity in the developing midbrain. Development 124: 959-969.

• Leonardo ED, Hinck L, Masu M, Keino-Masu K, Fazeli A, Stoeckli ET, Ackerman SL, Weinberg RA, Tessier-Lavigne M (1997a) Guidance of developing axons by netrin-1 and its receptors. Cold Spring Harb Symp Quant Biol 62: 467-478.

• Leonardo ED, Hinck L, Masu M, Keino-Masu K, Ackerman SL, Tessier-Lavigne M (1997b) Vertebrate homologues of C. elegans UNC-5 are candidate netrin receptors. Nature 386: 833-838.

• Lesch KP, Wolozin BL, Murphy DL, Riederer P (1993) Primary structure of the human platelet serotonin uptake site: identity with the brain serotonin transporter. J Neurochem 60: 2319-2322.

• Leslie MJ, Bennett-Clarke CA, Rhoades RW (1992) Serotonin 1B receptors form a transient vibrissa-related pattern in the primary somatosensory cortex of the developing rat. Dev Brain Res 69: 143-148.

• Levi-Montalcini R (1987) The nerve growth factor 35 years later. Science 237: 1154-1162.

• Levin BE, Craik RL, Hand PJ (1988) The role of neurotrophin in adult somatosensory (SmI) cortical metabolism and plasticity. Brain Res 443: 261-271.

• Levine ES, Crozier RA, Black IB, Plummer MR (1998) Brain-derived neurotrophic factor modulates hippocampal synaptic transmission by increasing N-methyl-D-aspartic acid receptor activity. Proc Natl Acad USA 95: 10235-10239.

• Levitt P, Moore RY (1978) Developmental organization of raphe neuron groups in the rat. Anat Embryol 154: 241-251.

• Levitt P, Pintar JE, Breakefield XO (1982) Immunocytochemical demonstration of monoamine oxidase B in rat astrocytes and serotoninergic neurons. Proc Natl Acad Sci USA 79: 6385-6389.

• Levitt P, Harvey JA, Friedman E, Simansky K, Murphy EH (1997) New evidence for neurotransmitter influences on brain development. Trends Neurosci 20: 269-274.

• Lewinsohn R, Glover W, Sandler (1980) Development of benzylamine oxidase and monoamine oxidase A and B in man. Biochem Pharmacol 29: 1221-1230.

• Lichtensteiger W, Mutzner U, Langemann H (1967) Uptake of 5-hydroxytryptamine and 5-hydroxytryptophan by neurons of the central nervous system normally containing catecholamines. J Neurochem 14: 489-497.

• Li Y, Erzurumlu RS, Chen C, Jhaveri S, Tonegawa S (1994) Whisker-related neuronal patterns fail to develop in the trigeminal brainstem nuclei of NMDAR1 knockout mice. Cell 76: 427-437.

• Lidov HGW, Rice FL, Molliver ME (1978) The organisation of the catecholamine innervation of the somatosensory cortex: The barrel field of the mouse. Brain Res 153: 577-584.

• Lidov HGW, Molliver ME (1982a) An immunohistochemical study of serotonin neuron development in the rat: ascending pathways and terminal fields. Brain Res Bull 8: 389-430.

• Lidov HGW, Molliver ME (1982b) Immunohistochemical study of the development of serotonergic neurons in the rat CNS. Brain Res Bull 9: 559-604.

• Lipton SA, Kater SB (1989) Neurotransmitter regulation of neuronal outgrowth, plasticity and survival. Trends Neurosci 12: 265-270.

• Liu KP, Tamir H, Hsiung S, Adelsberg M, Gershon MD (1987) Prenatal development of serotonin binding protein in relation to order transmitted-related characteristics of central serotoninergic neurons. Dev Brain Res 32: 31-41.

• Liu JP, Lauder JM (1991) Serotonin and nialamide differentially regulate survival and growth of cultured serotonin and catecholamine neurons. Brain Res Dev Brain Res 62: 297-305.

• Liu J, Lauder JM (1992a) Serotonin promotes region-specific glial influences on cultured serotonin and dopamine neurons. Glia 5: 306-317.

• Liu J, Lauder JM (1992b) S-100β and insuline-like growth factor-II differentially regulate growth and developing serotonin and dopamine neurons *in vitro*. J Neurosci Res 33: 248-256.

• Liu J, Merlie JP, Todd RD, O'Malley KL (1997) Identification of cell-specific promoter elements associated with the rat tyrosine hydroxylase gene using transgenic founder analysis. Brain Res Mol Brains Res 50: 33-42.

• Livesey FJ, Hunt SP (1997) Netrin and netrin receptor expression in the embryonic mammalian nervous system suggests roles in retinal, striatal, nigral, and cerebellar development. Mol Cell Neurosci 8: 417-429.

• Lo DC (1995) Neurotrophic factors and synaptic plasticity. Neuron 15: 979-981

• Lo L, Tiveron MC, Anderson DJ (1998) MASH1 activates expression of the paired homeodomain transcription factor Phox2a, and couples pan-neuronal and subtype-specific components of autonomic neuronal identity. Development 125: 609-620.

• Loeb EP, Chang FLF, Greenough WT (1987) Effects of neonatal 6-hydroxydopamine treatment upon morphological organization of the posteromedialbarrel subfield in mouse somatosensory cortex. Brain Res 403: 113-120.

• Loizou LA (1969) The development of monoamine-containing neurones in the brain of the albino rat. J Anat 104: 588.

• Loizou (1972) The postnatal ontogeny of monoamine-containing neurones in the central nervous system of the albino rat. Brain Res 40: 395-418.

• Lotto B, Upton L, Price DJ, Gaspar P (1999) Serotonin receptor activation enhances neurite outgrowth of thalamic neurones in rodents. Neurosci Lett 269: 87-90.

• Lorente de No' R (1922) La corteza cerebral del raton. Trab Lab Invest Biol (Madrid) 20: 41-78.

• Lorente de No' R (1949) Cerebral cortex: architectonics intracortical connections. In "Physiology of the nervous system". Fulton j (Ed), Oxford, Oxford UP, pp 274-301.

• Loughlin SE, Foote SL, Bloom FE (1986) Efferent projections of nucleus locus coeruleus: topographic organization of cell origin demonstrated by three-dimensional reconstruction. Neuroscience 18: 291-306.

• Lumsden A (1990) The development and significance of hindbrain segmentation. Sem Dev Biol 1:117-125.

• Lumsden A, Krumlauf R (1996) Patterning the vertebrate neuraxis. Science 274: 1109-1114.

• Lund RD, Mustari MJ (1977) Development of the geniculocortical pathways in rats. J Comp Neurol 173: 289-305.

• Lundell MJ, Hirsch M-R (1998) Eagle is required for the specification of serotonin neurons and other neuroblast 7-3 progeny in the Drosophila CNS. Development 125: 463-472.

• Luque JM, Kwan SW, Abell CW, Da Prada M, Richards JG (1995) Cellular expression of mRNAs encoding monoamine oxidase A and B in the rat central nervous system. J Comp Neurol 363: 665-680.

• Lyons WE, Mamounas LA, Ricaurte GA, Coppola V, Reid SW, Bora SH, Wihler C, Koliatsos VE, Tessarollo L (2000) Brain-derived neurotrophic factor-deficient mice develop aggressiveness and hyperphagia in conjunction with brain serotonergic abnormalities. Proc Natl Acad Sci USA 96: 15239-15244.

• Ma PM (1993) Barrelettes-architectonic vibrissal representations in the brainstem trigeminal complex of the mouse. II. Normal postnatal development. J Comp Neurol 327: 376-397.

• McAllister AK, Lo DC, Katz LC (1995) Neurotrophins regulate dendritic growth in developing visual cortex. Neuron 15: 791-803.

• McAllister AK, Katz LC, Lo DC (1997) Opposing roles for endogenous BDNF and NT-3 in regulating cortical dendritic growth. Neuron 18: 767-778.

• McAllister AK, Katz LC, Lo DC (1999) Neurotrophins and synaptic plasticity. Annu Rev Neurosci 22: 295-318.

• McCandlish C, Waters RS, Cooper MG (1989) Early development of the representation of the body surface in SI cortex barrel field in neonatal rats as demonstrated with peanut agglutinin binding: evidence for differential development within the rattunculus. Exp Brain Res 77: 425-431.

• McCobb DP, Cohan CS, Connor JA, Kater SB (1988a) Interactive effects of serotonin and acetylcholine on neurite elongation. Neuron 1: 377-385.

•McCobb DP, Haydon PG, Kater SB (1988b) Dopamine and serotonin inhibition of neurite elongation of different identified neurons. J Neurosci Res 19: 19-26.

• MacKenzie FJ, James MD, Wilson CA (1988) Changes in dopamine activity in the zona incerta (ZI) over the rat oestrous cycle and the effects of lesions of the ZI on the cyclicity : further evidence that the incerto-hypothalamic tract has a stimulatory role in the control of LH release. Brain Res 444: 75-83.

• Maffei L, Berardi N, Domenici L, Parisi V, Pizzorusso T (1992) Nerve growth factor (NGF) prevents the shift in ocular dominance column distribution of visual cortical neurons in monocularly deprived rats. J Neurosci 12: 4651-4662.

• Mamounas LA, Altar CA, Blue ME, Kaplan DR, Tessarollo L, Lyons WE (2000) BDNF promotes the regenerative sprouting, but not survival, of injured serotonergic axons in the adult rat brain. J Neurosci 20: 771-782.

• Huang ZJ, Kirkwood A, Pizzorusso T, Porciatti V, Morales B, Bear MF, Maffei L, Tonegawa S (1999) BDNF regulates the maturation of inhibition and the critical period of plasticity in mouse visual cortex. Cell 98: 739-755.

• McLean JH, Shipley MT (1988) Postmitotic, postmigrational expression of tyrosine hydroxylase in the olfactory bulb dopaminergic neurons. J Neurosci 8: 3658-3669.

• Magyar K, Szende B, Lengyel J, Tarczali J, Szatmary I. 1998. The neuroprotective and neuronal rescue effects of (-)-deprenyl. J Neural Transm (Suppl 52): 109-123.

• Maier DL, Mani L, Donovan SL, Soppet D, Tessarollo L, McCasland J, Meiri KF (1999) Disrupted cortical map and absence of cortical barrels in growth-associated protein (GAP)-43 knockout mice. Proc Natl Acad Sci USA 96: 9397-9402.

• Maitre L, Delini-Stula A, Waldemeier PC (1976) Relations between the degree of monoamine oxidase inhibition and some psycho-pharmacological responses to monoamine oxidase inhibitors in rat. In "Monoamine oxidase and its inhibition", Ciba Foundation Symposium 39, Amsterdam, Elsevier, pp 247-267.

• Mantle TJ, Garrett NJ, Tipton KF (1976) The development of monoamine oxidase in rat liver and brain. FEBS Lett 64: 227-230.

• Marin-Padilla M (1971) Early prenatal ontogenesis of the cerebral cortex (neocortex) of the cat (felis domestica): a golgi study. I. The primordial neocortical organization. Z Anat Entwicklungsgesch 134: 117-145.

• Marin-Padilla M (1978) Dual origin of the mammalian neocortex and evolution of the cortical plate. Anat Embryol 152: 109-126.

• Masana Y, Wanaka A, Kato H, Asai T, Tohyama M (1993) Localization of trkB mRNA in postnatal brain development. J Neurosci Res 35: 468-479.

• Maroteaux L, Saudou F, Amlaiky N, Boschert U, Plassat JL, Hen R (1992) The mouse 5-HT1D receptor; cloning, functional expression and localization in motor centers. Proc Natl Acad Sci USA 89: 3020-3024.

• Mastick GS, Davis NM, Andrews GL, Easter jr SS (1997) Pax-6 functions in boundary formation and axon guidance in the embryonic mouse forebrain. Development 124:1985-1997.

• Matsunami H, Takeichi M (1995) Fetal brain subdivisions defined by R- and E-cadherin expressions: evidence for the role of cadherin activity in region-specific, cell-cell adhesion. Dev Biol 172: 466-478.

• Medina L, Puelles L, Smeets WJAJ (1994) Development of catecholamine systems in the brain of the lizard *Gallotia galloti*. J Comp Neurol 350:41-62.

• Melamed E, Rosenthal J, Youdim MBH (1990) Immunity of fetal mice to prenatal administration of the dopaminergic neurotoxin 1-methyl-4-phenyl-1,2,3,6-tetrahydropyridine. J Neurochem 55: 1427-1431.

• Meltzer HY, Lowy MT (1987) The serotonin hypothesis of depression. In "Psychopharmacology: the third generation of progress". Meltzer HY (Ed), New York, Raven Press, pp 513-526.

• Ming G, Song H, Berninger B, Inagaki N, Tessier-Lavigne M, Poo MM (1999) Phospholipase C-gamma and phosphoinositide 3-kinase mediate cytoplasmic signaling in nerve growth cone guidance. Neuron 23: 139-148.

• Minichiello L, Piehl F, Vazquez E, Schimmang T, Hokfelt T, Represa J, Klein R (1995) Differential effects of combined trk receptor mutations on dorsal root ganglion and inner ear sensory neurons. Development 121: 4067-4075.

• Mitrovic N, Schachner M (1996) Transient expression of NADPH diaphorase activity in the mouse whisker to barrel field pathway. J Neurocytology 25: 429-437.

• Miyashita-Lin EM, Hevner R, Wassarman KM, Martinez S, Rubenstein JLR (1999) Early cortical regionalization in the absence of thalamic innervation. Science 285: 906-909.

• Modigh K, Balldin J, Eden S, Granerus AK, Wahlinder J (1971) Electroconvulsive therapy and receptor sensitivity. Arch Psych Scand 63 (Suppl. 290): 91-99.

• Molnar Z, Blakemore C (1995) How do thalamic axons find their way to the cortex? Trends Neurosci 9: 389-396.

• Moore RY, Bloom FE (1979) Central catecholamine neurons systems: Anatomy and physiology of the norepinephrine and epinephrine systems. Annu Rev Neurosci 2: 113-168.

• Moore RY (1981) The anatomy of central serotonin neuron system in the rat brain. In "Serotonin neurotransmission and behavior". Jacobs BL, Gelperin A (Eds), Cambridge (MA), MIT Press, pp 35-71.

• Moore DR, Russel A, Cathcart NK (1995) Lateral superior olive projections to the inferior colliculus in normal and unilaterally deafened ferrets. J Comp Neurol 357: 204-216.

• Morell R, Friedman TB, Moeljopawiro S, Hartono, Soewito, Asher JH Jr (1992) A frameshift mutation in the HuP2 paired domain of the probable human homolog of murine Pax-3 is responsible for Waardenburg syndrome type 1 in an Indonesian family. Hum Mol Genet 1: 243-247.

• Morin X, Cremer H, Hirsch M-R, Kapur RP, Goridis C, Brunet JF (1997) Defects in sensory and autonomic ganglia and absence of locus coeruleus in mice deficient for the homeobox gene Phox2a. Neuron 18: 411-423.

• Muhr J, Jessell TM, Edlund T (1997) Assignment of early caudal identity to neural plate cells by a signal from caudal paraxial mesoderm. Neuron 19: 487-502.

• Munoz A, Liu XB, Jones EG (1999) Development of metabotropic glutamate receptors from trigeminal nuclei to barrel cortex in postnatal mouse. J Comp Neurol 409: 549-566.

• Murphy DL, Donelly CH (1974) Monoamine oxidase in man: enzyme characteristics in platelets, plasma, and other tissus. In " Neuropsychopharmacology of monoamine and their regulatory enzymes". Udsin E (Ed), New York, Raven Press, pp 71-85.

• Murphy DL, Sims KB, Karoum F, de La Chapelle A, Norio R, Sankila EM, Breakefield XO (1990) Marked amine and amine metabolite changes in Norrie disease patients with an X chromosome deletion affecting monoamine oxidase. J Neurochem 54: 242-247.

• Nagatsu T (1995) Tyrosine hydroxylase: human isoforms, structure and regulation in physiology and pathology. Essays Biochem 30:15-35.

• Nakamura S, Akiguchi I, Kimura J (1993) A subpopulation of mouse striatal cholinergic neurons show monoamine oxidase activity. Neurosci Lett 161: 141-144.

• Nawa H, Pellymounter MA, Carnahan J (1994) Intraventricular administration of BDNF increases neuropeptide expression in newborn rat brain. J Neurosci 14: 3751-3765.

• Neff NH, Yang HY (1974) Another look at the monoamine oxidases and the monoamine oxidase inhibitor drugs. Life Sci 14: 2061-2074.

• Nef P, Larabee TM, Kagimoto K, Meyer UA (1990) Olfactory-specific cytochrome P450 (P450olf1; IIG1). Gene structure and developmental regulation. J Biol Chem 265: 2903-2907.

• Nelson DL, Herbert A, Glowinski J, Hamon M (1979) (3H) Harmaline as a specific ligand of MAOA. II. Measurement of the rates of MAO A during ontogenesis in the rat brain. J Neurochem 32: 1829-1836.

• Nestler EJ, Hope BT, Widnell KL (1993) Drug addiction: a model for the molecular basis of neural plasticity. Neuron 11: 995-1006.

• Nirenberg MJ, Chan J, Vaughan RA, Uhl GR, Kuhar MJ, Pickel VM (1997) Immunogold localization of the dopamine transporter: an ultrastructural study of the rat tegmental area. J Neurosci 17: 5255-5262.

• Northcutt RG, Kaas JH (1995) The emergence and evolution of mammalian neocortex. Trends Neurosci 18: 373-379.

• Ohyama K, Kawano H, Asou H, Fukuda T, Oohira A, Uyemura K, Kawamura K (1998) Coordinate expression of L1 and 6B4 proteoglycan/phosphacan is correlated with the migration of mesencephalic dopaminergic neurons in mice. Brain Res Dev 107: 219-226.

• O'Leary DD, Schlaggar BL, Tuttle R (1988) Specification of neocortical areas and thalamocortical connections. Annu Rev Neurosci 17: 419-439.

• O'Leary DDM (1989) Do cortical areas emerge from the protocortex? Trends Neurosci 12: 400-406.

• O'Leary DDM, Stanfield BB (1989) Selective elimination of axons extended by developing cortical neurons is dependent on regional locale: experiments utilizing fetal cortical transplants. J Neurosci 9: 2230-2246.

• O'Leary DDM, Ruff NL, Dyck RH (1994) Development, critical period plasticity, and adult reorganization of mammalian somatosensory systems. Curr Opin Neurobiol 4: 535-544.

• Olivier B, Mos J, Hartog J, Rasmussen D (1990) Serenics. Drugs News Perspect 3: 261-271.

• Olson L, Seiger A (1972) Early prenatal ontogeny of central monoamine neurons in the rat: Fluorescence histochemical observations. Z Anat Entwickl 139: 259-282.

• Oppenheim RW, Houenou LJ, Johnson JE, Lin LF, Li L, Lo AC, Newsome AL, Prevette DM, Wang S (1995) Developing motor neurons rescued from programmed and axotomy-induced cell death by GDNF. Nature 373: 344-346.

• Oreland L (1993) Monoamine oxidase in neuropsychiatric disorders. In "Monoamine oxidase; structure, function and altered function". Singer, T, Von Korff R, Murphy D (Eds), New York, Academic press, pp 379-387.

• Osterheld-Haas MC, Van der Loos H, Hornung JP (1994) Monoaminergic afferents to cortex modulate structural plasticity in the barrelfield of the mouse. Dev Brain Res 77: 189-202.

• Osterheld-Haas MC, Hornung JP (1996) Laminar development of the mouse barrel cortex: effects of neurotoxins against monoamines. Exp Brain Res 110: 183-195.

• Pacholczyk T, Blakely RD, Amara SG (1991) Expression cloning of a cocaine- and antidepressant –sensitive humam noradrenaline transporter. Nature 350: 350-354.

• Page IH (1968) Serotonin. Chicago, Year book medical publishers, Inc.

• Page IH (1976) The discovery of serotonin. Perspect Biol Med 20: 1-8.

• Palacios JM, Waeber C, Bruinvels AT, Hoyer D (1992) Direct visualization of serotonin 1D receptors in the human brain using a new radioiodinated radioligand. Mol Brain Res 13: 175.

• Parkinson J (1817) An essay on the shaking palsy. London.

• Parnavelas JG, Blue ME (1982) The role of noradrenergic system on the formation of synapses in the visual system of the rat. Dev Brain Res 3: 140-144.

• Paterson IA, Tatton WG (1998) Antiapoptotic actions of monamine oxidase B inhibitors. Adv Pharmacol 42 : 312-315.

• Pattyn A, Morin X, Cremer H, Goridis C, Brunet JF (1997) Expression and interactions of the two closely related homeobox genes Phox2a and Phox2b during neurogenesis. Development 124: 4065-4075.

• Paxinos G, Tork I, Tecott LH, Valentino KL (1991) Atlas of the developing rat brain. San Diego: Academic Press.

• Paxinos G, Ashwell KWS, Tork I. (1994) Atlas of the developing rat nervous system. San Diego: Academic Press.

• Pinon LG, Minichiello L, Klein R, Davies AM (1996) Timing of neuronal death in trkA, trkB and trkC mutant embryos reveals developmental changes in sensory neuron dependence on Trk signalling. Development 122: 3255-3261.

• Ponce A, Bueno E, Kentros C, Vega-Saenz de Miera E, Chow A, Hillman D, Chen S, Zhu L, Wu MB, Wu X, Rudy B, Thornhill WB (1996) G-protein-gated inward channel rectifier K+ channel proteins (GIRK1) are present in the soma and dendrites as well as in nerve terminals of specific neurons in the brain. J Neurosci 16: 1990-2001.

• Porsolt RD, Le Pichon M, Jalfre M (1977) Depression: a new animal model sensitive to antidepressant treatments. Nature 266: 730-732.

• Prakash N, Cohen-Cory S, Frostig RD (1996). Rapid and opposite effects of BDNF and NGF on the functional organization of the adult cortex *in vivo*. Nature 381: 702-706.

• Przyborski SA, Knowles BB, Ackerman SL (1998) Embryonic phenotype of Unc5h3 mutant mice suggests chemorepulsion during the formation of the rostral cerebellar boundary. Development 125: 41-50.

• Puelles L, Medina L (1994) Development of neurons expressing tyrosine hydroxylase and dopamine in the chicken brain: a comparative segmental analysis. In: Phylogeny and development of catecholamine systems in the CNS of vertebrates (WJAJ Smeeths and A Reiner, Eds). Cambridge: Cambridge University Press. p, 381-404.

• Puelles L (1995) A segmental morphological paradigm for understanding vertebrate forebrains. Brain Behav Evol 46: 319-337.

• Puelles L, Verney C (1998) Early neuromeric distribution of tyrosine hydroxylase-immunoreactive neurons in human embryos. J Comp Neurol 394: 283-308.

• Puschel AW, Gruss P, Westerfield M (1992) Sequence and expression pattern of pax-6 are highly conserved between zebrafish and mice. Development 114: 643-651.

• Puschel AW (1996) The semaphorins: a family of axonal guidance molecules? Eur J Neurosci 8: 1317-1321.

• Qian J, Bull MS, Levitt P (1992) Target-derived astroglia regulate axonal outgrowth in a region-specific manner. Dev Biol 149: 278-294.

• Rama-Krishna NS, Getchell ML, Tate SS, Margolis FL, Getchell TV (1992) Glutathione and g-glutamyl transpeptidase are differentially distributed in the olfactory mucosa of rats. Cell Tissue Res 270: 475-484.

• Rakic P (1976) Prenatal genesis of connections subserving ocular dominance in the rhesus monkey. Nature 261: 467-471.

• Rakic P (1977) Prenatal development of the visual system in rhesus monkey. Phil Trans Roy Soc. London B 278: 245-260.

• Rakic P (1981) Developmental events leading to laminar and areal organization of the neocortex. In "The organization of the cerebral cortex". Schmitt FO (Ed), Cambridge, MIT Press, pp 7-28.

• Rakic P (1988) Specification of cerebral cortical areas. Science 241: 170-176.

• Reid SNM, Romano C, Hughes T, Daw NW (1997) Developmental and sensory-dependent changes of phosphoinositide-linked metabotropic glutamate receptors. J Comp Neurol 389: 577-583.

• Reyes RB, Hill SY, Kupfer DJ (1983) Effects of acute doses of zimelidine on REM sleep in rats. Psychopharmacology 80: 214-216.

• Reznikov KY, Fulop Z, Hajos F (1984) Mosaicism of the ventricular layer as the developmental basis of neocortical columnar organization. Anat Embryol 170: 99-105.

• Rhoades RW, Bennett-Clarke CA, Chiaia NL, White FA, McDonald GJ, Haring HI, Jacquin MF (1990) Development and lesion induced reorganization of the cortical representation of the rat's body surface as revealed by immunochemistry for serotonin. J Comp Neurol 293: 190-207.

• Rhoades RW, Bennett-Clarke CA, Shi M-Y, Mooney RD (1994) Effects of 5-HT on thalamocortical synaptic transmission in the developing rat. J Neurophysiol 72: 2438-2450.

• Rice FL, Van der Loos H (1977) Development of the barrels and barrel field in the somatosensory cortex of the mouse. J Comp Neurol 171: 545-560.

• Riddle D, Richards A, Zsuppan F, Purves D (1992) Growth of the rat somatic sensory cortex and its constituent parts during postnatal development. J Neurosci 12: 3509-3524.

• Rocamora N, Welker E, Pascual M, Soriano E (1996). Upregulation of BDNF mRNA expression in the barrel cortex of adult mice after sensory stimulation. J Neurosci 16: 4411-4419.

• Roghani A, Feldman J, Kohan SA, Shirzadi A, Gundersen CB, Brecha N, Edwards RH. 1994. Molecular cloning of a putative vesicular transporter for acetylcholine. Proc Natl Acad Sci USA 91: 10620-10624.

• Romano C, Van de Pol AN, O'Malley KL (1996) Enhanced early developmental expression of the metabotropic glutamate receptor mGluR5 in rat brain: protein mRNA splice variants and regional distribution. J Comp Neurol 367: 403-412.

• Rörig B, Sutor B (1996) Serotonin regulates gap junction coupling in the developing rat somatosensory cortex. Eur J Neurosci 15: 7386-7400.

• Rose M (1929) Cytoarchitektonischer atlas der grosshirnrinde der maus. J Psychol Neurol (Lpz) 40: 1-51.

• Rosenblad C, Kirik D, Devaux B, Moffat B, Phillips HS, Bjorklund A (1999) Protection and regeneration of nigral dopaminergic neurons by neurturin or GDNF in a partial lesion model of Parkinson's disease after administration into the striatum or the lateral ventricle. Eur J Neurosci 11: 1554-1566.

• Rubenstein JL, Martinez S, Shimamura K, Puelles (1994) The embryonic vertebrate forebrain: the prosomeric model. Science 266:578-580.

• Ruggiero DA, Baker H, Joh TH, Reis DJ (1984) Distribution of catecholamine neurons in the hypothalamus and preoptic region of mouse. J Comp Neurol 223:556-582.

• Ruiz I Ataba (1998) The works of GLI and the power of Hedgehog. Nat Cell Biol 1: E147-E148.

• Rutherford LC, Nelson SB, Turrigiano GG (1998) BDNF has opposite effects on the quantal amplitude of pyramidal neuron and interneuron excitatory synapses. Neuron 21: 521-530.

• Sakurada K, Ohshima-Sakurada M, Palmer TD, Gage FH (1999) Nurr1, an orphan nuclear receptor, is a transcriptional activator of endogenous tyrosine hydroxylase in neural progenitor cells derived from the adult brain. Development 126: 4017-4026.

• Sala R, Viegi A, Rossi FM, Pizzorusso T, Bonanno G, Raiteri M, Maffei L (1995) Nerve growth factor and brain-derived neurotrophic factor increase neurotransmitter release in the rat visual cortex. Eur J Neurosci 10: 2185-2191.

• Samad TA, Kretzel W, Chambon P, Borrelli E (1997) Regulation of dopaminergic pathways by retinoids-activation of the d2 receptor promoter by members of the retinoic acid receptor retinoid x receptor family. Proc Natl Acad Sci USA 94: 14349-14354.

• Samsa JM, Baker PC, Hoff KM (1979) Monoamine oxidase inhibition and recovery in the mouse brain at various ages after birth. Biol. Neonate 35: 249-254.

• Sandler M, Reveley MA, Glover V (1981) Human platelet monoamine oxidase in health and disease: a review. J Clin Pathol 34: 407-413.

• Sanyanusin P, Norrish JH, Ward TA, Nebel A, McNoe LA, Eccles MR (1995) Genomic structure of the human PAX2 gene. Genomics 35: 258-261.

• Santos Rodriguez P, Dowling JE (1990) Dopamine induces neurite retraction in retinal horizontal cells via diacylglycerol and protein kinase C. Proc Natl Acad Sci USA 87: 2693-2697.

• Sasaki H, Hogan BLM (1994) HNF-3beta as a regulator of floor plate development. Cell 76: 103-115.

• Sasaki H, Hui C, Nakafuku M, Kondoh H (1997) A binding site for Gli proteins is essential for HNF-3beta floor plate enhancer activity in transgenics and can respond to Shh in vitro. Development 124: 1313-1322.

• Saucedo-Cardenas O, Quitanahau JD, Le WD, Smidt MP, Cox JJ, Demayo F, Burbach JPH, Coonneely OM (1998) Nurr1 is essential for the induction of the dopaminergic phenotype and the survival of ventral mesencephalic late dopaminergic precursor neurons. Proc Natl Acad Sci USA 95: 4013-4018.

• Saura J, Ketter M, Da Prada M, Richards JG (1992) Quantitative enzyme radioautography with ^{3}H-Ro 41-1049 and ^{3}H-Ro 19-6327 in vitro: localization and

abundance of MAO-A and MAO-B in rat CNS, peripheral organs, and human brain. J Neurosci 12: 1977-1999.

• Saura J, Nadal E, van den Berg B, Vila M, Bombi JA, Mahy N (1996) Localization of monoamine oxidases in human peripheral tissues. Life Sci 59: 1341-1349.

• Scatton B, Dennis T, Curet O (1984) Increase in dopamine and DOPAC levels in noradrenergic terminals after electrical stimulation of the ascending noradrenergic pathways. Brain Res 298: 193-196.

• Schambra UB, Lauder JM, Silver J (1992) Atlas of the prenatal mouse brain. San diego: Academic Press.

• Schlaggar BL, O'Leary DDM (1991) Potential of visual cortex to develop an array of functional units unique to the somatosensory cortex. Science 252: 1556-1560.

• Schlaggar BL, Fox K, O'Leary DDM (1993) Postsynaptic control of the somatotopic map and barrel patterning in rat somatosensory cortex. Nature 364: 623-626.

• Schlaggar BL, O'Leary DDM (1994) Early development of the somatotopic map in rat somatosensory cortex. J Comp Neurol 346: 80-96.

• Schlumpf M, Shoemaker WJ, Bloom FE (1980) Innervation of the embryonic rat cerebral cortex by catecholamine-containing fibers. J Comp Neurol 192: 361-376.

• Schroeter S, Blakely RD (1996) Drug target in the embryo. Studies on the cocaine- and antidepressant-sensitive serotonin transporter. Ann NY Acad Sci 801: 239-255.

• Seiger A, Olson L (1973) Late prenatal ontogeny of central monoamine neurons in the rat: Fluorescence histochemical observations. Z Anat Entwicklungsgesch 140: 281-318.

• Semina EV, Reiter RS, Murray JC (1997) Isolation of a new homeobox gene belonging to the Pitx/Rieg family: expression during lens development and mapping to the aphakia region on mouse chromosome 19. Hum Mol Genet 6: 2109-2016.

• Semina EV, Ferrell RE, Mintz-Hittner HA, Bitoun P, Alward WL, Reiter RS, Funkhauser C, Daack-Hirsch S, Murray JC (1998) A novel homeobox gene PITX3 is mutated in families autosomal-dominant cataracts and ASMD. Nat Genet 19: 167-170.

• Senft SL, Woolsey TA (1991a) Growth of thalamic afferents into mouse barrel cortex. Cereb Cortex 1: 308-335.

• Senft SL, Woolsey TA (1991b) Computer-aided analyses of thalamocortical afferent ingrowth. Cereb Cortex 1: 336-347.

• Serafini T, Colamarino SA, Leonardo ED, Wang H, Beddington R, Skarnes WC, Tessier-Lavigne M (1996) Netrin-1 is required for commissural axon guidance in the developing vertebrate nervous system. Cell 87: 1001-1014.

• Sermasi E, Margotti E, Cattaneo A, Domenici L (2000) TrkB signalling controls LTP but not LTD expression in the developing rat visual cortex. Eur J Neurosci 12: 1411-1419.

• Shatz CJ, Luskin MB (1986) Relationship between the geniculocortical afferents and their cortical target cells during development of the cat primary visual cortex. J Neurosci 6: 3655-3668.

• Shatz CJ, Chun JJM, luskin MB (1988) The role of the subplate in the development of the mammalian telencephalon. In Cerebral cortex, vol7: development and maturation of cerebral cortex". Peters A, Jones EG (Eds), New York, Plenum press, pp 35-58.

• Shatz CJ, Stryker MP (1988) Prenatal tetrodotoxin infusion blocks segregation of retinogeniculate afferents. Science 242: 87-89.

• Shatz CJ (1990) Impulse activity and the patterning of connections during CNS development. Neuron 5: 745-756.

• Shih JC (1991) Molecular basis of human MAO A and B. Neuropsychopharmacology 4: 1-7.

• Shih JC, Grimsby J, Chen K, Zhu QS (1993) Structure and promoter organization of human monoamine oxidase A and B genes. J Psychiatr Neurosci 18: 25-32.

• Shih JC, Grimsby J, Chen K (1997) Molecular biology of monoamine oxidase A and B: their role in the degradation of serotonin. In: Handbook of experimental pharmacology, Vol 129, Serotoninergic neurons and 5-HT receptors in the CNS. Baumgarten HG, Gothert M (Eds), Berlin, Springer-Verlag, pp 655-670.

• Shimada S, Kitayama S, Lin CL, Patel A, Nanthakumar E, Gregor P, Kuhar M, Uhl G (1991) Cloning and expression of a cocaine-dopamine transporter complementary DNA. Science 254: 577-578.

• Shimamura K, Hartigan DJ, Martinez S, Puelles L, Rubenstein JL (1995) Longitudinal organization of the anterior neural plate and neural tube. Development 121: 3923-3933.

• Shimamura K, Rubenstein JL (1997) Inductive interactions direct early regionalization of the mouse forebrain. Development 124: 2709-2018.

• Shimamura K, Martinez S, Puelles L, Rubenstein JL (1997) Patterns of gene expression in the neural plate and neural tube subdivide the embryonic forebrain into transverse and longitudinal domains. Dev Neurosci 19: 88-96.

• Schimmang T, Minichiello L, Vazquez E, San Jose I, Giraldez F, Klein R, Represa J (1995) Developing inner ear sensory neurons require TrkB and TrkC receptors for innervation of their peripheral targets. Development 121: 3381-1191.

• Shopsin B, Gershon S, Selzer G (1976) The neuropsychopharmacology of mania. In "Drug treatment of mental disorders". Simpson LL (Ed), New York, Raven Press, pp 175-193.

• Shu T, Valentino KM, Seaman C, Cooper HM, Richards LJ (2000) Expression of the netrin-1 receptor, deleted in colorectal cancer (DCC), is largely confined to projecting neurons in the developing forebrain. J Comp Neurol 416: 201-212.

• Sikich L, Hickok JM, Todd RD (1990) 5-HT1A receptors control neurite branching during development. Dev Brain Res 56: 269-274.

• Silos-Santiago I, Fagan AM, Garber M, Fritzsch B, Barbacid M (1997) Severe sensory deficit but normal CNS development in newborn mice lacking TrkB and TrkC tyrosine protein kinase receptors. Eur J Neurosci 10: 2045-2056.

• Simon (1995) Independent assignment of antero-posterior and dorso-ventral positional values in the developing chick hindbrain. Curr Biol 5: 205-214.

• Sims KB, de La Chapelle A, Norio R, Sankila EM, Hsu YPP, Rinehart WB, Corey TJ, Ozelius L, Powell JF, Bruns G, Gusella JF, Murphy DL, Breakefield XO (1989) Monoamine oxidase deficiency in males with an X chromosome deletion. Neuron 2: 1069-1076.

• Sims KB, Lebo RV, Benson G, Shalish C, Golbus MS, Breakefield XO (1992) The Norrie disease gene maps to a 150kb region chromosome Xp11.3. Hum Mol Genet 1: 83-89.

• Sitaram N, Nurnberger JI, Gershon EJ, Gallin JC (1982) Cholinergic regulation of mood and REM sleep: a potential model and marker for vulnerability to depression. Am J Psychiatry 139: 571-576.

• Skagerberg G, Lindvall O, Bjorklund A (1984) Origin, course and termination of the mesohabenular dopamine pathway in the rat. Brain Res 307:99-108.

• Sleight AJ, Marsden CA, Martin KF, and Palfreyman MG (1988) Relationship between extracellular 5-hydroxytryptamine and behaviour following monoamine oxidase inhibition and L-tryptophan. Br J Pharmacol 93: 303-310.

• Smart IHM, McSherry GM (1982) Growth patterns in the lateral wall of the mouse telencephalon. II. Histological changes during and subsequent to the period of isocortical neuron production. J Anat 134: 415-442.

• Smidt MP, van Schaick HS, Lanctot C, Tremblay JJ, Cox JJ, van der Kleij AA, Wolterink G, Drouin J, Burbach JP (1997) A homeodomain gene Ptx3 has highly restricted brain expression in mesencephalic dopaminergic neurons. Proc Natl Acad Sci USA 94: 13305-13310.

• Smith WK (1987) The stress analogy. Schiz Bull 13: 215-225.

• Son JH, Min N, Joh TH (1996) Early ontogeny of catecholaminergic cell lineage in brain and peripheral neurons monitored by tyrosine hydroxylase-lacZ transgene. Mol Brain Res 36: 300-308.

• Sotty F, Souliere F, Brun P, Chouvet G, Steinberg R, Soubrie P, Renaud B, Suaudchagny MF (1998) Differential effects of neurotensine on dopamine release in the caudal and rostral nucleus accumbens-a combined *in vivo* electrochemical and electrophysiological study. Neuroscience 85: 1173-1182.

• Specht LA, Pickel VM, Joh TH, Reis DJ (1977a) Light-microscopy immunocytochemical localization of tyrosine hydroxylase in prenatal rat brain. I. Early ontogeny. J Comp Neurol 199 223-253.

• Specht LA, Pickel VM, Joh TH, Reis DJ (1977b) Light-microscopy immunocytochemical localization of tyrosine hydroxylase in prenatal rat brain. II Late ontogeny. J Comp Neurol 199 255-276.

• Steinbusch HWM, Verhofstad AAJ, Joosten HWJ (1978) Localization of serotonin in the central nervous system by immunocytochemistry: description of a specific and sensitive technique and some applications. Neuroscience 3: 81.

• Steinbusch HWM (1981) Distribution of serotonin-immunoreactivity in the central nervous system of the rat-cell bodies and terminals. Neuroscience 6: 557-618.

• Steinbusch HWM, Verhofstad AAJ, Joosten HWJ, Golstein M (1982) Serotonin-immunoreactive cell bodies in the nucleus dorsomedialis hypothalami, in the substantia nigra, and in the area tegmentalis ventralis of Tsai: observations after pharmacological manipulations in the rat. In: Cytochemical Methods in Neuroanatomy, New York, Alan Liss Inc, pp 407-421.

• Steinbusch HWM, Nieuwenhuys R (1983) The raphe nuclei of the rat brainstem: a cytoarchitectonic and immunocytochemical study. In "Chemical neuroanatomy". Emson PC (Ed), New York, Raven Press, pp 131-207.

• Stettler O, Tavitian B, Moya KL (1996) Differential synaptic vesicle protein expression in the barrel field of developing cortex. J Comp Neurol 375: 321-332.

• Stoykova A, Gruss P (1994) Roles of Pax-genes in developing and adult brain as suggested by expression patterns. J Neurosci 14: 1395-1412.

• Stoykova A, Fritsch R, Walther C, Gruss P (1996) Forebrain patterning defects in Small eye mutant mice. Development 122: 3453-3465.

• Stoykova A, Gotz M, Gruss P, Price J (1997) Pax6-dependent regulation of adhesive patterning, R-cadherin expression and boundary formation in developing forebrain. Development 124: 3765-3777.

• Strolin-Benedetti M, Dostert P (1989) Monoamine oxidase, brain aging and degenerative diseases. Biochem Pharmacol 38: 555-561.

• Strolin-Benedetti M, Marrari P, Cini M, Da Prada M, Dostert P (1991) Effects of MAO inhibition on age-induced changes in tissue amino acid levels in mice and rats. In "Biological psychiatry, Vol 1". Rakani G, Brunello N, Fukuda T (Eds), Amsterdam, Excerpta Medica, pp 386-389.

• Strolin-Benedetti M, Dostert P, Tipton KF (1992) Developmental aspects of the monoamine-degrading enzyme monoamine oxidase. Dev Pharmacol Ther 18: 191-200.

• Suuronen T, Kolehmainen P, Salminen A (2000) Protective effect of L-deprenyl against apoptosis induced by okadaic acid in cultured neuronal cells. Biochem Pharmacol 59:1589-1595.

• Tanabe Y, Jessell TM (1996) Diversity and pattern in the developing spinal cord. Science 274: 1115-1123.

• Tan SS, Breen S (1993) adial mosaicism and tangential cell dispersion both contribute to mouse neocortical development. Nature 362: 638-640.

• Tatton WG, Chalmers-Redman RM (1996) Modulation of gene expression rather than monoamine oxidase inhibition: (-)-deprenyl-related compounds in controlling neurodegeneration. Neurology 47 (Suppl 3), S171-S183.

• Tecott L, Shtrom S, Julius D (1995) Expression of a serotonin-gated ion channel in embryonic neural and nonneural tissues. Mol Cell Neurosci 6: 43-55.

• Theil T, Alvarez-Bolado G, Walter A, Rüther U (1999) *Gli3* is required for *Emx* gene expression during dorsal telencephalon development. Development 126: 3561-3571.

• Thoenen H (1995) Neurotrophins and neural plasticity. Science 270: 593-597.

• Thor S, Thomas JB (1997) The Drosophila islet gene governs axon pathfinding and neurotransmitter identity. Neuron 18: 397-409.

• Thornton-Manning JR, Nikula KJ, Hotchkiss JA, Avila KJ, Rohrbacher KD, Ding X, Dahl AR (1997) Nasal cytochrome P450 2A: identification, regional localization, and metabolic activity toward hexamethylphosphoramide, a known nasal carcinogen. Toxicol Applied Pharmac 142: 22-30.

• Thorpe LW, Westlund KN, Kochersperger LM, Abell CW, Denney RM (1987) Immunocytochemical localization of monoamine oxidase A and B in human peripheral tissues and brain. J Histochem Cytochem 35: 217-236.

• Tinti C, Yang C, Seo H, Conti B, Kim C, Joh TH, Kim KS (1997) Structure/function relationship of the cAMP response element in tyrosine hydroxylase gene transcription. J Biol Chem 272: 19158-19164.

• Tipton KF (1989) Monoamine oxidase inhibitors as antidepressants. In "Biochemical and pharmacological aspects of depression", K.F. Tipton and M.B.H. Youdim (Eds), London, Taylor and Francis, pp 1-24.

• Tiveron MC, Hirsch MR, Brunet JF (1996) The expression pattern of the transcription factor Phox2 delineates synaptic pathways of the autonomic nervous system. J Neurosci 16: 7649-7660.

• Todd RD (1992) Neural development is regulated by classical neurotransmitters: dopamine D2 receptor stimulation enhance neurite outgrowth. Biol Psychiat 31: 794-807.

• Tohyama M, Shiosaka S, Sakanaka M, Takagi H, Senba E, Saitoh Y, Takahashi Y, Sakumoto T, Shimizu N (1980) Detailed pathways of the raphe dorsalis neuron to the cerebral cortex with use of horseradish peroxidase-3, 3',5, 5'-tetramethylbenzydine reaction as a tool for the fiber tracing technique. Brain Res 181: 433-439.

• Ton CC, Hirvonen H, Miwa H, Weil MM, Monaghan P, Jordan T, van Heyningen V, Hastie ND, Meijers-Heijboer H, Drechsler M, et al (1991) Positional cloning and characterization of a paired box- and homeobox-containing gene from the aniridia region. Cell 67:1059-1074.

• Trupp M, Arenas E, Fainzilber M, Nilsson AS, Sieber BA, Grigoriou M, Kilkenny C, Salazar-Grueso E, Pachnis V, Arumae U (1996) Functional receptor for GDNF encoded by the c-ret proto-oncogene. Nature 381: 785-789.

• Tsao LI, Ladenheim B, Andrews AM, Chiueh CC, Cadet JL, Su TP (1998) Delta opiod peptide (d-ala(2),d-Leu(5))enkephalin) bolks the long-term loss of dopamine transporters induced by multiple administrations of mathamphetamine-involvment of opiod receptors and reactive oxygen species. J Pharmacol Exp Ther 287: 322-331.

• Tucker A, Valera-Echevaria A, Puschel AW, Guthrie S (1996) Motor axon subpopulations respond differentially to the chemorepellent netrin-1 and semaphorin D. Neuron 18: 193-207.

• Twarog BM, Page IH (1953) Serotonin content of some mammalian tissues and urine and methods for its determination. Am J Physiol 175: 157-161.

• Twarog BM (1988) Serotonin: history and discovery. Comp Biochem Physiol 91: 21-24.

• Upton A L, Salichon N, Lebrand C, Ravary A, Blakely R, Seif I, Gaspar P (1999) Excess of Serotonin (5-HT) Alters the Segregation of Ispilateral and Contralateral Retinal Projections in Monoamine Oxidase A Knock-Out Mice: Possible Role of 5-HT Uptake in Retinal Ganglion Cells During Development. J Neurosci 19: 7007-7024.

• Uylings HBM, Van Eden CG, Parnavelas JG, Kalbeek A (1990) The prenatal and postnatal development of rat cerebral cortex. In " The cerebral cortex of the rat". Kolb B, Tees EC (Eds) Cambridge, MIT Press 35-76.

• Valarche I, Tissier-Seta JP, Hirsch MR, Martinez S, Goridis C, Brunet JF (1993) The mouse homeodomain protein Phox2 regulates Ncam promoter activity in concert

with Cux/CDP and is a putative determinant of neurotransmitter phenotype. Development 119: 881-896.

• Valzelli L (1981) Psychopharmacology of aggression: an overview. Int Pharmacolopsychiatry 16: 39-48.

• Van der Loos H, Woolsey TA (1973) Somatosensory cortex: structural alterations following early injury to sense organs. Science 179: 395-398.

• Van der Loos H, Welker E (1985) Development and plasticity of the somatosensory brain map. In "Development, organization, and processing in somatosensory pathways". Rowe M, Willis WD (Eds), New York, Alan Liss, pp 53-67.

• Van der Loos H, Welker E, Dorlf J, Hoogland PV (1991) Brain maps: development, plasticity and distribution of signals beyond. In "The neocortex, Ontogeny and Phylogeny". Finlay BL, Innocenti G, Sheich H (Eds). New York, Plenum Press. p, 229-236.

• Van Erp Taalman Kip MJ (1938) Lichaamsgrootte en hersenschors. Nordhoff, Groningen. 143.

• Van Hasterfeldt C, Moore B, Hartman BK (1986) Transient midline raphe glial structure in thedeveloping rat. J Comp Neurol 253: 175-184.

• Verney C, Berger B, Adrien J, Vigny A, Gay M (1982) Development of the dopaminergic innervation of the rat cerebral cortex. A light microscopic immunocytochemical study using anti-tyrosine hydroxylase antibodies. Brain Res 281: 41-52.

• Verney C, Gaspar G, Febvret A, Berger B (1988) Transient tyrosine hydroxylase-like immunoreactive neurons contain somatostatin and substance P in the developing amygdala and bed nucleus of the stria terminalis of the rat. Dev Brain Res 42: 45-58.

• Vitalis T, Cases O, Callebert J, Launay JM, Price DJ, Seif I, Gaspar P (1998) Effects of monoamine oxidase A inhibition on barrel formation in the mouse somatosensory cortex. Determination of a sensitive developmental period. J Comp Neurol 393: 169-184.

• Vitalis T, Cases O, Engelkamp D, Verney C, Price DJ (2000) Defects of tyrosine-hydroxylase-immunoreactive neurons in the brains of mice lacking the transcription factor Pax6. J Neurosci 20: 6501-6516.

• Vogt M (1982) Some functional aspects of central serotoninergic neurones. In "Biology of Serotoninergic Neurotransmission". Obsborn NN (Ed), Chishester, John Wiley and Sons, pp 299-316.

• Voitenko NN (1992) Age changes in brain monoamine oxidase in mice from four lines. Voprosoy Meditsinskoi Khimii. 38: 32-35.

• Von Bartheld CS, Byers MR, Williams R, Bothwell M (1996) Anterograde transport of neurotrophins and axodendritic transfer in the developing visual system. Nature 379: 830-833.

• Vongdokmai R (1980) Effect of protein malnutrition on development of mouse cortical barrels. J Comp Neurol 191: 283-294.

• Von Knorring AL, Bohman M, Von Knorring L, Oreland L (1985) Platelet MAO activity as a biological marker in subgroups of alcoholism Acta Psychiatr Scand 72: 51-58.

• Voorn P, Kalsbeek A, Jorritsma-Byham B, Groenewegen HJ (1988) The pre- and postnatal development of the dopaminergic cell groups in the ventral mesencephalon and the dopaminergic innervation of the striatum of the rat. Neuroscience 25: 857-887.

• Wadsworth WG, Bhatt H, Hedgecock EM (1996) Neuroglia and pioneer neurons express UNC-6 to provide global and local netrin cues for guiding migrations in C. elegans. Neuron 16: 35-46.

• Wallace JA, Petruz P, Lauder JM (1982) Serotonin immunocytochemistry in the adult and developing rat brain: methodological demonstration of sensory maps in the rat and mouse cerebral cortex. Brain Res 9: 171-129.

• Wallace JA, Lauder JM (1983) Development of the serotonergic system in rat embryo: an immunocytochemical study. Brain Res Bull 10: 459-479.

• Wallace MN (1987) Histochemical demonstration of sensory maps in the rat and mouse cerebral cortex. Brain Res 418: 178-182.

• Walther C, Gruss P (1991) Pax-6, a murine paired box gene, is expressed in developing CNS. Development 113: 1435-1449.

• Wang MZ, Jin P, Bumcrot DA, Marigo V, McMahon AP, Wang EA, Woolf T, Pang K (1995) Induction of dopaminergic phenotype in the midbrain by Sonic hedgehog protein. Nat Med 1: 1184-1188.

• Wang XH, Poo MM (1997) Potentiation of developing synapses by postsynaptic release of neurotrophin-4. Neuron 19: 825-835.

• Warburg M (1966) Norrie's disease: a congenital progressive oculo-acousticocerebral degeneration. Acta Ophtalmol 89: 1-47.

• Warren N, Price DJ (1997) Roles of Pax6 in murine diencephalic development. Development 124: 1573-1582.

• Watanabe E, Aono S, Matsui F, Yamada Y, Naruse I, Oohira A (1995) Distribution of a brain-specific proteoglycan, neurocan, and the corresponding mRNA during the formation of barrels in the rat somatosensory cortex. Eur J Neurosci 7: 547-554.

• Webber KM, Pennefather JN, \Head GA, Vandenbuuse M (1998) Endothelin induces dopamine release from rat striatum via endothelin-β receptors. Neuroscience 86: 1173-1180.

• Wechsler-Reya RJ, Scott MP (1999) Control of neuronal precursor proliferation in the cerebellum by Sonic Hedgehog. Neuron 22: 103-114.

• Wehr TA, Goodwin FK (1981) Biological rithms and psychiatry. In "American Handbook of psychiatry". Arieti S, Brodie HKH (Eds), New York, Basic books Vol.7, pp 46-74.

• Weinberger DR (1987) Implications of normal brain development for the pathogenesis of schizophrenia. Arch Gen Psychiatry 44: 660-669.

• Weiner RI, Findell PR, Kordon C (1988) Role of classic and peptide neuromediators in the neuroendocrine regulation of LH and Prolactine. In The Physiology of Reproduction. Knobill E, Neill J (Eds), New York, Raven Press, pp 1235-1281.

• Weiser M, Vega-Saez de Miera E, Kentros C, Moreno H, Franzen L, Hillman D, Baker H, Rudy B (1994) Differential expression of Shaw-related K+ channels in the rat central nervous system. J Neurosci 14: 949-972.

• Welker E, Van der Loos H (1986) Quantitative correlation between barrelfield size and the sensory innervation of the whisker pad: a comparative study in size strains of mice bred for different patterns of mystacial vibrissae. J Neurosci 6: 3355-3373.

• Welker C (1976) Receptive fields of barrels in the somatosensory neocortex of the rat. J Comp Neurol 166: 173-190.

• Welker E, Van der Loos H (1986) Quantitative correlation between barrel-field size and the sensory innervation of the whiskerpad: a comparative study of six strains of mice bred for different patterns of mystacial vibrissae. J Neurosci 6: 3355-3373.

• Welker E, Armstrong-James M, Bronchti G, Ourednik W, Gheorghita-Baechler F, Dubois R, Guernsey DL, Van der Loos H, Neumann PE (1996) Altered sensory processing in the somatosensory cortex of the mouse mutant barrelless. Science 271: 1864-1867.

• Westlund KN, Denney RM, Kochersperger LM, Rose RM, Abell CW (1985) Distinct monoamine oxidase A and B populations in primate brain. Science 230: 181-183.

• Westlund KN, Denney RM, Rose RM, Abell CW (1988) Localization of distinct monoamine oxidase A and monoamine oxidase B cell populations in human brainstem. Neuroscience 25: 439-456.

• Weyler W, Hsu YP, Breakefield XO (1990) Biochemistry and genetics of monoamine oxidase. Pharmac Ther 47: 391-417.

• Whitaker-Azmitia PM, Azmitia E (1989) Stimulation of astroglial serotonin receptors produces culture media which regulates growth of serotonergic neurons. Brain Res 497: 80-85.

• Whitaker-Azmitia PM, Shemer AV, Caruso J, Molino L, Azmitia EC (1990) Role of high affinity serotonin receptors in neuronal growth. Ann NY Acad Sci 600: 315-330.

• Whitaker-Azmitia PM (1992) Role of serotonin and other neurotransmitter receptors in the brain development: basis for developmental pharmacology. Pharm Rev 43: 553-561.

• Whitaker-Azmitia PM, Zhang X, Clarke C (1994) Effects of gestational exposure to oxidase inhibitors in rats: preliminary behavioral and neurochemical studies. Neuropsychopharmacology 11: 125-132.

• White EL, Weinfeld L, Lev DL (1997) A survey of morphogenesis during the early postnatal period in PMBSF barrels of mouse Sm1 cortex with emphasis on barrel D4. Somatosens Mot Res14: 34-55.

• Wiesel TN, Hubel DH (1965) Comparison of the effects of unilateral and bilateral eye closure on cortical unit responses in kittens. J Neurophysiol 28: 1029-1040.

• Wilkinson GA, Farinas I, Backus C, Yoshida CK, Reichardt LF (1997) Neurotrophin-3 is a survival factor In vivo for early mouse trigeminal neurons. J Neurosci 16: 7661-7669.

• Willoughby J, Glover V, Sandler M (1988) Histochemical localisation of MAO-A and -B in rat brain. J Neural Transm 74: 29-42.

• Wise SP, Jones EG (1978) Developmental studies of thalamocortical and commissural connections in the rat somatic sensory cortex. J Comp Neurol 178: 187-208.

• Witsow GJ, Piatigorsky J (1988) Lens crystallins: the evolution and expression of proteins for a highly specialized tissue. Annu Rev Biochem 57: 479-504.

• Wong DF, Wagner HN, Tune LE, Dannals RF, Pearlson GD, Links JM, Tamminga CA, Broussole EP, Ravert HT, Wilson AA, Toung JKT, Malat J, Williams JA, O'Tuama LA, Snyder SH, Kuhar MJ, Gjedde A (1986) Positron emission tomography reveals elevated D2 dopamine receptors in drug-naïve schizophrenics. Science 234: 1558-1563.

• Wong-Riley MTT, Welt C (1980) Histochemical changes in cytochrome oxidase of cortical barrels after vibrissal removal in neonatal and adult mice. Proc Natl Acad Sci USA 77: 2333-2337.

• Woolsey TA, Van der Loos H (1970) The structural organization of layer IV in the somatosensory region (S1) of mouse cerebral cortex. Brain Res 17: 205-242.

• Woolsey TA, Wann JR (1976) Areal changes in mouse cortical barrels following vibrissal damage at different postnatal ages. J Comp Neurol 170: 53-66.

• Woolsey TA (1990) Peripheral alteration and somatosensory development. In "Development of sensory systems in mammals". Coleman J (Ed), New-York, Wiley, pp 461-516.

• Xu B, Zang K, Ruff NL, Zhang YA, McConnel SK, Stryker MP, Reichardt LF (2000) Cortical degeneration in the absence of neurotrophin signaling: dendritic retraction and neuronal loss after removal of the receptor TrkB. Neuron 26: 233-245.

• Yacoubian TA, Lo DC (2000) Truncated and full-length TrkB receptors regulate distinct modes of dendritic growth. Nat Neurosci 3: 342-349.

• Yang C, Kim HS, Seo H, Kim KS (1998) Identification and characterization of potential cis-regulatory elements governing transcriptional activation of the rat tyrosine hydroxylase gene. J Neurochem 71: 1358-1368.

• Ye W, Shimamura K, Rubenstein JLR, Hynes MA, Rosenthal A (1998) FGF and Shh signals control dopaminergic and serotonergic cell fate in the anterior neural plate. Cell 93: 755-766.

• Young SN, Smith SE, Pihl RO, Ervin FR (1985) Tryptophan depletion causes a rapid lowering of mood in normal males. Psychopharmacology (Berl) 87: 173-177.

• Yu PH, Hertz L (1982) Differential expression of type A and type B monoamine oxidase of mouse astrocytes in primary cultures. J Neurochem 39: 1492-1495.

• Yue Y, Widmer DA, Halladay AK, Cerretti DP, Wagner GC, Dreyer JL, Zhou R (1999) Specification of distinct dopaminergic neural pathways: roles of the Eph family receptor EphB1 and ligand ephrin-B2. J Neurosci 19: 2090-2101.

• Zellmer E, Zhang Z, Greco D, Rhodes J, Cassel S, Lewis EJ (1995) A homeodomain protein selectively expressed in noradrenergic tissue regulates transcription of neurotransmitter biosynthetic genes. J Neurosci.15: 8109-8120.

• Zetterstrom RH, Solomin L, Mitsiadis T, Olson L, Perlmann T (1996a) Retinoid X receptor heterodimerization and developmental expression distinguish the orphan nuclear receptors NGFI-B, Nurr1, and Nor1. Mol Endocrinol 10: 1656-1666.

• Zetterstrom RH, Williams R, Perlmann T, Olson L (1996b) Cellular expression of the immediate early transcription factors Nurr1 and NGFI-B suggests a gene regulatory role in several brain regions including the nigrostriatal dopamine system. Brain Res Mol Brain Res 41: 111-120.

• Zetterstrom RH, Solomin L, Jansson L, Hoffer BJ, Olson L, Perlmann T (1997) Dopamine neuron agenesis in Nurr1-deficient mice. Science 276: 248-250.

• Zhu D, Antonarakis SE, Schmeckpeper BJ, Biergaarde PJ, Greb AE, Maumenee IH (1989) Microdeletion in the X-chromosome and prenatal diagnosis in a family with Norrie disease. Am J Genet 33: 485-488.

• Zureick JL, Metzer HY (1988) platelet MAO activity in hallucinating and paranoid schizophrenics: a review and meta-analysis. Biol Psychiatry 24: 63-78.

ANNEXES

Publication 1: **Vitalis T**, Cases O, Callebert J, Launay JM, Price DJ, Seif I, Gaspar P (1998) Effects of monoamine oxidase A inhibition on barrel formation in the mouse somatosensory cortex. Determination of a sensitive developmental period. J Comp Neurol 393: 169-184.

Publication 2: Cases O, Lebrand C, Giros B, **Vitalis T**, De Maeyer E, Caron MG, Price DJ, Gaspar P, Seif I (1998) Plasma membrane transporters of serotonin, dopamine, and norepinephrine mediate serotonin accumulation in atypical locations in the developing brain of monoamine oxidase A knock-outs. J Neurosci 18: 6914-6927.

Publication 3: **Vitalis T**, Cases O, Engelkamp D, Verney C, Price DJ (2000) Defects of tyrosine-hydroxylase-immunoreactive neurons in the brains of mice lacking the transcription factor Pax6. J Neurosci 20: 6501-6516.

THE JOURNAL OF COMPARATIVE NEUROLOGY 393:169–184 (1998)

Effects of Monoamine Oxidase A Inhibition on Barrel Formation in the Mouse Somatosensory Cortex: Determination of a Sensitive Developmental Period

TANIA VITALIS,[1,3] OLIVIER CASES,[1,2,3] JACQUES CALLEBERT,[4] JEAN-MARIE LAUNAY,[4] DAVID J. PRICE,[3] ISABELLE SEIF,[2] AND PATRICIA GASPAR[1]*
[1]INSERM U106, Hôpital de la Salpêtrière, 75651 Paris Cedex 13, France
[2]CNRS UMR 177, Institut Curie, 91405 Orsay Cedex, France
[3]Department of Physiology, Medical School, University of Edinburgh, Edinburgh EH8 9AG, Scotland
[4]Centre de Recherche C. Bernard "Pathologie Expérimentale et Communications Cellulaires" IFR6, Services de Biochimie, Hôpital Lariboisière, 75010 Paris, France

ABSTRACT

Genetic inactivation of monoamine oxidase A (MAOA) in C3H/HeJ mice causes a complete absence of barrels in the somatosensory cortex, and similar alterations are caused by pharmacological inhibition of MAOA in wild type mice. To determine when and how MAOA inhibition affects the development of the barrel field, the MAOA inhibitor clorgyline was administered to mice of the outbred strain OF1 for various time periods between embryonic day 15 (E15) and postnatal day 7 (P7), and the barrel fields were analyzed with cytochrome oxidase and Nissl stains in P10 and adult mice. High-pressure liquid chromatography measures of brain serotonin (5-HT) showed three- to eightfold increases during the periods of clorgyline administration. Perinatal mortality was increased and weight gain was slowed between P3 and P6. Clorgyline treatments from E15 to P7 or from P0 to P7 disrupted the formation of barrels in the anterior snout representation and in parts of the posteromedial barrel subfield (PMBSF). Treatments from P0 to P4 caused similar although less severe barrel field alterations. Clorgyline treatments only during embryonic life or starting on P4 caused no detectable abnormalities. In cases with barrel field alterations, a rostral-to-caudal gradient of changes was noted: Rostral barrels of the PMBSF were most frequently fused and displayed an increased size tangentially.

Thus, MAOA inhibition resulting in increased brain levels of 5-HT affects barrel development during the entire first postnatal week, with a sensitive period between P0 and P4. The rostral-to-caudal gradient of changes in the barrel field parallels known developmental gradients in the sensory periphery and in the maturation thalamocortical afferents. The observed barrel fusions could correspond to a default in the initial segregation of thalamic fibers or to a continued, exuberant growth of these fibers that overrides the tangential domain that is normally devoted to individual whiskers. J. Comp. Neurol. 393:169–184, 1998.

Indexing terms: serotonin; cerebral cortex; thalamocortical axons; barrels; clorgyline

A number of mechanisms underlying the formation and plasticity of cortical sensory maps have been uncovered by studying the barrel field in the rodent somatosensory cortex. The appeal of this system for developmental analyses lies in the fact that its precise topographical organization can be visualized readily: The peripheral tactile receptors associated with the whiskers are isomorphically

Grant sponsor: INSERM; Grant sponsor: CNRS; Grant sponsor: European Commission; Grant sponsor: University of Edinburgh; Grant sponsor: Wellcome Trust; Grant numbers: Biomed-2-PL962412 and Biotech Bio4CT-965048.

*Correspondence to: Dr. Patricia Gaspar, INSERM U106, Hôpital de la Salpêtrière, 47 Boulevard de l'Hôpital, 75651 Paris Cedex 13, France. E-mail: gaspar@infobiogen.fr

Received 12 May 1997; Revised 6 October 1997; Accepted 7 November 1997

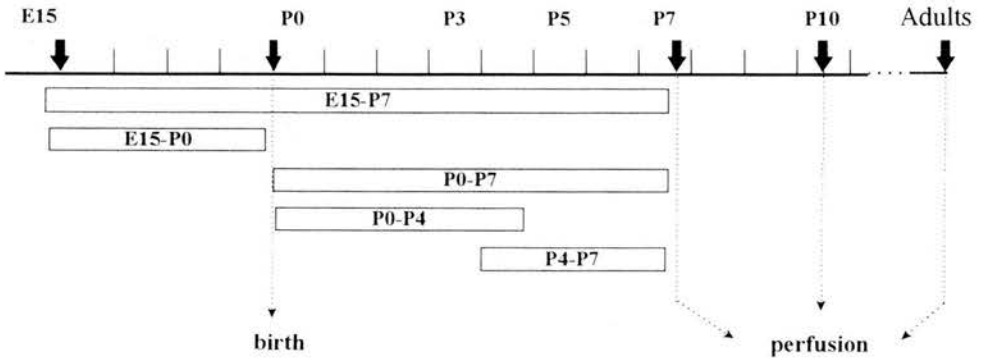

Fig. 1. Chart showing the different schedules of clorgyline treatment used in the present study are indicated with bars along a time scale that marks the days of pre- and postnatal development. E, embryonic day; P, postnatal day.

TABLE 1. Clorgyline- and Saline-Treated Pups and Dams Used in the Different Experiments in This Report[1]

Treatments	Dose (mg/kg)	Interval between injections (hours)	Period of the treatment	Dams (n)	P0 pups (n)	Animals analyzed (n)	Ages
Experiment 1: Optimization of clorgyline dosage							
Saline			E15–P7	4	51	10	P8, P10, P15
Clorgyline	5	24	E15–P7	3	37	14	P8, P15
Clorgyline	30	24	E15–P7	2	24	7	P8, P15
Clorgyline	5	8	E15–P7	2	16	5	P8, P15
Clorgyline	10	8	E15–P7	7	60	9	P8, P10
Experiment 2: Varying the period of clorgyline administration[2]							
Clorgyline	10	8	P0–P7	6	50	17	P8, P10, adults
Clorgyline	10	8	P0–P4	3	16	9	P10
Clorgyline	10	8	E15–P0	3	15	11	P10
Clorgyline	10	8	P4–P7	2	24	5	P10

[1]Animals that were used for immunocytochemistry and biochemical analyses are not counted in this Table.
[2]For all of these periods, saline-treated controls (n = 6) were analyzed in parallel with the clorgyline-treated mice. P, postnatal day; E, embryonic day.

represented as discrete elements, called barrelettes in the sensory relays of the brainstem, barreloids in the thalamic relay, and barrels in the primary somatosensory cortex (S1). In S1, barrels form clear units in layer IV, consisting of a ring of granular cells that surrounds a cell-sparse hollow containing the clustered terminal arbors of thalamic neurons (Woolsey and Van der Loos, 1970; Jensen and Killackey, 1987a). The crucial role of the sensory periphery in the formation of barrels was demonstrated early on. Lesioning a row of whiskers early in postnatal development causes defective formation of barrels in the corresponding cortical representation (Van der Loos and Woolsey, 1973; Woolsey and Wann, 1976; Belford and Killackey, 1980; Jeanmonod et al., 1981). Conversely, the presence of additional whiskers on the snout induces additional barrels to form in the cortex (Welker and Van der Loos, 1986). However, the nature of the signal conveyed by the periphery is still unclear, because blockade of neural activity with tetrodotoxin or bupivacaine does not alter barrel formation (Chiaia et al., 1992, 1994; Henderson et al., 1992). Nevertheless, normal glutamatergic neurotransmission appears to be necessary for the refinement of topographic order in the thalamocortical projection, because whisker-related patterns fail to develop in the brainstem, thalamus, and cortex of mice genetically deficient for the key subunit of the N-methyl-D-aspartate (NMDA) receptors (Li et al., 1994; Iwasato et al., 1996) and because pharmacological blockade of NMDA receptors in normal S1 disrupts the topographic refinement of the thalamocortical projection and the functional columnar organization of barrels (Fox et al., 1996).

Recently, defective formation of barrels has been shown to occur, despite the presence of normal peripheral receptors, in two other strains of mice. One strain is characterized by a spontaneous mutation, named "barrelless," located on the proximal segment of chromosome 11 (Welker et al., 1996). The other strain has a serendipitous knockout for the gene encoding monoamine oxidase A (MAOA) located on the X chromosome (Cases et al., 1995). In these two strains of mice, the tangential clustering of thalamocortical afferents is lacking, and granular neurons in layer IV do not form the characteristic rings. An excess of brain serotonin (5-HT) amounts during early postnatal development appears to be responsible for the abnormalities in the MAOA knockout mice, because lowering 5-HT amounts in the brain of developing pups allows normal barrels to form in S1 (Cases et al., 1996). Excess of 5-HT could alter two components of the normal developmental processes that underlie cortical barrel formation: The ingrowth of thalamocortical fibers and the differentiation of cortical neurons

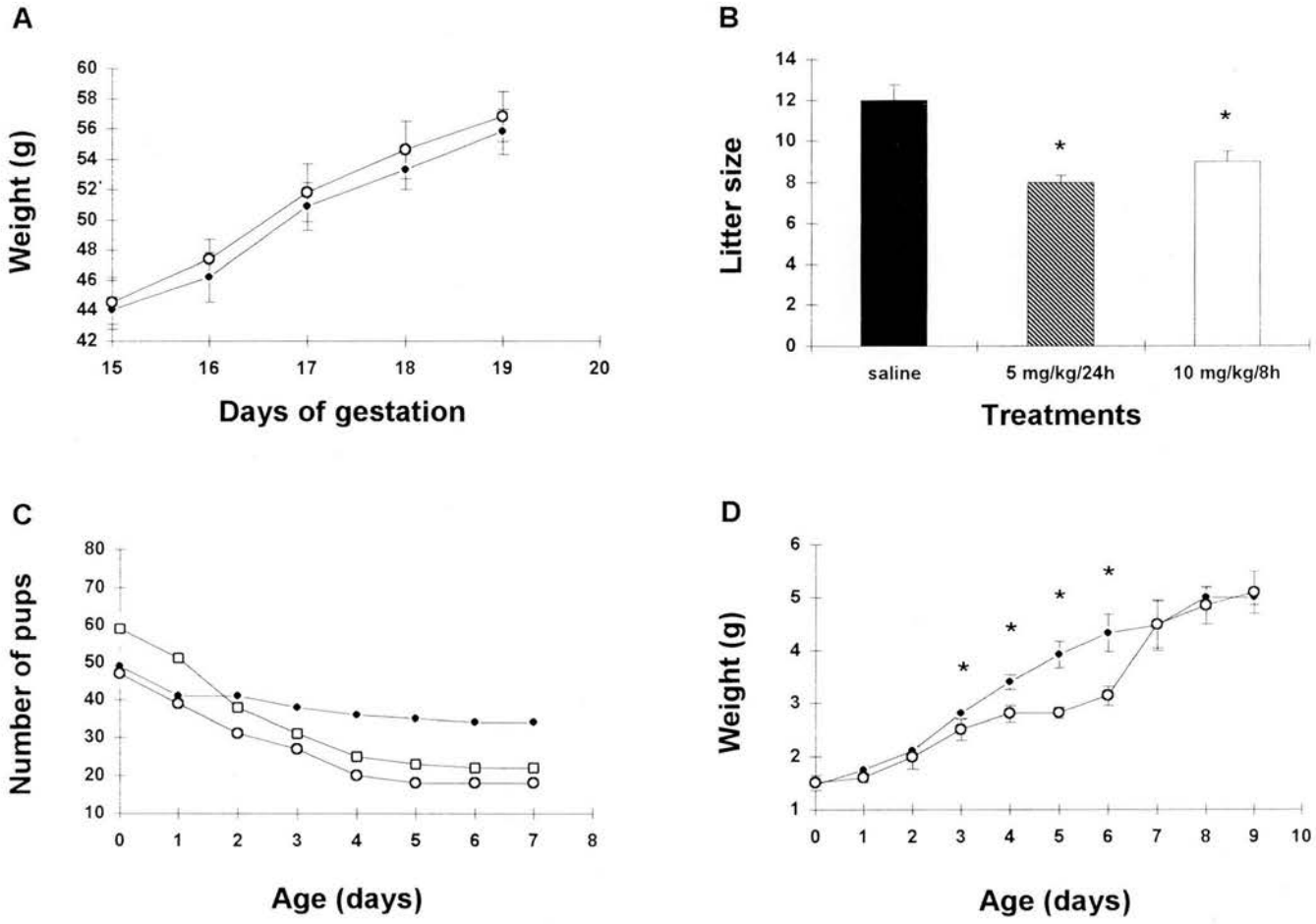

Fig. 2. General developmental effects of clorgyline administration. **A:** Weight increase in gram units (g) during pregnancy in dams injected with saline (solid circles; n = 5) and 10 mg/kg/8 hours clorgyline (open circles; n = 7). Mean ± S.E.M. **B:** Litter size at birth in mice treated with saline (n = 7), 5 mg/kg/24 hours clorgyline (n = 3), or 10 mg/kg/8 hours clorgyline (n = 7) from E15 to P0. Mean ± S.E.M. **C:** Survival of pups receiving injections of saline (solid circles) or 10 mg/kg/8 hours clorgyline from E15 to P7 (squares) or from P0 to P7 (open circles). **D:** Weight increase in grams of 10 mg/kg/8 hours clorgyline-treated pups from six litters (open circles) vs. saline-treated pups from five litters (solid circles). Injections were administered during the P0–P7 period. Mean ± S.E.M. Significant differences between groups ($P < 0.05$; Student's t-test) are indicated with an asterisk in B and D.

in layer IV. In mice, thalamocortical fibers reach the cortical anlage as early as embryonic day 15 (E15), invade the deep cortical layers in late embryonic life (Catalano et al., 1996), reaching the nascent layer IV in the lower cortical plate by P2. Barrel-like periodicities of the thalamocortical afferents become detectable on P3 (Senft and Woolsey, 1991a,b; Agmon et al., 1993) and are soon accompanied by changes in the distribution of the layer IV neurons: In Nissl-stained tangential sections, barrels first appear by P3.5 as oval-shaped patches of decreased packing density of perikarya. Clear, ring-like arrangements of granular neurons are observed by P5 (Rice and Van der Loos, 1977).

Although the exact targets of 5-HT in this intricate developmental process remain to be determined, there are strong arguments for a direct effect of 5-HT on the thalamocortical neurons originating from the ventrobasal (VB) thalamic nuclei. Serotonin receptors of the 5-HT_{1B} subtype are located transiently on VB terminals in the somatosensory cortex (Bennett-Clarke et al., 1993) and presynaptically inhibit the excitatory thalamocortical transmission, at least in vitro in brain slices (Rhoades et al., 1994). Furthermore, developing VB neurons transiently express the genes encoding the serotonin transporter (SERT) and the vesicular monoamine transporter (VMAT2). 5-HT, as a result, is taken up and stored in thalamocortical axons innervating S1 (Lebrand et al., 1996), giving the picture of a dense 5-HT^+ innervation of the barrel field during the first postnatal week (Fujimiya et al., 1986; D'Amato et al., 1987; Rhoades et al., 1990; Blue et al., 1991; Lebrand et al., 1996).

In the present study, we sought to obtain more precise information on the sensitive period during which increased levels of brain 5-HT affect barrel development. In our previous work, which focused on the absence of barrels in MAOA knockouts, we showed that, in wild-type C3H/HeJ mice, transient pharmacological inactivation of MAOA with clorgyline from P0 to P6 caused important and permanent barrel field abnormalities (Cases et al., 1996). The purpose of the present report, which was performed on

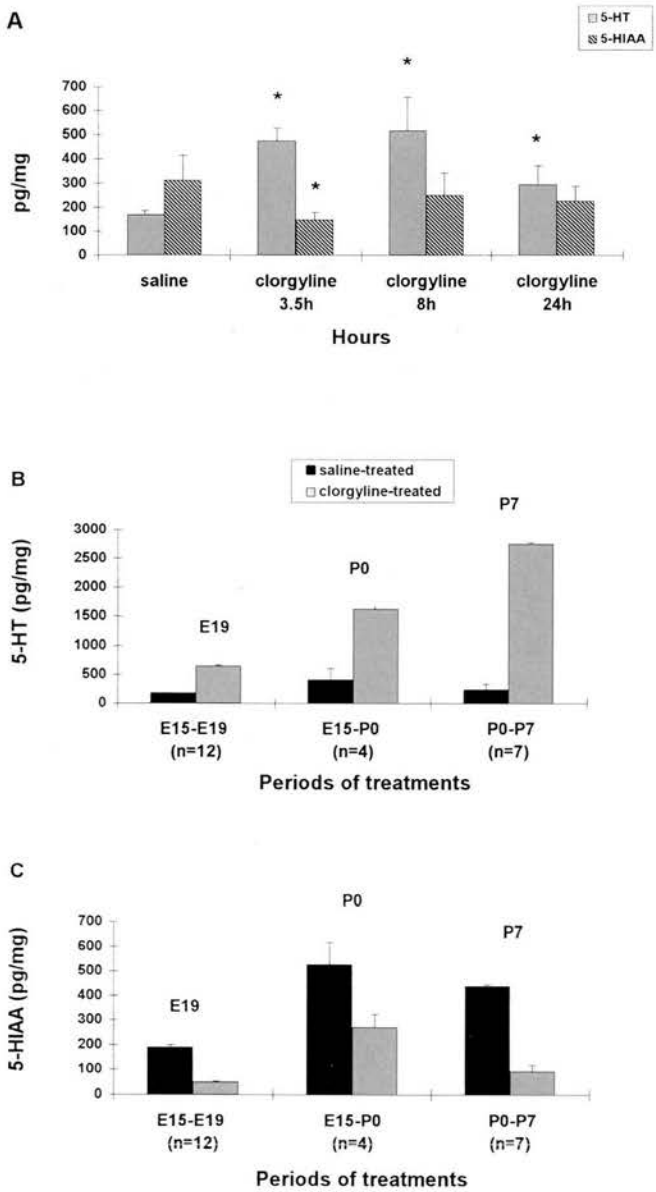

Fig. 3. **A:** Whole brain amounts of serotonin (5-HT; shaded bars) and 5-hydroxyindoleacetic acid (5-HIAA; hatched bars) in P3 pups after a single 10 mg/kg clorgyline injection. Pups were killed 3.5, 8.0, or 24.0 hours later (n = 5 for each point). Saline-treated controls were killed at the beginning (t = 0; n = 3) and at the end (t = +24 hours; n = 3) of the experiment. No difference was observed between these two control groups, which are pooled in the first histogram. Values are expressed in picograms per milligram of wet brain and represent the mean ± S.E.M. Asterisk indicates that the results are statistically significant ($P < 0.005$; Student's t-test). **B,C:** 5-HT (B) and 5-HIAA (C) amounts in whole brains of mice receiving repeated injections of saline (solid bars) or 10 mg/kg/8 hours clorgyline (shaded bars) following the E15–P7 schedule. Measures were performed at E19 (n = 12), P0 (n = 4), and P7 (n = 7). In A and B, all values of the clorgyline-treated group were statistically different from controls ($P < 0.005$; Student's t-test).

another strain of mice, the outbred OF1 strain, was to compare the extent of changes following a variety of clorgyline dosages and schedules in prenatal and early postnatal life and to provide a more detailed analysis of the pattern of barrel field abnormalities. We also analyzed the general physiological effects of the pharmacological treatments to determine whether any observed alterations of the barrel field could be related to the effects of MAOA inhibition on overall growth and development of the mice.

MATERIALS AND METHODS

Animals

Experiments were carried out on mice of the outbred strain OF1 (Iffa Credo, Orléans, France). All animal procedures were conducted in strict compliance with approved institutional protocols and in accordance with the provisions for animal care and use described in the Scientific Procedures on Living Animals Act of 1986. The day of birth was counted as postnatal day 0 (P0).

Pharmacological treatments

Clorgyline (5, 10, or 30 mg/kg; M-3778; Sigma-Aldrich, Strasbourg, France) or physiological saline was administered intraperitoneally to pregnant dams and subcutaneously to mouse pups by using a 30-gauge needle. Injections were given either daily or every 8 hours over the following developmental periods: E15–P0, E15–P7, P0–P4, P4–P7, and P0–P7 (Fig. 1). The first injection at P0 was made 4–8 hours after delivery. Each day, surviving pups were numbered and weighed. The total numbers of OF1 mice that were treated with the different dosages and schedules are indicated in Table 1.

Biochemical analysis

Embryos (E19) and P7 pups treated for various times with clorgyline (10 mg/kg/8 hours) or saline were decapitated after cold anesthesia 3 hours after the dams or the pups received their last injection. P0 pups born from treated mothers were killed in the same way, but, in this case, the delay with the last clorgyline injection to the mother was uncertain (between 3 and 10 hours). In addition, P3 pups were killed 3.5, 8, and 24 hours after a single clorgyline injection (10 mg/kg). The brains were rapidly frozen in liquid nitrogen and kept at −80°C. After homogenization of the whole brains, 5-HT, 5-hydroxyindoleacetic acid (5-HIAA), and tryptophan (Trp) amounts were measured with high-pressure liquid chromatography (HPLC) and fluorometric detection (Kema et al., 1993).

Histology

For Nissl and cytochrome oxidase (CO) stains, most animals were killed at P8 or P10 (Table 1). Some treated mice were killed as adults (at 2 months). Mice were deeply anesthetized with ether at P8 and P10 and with chloral hydrate (0.5 g/kg) as adults and were perfused transcardially with 4% paraformaldehyde in 0.1 M phosphate buffer, pH 7.4. After perfusion, brains were removed from the skull and weighed. One hemisphere was separated from the rest of the brain by a section through the internal capsule and was flattened between two glass slides separated by spacers. The rest of the brain was kept as one block. Blocks were postfixed overnight in the same buffered paraformaldehyde and were cryoprotected in 30% sucrose phosphate buffer. Serial, 40-µm-thick, frozen sections were obtained in the coronal or tangential planes.

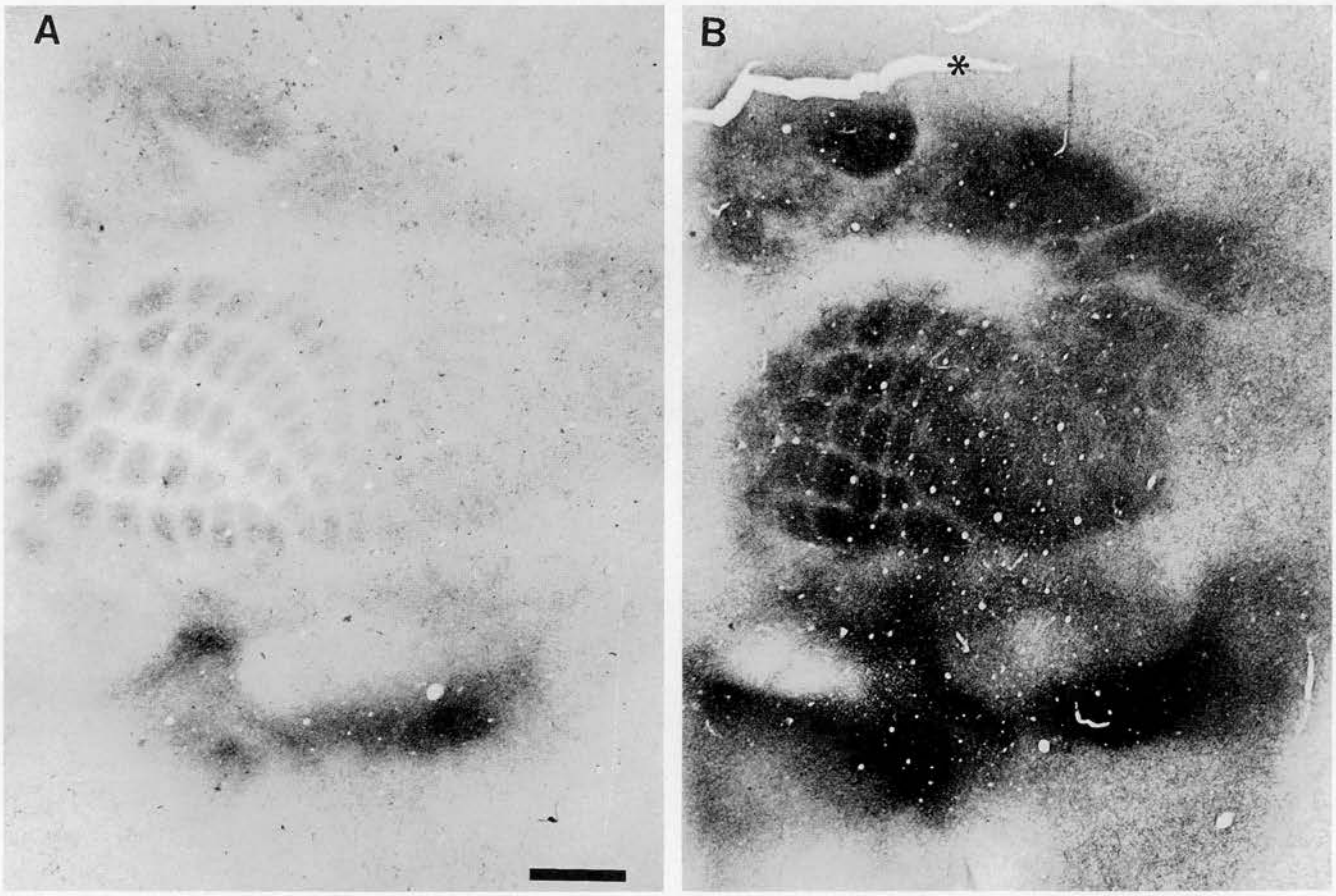

Fig. 4. Serotonin (5-HT) immunostaining in tangential sections of the flattened cortex at P7. **A:** In a saline-treated pup, moderate 5-HT immunostaining delineates the primary somatosensory cortex (S1) with a barrel pattern visible in the posteromedial barrel subfield (PMBSF) and the anterior snout (AS); the auditory cortex is also visible. **B:** In a P0–P7 clorgyline-treated pup, 5-HT immunostaining is more intense, obliterating the normal pattern of some barrels in S1. An artifactual crack on this section is indicated with an asterisk. Scale bar = 330 μm.

Alternate series of sections were used for CO, as described by Wong-Riley and Welt (1980), and for Nissl (0.025% thionine in acetate buffer, pH 5.5). 5-HT immunocytochemistry (rat monoclonal antibody from Harlan-Sera Laboratory, Loughborough, England; clone YC5/45, 1/50; Consolazione et al., 1981) was performed on frozen sections from animals killed at P0 and P7, as described previously by Lebrand et al. (1996).

Histological analysis

Barrels were examined in Nissl- or CO-stained coronal sections, and the entire barrel field was reconstructed from serial CO-stained tangential sections. The outlines of all CO-dense clusters (barrels, abnormally shaped barrels, all fused barrels) were drawn by using a camera lucida, and the drawings from consecutive sections were aligned by using blood vessels. Reconstructions from four to six animals were made for each administration schedule at 10 mg/kg/8 hours clorgyline.

From the reconstructions made with the 6.3× objective, we determined the total number of CO-dense clusters (barrels, abnormally shaped barrels, and fused barrels) in the posteromedial barrel subfield (PMBSF). To evaluate the topographical distribution of changes, the number of normal barrels were counted 1) along the five longitudinal rows (A–E) of the PMBSF and 2) along the eight transversal arcs (1–8) of the PMBSF (for nomenclature, see Rice and Van der Loos, 1977). The most caudal barrels (α, β, γ, and δ), which straddle barrel rows, were not counted in this scheme.

The surface area covered by the PMBSF and the anterior snout (AS) was outlined on reconstructions made with the 2.5× objective and was measured by using a morphometric software (Image Tool; The University of Texas Health Science Center, San Antonio, TX). The surface area of individual barrels was measured from reconstructions made with the 10× objective. Only unfused barrels in B1–B4, C1–C5, and D1–D5 in P0–P4 saline- or clorgyline-treated mice could be evaluated.

The thickness of cortical layers II–IV and layers II–VI were measured in Nissl-stained coronal sections by using an eyepiece graticule (10× objective). The thickness of layer IV was measured in CO-stained coronal sections (16× objective). Measurements were taken along a line perpendicular to the pial surface at two different levels: one in the PMBSF (level −1 posterior and −3.1 lateral to

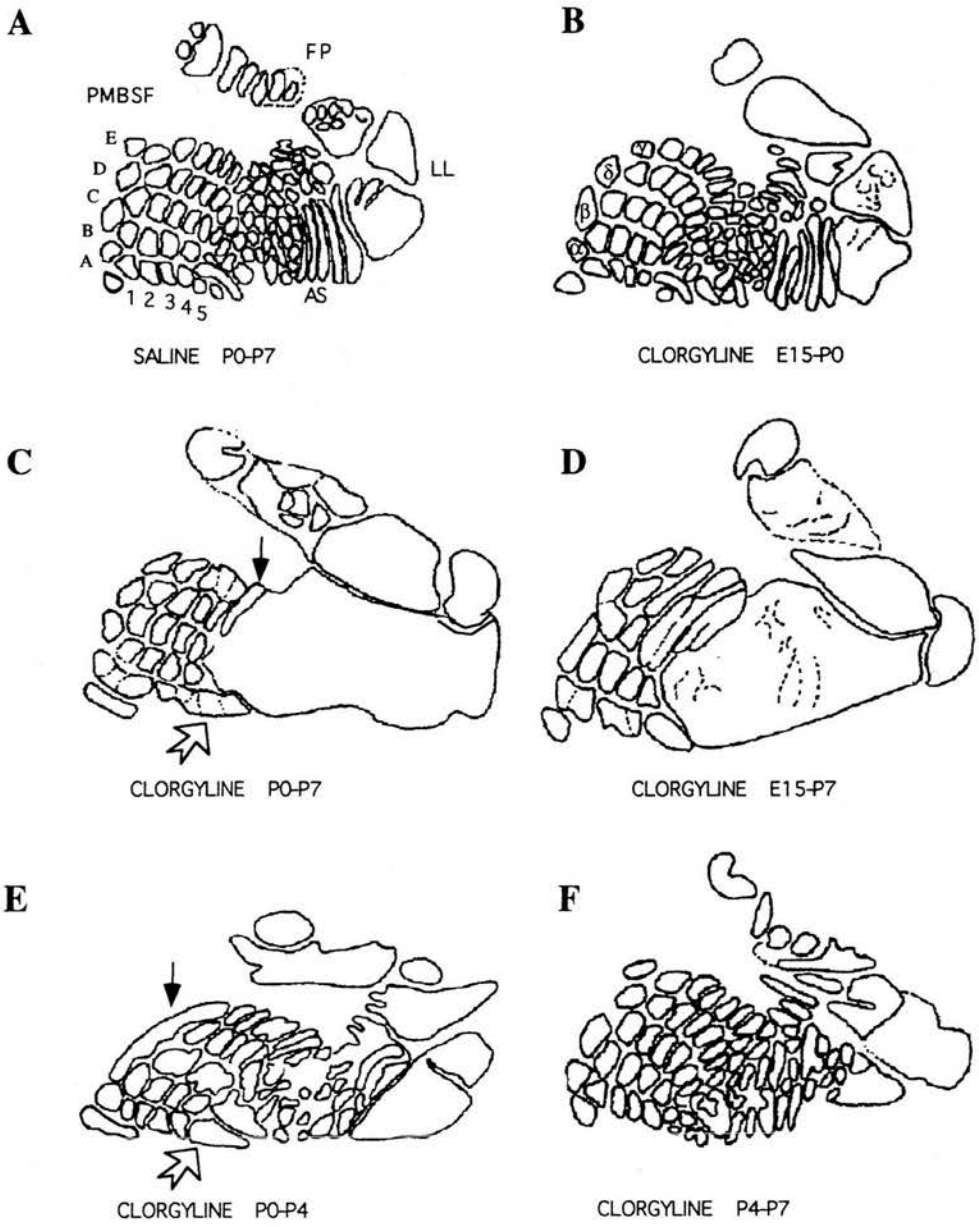

Fig. 5. Representative reconstructions of S1 were made from a complete series of cytochrome oxidase (CO)-stained tangential sections of flattened cortex. **A:** In a saline-treated pup, the different regions of the somatosensory representation are indicated: The large mystachial vibrissae (PMBSF), the anterior snout (AS), the lower lip (LL), and the forepaw (FP). These regions are separated by large septa. Each division is subdivided into barrels and stripes. **B:** Embryonic clorgyline injections (E15–P0) have no effects. **C,D:** Severe alterations are seen in protracted postnatal clorgyline treatments. A complete barrel fusion is seen in the AS, and partial row fusions (open arrow) or arc-fusions (solid arrow) are visible in the PMBSF. **E:** Early postnatal clorgyline administration (P0–P4) causes barrel disorganization and fusions in the LL, in the AS, and, to a lesser extent, in the PMBSF. **F:** P4–P7 clorgyline injections have no visible effects on formation of barrels in the different subfields.

Bregma) and the other in the AS (level +0.7 anterior and −3 lateral to Bregma).

RESULTS

Optimization of clorgyline dosage regime

We determined the minimal dose and frequency of administration of clorgyline capable of producing major alterations in the formation of the barrel field. After each of the various protocols listed in Table 1 (experiment 1), the barrel field was examined with Nissl and CO stains at P8. We started with a 5 mg/kg daily injection of clorgyline, a dose that is known to acutely inhibit MAOA activity by nearly 100% in adult rats and that does not produce obvious behavioral alterations (Green and Youdim, 1975; Sleight et al., 1988). After daily administrations from E15 to P7, a few abnormally shaped barrels were observed in CO-stained coronal sections (4 of 14 pups). Increasing the daily dose to 30 mg/kg did not produce more substantial modifications of the barrel field. Taking into account the

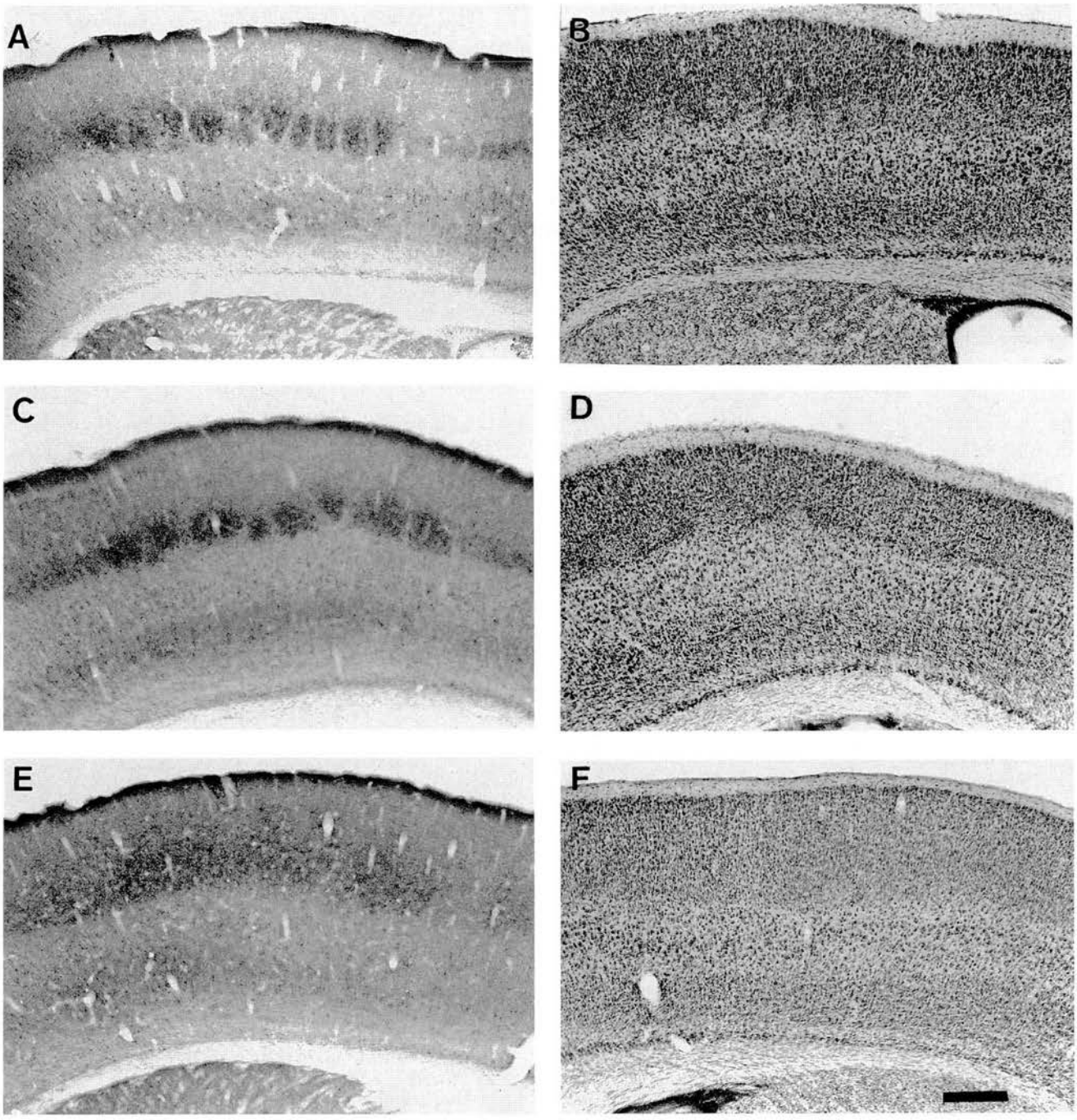

Fig. 6. Gradual alterations of the cortical barrels according to the period and the duration of the clorgyline treatment. **A,B:** Normal barrels are visible as blobs of increased cytochrome oxidase (CO) activity (A) or as clustered granular cells in layer IV (B) surrounding a cell-sparse hollow with Nissl staining. **C,D:** In P0–P4 clorgyline-treated pups, barrels appear larger than in controls on CO stains (C) and are less clearly defined cytoarchitecturally on Nissl stains (D). **E,F:** In P0–P7 clorgyline-treated pups, increased CO activity (E) and granular neurons (F) form a continuous band in layer IV. Scale bar = 320 μm.

higher rate of MAOA synthesis in pups (Nelson et al., 1979; Samsa et al., 1979), we then increased the frequency of clorgyline administration. Treating animals from E15 to P7 with 5 mg/kg/8 hours of clorgyline produced alterations in rostral barrels but had little effect on the PMBSF. The 10 mg/kg/8 hours regime led to constant and severe abnormalities throughout the barrel field. Therefore, the following report will deal mainly with the latter dosage regime.

General developmental and behavioral effects of clorgyline administration

In mothers treated from E15 to P0 (5 mg/kg/24 hours or 10 mg/kg/8 hours), we observed no effects of the clorgyline

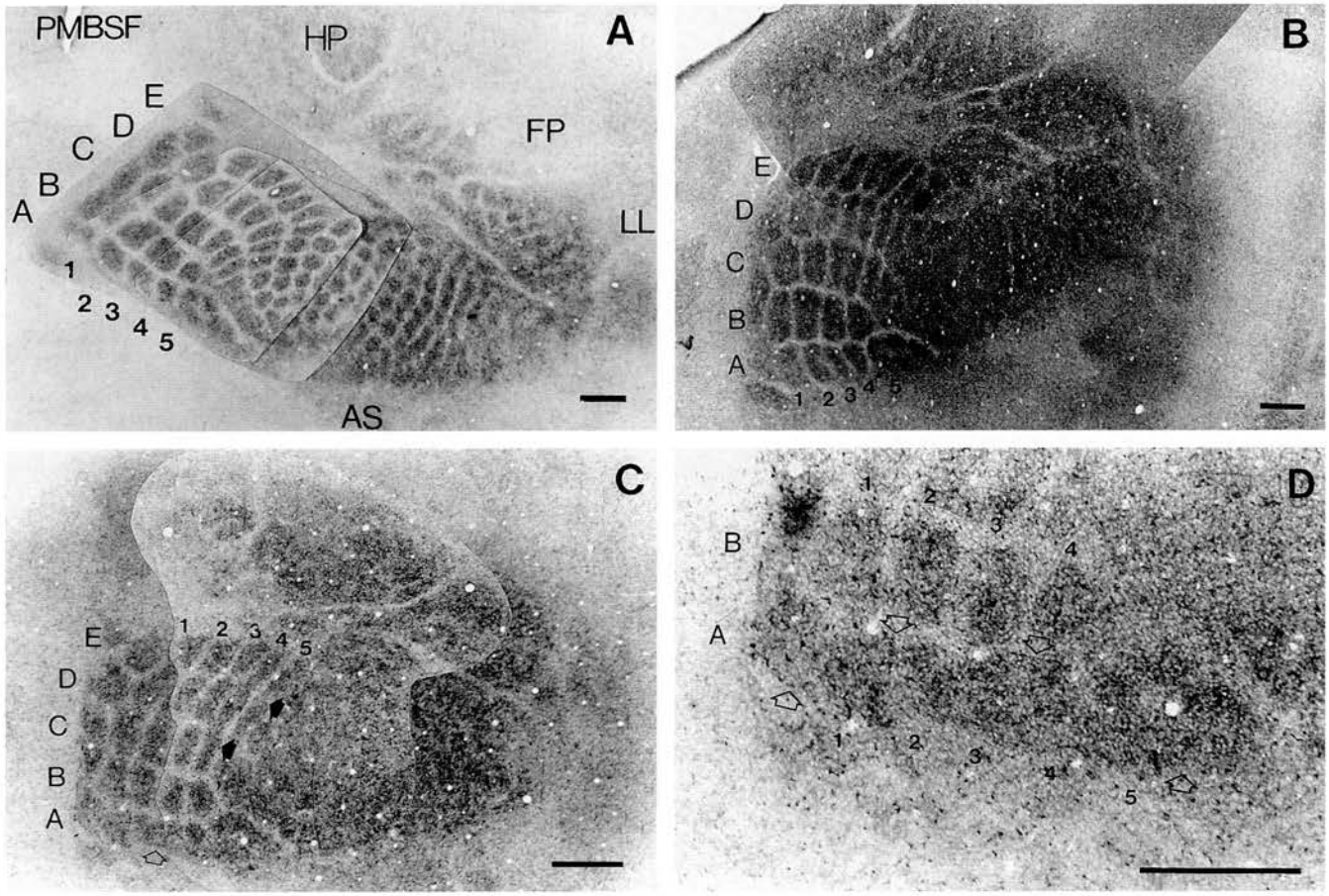

Fig. 7. Typical examples of barrel field alterations caused by monoamine oxidase A (MAOA) inhibition viewed on cytochrome oxidase (CO)-stained tangential sections. **A:** Reconstruction of S1 in a saline-treated mouse killed at P10 showing the different trigeminal subfields, posteromedial barrel subfield (PMBSF), anterior snout (AS), and lower lip (LL) as well as the hind paw (HP) and forepaw (FP) representations. The five rows in the PMBSF are indicated with letters from A to E, and the first five barrel arcs are indicated with numbers. **B:** An E15–P7 clorgyline-treated mouse killed at P10: Note the lack of barrels or cytochrome oxidase (CO^{+}) clusters in AS, LL, and FP. In the PMBSF, the most rostral barrels are lacking, with arc-like fusions of barrels along arc 5 (D5 and E5). **C:** A similar pattern of barrel field alterations is visible in a P0–P7 clorgyline-treated mouse killed at P8. Arc-like fusions of barrels along arc 4 (C4, D4, and E4) and arc 5 (D5 and E5) are indicated by solid arrows. A row-like fusion is also visible along row A (open arrow). **D:** High magnification of C, showing the fusion along row A delineated by arrows. Scale bars = 320 μm.

treatment on the duration of pregnancy, or weight increase during pregnancy (Fig. 2A). However, the size of the litters, which was evaluated 4–8 hours after delivery, was reduced by 30% (Fig. 2B), reflecting an increased perinatal mortality. Mortality of clorgyline-treated pups was considerably increased during the subsequent 4 days of postnatal life (Fig. 2C), with survival rates at P7 of 30% and 36% in the E15–P7 and P0–P7 administration schedules, respectively. Surviving clorgyline-treated pups at P3–P6 displayed a slight, temporary retardation of their growth curve relative to controls, but their growth returned to normal at P7 (Fig. 2D). Clorgyline-treated pups displayed some of the behavioral abnormalities described in the MAOA knockout pups (Cases et al., 1995), such as agitation, trembling, hunched posture, increased righting time (15–20 seconds instead of 1 second in controls), and abnormal rooting reflex. However, these behavioral alterations were less intense and were no longer observable 24 hours after the last injection.

Clorgyline-treated dams, contrary to saline-treated dams, showed almost constantly increased locomotor activity and excitability, even after the end of the treatment, which were probably due to the long-lasting effects of clorgyline in adults (Maitre et al., 1976). This could explain in part the high mortality rate of the pups observed in the E15–P7 group. Nursing and nurturing defects have also been noted previously when rat pups were treated with inhibitors of monoamine oxidases (Whitaker-Azmitia et al., 1994).

Biochemical abnormalities

To evaluate the duration of MAOA inhibition provoked by the administration of clorgyline, we measured the amounts of 5-HT and its metabolite, 5-HIAA, 3.5, 8, and 24 hours after a single subcutaneous injection at P3 (10 mg/kg; Fig. 3A). Judging by the reduction in the amounts of 5-HIAA, MAOA inhibition was maximal 3.5 hours after the injection (55% reduction from controls), and a partial recovery was observed by 8 hours (20–25% reduction from controls). 5-HT amounts were increased threefold by 3.5 and 8 hours after the injection.

Repeated injections of clorgyline (10 mg/kg/8 hours) over the P0–P7 period led to a more complete inhibition of

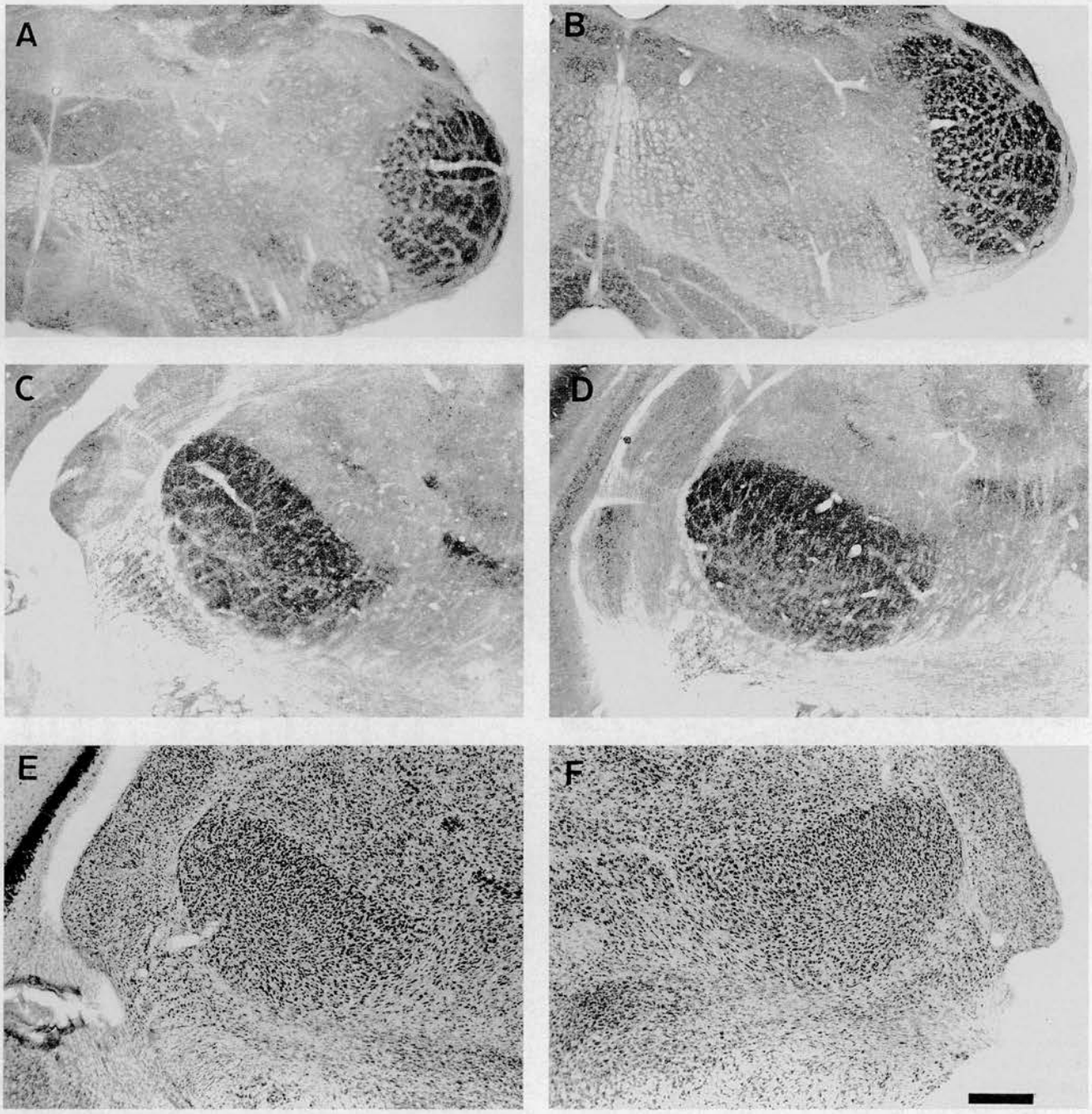

Fig. 8. Normal patterning in the lower stations of the somatosensory pathway in P10 pups. Different relays of the somatosensory pathway are shown with CO activity (**A–D**) and Nissl (**E,F**). Barrelettes have similar staining and distribution patterns in the trigeminal nucleus principalis of controls (A) and P0–P7 clorgyline-treated pups (B). Barreloids have similar staining and distribution in the ventrobasal thalamic nucleus of controls (C,E) and P0–P7 clorgyline-treated pups (D,F). Scale bar = 320 μm.

MAOA. There was a larger increase in 5-HT (eightfold; Fig. 3B), a larger decrease in 5-HIAA (80% reduction; Fig. 3C), and a 6% increase in Trp levels (not shown). Pharmacological inhibition with clorgyline was also effective in embryos. In E19 embryos taken from treated pregnant dams or in P0 pups born from treated mothers, the amounts of brain 5-HT were fourfold higher than in controls, whereas 5-HIAA was reduced by 70%, or 50% of the controls (Fig. 3C).

5-HT immunostaining

5-HT immunostaining at P7 was increased in the brainstem, diencephalon, and cerebral cortex of P0–P7 clorgyline-treated pups. This increase was also visible in P0 pups born to clorgyline-treated mothers. In tangential sections of the cerebral cortex of P7 clorgyline-treated pups, 5-HT immunolabeling was markedly increased in S1 as well as in the primary auditory and primary visual cortices. In

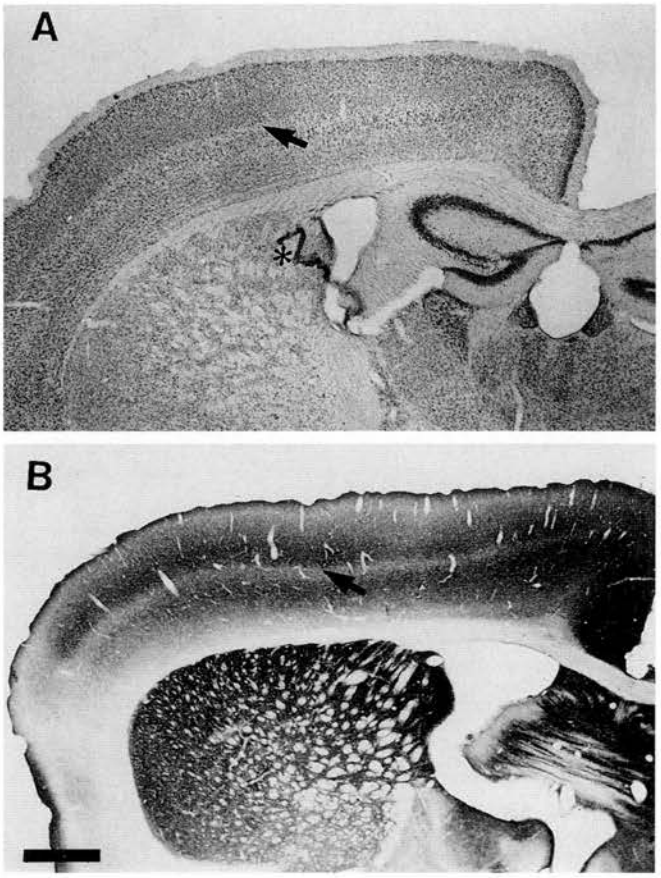

Fig. 9. Permanent alterations of layer IV in a 2-month-old mouse treated with 10 mg/kg/8 hours clorgyline from P0 to P7: Granular neurons observed with Nissl staining (the asterisk indicates a displaced fragment of the choroid plexus; **A**) and cytochrome oxidase (CO) activity (**B**) form a continuous band in layer IV instead of clustered granular cells (Fig. 7A) or blobs of increased CO activity (Fig. 7B). Scale bar = 640 μm.

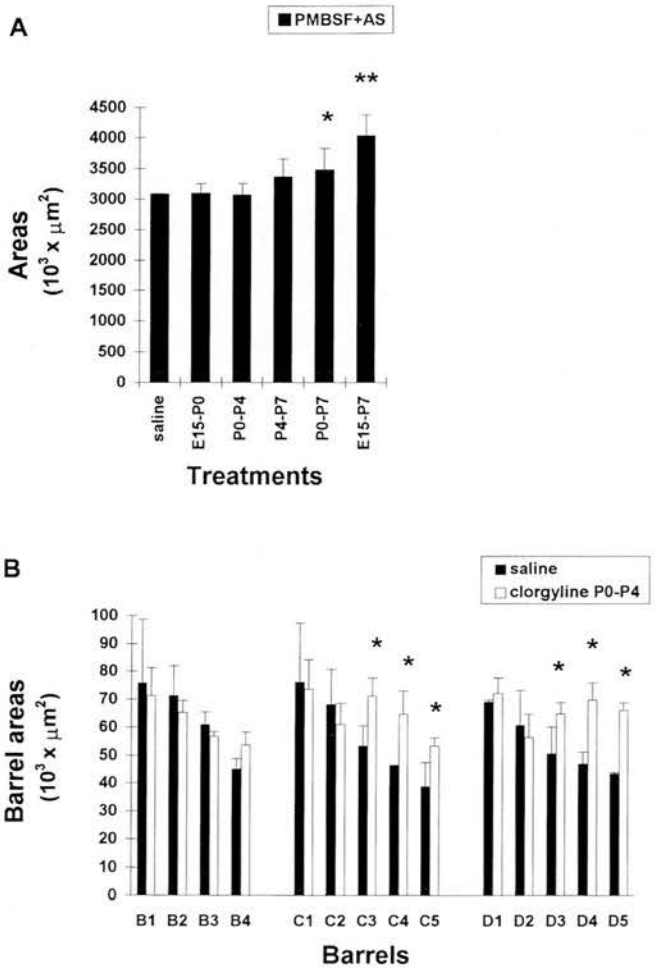

Fig. 10. **A:** Area of the posteromedial barrel subfield (PMBSF) plus the AS measured on cytochrome oxidase (CO) stains from pups treated with saline (n = 4) or 10 mg/kg/8 hours clorgyline during different periods: E15–P0 (n = 6), P0–P4 (n = 6), P4–P7 (n = 5), P0–P7 (n = 6), and E15–P7 (n = 4). Asterisks indicates that the results are statistically significant ($^*P < 0.025$, $^{**}P < 0.005$; Student's t-test). **B:** Histograms representing the area of individual CO-stained barrels after saline (n = 4) and P0–P4 clorgyline treatment (n = 6). Asterisk indicates that the results are statistically significant ($^*P < 0.05$; Student's t-test) between saline- and clorgyline-treated pups.

S1, the frontiers between cortical barrels were blurred (Fig. 4B).

Effects on the barrel field

The patterning of the barrels was affected diversely by the different schedules of clorgyline administration. In animals that received clorgyline treatments only during the embryonic period E15–P0, cortical barrels had a normal appearance on CO- and Nissl-stained coronal sections. On reconstructions from CO-stained tangential sections, the organization of S1 was similar to that of controls (Fig. 5A,B). Barrels and other characteristic CO-dense elements were distinguished in the four main domains of S1: The PMBSF, the AS, the lower lip (LL), and the forepaw (FP). They normally have different aspects and sizes in these different parts: They are largest and quadrangular in the PMBSF, smaller and roughly circular in the caudal part of the AS, have a stripe-like organization in the rostral part of the AS, and are the least sharply defined in LL and FP, where ovoid blobs are visible.

Severe alterations of the barrel field were observed in all pups that received clorgyline from E15 to P7 and from P0 to P7. On CO-stained coronal sections, barrels were distinguished only in a few cases: Large patches with blurred outlines were observed in the most caudal part of the PMBSF (Fig. 6E). Tangential reconstructions of S1 were made in 12 cases. In the AS, barrels or stripes were completely absent in 11 cases and, in one case, showed a few disorganized clusters. In the LL, CO^+ clusters or blobs were completely lacking in eight cases (Fig. 5C,D). In the PMBSF, some barrels were visible in all of the cases, but there were fusions of barrels within a given row, mainly in row A, or along the barrel arcs, mainly between the rostral barrels of rows C, D, and E (Fig. 7). Nissl-stained coronal sections did not show the characteristic clusters in layer IV of S1 (Fig. 6B); instead, granular neurons formed a uniform band with a moderate packing density (Fig. 6F). These cortical alterations were not accompanied by any obvious abnormalities in the barrelette or barreloid patterns of the lower sensory stations (Fig. 8). Furthermore,

TABLE 2. Number of Cytochrome Oxydase-Positive Clusters (Normal barrels, abnormal shaped barrels, or fused barrels) and Clearly Defined Barrels That Can Be Identified in the Posteromedial Barrel Subfield of P10 Pups Treated With Saline or Clorgyline (10 mg/kg/8 hours) During Different Periods[1]

	Saline	Clorgyline				
	P0–P7 (n = 5)	E15–P0 (n = 6)	E15–P7 (n = 4)	P0–P7 (n = 5)	P0–P4 (n = 6)	P4–P7 (n = 4)
CO clusters in the PMBSF	30*	29.5 ± 0.7*	17 ± 1.3**	19.4 ± 1.5**	23.8 ± 2.3***	29.7 ± 0.6*
Clearly defined barrels in the PMBSF	30*	29.5 ± 0.7*	12.3 ± 1.8**	14 ± 0.4**	19 ± 1.8***	29.7 ± 0.6*

[1]Counts were obtained from flattened reconstructions. Mean ± S.E.M. CO, cytochrome oxydase; PMBSF, posteromedial barrel subfield.
*Statistical difference between the different clorgyline schedules and the P0–P7-treated group ($P < 0.05$; Student's t-test).
**Statistical difference relative to the control group ($P < 0.05$; Student's t-test).

TABLE 3. Topographical Distribution of Barrel Alterations[1]

	Saline	Clorgyline				
	P0–P7 (n = 5)	E15–P0 (n = 6)	E15–P7 (n = 4)	P0–P7 (n = 5)	P0–P4 (n = 6)	P4–P7 (n = 4)
Rows						
A	5	5	1 ± 0.7**	1.6 ± 0.9**	3 ± 1.3*	4.7 ± 0.5
B	4	4	4	4	4	4
C	6	6	2**	3.2 ± 0.6**	4.2 ± 0.6*	6
D	7	7.5 ± 0.7	2.7 ± 0.9**	2.2 ± 0.3**	3.3 ± 1**	7
E	8	8	3 ± 0.7**	2.8 ± 0.6**	4.3 ± 0.7**	8
Arcs						
1	5	5	4.3 ± 0.9	4.4 ± 0.5	4.5 ± 0.6	5
2	5	5	4	4.4 ± 0.5	4 ± 0.7	5
3	5	5	2.3 ± 0.4**	2.8 ± 0.6**	4 ± 0.3*	5
4	5	5	1.7 ± 0.9**	2 ± 0.4**	4.3 ± 0.7	5
5	4	4	0	2 ± 0.4**	1.3 ± 1.0**	3.7 ± 0.4
6	3	2.7 ± 0.4	0	0.2 ± 0.3**	0.5 ± 0.5**	3
7	2	2	0	0	0.5 ± 0.7*	2
8	1	1	0	0	0.2 ± 0.3*	1

[1]Number of clearly defined barrels along rows and arcs of the PMBSF as identified on complete primary somatosensory cortex reconstructions. Analysis was done in P10 pups treated with saline or clorgyline (10 mg/kg/8 hours). Values represent the mean ± S.E.M. of n cases.
*Statistical difference relative to the saline group ($P < 0.05$; Student's t-test).
**Statistical difference relative to the saline group ($P < 0.01$; Student's t-test).

TABLE 4. Cortical Thickness in P10 Pups Treated With Saline or Clorgyline (10 mg/kg/8 hours) During Different Periods[1]

Treatment (number of pups)	Period of the treatment	Thickness of layers (μm)	
		II–IV	II–VI
Saline (n = 3)	P0–P7	467 ± 20	1,195 ± 34
Clorgyline (n = 6)	E15–P0	413 ± 32	1,023 ± 22
Clorgyline (n = 6)	P0–P4	410 ± 39	1,088 ± 90
Clorgyline (n = 6)	P0–P7	462 ± 24	1,169 ± 64

[1]Measures were obtained from Nissl-stained coronal sections at the level −1 mm posterior, −3.1 mm lateral to Bregma. Mean ± S.E.M.

cortical changes were permanent, because no barrels were distinguished on CO- and Nissl-stained coronal sections from four adult mice that had been treated with 10 mg/kg/8 hours of clorgyline from P0 to P7 (Fig. 9A,B).

Less severe alterations of the barrel field were visible in P0–P4 clorgyline-treated pups. In coronal sections, clustered, CO-stained blobs were observed in the caudal PMBSF (Fig. 6C) and also occasionally in coronal sections, through the anterior part of the barrel field. These CO clusters had irregular shapes and blurred contours. Tangential reconstructions of S1 were made in six cases. In the AS, barrels were completely lacking in only one case: The other five cases displayed barrel-like, CO^+ clusters, albeit with a disorganized appearance compared with controls (Fig. 5E). In the LL, segregation into blobs was absent in four cases. In the PMBSF, barrels were always distinguishable, but with some barrel fusions similar to those described previously along arcs or rows (Figs. 5E, 7). Nissl-stained coronal sections through S1 revealed a disorganized distribution of granular cells in layer IV with periodic differences in cellular density (Fig. 6D), suggesting that some architectonic differentiation had occurred.

In P4–P7 treated pups, barrels appeared to be normal on coronal sections, and, in all of the five reconstructed cases, all PMBSF barrels could be identified, and barrels were found in the AS (Fig. 5E). In the case illustrated, the patterning of the AS differed slightly from controls, but this is difficult to interpret, because there are some variations in the patterning of this subfield in normal animals.

To provide a quantitative comparison of the effect of these different treatments, we counted the total number of CO^+ clusters as well as the number of clearly formed barrels in the PMBSF (see Materials and Methods). These counts confirmed that clorgyline had more potent effects when it was administered during the E15–P7 and P0–P7 periods rather than only during the P0–P4 period, whereas a prenatal treatment did not significantly augment the deleterious developmental effect of clorgyline (Table 2). Furthermore, counts of the number of the normally formed barrels along the rows and arcs confirmed the impression of a topographical distribution of the barrel alterations: The reduction in the number of barrels was most severe in row A. Row B, which is formed of four caudal barrels appeared to be relatively spared. Normal barrels were also less frequent within rostral barrel arcs, comprising arcs 3–8 in the E15–P7 and P0–P7 clorgyline-treated pups and arcs 5–8 in the P0–P4 clorgyline-treated pups (Table 3). Barrel straddlers (α, β, γ, and δ), which were not included in the counts, appeared to be fused in about half of the clorgyline-treated cases (E15–P7, P0–P7, and P0–P4).

Morphometry

Brain weights were similar in P0–P7 clorgyline-treated mice (308 ± 30 mg) and P10 control mice (310 ± 7 mg). On Nissl-stained coronal sections, neither the thickness of cortical layers II–VI nor the thickness of the layers (II–IV) were significantly changed by any of the treatments (Table 4). By contrast, the thickness of layer IV, measured as the reactive CO-dense zone, was reduced by 10–20% (Table 5).

The surface area comprising the PMBSF and the AS in the tangential sections showed a significant (10–20%) increase in the P0–P7 and E15–P7 clorgyline-treated pups but appeared unchanged with the E15–P0, P0–P4, and P4–P7 treatments (Fig. 10A). Measurements of the individual barrel areas were taken in the P0–P4 clorgyline-treated pups, considering only the unfused barrels that could be identified in rows B, C, and D. Significant increases in size were noted for barrels C3–C5 and D3–D5, whereas changes were nonsignificant for the more caudal barrels C1, C2, D1, and D2 and for barrels B1–B4 (Fig. 10B). Measurements of individual barrel areas in the P4–P7 treated mice showed no significant difference from

TABLE 5. Thickness of Cortical Layer IV in P10 Pups Treated With Saline or Clorgyline (10 mg/kg/8 hours) During Different Periods[1]

Treatment (number of pups)	Period of the treatment	Thickness of layer IV (μm) at level to Bregma	
		−1, −3.1 mm	+0.7, −3 mm
Saline (n = 2)	P0–P7	203 ± 17	201 ± 2
Clorgyline (n = 6)	E15–P0	189 ± 20	207 ± 12
Clorgyline (n = 6)	P0–P4	169 ± 16	209 ± 14
Clorgyline (n = 6)	P0–P7	168 ± 8	177 ± 7

[1]Measures were obtained from CO-stained coronal sections at two different stereotaxic levels: −1 mm posterior and −3.1 mm lateral, and +0.7 mm anterior and −3 mm lateral, to Bregma. Mean ± S.E.M.

controls. Such measures were not feasible in the other treated groups because of the frequency of fused barrels.

DISCUSSION

The present study shows that pharmacological inhibition of MAOA activity during development irreversibly alters the formation of barrels in the mouse somatosensory cortex. The degree of cortical abnormality is strongly related to the time period during which MAOA activity is inhibited, with a critical period during the first 5 days of postnatal life but with more pronounced effects when MAOA inhibition is maintained throughout the first postnatal week.

Pharmacological blockade of MAOA activity: Evaluation of the present model and comparison with MAOA knockout mice

MAOs are key enzymes in the degradation pathway of monoamines. Two MAOs exist in the brain, MAOA and MAOB (for review, see Weyler et al., 1990). Although they are closely related in their gene structure (Shih, 1991), MAOA and MAOB differ in several characteristics: MAOA is abundant in noradrenergic neurons (Luque et al., 1995; Jahng et al., 1997), has a preferential affinity for 5-HT, and is selectively inhibited by clorgyline, whereas MAOB is abundant in serotoninergic neurons and glial cells, has a lower affinity for 5-HT, and is selectively inhibited by deprenyl. Compounds that inhibit MAOs exhibit antidepressant activity (for review, see Tipton, 1989). In rodents, developmental studies have shown that MAO activity in the brain appears early in ontogeny, by E15 (Bourgoin et al., 1977), with MAOA activity initially predominating over MAOB (Mantle et al., 1976). By P15, MAOA is maximal, whereas MAOB activity reaches 50% of adult values (Jourdikian et al., 1975).

In a transgenic mouse line characterized by the deletion of exons 2 and 3 of the gene encoding MAOA and resulting in the absence of measurable MAOA activity, we observed a peculiar developmental abnormality in S1, where layer IV cortical neurons and afferent thalamic fibers failed to organize in barrels (Cases et al., 1995, 1996). Similar, although less extensive, alterations were produced when the corresponding wild type mice (inbred strain C3H/HeJ) were treated with the MAOA inhibitor clorgyline (Cases et al., 1996). To generalize these findings, an important first step was to show that similar effects could be obtained in other mouse strains. In the present study, abnormalities in barrel formation were observed after MAOA inhibition in the OF1 mouse strain. We found that these alterations were similar to those observed in the C3H/HeJ mice. However, in parallel, unpublished studies, we observed variations of the effects of MAOA inhibition among different mouse strains. In F1 hybrids between the C57BL/6 and C3H/HeJ strains, clorgyline treatments from P0 to P7 induced only minor changes in the AS field, whereas treatment from P0 to P4 produced no visible cortical alterations (T. Vitalis and O. Cases, unpublished observations). Correspondingly, MAOA knockouts with a C57BL/6 genetic background, which were obtained by repeated back crossing, have some ill-defined barrels in the caudal PMBSF (I. Seif and P. Gaspar, unpublished observations). This suggests that, according to the mouse strain used, factors that modulate the levels or effects of 5-HT are differently regulated. Indeed, amounts of MAOs (Voitenko, 1992), tryptophan hydroxylase (Knapp et al., 1981; Daszuta et al., 1984; Kulikov et al., 1995), 5-HT receptors, and 5-HT transporter as well as the number of serotonergic raphe neurons (Daszuta and Portalier, 1985) appear to differ among inbred mouse strains.

The milder severity of alterations in clorgyline-treated mice compared with MAOA knockouts with identical genetic backgrounds could be due to incomplete inhibition of MAOA. Incomplete inhibition of MAOA might be particularly critical during specific periods, such as the perinatal period. Clorgyline is an irreversible inhibitor of MAOA, and the duration of its effects is linked to its elimination and the rate of synthesis of MAOA, with a replacement rate in MAO activity varying from 24 hours in rat or mouse pups (Nelson et al., 1979; Samsa et al., 1979) to 10–12 days in adult rats (Maitre et al., 1976). Present observations indicate that a partial recovery of MAOA activity occurs as soon as 8 hours after a single clorgyline administration at P3. Thus, although chronic administration of clorgyline every 8 hours resulted in near-complete inhibition of MAOA at P7, as reflected by the increased levels of brain 5-HT that mirrored the levels observed in the MAOA knockouts, there could be fluctuations in these levels. For instance, at P0, brain levels of 5-HT increased fourfold in pharmacologically treated vs. ninefold in MAOA knockouts, probably reflecting the difficulty of drug administrations during the perinatal period. A continuous mode of administration of clorgyline, such as that afforded by minipumps, would be needed to evaluate the importance of these fluctuations. A critical threshold of brain 5-HT might exist above which cortical abnormalities occur. Below such a level, compensatory mechanisms might be active: For instance, other neurotransmitters could antagonize the effects of 5-HT, or changes in number or affinity of 5-HT receptors and monoaminergic transporters could dampen the effects of 5-HT increase. Such compensations would become ineffective when the brain is overwhelmed with large amounts of 5-HT.

The present protocol is potentially flexible and could be applied to other useful experimental species, such as rats or felines, to determine whether similar effects of MAOA inhibition on the formation of cortical maps can be observed. The variability of effects observed between different mouse strains, however, is an indication that interspecies differences are to be expected.

Period sensitive to MAOA inhibition: Relationship to stages in barrel field development

The present pharmacological study, together with our previous observations in the MAOA knockout mice, allows us to narrow down the sensitive period during which

MAOA inhibition can alter the development of barrels. In the rodent trigeminal system, the formation of the cortical map and its differentiation into barrels results from a precisely timed sequence of events, which can be separated into three main epochs. The first period corresponds to the formation of a topographic map of the VB in the cortex. During fiber outgrowth, VB axons maintain a strictly ordered topography (Molnar and Blakemore, 1995; Catalano et al., 1996) that is in register with the peripheral topography initiated in the trigeminal nerve and is transmitted to the trigeminal nerve nuclei and to the VB (Erzurumlu and Killackey, 1983). None of these processes that occur during embryonic life are affected by MAOA inhibition. Indeed, clorgyline treatments during embryonic life caused no visible effects and did not increase significantly the postnatal effects of MAOA inhibition (E15–P7 compared with P0–P7 clorgyline treatments). Accordingly, in MAOA knockouts, inhibition of 5-HT synthesis during postnatal life (P0–P6) suffices to reverse the barrel field abnormalities (Cases et al., 1996). Furthermore, the topographic organization of the thalamocortical projection, revealed with anterograde tracers in adult MAOA knockouts, appeared to be normal (Cases et al., 1996).

The second major step is the formation of periphery-related clusters in S1. This process seems to be dictated by a tendency of thalamic terminal axons carrying information from a functional group of peripheral receptors (large vibrissa, sinus hair, or digits) to cluster together, first in layer VI, then in layer IV, where they induce the characteristic cellular, ring-like cytoarchitectonic differentiation (Rice and Van der Loos, 1977; Senft and Woolsey, 1991a,b; Agmon et al., 1993). These processes, which occur essentially during the first 4–5 days of postnatal life, appear to be most affected by the clorgyline treatments. Indeed, clorgyline treatments during the first 5 days of life sufficed to cause alterations in the barrel field, whereas clorgyline treatments after P4 caused no visible changes of the barrels. This time limit coincides with that disclosed for the effects of lesions of peripheral receptors (Woolsey and Wann, 1976; Belford and Killackey, 1980; Jeanmonod et al., 1981), indicating that the cytoarchitectonic differentiation of granular neurons in layer IV is an irreversible process once it has been initiated. The exact step that is disrupted by excess 5-HT during this 4-day period remains to be determined.

The third and last phase of barrel development extends probably until P21 and is characterized by the functional maturation of the barrels coinciding with an extensive collateral arborization of the thalamic axonal arbors within the confines of a given barrel (Agmon et al., 1993). A corresponding maturation of the cortical targets occurs with extensive dendritic remodeling: Formation of dendritic spines and synapses (White et al., 1997). The general result of these cellular events is growth in the size of individual barrels and in the total area of S1 (Rice and Van der Loos, 1977; Riddle et al., 1992). We could not detect a clear effect of clorgyline treatments between P4 and P7. However, the histological methods used in the present study do not allow us to monitor more subtle developmental events that could be affected by the excess of brain 5-HT, such as the fine topographic arrangement of thalamocortical afferents. For instance, early sensory deprivation or application of an NMDA-receptor antagonist to the cortex caused no cytoarchitectonic changes of the barrel field, although electrophysiological studies demonstrated the presence of topographically inappropriate thalamic projections (Fox, 1992; Fox et al., 1996).

An observation for which we do not yet have a clear interpretation is that barrel field changes were more important when MAOA inhibition was maintained until the end of the first postnatal week rather than just during the first 5 postnatal days. This difference could be interpreted as resulting from a delay in the cellular processes of barrel formation, which could still be reinitiated when MAOA inhibition ceases at P4 but not when it ceases at P7. However, in other experimental situations in which a delay in barrel formation was observed, such as that caused by 5-HT neurotoxins (Blue et al., 1991; Osterheld-Haas et al., 1994; Osterheld-Haas and Hornung, 1996) or protein malnutrition (Vongdokmai, 1980), a normal barrel field eventually formed, whereas the patterning of the barrel field remained abnormal after P0–P4 clorgyline treatments. The synergism of P4–P7 clorgyline treatments with the P0–P4 treatments could indicate that there are some later effects of 5-HT on barrel development but that these become apparent only when they are primed by an early effect during the initial stages of barrel development.

Gradients of changes in the barrel field

Barrel alterations in the representation of the whisker pad were not distributed uniformly: Effects were more marked in the rostral fields, where the small vibrissae are represented, than in the posterior field, where the large caudal vibrissae are represented. Indeed, barrel fusions were more frequent in the AS representation and in the rostral part of the PMBSF, where significant enlargements of "intact" individual barrels were also seen. Exceptions to this general trend were the largest and caudalmost barrels (α, β, γ, and δ), which were frequently fused.

Several hypotheses can be proposed to explain this phenomenon. The sequence of development of the face vibrissae proceeds from ocular to nasal, and this temporal sequence is replicated at least at the level of the trigeminal nerve and the brainstem (Erzurumlu and Killackey, 1983). A caudal-to-rostral sequence of emergence of periphery-related patterns has also been described in the somatosensory cortex. This can be seen in the acetylcholinesterase preparations of Schlaggar and O'Leary (1994), in which barrel-like patterning is visible in the PMBSF before it emerges in the AS. By using 5-HT immunostaining, which also reveals the thalamocortical afferents, Rhoades et al. (1990) described a clear caudal-to-rostral sequence of fiber clustering in S1. Later in development, boundary patterns of cortical glia (McCandlish et al., 1989) and markers of synaptogenesis (Stettler et al., 1996) were described as following a similar gradient of maturation. In this view, excess 5-HT would have more pronounced effects on the rostral, relatively immature thalamic fibers compared with the more mature caudal fibers, and the fact that we were not able to disrupt the caudalmost barrels, even when administering clorgyline before birth, could be due to insufficient MAOA inhibition during late embryonic and early postnatal life.

These gradients should also be considered in the context of a difference in the geometry and function of the peripheral receptors that are mapped in the caudal vs. the rostral parts of S1: The large vibrissae mapped in the PMBSF are more widely separate on the snout than the anterior sinus hair of the AS. Thus, large PMBSF vibrissae could be

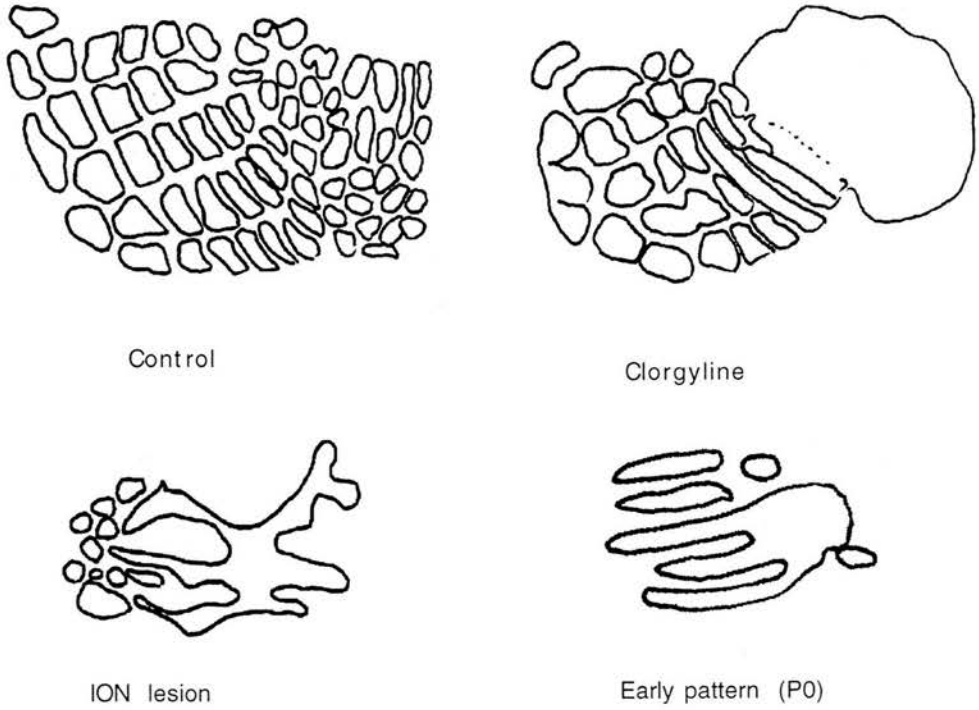

Fig. 11. Schematic representation of the barrel field (posteromedial barrel subfield [PMBSF] and anterior snout [AS]) pattern after MAOA inhibition compared with reported changes after infraorbital nerve transection (Killackey et al., 1994) and with described patterns of thalamocortical afferents in P0 rat pups (redrawn from Schlaggar and O'Leary, 1994).

expected to be functionally autonomous and to have asynchronous activity. This would provide a larger drive for segregation of afferents than in the case of the small AS vibrissae. If excess 5-HT antagonizes this process, then one could have more visible effects in the AS than in the PMBSF. This hypothesis derives from the general hypothesis that activity-dependent mechanisms are regulating the segregation of sensory afferents, following the principle that "cells that fire together wire together" (for review, see Shatz, 1990).

Effects of MAOA inhibition

It is important to consider whether the effects of clorgyline on barrel field development are due to a general effect on growth, because clorgyline administration caused a deficit in weight gain between P3 and P6. This is an unlikely explanation, however, because protein malnutrition in mice causes only a 2-day delay in the development of the barrels (Vongdokmai, 1980), and not a persistent absence of barrels as observed in this study. Despite our ignorance about the precise mechanism of 5-HT action in the developing somatosensory thalamocortical system, the developmental pattern of expression of 5-HT receptors in this system should be a good indication of the potential cellular targets of 5-HT.

In the cortex, pyramidal cells in layers II–III express functional 5-HT_2 receptors during development, and their activation reduces gap-junction coupling (Rörig and Sutor, 1996). Scattered cortical neurons have been shown to express the 5-HT_3 receptor gene (Tecott et al. 1995). However, it has not yet been determined whether layer IV neurons or glia express any 5-HT receptors during the critical period of barrel development.

On the other hand, developing VB thalamic fibers express both SERT (Lebrand et al., 1996) and the 5-HT_{1B} receptor subtype between E15 and P10 (Bennett-Clarke et al., 1993; Lebrand et al., unpublished observations). SERT causes 5-HT to accumulate in large excess in VB neurons when MAOA is inhibited (Cases et al., unpublished observations) and, thereby, could cause an abnormal development. Indeed, an abnormal tangential distribution of thalamocortical fibers in the clorgyline-treated mice was presently visualized with 5-HT immunocytochemistry. Excessive stimulation of the presynaptic 5-HT_{1B} receptor subtype might cause a complete inhibition of the excitatory neurotransmission in the thalamocortical circuit, interrupting any activity-dependent mechanism that could be responsible for the segregation of the thalamocortical axons. Alternatively, activation of the 5-HT_{1B} receptor subtype or internalization of 5-HT might also have a direct, trophic action on axonal growth that would mask the underlying segregation processes.

Indirect clues about the mechanisms underlying the effects of 5-HT may be drawn by comparing the effects of MAOA inhibition with those of different types of lesions. The fact that 5-HT has no instructive effects per se on barrel formation is demonstrated by the early lesions of the 5-HT system that cause no disruption in the general patterning of the barrel field (Blue et al., 1991; Bennett-Clarke et al., 1994; Osterheld-Haas et al., 1994). On the other hand, those studies suggest that 5-HT may have a trophic effect on thalamocortical and barrel development. In neonatal rat pups, 5,7-dihydroxytryptamine (5,7-DHT) or fenfluramine administration caused a decrease in the tangential area covered by individual barrels in the PMBSF (Bennett-Clarke et al., 1994, 1995), and a delay in the

laminar differentiation of layer IV was noted in 5,7-DHT-treated mice (Osterheld-Haas and Hornung, 1996). However, these findings are hampered by the possibility that 5,7-DHT could have a direct toxic effect on the developing thalamic neurons, because it may be taken up in these neurons by SERT.

5-HT could be acting as a modulator of peripheral influences derived from the periphery. Lesions of the infraorbital nerve (ION), the trigeminal branch that supplies the whisker pad, produced effects similar to that of MAOA inhibition, in that there was a loss of the characteristic thalamocortical clustering and a lack of cytoarchitectonic differentiation in layer IV. However, the pattern of PMBSF alterations resulting from such lesions differed: The deprived territory appeared atrophic and disorganized, with a main outline of the five barrel rows (Jensen and Killackey, 1987b; Killackey et al., 1994; Fig. 11). By contrast, clorgyline treatment during the sensitive period resulted in barrel fusions both within and across rows, with a general trend for hypertrophy, because there was an increase in the size of the trigeminal representation or of individual barrels. Furthermore, MAOA inhibition caused no visible alterations in the trigeminal nerve nucleus and VB, contrary to the effects of lesions (Durham and Woolsey, 1984; Killackey et al., 1994). These different patterns of alterations could indicate that peripheral lesions interrupt a trophic influence that originates from the peripheral receptors, whereas excess 5-HT does not. Anterograde transport of neurotrophic molecules from the periphery has been demonstrated recently in the chick developing visual system (Von Bartheld et al., 1996) and could well exist in the rodent somatosensory system, as suggested by recent observations (Chiaia et al., 1996; Wilkinson et al., 1997). In this respect, the effects of 5-HT may be viewed as being limited to the distalmost component of this ascending sensory pathway, which is the synaptic interaction of ingrowing terminals with their maturing cortical targets. Direct evidence derived from electrophysiological studies, pharmacology, single axonal reconstructions, and electron microscopy will be necessary to comprehend precisely what these effects are.

ACKNOWLEDGMENTS

We thank Peter Waldmeier (Research Department, Ciba-Geigy, Basel, Switzerland) for his pharmacological advice; Pascal Ezan and Katy Gillies for technical help; and Denis Lecren, Mark Rae, and B. McGrory for photographic and computer assistance. We also thank Jean-Pierre Hornung and Cecile Lebrand for helpful discussions.

LITERATURE CITED

Agmon, A., L.T. Yang, D.K. O'Dowd, and E.G. Jones (1993) Organized growth of thalamocortical axons from the deep tier of terminations into layer IV of developing mouse barrel cortex. J. Neurosci. *13:*5365–5382.

Belford, G.R. and H.P. Killackey (1980) The sensitive period in the development of the trigeminal system of the neonatal rat. J. Comp. Neurol. *193:*335–350.

Bennett-Clarke, C.A., M.J. Leslie, N.L. Chiaia, and R.W. Rhoades (1993) Serotonin 1B receptors in the developing somatosensory and visual cortices are located on thalamocortical axons. Proc. Natl. Acad. Sci. USA *90:*153–157.

Bennett-Clarke, C.A., M.J. Leslie, R.D. Lane, and R.W. Rhoades (1994) Effect of serotonin depletion on vibrissa-related patterns of thalamic afferents in the rat's somatosensory system. J. Neurosci. *14:*7594–7607.

Bennett-Clarke, C.A., R.D. Lane, and R.W. Rhoades (1995) Fenfluramine depletes serotonin from the developing cortex and alters thalamocortical organization. Brain Res. *702:*255–260.

Blue, M.E., R.S. Erzurumlu, and S. Jhaveri (1991) A comparison of pattern formation by thalamocortical and serotonergic afferents in the rat barrel field cortex. Cerebral Cortex *1:*380–389.

Bourgoin, S., F. Artaud, J. Adrien, F. Hery, J. Glowinski, and M. Hamon (1977) 5-Hydroxytryptamine catabolism in the rat brain during ontogenesis. J. Neurochem. *28:*415–422.

Cases, O., I. Seif, J. Grimsby, P. Gaspar, K. Chen, S. Pournin, U. Müller, M. Aguet, C. Babinet, J.C. Shih, and E. De Maeyer (1995) Aggressive behavior and altered amounts of brain serotonin and norepinephrine in mice lacking MAOA. Science *268:*1763–1766.

Cases, O., T. Vitalis, I. Seif, E. De Maeyer, C. Sotelo, and P. Gaspar (1996) Lack of barrels in the somatosensory cortex of monoamine oxidase A-deficient mice: Role of a serotonin excess during the critical period. Neuron *16:*297–307.

Catalano, S.M., R.T. Robertson, and H.P. Killackey (1996) Individual axon morphology and thalamocortical topography in developing rat somatosensory cortex. J. Comp. Neurol. *367:*36–53.

Chiaia, N.L., S.E. Fish, W.R. Bauer, C.A. Bennett-Clarke, and R.W. Rhoades (1992) Postnatal blockade of cortical activity by tetrodotoxin does not disrupt the formation of vibrissae-related patterns in the rat's somatosensory cortex. Dev. Brain Res. *66:*244–250.

Chiaia, N.L., S.E. Fish, W.R. Bauer, B.A. Figley, M. Eck, C.A. Bennett-Clarke, and R.W. Rhoades (1994) Effects of postnatal blockade of cortical activity with tetrodotoxin upon lesion-induced reorganization of vibrissae-related patterns in the somatosensory cortex of the rat. Dev. Brain Res. *79:*301–306.

Chiaia, N.L., C.A. Bennett-Clarke, R.S. Crissman, L. Zheng, M. Chen, and R.W. Rhoades (1996) Effect of neonatal axoplasmic transport attenuation in the infraorbital nerve on vibrissae-related patterns in the rat's brainstem, thalamus and cortex. Eur. J. Neurosci. *8:*1601–1612.

Consolazione, A., C. Milstein, B. Wright, and A.C. Cuello (1981) Immunocytochemical detection of serotonin with monoclonal antibodies. J. Histochem. Cytochem. *29:*1425–1430.

D'Amato, R., M.E. Blue, B.L. Largent, D.R. Lynch, D.J. Ledbetter, M.E. Molliver, and S.H. Snyder (1987) Ontogeny of the serotonergic projection to rat neocortex: Transient expression of a dense innervation to primary sensory areas. Proc. Natl. Acad. Sci. USA *84:*4322–4326.

Daszuta, A. and P. Portalier (1985) Distribution and quantification of 5-HT nerve cell bodies in the nucleus raphe dorsalis area of C57BL and BALBc mice. Relationship between anatomy and biochemistry. Brain Res. *360:*58–64

Daszuta, A., F. Hery, and M. Faudon (1984) In vitro 3H-serotonin (5-HT) synthesis and release in BALBc and C57BL mice. I. Terminal areas. Brain Res. Bull. *12:*559–563.

Durham, D. and T.A. Woolsey (1984) Effects of neonatal lesions on mouse central trigeminal pathways. J. Comp. Neurol. *223:*424–447.

Erzurumlu, R.S. and H.P. Killackey (1983) Development of order in the rat trigeminal system. J. Comp. Neurol. *213:*365–380.

Fox, K. (1992) A critical period for experience-dependent synaptic plasticity in rat barrel cortex. J. Neurosci. *12:*1826–1838.

Fox, K., B.L. Schlaggar, S. Glazewski, and D.D.M. O'Leary (1996) Glutamate receptor blockade at cortical synapses disrupts development of thalamocortical and columnar organization in somatosensory cortex. Proc. Natl. Acad. Sci. USA *93:*5584–5589.

Fujimiya, M., H. Kimura, and T. Maeda (1986) Postnatal development of serotonin nerve fibers in the somatosensory cortex of mice studied by immunohistochemistry. J. Comp. Neurol. *246:*191–201.

Green, A.R. and M.B.H. Youdim (1975) Effects of monoamine oxidase inhibition by clorgyline, deprenyl or tranylcypromine on 5-hydroxytryptamine concentrations in rat brain and hyperactivity following subsequent tryptophan administration. Br. J. Pharmacol. *55:*415–422.

Henderson, T.A., T.A. Woolsey, and M.F. Jacquin (1992) Infraorbital nerve blockade from birth does not disrupt central trigeminal pattern formation in the rat. Dev. Brain Res. *66:*146–152.

Iwasato, T., D.F. Chen, R.S. Erzurumlu, T. Sasaoka, and S. Tonegawa (1996) Disruption of whisker-specific patterns in the somatosensory cortex and subcortical areas of the rescued NMDAR1 knockout mice. Soc. Neurosci. Abstr. *22:*725.

Jahng, J.W., T.A. Houpt, T.C. Wessel, K. Chen, J.C. Shih, and T.H. Joh (1997) Localization of monoamine oxidase A and B mRNA in the rat brain by in situ hybridization. Synapse *25:*30–36

Jeanmonod, D., F.L. Rice, and H. Van der Loos (1981) Mouse somatosensory cortex: Alterations in the barrelfield following receptor injury at different early postnatal ages. Neuroscience *6:*1503–1535.

Jensen, K.F. and H.P. Killackey (1987a) Terminal arbors of axons projecting to the somatosensory cortex of the adult rat. I. The normal morphology of specific thalamocortical afferents. J. Neurosci. *7:*3529–3543.

Jensen, K.F. and H.P. Killackey (1987b) Terminal arbors of axons projecting to the somatosensory cortex of the adult rat. II. The altered morphology of thalamocortical afferents following neonatal infraorbital nerve cut. J. Neurosci. *7:*3544–3553.

Jourdikian, F., B. Tabakoff, and S.G.A. Alivisatos (1975) Ontogeny of multiple forms of monoamine oxidase in mouse brain. Brain Res. *93:*301–308.

Kema, I.P., A.M. Schellings, C.J. Hoppenbrouwers, H.M. Rutgers, E.G.E. de Vries, and F.A.J. Muskiet (1993) High performance liquid chromatographic profiling of tryptophan and related indoles in body fluids and tissues of carcinoid patients. Clin. Chim. Acta *221:*143–158.

Killackey, H.P., N.L. Chiaia, C.A. Bennett-Clarke, M. Eck, and R.W. Rhoades (1994) Peripheral influences on the size and organization of somatotopic representations in the fetal rat cortex. J. Neurosci. *14:*1496–1506.

Knapp, S., A.J. Mandell, P.V. Russo, A. Vitto, and K.D. Stewart (1981) Strain differences in kinetic and thermal stability of two mouse brain tryptophan hydroxylase activities. Brain Res. *230:*317–336.

Kulikov, A.V., E.Y. Kozlachkova, N.N. Kudryavstseva, and N.K. Popova (1995) Correlation between tryptophan hydroxylase activity in the brain and predisposition to pinch-induced catalepsy in mice. Pharmacol. Biochem. Behav. *50:*431–435.

Lebrand, C., O. Cases, C. Aldebrecht, A. Doye, C. Alvarez, S. El-Mestikawy, I. Seif, and P. Gaspar (1996) Transient uptake and storage of serotonin in developing thalamic neurons. Neuron *17:*823–835.

Li, Y., R.S. Erzurumlu, C. Chen, S. Jhaveri, and S. Tonegawa (1994) Whisker-related neuronal patterns fail to develop in the trigeminal brainstem nuclei of NMDAR1 knockout mice. Cell *76:*427–437.

Luque, J.M., S.W. Kwan, C.W. Abell, M. Da Prada, and J.D. Richards (1995) Cellular expression of mRNAs encoding monoamine oxidases A and B in the rat central nervous system. J. Comp. Neurol. *363:*665–680.

Maitre, L., A. Delini-Stula, and P.C. Waldemeier (1976) Relations between the degree of monoamine oxidase inhibition and some psychopharmacological responses to monoamine oxidase inhibitors in rat. In Monoamine Oxidase and its Inhibition, Ciba Foundation Symposium 39. Amsterdam: Elsevier, pp. 247–267.

Mantle, T.J., N.J. Garret, and K.F. Tipton (1976) The development of monoamine oxidase in rat liver and brain. FEBS Lett. *64:*227–230.

McCandlish, C., R.S. Waters, and N.G. Cooper (1989) Early development of the representation of the body surface in SI cortex barrel field in neonatal rats as demonstrated with peanut agglutinin binding: Evidence for differential development within the rat tunculus. Exp. Brain Res. *77:*425–431.

Molnar, Z. and C. Blakemore (1995) How do thalamic axons find their way to the cortex? Trends Neurosci. *9:*389–396.

Nelson, D.L., A. Herbert, J. Glowinski, and M. Hamon (1979) [3H]harmaline as a specific ligand of MAOA. II. Measurement of the rates of MAO A during ontogenesis in the rat brain. J. Neurochem. *32:*1829–1836.

Osterheld-Haas, M.C. and J.P. Hornung (1996) Laminar development of the mouse barrel cortex: Effects of neurotoxins against monoamines. Exp. Brain Res. *110:*183–195.

Osterheld-Haas, M.C., H. Van der Loos, and J.P. Hornung (1994) Monoaminergic afferents to cortex modulate structural plasticity in the barrelfield of the mouse. Dev. Brain Res. *77:*189–202.

Rhoades, R.W., C.A. Bennett-Clarke, N.L. Chiaia, F.A. White, G.J. McDonald, J.H. Haring, and M.F. Jacquin (1990) Development and lesion induced reorganization of the cortical representation of the rat's body surface as revealed by immunochemistry for serotonin. J. Comp. Neurol. *293:*190–207.

Rhoades, R.W., C.A. Bennett-Clarke, M.-Y. Shi, and R.D. Mooney (1994) Effects of 5-HT on thalamocortical synaptic transmission in the developing rat. J. Neurophysiol. *72:*2438–2450.

Rice, F.L. and H. Van der Loos (1977) Development of the barrels and barrel field in the somatosensory cortex of the mouse. J. Comp. Neurol. *171:*545–560.

Riddle, D., A. Richards, F. Zsuppan, and D. Purves (1992) Growth of the rat somatic sensory cortex and its constituent parts during postnatal development. J. Neurosci. *12:*3509–3524.

Rörig, B. and B. Sutor (1996) Serotonin regulates gap junction coupling in the developing rat somatosensory cortex. Eur. J. Neurosci. *15:*7386–7400.

Samsa, J.M., P.C. Baker, and K.M. Hoff (1979) Monoamine oxidase inhibition and recovery in the mouse brain at various ages after birth. Biol. Neonate *35:*249–254.

Schlaggar, B.L. and D.D.M. O'Leary (1994) Early development of the somatotopic map in rat somatosensory cortex. J. Comp. Neurol. *346:*80–96.

Senft, S.L. and T.A. Woolsey (1991a) Growth of thalamic afferents into mouse barrel cortex. Cerebral Cortex *1:*308–335.

Senft, S.L. and T.A. Woolsey (1991b) Computer-aided analyses of thalamocortical afferent ingrowth. Cerebral Cortex *1:*336–347.

Shatz, C.J. (1990) Impulse activity and the patterning of connections during CNS development. Neuron *5:*745–756.

Shih, J.C. (1991) Molecular basis of human MAO A and B. Neuropsychopharmacology *4:*1–7.

Sleight, A.J., C.A. Marsden, K.F. Martin, and M.G. Palfreyman (1988) Relationship between extracellular 5-hydroxytryptamine and behaviour following monoamine oxidase inhibition and L-tryptophan. Br. J. Pharmacol. *93:*303–310.

Stettler, O., B. Tavitian, and K.L. Moya (1996) Differential synaptic vesicle protein expression in the barrel field of developing cortex. J. Comp. Neurol. *375:*321–332.

Tecott, L., S. Shtrom, and D. Julius (1995) Expression of a serotonin-gated ion channel in embryonic neural and nonneural tissues. Mol. Cell. Neurosci. *6:*43–55.

Tipton, K.F. (1989) Monoamine oxidase inhibitors as antidepressants. In K.F. Tipton and M.B.H. Youdim (eds): Biochemical and Pharmacological Aspects of Depression. London: Taylor and Francis, pp. 1–24.

Van der Loos, H. and T.A. Woolsey (1973) Somatosensory cortex: Structural alterations following early injury to sense organs. Science *179:*395–398.

Voitenko, N.N. (1992) Age changes in brain monoamine oxidase in mice from four lines. Voprosoy Meditsinskoi Khimii. *38:*32–35.

Von Bartheld, C.S., M.R. Byers, R. Williams, and M. Bothwell (1996) Anterograde transport of neurotrophins and axodendritic transfer in the developing visual system. Nature *379:*830–833.

Vongdokmai, R. (1980) Effect of protein malnutrition on development of mouse cortical barrels. J. Comp. Neurol. *191:*283–294.

Welker, E. and H. Van der Loos (1986) Quantitative correlation between barrel-field size and the sensory innervation of the whiskerpad: A comparative study of six strains of mice bred for different patterns of mystacial vibrissae. J. Neurosci. *6:*3355–3373.

Welker, E., M. Armstrong-James, G. Bronchti, W. Ourednik, F. Gheorghita-Baechler, R. Dubois, D.L. Guernsey, H. Van der Loos, and P.E. Neumann (1996) Altered sensory processing in the somatosensory cortex of the mouse mutant barrelless. Science *271:*1864–1867.

Weyler, W., Y.P. Hsu, and X.O. Breakefield (1990) Biochemistry and genetics of monoamine oxidase. Pharmacol. Ther. *47:*391–417.

Whitaker-Azmitia, P.M., X. Zhang, and C. Clarke (1994) Effects of gestational exposure to monoamine oxidase inhibitors in rats: Preliminary behavioral and neurochemical studies. Neuropsychopharmacology *11:*125–132.

White, E.L., L. Weinfeld, and D.L. Lev (1997) A survey of morphogenesis during the early postnatal period in PMBSF barrels of mouse Sm1 cortex with emphasis on barrel D4. Somatosens. Motor Res. *14:*34–55.

Wilkinson, G.A., I. Farinas, C. Backus, C.K. Yoshida, and L.F. Reichardt (1997) Neurotrophin-3 is a survival factor in vivo for early mouse trigeminal neurons. J. Neurosci. *16:*7661–7669.

Wong-Riley, M.T.T. and C. Welt (1980) Histochemical changes in cytochrome oxidase of cortical barrels after vibrissal removal in neonatal and adult mice. Proc. Natl. Acad. Sci. USA *77:*2333–2337.

Woolsey, T. and H. Van der Loos (1970) The structural organization of layer IV in the somatosensory region (S1) of mouse cerebral cortex. Brain Res. *17:*205–242.

Woolsey, T.A. and J.R. Wann (1976) Areal changes in mouse cortical barrels following vibrissal damage at different postnatal ages. J. Comp. Neurol. *170:*53–66.

Plasma Membrane Transporters of Serotonin, Dopamine, and Norepinephrine Mediate Serotonin Accumulation in Atypical Locations in the Developing Brain of Monoamine Oxidase A Knock-Outs

Olivier Cases,[1] Cecile Lebrand,[2] Bruno Giros,[3] Tania Vitalis,[1] Edward De Maeyer,[4] Marc G. Caron,[5] David J. Price,[1] Patricia Gaspar,[2] and Isabelle Seif[4]

[1]Department of Physiology, Medical School, Teviot Place, Edinburgh EH8 9AG, Scotland, [2]Unité 106 et [3]Unité 288, Institut National de la Santé et de la Recherche Médicale, Hôpital de la Pitié-Salpêtrière, 75651 Paris Cedex 13, France, [4]Centre National de la Recherche Scientifique Unité Mixte de Recherche 146, Institut Curie, Bâtiment 110, 91405 Orsay Cedex, France, and [5]Department of Cellular Biology and Medicine, Duke University Center, Durham, North Carolina 27710

Genetic loss or pharmacological inhibition of monoamine oxidase A (MAOA) in mice leads to a large increase in whole-brain levels of serotonin (5-HT). Excess 5-HT in mouse neonates prevents the normal barrel-like clustering of thalamic axons in the somatosensory cortex. Projection fields of other neuron populations may develop abnormally. In the present study, we have analyzed the localization of 5-HT immunolabeling in the developing brain of MAOA knock-out mice. We show numerous atypical locations of 5-HT during embryonic and postnatal development. Catecholaminergic cells of the substantia nigra, ventral tegmental area, hypothalamus, and locus ceruleus display transient 5-HT immunoreactivity. Pharmacological treatments inhibiting specific monoamine plasma membrane transporters and genetic crosses with mice lacking the dopamine plasma membrane transporter show that the accumulation of 5-HT in these catecholaminergic cells is attributable to 5-HT uptake via the dopamine or the norepinephrine plasma membrane transporter. In the telencephalon, transient 5-HT immunolabeling is observed in neurons in the CA1 and CA3 fields of the hippocampus, the central amygdala, the indusium griseum, and the deep layers of the anterior cingulate and retrosplenial cortices. In the diencephalon, primary sensory nuclei, as well as the mediodorsal, centrolateral, oval paracentral, submedial, posterior, and lateral posterior thalamic nuclei, are transiently 5-HT immunolabeled. The cortical projections of these thalamic nuclei are also labeled. In the brainstem, neurons in the lateral superior olivary nucleus and the anteroventral cochlear nucleus are transiently 5-HT immunolabeled. None of these structures appear to express the monoamine biosynthetic enzyme L-aromatic amino acid decarboxylase. The administration of monoamine plasma membrane transporter inhibitors indicates that the 5-HT immunolabeling in these structures is attributable to an uptake of 5-HT by the 5-HT plasma membrane transporter. This points to neuron populations that form highly precise projection maps that could be affected by 5-HT during specific developmental stages.

Key words: monoamine oxidase; serotonin; serotonin transporter; dopamine transporter; norepinephrine transporter; brain development

Serotonin (5-HT) has been shown to modulate brain developmental events such as neural crest migration (Moiseiwitsch and Lauder, 1995), cortical neuronal differentiation (Ladvas et al., 1997), and the refinement of thalamocortical connections (Gu and Singer, 1995; Cases et al., 1996). We recently demonstrated that mice that cannot normally degrade 5-HT because of a genetic lack of monoamine oxidase A (MAOA) have greatly enhanced levels of 5-HT in the brain during early postnatal life (Cases et al., 1995) and display an abnormal development of the primary somatosensory cortex in which the barrel-like clustering of neurons and thalamic axons fails to occur (Cases et al., 1996). This can be prevented by reducing 5-HT levels in MAOA knock-outs during an early postnatal developmental period (Cases et al., 1996). Similarly, an abnormal development of the barrel field can be reproduced in wild-type mice by inhibiting MAOA pharmacologically during the same critical period (Cases et al., 1996; Vitalis et al., 1998). Interestingly, during this same critical period, somatosensory thalamic neurons that instruct the formation of the cortical barrels transiently express serotonergic markers such as the 5-HT_{1B} receptor (Bennett-Clarke et al., 1993), the 5-HT plasma membrane transporter SERT, and the vesicular monoamine transporter VMAT2 (Lebrand et al., 1996). The presence of these transporters allows an active internalization of 5-HT from the extracellular space into presynaptic terminals and its storage in vesicles (Lebrand et al., 1996). Thus, although somatosensory thalamic neurons do not produce 5-HT, they appear to transiently contain the amine. This phenomenon is amplified when the degradation of 5-HT is prevented by MAOA inhibitors (D'Amato et al., 1987; Lebrand et al., 1996; Vitalis et al., 1998) and is best observed

Received March 23, 1998; revised June 8, 1998; accepted June 10, 1998.

This work was funded by the European Commission (BMH4 CT97–2412 and Biotech Bio4CT-965048), the University of Edinburgh, the Institut National de la Santé et de la Recherche Médicale, the Centre National de la Recherche Scientifique, and the Curie Institute. We thank Pascal Ezan and Vincent Martinez for technical help, Denis Lecren for photographic assistance, and Diana Haranger for animal care.

Correspondence should be addressed to Olivier Cases, Department of Physiology, Medical School, Teviot Place, Edinburgh, EH8 9AG, Scotland.

in MAOA knock-outs. Indeed, this phenomenon was first strongly suggested by observations in MAOA knock-outs that showed unambiguously the transient presence of 5-HT in thalamic neurons (Lebrand et al., 1996).

As first reported here in detail, MAOA knock-outs have been a most powerful tool to identify neuronal populations in which 5-HT is internalized during development. We have determined whether each suspected case of 5-HT internalization is attributable to an heterologous expression of SERT or to a cross-binding to other monoamine plasma membrane transporters. Our previous immunocytochemical localization of 5-HT in MAOA knock-outs (Cases et al., 1995) in 8-d-old pups had suggested the possibility of an internalization by the catecholaminergic transporters, because 5-HT was observed in the brainstem catecholaminergic neurons (Cases et al., 1995). Monoaminergic plasma membrane transporters specific for 5-HT, dopamine, or norepinephrine belong to the family of Na^+/Cl^--dependent transporters and display a significant degree of amino acid identity (Amara and Kuhar, 1993; Giros and Caron, 1993; Nelson and Lill, 1994), but no clear evidence of significant cross-reactivity of catecholaminergic transporters with 5-HT *in vivo* has ever been reported.

We report here transient and abnormal 5-HT immunolabeling in a number of neuronal structures in the cerebral cortex, the hippocampal formation, the amygdala, the thalamus, the hypothalamus, and the brainstem. In most of the nonaminergic structures, specific inhibitors of SERT abolished the 5-HT immunolabeling. Indeed, these locations coincide with the transient expression pattern of SERT (Hansson et al., 1998; Lebrand et al., 1998). Interestingly, 5-HT immunolabeling of each of these structures has a developmental timing, suggesting that they may be sensitive to the effects of 5-HT during these specific periods. Furthermore, we analyzed in greater detail the abnormal localization of 5-HT in catecholaminergic structures. Using pharmacological experiments and genetic crosses with mice lacking the dopamine plasma membrane transporter (Giros et al., 1996), we determined that 5-HT uptake in catecholaminergic neurons can be entirely accounted for by the dopamine plasma membrane transporter (DAT) or the norepinephrine plasma membrane transporter (NET).

MATERIALS AND METHODS

Animals. MAOA knock-outs and their C3H/He controls were as described in Cases et al. (1995). MAOA–DAT double knock-outs and their diverse controls were obtained in the F2 progeny from crosses between the MAOA knock-outs and DAT knock-outs (Giros et al., 1996) having a mixed genetic background (129/Sv, C57BL/6, and DBA/2). MAOA knock-outs were analyzed at embryonic day 12 (E12), E15, E16, E17, E18, E19 (the day of the vaginal plug was counted as E1), postnatal day 0 (P0), P4, P7, P10, P15, P21, P28, P60, and 2–6 months (the day of birth was counted as P0). MAOA–DAT double knock-outs were analyzed at E16, E19, P0, P4, and P7. All mice lacking DAT were given hydrated food pellets on the cage floor, and it was not necessary to transfer offspring to foster mothers. Animal procedures were conducted in strict compliance with approved institutional protocols and in accordance with the provisions for animal care and use described in the *Scientific Procedures on Living Animals ACT 1986*.

Immunocytochemistry. 5-HT immunocytochemistry was performed using a rat anti-5-HT monoclonal antibody (1:50; Harlan, Sussex, UK). The specificity of this antibody has been demonstrated previously (Consolazione et al., 1981; Lebrand et al., 1996). Rabbit polyclonal antibodies were used for detection of tyrosine hydroxylase (TH) (1:5000; gift from A. Vigny) and L-aromatic amino acid decarboxylase (AADC) (1:1000; Protos Biotech) (Joh and Ross, 1983).

Embryonic and postnatal mice were transcardially perfused with saline, followed by 4% paraformaldehyde in 0.1 M phosphate buffer, pH 7.2. Whole embryos or brains were post-fixed 1–5 d in the same fixative and cryoprotected in 30% sucrose in 0.1 M phosphate buffer. Serial coronal sections (40 μm) were cut on a freezing microtome and immediately processed for 5-HT, TH, or AADC immunocytochemistry as described previously (Cases et al., 1996). In brief, sections were washed in 0.1 M phosphate buffer and incubated 1 hr in PBS+ (0.1 M PBS with 0.2% gelatin and 0.25% Triton X-100). Sections were incubated with the primary antibodies for 24 hr at 4°C. Then, sections were washed in PBS+ and incubated with secondary antibodies (biotinylated goat anti-rat for 5-HT immunocytochemistry or biotinylated swine anti-rabbit for AADC immunocytochemistry) (1:200; Dako, High Wycombe, UK) for 2 hr at room temperature. Sections were washed in PBS+ and incubated with a streptavidin–biotin–peroxidase complex (1:200; Amersham, Arlington Heights, IL) for 2 hr at room temperature. Sections were then reacted with a solution containing 0.02% diaminobenzidine, 0.6% nickel ammonium sulfate (Carlo Erba), and 0.003% H_2O_2 in 0.05 M Tris buffer, pH 7.6. Sections were mounted on 3-aminopropyltriethoxysilane-coated slides, dehydrated, and coverslipped in DePeX.

Some coronal sections were counterstained with a solution containing 1% methyl green in 70% ethanol.

Double 5-HT and TH immunofluorescence. Frozen cryostat sections (20 μm) were incubated in the 5-HT antiserum (clone YC5/45) (1:1000 of a 5× concentrated batch) mixed with the TH antiserum (1:5000) overnight at room temperature. After rinsing in PBS+, sections were incubated with rhodamine-conjugated anti-rat (1:100; Amersham) and fluorescein-conjugated anti-rabbit (1:70; Silenus, Hawthorne, Australia) for 2 hr at room temperature. Sections were rinsed in PBS for 30 min and mounted with glycerol–PBS (3:1).

In situ *hybridization.* To prepare the SERT cRNA probes, a cDNA fragment corresponding to nucleotides 1510–2009 of the transcript (Blakely et al., 1991) was amplified by PCR and subcloned into pBluescript SKII (Stratagene, La Jolla, CA). The plasmid was linearized with *Bam*HI (Boehringer Mannheim, Indianapolis, IN) for antisense RNA synthesis by T7 polymerase (Pharmacia, Piscataway, NJ) and with *Eco*RI (Boehringer Mannheim) for sense RNA synthesis by T3 polymerase (Boehringer Mannheim).

The *in vitro* transcription was performed using a kit from Promega (Madison, WI), and probes were labeled with ^{35}S-UTP (>1000 Ci/mmol; Amersham) as described by Fontaine and Changeux (1989). *In situ* hybridization for cRNA probes was performed using fresh frozen brain sections (15 μm thick). Tissue sections were post-fixed for 15 min in 4% paraformaldehyde, washed in PBS, acetylated, washed in PBS, dehydrated, and air-dried. Sections were covered with hybridization buffer containing 5×10^4 cpm/μl ^{35}S-SERT (12.5 μl/section) and then incubated overnight in a humid chamber at 48°C. Washes were then performed as described previously (Fontaine and Changeux, 1989). Autoradiograms were obtained by apposing the sections to β-max hyperfilms (Amersham) for 4 d. For histological analyses, the slides were dipped in photographic emulsion (NTB2; Eastman Kodak, Rochester, NY) and exposed for ~10 d. After development of the emulsion, the sections were counterstained with cresyl violet.

Pharmacological treatments. Drugs and vehicle (0.9% saline) were administered subcutaneously in P6–P7 pups. Four main administration protocols were used: (1) two injections at a 14 hr interval; (2) three injections at 4 hr intervals; (3) three injections at 10 hr intervals; and (4) seven injections at 4 hr intervals. All animals were killed 4–6 hr after the last injection. The drugs used were fluoxetine (10 or 30 mg/kg; Eli Lilly), paroxetine (50 mg/kg; Beecham), GBR12783 (10 or 30 mg/kg; gift of Dr. J. Constentin, Unité de Neuropsychopharmacology, Saint Etiénne de Rouvray, France), nisoxetine (10 or 30 mg/kg; Research Biochemicals, Natick, MA), or NO-711 (50 mg/kg; Research Biochemicals). Fluoxetine was also administered intraperitoneally to pregnant dams (30 mg/kg) during the E18–E19 developmental period. Embryos were removed by cesarean section and perfused 4 hr after the last injection.

RESULTS

Unusual localization of 5-HT-containing neurons in MAOA knock-outs

The immunocytochemical localization of 5-HT was performed in parallel in MAOA-deficient and normal mice during embryonic and postnatal development. In the following, we will focus our description on the localization of 5-HT-labeled structures in MAOA knock-outs that was not observed in normal mice. The

Table 1. Locations of nonraphe 5-HT-positive neurons in the brain of MAOA knock-outs

	E15 $n = 4$	E18 $n = 5$	P0 $n = 6$	P7 $n = 6$	P10 $n = 2$	P15 $n = 1$	P21 $n = 3$	Adult $n = 2$
Telencephalon								
Cingulate cortex (Cg1 + Cg2)	−	+++2	++2	++2	++2	−	−	−
Retrosplenial cortex	−	+++2	+2	−	−	−	−	−
Indusium griseum	−	+++3	+2	−	−	−	−	−
Hippocampus (CA1 + CA3)	−	+++3	+2	−	−	−	−	−
Amygdala	++1	+++1	+++1	−	−	−	−	−
Diencephalon								
Hypothalamic nuclei								
Periventricular preoptic	++2	++2	−	−	−	−	−	−
Suprachiasmatic preoptic	++2	++3	−	−	−	−	−	−
Suprachiasmatic	−	−	−	+1	++2	++2	+2	−
Paraventricular	++3	−	−	−	−	−	−	−
Arcuate	++2	++2	−	++1	++1	++1	−	−
Thalamic nuclei								
Mediodorsal	−	+2	+2	+++3	++3	−	−	−
Centrolateral	−	−	++2	+++2	++2	−	−	−
Oval paracentral	−	−	+3	+++3	++3	−	−	−
Submedial	−	++3	++3	++3	+3	−	−	−
Ventroposteromedial (VPM)	−	+++3	+++3	+++3	++3	−	−	−
Ventroposterolateral (VPL)	++2	+++3	+++3	+++3	++3	+2	−	−
VPM, parvicellular	+2	++3	+++3	++3	−	−	−	−
VPL, parvicellular	+2	++3	+++3	++3	−	−	−	−
Posterior	−	−	+2	++2	+2	−	−	−
Lateral posterior	−	−	−	+++2	++2	−	−	−
Dorsal lateral geniculate	++3	+++3	+++3	+++3	++3	+3	−	−
Medial geniculate ventral	−	+++3	+++3	+++3	++3	−	−	−
Medial geniculate medial	−	−	++2	+++3	++3	−	−	−
Medial geniculate dorsal	−	−	++2	+++3	++3	−	−	−
Brainstem								
Substantia nigra (A9)	++3	+++3	+++3	+++3	+++3	++3	++3	−
Ventral tegmental area (A10)	++3	+++3	+++3	+++3	+++3	+3	+3	−
Retrorubral field (A8)	++3	+++3	+++3	+++3	+++3	+3	+3	−
Lateral superior olivary n.	−	+2	++3	++3	−	−	−	−
Anteroventral cochlear n.	−	++2	−	−	−	−	−	−
Subcoeruleus (A5)	++3	++3	+++3	+++3	++3	++3	−	−
Locus coeruleus (A6/7)	+++3	+++3	+++3	+++3	+++3	+++3	++3	−

Staining intensity of neurons at prenatal and postnatal ages according to locations in the brain.
Cell staining: − none; + light staining; ++ moderate staining; +++ heavy staining.
Cell number: 1, few scattered cells; 2, moderate number of cells (10 to 50%); 3, majority of cells.

general distribution of these labeled structures is given in Tables 1 and 2. The nomenclature is taken from Schambra et al. (1992) and Paxinos et al. (1991) for embryonic stages and from Franklin and Paxinos (1994) for postnatal stages. For the normal distribution of 5-HT, see the descriptions of Steinbusch (1981) for adult rats and Lidov and Molliver (1982a,b) and Wallace and Lauder (1983) for developing rats and mice. Throughout the developing brain of MAOA knock-outs, the innervation originating in the raphe displayed a much increased 5-HT immunoreactivity, suggesting that extracellular levels of 5-HT could also be higher than in normal mice.

5-HT in catecholaminergic cell groups

As early as E12 or E15 and at least until P15 or P21, neuronal cell bodies in the substantia nigra (SN) (cell group A9), the ventral tegmental area (VTA) (A10), the retrorubral field (A8), the locus ceruleus (LC) (A6–A7), and the locus subceruleus (A5) displayed 5-HT immunolabeling in MAOA knock-outs (Table 1). In LC, cells were already intensely labeled at E12. Dendritic trees were not apparent in these neuronal populations. Double immunolabeling with antibodies to the catecholamine synthesizing enzyme TH showed that these 5-HT-containing neurons were catecholaminergic. The varicose 5-HT-positive terminal network contained no TH immunolabeling (Fig. 1). Double immunolabeling also showed that most of the TH-positive neurons contained detectable levels of 5-HT in MAOA knock-out embryos and pups, indicating that this immunolabeling was not limited to specific subpopulations of the A5–A10 catecholamine cell groups. It persisted until P28 in the dopaminergic A8–A10 cell groups, whereas it disappeared between P21 and P28 in the noradrenergic A5–A7 cell groups.

In contrast, rostral catecholaminergic cell groups were not 5-HT

Table 2. Locations of nonaminergic 5-HT-positive fibers in the brain of MAOA knock-outs

	E15 $n = 4$	E18 $n = 5$	P0 $n = 6$	P7 $n = 6$	P10 $n = 2$	P15 $n = 1$
Orbital cortex	*a*	*a*	−	+++	++	−
Gustatory cortex	*a*	*a*	+++	+++	++	−
Visceral cortex	*a*	*a*	+++	+++	++	−
Somatosensory cortex	*a*	*a*	+++	+++	++	−
Auditory cortex	*a*	*a*	+++	+++	++	−
Visual cortex	*a*	*a*	+++	+++	++	−
Thalamocortical tract	++	+++	+++	+++	++	−
Fimbria/Fornix	++	++	+	−	−	−
Ventral hippocampal commissure	++	++	+	−	−	−
Ventral fornix	++	++	−	−	−	−
Optic chiasm and tract	+++	+++	+++	++	+	−
Superior colliculus	−	++	+++	+++	+++	−
Inferior colliculus	−	−	+	++	−	−
Trigeminal tract	++	++	−	−	−	−

Staining intensity of fibers at prenatal and postnatal ages according to locations in the brain.
Fiber staining: − none; + light staining; ++ moderate staining; +++ heavy staining.
[a] Before birth, thalamocortical axons are still confined to the subplate.

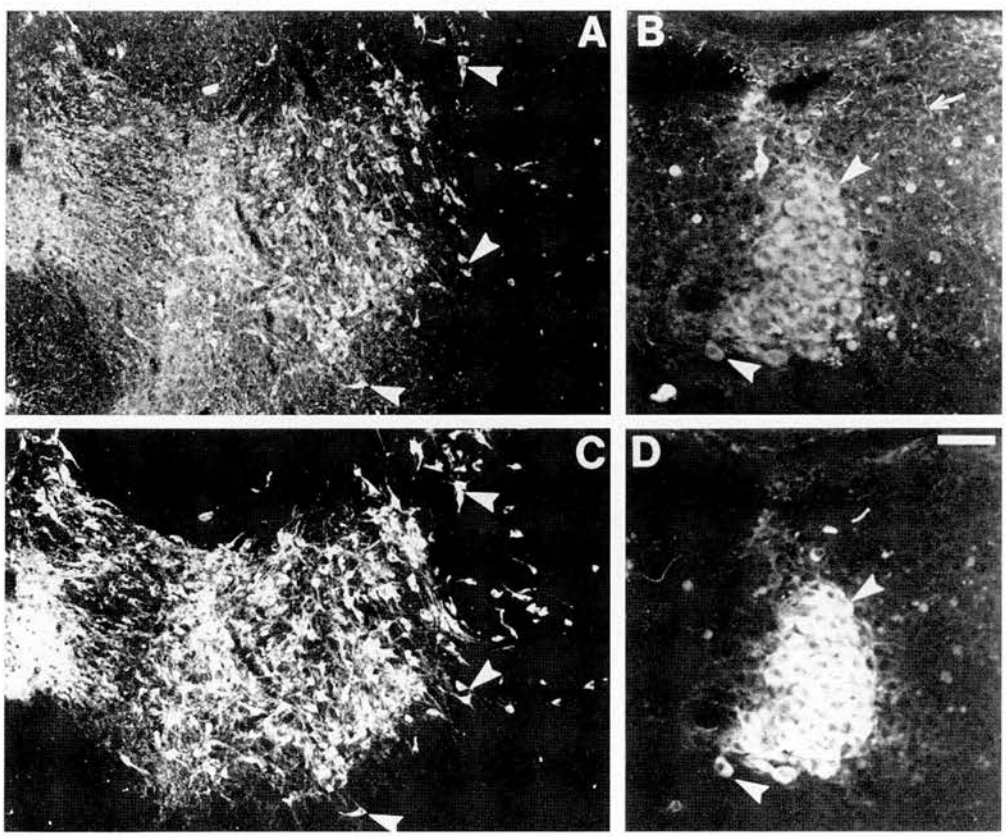

Figure 1. Catecholaminergic neurons accumulate 5-HT in P7 MAOA knock-outs. Coronal section through the SN–VTA complex (*A*, *C*) and the LC (*B*, *D*) were double immunostained with antibodies to 5-HT (*A*, *B*) and TH (*C*, *D*). As indicated by the *arrowheads*, almost all TH-positive neurons contain 5-HT immunolabeling. The varicose 5-HT-positive terminal network contains no TH immunolabeling (*arrow*). Scale bar (in *D*): *A*, *C*, 140 μm; *B*, *D*, 50 μm.

immunolabeled or lightly 5-HT immunolabeled. No 5-HT-containing neurons were observed in the olfactory bulb, whereas hypothalamic catecholaminergic cells showed moderate 5-HT immunolabeling during shorter developmental times than in the brainstem. Thus, 5-HT-containing neurons were observed in the periventricular preoptic (PVPO) and suprachiasmatic preoptic (SPO) nuclei, the paraventricular nucleus (PAVH), and the arcuate nucleus (Arc) primarily during late embryonic life with a transient upsurge for a few neurons in the Arc between P7 and P15 (Table 1).

5-HT in classically nonmonoaminergic cell groups

Telencephalon

In normal embryos and pups, we did not observe 5-HT-immunolabeled cell bodies in the telencephalon (Fig. 2*A*,*C*). In contrast, MAOA knock-out embryos and pups displayed 5-HT-containing neurons in cortical, hippocampal, or amygdaloid areas.

By E18, 5-HT-containing neurons were observed in the anterior cingulate cortex (ACG) in both its supra and pregenual parts

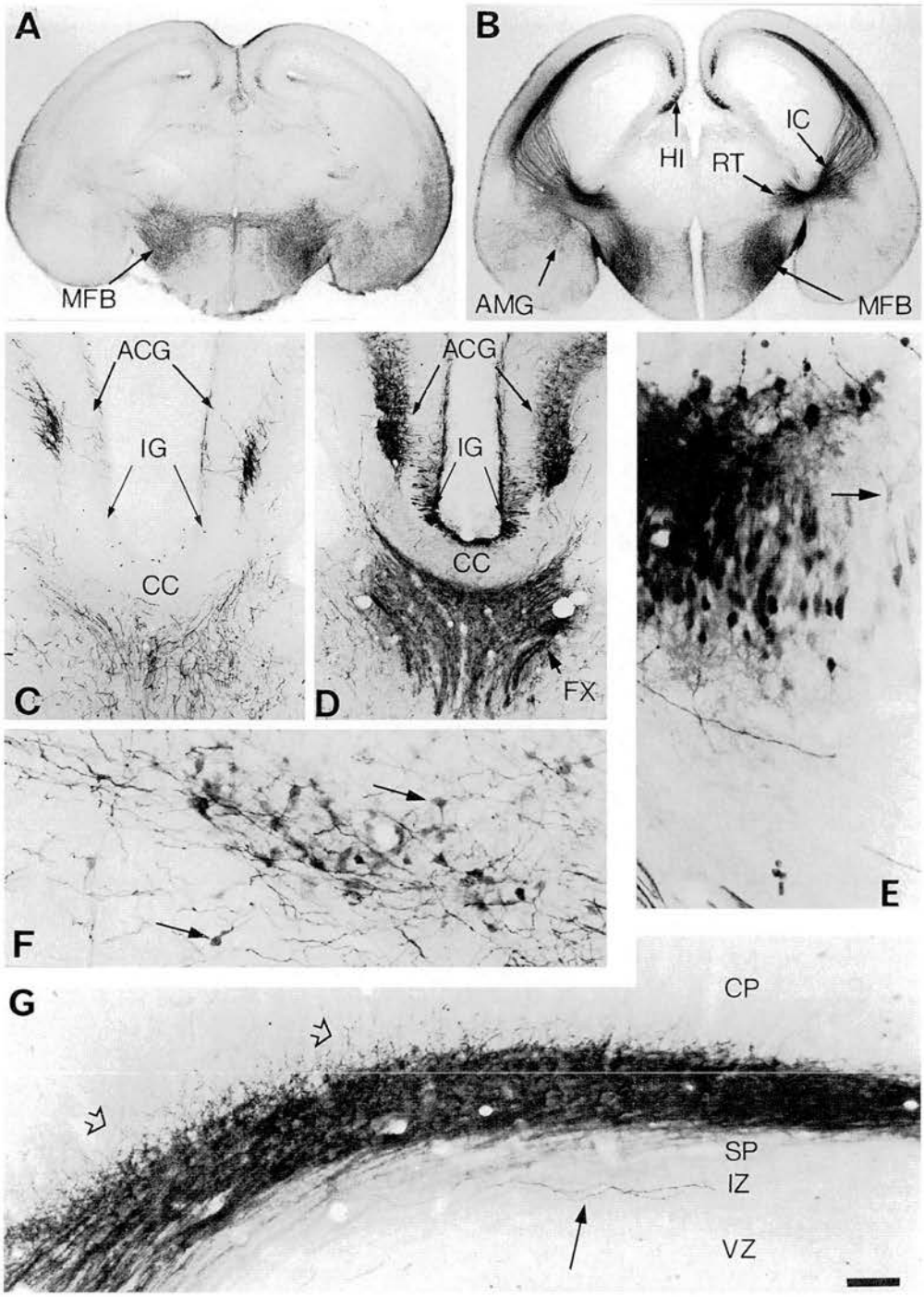

Figure 2. Atypical locations of 5-HT accumulation in the telencephalon of E18 MAOA knock-outs. Coronal brain sections are shown for controls (*A*, *C*) and MAOA knock-outs (*B*, *D–G*). *A*, In controls, 5-HT-immunostained fibers are primarily observed in the medial forebrain bundle (*MFB*). *B*, In MAOA knock-outs, 5-HT immunostaining of the MFB is increased, and a dense 5-HT immunolabeling is visible in the nucleus reticularis (*RT*), the thalamocortical fibers in the internal capsule (*IC*), the hippocampus (*HI*), and the amygdala (*AMG*). A higher magnification of the medial cortical area is shown in *C* and *D* at a more rostral level through the corpus callosum (*CC*), anterior cingulate cortex (*ACG*), and indusium griseum (*IG*). *C*, In controls, 5-HT immunoreactivity is only observed in terminal fibers or fiber tracts in the septum and ACG; the 5-HT-positive fibers in ACG form a bilaminar pattern in layer I and in the deep cortical layers. *D*, In MAOA knock-outs, 5-HT-positive fibers are more intensely stained, and additional labeling is visible in the fornix (*FX*) and in neuronal cell bodies in ACG and IG. *E*, A closer view of the 5-HT-immunolabeled cell bodies in the hippocampus reveals that these neurons have the morphological aspect of the principal pyramidal cells. *Arrow* indicates a neuron with a clear labeling of the dendritic tree. *F*, A closer view of the 5-HT immunolabeled neurons in the central nucleus of the amygdala. *Arrows* indicate neurons having a typical ovoid shape. *G*, Higher magnification of the 5-HT-positive thalamocortical fibers as they reach the cortical primordium. A dense network of fibers (fiber tracts and varicose fibers) is observed in the subplate (*SP*), with some fibers (*open arrows*) starting to penetrate in the cortical plate (*CP*). In contrast, a few long varicose fibers (*arrow*), probably representing afferents from the raphe, run in the intermediate zone (*IZ*). Only varicose fibers in SP and IZ were 5-HT immunoreactive in control mice, and this staining was much less intense than in MAOA knock-outs. *VZ*, Ventricular zone. Scale bar (in *G*): *A*, *B*, 625 μm; *C*, *D*, 150 μm; *E*, 27 μm; *F*, 40 μm; *G*, 33 μm.

(Fig. 2*B*,*D*) and in the granular (RSG) and agranular (RSA) retrosplenial cortex (Table 1). Their labeling generally appeared to be of medium intensity and was visible during late embryonic life until birth in RSG and RSA and until P10 in ACG (Fig. 3*A*). These 5-HT-containing neurons were located in the deep cortical layers (V–VI) and had the morphological appearance of pyramidal neurons (Fig. 3*C*). In normal mice, the corresponding cortical areas only displayed a dense network of thick serotonergic axons arranged in a bilaminar array (Fig. 2*A*,*C*).

By E17, 5-HT-containing neurons were observed in the hippocampal primordium. Their number sharply decreased by P0 (Table 1). As identified by the light 5-HT immunolabeling of their main dendrites, these neurons were pyramidal neurons in the indusium griseum (Fig. 2*D*) and in the CA1 and CA3 hippocampal fields (Fig. 2*B*,*E*). The efferent projections of these neurons most likely correspond to 5-HT-immunolabeled bundles observed in the fimbria, the ventral hippocampal commissure (containing the crossed projections from CA3 neurons), and the dorsal fornix from E18 to P0 (Fig. 2*D*). The subiculum, the other major output region of the hippocampal formation, did not show 5-HT-containing neurons. However, axons projecting through the ventral fornix known to contain subicular efferents appeared lightly 5-HT positive between E15 and E19. Correspondingly, pyramidal neurons in the dorsal subiculum, a projection area for the CA1

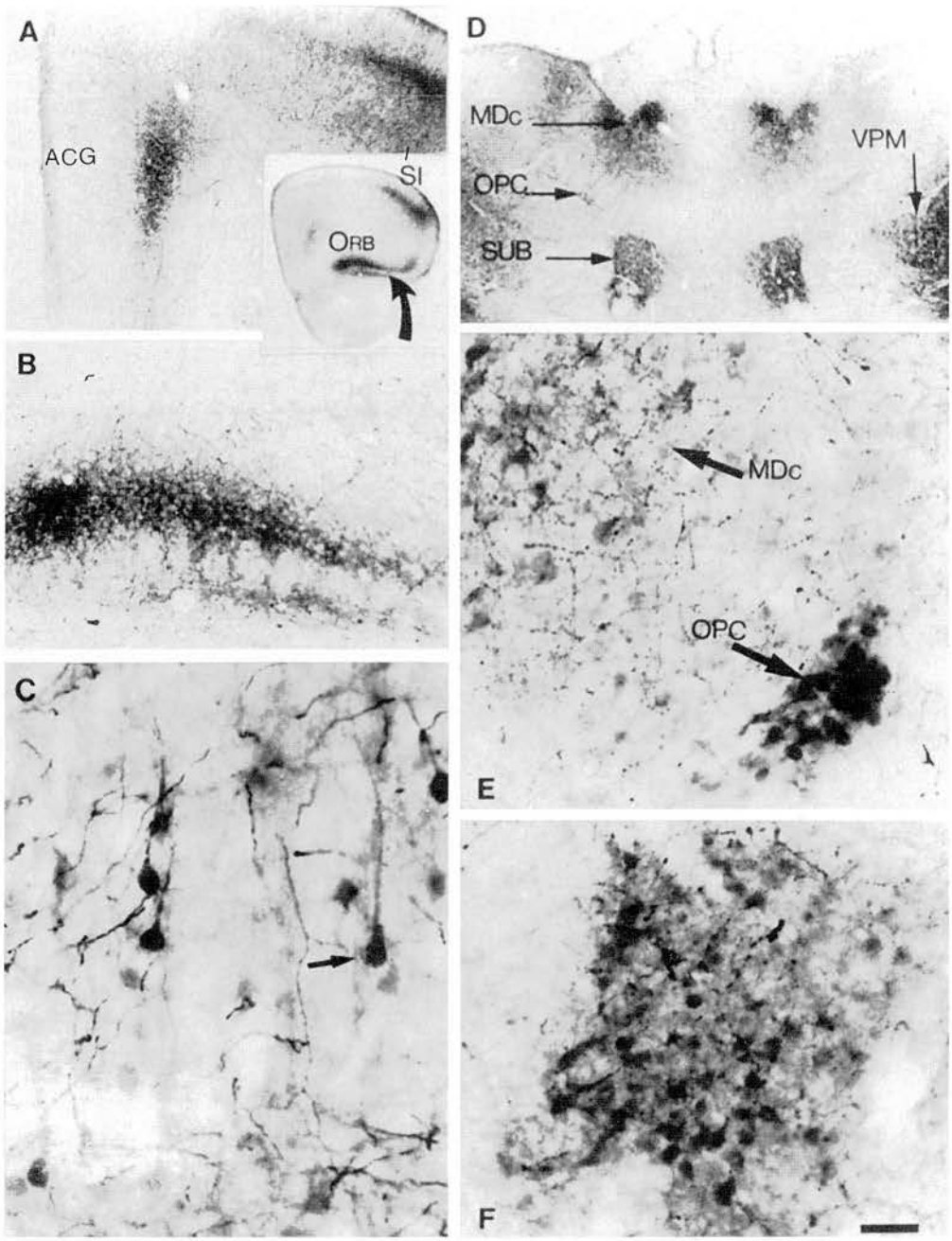

Figure 3. Atypical locations of 5-HT accumulation in the forebrain of P7 MAOA knock-outs. *A*, The coronal section through the frontal cortex shown in the *inset* indicates the position of unusual 5-HT immunolabeling in the orbital cortex (*ORB*) ventrally (*curved arrow*) and in the medial prefrontal and pregenual anterior cingulate cortex (*ACG*) medially; the primary somatosensory cortex (*SI*) was shown previously to be 5-HT-labeled in normal pups. *B*, At higher magnification, 5-HT immunolabeling in the orbital cortex is seen to be localized in a plexus of fine fibers in layer III. *C*, Higher magnification shows the presence of 5-HT-containing neurons in ACG. *Arrow* points to a neuron with a typical pyramidal shape. *D*, Coronal section through the thalamus showing strong 5-HT-immunolabeling in different thalamic nuclei. *MDc*, Central part of the mediodorsal nucleus; *SUB*, submedial nucleus; *OPC*, oval paracentral nucleus; *VPM*, ventroposteromedial nucleus. *E*, Higher magnification shows the presence of 5-HT-immunolabeled cell bodies in MDc and OPC. *F*, Higher magnification shows the presence of 5-HT-immunolabeled cell bodies in SUB. Scale bar (in *E*): *inset*, 820 μm; *A*, *B*, *D*, 150 μm; *C*, 19 μm; *E*, *F*, 24 μm.

pyramidal neurons, showed transient expression of SERT mRNA (Lebrand et al., 1998).

Finally, 5-HT-containing neurons were observed at the periphery of the central nucleus of the developing amygdala between E15 and P0 (Table 1). These neurons had a piriform shape with generally two to three primary dendrites and displayed medium to intense 5-HT immunolabeling (Fig. 2*F*).

Diencephalon

5-HT-containing cell bodies were found in primary sensory thalamic nuclei of the diencephalon of normal mice essentially between P4 and P7. In MAOA knock-outs, 5-HT immunolabeling was also seen in embryos and pups in other thalamic nuclei and in the suprachiasmatic nucleus.

Thalamus. We have shown previously that in normal pups, neurons in the somatosensory ventroposterolateral (VPL) and ventroposteromedial (VPM) nuclei, the visual dorsal lateral geniculate nucleus (DLG), and the auditory ventral medial geniculate nucleus (MGV) are transiently 5-HT immunoreactive (Lebrand et al., 1996). The 5-HT immunolabeling of these thalamic neurons was considerably increased in MAOA knock-outs of corresponding ages. While in normal mice the 5-HT immunolabeling is concentrated in the axonal compartment with only a faint diffuse labeling of the cell bodies, MAOA knock-outs displayed a clear and intense immunostaining of both individual cell bodies and axons running in the internal capsule or projecting to the reticular thalamic nucleus. Furthermore, the 5-HT immunolabeling was visible over a larger developmental period than in controls. In normal pups, 5-HT immunolabeling was noted at P4 and P7 in cell bodies and at P0, P7, and P10 in thalamocortical

fibers. In MAOA knock-outs, it was noted already at the earliest embryonic age examined (E15) in VPL and DLG and persisted until P15 (Table 1).

MAOA knock-outs displayed neuronal labeling in additional nuclei (Table 1). The visceral parvicellular part of VPL and the gustatory parvicellular part of the VPM displayed very strong 5-HT immunolabeling. Less intensely labeled neurons were observed in the central part of the mediodorsal nucleus (MDc) (Fig. 3*D*,*E*), the nociceptive submedial nucleus (SUB) (Fig. 3*D*,*F*), the oval paracentral nucleus (Fig. 3*D*,*E*), the rostral part of the posterior nucleus, the centrolateral nucleus (small patches of cells), the rostrolateral part of the lateral posterior nucleus, and the dorsal and medial parts of the medial geniculate nucleus (Table 1).

Sensory thalamocortical axons arising from the dorsal thalamus displayed intense 5-HT immunolabeling in MAOA knock-outs as early as E15 (at P0 in normal mice) (Table 2). By E18, the 5-HT immunolabeled thalamocortical axons reach the subplate through the internal capsule forming a dense plexus in the subplate (Fig. 2*B*,*G*, see also 5*C*). Later in development, a dense plexus was visible in the layers IV and VI of the primary somatosensory, auditory, visual, gustatory, and visceral cortices (Table 2). A plexus of moderate density was visible in the secondary somatosensory, auditory, and visual cortices between P4 and P10. Projections from the MDc and SUB were labeled in layer II–III of the lateral and ventral orbital cortex (Fig. 3*B*; Table 2) between P4 and P10, whereas a 5-HT-positive plexus was not observed in this part of the cortex in normal mice.

Hypothalamus. 5-HT-containing neurons were observed in the ventral and medial zones of the suprachiasmatic nucleus (SCN) during a protracted period of postnatal life (Table 1), whereas only a dense serotonergic innervation was present in normal mice (van den Pol and Tsujimoto, 1985; van den Pol, 1986). A positive correlation was found between the amount of label in individual cell bodies and the number or size of the 5-HT varicosities in close contact with the soma.

Brainstem

In MAOA knock-outs, 5-HT-containing neurons were observed in two auditory relays, the anteroventral cochlear nucleus and the lateral superior olivary nucleus (LSO) (Fig. 4*A*, Table 1). The major auditory center, the inferior colliculus (IC), did not contain 5-HT-positive cell bodies. In LSO, the 5-HT-positive cell bodies were in the lateral and central parts of the nucleus, as determined by counterstaining with methyl green, and immunostaining increased from central to lateral along the tonotopic axis. During the same period, 5-HT-positive bundles of fibers entering the IC and a dense 5-HT-positive plexus in the central nucleus of the IC were also observed (Fig. 4*B*,*D*, Table 2). The distribution resembled that of LSO efferent fibers.

In the somatosensory pathway, 5-HT immunolabeling was not observed in neurons of the principal nucleus of the trigeminal, although primary sensory fibers entering this nucleus were transiently 5-HT immunolabeled (our unpublished observations) (Table 2). Retinal afferents were transiently 5-HT immunolabeled (Figs. 4*B*, 5*C*; Table 2) (Upton et al., 1997; our unpublished observations). Other projections from peripheral neurons were 5-HT immunoreactive and will be described in separate reports (our unpublished observations).

AADC in 5-HT-containing neurons

The presence of 5-HT in atypical locations in developing mice could reflect a local synthesis of 5-HT. We determined whether the biosynthetic enzyme AADC is present at these sites at E18, P0, P7, P10, and P21 in MAOA knock-outs and normal controls. At all ages, the AADC immunolabeling was normally localized in the serotonergic, noradrenergic, and dopaminergic cell bodies and fibers, as well as in the 14 "D" groups of AADC-expressing cells (for review, see Jaeger et al., 1984). No AADC-containing neurons were observed in the cortex, amygdala, hippocampal formation, and thalamus (Fig. 5*A*,*B*,*D*). 5-HT-containing neurons in LSO and the anteroventral cochlear nucleus also lacked AADC.

Pharmacological treatments with inhibitors of transporters

To determine whether the 5-HT immunolabeling is caused by an uptake of 5-HT, MAOA knock-outs were injected with inhibitors of the monoaminergic transporters. Repeated administration of fluoxetine, a selective inhibitor of 5-HT uptake, to pregnant MAOA knock-out dams (30 mg/kg, seven injections at 4 hr intervals) completely eliminated 5-HT-immunolabeling in the nonaminergic 5-HT-containing neurons of the cortex, hippocampus, thalamus, and LSO of E19 embryos without affecting 5-HT immunolabeling in the catecholaminergic cell groups (data not shown). Similarly, in P7 MAOA knock-outs, repeated administration (three injections at 10 hr intervals) of the SERT inhibitors fluoxetine (30 mg/kg) or paroxetine (50 mg/kg) abolished 5-HT immunolabeling in all the thalamic nuclei and in the corresponding cortical projection areas (Fig. 6*C*), although a very faint labeling was still observed in the thalamocortical fibers in the internal capsule and in a few cell bodies. In contrast, fluoxetine or paroxetine treatments increased 5-HT immunolabeling in all the catecholaminergic cell groups (even after a single injection 6 hr before perfusion) (Fig. 6*A*,*B*). It was particularly apparent for Arc neurons (Fig. 7*A*) and for SN neurons and SN axonal terminals. Indeed, a fine 5-HT immunolabeled network was readily visible in the striatum after such treatments. Nisoxetine (10 or 30 mg/kg, two injections), a selective inhibitor of norepinephrine uptake, eliminated 5-HT immunolabeling in noradrenergic neurons (Fig. 6*D*) without affecting 5-HT immunolabeling in SN (Fig. 6*E*) and thalamic nuclei (Fig. 6*F*). GBR12783 (10 or 30 mg/kg, two injections), a selective inhibitor of dopamine uptake, abolished 5-HT immunolabeling in dopaminergic neurons (Fig. 6*H*) without affecting 5-HT immunolabeling in LC (Fig. 6*G*) or thalamic nuclei (Fig. 6*I*). Curiously, neither blocking 5-HT uptake with fluoxetine nor blocking catecholamine uptake with GBR12783 or nisoxetine could diminish the number of 5-HT-containing neurons in SCN. On the contrary, fluoxetine or paroxetine treatments enhanced neuronal staining in SCN (Fig. 7*B*). Treatment with NO-711 (50 mg/kg, three injections), a specific inhibitor of GAT-1, a neuronal GABA transporter that shares structural similarities with monoaminergic transporters, did not diminish the number of 5-HT-containing neurons in SCN.

MAOA–DAT double knock-out mice

We generated double knock-outs by crossing MAOA knock-outs and DAT knock-out mice (Giros et al., 1996). In contrast to MAOA knock-outs, MAOA–DAT double knock-out mice showed a total lack of 5-HT immunolabeling in the dopaminergic neurons of the SN–VTN complex (Fig. 8), PAVH, and Arc between E16 and P7, whereas 5-HT immunolabeling was main-

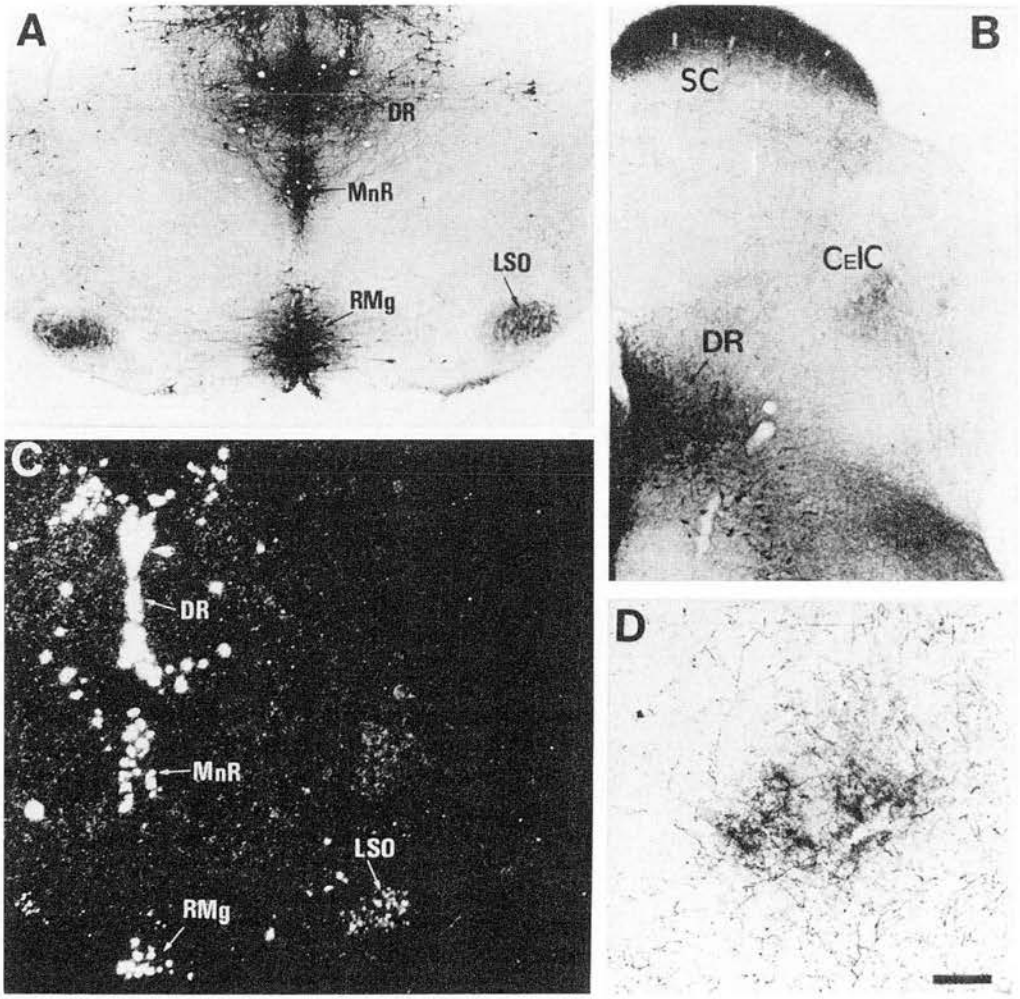

Figure 4. 5-HT uptake in neurons of the LSO. Coronal sections through the brainstem of P7 MAOA knock-outs (*A*, *B*, *D*) and control (*C*). *A*, 5-HT immunoreactivity is normally localized in 5-HT-producing neurons of the dorsal raphe (*DR*), median raphe (*MnR*), and raphe magnus (*RMg*) and is abnormally localized in auditory neurons of LSO. *B*, 5-HT immunolabeling is found in the projection area of LSO neurons in the central nucleus of the inferior colliculus (*CEIC*). See higher magnification in *D*. 5-HT immunolabeling is also visible in the stratum zonale and stratum griseum of the superior colliculus (*SC*) and is primarily contained in retinal afferents (A. L. Upton, N. Salichon, I. Seif, and P. Gaspar, personal communication). *C*, *In situ* hybridization with a radiolabeled SERT riboprobe shows the presence of SERT RNA in LSO neurons and in the raphe nuclei. *D*, At higher magnification, 5-HT immunolabeling in CEIC is not seen in cell bodies but in auditory afferents, presumably from LSO, as suggested by the trajectory of corresponding fiber bundles in adjacent sections. Scale bar (in *D*): *A–C*, 200 μm; *D*, 80 μm.

tained in LC (Fig. 8), MGV (Fig. 8), and the other thalamic nuclei, and SCN (data not shown) 5-HT immunolabeling was also maintained in PVSO, SPO, and SCN (data not shown).

Using MAOA–DAT double knock-out pups, we determined whether the previously reported behavioral abnormalities of MAOA single knock-out pups, such as tremor, myoclonus, agitation, frantic running, biting, and abnormal postures (Cases et al., 1995), could be related to the presence of 5-HT in dopamine neurons. MAOA–DAT double knock-out pups, but not DAT single knock-out pups, displayed the same behavioral abnormalities as MAOA single knock-out pups. Conversely, MAOA–DAT double knock-outs, but not MAOA single knock-outs, showed the same lethality as DAT single knock-outs at weaning age, which was prevented in both cases by supplementing the diet with hydrated food.

SERT RNA in nonmonoaminergic 5-HT-containing neurons

In a companion study using *in situ* hybridization and immunocytochemistry (Lebrand et al., 1998), we have analyzed the spatiotemporal expression patterns of SERT, DAT, and NET in developing normal mice, focusing on the forebrain and catecholaminergic groups. These normal patterns proved to be in good agreement with our spatiotemporal and pharmacological analyses of 5-HT accumulation in MAOA knock-outs. All of the nonmonoaminergic 5-HT-containing neurons observed in the forebrain of MAOA knock-outs appeared to transiently express SERT RNA in normal mice, except the amygdala and SCN neurons, in which no RNA expression of SERT, DAT, or NET could be found. Similarly, normal brainstem and midbrain catecholaminergic neurons did not show SERT RNA expression, whereas they expressed DAT or NET RNA abundantly. Here, we show additionally that SERT RNA is expressed in neurons of the LSO in normal mice (Fig. 4*C*).

DISCUSSION

In this report, we describe that in the developing CNS of MAOA knock-outs, 5-HT immunoreactivity is abnormally and transiently localized in catecholaminergic and nonmonoaminergic neurons.

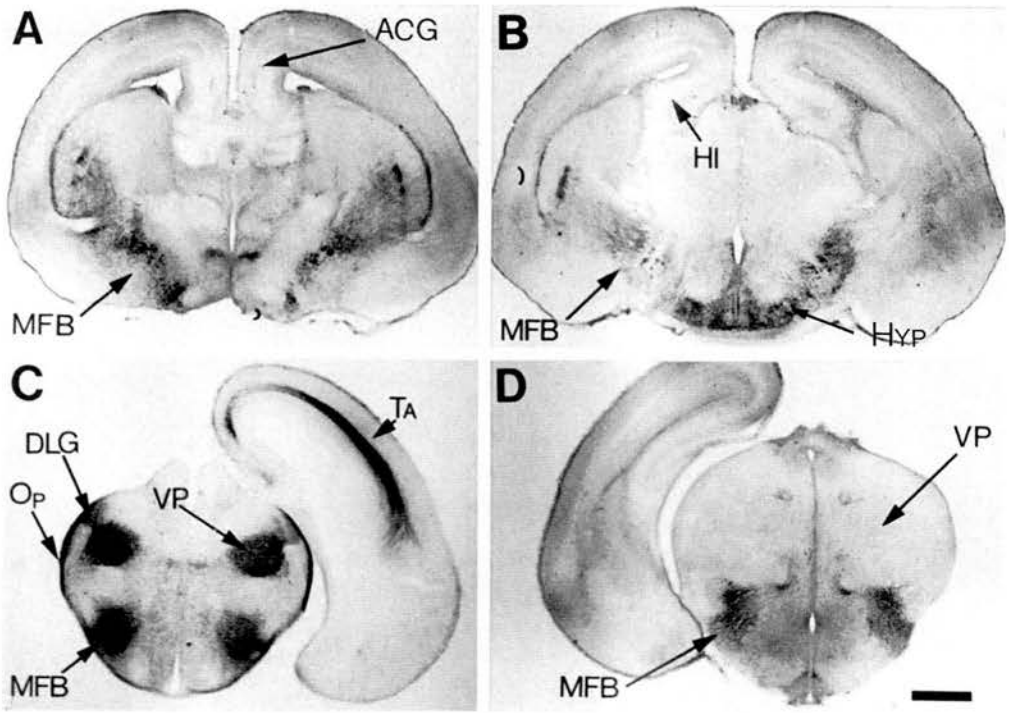

Figure 5. Immunocytochemical localization of AADC in E18 MAOA knock-outs. *A*, *B*, As viewed on coronal brain sections from rostral (*A*) to caudal (*B*), AADC immunoreactivity is localized in terminal fibers in the striatum, cortex, and hippocampus and in fiber tracts in the MFB or stria terminalis. AADC immunostaining of perikarya appears to be limited to catecholaminergic and D-group (Jaeger et al., 1984) neurons in the hypothalamus (*HYP*). *C*, *D*, Coronal sections at comparable levels of the diencephalon are shown with 5-HT (*C*) and AADC immunostaining (*D*); both antisera label fibers in the MFB. On the other hand, the dense 5-HT immunolabeling of the ventroposterior complex (*VP*), dorsal lateral geniculate nucleus (*DLG*), thalamocortical fibers (*TA*), and optic tract (*OP*) has no visible counterpart with AADC immunostaining. Scale bar (in *D*): *A–D*, 625 μm.

This is attributable to the lack of the normal degradation pathway of 5-HT and to the existence of functional transport of 5-HT, either by SERT, which is transiently expressed in nonmonoaminergic neurons, or by DAT and NET in catecholaminergic neurons. These abnormal accumulations of 5-HT during development could underlie some of the developmental and behavioral abnormalities that are observed in MAOA knock-outs (Cases et al., 1995).

Mechanisms of 5-HT accumulation in MAOA knock-outs

Early descriptions of rodent serotonergic systems in adult (Steinbusch, 1981) or during development (Lidov and Molliver, 1982a,b; Wallace and Lauder, 1983) have localized 5-HT exclusively in the neurons of the raphe complex (B1–B9) and in their widespread axonal arbors throughout the brain and spinal cord. However, recent studies during early postnatal development have questioned this view by showing that the transient dense 5-HT innervation of the primary somatosensory, visual, and auditory cortices (Fujimiya et al., 1986; D'Amato et al., 1987; Rhoades et al., 1990) is related to a 5-HT uptake in the corresponding thalamocortical neurons (Lebrand et al., 1996). This 5-HT uptake in developing thalamic neurons is attributable to the transient expression of SERT. More recent studies with *in situ* hybridization (Hansson et al., 1998; Lebrand et al., 1998) or autoradiographic binding (Bruning et al., 1997) have shown extensive sites of SERT expression during CNS development, both in the diencephalon and the telencephalon, and there appears to be an excellent correlation between the spatiotemporal pattern of SERT expression and 5-HT accumulation patterns that are detected in MAOA knock-outs in the cortex, hippocampus, and thalamus. The demonstration that 5-HT is only taken up but is not synthesized locally in these neurons is established by the lack of AADC, the last biosynthetic enzyme in the 5-HT biosynthesis pathway, in the developing cortical, hippocampal, or thalamic neurons. Furthermore, the 5-HT labeling of these structures was abolished by selective inhibitors of 5-HT uptake such as fluoxetine or paroxetine. It is noteworthy that these uptake inhibitors had to be administered repeatedly and at least during 24 hr to abolish the immunolabeling of the large thalamocortical fibers at P7, suggesting that 5-HT can be extremely resilient in neurons that lack MAOA. This resilience may be partly linked to a storage of 5-HT into vesicles via the vesicular monoamine transporter VMAT2, because VMAT2 RNA expression is observed in thalamic sensory neurons (Lebrand et al., 1996). If 5-HT was indeed stored into synaptic vesicles in these neurons, it could be released in an activity-dependent manner in normal mice. In MAOA knock-outs, such a release could be blocked by excess extracellular 5-HT acting on the inhibitory 5-HT_{1B} receptors that are present on thalamocortical fibers (Rhoades et al., 1994); this would counterbalance the lack of 5-HT replenishment during fluoxetine treatments. In comparison with MAOA knock-outs, normal mice displayed a much more limited 5-HT immunolabeling; 5-HT was not detected in any of the neurons that transiently express SERT during embryonic life, and during postnatal life, 5-HT was only sometimes visible in primary sensory thalamic cell bodies but was never observed in the other dorsal thalamic neurons, cortex, or hippocampus. These observations suggest that in normal conditions 5-HT is rapidly degraded in these neurons or is present in a labile compartment with a rapid turnover (e.g., immediate release and degradation in the extracellular space).

Besides the 5-HT accumulation in the neurons that transiently express SERT, MAOA knock-outs accumulated 5-HT in the major catecholaminergic cell groups of the brainstem and hypothalamus. This accumulation is mediated by DAT in the A8–A10 dopaminergic complex and in the hypothalamic PAVH and Arc, as demonstrated after pharmacological treatments and our observations in double knock-out mice that lack both DAT and MAOA. In the noradrenergic cell groups, 5-HT is taken up through NET, as indicated by our pharmacological blocking experiments. Previous pharmacological studies *in vitro* have shown

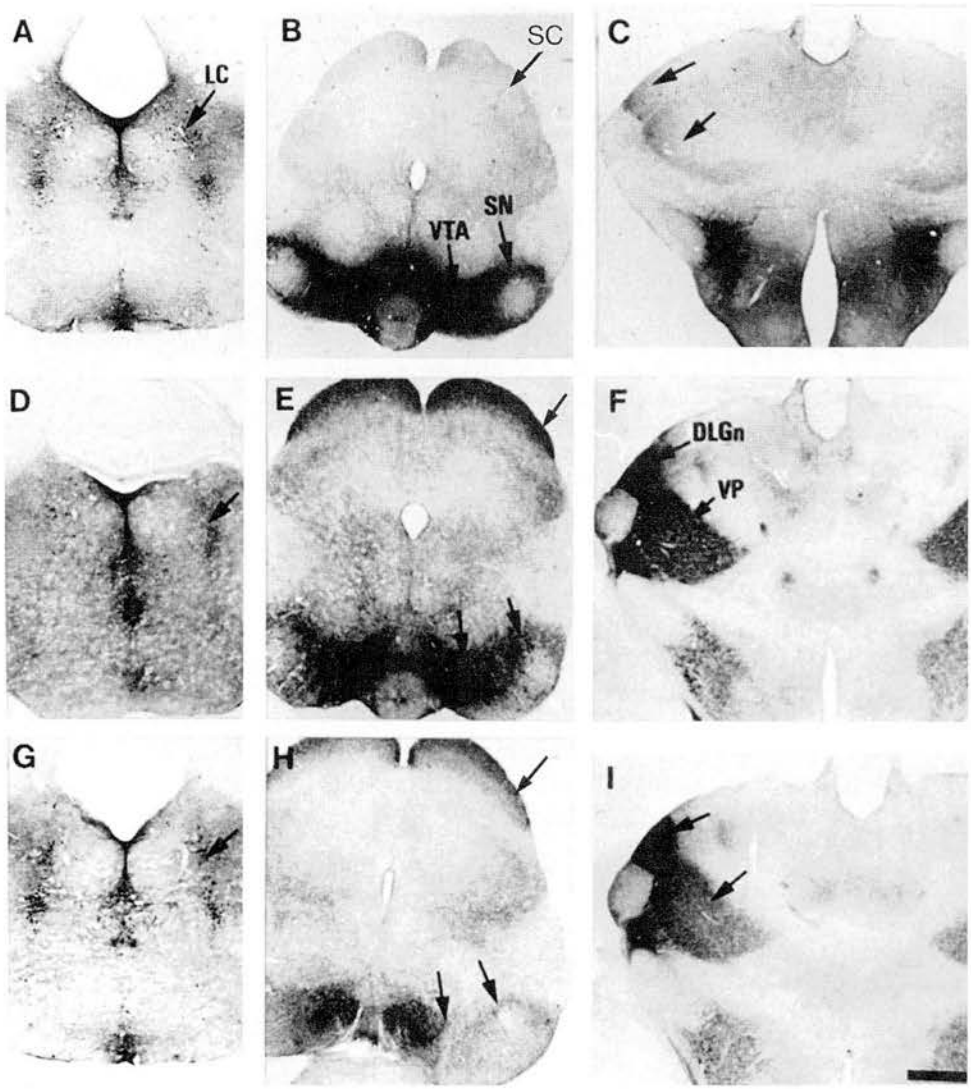

Figure 6. Changes of 5-HT immunoreactivity in P7 MAOA knock-outs after administration of selective inhibitors of monoaminergic transporters. Comparable coronal brain sections are shown in the metencephalon (*A*, *D*, *G*), mesencephalon (*B*, *E*, *H*), and diencephalon (*C*, *F*, *I*), after repeated administration of fluoxetine (*A–C*), nisoxetine (*D–F*), or GBR12783 (*G–I*) at P6 and P7. Control brain sections obtained from untreated MAOA knock-outs are not shown. 5-HT immunolabeling of the raphe nuclei is not visibly affected by any pharmacological treatment, although the staining of the fine varicose afferents from the raphe is reduced by the fluoxetine treatment. *A–C*, Fluoxetine, a selective inhibitor of SERT, causes the disappearance of 5-HT immunolabeling in the SC (*B*) and thalamus at the level of DLGn and VP (*C*) but increases staining of dopaminergic neurons in the SN and VTA (*B*), with no visible change in the LC (*A*). *D–F*, Nisoxetine, a selective inhibitor of NET, greatly reduces 5-HT immunolabeling in the LC (*D*) but does not cause changes of staining in the SN, VTA, SC (*E*), or thalamus (*F*). *G–I*, GBR12783, a selective inhibitor of DAT, abolishes 5-HT immunolabeling in the SN and VTA (*H*) but not in the LC (*G*), SC (*H*), or thalamus (*I*). Scale bar (in *I*): *A–I*, 625 μm.

that in transfected cell lines expressing DAT or NET, 5-HT cannot competitively inhibit catecholamine uptake (Giros et al., 1991; Pacholczyk et al., 1991). However, the kinetics of 5-HT transport in such cell lines have not been investigated, and the possibility should be considered that in native monoaminergic neurons, transporters have higher affinities for 5-HT than in *in vitro* expression systems.

Shaskan and Snyder (1970) showed that brain slices of striatum and hypothalamus displayed both high- and low-affinity uptake sites for 5-HT and suggested that the low-affinity uptake reflected an uptake in catecholaminergic terminals. Similar observations were made in autoradiographic studies after uptake of tritiated monoamines in brain slices (Berger and Glowinski, 1978; Doucet et al., 1988). *In vivo*, 5-HT accumulation was noted in dopaminergic neurons of the SN (Steinbush et al., 1982), hypothalamus (Lichtensteiger et al., 1967; Chan-Palay, 1977; Beaudet and Descarries, 1979), and pituitary intermediate lobe (Vanhatalo and Soinila, 1994) after supplementing animals with exogenous 5-HT or the 5-HT precursor L-tryptophan and blocking 5-HT degradation with inhibitors of monoamine oxidases. Arai et al. (1995) showed that when adult rats are injected with the 5-HT precursor 5-hydroxytryptophan (5-HTP), 5-HT accumulates in SN neurons, whether MAO inhibitors are added or not. They concluded that 5-HT was synthesized by the SN neurons (although it was not investigated whether DAT plays a role in this 5-HTP effect) and that the amine was not rapidly degraded in these neurons. The latter observation suggests that in MAOA knock-outs, increased extracellular levels of 5-HT surrounding SN neurons could be more critical than the lack of 5-HT degradation by MAOA in these neurons. In any case, in MAOA knock-outs, the intensity of 5-HT immunolabeling in individual SN neurons appeared to correlate with the abundance of 5-HT terminal innervation in close association with the cell body. It is not known whether within these structures rich in extracellular 5-HT the density of DAT sites on the surface of the dopaminergic cell body is high enough to cause an efficient uptake of 5-HT. Quite the opposite, it has been reported that DAT is primarily localized to dendritic and axonal plasma membranes (Ciliax et al., 1995; Nirenberg et al., 1997), although this was studied in adult rats, and it is known that DAT expression varies with age (Coulter et al., 1996).

5-HT immunolabeling in catecholaminergic neurons was observed as early as E12 in MAOA embryos. This suggests efficient release of 5-HT from raphe fibers at E12, as well as efficient DAT and NET uptake at this age. In postnatal MAOA knock-outs, the

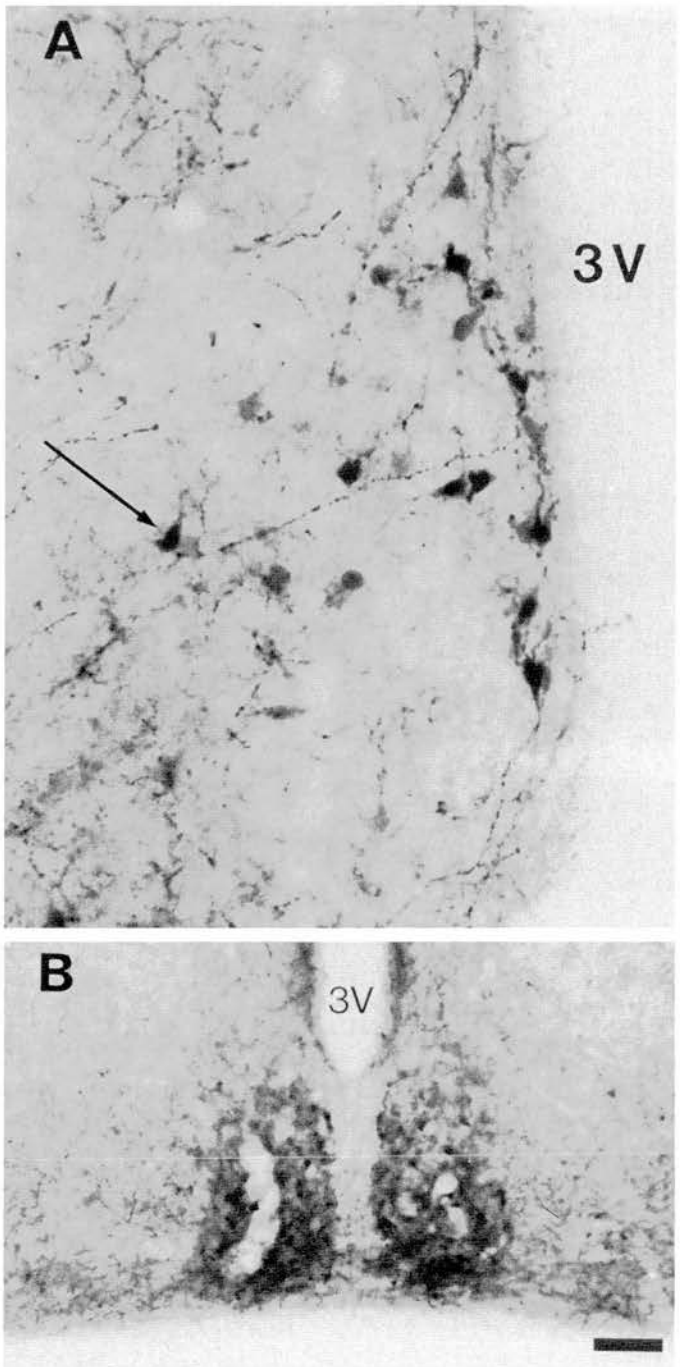

Figure 7. Increase in the number of 5-HT-containing neurons in the hypothalamus of P7 MAOA knock-outs after fluoxetine treatments. Control brain sections obtained from untreated MAOA knock-outs are not shown. *A*, The number of 5-HT-containing neurons is increased in the Arc. *Arrow* indicates a dorsal periventricular neuron. *B*, The number of 5-HT-containing neurons is increased in the SCN. *3V*, Third ventricle. Scale bar (in *B*): *A*, 24 μm; *B*, 90 μm.

5-HT-immunolabeling of catecholaminergic neurons was noted only during the first 3 weeks of postnatal life when brain 5-HT levels are highest (Cases et al., 1995). Thereafter, 5-HT immunolabeling diminished and eventually disappeared in catecholaminergic neurons, in relationship with the relative normalization of 5-HT levels because of the compensatory activity of the monoamine oxidase B (MAOB), possibly in association with intervening glial processes. When MAOB activity was pharmacologically inhibited in 5-month-old MAOA knock-outs, the 5-HT immunolabeling of catecholaminergic neurons reappeared (our unpublished observations).

One developmental localization of 5-HT in MAOA knock-outs that could not be clarified by the present pharmacological blocking experiments is the localization of 5-HT in neurons of the ventral and medial zones of the SCN. No SERT, DAT, or NET expression has been detected in these neurons (Lebrand et al., 1998). However, a very low expression of SERT might be sufficient, because 5-HT-labeled neurons in SCN benefit from an abundant 5-HT innervation originating in the raphe, and our pharmacological treatments cannot achieve total inhibition of SERT. Alternatively, 5-HT could be taken up by another transporter, such as a putative melatonin transporter (Helton et al., 1993; Liu et al., 1997).

Functional consequences of 5-HT accumulation in MAOA knock-outs

The functional consequences of 5-HT accumulation in the catecholaminergic neurons of MAOA knock-outs could not be predicted. Comparison of MAOA–DAT double knock-outs and MAOA single knock-outs failed to reveal developmental or behavioral consequences of 5-HT accumulation in dopaminergic neurons. MAOA–DAT double knock-outs lacked cortical barrels (our unpublished observations). Similarly, MAOA–DAT double knock-out pups displayed the flagrant behavioral abnormalities of MAOA knock-out pups (Cases et al., 1995), such as trembling. In fact, 5-HT accumulation in catecholaminergic neurons could be less detrimental to catecholaminergic function than the presence of excess extracellular 5-HT.

A particularly important feature of the spatiotemporal pattern of nonmonoaminergic 5-HT-containing neurons in MAOA knock-outs is the preferential localization of 5-HT uptake to glutamatergic neurons that form precise projection maps, which may be regarded as an indirect indication that extracellular 5-HT levels modulate the formation of these maps. We have described previously that somatosensory thalamocortical fibers, which accumulate large amounts of 5-HT in MAOA knock-out pups, develop abnormally, because they do not form proper axonal branches and barrel clusters in layer IV of the somatosensory cortex (Cases et al., 1996). Remarkably, as shown in the present report, thalamocortical fibers take up 5-HT from their initial outgrowth in MAOA knock-out embryos. This suggests that in normal mice, 5-HT has an effect on these fibers before they reach their specific cortical targets. However, in MAOA knock-outs, excess 5-HT does not seem to disrupt the major embryonic guidance mechanisms of the somatosensory thalamic fibers, because a normal barrel pattern can be obtained by decreasing 5-HT levels postnatally.

As in the case of the somatosensory cortex, postnatal alterations could be expected to occur in the primary visual, auditory, gustatory, and visceral thalamocortical projections that also display intense 5-HT accumulation during a critical period of their development. The presence of 5-HT immunoreactivity in neurons of the SUB, which relays thermoceptive and nociceptive information (Yoshida et al., 1991, 1992; Roberts and Dong, 1994), and in neurons of the central part of the MDc, which receives inputs from olfactory-related structures (Price and Slotnick, 1983; Groenewegen et al., 1990), also suggests that these thalamic neurons have a critical period during which the spatial tuning of their projections to the orbital cortex is sensitive to 5-HT.

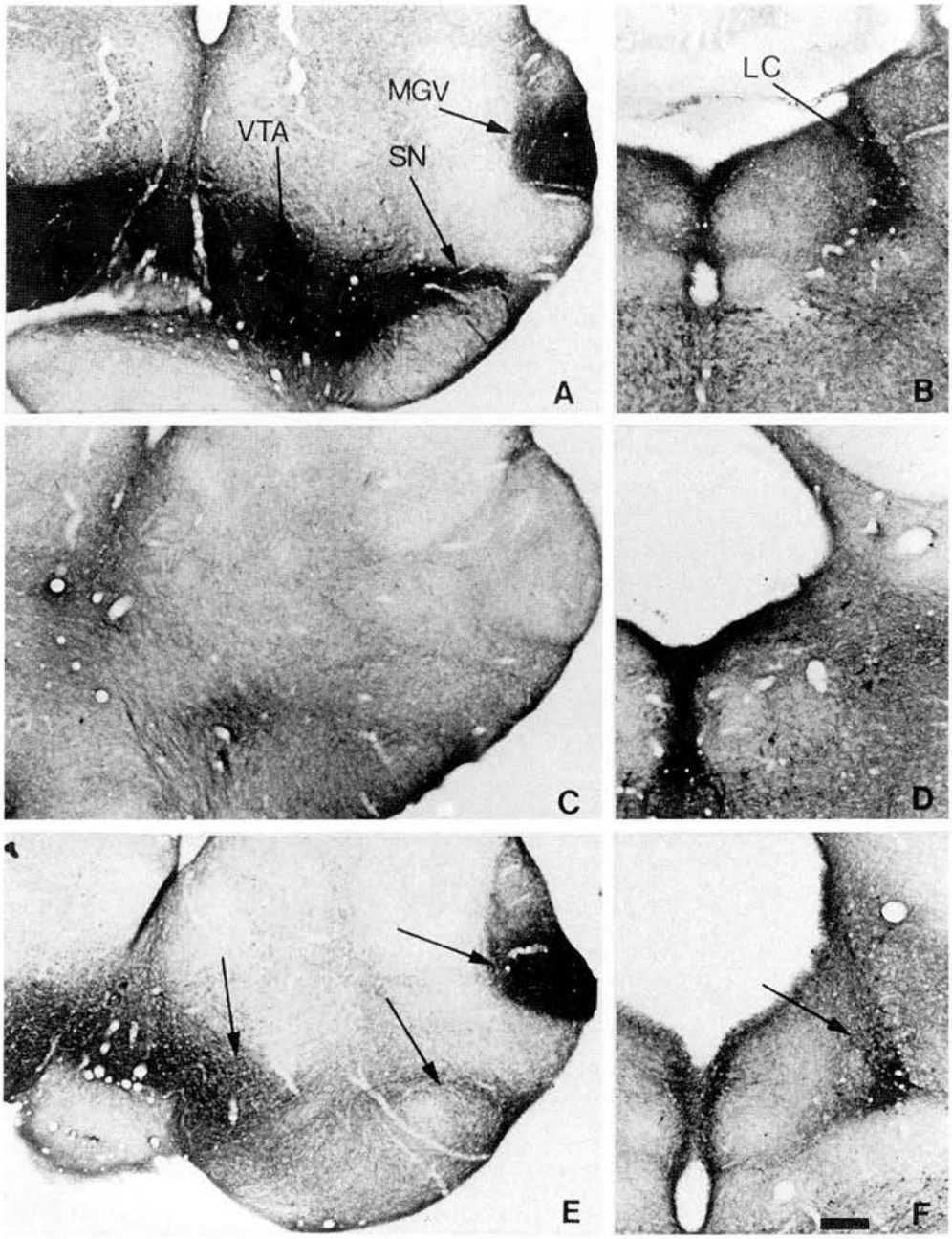

Figure 8. Lack of 5-HT accumulation in dopaminergic cell bodies of P7 MAOA–DAT double knock-outs. Comparable coronal brain sections are shown in the metencephalon (*A*, *C*, *E*) and the pons (*B*, *D*, *F*) of mice knock-outs for MAOA (*A*, *B*), DAT (*C*, *D*), or both MAOA and DAT (*E*, *F*). *A*, *B*, In the MAOA single knock-out, 5-HT-containing neurons are observed in the MGV, SN, VTA, and LC. *C*, *D*, In contrast, in the DAT single knock-out, no 5-HT-containing neurons are observed in the MGV, SN, VTA, and LC. *E*, *F*, In the MAOA–DAT double knock-out, 5-HT-containing neurons are still observed in the MGV and LC but are no longer observed in the SN and VTA. Scale bar: *A–F*, 265 μm.

Changes in the orbital cortex would be interesting to investigate in adult MAOA knock-outs, which display altered sexual, aggressive, and nociceptive behaviors (Cases et al., 1995; Kim et al., 1997). The orbital cortex is implicated in complex olfactory behaviors, such as olfactory-guided male sexual behavior (Eichenbaum et al., 1980; Sapolsky and Eichenbaum, 1980; Slotnick and Kaneko, 1981) and intermale aggression (De Bruin et al., 1983; De Bruin, 1990; Kolb and Gibb, 1990). In addition to causing developmental defects possibly leading to behavioral alterations in adult MAOA knock-outs, the considerable levels of 5-HT in the brain of MAOA knock-outs during the first 2 postnatal weeks have been shown to acutely cause much exaggerated behavioral responses. For example, P12 pups display defensive biting and prolonged responses to tail pinches. These behaviors may involve the orbital cortex and the SUB.

Abnormal segregation of neuronal projections in MAOA knock-outs is not confined to cortical fields and has been observed in the lower brain. In a preliminary report, we indicated that the segregation of contralateral and ipsilateral retinal projections is abnormal in the dorsal lateral geniculate thalamus of MAOA knock-outs (Upton et al., 1997; A. L. Upton, N. Salichon, I. Seif, and P. Gaspar, personal communication). This suggests that the projections from the LSO, which is involved in binaural hearing, could also be altered (Shneiderman and Henkel, 1987; Rietzel and Friauf, 1998). LSO neurons receive glutamatergic excitatory and glycinergic inhibitory neurons originating from the ipsilateral and contralateral ear, respectively, along an exquisitely organized tonotopic gradient (Caird and Klinke, 1983). During perinatal development, there is a shift in the effects of glycinergic inputs received by LSO neurons that have depolarizing effects before P8 and hyperpolarizing effects thereafter (Kandler and Friauf, 1995). LSO projects to the central nucleus of the inferior

colliculus. Most of the ipsilateral projection is glycinergic and most of the contralateral projection is glutamatergic, although this remains controversial (Glendenning et al., 1992; Moore et al., 1995; Saint Marie, 1996), and there appears to be little overlap of the ipsilateral and contralateral terminals (Shneiderman and Henkel, 1987). In MAOA knock-outs, 5-HT-positive neuronal cell bodies were observed in the lateral and central LSO (a region that responds to lower sound frequencies). Immunocytochemical and tracing experiments are needed to establish the nature of these 5-HT-containing neurons (glycinergic or glutamatergic) and the degree of patterning of their projections.

In the anterior cingulate cortex, a part of the brain involved in attention, 5-HT immunolabeling was located in pyramidal-like neurons of the deep layers of the cortical plate. The topography and morphology of these 5-HT-accumulating neurons resemble that of the pioneering callosal neurons that have been described in the rat cingulate cortex (Koester and O'Leary, 1994). In rabbits, prenatal exposure to cocaine, a general inhibitor of monoamine uptake systems, alters the bundling of apical dendrites of anterior cingulate pyramidal cells (Levitt et al., 1997), and in male rats, prenatal exposure reduces the midsagittal area of the corpus callosum (Ojima et al., 1996). It could be speculated that 5-HT has an effect on the differentiation and growth of these cortical neurons and that cocaine acts in part by elevating extracellular levels of 5-HT.

In conclusion, our study points to particular neurons that could develop abnormal projections in children exposed to drugs enhancing brain levels of 5-HT or in individuals having a genetic deficiency in MAOA (Brunner et al., 1993; Lenders et al., 1998) or SERT. This study also emphasizes how mice that have been genetically modified, here with a null mutation of the MAOA gene, could be a most valuable model to exacerbate and visualize unexpected mechanisms.

REFERENCES

Amara SG, Kuhar MJ (1993) Neurotransmitter transporters: recent progress. Annu Rev Neurosci 16:73–93.

Arai R, Karasawa N, Nagatsu T, Nagatsu I (1995) Exogenous L-hydroxytryptophan is decarboxylated in neurons of the substantia nigra pars compacta and locus coeruleus of the rat. Brain Res 669:145–149.

Beaudet A, Descarries L (1979) Radioautographic characterization of a serotonin-containing nerve cell group in the adult rat hypothalamus. Brain Res 160:231–243.

Bennett-Clarke CA, Leslie MJ, Chiaia NL, Rhoades RW (1993) Serotonin 1B receptors in the developing somatosensory and visual cortices are located on thalamocortical axons. Proc Natl Acad Sci USA 90:153–157.

Berger B, Glowinski J (1978) Dopamine uptake in serotoninergic terminals *in vitro*: a valuable tool for the histochemical differentiation of catecholaminergic and serotoninergic terminals in rat cerebral structures. Brain Res 147:29–45.

Blakely RD, Berson HE, Fremeau RT, Caron MG, Peek MM, Prince HK, Bradley CC (1991) Cloning and expression of a functional serotonin transporter from rat brain. Nature 354:66–70.

Bruning G, Liangos O, Baumgarten HG (1997) Prenatal development of the serotonin transporter in mouse brain. Cell Tissue Res 289:211–221.

Brunner HG, Nelen M, Breakefield XO, Ropers HH, Van Oost BA (1993) Abnormal behavior associated with a point mutation in the structural gene for monoamine oxidase A. Science 262:578–580.

Caird DM, Klinke R (1983) Processing of binaural stimuli by cat superior olivary complex neurons. Exp Brain Res 52:385–399.

Cases O, Seif I, Grimsby J, Gaspar P, Chen K, Pournin S, Muller U, Aguet M, Babinet C, Shih JC, De Maeyer E (1995) Aggressive behavior and altered amounts of brain serotonin and norepinephrine in mice lacking MAOA. Science 268:1763–1766.

Cases O, Vitalis T, Seif I, De Maeyer E, Sotelo C, Gaspar P (1996) Lack of barrels in the somatosensory cortex of monoamine oxidase A-deficient mice: role of serotonin excess during the critical period. Neuron 16:297–307.

Chan-Palay V (1977) Indoleamine neurons and their processes in the normal rat brain and in chronic diet-induced thiamine deficiency]demonstrated by uptake of ^{3}H-serotonin. J Comp Neurol 176:467–493.

Ciliax BJ, Heilman C, Demchyshyn LL, Pristupa ZB, Ince E, Hersch SM, Niznik HM, Levey AL (1995) The dopamine transporter: immunochemical characterization and localization in brain. J Neurosci 15:1714–1723.

Consolazione A, Milstein C, Wright B, Cuello AC (1981) Immunocytochemical detection of serotonin with monoclonal antibodies. J Histochem Cytochem 29:1425–1430.

Coulter CL, Happe HK, Murrin LC (1996) Postnatal development of the dopamine transporter: a quantitative autoradiographic study. Dev Brain Res 92:172–181.

D'Amato R, Blue ME, Largent BL, Lynch DR, Ledbetter DJ, Molliver ME, Snyder SH (1987) Ontogeny of the serotonergic projection to rat neocortex: transient expression of a dense innervation of primary sensory areas. Proc Natl Acad Sci USA 84:4322–4326.

De Bruin JPC (1990) Social behaviour and the prefrontal cortex. Prog Brain Res 85:485–497.

De Bruin JPC, Van Oyen HGM, Van De Poll N (1983) Behavioural changes following lesions of the orbital prefrontal cortex in male rats. Behav Brain Res 10:209–232.

Doucet G, Descarries L, Audet MA, Garcia S, Berger B (1988) Radioautographic method for quantifying regional monoamine innervations in the rat brain. Application to the cerebral cortex. Brain Res 441:233–259.

Eichenbaum H, Shedlack KJ, Eckmann KW (1980) Thalamocortical mechanisms in odor-guided behavior. I. Effects of lesions of the mediodorsal thalamic nucleus and frontal cortex and olfactory discrimination in the rat. Brain Behav Evol 17:255–275.

Fontaine B, Changeux JP (1989) Localization of nicotinic acetylcholine receptor α-subunit transcripts during myogenesis and motor endplate development in the chick. J Cell Biol 108:1025–1037.

Franklin KBJ, Paxinos G (1994) The mouse brain in stereotaxic coordinates. San Diego: Academic.

Fujimiya M, Kimura H, Maeda T (1986) Postnatal development of serotonin nerve fibers in the somatosensory cortex of mice studied by immunochemistry. J Comp Neurol 246:191–201.

Giros B, Caron MG (1993) Molecular characterization of the dopamine transporter. Trends Pharmacol Sci 14:43–49.

Giros B, El Mestikawy S, Bertrand L, Caron MG (1991) Cloning and functional characterization of a cocaine-sensitive dopamine transporter. FEBS Lett 295:149–154.

Giros B, Jaber M, Jones SR, Wightman RM, Caron MG (1996) Hyperlocomotion and indifference to cocaine and amphetamine in mice lacking the dopamine transporter. Nature 379:606–612.

Glendenning KK, Baker BN, Hutson KA, Masterton RB (1992) Acoustic chiasm V: inhibition and excitation in the ipsilateral and contralateral projections of LSO. J Comp Neurol 319:100–122.

Groenewegen HJ, Berendse HW, Wolters JG, Lohman AHM (1990) The anatomical relationship of the prefrontal cortex with the striatopallidal system, the thalamus and the amygdala: evidence for a parallel organization. Prog Brain Res 85:95–118.

Gu Q, Singer W (1995) Involvement of serotonin in developmental plasticity of kitten visual cortex. Eur J Neurosci 7:1146–1153.

Hansson SR, Mezey E, Hoffman BJ (1998) Serotonin transporter messenger RNA in the developing rat brain: early expression in serotonergic neurons and transient expression in non-serotonergic neurons. Neuroscience 83:1185–1201.

Helton RA, Harrison WA, Kelley K, Kane MA (1993) Melatonin interactions with cultured murine B16 melanoma cells. Melanoma Res 3:403–413.

Jaeger CB, Ruggiero DA, Albert VR, Joh TH, Reis DJ (1984) Immunocytochemical localization of aromatic-L-amino acid decarboxylase. In: Handbook of chemical neuroanatomy, Vol 2, Classical transmitters in the CNS, Pt I (Bjorklund A, Hokfelt T, eds), pp 387–408. Amsterdam: Elsevier.

Joh TH, Ross ME (1983) Preparation of catecholamine synthesizing enzymes as immunogen for immune histochemistry. In: Immunochemistry, IBRO Handbook series, Vol 3 (Cuello AC, ed), pp 121–151. Chichester, England: Wiley.

Kandler K, Friauf E (1995) Development of glycinergic and glutamater-

gic synaptic transmission in the auditory brainstem of perinatal rats. J Neurosci 15:6890–6904.
Kim JJ, Shih JC, Chen K, Chen L, Bao S, Maren S, Anagnostaras SG, Fanselow MS, De Maeyer E, Seif I, Thompson RF (1997) Selective enhancement of emotional, but not motor, learning in monoamine oxidase A-deficient mice. Proc Natl Acad Sci USA 94:5929–5933.
Koester SE, O'Leary DDM (1994) Axons of early generated neurons in cingulate cortex pioneer the corpus callosum. J Neurosci 14:6608–6620.
Kolb B, Gibb R (1990) Anatomical correlates of behavioural change after neonatal prefrontal lesions in rats. Prog Brain Res 85:241–256.
Ladvas AA, Blue ME, Lincoln J, Parnavelas JG (1997) Serotonin promotes the differentiation of glutamate neurons in organotypic slice cultures of the developing cerebral cortex. J Neurosci 17:7872–7880.
Lebrand C, Cases O, Aldebrecht A, Doye A, Alvarez C, El Mestikawy S, Seif I, Gaspar P (1996) Transient uptake and storage of serotonin in developing thalamic neurons. Neuron 17:823–835.
Lebrand C, Cases D, Wehrle R, Blakely RD, Edwards RH, Gaspar P (1998) Transient developmental expression of monoamine transporters in the rodent forebrain. J Comp Neurol, in press.
Lenders JW, Brunner HG, Murphy DL, Eisenhofer G (1998) Genetic deficiencies of monoamine oxidase enzymes: a key to understanding the function of the enzyme in humans. Adv Pharmacol 42:297–301.
Levitt P, Harvey JA, Friedman E, Simansky K, Murphy EH (1997) New evidence for neurotransmitter influences on brain development. Trends Neurosci 20:269–274.
Lichtensteiger W, Mutzner U, Langemann H (1967) Uptake of 5-hydroxytryptamine and 5-hydroxytryptophan by neurons of the central nervous system normally containing catecholamines. J Neurochem 14:489–497.
Lidov HGW, Molliver ME (1982a) An immunohistochemical study of serotonin neuron development in the rat: ascending pathways and terminal fields. Brain Res Bull 8:389–430.
Lidov HGW, Molliver ME (1982b) Immunohistochemical study of the development of serotonergic neurons in the rat CNS. Brain Res Bull 9:559–604.
Liu C, Weaver DR, Jin X, Shearman LP, Pieschl RL, Gribkoff VK, Reppert SM (1997) Molecular dissection of two distinct actions of melatonin on the suprachiasmatic circadian clock. Neuron 19:91–102.
Moiseiwitsch JR, Lauder JM (1995) Serotonin regulates mouse cranial neural crest migration. Proc Natl Acad Sci USA 92:7182–7186.
Moore DR, Russel FA, Cathcart NC (1995) Lateral superior olive projections to the inferior colluculus in normal and unilaterally deafened ferrets. J Comp Neurol 357:204–216.
Nelson N, Lill H (1994) Porters and neurotransmitter transporters. J Exp Biol 196:213–228.
Nirenberg MJ, Chan J, Vaughan RA, Uhl GR, Kuhar MJ, Pickel VM (1997) Immunogold localization of the dopamine transporter: an ultrastructural study of the rat tegmental area. J Neurosci 17:5255–5262.
Ojima K, Abiru H, Fukui Y (1996) Effects of cocaine on the rat cerebral commissure. Int J Dev Neurosci 14:649–654.
Pacholczyk T, Blakely RD, Amara SG (1991) Expression cloning of a cocaine- and antidepressant-sensitive human noradrenaline transporter. Nature 350:350–354.
Paxinos G, Tork I, Tecott LH, Valentino KL (1991) Atlas of the developing rat brain. San Diego: Academic.
Price JL, Slotnick BM (1983) Dual olfactory representation in the rat thalamus: an anatomical and electrophysiological study. J Comp Neurol 215:63–77.
Rhoades RW, Bennett-Clarke CA, Chiaia NL, White FA, McDonald GJ, Haring JH, Jacquin MF (1990) Development and lesion induced reorganization of the cortical representation of the rat's body surface as revealed by immunochemistry for serotonin. J Comp Neurol 293:190–207.
Rhoades RW, Bennett-Clarke CA, Shi MY, Mooney RD (1994) Effects of 5-HT on thalamocortical synaptic transmission in the developing rat. J Neurophysiol 72:2438–2450.
Rietzel H-J, Friauf E (1998) Neuron types in the rat superior olive and developmental changes in the complexity of their dendritic arbors. J Comp Neurol 390:20–40.
Roberts VJ, Dong WK (1994) The effect of thalamic nucleus submedius lesions on nociceptive responding in rats. Pain 57:341–349.
Saint Marie RL (1996) Glutamatergic connections of the auditory midbrain: selective uptake and axonal transport of D-(^{3}H)aspartate. J Comp Neurol 373:255–270.
Sapolsky RM, Eichenbaum H (1980) Thalamocortical mechanisms in odor-guided behavior. II. Effects of lesions of the mediodorsal thalamic nucleus and frontal cortex on odor preferences and sexual behavior in the hamster. Brain Behav Evol 17:276–290.
Schambra UB, Lauder JM, Silver J (1992) Atlas of the prenatal mouse brain. San Diego: Academic.
Shaskan EG, Snyder SH (1970) Kinetics of serotonin accumulation into slices from rat brain: relationship to catacholamine uptake. J Phar Exp Ther 175:404–418.
Shneiderman A, Henkel CK (1987) Banding of lateral superior olivary nucleus afferents in the inferior colliculus: a possible substrate for sensory integration. J Comp Neurol 266:519–534.
Slotnik BM, Kaneko N (1981) Role of the mediodorsal thalamic nucleus in olfactory discrimination learning in rats. Science 214:91–92.
Steinbusch HWM (1981) Distribution of serotonin-immunoreactivity in the central nervous system of the rat-cell bodies and terminals. Neuroscience 6:557–618.
Steinbusch HWM, Verhofstad AAJ, Joosten HWJ, Golstein M (1982) Serotonin-immunoreactive cell bodies in the nucleus dorsomedialis hypothalami, in the substantia nigra, and in the area tegmentalis ventralis of Tsai: observations after pharmacological manipulations in the rat. In: Cytochemical methods in neuroanatomy, pp 407–421. New York: Liss.
Upton AL, Lebrand C, Salichon N, Ezan P, Seif I, Gaspar P (1997) Serotonin uptake in retinal ganglion cells during development of normal and MAOA-knockout mice. Soc Neurosci Abstr 23:639.
van den Pol AN (1986) Gamma-aminobutyrate, gastrin releasing peptide, serotonin, somatostatin, and vasopressin: ultrastructural immunocytochemical localization in presynaptic axons in the suprachiasmatic nucleus. Neuroscience 17:643–659.
van den Pol AN, Tsujimoto KL (1985) Neurotransmitters of the hypothalamic suprachiasmatic nucleus: immunocytochemical analysis of 25 neuronal antigens. Neuroscience 15:1049–1086.
Vanhatalo S, Soinila S (1994) Pharmacological characterization of serotonin synthesis and uptake suggest a false neurotransmitter role for serotonin in the pituitary intermediate lobe. Neurosci Res 21:143–149.
Vitalis T, Cases O, Callebert J, Launay JM, Price DJ, Seif I, Gaspar P (1998) Effects of monoamine oxidase A inhibition on barrel formation in the mouse somatosensory cortex. Determination of a sensitive developmental period. J Comp Neurol 393:169–184.
Wallace JA, Lauder JM (1983) Development of the serotonergic system in rat embryo: an immunocytochemical study. Brain Res Bull 10:459–479.
Yoshida A, Dostrovsky JO, Sessle BJ, Chiang CY (1991) Trigeminal projections to the nucleus submedius of the thalamus in the rat. J Comp Neurol 307:609–625.
Yoshida A, Dostrovsky JO, Chiang CY (1992) The afferent and efferent connections of the nucleus submedius in the rat. J Comp Neurol 324:115–133.

Defects of Tyrosine Hydroxylase-Immunoreactive Neurons in the Brains of Mice Lacking the Transcription Factor Pax6

Tania Vitalis,[1] Olivier Cases,[1,2] Dieter Engelkamp,[3] Catherine Verney,[2] and David J. Price[1]

[1]Department of Biomedical Sciences, Medical School, Edinburgh EH8 9AG, Scotland, [2]Institut National de la Santé et de la Recherche Médicale U106, Hôpital de la Salpêtrière, 75651 Paris Cedex 13, France, and [3]Medical Research Council Human Genetics Unit, Western General Hospital, Edinburgh, EH4 2XU, Scotland

In the CNS, the lack of the transcription factor Pax6 has been associated with early defects in cell proliferation, cell specification, and axonal pathfinding of discrete neuronal populations. In this study, we show that Pax6 is expressed in discrete catecholaminergic neuronal populations of the developing ventral thalamus, hypothalamus, and telencephalon. In mice lacking Pax6, these catecholaminergic populations develop abnormally: those in the telencephalon are reduced in cell number or absent, whereas those in the ventral thalamus and hypothalamus are greatly displaced and densely packed. Catecholaminergic neurons of the substantia nigra (SN) and the ventral tegmental area (VTA) do not express Pax6 protein. Nevertheless, mice lacking Pax6 display an altered pathfinding of SN–VTA projections: instead of following the route of the medial forebrain bundle ventrally, most of the SN–VTA projections are deflected dorsorostrally at the pretectal–dorsal thalamic transition zone and in the dorsal thalamic alar plate. Moreover, some catecholaminergic neurons are displaced dorsally to an ectopic location at the pretectal–dorsal thalamic transition zone. Interestingly, from the pretectal–dorsal thalamic to the dorsal thalamic–ventral thalamic transition zones, mice lacking Pax6 display an ectopic ventral to dorsal expansion of the chemorepellant/chemoattractive molecule, Netrin-1. This may be responsible for both the altered pathway of catecholaminergic fibers and the ectopic location of catecholaminergic neurons in this region.

Key words: catecholaminergic neuron; Pax6; netrin; proliferation; adhesion; axonal pathfinding

Recently, a neuromeric model for catecholaminergic (CA) neuronal development has been proposed in several species, including lizard (Medina et al., 1994), chick (Puelles and Medina, 1994), and human (Puelles and Verney, 1998). In this model, it is proposed that permanent or transient CA (dopaminergic and noradrenergic) neurons are generated in or near the region that they occupy in the adult, rather than being generated at a few localized sources and distributed through migration (Olson and Seiger, 1972). Despite the apparent anatomical diversity of noradrenergic (NA) and dopaminergic (DA) neurons, it appears that their early specification relies on a small number of molecules. For instance, essential transcription factors such as Mash1, Phox2a, and Phox2b have been implicated in controlling the specification of all noradrenergic neurons (Pattyn et al., 1997; Hirsh et al., 1998). It appears that the two secreted molecules sonic hedgehog (SHH) and fibroblast growth factor 8 are critical for the specification of DA neurons, and the stereotypic location of most DA neurons along the anteroposterior and dorsoventral axes is defined by the integration of these two signals (Ye et al., 1998).

Gene expression studies have shown that the transcription factor Pax6 is transiently expressed in areas containing discrete CA neurons in the mesencephalon, the ventral thalamus, the hypothalamus (Stoykova and Gruss, 1994), and the olfactory bulb (Dellovade et al., 1998). *Pax6* is a member of a highly conserved gene class and encodes a transcription factor containing a paired domain and a homeodomain (Callaerts et al., 1997). The spatiotemporal expression of *Pax6*, from E8.5 to adulthood, suggested that Pax6 plays key roles in CNS development (Walther and Gruss, 1991). Indeed, mice lacking Pax6 display early defects in axonal pathfinding (Mastick et al., 1997), in the specification of several prosomeric transition zones (Stoykova et al., 1996; Grindley et al., 1997), in cell proliferation (Warren and Price, 1997), in the specification of motor (Ericson et al., 1997) cell subtypes, and in cell migration (Caric et al., 1997; Brunjes et al., 1998; Engelkamp et al., 1999).

In the present study, we first defined the localization of the Pax6 protein in CA [tyrosine hydroxylase-immunoreactive (TH-IR)] populations during development. We then investigated the role of Pax6 in these populations by looking at their development in mice lacking Pax6. We found that developing TH-IR neurons of the ventral thalamus [zona incerta (Zi)], hypothalamus (paraventricular nucleus), olfactory bulb, and basal telencephalon (anterior olfactory nucleus, piriform cortex, anterior amygdala, and olfactory tubercle) display high levels of Pax6 protein during a critical period of their development. Despite severe positional alterations, diencephalic and hypothalamic TH-IR neurons were identified in mice lacking Pax6, showing that Pax6 is not necessary for their specification. In contrast, TH-IR neurons were greatly reduced in number in the basal telencephalon and the remaining olfactory bulb. In addition, we found that ectopic TH-IR neurons were distributed ventrodorsally along the pretectal–dorsal thalamic transition zone and that TH-IR fibers were misguided in this zone and in the dorsal thalamic alar plate. Interestingly, this region displayed an increased and ectopic expression of the SHH-induced chemorepellant/chemoattractive molecule, Netrin-1 (Leonardo et al., 1997; Lauderdale et al., 1998), which might contribute to its having altered cues for cell migration and axonal navigation.

MATERIALS AND METHODS

Animals. The original small-eye ($Pax6^{scy}$) mutation arose spontaneously in a stock called "CSR" and was subsequently outcrossed. The genetic background of the small-eye strain used in this study was derived from the

Received Feb. 22, 2000; revised May 1, 2000; accepted June 14, 2000.

This work was funded by the European Commission (BMH4 CT97-2412), the University of Edinburgh, the Institut National de la Santé et de la Recherche Médicale, and the Centre National de la Recherche Scientifique. We thank Luis Puelles, Patricia Gaspar, and Veronica van Heyningen for helpful discussions during the preparation of this manuscript. We thank Matt Kaufman for mutant mice and for his advice throughout this study. We thank Marc Tessier-Lavigne and Andreas Puschel for kindly providing excellent probes, cheerful encouragement, and advice. We thank Linda Sharp for confocal assistance and Grace Grant for efficient technical help. We also greatly thank Brendan McGrory for his enthusiasm and patient assistance with photography.

Correspondence should be addressed to Tania Vitalis, Department of Biomedical Sciences, Medical School, Teviot Place, Edinburgh, EH8 9AG, Scotland. E-mail: tvitalis@srv4.med.ed.ac.uk.

Dr. Engelkamp's present address: Max Planck Institut für Hirnforschung, Deutschordenstrasse 46, 60528 Frankfurt, Germany.

 0270-6474/00/206501-16$15.00/0

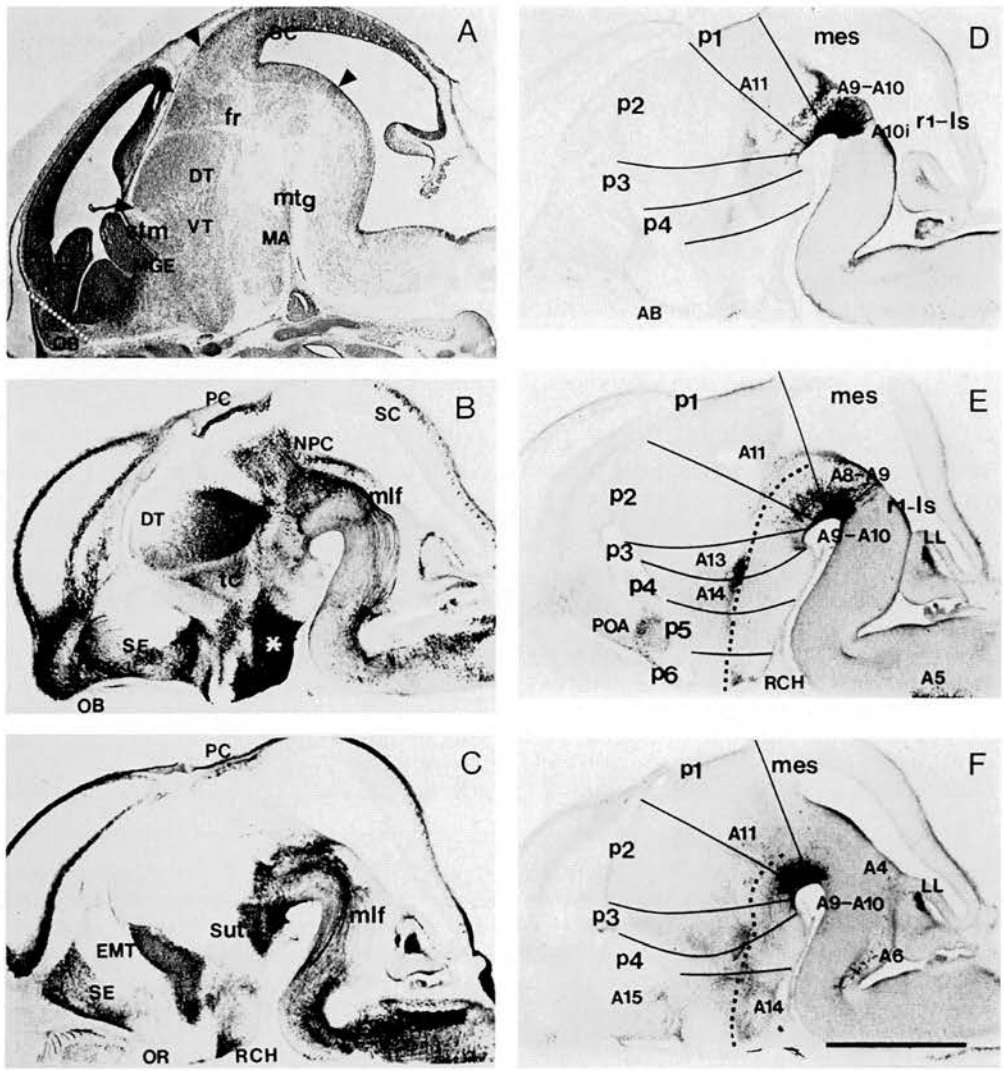

Figure 1. Determination of the neuromeric organization of TH-IR neurons in E14.5 wild-type embryos. Sagittal sections stained for Nissl (*A*) or immunoreacted for calbindin (*B*) or calretinin (*C*) have provided the prosomeric landmarks used for the determination of the segmental organization of TH-IR groups as shown in *D–F*. *A*, The section shows constrictions in the neural wall and regions of low cell densities associated with prosomeric boundaries. *Arrowheads* indicate, from caudal to rostral, the isthmic constriction, the caudal limit of the posterior commissure (*PC*) at the mesencephalic (*mes*)–p1 boundary, the fasciculus retroflexus (*fr*) at the p1–p2 boundary (in *p2*), and the stria medullaris (*stm*) at the p3–p4 boundary. The *dotted line* represents the angle used for coronal sectioning. *B*, Calbindin immunoreactivity shows the posterior commissure in the roof of p1, the nucleus of the posterior commissure (*NPC*) in p1, the dorsal thalamus (*DT*) in p2 alar plate, and thalamocortical axons (*tc*) running through p3 alar plate. The *asterisk* marks a strong immunoreactive hypothalamic region in p5 and p6 basal plate. The septum (*SE*) and olfactory bulb (*OB*) are also strongly immunoreactive. *C*, Calretinin immunoreactivity shows the posterior commissure, the subthalamic nucleus (*Sut*) in p4 basal plate, the thalamic eminence (*EMT*) in p4 alar plate, and the retrochiasmatic area (*RCH*) in p6 basal plate. The septum (*SE*) is also strongly immunolabeled. *D–F*, The prosomeric boundaries (*continuous black lines*) and basal–alar limit (*dotted lines*) are deduced from the adjacent sections stained for calretinin or calbindin. Note that *B*, *C*, and *E* are alternate sections. *D*, Medial section showing a subgroup of A11 organized along the fasciculus retroflexus and the A9–A10 complex. Note that A9 is located in the basal plate and extends from mes to p2, whereas A10 is located in the floor plate and extends from the isthmic (*A10i*) region to p3. *E*, A more lateral section than shown in *D* showing A11 extending from mes to p2 and the diencephalic and hypothalamic groups: *A13* in *p3*, *A14* in *p4*, and *RCH* and anterior preoptic (*POA*) areas in p6. *F*, A lateral section shows additional groups in the hypothalamus (*A14* subgroups in p5 basal and alar plates) and in the telencephalon (*A15*). *AB*, Anterobasal nucleus; *Is*, isthmus; *LGE*, ganglionic eminence, lateral part; *LL*, lateral lemniscal area; *MA*, mammillary region; *mes*, mesencephalon; *MGE*, ganglionic eminence, medial part; *mlf*, medial longitudinal fasciculus; *mtg*, mammillotegmental tract; *OR*, optic recess; *p1–p3*, prosomeres; *r1*, rhombomere 1; *SC*, superior colliculus. Scale bar, *A–F*, 4 mm.

outbred Swiss background. The mating of Pax6^{sey}/+ (small-eye heterozygotes) was confirmed by the presence of a vaginal plug the following morning. This was designated embryonic day 0.5 (E0.5). Experiments were performed on E11.5, E12.5, E13.5, E14.5, E16.5, E17.5, and E18.5 embryos. Embryos were dissected from deeply anesthetized mothers into cold PBS on ice and examined under a dissecting microscope. Homozygous Pax6^{sey}/Pax6^{sey} embryos were easily distinguished by their absence of eyes and characteristic craniofacial phenotype of foreshortened upper jaw. From E12.5, heterozygotes (Pax6^{sey}/+) were distinguished by the characteristic appearance of their iris lacking its inferior margin (Kaufman et al., 1995). In each experiment, wild-type and Pax6^{sey}/Pax6^{sey} embryos were obtained from the same litter. Some additional experiments were also performed on embryos and postnatal and adult mice of the Swiss genetic background. Animal procedures were conducted in strict compliance with approved institutional protocols and in accordance with the provisions for animal care and use described in the *Scientific Procedures on Living Animals ACT 1986*. In all the experiments, adult mice were anesthetized with 0.3 ml 25% urethane injected intraperitoneally.

Immunocytochemistry. E11.5, E12.5, and E13.5 embryos were fixed by immersion in 4% paraformaldehyde in 0.1 M phosphate buffer (PB), pH 7.6. Embryos from E14.5 to E19.5 and postnatal mice were perfused transcardially with saline followed by 4% paraformaldehyde in PB. Whole embryos or brains were post-fixed for 2–5 d in the same fixative and cryoprotected in 30% sucrose in PB. Serial coronal or sagittal sections (40 μm) were cut on a freezing microtome and immediately processed for immunocytochemistry. In brief, sections were incubated with the primary antibodies diluted in PBS+ (0.1 M PBS with 0.2% gelatin and 0.25% Triton X-100) overnight at 4°C. Rabbit polyclonal anti-TH antibodies (1:8000, kind gift of A. Vigny, or 1:800, Protos Biotech), rabbit polyclonal anti-calretinin antibody (1:10,000: Swant), rabbit polyclonal anti-calbindin antibody (1:20,000; Swant), rat monoclonal anti-L1 antibody (1:50, Roche Diagnostics), and rat monoclonal anti-NCAM antibody (1:50; Roche Diagnostics) were used. Biotinylated goat anti-rabbit and biotinylated goat anti-rat (1:200, Dako, Glostrup, Denmark) were used as secondary antibodies and revealed with a streptavidin–biotin–peroxidase complex (1:200, Amersham, Buckinghamshire, UK). Sections were then reacted with a solution containing 0.02% diaminobenzidine, 0.6% nickel ammonium sulfate, and 0.003% H_2O_2 in 0.05 M Tris buffer, pH 7.6 (DAB-Ni). From these sections, the total number of TH-IR neurons in A14 paraventricular hypothalamic nucleus (PAVH) and the diameters of randomly selected TH-IR neurons (n = 20) were measured in A14PAVH from E17.5 wild-type (n = 4) and Pax6^{sey}Pax6^{sey} (n = 4) embryos.

Double Pax6 and TH immunocytochemistry. Whole embryos (E11.5, E12.5, E14.5, E16.5, E17.5, and E18.5) and dissected postnatal (P0, P2, P4, and P9) and adult brains (5 and 16 weeks old) were immediately frozen in isopentane (−40°C) and stored at −80°C until sectioning. Coronal and sagittal sections (10–14 μm) were cut on a cryostat and processed the same day. Sections were dried at room temperature, fixed for 10 min in methanol/acetone (1:1; −20°C), dried for 15 min at room temperature, hydrated for 5 min in PBS, and blocked for 15 min in a solution containing 2% bovine serum albumin, 2% sheep serum, 7% glycerol, and 0.2% Tween 20 (BS). Sections were then incubated overnight at room temperature with three different antibodies: a rabbit polyclonal anti-TH antibody (1:5000, kind gift of A. Vigny) and two mouse monoclonal anti-PAX6 antibodies [AD1.5.6 and AD2.35; 1:50 in embryos and 1:30 in adults (Engelkamp et al., 1999)] diluted in BS. Sections were washed in PBS 0.2% Tween 20 (PBST) and incubated for 1 hr with secondary antibodies [TRITC anti-mouse antibody, 1:200 (Vector Laboratories, Burlingame, CA), and FITC anti-rabbit antibody, 1:200 (Sigma, St. Louis, MO)], diluted in PB. Sections were washed in PBST and analyzed with a Leica (Nussloch, Germany)

Table 1. Mapping of the main TH-IR groups in E14.5 mouse brain

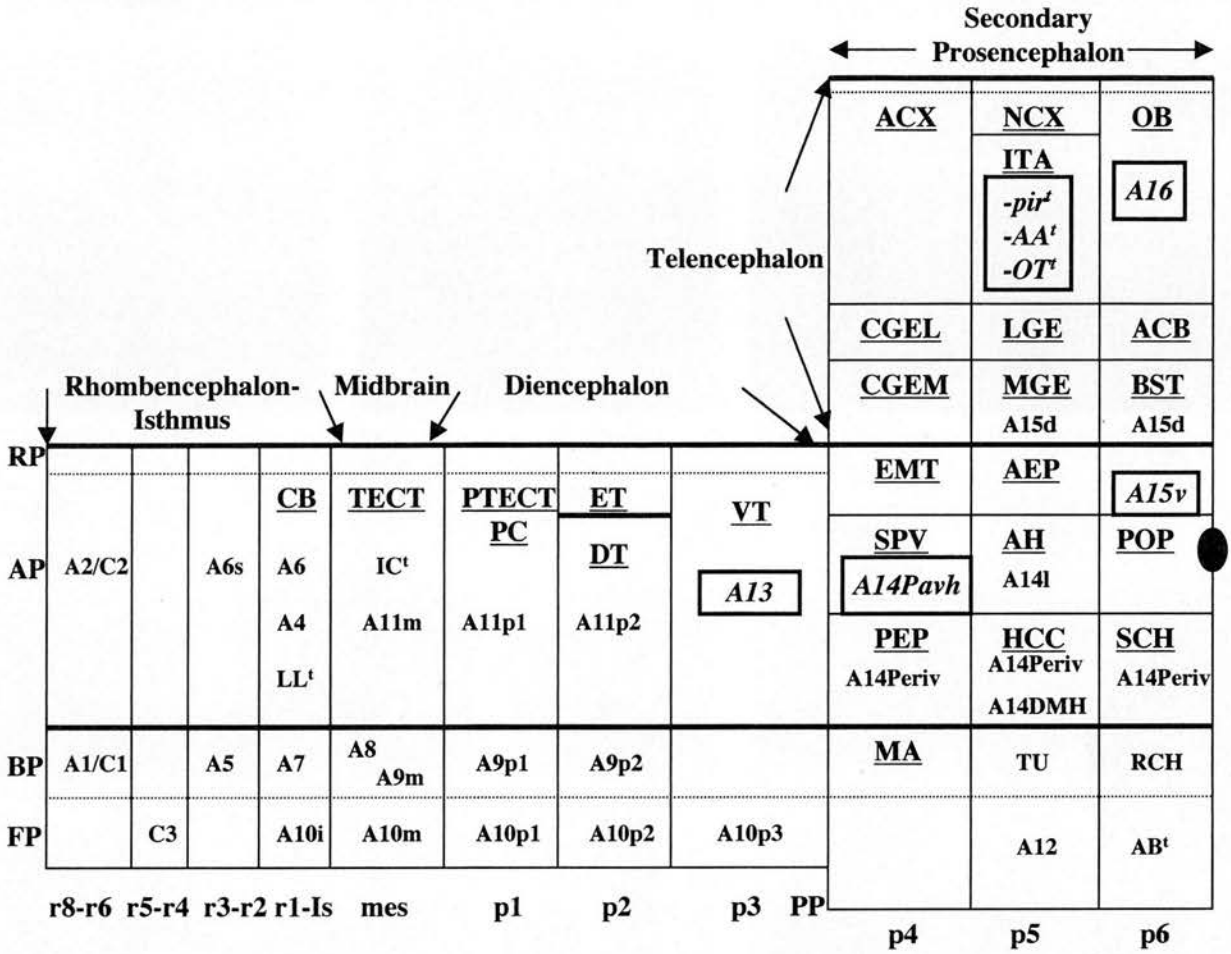

We used the same neuromeric criteria as those applied to describe the early neuromeric TH-IR neurons in human embryos (Puelles and Verney, 1998). According to the models described in Lumsden (1990), Krumlauf (1994), Rubenstein et al. (1994), Puelles (1995), and Guthrie (1996) (see also Material and Methods, Nomenclature), the different neuromeres are individualized by longitudinal and transverse black bars, and the different histogenetic fields are labeled in black capitals. The optic recess is marked with a black circle. In this scheme, the different TH-IR groups are mapped. Groups displaying a transient tyrosine hydroxylase immunoreactivity are labeled with a superscript "t". Each subgroup was labeled according to its location; for instance, the isthmic component of A10 is labeled A10i where "i" stands for the isthmus, except for the transient TH-IR groups located in the piriform cortex (pir), the anterior amygdala (AA), and the olfactory tubercle (OT), which appear in the intermediate telencephalic territory (ITA), the region from which they are supposed to be derived (Fernandez et al., 1998). TH-IR groups displaying Pax6 immunoreactivity appear in boxed black italics. A1–A17, Catecholaminergic groups; AB, anterobasal nuclei; ACB, nucleus accumbens; ACX, archicortex; AEP, entopeduncular area; AH, anterior hypothalamus; AP, alar plate; BP, basal plate; BST, bed nucleus of stria terminalis; C1–C3, putative adrenergic groups; CB, cerebellar primordium; CGEL, caudal ganglionic eminence, lateral part; CGEM, caudal ganglionic eminence, medial part; DMH, dorsal medial hypothalamic nucleus; DT, dorsal thalamus; ET, epithalamus; FP, floor plate; HCC, hypothalamic cell cord; IC, inferior colliculus; Is, isthmus; LGE, lateral ganglionic eminence; LL, lateral lemniscus; MA, mammillary region; mes, mesencephalon; MGE, medial ganglionic eminence; OB, olfactory bulb; p1–p6, prosomeres; PC, posterior commissure; PAVH, paraventricular hypothalamic nucleus; PEP, posterior entopeduncular area; PF, prechordal floor plate; POA, anterior preoptic area; POP, posterior preoptic area; PP, prechordal plate; PTECT, pretectum; r1–r8, rhombomeres; RCH, retrochiasmatic nucleus; RP, roof plate; SCH, suprachiasmatic nucleus; SPV, supraoptic/paraventricular region; EMT, thalamic eminence; TECT, midbrain tectum; TU, tuberal hypothalamic region; VT, ventral thalamus.

confocal microscope. In addition, alternate sections immunostained with anti-TH antibody or anti-PAX6 antibody or Nissl-stained were analyzed in parallel.

Morphometric analysis. Free-floating sections (45 μm) were processed for TH immunocytochemistry as described above, except that immunolabeling was revealed using an FITC anti-rabbit antibody (1:200, Dako). Propidium iodide, a nuclear dye (1/10,000, Molecular Probes, Eugene, OR), was added during the last 10 min of incubation with the secondary antibody. Our analysis was performed on sections obtained from four wild-type and four Pax6^{sey}/Pax6^{sey} embryos. In each case, seven sections from wild-type embryos and five sections from Pax6^{sey}/Pax6^{sey} embryos taken through the Zi and the dorsomedial hypothalamic nucleus (DMH) were selected. By confocal microscopy (Leica), each section was resectioned into serial 7-μm-thick sections. To estimate the volume of A13 and A14DMH in wild-type and Pax6^{sey}/Pax6^{sey} embryos, the surface area of these nuclei in each section was measured using Leica TCNS software. For each brain, volumes were obtained by multiplying each area by the thickness of tissue between sections and summing the values. To estimate cell densities in A13 and A14DMH, the same sections were analyzed. In the areas defined by TH immunoreactivity, all propidium-labeled nuclei and all cells with a visible TH immunostaining were counted, and the averages of total cell density and of TH-IR neuronal density (per millimeter cubed) were calculated for each nucleus. From these sections, the diameters of randomly selected TH–IR neurons (n = 30) were measured in A13 and A14DMH in wild-type and Pax6^{sey}/Pax6^{sey} embryos using the same software.

Proliferation of tyrosine hydroxylase neurons. Pregnant mice were injected with a single dose of bromodeoxyuridine (BrdU; 25 mg/kg in sterile saline, i.p.) on E9.75, E10.5, E11.5, and E12.5 and were killed when embryos reached E17.5. Embryos were perfused transcardially with saline followed by 4% paraformaldehyde in PB, and brains were dissected, post-fixed overnight in the same fixative, and cryoprotected in 10% sucrose in PB. Brains were embedded in a solution containing 7% gelatin and 10% sucrose and frozen in isopentane. Alternate coronal sections (20 μm) were cut on a cryostat and processed for sequential immunolabeling. Half of the alternate sections were reacted for both TH and BrdU. Sections were first processed for TH immunocytochemistry as described above except that only DAB was used (0.03% DAB, 0.01% hydrogen peroxide in 0.1 M PBS). Then, sections were washed in TBS (0.09% NaCl, 50 mM Tris, pH 7.6), incubated for 8 min in 1 M HCl at 60°C, washed for 4 min with tap water, rinsed in TBS, incubated for 10 min in 20% rabbit serum in TBS, and finally incubated overnight with a solution containing mouse anti-BrdU (1:200, Becton-Dickinson) in 20% rabbit serum–TBS. Sections were washed in TBS, incubated for 2 hr with a biotinylated rabbit anti-mouse (1:200, Dako) in 20% rabbit serum–TBS, washed in TBS, incubated with a streptavidin–biotin–peroxidase complex (1:200, Amersham) for 2 hr at room temperature, and revealed with the DAB-Ni protocol (see above). The other half was Nissl-stained. To estimate the number of BrdU-labeled

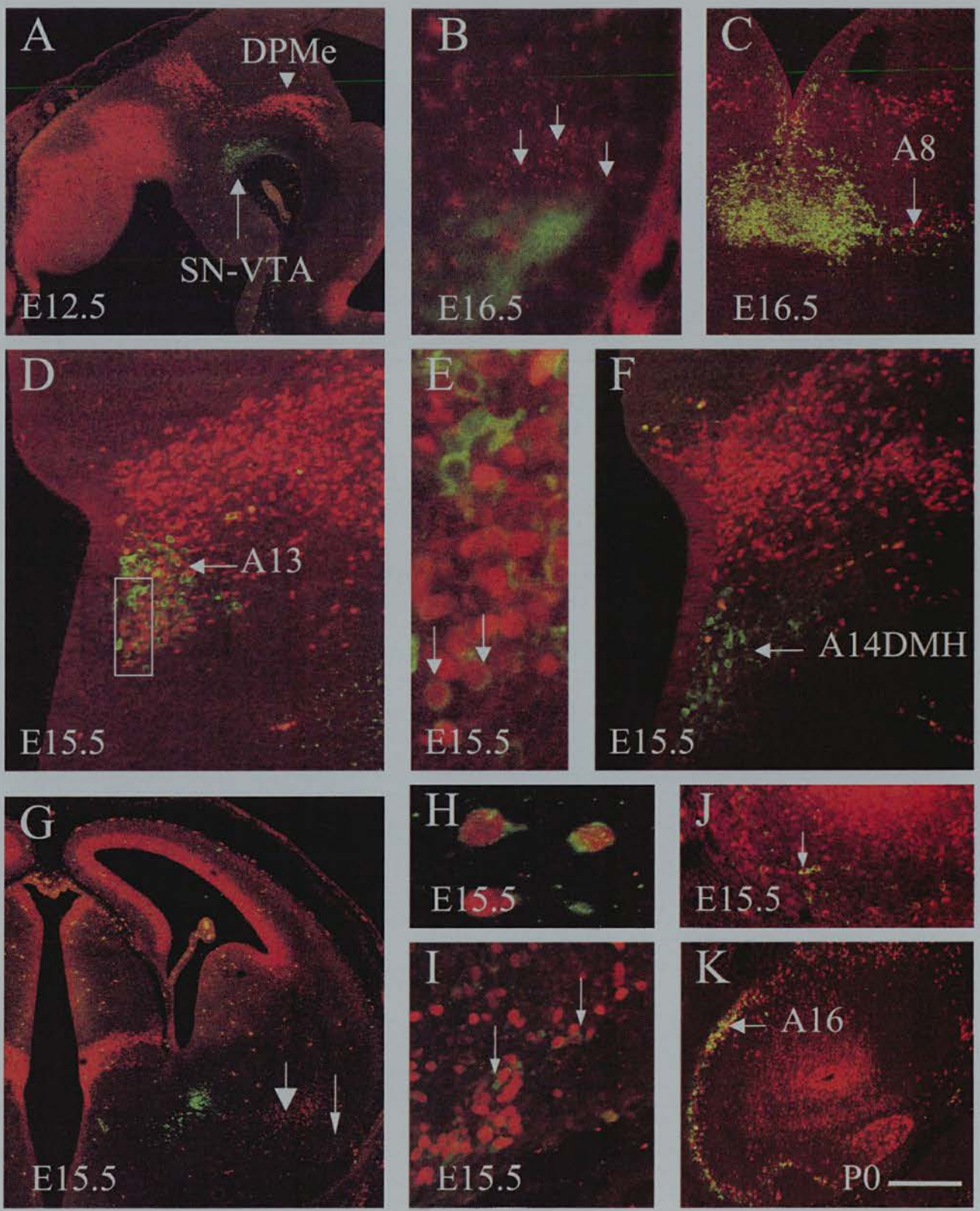

Figure 2. Pax6 protein expression in discrete developing TH-IR groups. Sections through the A8–A10 complex (*A–C*), the diencephalon and the hypothalamus (*D–F*), and the telencephalon (*G–K*) were double-immunostained with antibodies to TH (*green*; cytoplasmic staining) and Pax6 (*red*; nuclear staining). *A–C*, Absence of Pax6 and TH colocalization in the SN–VTA (A9–A10) complex and the retrorubral field (A8). *A*, The sagittal section shows a lack of Pax6 immunoreactivity in the developing SN–VTA of E12.5 embryo. Note the strong Pax6 immunolabeling of the deep mesencephalic nucleus (*DPMe*). *B*, The coronal section shows Pax6 immunoreactive cells (*short arrows*) in close proximity with TH-IR neurons of the dorsal part of the SN in E16.5 embryo. *C*, The coronal section shows Pax6 immunoreactive cells in the retrorubral field close to A8 neurons. *D*, The coronal section shows the colocalization of TH and Pax6 in A13 neurons of the zona incerta in the ventral thalamus. *E*, Higher magnification of the *box* shown in *D* showing individual double-immunolabeled cells *(white arrows)*. Note the presence of TH-IR neurons (A13d) that do not express Pax6 (*white arrow*). *F*, The coronal section shows the lack of Pax6 immunoreactivity in A14DMH neurons of the hypothalamus. *G*, Coronal section showing Pax6-immunoreactive cells in the basal telencephalon. Pax6-immunoreactive cells are located in the anterior amygdala (*large arrowhead*) and the region of the piriform cortex (*small arrowhead*). Note Pax6 immunoreactive cells also in the cerebral cortex, hypothalamus, and ventral thalamus. *H*, Higher (*Figure legend continues*)

cells, a minimum of six sections taken through Zi and DMH were selected. On each section, A13 and A14DMH were identified, and the number of TH-IR neurons heavily labeled (defined as having >50% of the nucleus immunolabeled) for BrdU was estimated using 40× and 100× objectives. Only heavily labeled cells were counted because they would have been generated at the time of BrdU administration, whereas many lightly labeled cells would have been the products of further progenitor cell divisions (Gillies and Price, 1993). For each age of BrdU injection, wild-type ($n = 4$) and Pax6^{sey}/Pax6^{sey} ($n = 4$) embryos were obtained from at least two independent litters. In addition, the total number of TH-IR neurons in A13 and A14DMH was estimated from these sections in wild-type ($n = 6$) and Pax6^{sey}/Pax6^{sey} ($n = 6$) embryos.

Nissl staining and counterstaining. Complete series of parasagittal and coronal paraffin sections (10 μm) obtained from E11.5, E12.5, E14.5, E16.5, and E18.5 wild-type and Pax6^{sey}/Pax6^{sey} embryos were Nissl-stained in a solution containing 0.05% thionin in acetic acid, pH 5.5.

In situ *hybridization.* E11.5, E12.5, E13.5, E14.5, E16.5, and E19.5 wild-type and Pax6^{sey}/Pax6^{sey} embryos were dissected in PBS, fixed, and cryoprotected overnight in 4% paraformaldehyde–30% sucrose. Sections (80–100 μm thick) were obtained on a freezing microtome, washed in PBS 0.1% Tween 20 (PTW), dehydrated for 20 min in methanol, and rehydrated in PTW before hybridization. Hybridization was performed as described in Henrique et al. (1995). Briefly, sections were treated with proteinase K (10 mg/ml) for 10 min, rinsed in PTW, fixed for 20 min in 4% paraformaldehyde–0.2% glutaraldehyde, rinsed in PTW, rinsed in the hybridization medium (50% formamide, 1.3× SSC, 50 mM EDTA, 0.2% Tween 20, 10% 3-[(3-cholamidopropyl)dimethylammonio]-1-propanesulfonic acid, 100 mg/ml heparin) at room temperature until the sections settled, and rinsed in the hybridization medium (HM) at 65°C before hybridization. Sections were then hybridized overnight at 65°C with digoxigenin-labeled (Roche Diagnostics) riboprobes for Netrin-1 (kind gift of M. Tessier-Lavigne; *Eco*RI, T3: antisense; *Sac*I, T7: sense) or Pax6 (kind gift of S. Saule; *Pst*I, T3: antisense; *Hin*dIII, T7: sense). The following day, sections were rinsed in HM (2 × 30 min, 65°C), washed in a 1:1 mixture of HM and MABT (100 mM maleic acid, 150 mM NaCl, pH 7.5, 0.1% Tween 20) for 10 min at 65°C and 15 min at room temperature, incubated for 1 hr in MABT with 2% blocking reagent (Roche Diagnostics), and incubated for 4 hr in MABT with 2% blocking reagent and 20% heat-treated sheep serum (MABT+), and finally incubated overnight with anti-digoxigenin antibody conjugated with alkaline phosphatase (1:2000, Roche Diagnostics) in MABT+. Sections were washed in MABT for 4 hr and in a mixture of 100 mM NaCl, 100 mM Tris-HCl, pH 9.5, 50 mM $MgCl_2$, and 0.1% Tween 20 for 20 min before the enzymatic color detection with the nitro blue tetrazolium/5-bromo-4-chloro-3-indolyl phosphate substrate (Roche Diagnostics).

Nomenclature. On the basis of gene expression domains and anatomical features (constrictions in the neural wall and regions of low cell density), the brain has been subdivided into neuromeres. The rhombomeric and mesencephalic organizations have been described by Lumsden (1990), Krumlauf (1994), and Guthrie (1996), and the prosomeric organization has been described in Rubenstein et al. (1994) and Puelles (1995). Eight consecutive rhombomeres (r1–r8), the isthmus (Is), and the mesencephalon (mes) are identified in the rhombencephalon and midbrain. Note that rhombomere 1 and isthmus are represented as a single entity (r1–Is) in this scheme. According to the prosomeric model, the forebrain is subdivided into six transverse domains called prosomeres (p1–p6). The diencephalon develops in prosomeres 1–3 (p1–p3), and the secondary prosencephalon (hypothalamus, preoptic areas, and its hyper-alar extension, the telencephalon) develops in p4–p6. In addition, these transverse domains are subdivided dorsoventrally into roof plate, alar plate, basal plate, and floor plate or prechordal plate (from p4) (Shimamura at al., 1995). Telencephalic organization refers also to the work of Fernandez et al. (1998). Our anatomical description refers to the atlas of the developing rat brain (Paxinos, 1991), the atlas of the mouse brain (Franklin and Paxinos, 1995), and the chemoarchitectonic atlas of the developing mouse brain (Jacobowitz and Abbott, 1998). To describe the permanent TH-IR cell groups (A1–A17), we have mainly used the nomenclature of Hokfelt et al. (1984) and Jacobowitz and Abbott (1998). The description of the distribution of TH-IR neurons in the hypothalamus and preoptic regions also refers to the work of Ruggiero et al. (1984) and Foster (1994). A14 complex was subdivided into subgroups relative to their main anatomical locations. In addition, some transient TH-IR neuronal populations have already been described in the developing CNS (Jaeger and Joh, 1983; Verney et al., 1988; Nagatsu et al., 1990).

RESULTS

Neuromeric location of TH-immunoreactive groups in E14.5 wild-type embryos

So far, no description of the neuromeric location of permanent and transient TH-IR groups is available in developing mice despite the increasing references to the neuromeric organization of the brain (Bulfone et al., 1993; Rubenstein et al., 1994; Puelles, 1995; Shimamura et al., 1995, 1997). In this study we first provide a comprehensive neuromeric location of the different TH-IR groups in E14.5 wild-type mice. At this age, most of the permanent TH-IR groups (A1–A17) (Hokfelt et al., 1984) occupy their definitive position, some transient TH-IR groups are detected, and the neuromeric limits are still visible. The topological landmarks necessary for the description of the neuromeric organization were obtained by studying alternate sections stained for Nissl (Fig. 1*A*) or for several differentiation markers, principally, the two calcium-binding proteins calbindin (Fig. 1*B*) and calretinin (Fig. 1*C*), which display complementary immunoreactive patterns [Jacobowitz and Abbott (1998) and Fig. 1]. The neuromeric location of the main discrete TH-IR groups is shown in Figure 1*D–F* and detailed in Table 1. The description of TH-IR groups that did or did not display Pax6 immunoreactivity in wild-type mice is presented within this framework (see below and Table 1).

Colocalization of Pax6 and TH immunoreactivities

TH-immunoreactive neurons displaying Pax6 immunoreactivity (Table 1)

Pax6 immunoreactivity was detected in three dopaminergic groups of the forebrain. In the alar plate of the ventral thalamus, a subpopulation (~40%) of TH-IR neurons of the zona incerta (A13) displayed a strong and transient Pax6 immunoreactivity from E12.5 to P9 (Fig. 2*D,E*). This subpopulation corresponds to the body of A13. In the hypothalamus, TH-IR neurons of the magnocellular part of the hypothalamic paraventricular nucleus displayed transient Pax6 immunoreactivity from E14.5 to P2 (A14PAVH in Table 1; data not shown). TH-IR neurons of the supraoptic nucleus (A15v) display also a transient Pax6 immunoreactivity from P0 to P9 (Table 1; data not shown). In the telencephalon, transient TH-IR neurons located in the anterior olfactory nucleus (A16AON) displayed Pax6 immunoreactivity from E14.5 to E18.5 (Table 1; data not shown). Transient TH-IR neurons of the piriform cortex, the olfactory tubercle, and the anterior amygdala display Pax6 immunoreactivity from E14.5 to E18.5 (Fig. 2 *G–I*). In the olfactory bulb (A16OB), TH-IR external tufted cells displayed Pax6 immunoreactivity from E14.5 and TH-IR periglomerular interneurons from E18.5 (Fig. 2*J,K*, Table 1).

TH-immunoreactive neurons not displaying Pax6 immunoreactivity (Table 1)

Noradrenergic (A1–A7) and adrenergic (C1–C3) neurons of the brainstem never displayed Pax6 immunoreactivity (Table 1). Dopaminergic neurons of the ventral tegmental area (A10i, A10m, A10p1, A10p2, and A10p3) in the floor plate, of the substantia nigra (A9m, A9p1, and A9p2), and of the retrorubral field (A8) in the basal plate, and of A11 complex (A11m, A11p1, A11p2) in the alar plate did not display Pax6 immunoreactivity throughout development (Fig. 2*A–C*). In the hypothalamus, the TH-IR groups listed below did not display Pax6 immunolabeling at any stage of development: the lateral hypothalamic nucleus (A14l), the medial preoptic area (POA and A14d), the arcuate nucleus (A12). In the telencephalon, TH-IR neurons of the bed nucleus of the stria terminalis (A15d) did not display Pax6 immunoreactivity. Al-

←

magnification of *G* showing individual double-labeled neurons at the level of the anterior amygdala. *I,* Higher magnification of *G* showing individual double-labeled neurons at the level of the piriform cortex (*arrows*). *J, K,* Coronal sections of the olfactory bulb. *J,* TH-IR external tufted cells display a strong Pax6 immunostaining in E15.5 embryo (*small arrow*). *K,* Both TH-IR periglomerular neurons and TH-IR external tufted cells in A16 display Pax6 immunoreactivity at P0. Scale bar: *A, G,* 6 mm; *B, C,* 4 mm; *D, F, J,* 1 mm; *E,* 0.25 mm; *H,* 0.12 mm; *I,* 0.5 mm; *K,* 5 mm.

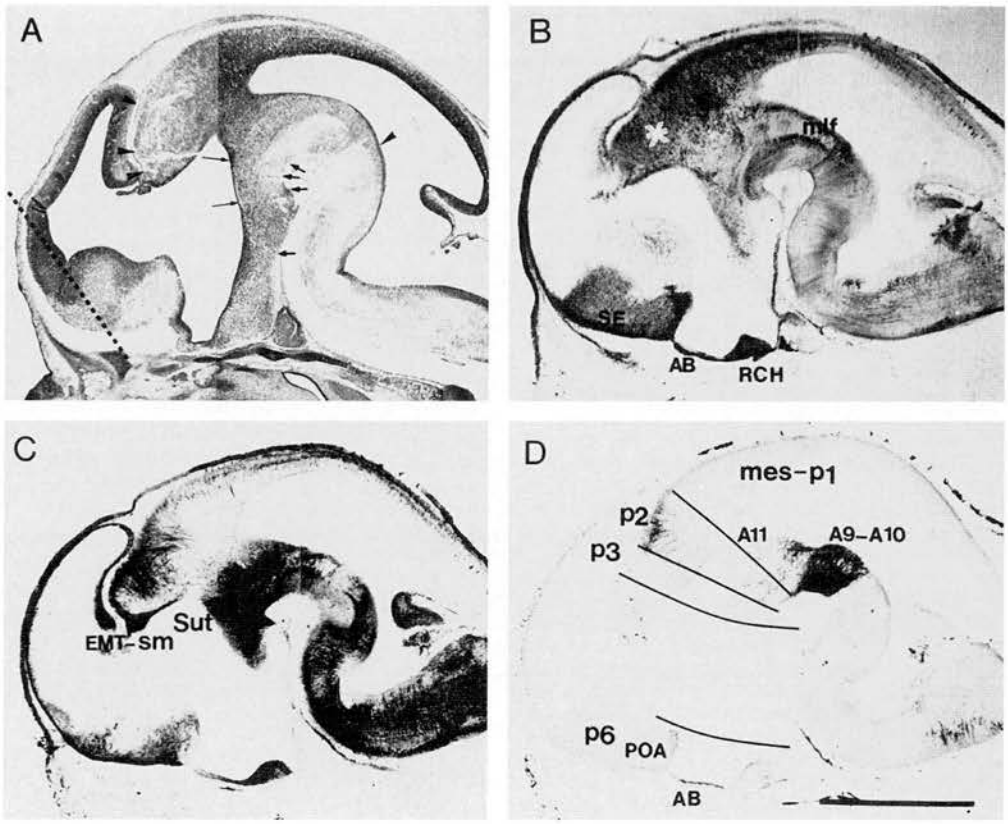

Figure 3. Determination of the presumptive neuromeric organization of TH-IR groups in E14.5 Pax6^{sey}/Pax6^{sey} embryos. Nissl-staining (*A*) and immunolabeling for calbindin (*B*) or calretinin (*C*) have provided prosomeric landmarks used for the determination of the segmental organization of TH-IR groups (*D*). *A*, The sagittal section shows constrictions in the neural wall and regions of low cell densities associated with neuromeric boundaries. From caudal to rostral, *arrowheads* point to the isthmic constriction and the presumptive, p1–p2, p2–p3, and p3–p4 boundaries. *Thin arrows* point to the presumptive p2–p3 and p3–p4 boundaries. *Arrows* point to the presumptive p1–p2, p2–p3, p3–p4, and p4–p5 boundaries. The *dotted line* represents the angle used for coronal sectioning. *B*, The sagittal section immunoreacted for calbindin shows a normal medial longitudinal fasciculus (*mlf*), retrochiasmatic (*RCH*) and anterobasal (*AB*) areas, and septum (*SE*). The *white star* indicates the lack of clustering of the presumptive dorsal thalamus and the lack of thalamocortical axons. *C*, Sagittal section immunoreacted for calretinin shows normal immunoreactivity in the thalamic eminence (*EMT*), the stria medullaris (*sm*), and the subthalamic nucleus (*Sut*) in p4. *D*, The sagittal section immunoreacted for TH shows numerous groups and complexes: *A11*, *A9–A10*, and in anterobasal and preoptic (*POA*) areas. The limit between *mes* and *p1* is not indicated because this neuromeric limit is altered in the mutant (Mastick et al., 1997). Scale bar: *A–D*, 4 mm.

though no colocalization of TH and Pax6 was observed in TH-IR neurons of the dorsal medial hypothalamic nucleus (Fig. 2*F*, *A14DMH*), Pax6 was expressed in the neuroepithelium of A14DMH during its period of genesis (from E9.75 to E12.5; see below).

An overview of defects in Pax6^{sey}/Pax6^{sey} embryos

From E10.5 to E14.5, Pax6^{sey}/Pax6^{sey} embryos displayed a delay in their growth. A marked difference in their crown-rump length was observed at E11.5 (wild type: 4.8 ± 0.3 mm, n = 15; Pax6^{sey}/Pax6^{sey}: 3.8 ± 0.33 mm, n = 15). By E14.5, wild-type and Pax6^{sey}/Pax6^{sey} embryos displayed no significant difference in their crown-rump length (wild type: 11.7 ± 0.07 mm, n = 30; Pax6^{sey}/Pax6^{sey}: 11.1 ± 0.1 mm, n = 30). By E17.5, brain weights were similar in wild-type and Pax6^{sey}/Pax6^{sey} embryos (wild type: 0.76 ± 0.07 gm, n = 30; Pax6^{sey}/Pax6^{sey}: 0.74 ± 0.06 gm, n = 25). Some brain regions in Pax6^{sey}/Pax6^{sey} embryos have been shown to display higher than normal cell densities (Schmahl et al., 1993; Caric et al., 1997), and there may be hypertrophy of brain regions in response to an increased SHH expression. This may compensate for the reduction of some structures such as the olfactory bulbs and, for example, the decrease of the cortical thickness.

TH-IR groups that did or did not display Pax6 immunoreactivity were described in Pax6^{sey}/Pax6^{sey} embryos within the same framework used above (see Fig. 3 for a general overview at E14.5). We observed several alterations in both Pax6-expressing TH-IR populations and TH-IR neurons that did not express Pax6, such as SN and VTA neurons. Noradrenergic (A1–A7) and adrenergic (C1–C3) neurons and mesencephalic dopaminergic neurons of A8, which did not express Pax6 (Table 1), displayed no delay and appeared normally organized in Pax6^{sey}/Pax6^{sey} embryos. The following description will focus on TH-IR groups displaying alterations.

Defects in Pax6-immunoreactive components of the incerto-hypothalamic axis

The incerto-hypothalamic axis (Bjorklund et al., 1975) includes TH-IR neurons of A11–A14. In this structure in normal animals, TH-IR neurons appear fused together along an axis extending from the mesencephalon to the anterior hypothalamus. In this structure, TH-IR neurons are arranged either in discrete nuclei (A12, A13, A14PAVH, and A14DMH) or in a periventricular position (A11, A14Periv). A13 and A14PAVH express Pax6 transiently during development, whereas A11, A12, A14DMH, A14Periv, and A14l do not express Pax6.

Cell generation

In E11.5 wild-type embryos, it was possible to identify scattered TH-IR neurons in the ventral thalamus at the level of the primordium of A13 and a few medium-sized TH-IR neurons of the A14 complex in p4 and p5. These cells were more numerous by E12.5 (Fig. 4*A*). In Pax6^{sey}/Pax6^{sey} embryos, the A13 and A14 primordia appeared with a 2 d delay (Fig. 4*A,B*), and when they first appeared, they contained fewer TH-IR neurons than in wild-type embryos (50% reduction estimated). This delay did not persist. By E17.5, the total numbers of TH-IR profile counts in mutants and wild types were similar in A13 (n = 600 ± 65, from six wild types; n = 524 ± 60, from six mutants; values are means ± SEM), in A14DMH (n = 510 ± 40, from six wild types; n = 486 ± 60, from six mutants), and in A14PAVH (n = 40 ± 4, from four wild types; n = 38 ± 3, from four mutants). Because the mean diameters of TH-IR neuronal cell bodies were similar in wild-type (A13, n = 10 μm ± 0.7; A14DMH, n = 11 μm ± 0.7; A14PAVH, n = 12 μm ± 0.9; values are means ± SEM from 30 TH-IR neurons from four wild types) and Pax6^{sey}/Pax6^{sey} embryos (A13, n = 11 μm ± 0.6; A14DMH, n = 10.5 μm ± 1.0; A14PAVH, n = 11.5 μm ± 0.4, values are means ± SEM from 30 TH-IR neurons from four mutants), this indicates that there is no difference in TH-IR cell number in these structures.

Although Pax6 is expressed in differentiated TH-IR neurons of A13 and A14PAVH but not A14DMH, Pax6 is expressed during the time of genesis of all of these TH-IR populations. We have investigated a possible delay in cell generation of the cells destined for these groups in Pax6^{sey}/Pax6^{sey} embryos. Cell proliferation was studied by analyzing BrdU incorporation into S-phase cells and

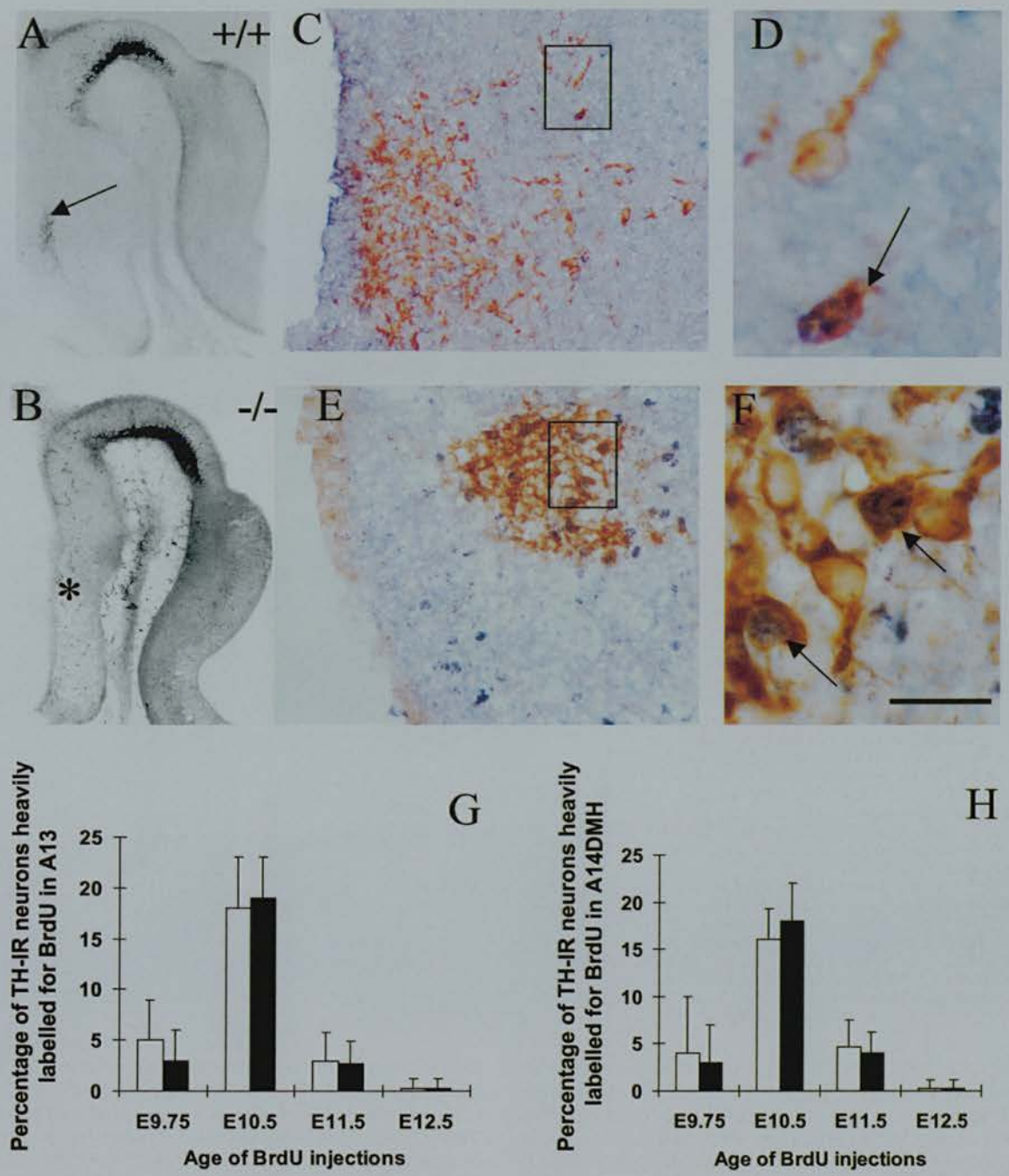

Figure 4. Delay in the appearance of a TH phenotype in A13 and A14DMH is not caused by a cell proliferation defect. *A*, *B*, Sagittal sections of E12.5 wild-type (*A*) and Pax6^{sey}/Pax6^{sey} (*B*) embryos immunolabeled for TH. *A*, *Arrow* points to the A13 and A14 primordia. *B*, The *black asterisk* indicates the presumptive location of the A13 and A14 primordia in the mutant; note the lack of TH-IR neurons in these regions. *C–F*, Double immunolabeling for TH and BrdU of E17.5 wild-type (*C*, *D*) and Pax6^{sey}/Pax6^{sey} embryos (*E*, *F*) at the level of A13. BrdU was injected on E10.5. *D*, *F*, *Arrows* point to TH–BrdU double-labeled neurons. *G*, *H*, Histograms showing similar mean percentages (±SEM) of TH-IR neurons darkly labeled for BrdU in A13 (*G*) and A14DMH (*H*) in wild-type (*white bars*) and Pax6^{sey}/Pax6^{sey} (*black bars*) E17.5 embryos after injections of BrdU on E9.75–E12.5. Scale bar: *A*, *B*, 2 mm; *C*, *E*, 0.5 mm; *D*, *F*, 0.1 mm.

visualizing them at E17.5 using anti-BrdU and anti-TH antibodies (Fig. 4*C–F*). To identify the embryonic stages at which the neurons of these nuclei are generated, a single injection was applied at four different developmental stages: E9.75, E10.5, E11.5, and E12.5. The number of BrdU–TH-positive cells and TH-positive cells was determined on coronal sections at E17.5. The labeling index was calculated as the percentage of the total number of TH-positive cells that were BrdU–TH-positive. In wild-type embryos, A13 and A14DMH are generated from E9.75 to E11.5 with a peak at E10.5 (Fig. 4*G*,*H*, *white bars*). In Pax6^{sey}/Pax6^{sey} embryos, the labeling index after each injection was unchanged and no delay was observed (Fig. 4*G*,*H*, *black bars*), suggesting that cell generation is unaffected in A13 and A14DMH.

Positional alterations

In wild-type embryos, A13, A14DMH, and A14PAVH were populated by large TH-IR neurons and appeared fused with each other from E14.5 (Figs. 1*F*, 5*A*,*C*). In Pax6^{sey}/Pax6^{sey} embryos, A13, A14DMH, and A14PAVH appeared greatly disjoined and abnormally shaped (Fig. 5*E–G*). In wild-type embryos, three distinct A13 subgroups were observed from E16.5 (Hokfelt et al., 1984): a dorsal group (A13d), a lateral group (Fig. 5*B*, *A13L*), and a medial group

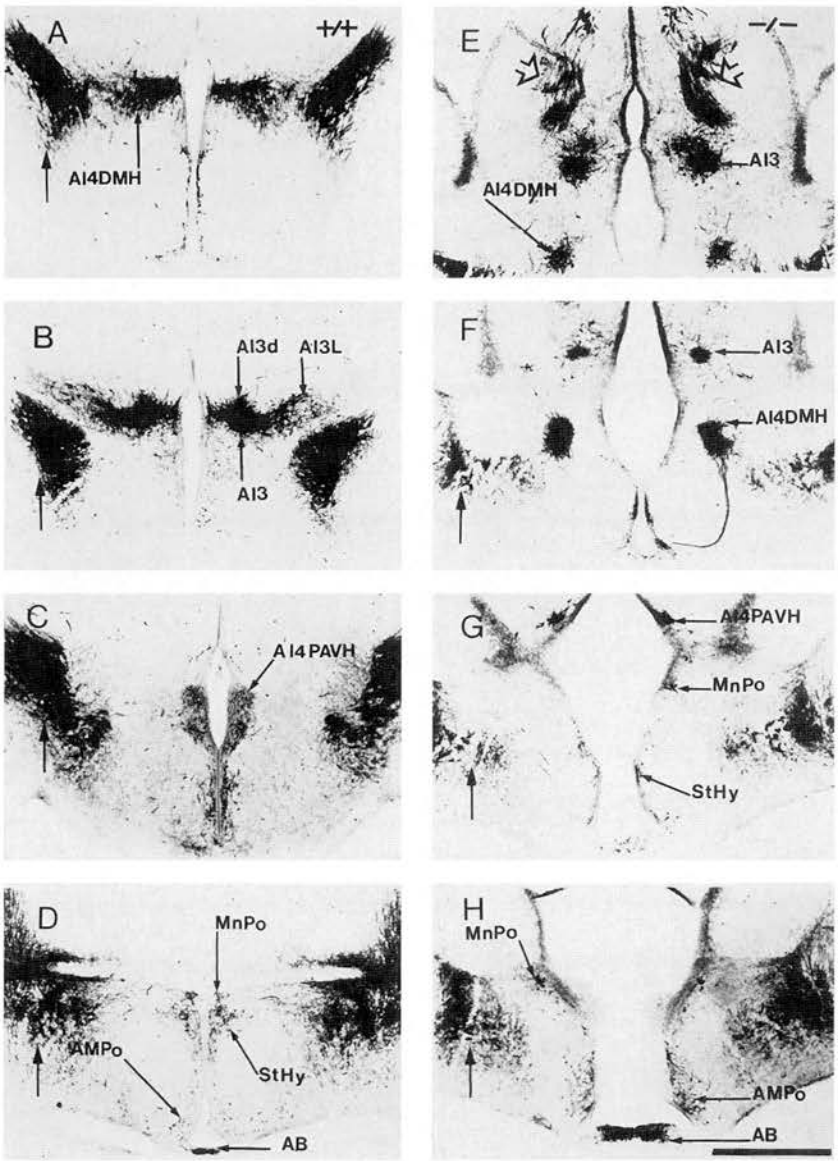

Figure 5. Alterations of the incerto-hypothalamic axis in E18.5 Pax6^{sey}/Pax6^{sey} embryos. Coronal sections are shown for wild-type (*A–D*) and Pax6^{sey}/Pax6^{sey} (*E–H*) embryos and are organized from caudal (*top*) to rostral (*bottom*). *A–C*, The components of the incerto-hypothalamic axis, A13, A14PAVH, and A14DMH appear fused together in wild-type embryos. The medial forebrain bundle is also indicated in *A–D* and *F–H* (*large unlabeled arrows*). *A*, *Arrow* indicates TH-IR neurons of the A14DMH complex. *B*, TH-IR neurons of A13 are divided into three distinct groups: a dorsal group (*A13d*), a lateral group (*A13L*), and a medial group A13 (*A13*). *C*, *Arrow* indicates TH-IR neurons of the paraventricular hypothalamic nucleus (*A14PAVH*). *D*, Rostral section at the level of the anterior commissure showing TH-IR neurons located in the medial preoptic nucleus (*MnPo*), the striato-hypothalamic nucleus (*StHy*), and the anterobasal region (*AB*). *E–G*, In Pax6^{sey}/Pax6^{sey} embryos, the components of the incerto-hypothalamic axis are completely disjoined and display abnormally high packing of the neurons. *E*, *Arrows* indicate *A13* and *A14DMH*. *Open arrows* indicate abnormally located TH-IR fibers originating from the SN–VTA. *F*, *Arrows* indicate *A13* and *A14DMH*. Projections from A14DMH to the area of the arcuate nucleus–median eminence are abnormally highly fasciculated. *G*, *H*, *Arrows* indicate the location of *A14PAVH*, *StHy*, the anterior medial preoptic nucleus (*AMPo*), *MnPo*, and *AB*. Scale bar: *A–H*, 2 mm.

(A13) (Fig. 5*B*). In Pax6^{sey}/Pax6^{sey} embryos, only two subgroups were identified in A13; they were displaced laterally from the third ventricle and appeared as a ventral round-shaped group (Fig. 5*E*,*F*) and as a dorsal group (Fig. 5*F*). The presumptive A14PAVH was observed more rostrally, as a small nucleus densely packed with few TH-IR neurons (Fig. 5*G*). The presumptive A14DMH group was laterally displaced and organized as an ovoid-shaped nucleus (Fig. 5*E*,*F*).

Cellular segregation

In wild-type embryos, the structures of the incerto-hypothalamic axis, Zi, DMH, and PAVH are each composed of several neuronal groups with different phenotypes, such as TH, neurotensin, or vasopressin neurons. In these structures, TH-IR neurons are mixed with other cell types that do not express TH (Fig. 6*A*). In Pax6^{sey}/Pax6^{sey} embryos, TH-IR neurons constituting A13, A14DMH, and A14PAVH appeared more highly clustered (Fig. 6*B*). As described above, the total number of TH-IR neurons in A13, A14DMH, and A14PAVH are the same in the wild-type and Pax6^{sey}/Pax6^{sey} embryos (Fig. 6*C–F*); however, the volume occupied by A13 and A14DMH was smaller in Pax6^{sey}/Pax6^{sey} embryos (Fig. 6*C*). Interestingly, although the mean cellular density was similar between wild-type and Pax6^{sey}/Pax6^{sey} embryos (Fig. 6*D*), the cellular density of TH-IR neurons in these structures was higher in Pax6^{sey}/Pax6^{sey} embryos (Fig. 6*F*), indicating a higher segregation of TH-IR neurons in these structures as estimated by the increased percentage of TH-IR neurons within them (Fig. 6*E*). TH-IR neurons were more clustered or less mixed with cell types that did not express TH. This suggests altered adhesive properties of cells composing the Zi and DMH in Pax6^{sey}/Pax6^{sey} embryos.

Defects of TH-immunoreactive neurons in the telencephalon of Pax6^{sey}/Pax6^{sey} embryos

In wild-type embryos, from E14.5, TH-IR neurons were observed at the level of the bed nucleus (Fig. 7*A*, *A15d*) and the anterior olfactory nucleus (A16AON) (Nagatsu et al., 1990) (Fig. 8*C*). In Pax6^{sey}/Pax6^{sey} embryos, A15d was greatly reduced in cell number (Fig. 7*C*), whereas A16AON was absent by E14.5 (Fig. 8*G*). In wild-type embryos, TH-IR neurons were also observed in the olfactory bulb as soon as E16.5 (Fig. 8*D*). Based on their age, large soma size, and the location in the developing glomerular layer, these neurons probably correspond to external tufted cells. By E18.5, a large number of TH-IR neurons were observed in the glomerular layer of the olfactory bulb, corresponding to both external tufted cells and the earliest population of periglomerular interneurons. In Pax6^{sey}/Pax6^{sey} embryos, from E16.5, only a few lightly labeled TH-IR neurons were observed at the level of the residual olfactory bulb (Fig. 8*G*). Evidence for the development of a residual olfactory structure is provided by calretinin and calbindin immunoreactivities (Fig. 8*E*,*F*). In this structure, TH-IR

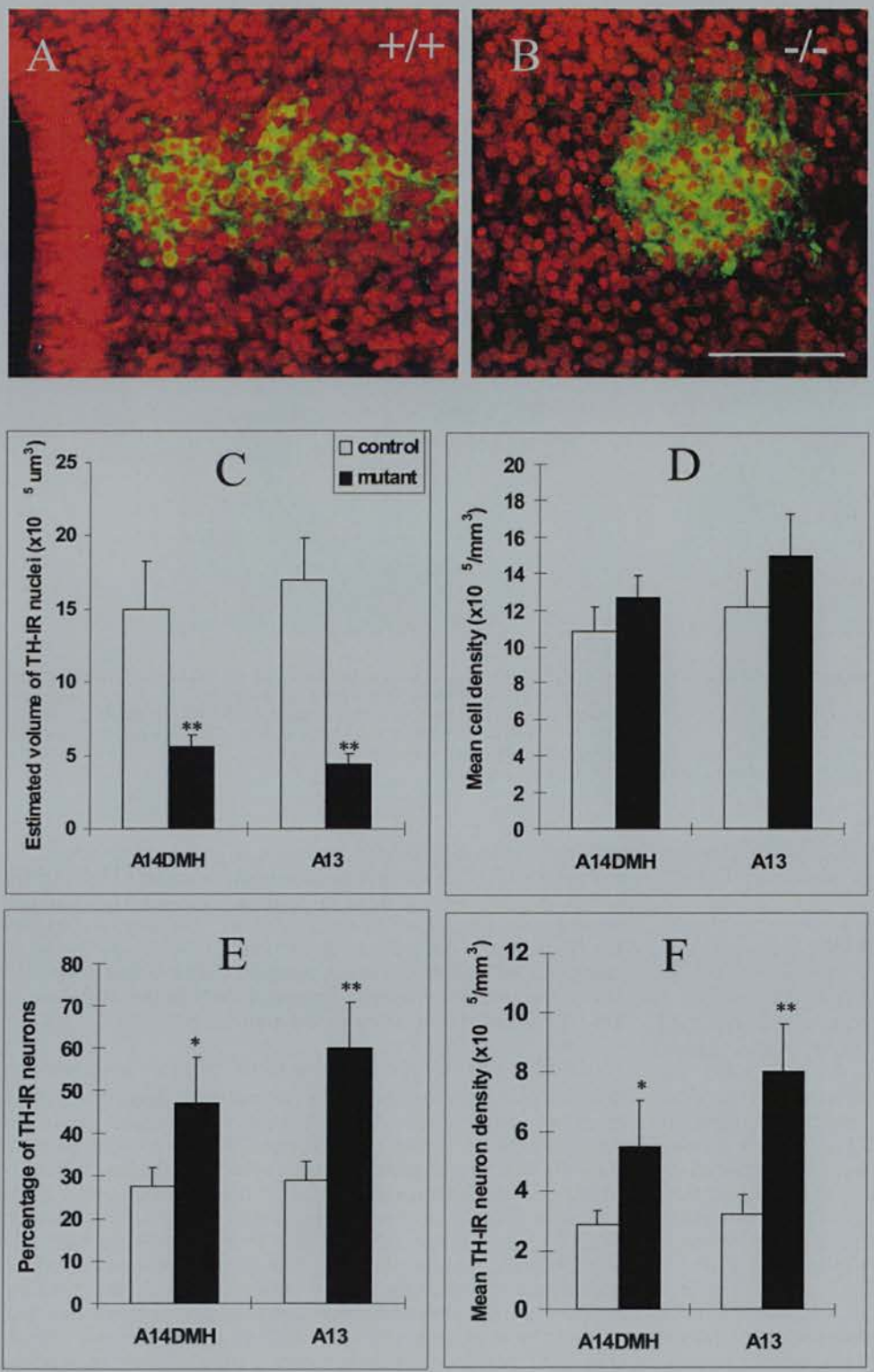

Figure 6. Increased cellular segregation of TH-IR neurons in A13 and A14DMH of mice lacking Pax6. TH was revealed with fluorescein-coupled antibodies (*green* in *A* and *B*), and nuclei were revealed on the same sections with propidium iodide (*red* in *A* and *B*). Pictures show the addition of two confocal images acquired simultaneously with a two-channel excitation beam. *A*, In A13 in the wild-type embryo, TH-IR neurons were mixed with non-TH-IR neurons. *B*, In Pax6^{sey}/Pax6^{sey} embryos, TH-IR neurons of A13 appeared more densely clustered and more segregated from the non-TH-IR neurons. *C*, Histogram shows the estimated volume occupied by TH-IR neurons in A14DMH and A13 in wild-type (*white bars*) and Pax6^{sey}/Pax6^{sey} (*black bars*) embryos. *D*, Histogram shows that the mean cell density of propidium-positive nuclei in A14DMH and A13 was similar in wild-type (*white bars*) and Pax6^{sey}/Pax6^{sey} (*black bars*) embryos. *E*, Histogram shows a significant increase of the percentage of TH-IR neurons compared with the total number of propidium-positive nuclei in A14DMH and A13 of Pax6^{sey}/Pax6^{sey} embryos. *F*, Histogram shows a significant increase in the density of TH-IR neurons in A14DMH and A13 in Pax6^{sey}/Pax6^{sey} embryos. *C–F*, Significant differences with Student's *t* test between groups are indicated: $*p < 0.05$; $**p < 0.01$. Scale bar: *A*, *B*, 0.75 mm.

neurons were scattered but differentiated: they were large with angular shapes and short processes probably corresponding to the external tufted cells (Fig. 8*H*). The reduction in the mutant of TH-IR neurons in A15d (Fig. 7*C*) and A16 (data not shown) persisted in older Pax6^{sey}/Pax6^{sey} embryos. No small TH-IR neurons corresponding to the periglomerular interneurons were observed in older Pax6^{sey}/Pax6^{sey} embryos.

In wild-type embryos, from E16.5, TH-IR neurons were observed at the level of the strio-hypothalamic nuclei (Fig. 5*D*). In Pax6^{sey}/Pax6^{sey} embryos, despite the lack of the anterior commissure, TH-IR neurons were observed at the presumptive level of the strio-hypothalamic nucleus (Fig. 5*H*).

In addition, transient TH-IR neurons were observed in the piriform cortex (Fig. 7*A*,*B*, near A15v) from E14.5 to E18.5 and in the anterior amygdala (data not shown) and olfactory tubercle (data not shown) from E16.5 to E18.5 in wild-type embryos. In Pax6^{sey}/Pax6^{sey} embryos, TH-IR neurons were rare, round, and pale ($n = 15 \pm 4$, values are mean ± SEM from four mutants; $n = 90 \pm 10$, values are mean ± SEM from four wild types) at the presumptive level of the anterior amygdala. By E18.5, TH-IR neurons were not detected, and no pyknotic profiles were observed in this region. This suggests that these neurons were generated and had progressively lost their ability to maintain TH expression. TH-IR neurons were never observed in the presumptive olfactory

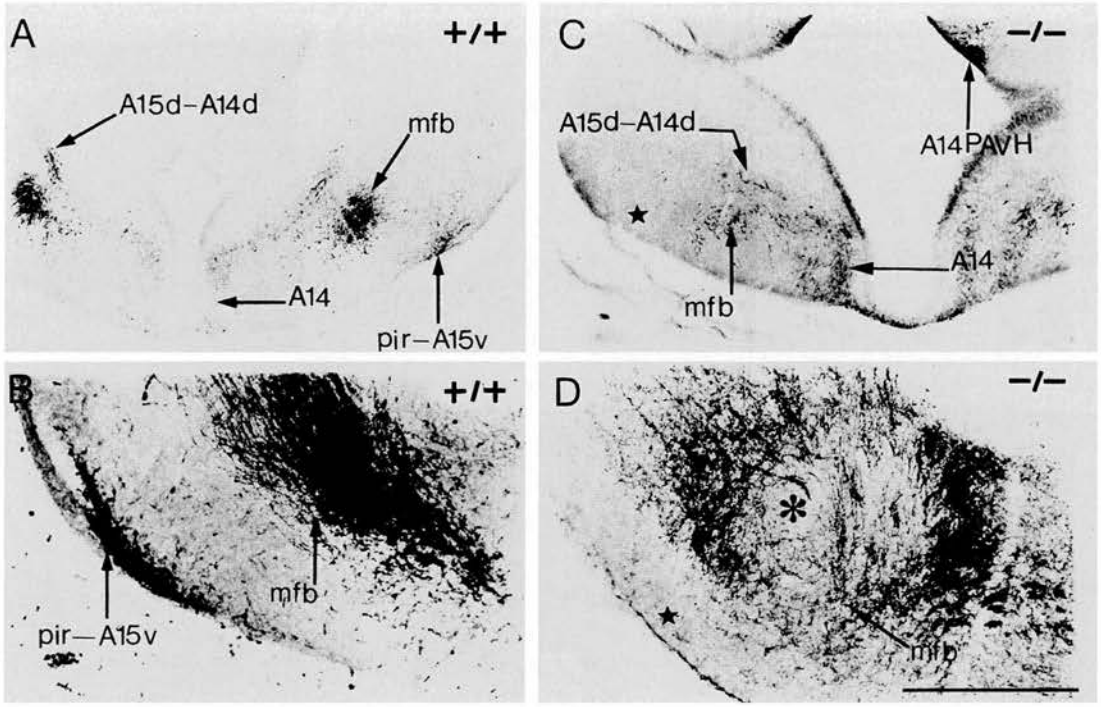

Figure 7. Defects of the telencephalic TH-IR neurons in Pax6^{sey}/Pax6^{sey} embryos. Coronal sections through the basal telencephalon and hypothalamus of E14.5 (*A*, *C*) and E18.5 (*B*, *D*) wild-type (*A*, *B*) and Pax6^{sey}/Pax6^{sey} (*C*, *D*) embryos. *A*, The section shows both the transient TH-IR neurons of the piriform cortex (*pir*) and the permanent TH-IR groups of *A15v* and *A15d* in continuation with *A14d*. Note the location of the medial forebrain bundle (*mfb*). *B*, High magnification of the *pir–A15v* area. *C*, The section shows a reduced A15d still in continuation with A14d. The *black star* indicates the lack of pir–A15v at the presumptive level of the rhinal fissure. *D*, The lack of pir–A15v persists in older age embryos (*black star*). The *large asterisk* indicates the abnormal swirl of TH-IR fibers at the medial forebrain bundle (*mfb*). Scale bar: *A–E*, 2 mm.

tubercle, the piriform cortex (Fig. 7*C*,*D*), and the neighboring hypothalamic A15v (Fig. 7*C*) and at any age studied in Pax6^{sey}/Pax6^{sey} embryos.

Defects in TH-immunoreactive groups not expressing Pax6

Defects in the SN–VTA (A9–A10) and A11 complex

In wild-type embryos, from E11.5 to E13.5, TH-IR neurons of the primordium of the ventral tegmental area (A10i, A10m, A10p1, A10p2, and A10p3) and of the substantia nigra (A9m, A9p1, and A9p2) migrate radially from their proliferative zones to more superficial positions (Kawano et al., 1995). These cells are shown in Figure 9*A*. In Pax6^{sey}/Pax6^{sey} embryos, by E11.5, TH-IR neurons of A9m and A9p1 and of A10m and A10p1 were normally radially organized, suggesting that they were normally migrating to their ventral positions (data not shown). At this age, TH-IR neurons of A10p2 and A10p3, in the p2-p3 floor plate of the mutants, were less numerous than in wild type (75% reduction estimated), probably because of a delayed TH expression. By E12.5, although sagittal mediolateral sections of wild-type embryos showed that the oldest TH-IR neurons of A9p1 and A9p2 were oriented caudorostrally in p1 and p2, in Pax6^{sey}/Pax6^{sey} embryos, very few radially oriented TH-IR neurons were observed on medial-most sections in mes, p1, p2, and p3. Strikingly, in mediolateral and lateral sections, TH-IR neurons of A9 were abnormally positioned along the presumptive p1–p2 transition zone (Fig. 9, compare *E* with *A*).

In wild-type embryos, the number of radially oriented TH-IR neurons detected in the vicinity of the ventricular surface gradually decreased by E13.5. By E14.5, most A9 and A10 neurons had reached their final locations in more superficial positions of the ventral floor plate and basal plate, respectively, and were oriented parallel to the ventral pial surface. From E16.5, TH-IR neurons of the A9 complex displayed their characteristic "inverted fountain" pattern (Hanaway et al., 1971; Kawano et al., 1995). This arrangement was even more striking in embryos of older stages (Fig. 9*B*). Strikingly, in Pax6^{sey}/Pax6^{sey} embryos, from E16.5, defects in the topography of A9 neurons were accentuated at the p1–p2 border, and in p2, A9 did not show its characteristic inverted fountain organization (Fig. 9, compare *F* and *B*). On sagittal sections, TH-IR neurons accumulated abnormally at the p1–p2 border in Pax6^{sey}/Pax6^{sey} embryos (Fig. 9, compare *C* with *G* and *D* with *H*). Taken together, these results suggest defects in the migration of TH-IR A9 and A10 neurons in the mutant.

TH-IR fiber pathway alterations in Pax6^{sey}/Pax6^{sey} embryos

In wild-type embryos, by E11.5, nigrostriatal and mesocortical fibers originating from A9 and A10 followed the pathway of the medial forebrain bundle (mfb) in mes, p1, p2, p3, and p4 basal plate. By E14.5, nigrostriatal fibers terminated in the lateral portion of the caudate-putamen (Fig. 10*A*), whereas mesocortical fibers continued rostrally to reach the prefrontal cortex and the striatum by E15.5. In addition, a few TH-IR fibers originating from A10 were observed running along the fasciculus retroflexus toward the epithalamus (Skagerberg et al., 1984). By E18.5, the caudate-putamen and the globus pallidus were homogeneously labeled, and a denser band of terminals was visible under the external capsule (Fig. 10*K*). Mesocortical fibers emerged from mfb and entered the olfactory tubercle or ramified into the ventral lateral part of the nucleus accumbens (Fig. 10*K*). The remaining mesocortical TH-IR fibers turned dorsally to enter the medial, prefrontal, and anterior cingulate cortices (Verney et al., 1982; Voorn et al., 1988; present study).

In Pax6^{sey}/Pax6^{sey} embryos, by E11.5, most TH-IR fibers did not follow the pathway of mfb. Fibers were misguided along the presumptive p1–p2 transition zone where they followed a straight ventrodorsal course (Fig. 10*B*,*C*). A few fibers originating from the more rostral and ventromedial neurons of the A9–A10 complex followed the pathway of the presumptive mfb (Fig. 10*D*), although they only reached p4 by E12.5. By E14.5, misguided TH-IR fibers looped in the roof of p2, plunged mediolaterally after the presump-

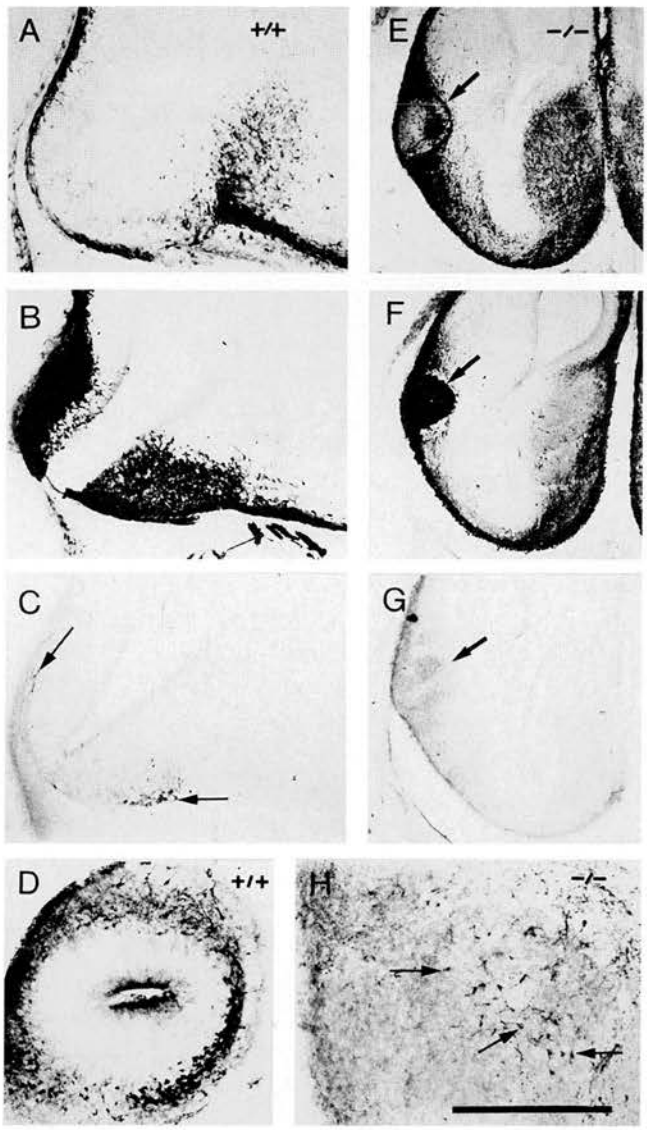

Figure 8. Delay and diminution in the number of A16 neurons in the anterior olfactory nucleus and the residual olfactory structure of Pax6^{sey}/Pax6^{sey} embryos. Sagittal (*A–C*) and coronal (*D–H*) sections are shown for E14.5 (*A–C*, *E–G*) and E16.5 (*D*, *H*) wild-type (*A–D*) and Pax6^{sey}/Pax6^{sey} (*E–H*) embryos. Alternate sections are immunostained for calbindin (*A*, *E*), calretinin (*B*, *F*), or TH (*C*, *F*). *A*, Calbindin immunoreactivity labels short axon cells of the olfactory bulb. *B*, Calretinin immunoreactivity labels mitral and tufted cells of the olfactory bulb. *C*, *Arrows* indicate neurons of A16 in the anterior olfactory bulb in A16AON. *D*, Section showing TH-IR external tufted cells in the olfactory bulb of E16.5 wild-type embryo. *E*, Calbindin immunoreactivity strongly labels cells that may correspond to short axon cells. *F*, Calretinin immunoreactivity strongly labels cells that may correspond to the mitral and tufted cells of the remaining olfactory bulb. *G*, TH-IR neurons are absent in the remaining olfactory structure of E14.5 Pax6^{sey}/Pax6^{sey} embryo. *E–G*, *Arrow* points to the residual olfactory structure. *H*, High magnification shows scattered TH-IR neurons with short processes (*arrows*) in the residual olfactory bulb of E16.5 Pax6^{sey}/Pax6^{sey} embryo. Scale bar: *A–C*, *E–G*, 2 mm; *D*, *H*, 1 mm.

tive p2–p3 border, and turned rostroventrally in p3 basal plate to reach and follow the pathway of the presumptive mfb in p4 and p5 (Fig. 10*E–J*). In addition, few TH-IR fibers looped rostrally in presumptive p2 alar plate (Fig. 10*E*,*G*). In their ascending and descending courses, TH-IR fibers appeared abnormally highly fasciculated (Fig. 10*H*). At the presumptive level of the internal capsule and the optic tract, TH-IR fibers swirled just before they entered the caudate putamen (Fig. 7*D*). From E18.5, at least some TH-IR fibers reached the same rostral levels as observed in wild-type embryos, although the number of terminals was greatly reduced, particularly in the olfactory tubercle (Fig. 10*L*).

General fiber pathway alterations in Pax6^{sey}/Pax6^{sey} embryos

Using the neuronal cell adhesion molecules NCAM and L1 as general markers of most axonal pathways, we analyzed whether alterations of TH-IR axons in the presumptive diencephalon were a selective defect of catecholaminergic fibers or a general defect of all ascending and descending fibers.

NCAM (from E11.5 to E13.5) and L1 (from E14.5) immunoreactivities revealed most of the fiber pathways traveling in the diencephalon. In wild-type embryos, the posterior, pretectal, and tectal commissures, the fasciculus retroflexus, and the stria medullaris were labeled with NCAM (Fig. 11*B*) or L1 (Fig. 11*E*). In addition, the zona limitans intrathalamica (Zli) at the p2–p3 boundary displayed NCAM immunoreactivity from E11.5 to E13.5 (Fig. 11*B*).

In Pax6^{sey}/Pax6^{sey}embryos, fibers traveling medially followed a normal trajectory in the basal plate of the rhombencephalon, mes, p1, p2, and p3, whereas fibers located laterally in basal plate and alar plate were misguided at the presumptive p1–p2 transition zone and in p2 alar plate (Fig. 11*D*,*F*). In p2, most of the L1 immunoreactive fibers were highly fasciculated into several straight and parallel bundles (Fig. 11*F*). In the roof of p2, most fibers looped and descended at the presumptive p2–p3 limit.

Altered expression of the chemorepellent/chemoattractive molecule Netrin-1 in Pax6^{sey}/Pax6^{sey} embryos

In Pax6^{sey}/Pax6^{sey} embryos, from E11.5, the developmental expression of Netrin-1 was roughly normal in the rhombencephalic and mesencephalic floor plate, along the floor of the fourth ventricle and along the wall of the lateral ventricle (Fig. 12). From E13.5, Netrin-1 was normally expressed in the striatum and from E14.5 in the vicinity of the SN–VTA complex (Livesey and Hunt, 1997) (Fig. 12*A*,*C*). However, an abnormally high and expanded expression of Netrin-1 was observed from the presumptive p1–p2 transition zone to the p2–p3 transition zone. Instead of being expressed in the ventral part of the diencephalic basal plate and in the Zli (Fig. 12*C*), Netrin-1 expression was expanded in all of the basal plate and the most ventral part of the presumptive alar plate (Fig. 12*D*). This altered Netrin-1 expression persisted and was correlated with increased and expanded expression of SHH reported previously (Grindley et al., 1997) (data not shown). The comparison of the pattern of Netrin-1 expression with TH-IR immunoreactivity (compare Figs. 12*D* and 10*E*,*H*) showed that TH-IR fibers and neurons seemed orientated abnormally toward the increased and ectopic Netrin-1 expression located at the pretectal–dorsal thalamic transition zone.

DISCUSSION

Our results in normal mice are in good agreement with previous comparative analyses on catecholaminergic systems in sauropsides (Medina et al., 1994) and humans (Puelles and Verney, 1998). The main TH-IR neurons clearly arise independently along the whole brain axis. Table 1 shows the resulting topological map of these groups. This mosaic pattern strongly suggests that this phenotype is generated by the combinatorial effects of regionally expressed transcription factors, such as Pax6, and diffusable morphogens such as SHH or FGF8. Differences between groups of TH-IR neurons may be caused by differences in the factors they express and the signals they receive.

It has been suggested that Pax6 could be a good candidate for controlling the proliferation, specification, or maintenance of discrete CA populations (Stoykova and Gruss, 1994; Dellovade et al., 1998). Our study indicates that discrete CA populations in the diencephalon, the hypothalamus, and the basal telencephalon express Pax6, either permanently or transiently. By analyzing mice lacking Pax6, we show that Pax6 is not necessary for the specification and time of generation of diencephalic and hypothalamic DA neurons but is needed for the normal packing and segregation of these cells. The lack of Pax6 leads also to a virtual absence of

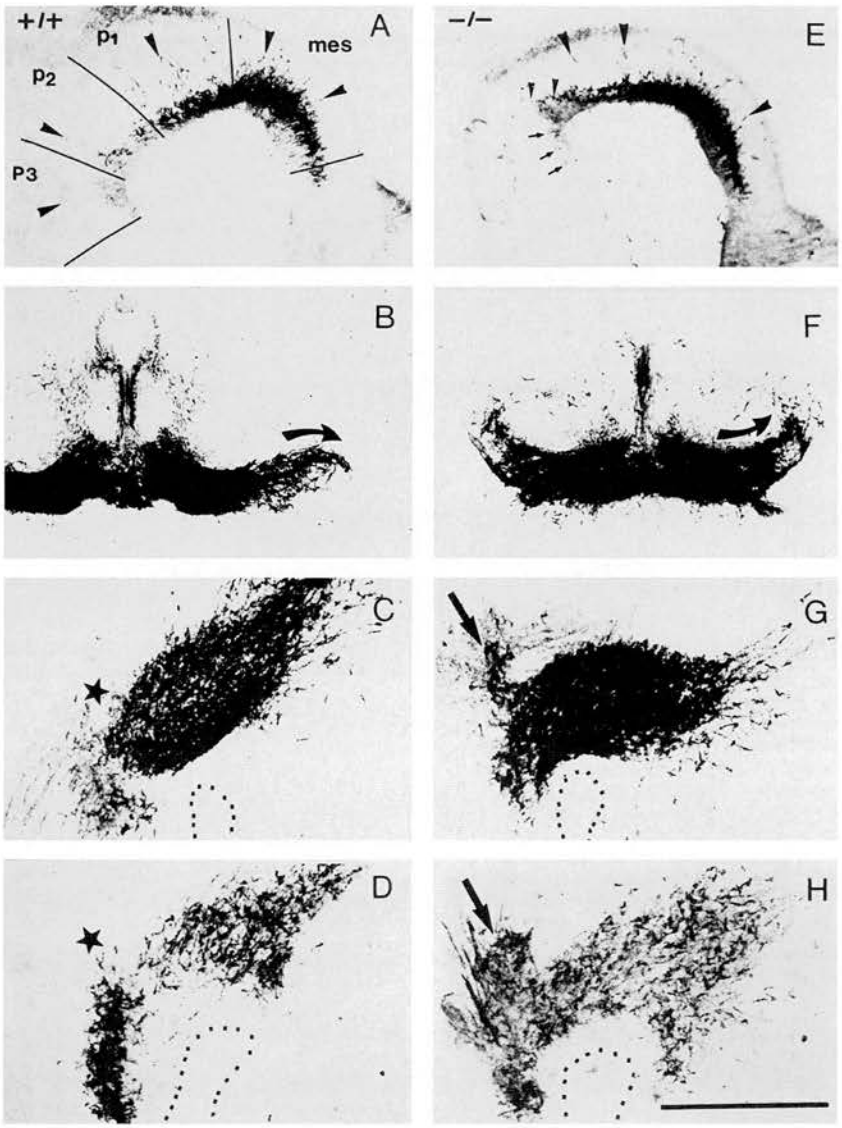

Figure 9. Developmental defects of the SN–VTA complex in Pax6^{sey}/Pax6^{sey} embryos. *A*, Sagittal section showing the developing SN–VTA complex of E12.5 wild-type embryo. *Arrowheads* indicate the radially oriented TH-IR neurons from *mes* to *p3*. Note that TH-IR neurons of A10 in p3 (A10p3) display a less intense immunoreactivity. *B*, Coronal section of E18.5 wild-type embryo showing the characteristic topographical inverted fountain-like organization of the SN–VTA complex. *C*, *D*, Medial (*C*) and lateral (*D*) sagittal sections of E18.5 wild-type embryo showing the organization of the SN–VTA complex. *E*, Sagittal section of the developing SN–VTA complex in E12.5 Pax6^{sey}/Pax6^{sey} embryo showing the abnormal topographical organization of TH-IR neurons in *p1* and *p2* (*small arrowheads*). *Small arrows* point to A10p3; *large arrowheads* point to radially migrating TH-IR neurons. *F*, The coronal section shows the abnormal topographical organization of the SN–VTA complex in an E18.5 Pax6^{sey}/Pax6^{sey} embryo. *B*, *F*, *Curved arrows* emphasize the topographical organization of dopaminergic neurons of the SN and the main direction of their neuropils. *G*, *H*, Medial (*G*) and lateral (*H*) sagittal sections of E18.5 Pax6^{sey}/Pax6^{sey} embryo. The *arrows* point to TH-IR neurons abnormally located along the p1–p2 border and in p2. *C*, *D*, The *black star* indicates the lack of TH-IR neurons in wild-type embryo at the corresponding location where ectopic TH-IR neurons are seen in the mutant. Scale bar: *A*, *E*, 2 mm; *B*, *F*, 1 mm; *C*, *D*, *G*, *H*, 0.5 mm.

TH-IR neurons in the basal telencephalon. We also describe non-cell autonomous defects among DA neurons of the SN–VTA complex: some are abnormally located, and the medial forebrain bundle, the major ascending pathway of DA neurons, is misrouted.

Dopaminergic populations expressing Pax6

Diencephalic and hypothalamic TH-IR neurons: cell adhesion defect

The neuroepithelium of prosomeres 3, 4, and 5 expresses Pax6 during the time of genesis of diencephalic and hypothalamic TH-IR neurons. Our study indicates that differentiated TH-IR neurons of A13 and A14PAVH continue to express Pax6 until the first postnatal days, whereas A14DMH does not. In mice lacking Pax6, these populations differentiate but display a 1–2 d delay in their appearance. Because previous studies have shown abnormally low proliferative rates in the entire diencephalic alar plate of mice lacking Pax6 (Warren and Price, 1997), we looked for a delay in the genesis of these TH-IR groups. Our results clearly indicate no significant delay in genesis in A13 and A14DMH and no reduction in cell number of TH-IR neurons in A13, A14PAVH, and A14DMH.

In mice lacking Pax6, A13, A14PAVH, and A14DMH, TH-IR neurons display an increase in cell density, suggesting altered adhesive properties. Previous studies have suggested that Pax6 regulates the expression of adhesion molecules (Stoykova et al., 1997; Meech et al., 1999). In mice lacking Pax6, there is a loss of R-cadherin expression in areas in which this gene is normally coexpressed with Pax6. Moreover, it has been shown that the segregation normally observed in aggregates of cortical and striatal cells in an *in vitro* assay is lost in mice lacking Pax6 (Stoykova et al., 1997). This could be explained by a model in which loss of Pax6 disrupts the adhesive mechanisms involving R-cadherin, thereby increasing cell mixing and leading to some of the morphological disruptions observed. Interestingly, TH-IR neurons in A13, A14PAVH, and A14DMH do not display a particular scattering or increased cell mixing, as might be expected, but paradoxically they are more densely packed in roundish cell clusters. We suggest that the selective loss of some adhesion molecules (such as R-cadherins) may alter the balance between heterophilic and homophilic interactions in such a way that some cells may have reduced ability to adhere to other types of cells and may have a tendency to adhere more strongly to cells of their own type.

Telencephalic populations: cell migration/maintenance defect

In the olfactory bulb, Pax6 is expressed from E15.5 in TH-IR external tufted cells and from E18.5 in TH-IR periglomerular interneurons. In mice, external tufted cells are born between E13 and E18 (Hinds, 1968a,b) and proliferate in the ventricular zone of the olfactory bulb. In mice lacking Pax6, we observe rare TH-IR neurons in the region of the olfactory structure, and their onset of TH expression and morphology correspond to those expected for external tufted cells. This suggests that Pax6 is important for the

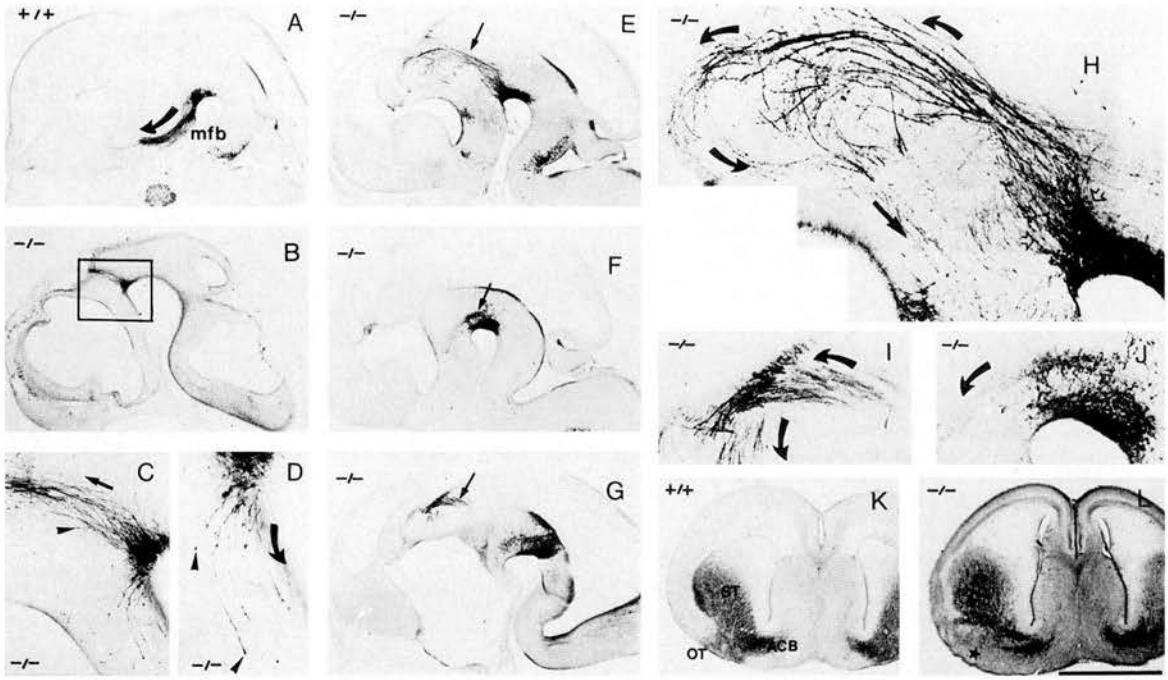

Figure 10. Alterations of TH-IR fibers pathway in Pax6^{sey}/Pax6^{sey} embryos. Sagittal (*A–J*) and coronal (*K*, *L*) sections are shown for wild-type (*A*, *K*) and Pax6^{sey}/Pax6^{sey} (*B–J*, *L*) embryos. Embryos were sectioned at E11.5 (*B–D*), E14.5 (*A*, *E–J*), and E18.5 (*K*, *L*). *Large arrows* indicate the direction of the fibers. *A*, *Large arrow* indicates the direction of the medial forebrain bundle (*mfb*), the major fiber pathway originating from TH-IR neurons of the SN–VTA complex. *B*, The sagittal section shows early alterations of TH-IR fiber pathway. *C*, *D*, *Small arrowheads* point to growth cones. *C*, Higher magnification of area outlined in *B*, showing that most of the TH-IR fibers are abnormally deflected dorsally after the presumptive pretectal–dorsal thalamic boundary. *D*, Higher magnification of area outlined in *B* shows that some TH-IR fibers are not deflected dorsally. *E*, A lateral section shows a high number of fibers from the SN–VTA complex misguided in the diencephalic alar plate (*arrow*). *F*, A mediolateral section of Pax6^{sey}/Pax6^{sey} embryos indicating neurons of the SN and their projections. *Arrow* indicates some TH-IR neurons of the SN that are not misguided. *G*, A medial section shows TH-IR fibers looping in the roof of the diencephalon (*arrow*). *H*, *I*, *J*, Higher magnifications of *E*, *G*, *and F*, respectively. *H*, Reconstruction of TH-IR fiber pathway. *K*, The coronal section shows the main projecting areas of TH-IR fibers, the striatum (*ST*), the nucleus accumbens (*ACB*), and the olfactory tubercle (*OT*). *L*, TH-IR fibers terminated normally in the striatum and the nucleus accumbens of Pax6^{sey}/Pax6^{sey}embryo. The *black star* indicates a lack of terminals in the olfactory tubercle. Scale bar: *A*, *E–G*, *K*, *J*, 4 mm; *B*, 2 mm; *C*, *H–J*, 1 mm; *D*, 0.5 mm.

specification of external tufted cells in the olfactory bulb. Proliferation defects may account for the low number of external tufted cells. Alternatively, because mice lacking Pax6 fail to develop a nasal olfactory epithelium, this dramatic reduction could be attributable to the lack of induction by primary olfactory afferents (McLean and Shipley, 1988; Baker and Farbman, 1993; Cigola et al., 1998).

In contrast to external tufted cells, periglomerular cells are born from E18 and arise along the anterior subventricular zone (Hinds, 1968a,b; Betarbet et al., 1996). In mice lacking Pax6, no TH-IR periglomerular interneurons are observed in late embryos or neonatal pups. Interestingly, Pax6^{sey}/+ heterozygote mice display a dramatic and specific decrease of TH-IR periglomerular interneurons, whereas external tufted cells are preserved. This reduction has been correlated to a progressive diminution in primary afferents (Dellovade et al., 1998).

Pax6 is strongly and transiently expressed in all TH-IR neurons of the piriform cortex, olfactory tubercle, and anterior amygdala. Recently, it has been suggested that cells populating these structures may be derived in part from a transient structure, the intermediate telencephalic territory (ITA), located at the transition zone between the neocortex and the lateral ganglionic eminence. Pax6 is expressed (from E12.5 to E14.5) in both proliferating cells and cells located near or in migrating neurons of the lateral cortical migratory stream derived from ITA (our unpublished results). When cells reach their targets, most of them express Pax6 during the formation of the different structures of the basal telencephalon. In mice lacking Pax6, ITA is dramatically altered: radial glial fascicles do not form at the cortical-ganglionic eminence transition zone and the expression of R-cadherin and the extracellular matrix molecule tenascin-C is lost (Stoykova et al., 1997). Interestingly, cellular migration in the lateral cortical migratory stream occurs in Pax6^{sey}/Pax6^{sey} embryos, although cells fail to stop in their final locations in the basal telencephalon and continue to migrate to the pial surface of the brain (Brunjes et al., 1998). We observe that the transient TH-IR neurons of the piriform cortex, the anterior amygdala, and the olfactory tubercle are decreased in number and fail to maintain TH expression in Pax6^{sey}/Pax6^{sey} embryos. We suggest that the absence of TH immunoreactivity in these cells may be because of the failure of TH induction or maintenance of TH expression in these migrating neurons that do not recognize a "stop signal " in the basal telencephalon.

Defects in catecholaminergic populations not expressing Pax6

Although TH-IR neurons of the SN–VTA complex never display Pax6 immunoreactivity, we show in mice lacking Pax6 an abnormal location of TH-IR neurons and an altered pathway of catecholaminergic fibers along the pretectal–dorsal thalamic transition zone and in the alar plate of the dorsal thalamus. The abnormal location of TH-IR neurons might be caused by either an ectopic genesis induced by altered expression of morphogenetic molecules or an altered migratory behavior induced by changes in the navigational environment.

Ectopic genesis of TH-IR neurons

Pax6^{sey}/Pax6^{sey} mice display an early abnormal ventral to dorsal expansion of the signaling secreted morphogen SHH and the SHH-induced gene, the winged helix transcription factor hepatocyte nuclear factor 3β (HNF-3β) at the level of the pretectal–dorsal thalamic transition zone and in the alar plate of the dorsal thalamus (Grindley et al., 1997) (our unpublished observation).

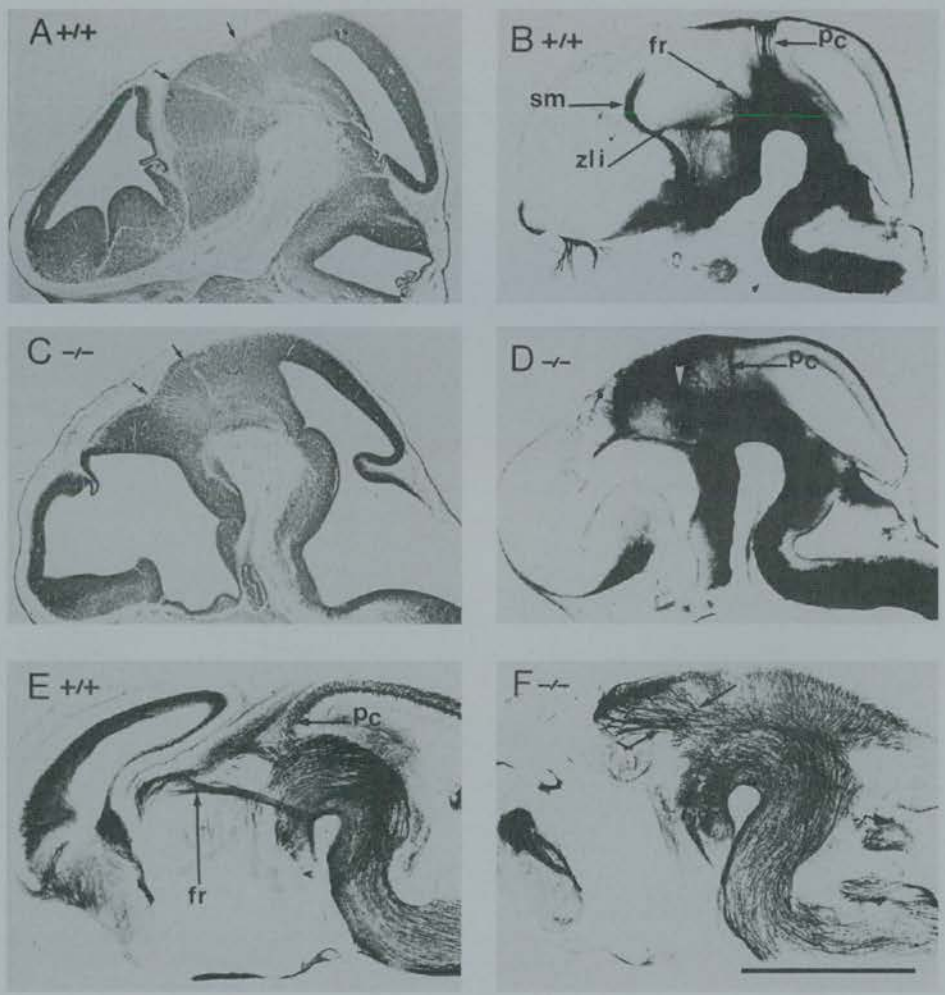

Figure 11. Alterations of specific fiber pathways in Pax6^{sey}/Pax6^{sey} embryos. Sagittal sections are shown for E12.5 wild-type (*A*, *B*) and Pax6^{sey}/Pax6^{sey} (*C*, *D*) embryos. Nissl-stained sections (*A*, *C*) are shown in parallel with sections immunoreacted for NCAM (*B*, *D*). *A*, *C*, The sagittal section shows constrictions and regions of low cell densities associated with prosomeric boundaries. *A*, C, *Arrows* indicate, from caudal to rostral, the mes–p1 boundary and the p1–p2 boundary. *B*, NCAM immunoreactivity reveals ascending and descending fibers of the posterior commissure (*pc*), the fasciculus retroflexus (*fr*), the stria medullaris (*sm*), and thalamic axons. A cellular labeling also reveals the zona limitans intrathalamica (*zli*). *D*, A remaining *pc* is distinguishable in p1 but most of the fiber tracts are misguided in the diencephalon (*white arrowhead*). *E*, *F*, Sagittal sections immunoreacted for L1 are shown for E18.5 (*E*), wild-type, and (*F*) Pax6^{sey}/Pax6^{sey} embryos. *E*, The sagittal section shows the posterior commissure (*pc*) in the caudal part of the pretectum and the fasciculus retroflexus (*fr*) at the pretectal–dorsal thalamic transition zone. *F*, The sagittal section shows aberrant fiber pathways in the pretectal and dorsal thalamic alar plate (between the *arrows*). Note that fibers traveling in the lower part of the basal plate and in the floor plate maintain a normal trajectory. Scale bar: *A–D*, 4 mm; *E*, *F*, 8 mm.

There is evidence that HNF-3β, SHH, and FGF8 create induction sites for TH-IR neurons along the dorsoventral axis (Sasaki and Hogan, 1994; Hynes et al., 1995; Wang et al., 1995; Ye et al., 1998). It is possible that the early ectopic SHH and HNF-3β expression domains in Pax6^{sey}/Pax6^{sey} mice induce ectopic catecholaminergic neurons.

Changes in navigational environment

Clearly a complex set of attractive and repulsive guidance molecules is provided in the environment. Ectopic expression of SHH or FGF8 could induce an ectopic expression of guidance cues, leading to the misrouting of growth cones or defects in cellular

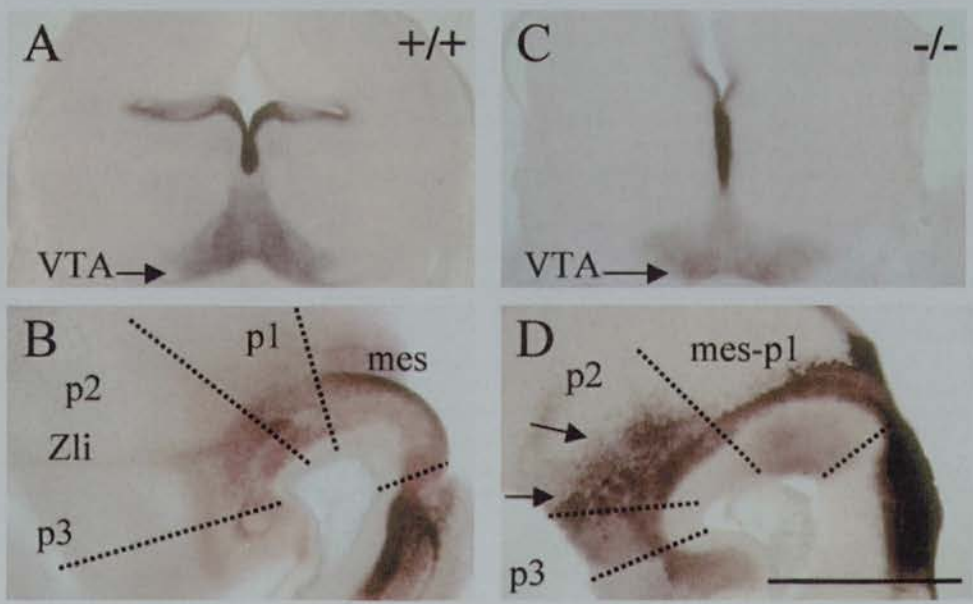

Figure 12. Alteration of Netrin-1 expression in the diencephalon of Pax6^{sey}/Pax6^{sey} embryos. Coronal (*A*, *C*) and sagittal (*B*, *D*) sections of E14.5 (*B*, *D*) and E16.5 (*A*, *C*) wild-type (*A*, *B*) and Pax6^{sey}/Pax6^{sey} (*C*, *D*) embryos. *A*, In the mesencephalon, Netrin-1 is expressed at the level of the SN–VTA complex. *B*, The sagittal section shows Netrin-1 expression in the floor of the fourth ventricle and in the basal plate of *p1*, *p2*, and *p3*. Note also a weak expression along the zona limitans intrathalamica (*Zli*). *C*, The coronal section shows a normal Netrin-1 expression at the level of the SN–VTA complex. *D*, In the diencephalon, Netrin-1 expression is increased and expanded dorsally. *Arrows* indicate the dorsal expansion in the ventral and dorsal thalamic alar plates. *mes*, Mesencephalon. Scale bar: *A*, *C*, 4 mm; *B*, *D*, 2 mm.

migration. For instance, it has been shown recently that ectopic expression of Hedgehog molecules induces ectopic Netrin-1 expression in the CNS of zebrafish embryos (Lauderdale et al., 1998). In mice lacking Pax6, the early ventral to dorsal expansion of SHH (Grindley et al., 1997) coincides with the ventral to dorsal expansion of Netrin-1. Netrin-1 is a laminin-related secreted protein with critical roles in axon guidance (Leonardo et al., 1997) and cell migration (Przyborski et al., 1998; Bloch-Gallego et al., 1999) that induces either attractive or repulsive responses, depending on the netrin receptor expressed. Normally, TH-IR neurons of the SN–VTA complex migrate in two phases: first, radially along tenascin-bearing glial processes, and second, tangentially, giving the SN its characteristic inverted fountain shape (Hanaway et al., 1971; Kawano et al., 1995). In $Pax6^{sey}/Pax6^{sey}$ embryos, the radial migration of SN–VTA neurons occurs normally (our unpublished results). Later, the rostral pretectal SN–VTA neurons are disorientated at the pretectal–dorsal thalamic transition zone near the expansion of Netrin-1 expression, and ectopic TH-IR neurons in the dorsal thalamus are disorientated and appear to be migrating away from the expanded Netrin-1 expression.

Nearly all SN–VTA projections are also misrouted at the pretectal–dorsal thalamic transition zone. Instead of following the medial forebrain bundle ventrally, SN–VTA projections are deflected rostrodorsally away from the expanded Netrin-1 expression. Taken together, we speculate that Netrin-1 has a chemorepellant activity on both the tangential migration and the pathfinding of SN–VTA neurons.

In conclusion, our study indicates that Pax6 is directly or indirectly involved in the adhesion and migration of discrete catecholaminergic populations and the maintenance of their phenotype. Second, Pax6 has a primordial role in determining the correct navigational environment for early diencephalic axonal pathfinding.

REFERENCES

Baker H, Farbman AL (1993) Olfactory afferent regulation of the dopamine phenotype in fetal rat olfactory system. Neuroscience 52:115–134.

Betarbet R, Zigova T, Bakay RA, Luskin MB (1996) Dopaminergic and GABAergic interneurons of the olfactory bulb are derived from the neonatal subventricular zone. Int J Dev Neurosci 14:921–930.

Bjorklund A, Lindvall O, Nobin A (1975) Evidence of an incerto-hypothalamic dopamine neurone system in the rat. Brain Res 89:29–42.

Bloch-Gallego E, Ezan F, Tessier-Lavigne M, Sotelo C (1999) Floor plate and netrin-1 are involved in the migration and survival of inferior olivary neurons. J Neurosci 19:4407–4420.

Brunjes PC, Fisher M, Grainger R (1998) The small-eye mutation results in abnormalities in the lateral cortical migratory stream. Dev Brain Res 110:121–125.

Bulfone A, Puelles L, Porteus MH, Frohman MA, Rubenstein JLR (1993) Spatially restricted expression of Dlx-1, Dlx2 (Tes-1), Gbx-2 and Wnt-3 in the embryonic day 12.5 mouse forebrain defines potential transverse and longitudinal segmental boundaries. J Neurosci 13:3155–3172.

Callaerts P, Halder G, Gehring WJ (1997) PAX-6 in development and evolution. Annu Rev Neurosci 20:483–532.

Caric D, Gooday D, Hill RE, McConnell SK, Price DJ (1997) Determination of the migratory capacity of embryonic cortical cells lacking the transcription factor Pax-6. Development 124:5087–5096.

Cigola E, Volpe BT, Li JW, Franzen L, Baker H (1998) Tyrosine hydroxylase expression in primary cultures of olfactory bulb: role of L-type calcium channels. J Neurosci 18:7638–7649.

Dellovade TL, Pfaff DW, Schwanzel-Fukuda M (1998) Olfactory bulb development is altered in small-eye (Sey) mice. J Comp Neurol 402:402–418.

Engelkamp D, Rashbass P, Seawright A, van Heyningen V (1999) Role of *Pax6* in development of the cerebellar system. Development 126:3583–3596.

Ericson J, Rashbass P, Schedl A, Brenner-Morton S, Kawakami A, Van Heyningen V, Jessel TM, Briscoe J (1997) Pax6 controls progenitor cell identity and neuronal fate in response to graded Shh signalling. Cell 90:169–180.

Fernandez AS, Pieau C, Reperant J, Boncinelli E, Wassef M (1998) Expression of the Emx-1 and Dlx-1 homeobox genes defines three molecularly distinct domains in the telencephalon of mouse, chick, turtle and frog embryos: implications for the evolution of telencephalic subdivisions in amniotes. Development 125:2099–2111.

Foster GA (1994) Ontogeny of catecholaminergic neurons in the central nervous system of mammalian species: general aspects. In: Phylogeny and development of catecholamine systems in the CNS of vertebrates (Smeeths WJAJ, Reiners A, eds), pp 405–434. Cambridge: Cambridge UP.

Franklin KBJ, Paxinos G (1995) The atlas of the mouse brain. San Diego: Academic.

Gillies K, Price DJ (1993) The fates of cells in the developing cerebral cortex of normal and methylazoxymethanol acetate-lesioned mice. Eur J Neurosci 5:73–84.

Grindley JC, Hargett LK, Hill RE, Ross A, Hogan BLM (1997) Disruption of Pax6 function in mice homozygous for the Pax6Sey-1Neu mutation produces abnormalities in the early development and regionalization of the diencephalon. Mech Dev 64:111–126.

Guthrie S (1996) Patterning the hindbrain. Curr Opin Neurobiol 6:41–48.

Hanaway J, McConnell JA, Netsky MG (1971) Histogenesis of the substantia nigra, ventral tegmental area of Tsai and interpeduncular nucleus: an autoradiographic study of the mesencephalon in the rat. J Comp Neurol 142:59–74.

Henrique D, Adam J, Myat A, Chitnis A, Lewis J, Ish-Horowicz D (1995) Expression of a Delta homologue in prospective neurons in the chick. Nature 375:787–790.

Hinds JW (1968a) Autoradiographic study of histogenesis in the mouse olfactory bulb. I. Time of origin of neurons and neuroglia. J Comp Neurol 134:287–304.

Hinds JW (1968b) Autoradiographic study of histogenesis in the mouse olfactory bulb. II. Cell proliferation and migration. J Comp Neurol 134:305–322.

Hirsh MR, Tiveron MC, Guillemot F, Brunet JF, Goridis C (1998) Control of noradrenergic expression by MASH1 in the central and peripheral nervous system. Development 125:599–608.

Hokfelt T, Matensson A, Bjorklund S, Kleinau S, Goldstein M (1984) Distributional maps of tyrosine hydroxylase-immunoreactive neurons in the rat brain. In: Handbook of chemical neuroanatomy. Classical transmitters in the CNS, Vol 2 (Bjorklund A, Hokfelt T, eds), pp 227–379. Amsterdam: Elsevier.

Hynes M, Porter JA, Chiang C, Chang D, Tessier-Lavigne M, Beachy PA (1995) Induction of midbrain dopaminergic neurons by sonic hedgehog. Neuron 15:35–44.

Jacobowitz DM, Abbott LC (1998) Chemoarchitectonic atlas of the developing mouse brain. Boca Raton, FL: CRC.

Jaeger CB, Joh TH (1983) Transient expression of tyrosine hydroxylase in some neurons of the developing inferior colliculus of the rat. Dev Brain Res 11:128–132.

Kaufman MH, Chang HH, Shaw JP (1995) Craniofacial abnormalities in homozygous Small eye (Sey/Sey) embryos and newborn mice. J Anat 186:607–617.

Kawano H, Ohyama K, Kawamura K, Nagatsu I (1995) Migration of dopaminergic neurons in the embryonic mesencephalon of mice. Dev Brain Res 86:101–113.

Krumlauf R (1994) Hox genes in vertebrate development. Cell 78:191–201.

Lauderdale JD, Pasquali SK, Fazel R, van Eeden FJ, Schauerte HE, Haffter P, Kuwada JY (1998) Regulation of netrin-1a expression by hedgehog proteins. Mol Cell Neurosci 11:194–205.

Leonardo ED, Hinck L, Masu M, Keino-Masu K, Fazeli A, Stoeckli ET, Ackerman SL, Weinberg RA, Tessier-Lavigne M (1997) Guidance of developing axons by netrin-1 and its receptors. Cold Spring Harb Symp Quant Biol 62:467–478.

Livesey FJ, Hunt SP (1997) Netrin and netrin receptor expression in the embryonic mammalian nervous system suggests roles in retinal, striatal, nigral, and cerebellar development. Mol Cell Neurosci 8:417–429.

Lumsden A (1990) The development and significance of hindbrain segmentation. Semin Dev Biol 1:117–125.

Mastick GS, Davis NM, Andrews GL, Easter Jr SS (1997) Pax-6 functions in boundary formation and axon guidance in the embryonic mouse forebrain. Development 124:1985–1997.

McLean JH, Shipley MT (1988) Postmitotic, postmigrational expression of tyrosine hydroxylase in the olfactory bulb dopaminergic neurons. J Neurosci 8:3658–3669.

Medina L, Puelles L, Smeets WJAJ (1994) Development of catecholamine systems in the brain of the lizard *Gallotia galloti*. J Comp Neurol 350:41–62.

Meech R, Kallunki P, Edelman GM, Jones FS (1999) A binding site for homeodomain and Pax proteins is necessary for L1 cell adhesion molecule gene expression by Pax-6 and bone morphogenetic proteins. Proc Natl Acad Sci USA 96:2420–2425.

Nagatsu I, Komori K, Takeuchi T, Sakai M, Yamada K, Karasawa N (1990) Transient tyrosine hydroxylase neurons in the region of the anterior olfactory nucleus of pre- and postnatal mice do not contain dopamine. Brain Res 511:55–62.

Olson L, Seiger A (1972) Early prenatal ontogeny of central monoamine neurons in the rat: fluorescence histochemical observations. Z Anat Entwicklungsgesch 139: 259–282.

Pattyn A, Morin X, Cremer H, Goridis C, Brunet JF (1997) Expressions and interactions of the two closely related homeobox genes Phox2a and Phox2b during neurogenesis. Development 124:4065–4075.

Paxinos G (1991) The atlas of the developing rat brain. San Diego: Academic.

Przyborski SA, Knowles BB, Ackerman SL (1998) Embryonic phenotype of Unc5h3 mutant mice suggests chemorepulsion during the formation of the rostral cerebellar boundary. Development 125:41–50.

Puelles L (1995) A segmental morphological paradigm for understanding vertebrate forebrains. Brain Behav Evol 46:319–337.

Puelles L, Medina L (1994) Development of neurons expressing tyrosine hydroxylase and dopamine in the chicken brain: a comparative segmental analysis. In: Phylogeny and development of catecholamine systems in the CNS of vertebrates (Smeeths WJAJ, Reiner A, eds), pp 381–404. Cambridge: Cambridge UP.

Puelles L, Verney C (1998) Early neuromeric distribution of tyrosine hydroxylase-immunoreactive neurons in human embryos. J Comp Neurol 394:283–308.

Rubenstein JL, Martinez S, Shimamura K, Puelles (1994) The embryonic vertebrate forebrain: the prosomeric model. Science 266:578–580.

Ruggiero DA, Baker H, Joh TH, Reis DJ (1984) Distribution of catecholamine neurons in the hypothalamus and preoptic region of mouse. J Comp Neurol 223:556–582.

Sasaki H, Hogan BLM (1994) HNF-3β as a regulator of floor plate development. Cell 76:103–115.

Schmahl W, Knoediseder M, Favor J, Davidson D (1993) Defects of neuronal migration and the pathogenesis of cortical malformations are associated with small eye (sey) in the mouse, a point mutation of the Pax-6 locus. Acta Neuropathol 86:126–135.

Shimamura K, Hartigan DJ, Martinez S, Puelles L, Rubenstein JL (1995) Longitudinal organization of the anterior neural plate and neural tube. Development 121:3923–3933.

Shimamura K, Martinez S, Puelles L, Rubenstein JL (1997) Patterns of gene expression in the neural plate and neural tube subdivide the embryonic forebrain into transverse and longitudinal domains. Dev Neurosci 19:88–96.

Skagerberg G, Lindvall O, Bjorklund A (1984) Origin, course and termination of the mesohabenular dopamine pathway in the rat. Brain Res 307:99–108.

Stoykova A, Gruss P (1994) Roles of Pax-genes in developing and adult brain as suggested by expression patterns. J Neurosci 14:1395–1412.

Stoykova A, Fritsch R, Walther C, Gruss P (1996) Forebrain patterning defects in Small eye mutant mice. Development 122:3453–3465.

Stoykova A, Gotz M, Gruss P, Price J (1997) Pax6-dependent regulation of adhesive patterning, R-cadherin expression and boundary formation in developing forebrain. Development 124:3765–3777.

Verney C, Berger B, Adrien J, Vigny A, Gay M (1982) Development of the dopaminergic innervation of the rat cerebral cortex. A light microscopic immunocytochemical study using anti-tyrosine hydroxylase antibodies. Brain Res 281:41–52.

Verney C, Gaspar G, Febvret A, Berger B (1988) Transient tyrosine hydroxylase-like immunoreactive neurons contain somatostatin and substance P in the developing amygdala and bed nucleus of the stria terminalis of the rat. Dev Brain Res 42:45–58.

Voorn P, Kalsbeek A, Jorritsma-Byham B, Groenewegen HJ (1988) The pre- and postnatal development of the dopaminergic cell groups in the ventral mesencephalon and the dopaminergic innervation of the striatum of the rat. Neuroscience 25:857–887.

Walther C, Gruss P (1991) Pax-6, a murine paired box gene, is expressed in developing CNS. Development 113:1435–1449.

Wang MZ, Jin P, Bumcrot DA, Marigo V, McMahon AP, Wang EA, Woolf T, Pang K (1995) Induction of dopaminergic phenotype in the midbrain by Sonic hedgehog protein. Nat Med 1:1184–1188.

Warren N, Price DJ (1997) Roles of Pax6 in murine diencephalic development. Development 124:1573–1582.

Ye W, Shimamura K, Rubenstein JLR, Hynes MA, Rosenthal A (1998) FGF and Shh signals control dopaminergic and serotonergic cell fate in the anterior neural plate. Cell 93:755–766.